Title
Nickel-Catalyzed Reactions of Amides and New Methods for the Synthesis of Nitrogen-Containing Heterocycles

Author
Simmons, Bryan Joseph

Publication Date
2019

Peer reviewed|Thesis/dissertation

UNIVERSITY OF CALIFORNIA

Los Angeles

Nickel-Catalyzed Reactions of Amides and New Methods for the Synthesis of Nitrogen-Containing Heterocycles

A dissertation submitted in partial satisfaction of the

requirements for the degree Doctor of Philosophy

in Chemistry

by

Bryan Joseph Simmons

2019

ABSTRACT OF THE DISSERTATION

Nickel-Catalyzed Reactions of Amides and

New Methods for the Synthesis of Nitrogen-Containing Heterocycles

by

Bryan Joseph Simmons

Doctor of Philosophy in Chemistry

University of California, Los Angeles, 2019

Professor Neil K. Garg, Chair

This dissertation is divided into two main themes concerning transition metal-mediated methodologies and the synthesis of nitrogen-containing heterocycles. The first part of this dissertation focuses on the development of three new reaction pathways utilizing nickel and palladium. The impact of transition metals in the field of synthetic organic chemistry cannot be overstated, with the 2010 Nobel Prize being awarded for the use of palladium cross-coupling in organic synthesis. The second part of this dissertation aims to expand the synthetic toolbox towards the generation of nitrogen-containing heterocycles. With over 100 FDA-approved drugs containing a nitrogen atom, new methodologies toward these scaffolds remain highly sought after.

Chapters One, Two, and Three focus on the development of new methodologies utilizing nickel and palladium catalysis. Chapters One and Two describe our efforts towards the functionalization of the amide moiety. Although amides were once thought to be unreactive due to their resonance stabilization, we sought to probe the utility of amides as a functional group handle. Chapter One focuses on the alkylation of amides using nickel and an organozinc source to generate sp^2–sp^3 C–C bonds. Chapter Two showcases a methodology to convert secondary and tertiary amides to their corresponding amines using a silane reducing agent and nickel catalysis. Chapter Three discusses an academic and industrial collaboration towards the synthesis of tetra-*ortho*-substituted biaryls using palladium catalysis. These studies culminated in an extensive computational analysis of the reaction mechanism and the synthesis of numerous atropisomeric biaryls.

Chapters Four, Five, and Six detail new methodologies towards the generation of nitrogen-containing heterocycles. With the nitrogen atom being prevalent in numerous FDA-approved drugs, facile routes towards their incorporation remain highly valued. Chapter Four illustrates the elusive 3,4-piperidyne's use in a variety of cycloaddition reactions. This study led to the formation of numerous annulated piperidines and exemplifies the utility of our methodology. Chapters Five and Six utilize the interrupted Fischer indolization reaction to produce an assortment of furanoindoline and pyrrolidinoindoline products. Chapter Five centers on the synthesis of the aza-analogues of these products by employing pyridylhydrazines. A computational study was undertaken to determine the cause of success or failure in this transformation. Chapter Six describes a variation of interrupted Fischer indolization methodology performed in a microfluidic device, which should enable its use in medicinal chemistry.

The dissertation of Bryan Joseph Simmons is approved.

Yi Tang

Hosea Martin Nelson

Kendall N. Houk

Neil Kamal Garg, Committee Chair

University of California, Los Angeles

2019

“I’m Uncle Bryan, I do science.”

– Grace Simmons, Five Years Old

For my family

TABLE OF CONTENTS

LIST OF FIGURES

CHAPTER ONE

CHAPTER TWO

CHAPTER THREE

CHAPTER FIVE

LIST OF SCHEMES

CHAPTER ONE

CHAPTER THREE

CHAPTER FOUR

CHAPTER FIVE

CHAPTER SIX

LIST OF TABLES

CHAPTER ONE

CHAPTER TWO

CHAPTER THREE

CHAPTER FOUR

CHAPTER FIVE

CHAPTER SIX

LIST OF ABBREVIATIONS

α	alpha
$[\alpha]_D$	specific rotation at wavelength of sodium D line
Å	angstrom
β	beta
c	concentration for specific rotation measurements
γ	gamma
m/z	mass to charge ratio
μ	micro
π	pi
Ac	acetyl, acetate
AcOH	acetic acid
AIBN	azobisisobutyronitrile
app.	apparent
aq.	aqueous
Boc	*tert*-butoxycarbonyl
Boc_2O	di-*tert*-butyl dicarbonate
Bn	benzyl
br	broad
Bu	butyl
i-Bu	isobutyl
n-Bu	butyl (linear)
t-Bu	*tert*-butyl
t-BuOH	*tert*-butyl alcohol
Bz	benzoyl
°C	degrees Celsius
calcd	calculated
cat.	catalytic
Cbz	carboxybenzyl
cod	1,5-cyclooctadiene
d	doublet
dba	dibenzylideneacetone
dr	diastereomeric ratio

DCE	1,2-dichloroethane
Dess–Martin	Dess–Martin Periodinane
DIBAL-H	diisobutylaluminium hydride
DIC	*N,N*′-diisopropylcarbodiimide
DMA	Dimethylacetamide
DMAP	4-dimethylaminopyridine
dme	dimethoxyethane
DMF	*N*,*N*-dimethylformamide
DMSO	dimethyl sulfoxide
dppf	1,1′-bis(diphenylphosphino)ferrocene
ee	enantiomeric excess
er	enantiomeric ratio
equiv	equivalent
EDC•HCl	1-ethyl-3-(3-dimethylaminopropyl)carbodiimide hydrochloride
Et_3N	triethylamine
ESI	electrospray ionization
Et	ethyl
g	gram(s)
h	hour(s)
HOBt	hydroxybenzatriazole
HRMS	high resolution mass spectroscopy
Hz	hertz
IBX	2-iodoxybenzoic acid
IR	infrared (spectroscopy)
J	coupling constant
L	liter
LDA	Lithium diisopropylamide
m	meta
m	multiplet or milli
min	minute(s)
mol	mole(s)
mp	melting point
M	molecular mass
Me	methyl

MHz	megahertz
MS	molecular sieves
NBS	*N*-bromosuccinimide
NMR	nuclear magnetic resonance
nM	Nanomolar
Ns	nosyl
[O]	oxidation
OTf	trifluoromethanesulfonate (triflate)
ppts	para-toluenesulfonic acid
pH	hydrogen ion concentration in aqueous solution
PMHS	polymethylhydrosiloxane
ppm	parts per million
Ph	phenyl
Piv	pivaloyl
Pr	propyl
i-Pr	isopropyl
PSI	Pounds per square inch
q	quartet
quint.	quintet
R_f	retention factor
s	singlet
sat.	saturated
sext.	sextet
SFC	supercritical fluid chromatography
SiPr	1,3-Bis(2,6-diisopropylphenyl)-1,3-dihydro-2*H*-imidazol-2-ylidene
t	triplet
trig	trigonal
TFA	trifluoroacetic acid
THF	tetrahydrofuran
TLC	thin layer chromatography
TMS	trimethylsilyl
Ts	Tosyl
UV	ultraviolet

ACKNOWLEDGEMENTS

To begin, I would like to thank my advisor Prof. Neil K. Garg. As a kid with limited chemical knowledge, coming from a small liberal arts school, Neil took a risk accepting me into his lab. I like to believe he saw a potential in me that I had yet to see in myself. When I considered joining the lab, the chatter surrounding Neil was about how great of a chemist he was. Although true, he was much more than this. Above all else, Neil was everyone's personal advocate. Whether it was an award nomination or trying to acquire an industrial position, Neil would be the first one to support you. It was this constant encouragement that I became so appreciative of and have tried to emulate throughout my life. I thank him for all the time he's spent on my personal and professional development and for giving me a chance (or two).

I would also like to acknowledge the rest of my doctoral committee: Professors Ken Houk, Yi Tang, and Hosea Nelson. Their guidance and support throughout my graduate career has been invaluable and I thank them for serving on my committee.

I would also like to thank those who were directly responsible for sparking my love of science. Mr. Van Duzee's molecular biology class was my first exposure to the microscopic world and from that first day, when I peered into a microscope, I knew I would never turn back. Upon starting at California Lutheran University, I was fortunate to join the research lab of Dr. John Tannaci. His infectious love of organic chemistry drove me away from looking at cells and I quickly devoted myself to organic synthesis. It was in his lab that I had my first taste of research, and although quite bitter at times, his passion for science solidified my idea to be a synthetic chemist. I was also fortunate to consider Dr. Tannaci a good friend. Between the bar hopping around Thousand Oaks and the late night barbeques and "diet cokes", I enjoyed the time we shared together. Now if only you'd reply to an email! I was also lucky to work alongside a

number of incredibly bright chemists during my time there. From my roommates Mike Mayers and Scott Lombardi, to the rest of the summer crew, Vanessa Orr and Steven Boggess, my early chemistry career would not have been nearly as enjoyable without you. I would also like to acknowledge Professors Butcher, Quinlan, and Kingsbury for constantly pushing me to enter into graduate school and pursue a doctorate degree. This one's for you.

As I am about to embark on my next chapter as a medicinal chemist at Celgene… BMS? no, Celgene, I would like to thank those that helped guide my decision. To everyone at Boehringer Ingelheim, especially Drs. Senanayake, Sieber, Patel, and Qu. The conversations we shared about life as an industrial chemist and the encouragement to pursue this career proved invaluable in my decision to enter into industry. I would also like to thank the entire John lab at UCLA for opening the world of medicinal chemistry to me. What started out as a collaboration to survey our lab's compounds turned into a two-year partnership aimed at helping millions of patients dealing with Alzheimer's. Every day on this project gave me the opportunity to learn a new skill. Whether it was understanding how high-throughput assays are run from Jesus Campagna to methods on delivering your compound to mice with Tina Bilousova, the highly multi-disciplinary nature of our collaboration helped me feel secure in my decision to become a medicinal chemist.

When I joined Neil's lab, I was fortunate to be a part of 5229. Although I did not know it at the time, the individuals I met during my tenure in this room I now consider my family. The post-doc at the time, and my direct mentor, was Dr. Travis McMahon. I will never forget the first time I met Travis, with his stained t-shirt from high school and haircut out of an early 90's teen drama. His love of diet cokes and muffins was infectious and I still think of him every time I purchase one. I want to thank Travis for his patience in training me and for instilling in me the

idea that I should always know what every reagent is doing before putting it into my flask. The next oldest students in 5229 were Michael Corsello and Jose Medina. Mike bud or Luigi as I later called him, played a huge role in my graduate career. Whether it was his boisterous belly laugh or the nightly dance sessions to Queen, Mike always knew how to put a smile on my face. His chemical knowledge was also second to none. He would be the first one to question me about a mechanism or to check in on how my reaction went. I appreciated the time I got to spend with him and am looking forward to opening "Bry Guy's Pizzeria" when we are both old and decrepit. Jose bud or as he was colloquially known, "Bud", was one of the hardest working members of the Garg Lab. If he wasn't looking at cat videos during his lunch break, Bud was at his hood working towards one of his numerous first author publications. He also had exquisite taste in music and I was fortunate to accompany him to various concerts throughout LA. With us both residing in Southern California, I'm looking forward to continuing our friendship. The next oldest student in lab and someone who I was closest with during my time was Elias "Starboy" Picazo. Elias has this uncanny ability to see the positives in all aspects of life. When graduate school started to beat me down, Eli would be there with some random shower thought from Reddit or words of motivation he picked up from a Justin Beiber song. Elias was also one of the brightest individuals I have ever met and there is no ceiling to his potential. I thank him for his friendship and mentorship throughout the four years I was fortunate enough to work alongside him. After getting to spend the better part of a year with these four fine gentlemen, Travis left for bigger and better things. In an attempt to replace his prowess in lab, a new French post-doc, Dr. Marie Hoffmann, was brought on. Though we questioned whether or not she would be able to fit in to our lab culture, Marie did much more than that. Her aggressive but caring nature was a perfect fit and she quickly became the fifth "bud" of 5229. It was Marie who instilled in me the

importance of understanding everything about your NMR spectrum and forced me into understanding the difference between a doublet of triplets and a doublet of doublet of doublet of doublets. I also got to spend numerous late nights with Marie and enjoyed the time we had wandering aimlessly (perhaps drunkenly) through the streets of LA.

Although I was fortunate to share the glory days of 5229 with the individuals mentioned above, numerous other lab members greatly impacted my time in graduate school. When I joined the lab, two fifth year graduate students took it upon themselves to get to know me. Joel Smith was an absolute wiz when it came to anything synthetic chemistry related and he quizzed me often on mechanisms. Noah Fine Nathel had one of the darkest senses of humor of anyone I have met but was simultaneously caring and compassionate. When I began to question if I should leave the program or not, it was Noah that talked me off the ledge, and for this, I will forever be grateful to him. It was this selfless act that has led me to always make time for younger students, no matter how busy or stressed I may be.

The next youngest class contained two of the happiest-go-luckiest individuals. Tejas Shah and Liana Hie were incredibly hardworking and set an example for what a younger student should aspire to be. Tejas also was the labs de-facto party planner (even though Jesus would invite everyone over without him knowing). I appreciate all their help during the time we spent together. True!!!

Accompanying Mike and Jose in lab were Nick Weires and Jesus Moreno. Nick was someone you could count on to always be chippy and have a pep in his step. Literally, Nick walked on his toes and it was impressive. In one of my first projects, Nick was kind enough to join me and help guide me through what it takes to bring a project from infancy to completion. As we found out together on this journey, and contrary to popular beliefs, organozincs are hell to

make. I always appreciated his positive attitude and his outlook on life. On the other end of the positive attitude spectrum, was Jesus Moreno. Jesus always found something wrong with the world, but boy did I love him for that. Jesus was an incredibly bright chemist and an even bigger Chivas fan. I've lost count how many nights I spent in his apartment watching Liga MX and trying to calm him down from throwing his beer through the TV. On a serious note, I consider Jesus one of my dearest friends and I am extremely lucky to have gotten to know him. Once he no longer has to pay Merck back his signing bonus, you can bet I will be recruiting him to San Diego. Who else am I going to go see Tame Impala with?!

Having to deal with me for four years, alongside Elias, were Emma Baker and Junyong Kim. Like Noah, Emma had a dark sense of humor, and needless to say, we got along very well. Her love of cats and Hawaiian shirts have changed my wardrobe for the better (although some may say otherwise). I've also enjoyed how much closer we have grown after her time in Neil's lab. I now look for her in Trader Joe's anytime I'm trying to find the perfect potato. Junyong, Juny, or June puppy as he is known around certain parts of LA, was notorious for his laugh and his impeccable work ethic. On that note, Junyong also taught me it was okay to nap in lab, just so long as you have a reaction running in your hood. Like Elias, I can't wait to see what he does in his independent career and any young budding chemist would be fortunate to have him as their advisor.

I would be remiss to not mention those in my year. Graduate school is definitely a journey and I was fortunate to have two amazing people by my side. Joyann Barber is the bubbliest and most optimistic person I know. Her positive attitude on life is infectious and I look forward to potentially being neighbors down in San Diego! Lucas Morrill, someone who I criticized heavily when I first met due to his sandals and tie dye t-shirt, became one of my closest

friends and confidants. If Lucas wasn't enjoying his 10-lb bar of chocolate, you could find him at my hood reminiscing about the old days (mostly us getting yelled at in subgroup). From getting beers after work, playing golf on the weekends, or talking about what our futures hold, I've enjoyed the time we have spent together. I know he's going to do amazing work at Amgen and I am already looking forward to our beer tours in San Diego.

At some point in your graduate career you go from being the mentee to being the mentor, and I was fortunate enough to mentor and befriend a number of younger students. The class below consisted of a number of strong personalities: Jacob Dander, Michael Yamano, Robert Susick, and Jordan Dotson. I had the chance to work along side Jacob during my first year and lucky enough to do the same during my last. Jacob is the epitome of an intellectual and is the resident dictionary of our lab. His quick wit and love for all things political have forced me to stay abreast on current affairs. I don't know where his life will take him, but you can be damn sure he has my vote in the future. Dander 2040. Another member of his cohort that I was able to get to know during my tenure is Michael Yamano. Although I questioned his choice in music (and hockey team) almost daily, his love for science is infectious. If there was ever chemistry to try, the odds were that Michael had already tried it. He also had a love for Las Vegas and I enjoyed losing all our money playing craps together. Also, since he cannot argue with me in my thesis, no Michael, a pop-tart is not a ravioli and how dare you even consider it one. I am also thankful for the time I got to spend with Robert Susick. Though quite tall, Robert and I always saw eye to eye when it came to music and podcast. His enjoyment (obsession?) of League of Legends also found me by his side watching the tournament live. Rob was also a fantastic chemist and I was fortunate to get to know him. #TeamMoonPie. Jordan Dotson was the last member of this cohort and though I did not get to know him well, as he became a joint student

later in his career, his comments in group meeting could only come from someone well-versed in the chemical literature. I wish him the best of luck with his future endeavors.

The next class, which consisted of some of the brightest minds in our lab, was Melissa Ramirez, Tim Boit, and Sarah Anthony. Melissa joined the craziness of 5229 and became an integral part of the lab. Besides being an excellent computational chemist, Melissa had an uncanny ability to stay perfectly still. While working in the office, Melissa was so subtle with her movements that the lights in the office turned off. Don't ever change Melissa. Tim, like Joel and Mike before him, was an encyclopedia of knowledge when it came to organic chemistry. It has been a joy to see him progress as a quiet lost soul, into a budding chemist taking the reigns of the lab. I would wish him good luck in his independent career, but there isn't a person alive that doubts him. If there is anyone besides my cohort that understands what five years of graduate school is like, it is Sarah Anthony. Having started as an undergraduate shortly after my arrival, Sarah has been here since day one. Known for her boisterous personality, Sarah is not one to be timid when it comes to how she feels. Besides having a strong personality, Sarah is also incredibly strong when it comes to synthetic chemistry. There is not a single reaction that Sarah won't attempt and I know she is going to do amazing work with her remaining time here. I've also been fortunate to get to know Sarah on a more personal level and I've cherished the late nights and empty wine bottles we've produced. I'm excited to see what the future holds for us.

I was fortunate to get to know the following class of Rachel Knapp, Francesca Ippoliti, and Jason Chari. Although she would probably deny it, Rachel and I are very much alike. We both come from Italian families, we both have a love for classic rock, and we both have had the same roommate (she who must not be named). Rachel is also a fantastic chemist and I can't think of anyone I would rather have take over the Alzheimer's project. Oh, say hi to Shelby for me.

Francesca, or as I always liked to call her, Franny, is a bright and energetic person, even with her Minnesotan accent. Any time I read the label of a wine bottle, I will always do it in her voice. You and Josh are always welcome to come visit me in San Diego! Jason Chari has to be the nicest person I have ever met. There no doubt you'll do great things in grad school.

As I became a fifth year, I swore I would never spend my time getting to know the first years, and although I tried to make that come to fruition, they all became good friends. Katie Spence and Milauni (Moana) Mehta, or the dynamic duo, always seemed to be the reason behind my headaches. Whether it was the late night texts (please stop texting me) or the new age slang (which I still don't understand and never want to), they were constantly brightening up my day. Best of luck over your next five years, you'll need it. Hey Milauni, you up? The third musketeer in that class was Andrew Kelleghan. Though I did not get to know Andrew well, I've enjoyed the conversations we have had. Good luck with the other two.

Last but not least, there is the post-doc Evan Darzi. Sharing a room with you (again) over the last year has been a joy. From the constant sports talk to your exquisite taste in music (except mouthsounds… never again), I'm glad we've gotten to reconnect. You're an exceptional chemist and an even better father. I've really enjoyed getting to know you over the last few years and I wish you all the best moving forward.

From the day I started to when I will be getting hooded, the most constant part of graduate school has been my family and friends. To Josh and Danielle, thank you for always taking an interest in my rather nerdy endeavor. Your constant questions about anything "science" related always put a smile on my face, even if my answer was straight from Wikipedia. You're both amazing people and I'm glad I get to call you my friends. Now hurry up and get married. To Chloe Vieira, thank you. No words can really do justice how much you have helped me

during my time here. From proofreading my applications to grad school, to putting up with me for three years, you are a truly exceptional person. I consider you my closest friend and someone I have always looked up to. You are going to do amazing things with your life and I'm excited to be able to witness all of them. To the friends I've made during my time at UCLA, thank you for your support. Over the past three years, Margeaux Miller has been my partner in crime when it comes to musicals and plays. However, the biggest contributions came from my teachings of genres and sub-genres of metal music. She is much better off because of it. For some reason, Margeaux also allowed me to be her life coach, not sure how that turned out, but I'm honored to have held the title. You're an amazing person and I'm excited to try all the vegan restaurants in San Diego with you. To Dalton Steele, Janice Lin, and Leibniz Hang, thank you for all the fun times. Cume prep would not have been the same without you. I would also like to acknowledge Mike Jung for allowing me to get my ass kicked in racquetball every week. Although the student started to become the master towards the end, our games were always a nice reprieve from lab work. Lastly, I would like to thank Ricky Ruiz for all his hard work and dedication to the department. I will miss our daily conversations and run-ins at the grocery store. When you strike it big at the casino, don't forget about me.

Being raised by a small village of Italians, there was never a chance my family wouldn't be involved in every aspect of my life. To my aunts, uncles, and cousins, thank you for everything you have done for me. From the persistent love and support, to always being confused about what I do, and whether Saturday or Sunday was my day off, you have always stood by me. I couldn't ask for a better family. To my nieces Grace and Olivia, thank you for being a little shining glimmer of hope during my time in graduate school. When reactions stopped working and the pressure of my surroundings started to cave in, I always had you two.

The late night video chats where Olivia would just run in circles or where Grace would prop me up so I can see her eat dinner, were always the highlight of my day. I know you two will never remember what Uncle Bryan went through during this process, but I hope you realize that if I can do this, there is nothing you can't accomplish. I love you two to death and I'm so excited to see you grow up and change the world. To my brother Brandon, thank you for always being a role model. Through all the adversity you have faced in your life, you've always come out stronger. Growing up with you has been an experience to say the least, but I've enjoyed every minute of it. You're still a jackass, and that will never change, but you'll always be my brother. Oh, and Brandon, can I talk to you now? Lastly, to my parents, Michael and JoAnn, you two have always been my biggest supporters. From the times when I thought I couldn't continue, to the highest points in my life, you two were always there for me. You've taught me how to be an adult, how to put others before myself, and how hard work and dedication will allow you to accomplish anything. None of this would have been possible without your countless acts of unselfishness, love, and support. Every day I spent here was to make you proud and to show you what kind of son *you* raised. Thank you for everything. I love you both.

From when I joined the lab to where I sit now writing my thesis, graduate school has proven to be many things. For one, graduate school has been an introspective experience. It's forced me to understand my strengths and weakness, my limitations, and my wants. It's forced me to love myself, to truly understand what makes me happy, and what I want out of life. Some of the lowest moments of my life have come from this experience, but so have some of the best. When I was about to start graduate school, I was told this experience would leave me with Stockholm syndrome. The idea that when you are struggling to get through every day, when all your reactions are failing and you have deadlines to meet, that you would hate the experience.

When you begin to wrap up though, and have time to reflect on what the experience was like, the friends you made, the laughs and tears you shared, you would begin to realize that an opportunity like this doesn't come often. You start to understand how lucky you were to be apart of something bigger than yourself. We always ask the question, knowing what we know now, would we do graduate school again? For me, the answer is simple. I would.

BIOGRAPHICAL SKETCH

Education:

University of California, Los Angeles, CA

- Ph.D. in Organic Chemistry, anticipated Spring 2019, Advisor: Neil K. Garg
- NSF Graduate Research Fellowship, 2016–2019
- UCLA Anderson Business Foundations Certificate, 2018

California Lutheran University, Thousand Oaks, CA

- B.S. in Chemistry, *Cum Laude*, 2014

Professional and Academic Experience:

Graduate Research Assistant: University of California, Los Angeles, CA

- July 2014 – present; Advisor: Prof. Neil K. Garg.
- Advanced material towards the first 3,4-azacyclohexyne and synthesized various medicinally privileged piperidine heterocycles.
- Discovered the nickel-catalyzed alkylation of amides for the formation of alkyl ketones.
- Developed a mild and scalable nickel-catalyzed reduction of amides to furnish amines utilizing an air-stable nickel source.
- Generated complex heterocyclic scaffolds through an interrupted Fischer azaindolization cyclization.
- Discovered novel nSMase2 and AChE inhibitors for the potential treatment of neurodegenerative diseases (Collaboration with Prof. Varghese John, UCLA).
- Aided in the development of an interrupted Fischer indolization methodology using a microfluidic reactor (Collaboration with Prof. Varghese John, UCLA).

Chemical Development Intern: Boehringer Ingelheim, Ridgefield, CT

- May–August 2017; Advisors: Dr. Joshua Sieber, Dr. Chris Senanayake
- Expanded the substrate scope for the palladium-catalyzed cross-coupling of tetra-ortho substituted biaryls.

Undergraduate Research Assistant: Cal. Lutheran University, Thousand Oaks, CA

- July 2012 – May 2014; Advisor: Prof. John F. Tannaci
- Synthesized conjugated polymers for use in organic photovoltaics (collaboration with Prof. Barry C. Thompson, USC).
- Developed palladium-catalyzed C–H activation methodology for small-molecule systems.

Honors and Awards:

- Medicinal and Bioorganic Chemistry Foundation Scholar (2019)
- Seaborg Symposium Poster Prize, UCLA, (2014, 2017)
- NSF Graduate Research Fellowship, UCLA, 2016–2019
- Hanson-Dow Excellence in Teaching Award, UCLA, 2015
- NSF Graduate Research Fellowship Honorable Mention, UCLA, 2015
- UCLA University Fellowship, UCLA, 2014
- Graduation Honors: *Cum Laude*, Cal. Lutheran University, 2014
- Swenson Fellowship for Undergraduate Research, Cal. Lutheran University, 2013
- Cal. Lutheran University Guarantee Scholarship, 2010–2014

Publications

1. **Preparation of Azacyclotridecane via a Nickel-Catalyzed Reduction.** Bryan J. Simmons, Melissa Ramirez, Neil K. Garg. *Org. Synth.* (*manuscript submitted*).
2. **Synthesis of Fused Indolines by Interrupted Fischer Indolization in a Microfluidic Reactor.** Alexander Tuan-Huy Duong, Bryan J. Simmons, Mohammad Parvez Alam, Jesus Campagna, Neil K. Garg, Varghese John. *Tetrahedron Lett.* **2019**, *60*, 322–326.
3. **Computationally Assisted Mechanistic Investigation and Development of Pd-Catalyzed Asymmetric Suzuki–Miyaura and Negishi Cross-Coupling Reactions for Tetra-ortho-Substituted Biaryl Synthesis.** Nitinchandra D. Patel, Joshua D. Sieber, Sergei Tcyrulnikov, Bryan J. Simmons, *et. al. ACS Catal.* **2018**, *8*, 10190–10209.
4. **Understanding and Interrupting the Fischer Azaindolization Reaction.** Bryan J. Simmons, Marie Hoffmann, Pier Alexander Champagne, Elias Picazo, Katsuya Yamakawa, Lucas A. Morrill, K. N. Houk, and Neil K. Garg. *J. Am. Chem. Soc.* **2017**, *139*, 14833–14836.
5. **Nickel-Catalyzed Reduction of Secondary and Tertiary Amides.** Bryan J. Simmons, Marie Hoffmann, Jaeyeon Hwang, Mortiz K. Jackl, and Neil K. Garg. *Org. Lett.* **2017**, *19*, 1910–1913.
6. **Nickel-Catalyzed Alkylation of Amide Derivatives.** Bryan J. Simmons,† Nicholas A. Weires,† Jacob E. Dander, and Neil K. Garg. *ACS Catal.* **2016**, *6*, 3176–3179.
7. **Generation and Regioselective Trapping of a 3,4-Piperidyne for the Synthesis of Functionalized Heterocycles.** Travis C. McMahon,† Jose M. Medina,† Yun-Fang Yang, Bryan J. Simmons, K. N. Houk, and Neil K. Garg. *J. Am. Chem. Soc.* **2015**, *137*, 4082–4085.

Patents:

1. **Inhibitors of nSMase2.** Varghese John, Tina Bilousova, Barbara Jagodzinska, Neil K. Garg, Bryan J. Simmons, Kanagasabai Vadivel. US Provisional Patent Application No. 62/746,768.

CHAPTER ONE

Nickel-Catalyzed Alkylation of Amide Derivatives

Bryan J. Simmons[†], Nicholas A. Weires[†], Jacob E. Dander, and Neil K. Garg.

ACS Catal. **2016**, *6*, 3176–3179.

1.1 Abstract

We report the first catalytic alkylation of amide derivatives, which relies on the use of non-precious metal catalysis. Amide derivatives are treated with organozinc reagents utilizing nickel catalysis to yield ketone products. The methodology is performed at ambient temperature and is tolerant of variation in both coupling partners. A precursor to a nanomolar glucagon receptor modulator was synthesized using the methodology, underscoring the mild nature of this chemistry and its potential utility in pharmaceutical synthesis. These studies are expected to further promote the use of amides as synthetic building blocks.

1.2 Introduction

The ability to activate traditionally unreactive functional groups as synthons continues to be a vital area of research. One particularly stable functionality is the amide.[1] The resonance stabilization of amides has been well understood for decades;[1,2] consequently, the use of amides in C–N bond cleavage reactions has remained limited. Recently, however, there has been much interest in breaking amide C–N bonds to forge new C–heteroatom and C–C bonds.[3,4,5,6,7] Such methodologies provide new tactics to prepare acyl derivatives, but with the key benefit of amide

stability. The use of amides in multistep synthesis, followed by selective C–N bond activation and coupling, should ultimately prove advantageous in the synthesis of complex molecules.

The present study focuses on activating and coupling amides to build acyl C–C bonds in an intermolecular fashion (Figure 1.1). Such a catalytic methodology would complement Weinreb amide chemistry, but without the use of highly basic and pyrophoric organometallic reagents.[8] Prior contributions in this area include Suzuki–Miyaura couplings (**1.1→1.2**) reported by Zou (Pd),[4] Szostak (Pd),[5] and our laboratory (Ni).[3b] In each of these cases, the nucleophilic coupling partner was restricted to *aryl* boronate species, thus limiting the application of this methodology. The corresponding *alkylative* coupling (**1.1→1.3**) would be highly desirable given the prevalence of alkyl ketones in molecules of biological importance and the versatility of alkyl ketones as synthetic building blocks. Herein, we report the first alkylative cross-coupling of amide derivatives.

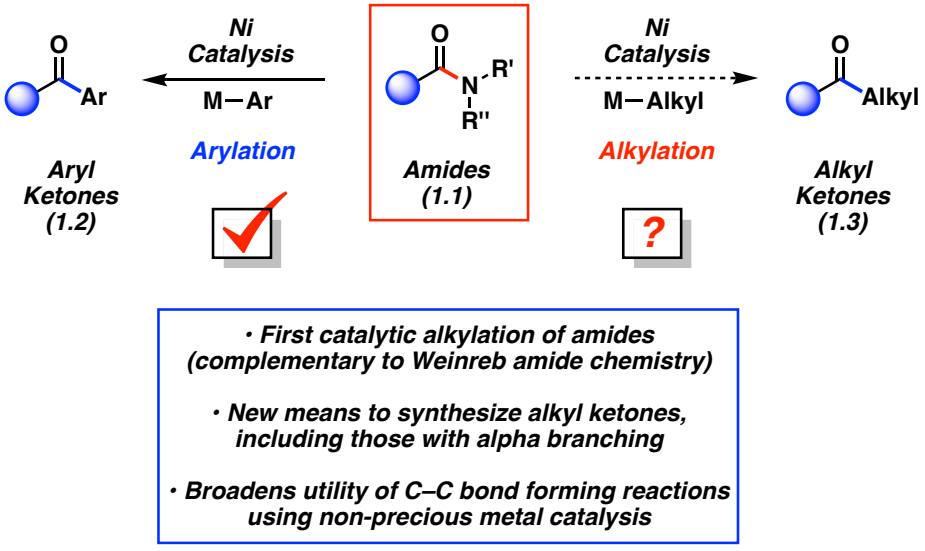

Figure 1.1. Nickel-catalyzed C–C bond forming reactions from amides.

Following unsuccessful attempts to couple amide derivatives with aliphatic boronic acids and esters, we opted to pursue the use of organozinc reagents as cross-coupling partners.[9] Our earlier studies have relied on the use of nickel catalysis for amide C–N bond activation,[3] which is notable given that nickel is less expensive, more abundant, and displays a lower CO_2 footprint compared to its precious metal counterpart, palladium.[10] Catalytic acyl couplings[11] with organozinc reagents are well precedented using acid halides (Pd or Ni),[12] anhydrides (Pd, Ni, or Rh),[12a,13] and thioesters (Pd or Ni),[12a,b,14] but the corresponding coupling of amides has not been reported.

1.3 Development of the Coupling Using Amides with Various *N*-Substituents

To initiate our study, we examined the coupling of naphthamides **1.4** with benzylzinc bromide (**1.5**) in the presence of catalytic $Ni(cod)_2$ and the NHC ligand SIPr in THF (Table 1.1). Although several amide derivatives failed to undergo the coupling (entries 1–3), we were delighted to find that *N*-alkyl,Boc and *N*-alkyl,Ts derivatives could be utilized (entries 4–5, respectively).[15] *N*-Alkyl,Ts amides (e.g., **1.4e**) are well suited for use in multistep synthesis.[16] It should be noted that the successful reactions of **1.4d** and **1.4e** proceeded at room temperature, which compares favorably to the few existing examples of catalytic amide C–N bond activation (ca. 50–160 °C)[3,4,5,6,7] and highlights the mild nature of this coupling.

Table 1.1. Survey of amide *N*-substituents in the coupling of substrates **1.4** with **1.5**.[a]

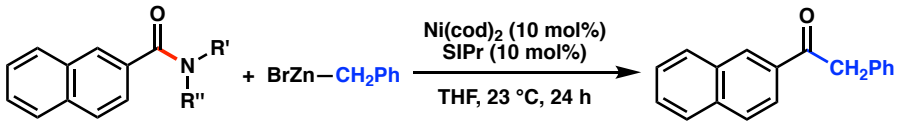

1.4 *1.5* *1.6*

Entry	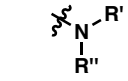	*Recovered 1.4*	*Yield of Ketone 1.6*[b]
1	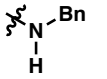 *1.4a*	*100%*	*0%*
2	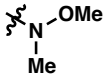 *1.4b*	*51%*	*0%*
3	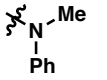 *1.4c*	*100%*	*0%*
4	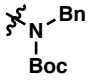 *1.4d*	*40%*	*60%*
5	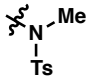 *1.4e*	*17%*	*81%*

[a] Conditions: $Ni(cod)_2$ (10 mol%), SIPr (10 mol%), substrate **1.4** (1.0 equiv), benzylzinc bromide (**1.5**, 1.5 equiv) and THF (1.0 M) at 23 °C for 24 h. [b] Yields determined by ^1H NMR analysis using hexamethylbenzene as an internal standard.

1.4 Scope of the Coupling with Respect to the Amide Substrate

Having found that the alkylative coupling of amide derivatives was indeed possible,[17] we evaluated the scope of the amide substrate (Table 1.2). The use of the parent naphthyl substrate gave **1.6** in 80% isolated yield. Additionally, it was found that the methodology was not restricted to extended aromatics. For example, the substrate derived from benzoic acid coupled smoothly to furnish **1.7** in 74% yield. Substrates bearing electron-donating groups could also be employed, as demonstrated by the formation of **1.8**–**1.10**. From the latter two cases, it should be emphasized that the presence of tertiary amines does not hinder catalysis. As shown by the

formation of **1.11** and **1.12**, the electron-withdrawing –F and –CF_3 substituents were also tolerated.[18]

Table 1.2. Scope of the amide substrate.[a]

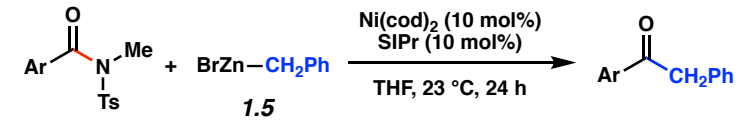

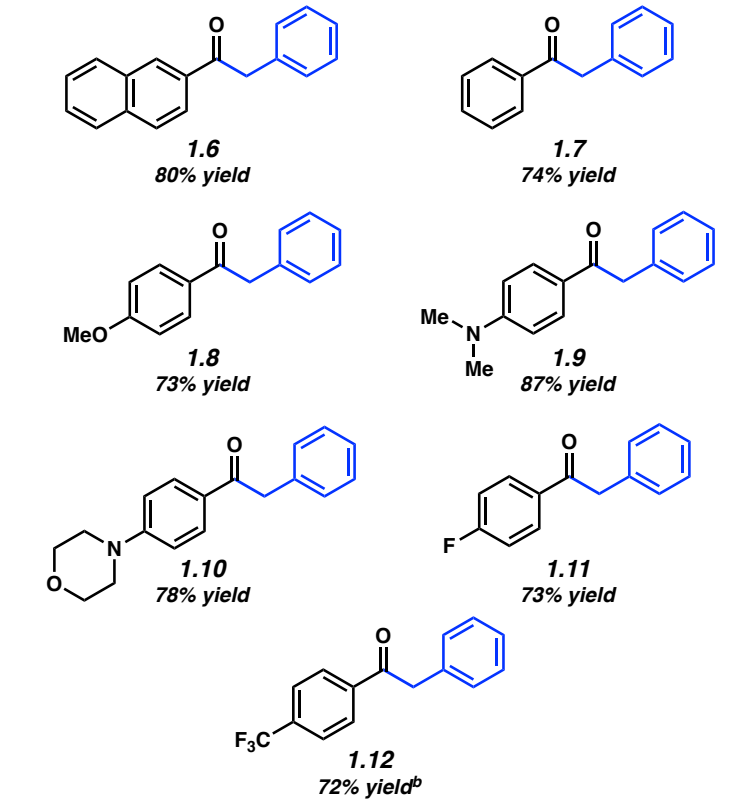

[a] Conditions unless otherwise stated: $Ni(cod)_2$ (10 mol%), SIPr (10 mol%), substrate (1.0 equiv), benzylzinc bromide (**1.5**, 1.5 equiv) and THF (1.0 M) at 23 °C for 24 h. Yields shown reflect the average of two isolation experiments. [b] The corresponding *N*-Bn,Boc benzamide derivative was used.

1.5 Scope of the Coupling with Respect to the Organozinc Species

We also examined the scope of the organozinc reagent in this methodology (Table 1.3).[19,20] *n*-Propylzinc bromide was successfully employed to furnish **1.13** in 80% yield. To

assess the tolerance of the methodology toward β-branching, neopentylzinc iodide, a very hindered nucleophile was tested and found to undergo the desired coupling to furnish **1.14**. α-Branched nucleophiles could also be employed, as judged by the formation of **1.15** and **1.16**. Notably, couplings utilizing secondary organozinc reagents are known to be challenging.[21] Finally, cyclopentyl and cyclohexyl organozinc reagents underwent the desired coupling in good yields to deliver products **1.17** and **1.18**, respectively.

Table 1.3. Scope of the organozinc coupling partner.[a]

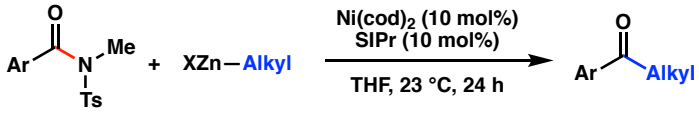

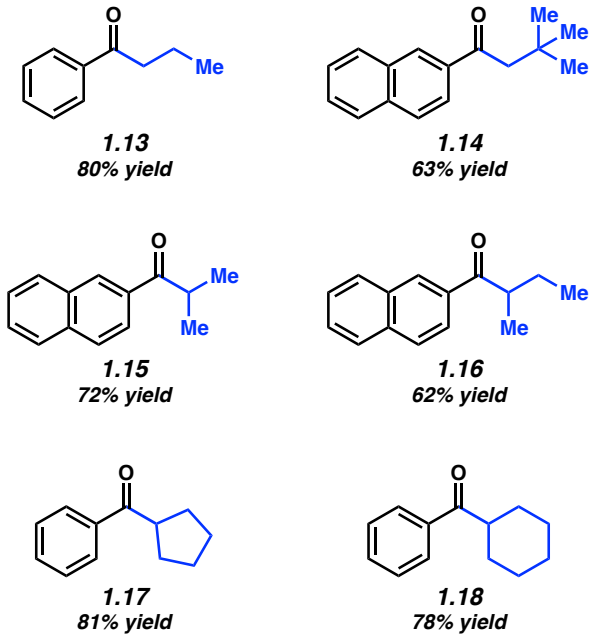

[a] Conditions unless otherwise stated: $Ni(cod)_2$ (10 mol%), SIPr (10 mol%), substrate (1.0 equiv), organozinc reagent (1.5 equiv) and THF (1.0 M) at 23 °C for 24 h. Yields shown reflect the average of two isolation experiments.

1.6 Demonstration of Coupling on Gram-Scale

The alkylative cross-coupling methodology was further probed in a synthetic application (Scheme 1.1). On gram-scale, amide derivative **1.19** was coupled with cyclohexylzinc iodide (**1.20**) using our optimal nickel-catalyzed reaction conditions. This transformation provided ketone **1.21** in 71% yield without disturbing the ester.[22] Ketone **1.21** is an intermediate in Pfizer's synthesis of the glucagon receptor modulator **1.22**.[23] The cross-coupling route to **1.21** provides a favorable alternative to the known Weinreb amide displacement chemistry described in the literature, which proceeds in 34% yield.[23]

Scheme 1.1. Gram-scale coupling to form ketone **1.21**.

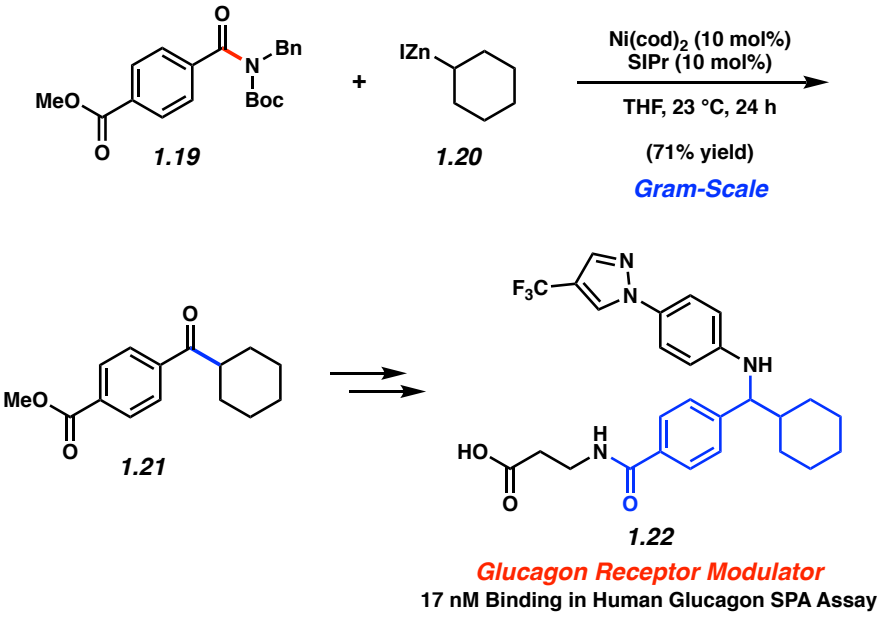

1.7 Conclusion

In summary, we have developed the first catalytic alkylation of amide derivatives. The transformation involves the coupling of *N*-alkyl,Ts or *N*-alkyl,Boc amides with organozinc reagents using nickel catalysis. The methodology proceeds at room temperature and is tolerant of

variation in both the substrate and nucleophilic coupling partner. The synthesis of **1.21** underscores the mildness and scalability of this methodology, along with the applicability of this technology to pharmaceutical synthesis. As such, we expect these studies will further promote the use of amides as synthetic building blocks for use in drug and natural product synthesis.

1.8 Experimental Section

1.8.1 Materials and Methods

Unless stated otherwise, reactions were conducted in flame-dried glassware under an atmosphere of nitrogen and commercially obtained reagents were used as received. Non-commercially available substrates were synthesized following protocols specified in Section 1.8.2.1 in the Experimental Procedures. Prior to use, tetrahydrofuran was purified by distillation and taken through five freeze-pump-thaw cycles. Iodine was obtained from Spectrum Chemical. Benzyl bromide, 1-bromopropane, 1-iodo-2,2-dimethylpropane, 2-bromopropane, 2-bromobutane, iodocyclohexane, bromocyclopentane, acid chlorides **1.23**, **1.27**, and carboxylic acid **1.25** were obtained from Sigma–Aldrich and used as received. *N*,4-Dimethylbenzenesulfonamide (**1.24**) and carboxylic acid **1.29** were obtained from Combi-Blocks. $Ni(cod)_2$, SIPr, and Zn powder (325 mesh, 99.9%) were obtained from Strem Chemicals and stored in a glove box. Anhydrous lithium chloride (99%) was obtained from Alfa Aesar and stored in a glove box. Chlorotrimethylsilane and 1,2-dibromoethane were obtained from Alfa Aesar and Sigma–Aldrich, respectively, and distilled before use. Reaction temperatures were controlled using an IKA mag temperature modulator, and unless stated otherwise, reactions were performed at room temperature (approximately 23 °C). Thin-layer chromatography (TLC) was conducted with EMD gel 60 F254 pre-coated plates (0.25 mm for analytical chromatography and

0.50 mm for preparative chromatography) and visualized using a combination of UV, anisaldehyde, and potassium permanganate staining techniques. Silicycle Siliaflash P60 (particle size 0.040–0.063 mm) was used for flash column chromatography. ^{1}H NMR spectra were recorded on Bruker spectrometers (at 300, 400, and 500 MHz) and are reported relative to residual solvent signals. Data for ^{1}H NMR spectra are reported as follows: chemical shift (δ ppm), multiplicity, coupling constant (Hz), integration. Data for ^{13}C NMR are reported in terms of chemical shift (at 75 and 125 MHz). ^{19}F NMR spectra were recorded on Bruker spectrometers (at 282 MHz) and reported in terms of chemical shift (δ ppm). IR spectra were recorded on a Perkin-Elmer UATR Two FT-IR spectrometer and are reported in terms of frequency absorption (cm^{-1}). High-resolution mass spectra were obtained on Thermo Scientific™ Exactive Mass Spectrometer with DART ID-CUBE.

1.8.2 Experimental Procedures

1.8.2.1 Syntheses of Amide Substrates

Representative Procedure A for the synthesis of amide substrates from Tables 1.1, 1.2, and 1.3 (synthesis of amide 1.4e is used as an example).

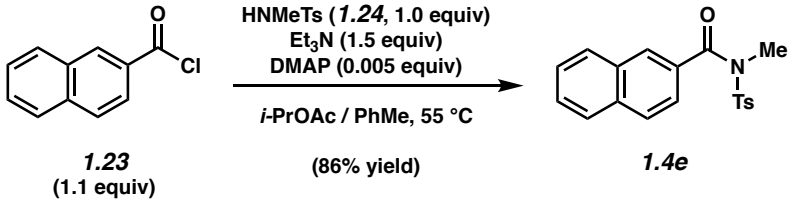

To a solution of sulfonamide **1.24** (3.00 g, 16.2 mmol, 1.0 equiv), DMAP (9.9 mg, 0.081 mmol, 0.005 equiv), triethylamine (3.40 mL, 24.3 mmol, 1.5 equiv), and *i*-PrOAc (35.2 mL) at 55 °C was added dropwise a solution of acid chloride **1.23** (3.41 g, 17.8 mmol, 1.1 equiv) in toluene (10.0 mL, 0.46 M in total) over 1 min. The reaction mixture was stirred at 55 °C for 1 h.

After cooling the reaction mixture to room temperature, the reaction was quenched by the addition of 1.0 M aqueous HCl (10 mL). The resulting biphasic mixture was transferred to a separatory funnel with EtOAc (30 mL) and extracted with EtOAc (3 x 30 mL). The organic layers were combined, dried over Na_2SO_4, and the volatiles were removed under reduced pressure. The resulting crude residue was purified by flash chromatography (24:1 Hexanes:EtOAc → 14:1 Hexanes:EtOAc → 9:1 Hexanes:EtOAc) to yield amide **1.4e** (5.2 g, 86% yield) as a white solid. Amide **1.4e**: mp: 96–98 ºC; R_f 0.50 (7:3 Hexanes:EtOAc); ^{1}H NMR (500 MHz, $CDCl_3$): δ 8.07–8.06 (s, 1H), 7.87–7.84 (m, 5H), 7.62–7.53 (m, 3H), 7.34–7.32 (m, 2H), 3.34 (s, 3H), 2.44 (s, 3H); ^{13}C NMR (125 MHz, $CDCl_3$): δ 171.9, 145.2, 135.6, 135.1, 132.5, 132.0, 130.0, 129.9, 129.3, 128.8, 128.5, 128.5, 128.2, 127.3, 124.9, 36.0, 22.0; IR (film): 3060, 2954, 2922, 1682, 1356 cm^{-1}; HRMS-ESI (*m/z*) $[M + H]^+$ calcd for $C_{19}H_{18}NO_3S$, 340.10074; found 340.09984.

Representative Procedure B for the synthesis of amide substrates from Tables 1.1, 1.2, and 1.3 (synthesis of amide 1.26 is used as an example).

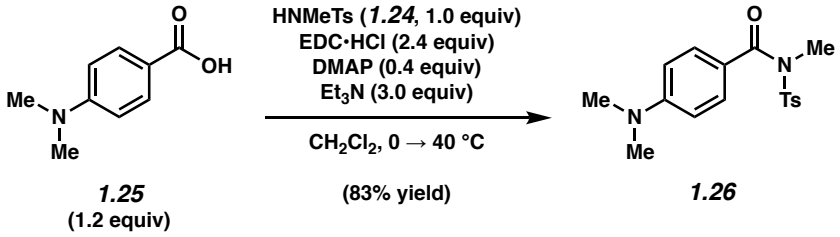

To a solution of sulfonamide **1.24** (1.00 g, 5.40 mmol, 1.0 equiv), EDC•HCl (2.48 g, 13.0 mmol, 2.4 equiv), DMAP (263 mg, 2.16 mmol, 0.4 equiv), triethylamine (2.30 mL, 16.2 mmol, 3.0 equiv), and CH_2Cl_2 (15.4 mL, 0.35 M) at 0 °C was added carboxylic acid **1.25** (1.07 g, 6.48 mmol, 1.2 equiv) as a solid in one portion. The reaction mixture was allowed to come to room temperature and then stirred at 40 °C for 16 h. After cooling to room temperature, the reaction

mixture was transferred to a separatory funnel with EtOAc (30 mL) and washed with 1.0 M aqueous HCl (2 x 10 mL), followed by 1.0 M aqueous NaOH (2 x 10 mL), and deionized water (10 mL). The organic layer was dried over Na_2SO_4, and the volatiles were removed under reduced pressure. The resulting crude residue was purified by flash chromatography (20:1 Benzene:Et_2O) to yield amide **1.26** (1.48 g, 83% yield) as an off-white solid. Amide **1.26**: mp: 104–106 ºC; R_f 0.52 (3:2 Hexanes:EtOAc); ^{1}H NMR (500 MHz, $CDCl_3$): δ 7.85 (d, J = 8.2, 2H), 7.65 (d, J = 9.0, 2H), 7.31 (d, J = 8.2, 2H), 6.63 (d, J = 8.9, 2H), 3.20 (s, 3H), 3.05 (s, 6H), 2.43 (s, 3H); ^{13}C NMR (125 MHz, $CDCl_3$): δ 172.0, 153.7, 144.7, 135.5, 132.3, 129.8, 128.8, 120.5, 110.8, 40.4, 36.4, 21.9; IR (film): 3060, 2917, 2823, 1672, 1600 cm^{-1}; HRMS-ESI (*m/z*) [M + H]$^+$ calcd for $C_{17}H_{21}N_2O_3S$, 333.12729; found 333.12611.

Note: Supporting information for the syntheses of some amides shown in Tables 1.1, 1.2, and 1.3, and Scheme 1.1 have previously been reported: **1.4a**,[24a] **1.4b**,[24b] **1.4c**,[24c] **1.4d**,[24d] **1.19**,[24d] **1.36**,[24e] **1.37**,[24f] **1.38**.[24d] Syntheses for the remaining substrates shown in Tables 1.1, 1.2, and 1.3 are as follows:

Any modifications of the conditions shown in the representative procedures above are specified in the following schemes.

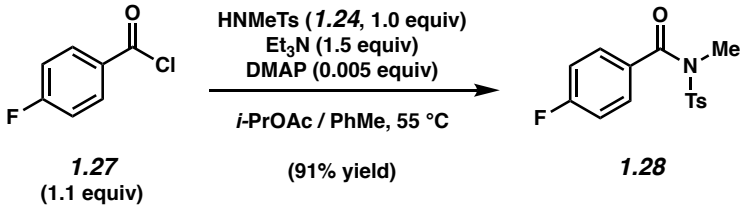

Amide 1.28. Followed representative procedure A. Purification by flash chromatography (9:1 Hexanes:EtOAc) generated amide **1.28** (91% yield) as a white solid. Amide **1.28**: mp: 80–83 °C; R_f 0.54 (7:3 Hexanes:EtOAc); ^{1}H NMR (500 MHz, $CDCl_3$): δ 7.77 (d, J = 8.3, 2H), 7.62–7.59

(m, 2H), 7.33 (d, J = 8.0, 2H), 7.12–7.08 (m, 2H), 3.24 (s, 3H), 2.45 (s, 3H); ^{13}C NMR (125 MHz, $CDCl_3$): δ 171.0, 165.3 (d, J_{C-F} = 253.9), 145.4, 135.3, 131.7 (d, J_{C-F} = 9.1) 131.1 (d, J_{C-F} = 3.3), 130.1, 128.6, 115.8 (d, J_{C-F} = 22.2), 35.8, 22.0; ^{19}F NMR (282 MHz, $CDCl_3$): δ 106.1; IR (film): 3074, 2954, 2924, 1683, 1596 cm^{-1}; HRMS-ESI (*m/z*) [M + H]$^+$ calcd for $C_{15}H_{15}FNO_3S$, 308.07567; found 308.07463.

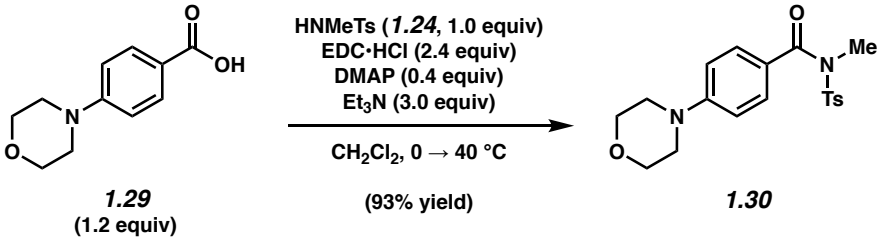

Amide 1.30. Followed representative procedure B. Purification by flash chromatography (1:1 Hexanes:EtOAc) generated amide **1.30** (93% yield) as a white solid. Amide **1.30**: mp: 141–143 ºC; R_f 0.60 (3:7 Hexanes:EtOAc); ^{1}H NMR (500 MHz, $CDCl_3$): δ 7.83 (d, J = 8.3, 2H), 7.63 (d, J = 8.8, 2H), 7.32 (d, J = 8.3, 2H), 6.84 (d, J = 8.8, 2H), 3.85 (t, J = 4.8, 4H), 3.29 (t, J = 4.8, 4H), 3.21 (s, 3H), 2.43 (s, 3H); ^{13}C NMR (125 MHz, $CDCl_3$): δ 171.7, 154.3, 144.9, 135.4, 131.8, 129.9, 128.8, 124.1, 113.5, 66.9, 47.9, 36.3, 22.0; IR (film): 3049, 2964, 2854, 1673, 1601 cm^{-1}; HRMS-ESI (*m/z*) [M + H]$^+$ calcd for $C_{19}H_{23}N_2O_4S$, 375.13785; found 375.13717.

1.8.2.2 Preparation of Organozinc Halides

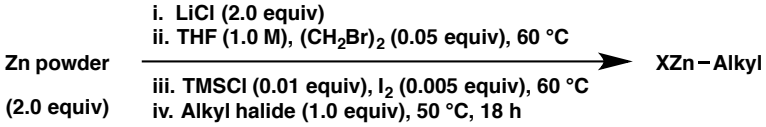

Following a modification of the procedure reported by Knochel,[25] a flame-dried 25 mL round bottom flask equipped with a magnetic stir bar and rubber septum was brought into a glove box

where Zn powder (650 mg, 10.0 mmol, 2.0 equiv, Strem 325 mesh) and anhydrous LiCl (420 mg, 10.0 mmol, 2.0 equiv) were added. The flask was then removed from the glove box and heated with a heat gun for 10 min under high vacuum, cooled to room temperature, and then backfilled with N_2. Freshly distilled THF (5.0 mL) and 1,2-dibromoethane (22 μL, 0.25 mmol, 0.05 equiv) were added via syringe and the reaction mixture was heated at 60 °C for 20 min. After cooling to room temperature, freshly distilled TMSCl (6 μL, 0.05 mmol, 0.01 equiv) followed by a solution of I_2 (6.4 mg, 0.025 mmol, 0.005 equiv) in THF (25 μL, 1.0 M) were added via syringe and the reaction mixture was heated again at 60 °C for 20 min. After cooling to room temperature, the alkyl halide (5.0 mmol, 1.0 equiv) was added dropwise via syringe over 1 min. A flame-dried air condenser was attached to the flask under N_2 and the reaction vessel was heated at 50 °C for 18 h. The reaction mixture was cooled to room temperature and allowed to stand for 1 h before the supernatant fluid was transferred to a flame-dried schlenk flask via syringe. The concentration of the organozinc halide was determined by iodometric titration using Knochel's procedure.[26]

Note: The use of organozinc reagents with lower titers led to lower yields in the subsequent coupling reactions.

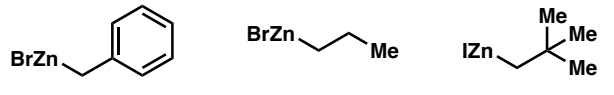

(***1.5***, 0.90–0.94 M)

(***1.31***, 0.94 M)

(***1.32***, 0.52 M)

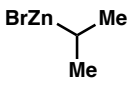

(***1.33***, 0.89 M)

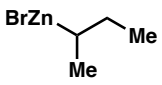

(***1.34***, 0.86 M)

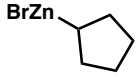

(***1.35***, 0.95 M)

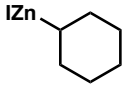

(***1.20***, 0.94 M)

1.8.2.3 Initial Survey of Naphthamide Substrates with Benzylzinc Bromide (1.5)

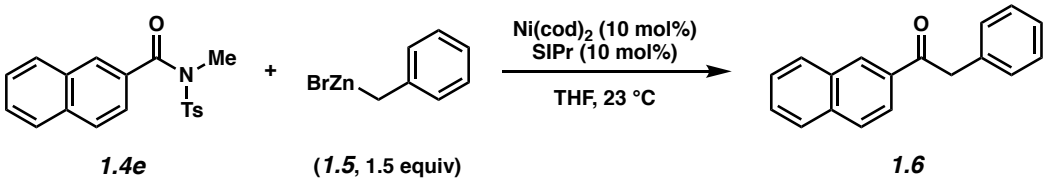

1.4e (*1.5*, 1.5 equiv) *1.6*

Representative Procedure for alkylation reactions of naphthamides from Tables 1.1, 1.2, 1.4, and 1.5 (coupling of amide 1.4e and benzylzinc bromide (1.5) is used as an example). A 1-dram vial was charged with a magnetic stir bar and flame-dried under reduced pressure, and then allowed to cool under N_2. Amide substrate **1.4e** (67.8 mg, 0.200 mmol, 1.0 equiv) and hexamethylbenzene (3.2 mg, 0.020 mmol, 0.1 equiv) were added, and the vial was flushed with N_2. The vial was taken into a glove box and charged with $Ni(cod)_2$ (5.5 mg, 0.020 mmol, 10 mol%) and SIPr (7.8 mg, 0.020 mmol, 10 mol%). Subsequently, THF (0.20 mL, 1.0 M) was added, and the vial was removed from the glove box and the reaction was allowed to stir at 23 °C for 1 h. Concurrently, the benzylzinc bromide solution (**1.5**) was heated in a water bath at 50 °C for 1 h. A portion of the preheated solution of **1.5** (333 μL, 0.300 mmol, 1.5 equiv, 0.90 M in THF) was then added to the reaction mixture dropwise via syringe over 3 sec. The vial was then capped with a Teflon-lined screw cap under a flow of N_2. The reaction mixture was allowed to stir at 23 °C for 24 h. The reaction was quenched by the addition of a saturated aqueous solution of NH_4Cl (0.5 mL), and the resulting aqueous layer was extracted with EtOAc (3 x 2 mL). The combined organics were filtered over a plug of silica gel (10 mL of EtOAc eluent). The volatiles were removed under reduced pressure, and the yield was determined by ^1H NMR analysis with hexamethylbenzene as an internal standard.

Any modifications of the conditions shown in the representative procedure above are specified below in Tables 1.4 and 1.5.

Table 1.4. Initial survey of naphthamide substrates with benzylzinc bromide (**1.5**).[a]

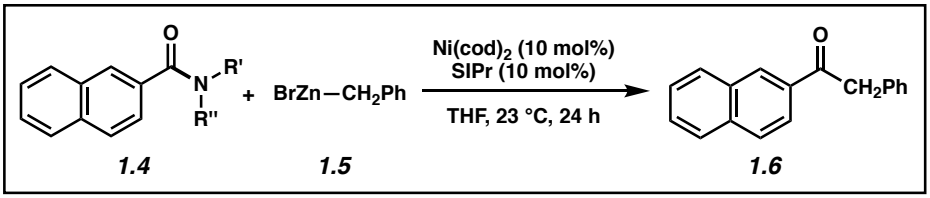

1.4 *1.5* *1.6*

Entry			*Recovered 1.4*	*Yield of Ketone 1.6*
1		*1.4a*	*100%*	*0%*
2	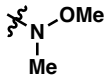	*1.4b*	*51%*	*0%*
3		*1.4c*	*100%*	*0%*
4		*1.4d*	*40%*	*60%*
5		*1.4e*	*17%*	*81%*

[a] **Yields were determined by ^{1}H NMR analysis using hexamethylbenzene as an internal standard.**

1.8.2.4 Relevant Control Experiments in the Alkylation of Amide 1.4e

Table 1.5. Relevant control experiments in the alkylation of amide **1.4e**.[a]

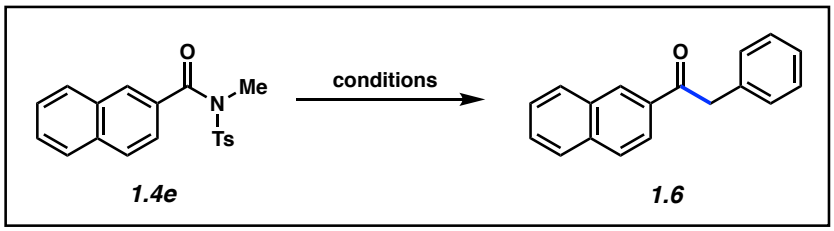

Reaction Conditions	Experimental Results 1.4e	1.6
BnZnBr (1.5 equiv), $Ni(cod)_2$ (10 mol%), SIPr (10 mol%) THF (1.0 M), 23 °C, 24 h	17%	81%
Control Experiments:		
BnZnBr (1.5 equiv) THF (1.0 M), 23 °C, 24 h	100%	0%
BnZnBr (1.5 equiv), SIPr (10 mol%) THF (1.0 M), 23 °C, 24 h	100%	0%
BnZnBr (1.5 equiv), $Ni(cod)_2$ (10 mol%) THF (1.0 M), 23 °C, 24 h	33%	35%[b]

[a] Yields were determined by ^1H NMR analysis using hexamethylbenzene as an internal standard.
[b] Some conversion to the ketone was observed in the absence of SIPr, but in greatly diminished yield relative to the experiment run with both $Ni(cod)_2$ and SIPr. Additionally, use of these conditions with other substrates was even less successful.

1.8.2.5 Scope of Methodology

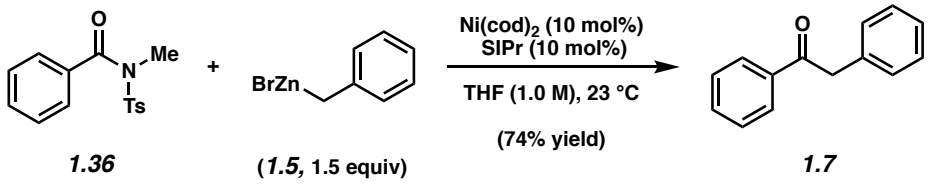

1.36 (*1.5,* 1.5 equiv) *1.7*

Representative Procedure (coupling of amide 1.36 and benzylzinc bromide (1.5) is used as an example). Ketone 1.7. A 1-dram vial was charged with a magnetic stir bar and flame-dried under reduced pressure, and then allowed to cool under N_2. Amide substrate **1.36** (57.8 mg, 0.200 mmol, 1.0 equiv) was added, and the vial was flushed with N_2. The vial was taken into a glove box and charged with $Ni(cod)_2$ (5.5 mg, 0.020 mmol, 10 mol%) and SIPr (7.8 mg, 0.020 mmol, 10 mol%). Subsequently, THF (0.20 mL, 1.0 M) was added, and the vial was removed from the glove box and the reaction was allowed to stir at 23 °C for 1 h. Concurrently, the benzylzinc bromide solution (**1.5**) was heated in a water bath at 50 °C for 1 h. A portion of the preheated solution of **1.5** (319 μL, 0.300 mmol, 1.5 equiv, 0.94 M in THF) was then added to the reaction mixture dropwise via syringe over 3 sec. The vial was then capped with a Teflon-lined screw cap under a flow of N_2. The reaction mixture was allowed to stir at 23 °C for 24 h. The reaction was quenched by the addition of a saturated aqueous solution of NH_4Cl (0.5 mL), and the resulting aqueous layer was extracted with EtOAc (3 x 2 mL). The combined organics were filtered over a plug of silica gel (10 mL of EtOAc eluent). The volatiles were removed under reduced pressure, and the crude residue was purified by preparative thin-layer chromatography (5:1 Hexanes:EtOAc) to yield ketone product **1.7** (74% yield, average of two experiments) as a white solid. Ketone **1.7**: R_f 0.54 (5:1 Hexanes:EtOAc). Spectral data match those previously reported.[27]

Any modifications of the conditions shown in the representative procedure above are specified in the following schemes, which depict all of the results shown in Tables 1.2 and 1.3.

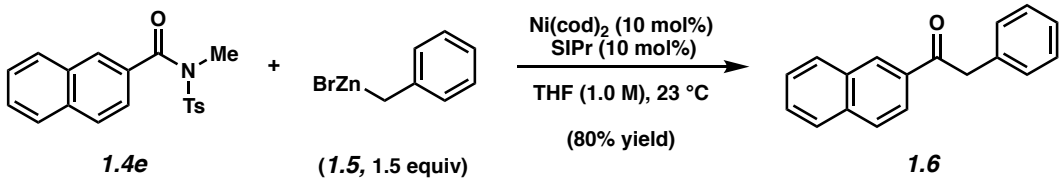

Ketone 1.6. Purification by preparative thin-layer chromatography (5:1 Hexanes:EtOAc) generated ketone **1.6** (80% yield, average of two experiments) as a white solid. Ketone **1.6**: R_f 0.53 (5:1 Hexanes:EtOAc). Spectral data match those previously reported.[27]

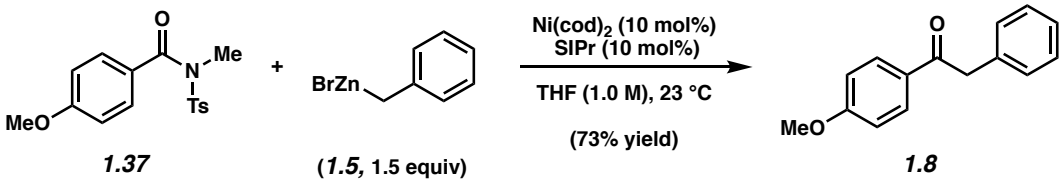

Ketone 1.8. Purification by preparative thin-layer chromatography (4:1 Hexanes:EtOAc) generated ketone **1.8** (73% yield, average of two experiments) as a white solid. Ketone **1.8**: R_f 0.46 (4:1 Hexanes:EtOAc). Spectral data match those previously reported.[28]

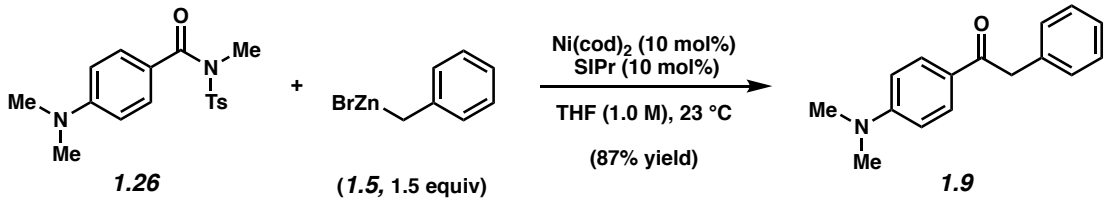

Ketone 1.9. Purification by flash chromatography (8:1:1 PhH:Et_2O:CH_2Cl_2) generated ketone **1.9** (87% yield, average of two experiments) as a white solid. Ketone **1.9**: R_f 0.46 (8:1:1 PhH:Et_2O:CH_2Cl_2). Spectral data match those previously reported.[29]

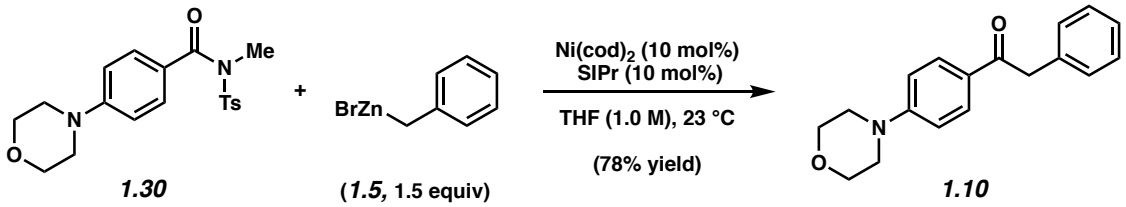

Ketone 1.10. Purification by flash chromatography (10:5:1 $CHCl_3$:Hexanes:CH_3CN) followed by preparative thin-layer chromatography (10:2:1 $CHCl_3$:Hexanes:CH_3CN) generated ketone **1.10** (78% yield, average of two experiments) as a white solid. Ketone **1.10**: mp: 138–139 °C; R_f 0.64 (3:2 Hexanes:EtOAc); ^{1}H NMR (500 MHz, CD_3CN): δ 7.94–7.88 (m, 2H), 7.33–7.19 (m, 5H), 6.95–6.89 (m, 2H), 4.21 (s, 2H), 3.77–3.73 (m, 4H), 3.29–3.24 (m, 4H); ^{13}C NMR (125 MHz, CD_3CN): δ 196.8, 155.5, 137.1, 131.4, 130.6, 129.4, 127.9, 127.4, 114.1, 67.1, 48.1, 45.5; IR (film): 3042, 2957, 2857, 2840, 1675, 1595 cm^{-1}; HRMS-ESI (*m/z*) $[M + H]^+$ calcd for $C_{11}H_8O_2$, 282.14940; found 282.14800.

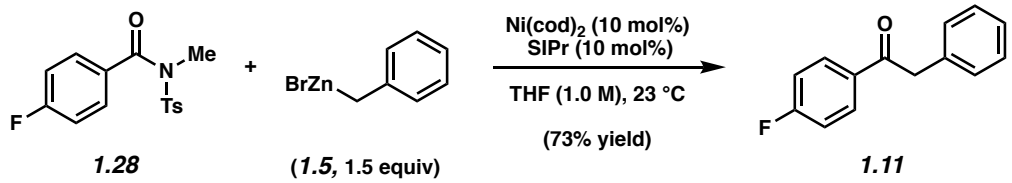

Ketone 1.11. Purification by preparative thin-layer chromatography (5:1 Hexanes:EtOAc) generated ketone **1.11** (73% yield, average of two experiments) as a white solid. Ketone **1.11**: R_f 0.50 (5:1 Hexanes:EtOAc). Spectral data match those previously reported.[27]

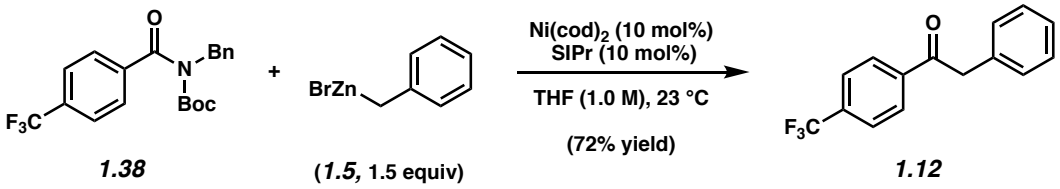

Ketone 1.12. Purification by flash chromatography (100% PhH) generated ketone **1.12** (72% yield, average of two experiments) as a white solid. Ketone **1.12**: R_f 0.68 (100% PhH). Spectral data match those previously reported.[30]

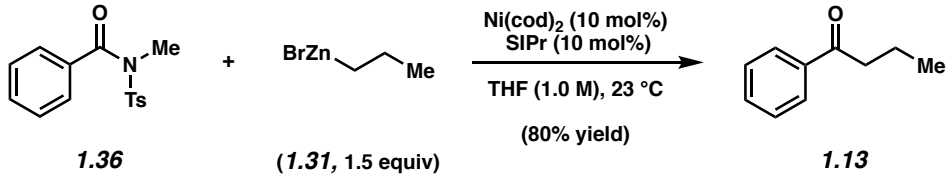

Ketone 1.13. Purification by preparative thin-layer chromatography (5:1 Hexanes:EtOAc) generated ketone **1.13** (80% yield, average of two experiments) as a colorless oil. Ketone **1.13**: R_f 0.57 (5:1 Hexanes:EtOAc). Spectral data match those previously reported.[27]

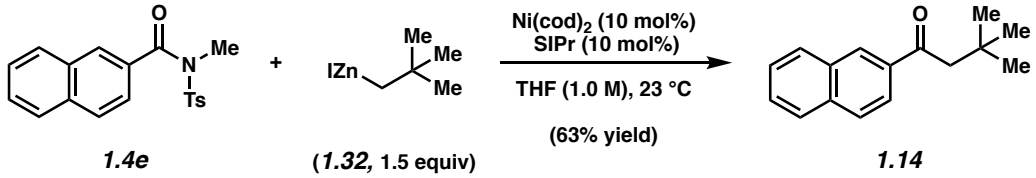

Ketone 1.14. Purification by preparative thin-layer chromatography (5:1 Hexanes:EtOAc) generated ketone **1.14** (63% yield, average of two experiments) as a colorless oil. Ketone **1.14**: R_f 0.63 (5:1 Hexanes:EtOAc). Spectral data match those previously reported.[31]

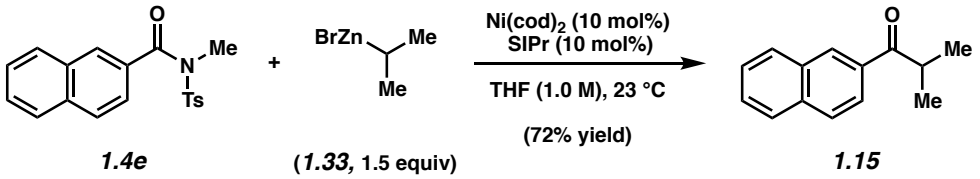

1.4e (*1.33,* 1.5 equiv) *1.15*

Ketone 1.15. Purification by preparative thin-layer chromatography (5:1 Hexanes:EtOAc) generated ketone **1.15** (72% yield, average of two experiments) as a colorless oil. Ketone **1.15**: R_f 0.64 (5:1 Hexanes:EtOAc). Spectral data match those previously reported.[32]

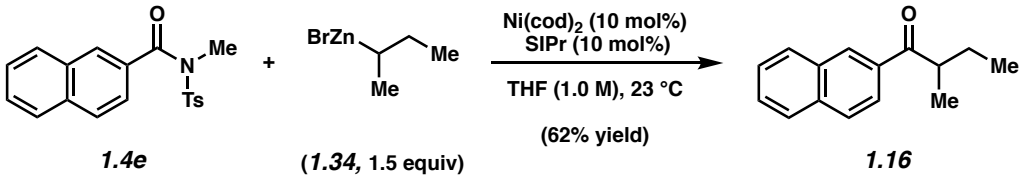

1.4e (*1.34,* 1.5 equiv) *1.16*

Ketone 1.16. Purification by preparative thin-layer chromatography (5:1 Hexanes:EtOAc) generated ketone **1.16** (62% yield, average of two experiments) as a colorless oil. Ketone **1.16**: R_f 0.44 (10:1 Hexanes:EtOAc); ^{1}H NMR (500 MHz, C_6D_6): δ 8.35 (br s, 1H), 8.13 (dd, J = 8.6, 1.6, 1H), 7.63 (d, J = 7.9, 1H), 7.56 (d, J = 8.6, 1H), 7.53 (d, J = 7.9, 1H) 7.27–7.19 (m, 1H), 3.26–3.18 (m, 1H), 1.93–1.83 (m, 1H), 1.48–1.38 (m, 1H), 1.14 (d, J = 6.9, 3H), 0.83 (t, J = 7.5, 3H);^{13}C NMR (125 MHz, CD_3CN): δ 205.3, 136.4, 135.2, 133.7, 130.7, 130.5, 129.5, 129.4, 128.6, 127.8, 125.0, 42.7, 27.6, 17.2, 12.0; IR (film): 3060, 2965, 2932, 2875, 1677, 1625 cm^{-1}; HRMS-ESI (*m/z*) $[M + H]^+$ calcd for $C_{11}H_8O_2$, 213.12794; found 213.12691.

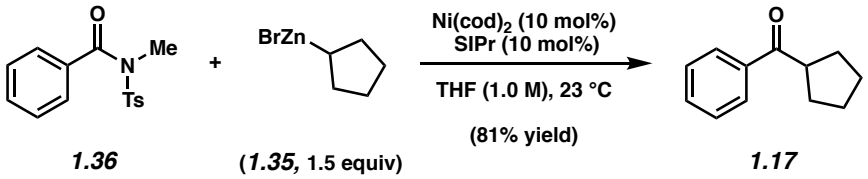

1.36 (*1.35,* 1.5 equiv) *1.17*

Ketone 1.17. Purification by preparative thin-layer chromatography (5:1 Hexanes:EtOAc) generated ketone **1.17** (81% yield, average of two experiments) as a colorless oil. Ketone **1.17**: R_f 0.64 (5:1 Hexanes:EtOAc). Spectral data match those previously reported.[33]

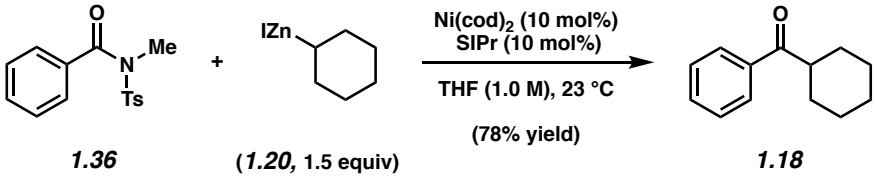

1.36 (*1.20,* 1.5 equiv) *1.18*

Ketone 1.18. Purification by preparative thin-layer chromatography (5:1 Hexanes:EtOAc) generated ketone **1.18** (78% yield, average of two experiments) as a colorless oil. Ketone **1.18**: R_f 0.54 (5:1 Hexanes:EtOAc). Spectral data match those previously reported.[34]

1.8.2.6 Gram-Scale Alkylation to Form Ketone 1.21

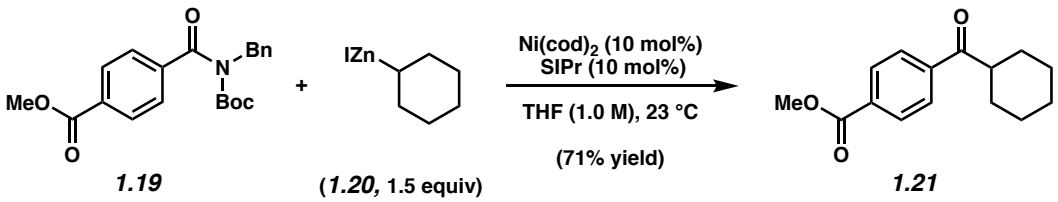

1.19 (*1.20,* 1.5 equiv) *1.21*

Ketone 1.21. A 20 mL scintillation vial was charged with a magnetic stir bar and flame-dried under reduced pressure, and then allowed to cool under N_2. Amide substrate **1.19** (1.00 g, 2.71 mmol, 1.0 equiv) was added, and the vial was flushed with N_2. The vial was taken into a glove box and charged with $Ni(cod)_2$ (74.5 mg, 0.270 mmol, 10 mol%) and SIPr (106 mg, 0.270 mmol, 10 mol%). Subsequently, THF (2.7 mL, 1.0 M) was added, and the vial was removed

from the glove box and the reaction was allowed to stir at 23 °C for 1 h. Concurrently, the cyclohexylzinc iodide solution (**1.20**) was heated in a water bath at 50 °C for 1 h. A portion of the preheated solution of **1.20** (4.32 mL, 4.07 mmol, 1.5 equiv, 0.94 M in THF) was then added to the reaction mixture dropwise via syringe over 5 sec. The vial was then capped with a Teflon-lined screw cap under a flow of N_2. The reaction mixture was allowed to stir at 23 °C for 24 h. The reaction was quenched by the addition of a saturated aqueous solution of NH_4Cl (3 mL), and the resulting aqueous layer was extracted with EtOAc (3 x 5 mL). The combined organics were filtered over a plug of silica gel (50 mL of EtOAc eluent). The volatiles were removed under reduced pressure, and the crude residue was purified by flash chromatography (24:1 Hexanes:EtOAc) to yield ketone product **1.21** (472 mg, 71% yield) as a pale yellow solid. Ketone **1.21**: R_f 0.50 (5:1 Hexanes:EtOAc). Spectral data match those previously reported.[35]

1.9 Spectra Relevant to Chapter One:

Nickel-Catalyzed Alkylation of Amide Derivatives

Bryan J. Simmons[†], Nicholas A. Weires[†], Jacob E. Dander, and Neil K. Garg.

ACS Catal. **2016**, *6*, 3176–3179.

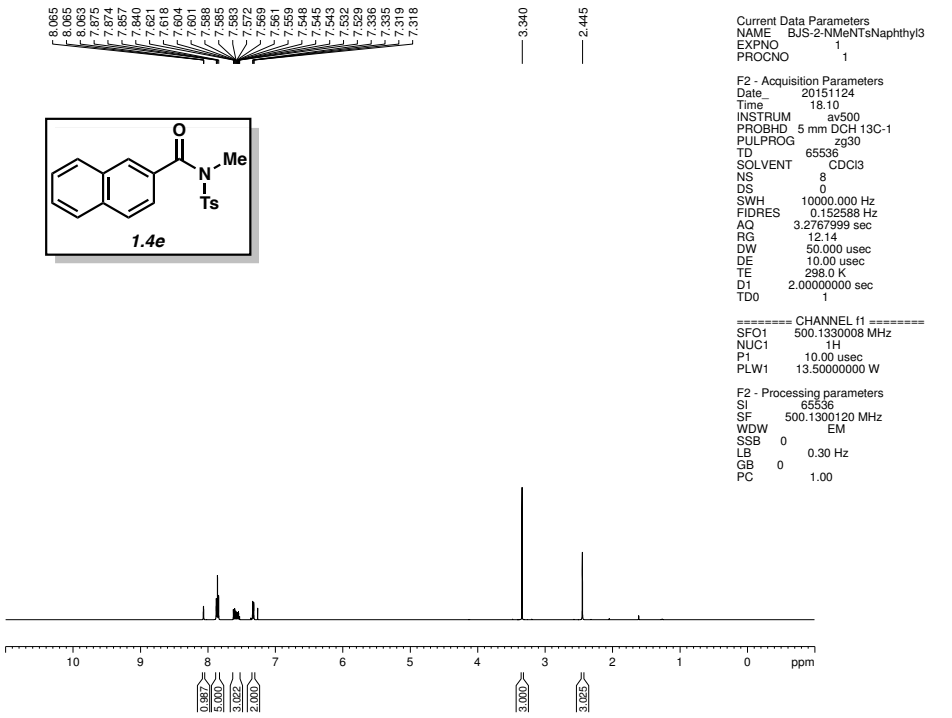

Figure 1.2 ^{1}H NMR (500 MHz, $CDCl_3$) of compound **1.4e**.

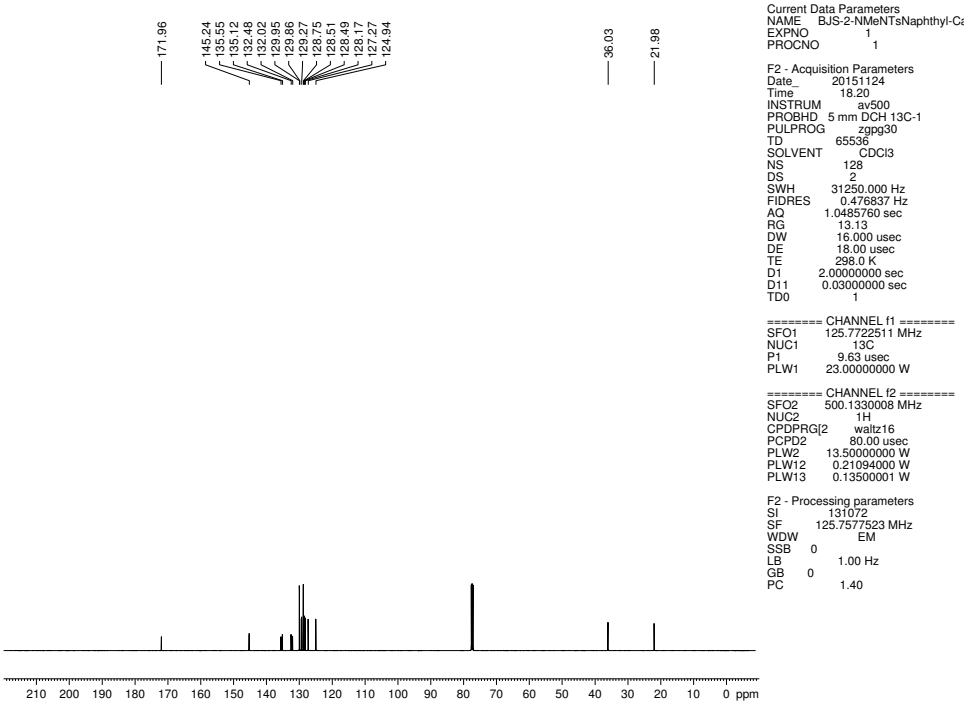

Figure 1.3 ^{13}C NMR (125 MHz, $CDCl_3$) of compound **1.4e**.

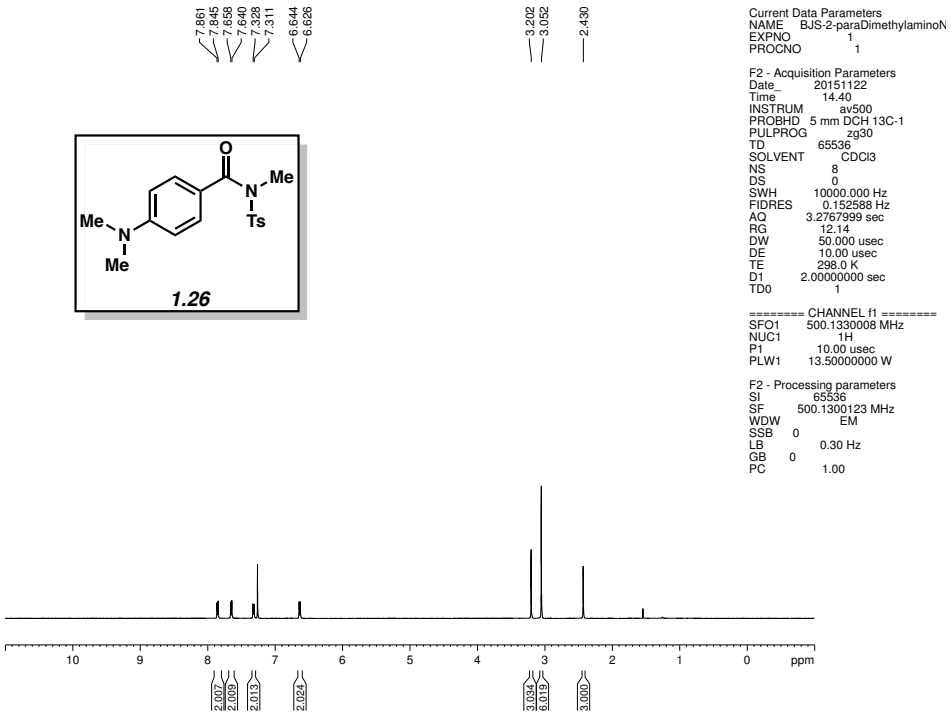

Figure 1.4 ^{1}H NMR (500 MHz, $CDCl_3$) of compound **1.26**

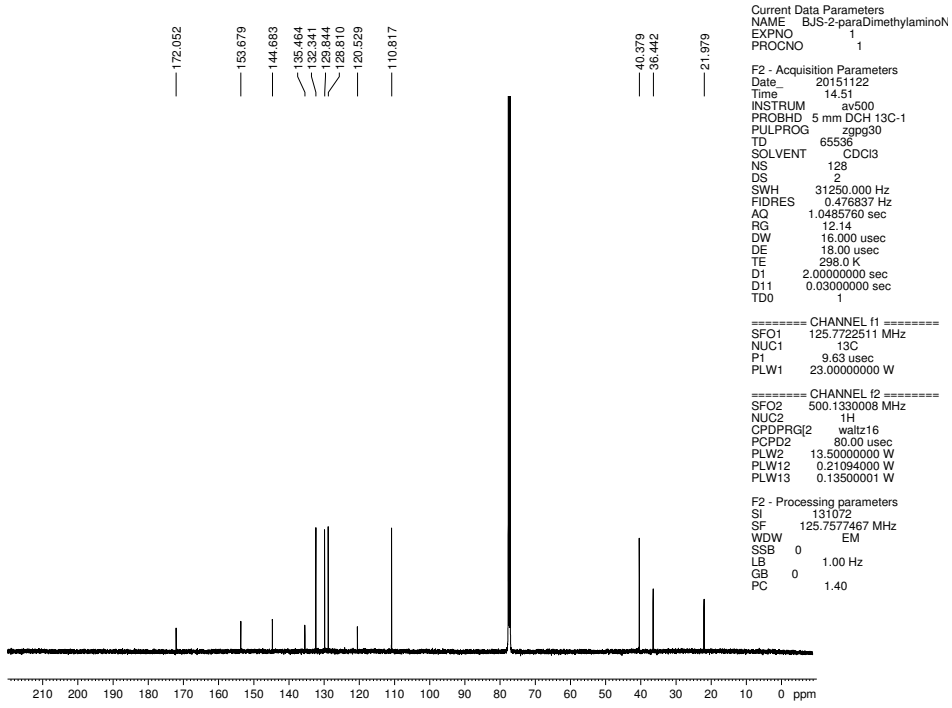

Figure 1.5 ^{13}C NMR (125 MHz, $CDCl_3$) of compound **1.26**.

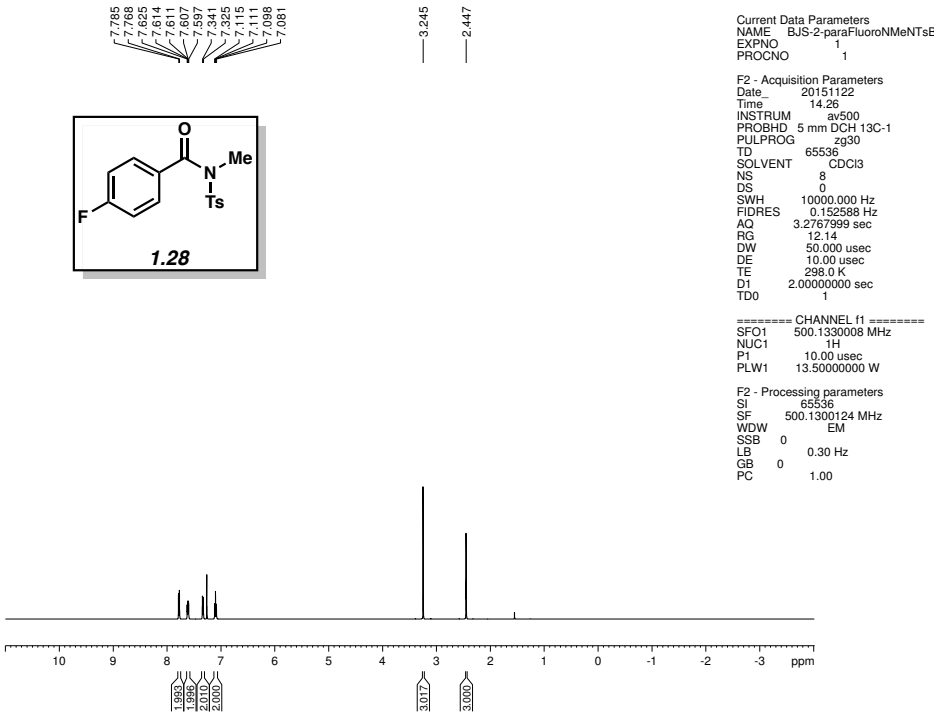

Figure 1.6 ^{1}H NMR (500 MHz, $CDCl_3$) of compound **1.28**

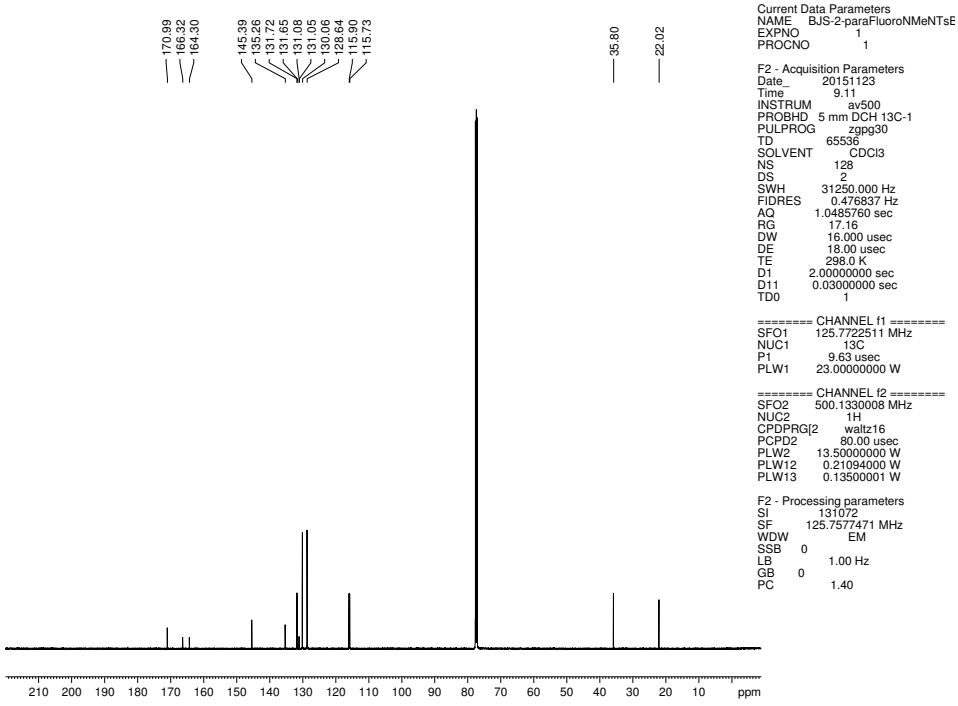

Figure 1.7 ^{13}C NMR (125 MHz, $CDCl_3$) of compound **1.28**.

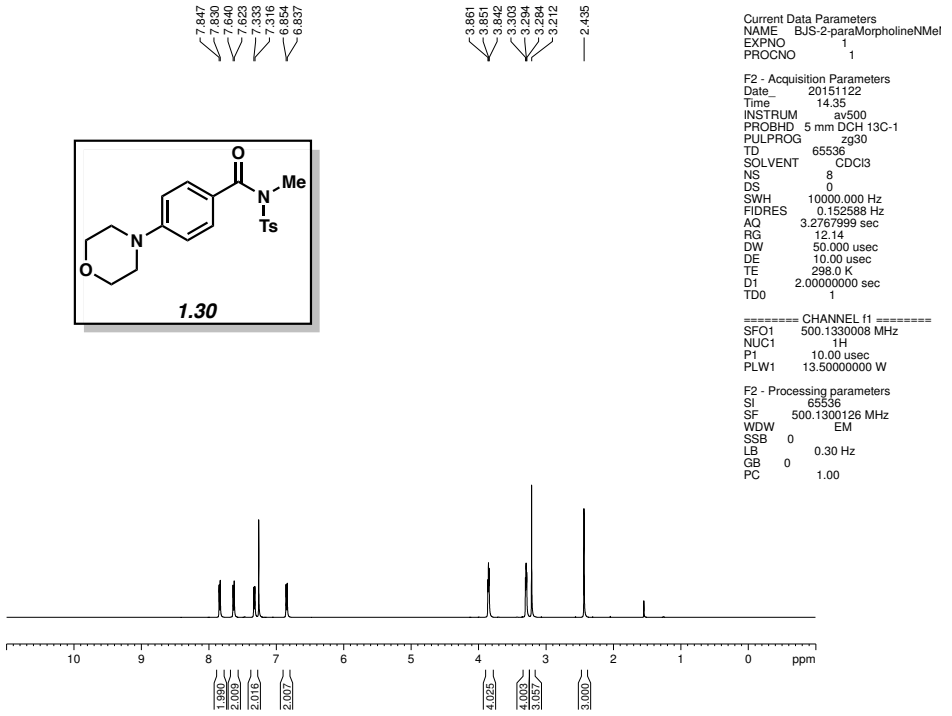

Figure 1.8 ^{1}H NMR (500 MHz, $CDCl_3$) of compound **1.30**.

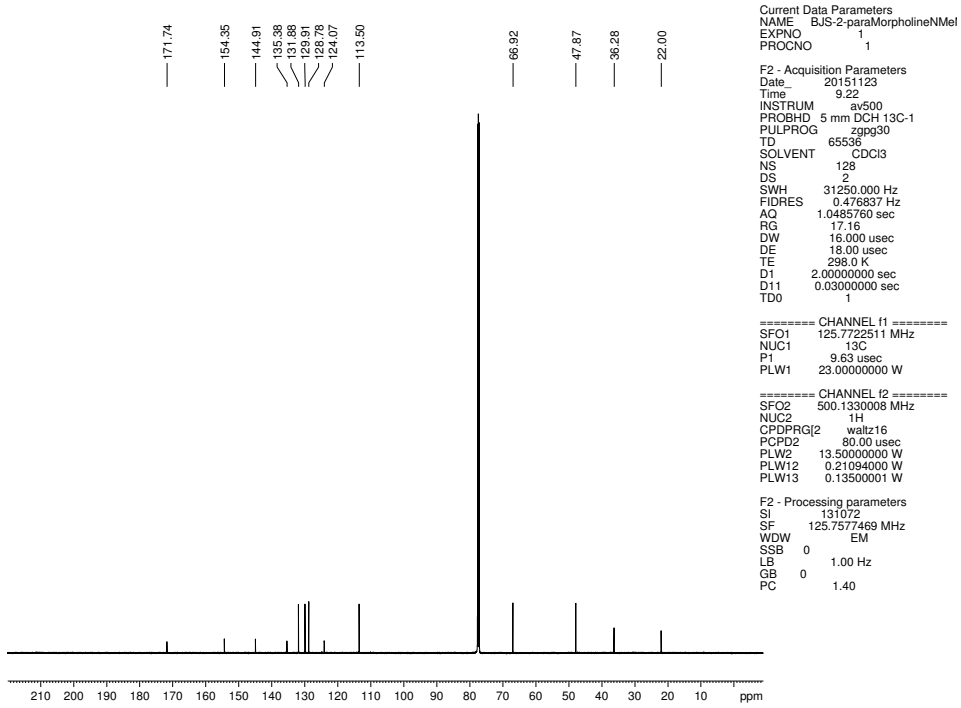

Figure 1.9 ^{13}C NMR (125 MHz, $CDCl_3$) of compound **1.30**.

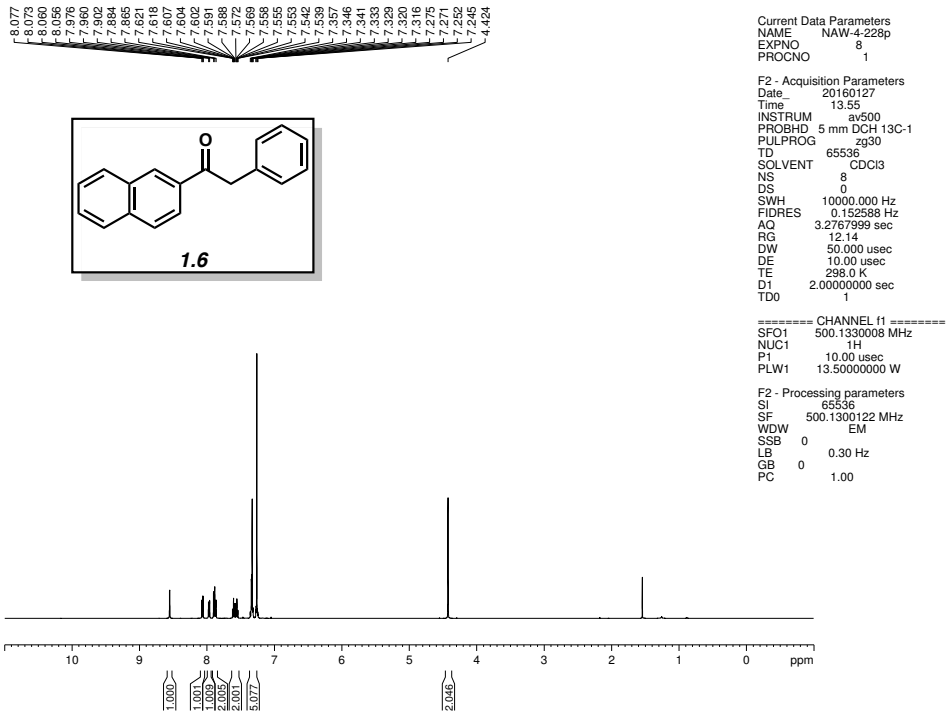

Figure 1.10 ^{1}H NMR (500 MHz, $CDCl_3$) of compound **1.6**.

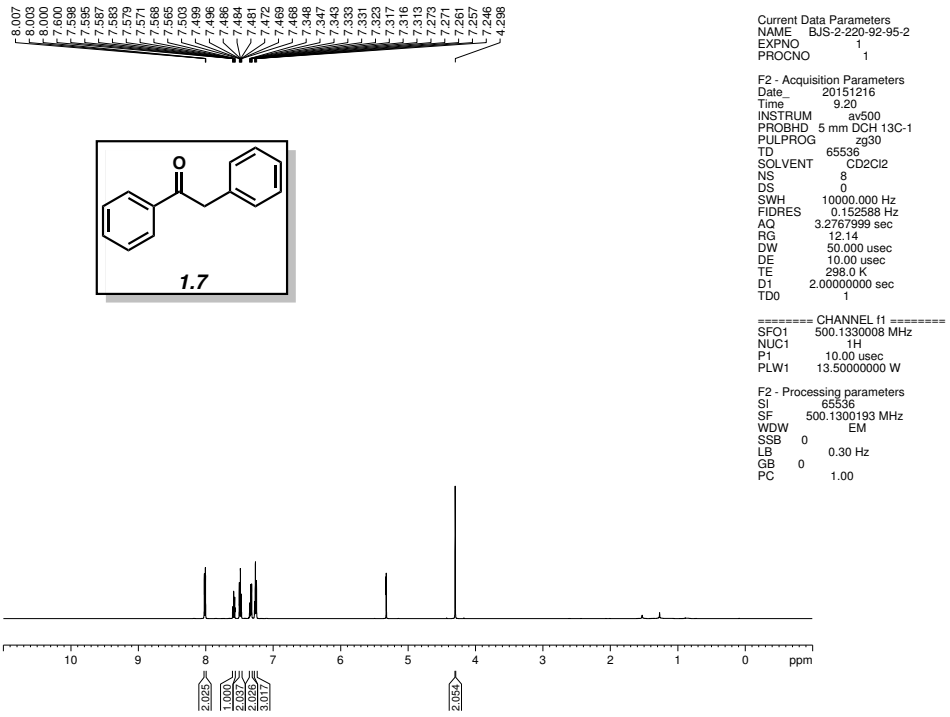

Figure 1.11 ^{1}H NMR (500 MHz, $CDCl_3$) of compound **1.7**.

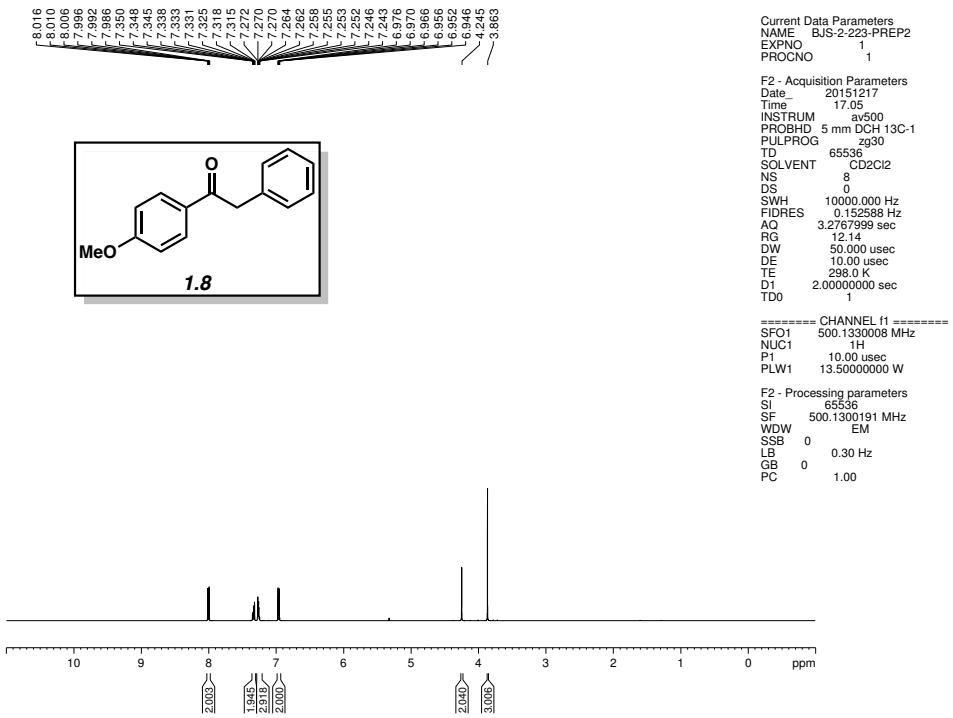

Figure 1.12 ^{1}H NMR (500 MHz, $CDCl_3$) of compound **1.8**.

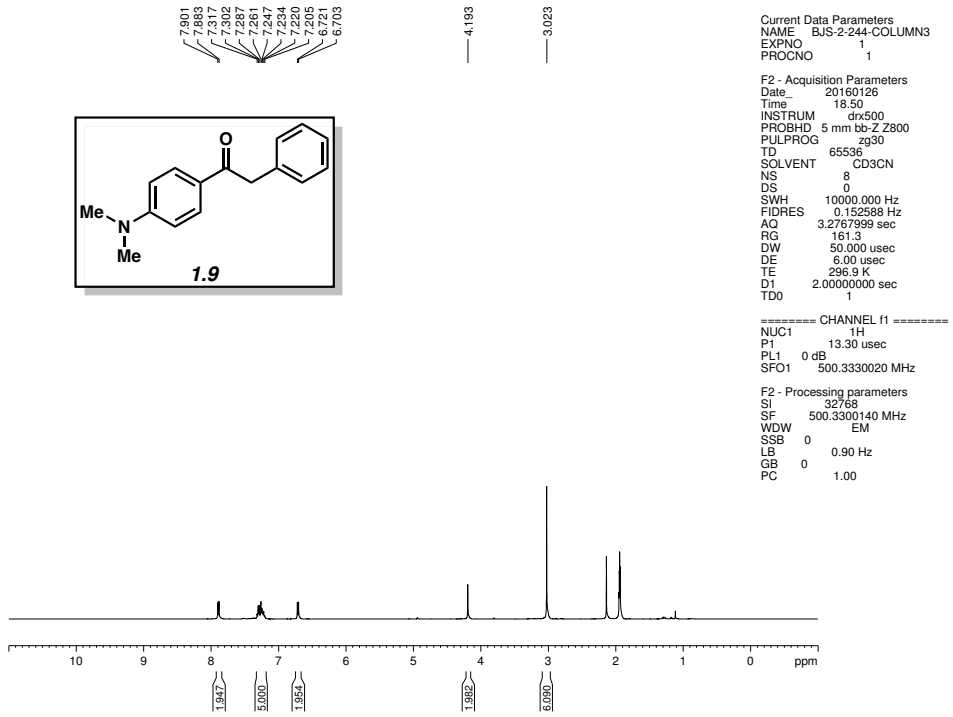

Figure 1.13 ^{1}H NMR (500 MHz, $CDCl_3$) of compound **1.9**.

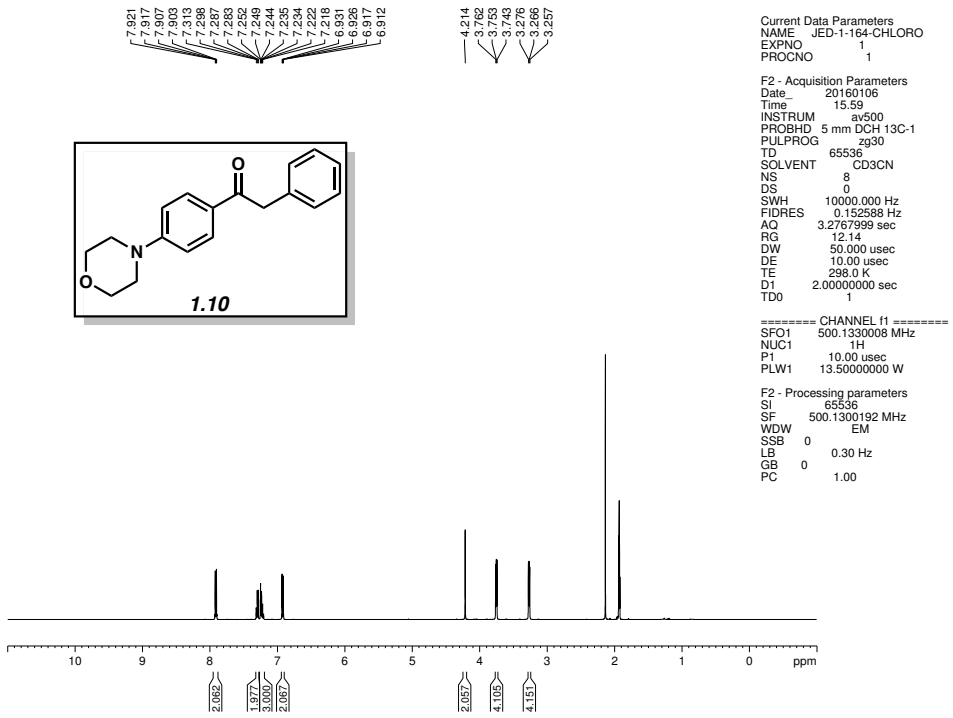

Figure 1.14 ^{1}H NMR (500 MHz, $CDCl_3$) of compound **1.10**.

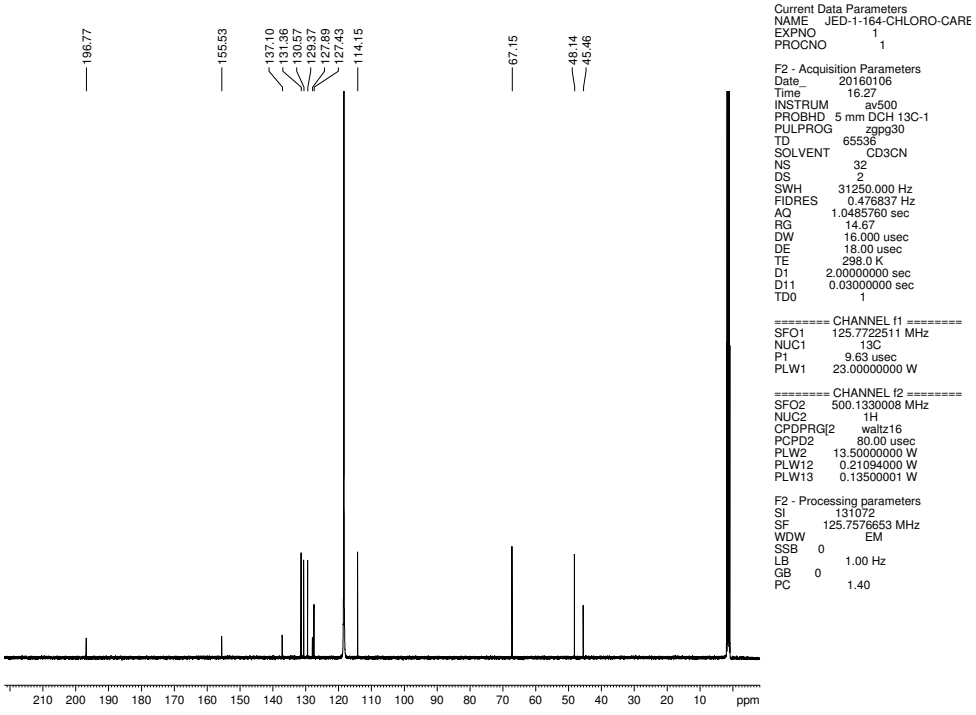

Figure 1.15 ^{13}C NMR (125 MHz, $CDCl_3$) of compound **1.10**.

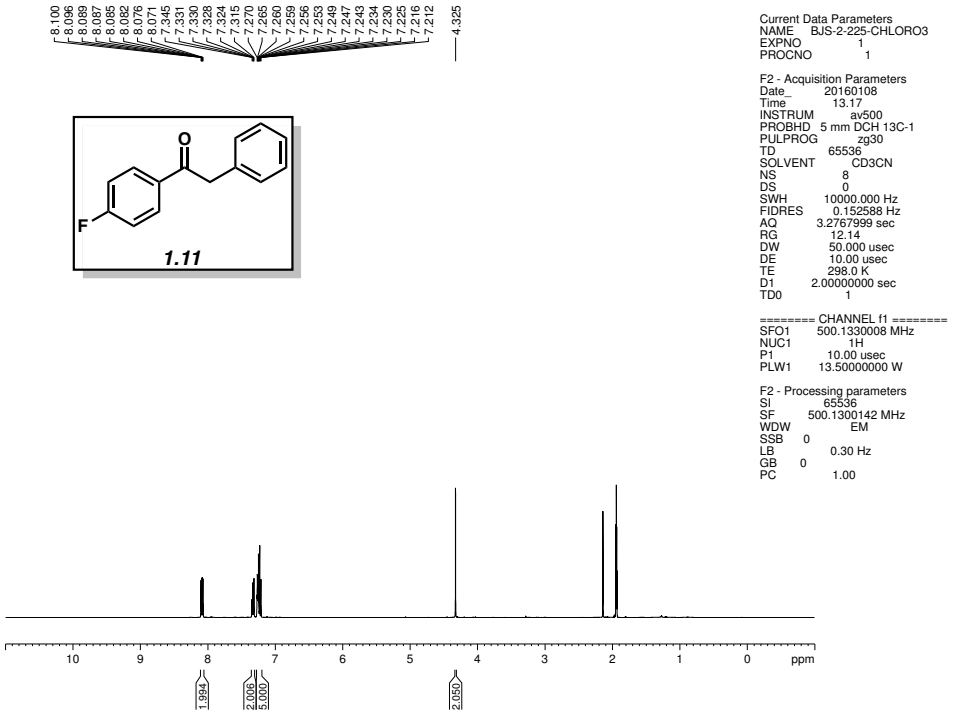

Figure 1.16 ^{1}H NMR (500 MHz, $CDCl_3$) of compound **1.11**.

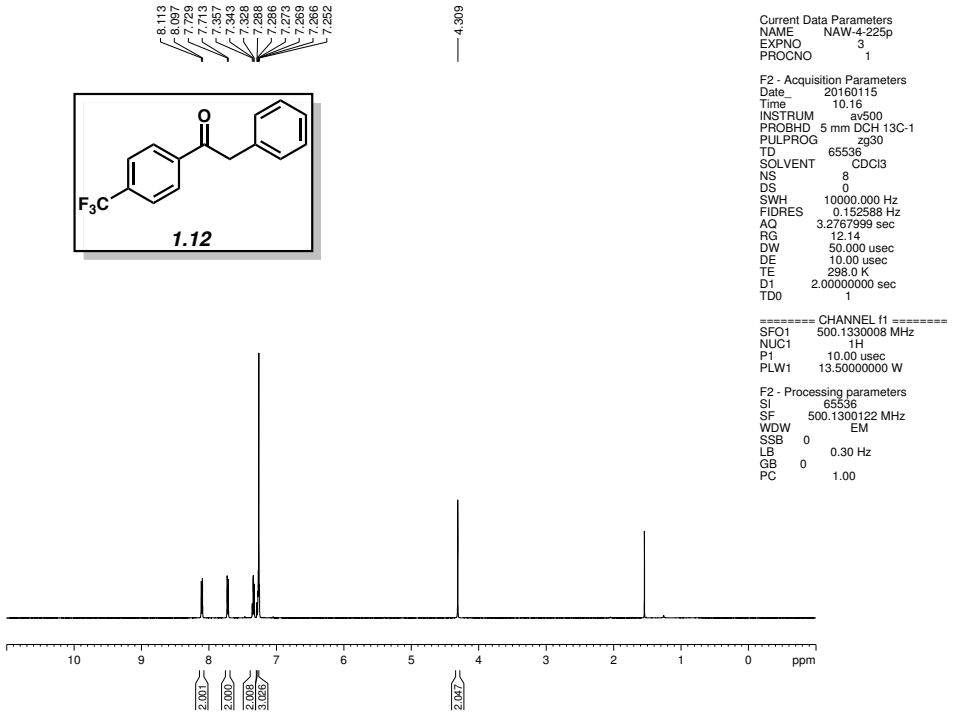

Figure 1.17 ^{1}H NMR (500 MHz, $CDCl_3$) of compound **1.12**.

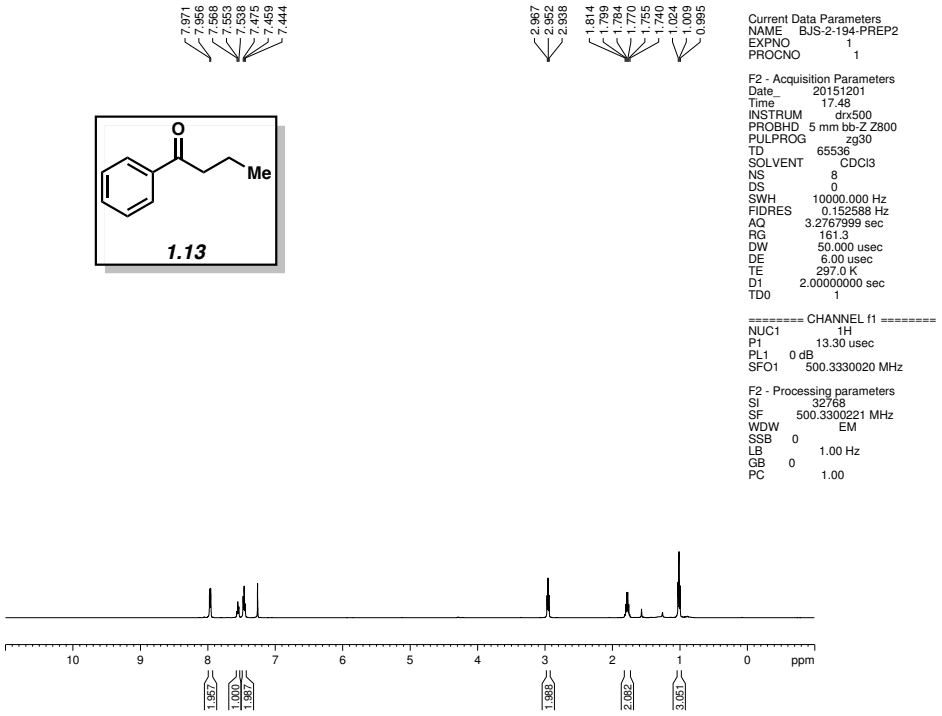

Figure 1.18 ^{1}H NMR (500 MHz, $CDCl_3$) of compound **1.13**.

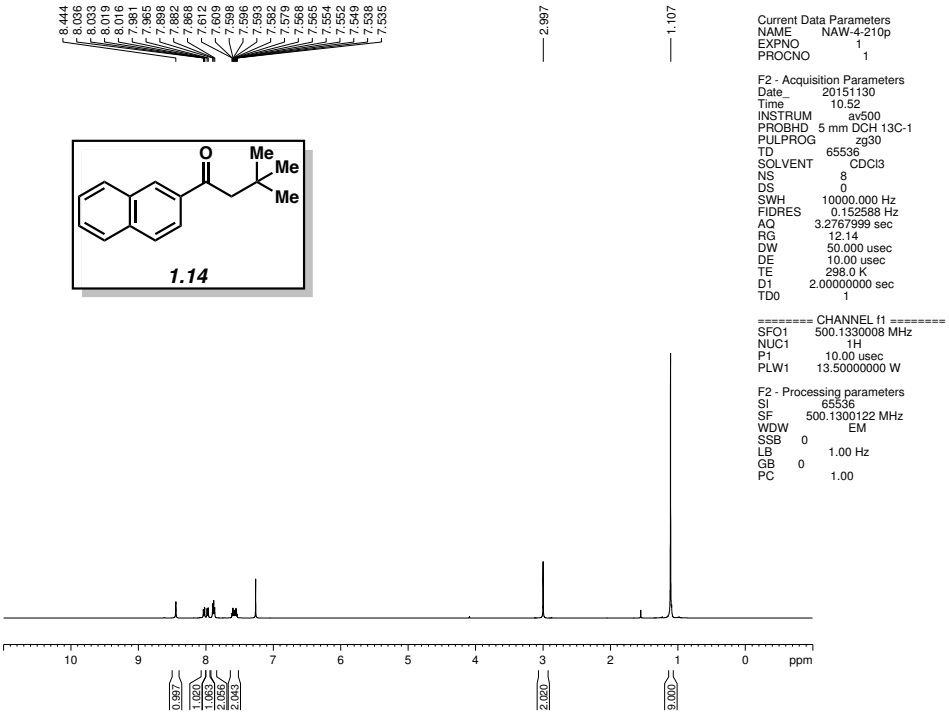

Figure 1.19 ^{1}H NMR (500 MHz, $CDCl_3$) of compound **1.14**.

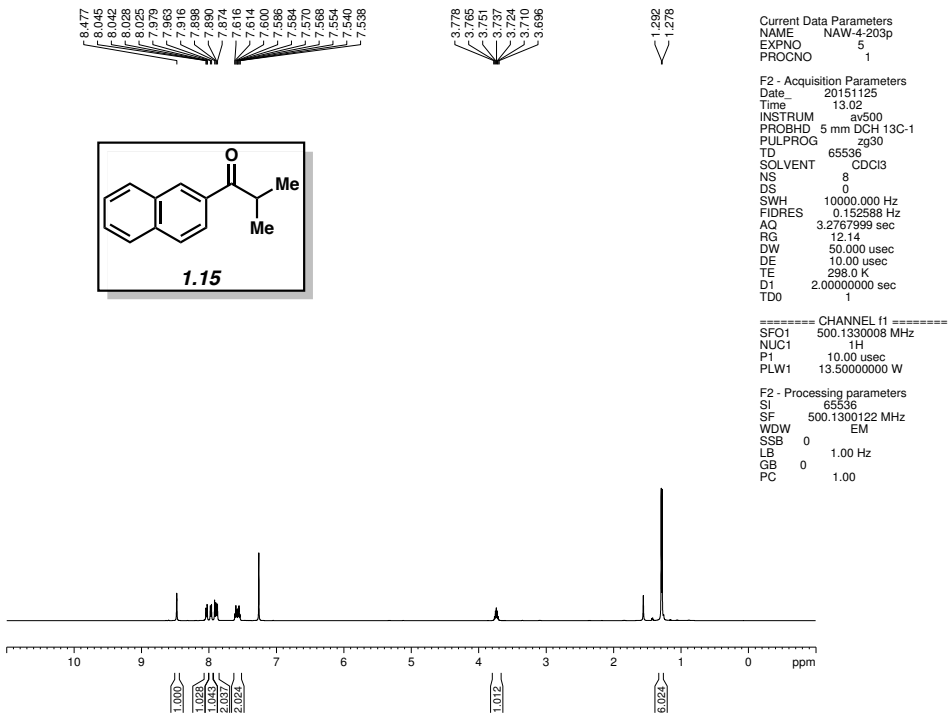

Figure 1.20 ^{1}H NMR (500 MHz, $CDCl_3$) of compound **1.15**.

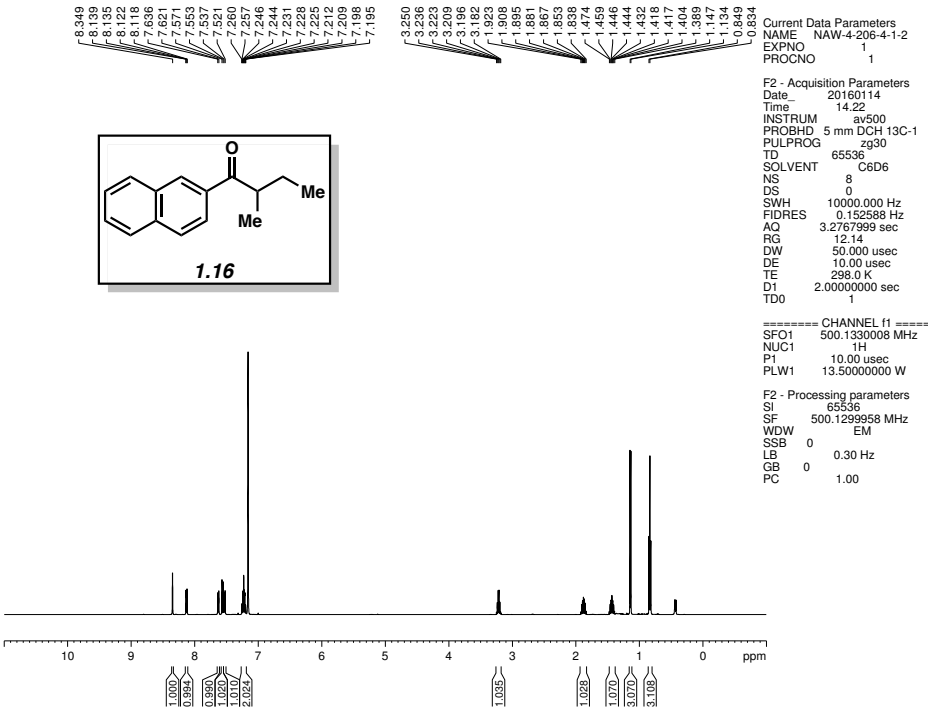

Figure 1.21 ^{1}H NMR (500 MHz, $CDCl_3$) of compound **1.16**.

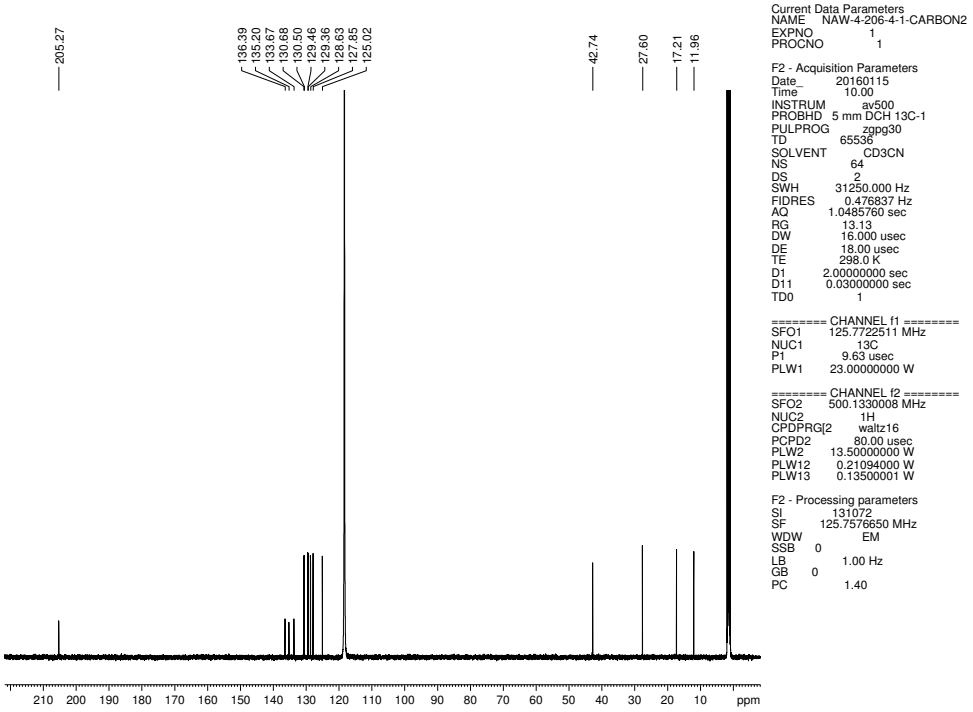

Figure 1.22 ^{13}C NMR (125 MHz, $CDCl_3$) of compound **1.16**.

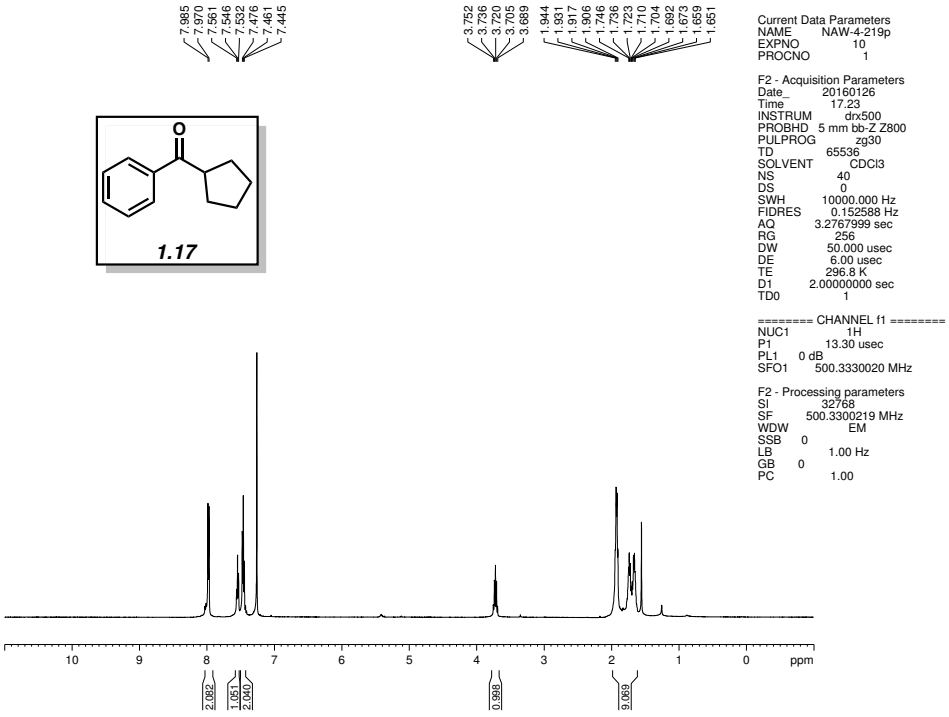

Figure 1.23 ^{1}H NMR (500 MHz, $CDCl_3$) of compound **1.17**.

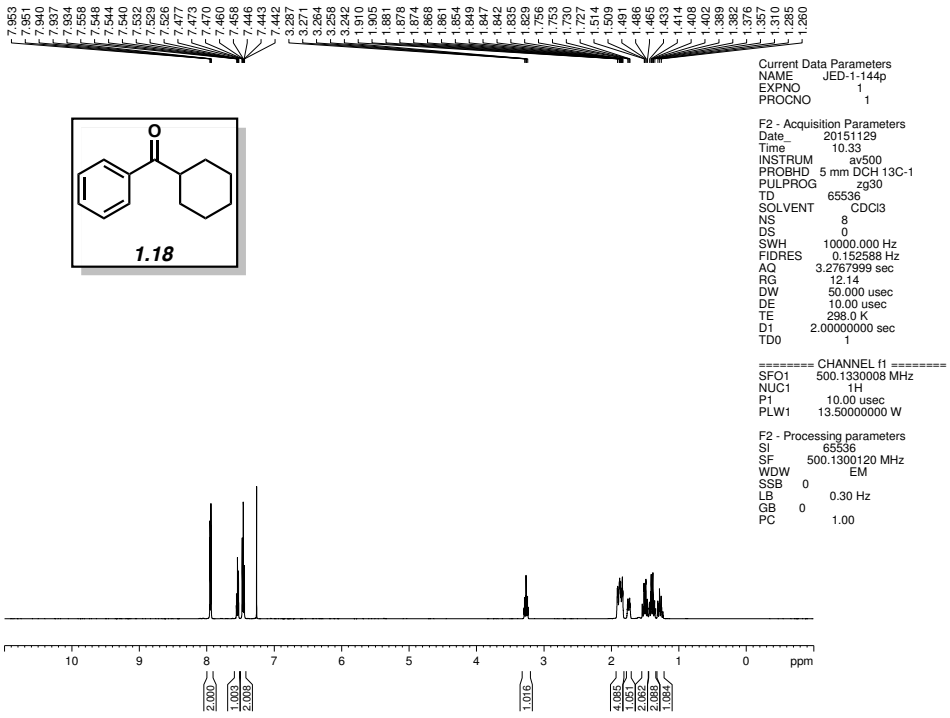

Figure 1.24 ^{1}H NMR (500 MHz, $CDCl_3$) of compound **1.18**.

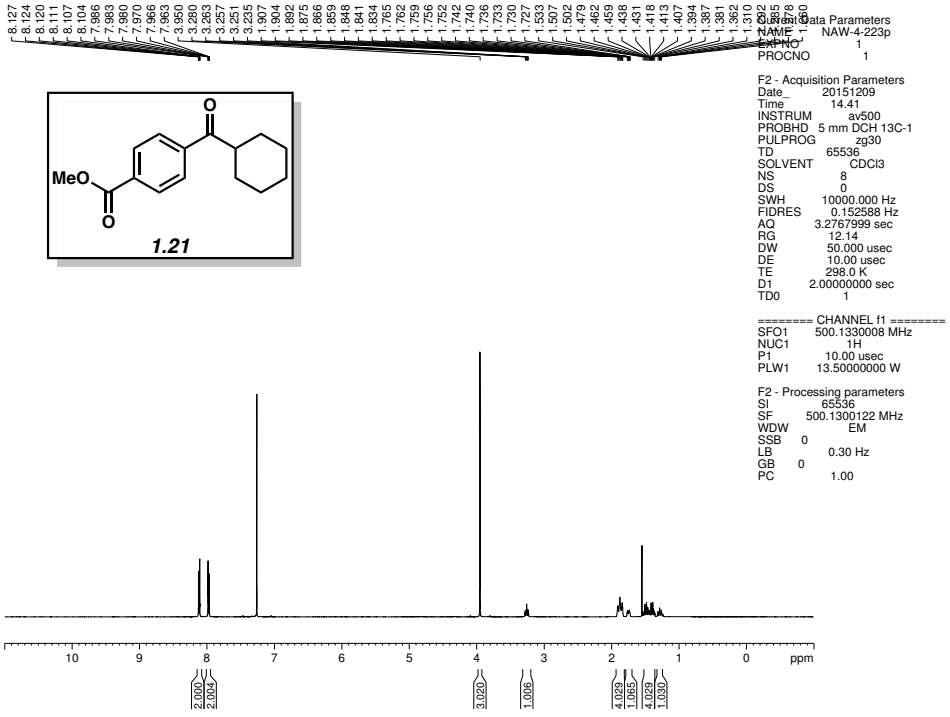

Figure 1.25 ^{1}H NMR (500 MHz, $CDCl_3$) of compound **1.21**.

1.10 Notes and References

(1) Greenberg, A.; Breneman, C. M.; Liebman, J. F. Eds. *The Amide Linkage: Structural Significance in Chemistry, Biochemistry, and Materials Science*; Wiley: New York, 2003; 1–672.

(2) Pauling, L.; Corey, R. B. *Proc. Natl. Acad. Sci. USA* **1951**, *37*, 729–740.

(3) (a) Hie, L.; Fine Nathel, N. F.; Shah, T. K.; Baker, E. L.; Hong, X.; Yang, Y.-F.; Liu, P.; Houk, K. N.; Garg, N. K. *Nature* **2015**, *524*, 79–83. (b) Weires, N. A.; Baker, E. L.; Garg, N. K. *Nat. Chem.* **2016**, *8*, 75–79.

(4) Li, X.; Zou, G. *Chem. Commun.* **2015**, *51*, 5089–5092.

(5) (a) Meng, G.; Szostak, M. *Org. Lett.* **2015**, *17*, 4364–4367. (b) Meng, G.; Szostak, M. *Org. Biomol. Chem.* **2016**, *14*, 5690–5707.

(6) For the activation of strained β-lactams using Pd, see: Yada, A.; Okajima, S.; Murakami, M. *J. Am. Chem. Soc.* **2015**, *137*, 8708–8711.

(7) For amide activation, accompanied by decarbonylation, see: (a) Meng, G.; Szostak, M. *Angew. Chem., Int. Ed.* **2015**, *54*, 14518–14522. (b) Meng, G.; Szostak, M. *Org. Lett.* **2016**, *18*, 796–799.

(8) Nahm, S.; Weinreb, S. M. *Tetrahedron Lett.* **1981**, *22*, 3815–3818.

(9) Organozinc halides are functional group tolerant and are not known to undergo nucleophilic attack on ketones, esters, or amides (including Weinreb amides). For pertinent discussions, see: (a) Cárdenas, D. J. *Angew. Chem., Int. Ed.* **2003**, *42*, 384–387. (b) Knochel, P.; Singer, R. D. *Chem. Rev.* **1993**, *93*, 2117–2188.

(10) (a) Rosen, B. M.; Quasdorf, K. W.; Wilson, D. A.; Zhang, N.; Resmerita, A.-M.; Garg, N. K.; Percec, V. *Chem. Rev.* **2011**, *111*, 1346–1416. (b) Tasker, S. Z.; Standley, E. A.; Jamison, T.

F. *Nature* **2014**, *509*, 299–309. (c) Mesganaw, T.; Garg, N. K. *Org. Process Res. Dev.* **2013**, *17*, 29–39. (d) Ananikov, V. P. *ACS Catal.* **2015**, *5*, 1964–1971.

(11) For the coupling of acid chlorides with alkyl Grignard reagents, see: Scheiper, B.; Bonnekessel, M.; Krause, H.; Fürstner, A. *J. Org. Chem.* **2004**, *69*, 3943–3949.

(12) (a) Zhang, Y.; Rovis, T. *J. Am. Chem. Soc.* **2004**, *126*, 15964–15965. (b) Cherney, A. H.; Reisman, S. E. *Tetrahedron* **2014**, *70*, 3259–3265. (c) Harada, T.; Kotani, Y.; Katsuhira, T.; Oku, A. *Tetrahedron Lett.* **1991**, *32*, 1573–1576. (d) Negishi, E.-i.; Bagheri, V.; Chatterjee, S.; Luo, F.-T.; Miller, J. A.; Stoll, A. T. *Tetrahedron Lett.* **1983**, *24*, 5181–5184. (e) Iwai, T.; Nakai, T.; Mihara, M.; Ito, T.; Mizuno, T.; Ohno, T. *Synlett* **2009**, 1091–1094. (f) Grey, R. A. *J. Org. Chem.* **1984**, *49*, 2288–2289. (g) Sato, T.; Naruse, K.; Enokiya, M.; Fujisawa, T. *Chem. Lett.* **1981**, *10*, 1135–1138.

(13) (a) Wang, D.; Zhang, Z. *Org. Lett.* **2003**, *5*, 4645–4648. (b) Cook, M. J.; Rovis, T. *Synthesis* **2009**, 335–338. (c) Bercot, E. A.; Rovis, T. *J. Am. Chem. Soc.* **2002**, *124*, 174–175. (d) Bercot, E. A.; Rovis, T. *J. Am. Chem. Soc.* **2005**, *127*, 247–254. (e) Johnson, J. B.; Cook, M. J.; Rovis, T. *Tetrahedron* **2009**, *65*, 3202–3210. (f) Rogers, R. L.; Moore, J. L.; Rovis, T. *Angew. Chem., Int. Ed.* **2007**, *46*, 9301–9304. (g) Bercot, E. A.; Rovis, T. *J. Am. Chem. Soc.* **2004**, *126*, 10248–10249. (h) Johnson, J. B.; Yu, R. T.; Fink, P.; Bercot, E. A.; Rovis, T. *Org. Lett.* **2006**, *8*, 4307–4310. (i) Johnson, J. B.; Bercot, E. A.; Rowley, J. M.; Coates, G. W.; Rovis, T. *J. Am. Chem. Soc.* **2007**, *129*, 2718–2725. (j) Cook, M. J.; Rovis, T. *J. Am. Chem. Soc.* **2007**, *129*, 9302–9303.

(14) (a) Tokuyama, H.; Yokoshima, S.; Yamashita, T.; Fukuyama, T. *Tetrahedron Lett.* **1998**, *39*, 3189–3192. (b) Mori, Y.; Seki, M. *Tetrahedron Lett.* **2004**, *45*, 7343–7345. (c) Shimizu, T.; Seki, M. *Tetrahedron Lett.* **2002**, *43*, 1039–1042. (d) Miyazaki, T.; Han-ya, Y.; Tokuyama, H.;

Fukuyama, T. *Synlett* **2004**, 477–480. (e) Shimizu, T.; Seki, M. *Tetrahedron Lett.* **2001**, *42*, 429–432. (f) Mori, Y.; Seki, M. *Adv. Synth. Catal.* **2007**, *349*, 2027–2038.

(15) The role of the *N*-substituents in amide C–N bond cleavage reactions is currently under investigation and will be described elsewhere in due course.

(16) *N*-Alkyl,Ts amides can be readily prepared by sulfonamide coupling of the corresponding carboxylic acid or acid halide (see the SI). For a discussion of the robustness of sulfonamides and their stability, see: Searles, S.; Nukina, S. *Chem. Rev.* **1959**, *59*, 1077–1103.

(17) Substrates derived from aliphatic carboxylic acids do not couple under the reported reaction conditions; studies to overcome this limitation are currently underway.

(18) Lower yields of **1.12** were obtained using the corresponding *N*-Me,Ts benzamide substrate. Generally, amides derived from electron-poor arenes were found to couple in higher yields when the *N*-Bn,Boc derivatives were employed.

(19) The organozinc bromide or iodide was used in accord with literature precedent for the formation of each organozinc species. Generally, alkyl bromides and iodides are known to undergo organozinc formation more readily than alkyl chlorides; see ref. 9b.

(20) Although primary and secondary organozinc species were well tolerated in the coupling, it was found that couplings with tertiary organozinc halides and organozinc reagents bearing heterocycles, acetals, and esters gave only trace amounts of product.

(21) Han, C.; Buchwald, S. L. *J. Am. Chem. Soc.* **2009**, *131*, 7532–7533.

(22) For the Ni-catalyzed activation of methyl esters, see: Hie, L.; Fine Nathel, N. F.; Hong, X.; Yang, Y.-F.; Houk, K. N.; Garg, N. K. *Angew. Chem., Int. Ed.* **2016**, *55*, 2810–2814. See ref. 10 for alternative examples of ester activation using nickel catalysis.

(23) Apnes, G. E.; Didluk, M. T.; Filipski, K. J.; Guzman-Perez, A.; Lee, E. C. Y.; Pfefferkorn, J. A.; Stevens, B. D.; Tu, M. M. Glucagon Receptor Modulators. U. S. Patent 20120202834, August 9th, 2012.

(24) (a) Allen, C. L.; Davulcu, S.; Williams, J. M. J. *Org. Lett.* **2010**, *12*, 5096–5099. (b) Krishnamoorthy, R.; Lam, S. Q.; Manley, C. M.; Herr, R. J. *J. Org. Chem.* **2010**, *75*, 1251–1258. (c) Baroudi, A.; Alicea, J.; Flack, P.; Kirincich, J.; Alabugin, I. V. *J. Org. Chem.* **2011**, *76*, 1521–1537. (d) Weires, N. A.; Baker, E. L.; Garg, N. K. *Nat. Chem.* **2016**, *8*, 75–79. (e) Yates, M. H.; Kallman, N. J.; Ley, C. P.; Wei, J. N. *Org. Process Res. Dev.* **2009**, *13*, 255–262. (f) Inamoto, Y.; Kaga, Y.; Nishimoto, Y.; Yasuda, M.; Baba, A. *Org. Lett.* **2013**, *15*, 3452–3455.

(25) Krasovskiy, A.; Malakhov, V.; Gavryushin, A.; Knochel, P. *Angew. Chem., Int. Ed.* **2006**, *45*, 6040–6044.

(26) Krasovskiy, A.; Knochel, P. *Synthesis* **2006**, 890–891.

(27) Zhao, B.; Lu, X. *Tetrahedron Lett.* **2006**, *47*, 6765–6768.

(28) Ahmad, I.; Pathak, V.; Vasudev, P. G.; Maurya, H. K.; Gupta, A. *RSC Adv.* **2014**, *4*, 24619–24634.

(29) Dolhem, E.; Barhdadi, R.; Folest, J. C.; Nédelec, J. Y.; Troupel, M. *Tetrahedron* **2001**, *57*, 525–529.

(30) Takemiya, A.; Hartwig, J. F. *J. Am. Chem. Soc.* **2006**, *128*, 14800–14801.

(31) Klemm, L. H.; Solomon, W. C.; Tamiz, A. P. *J. Org. Chem.* **1998**, *63*, 6503–6510.

(32) Jean, M.; Renault, J.; Uriac, P.; Capet, M.; van de Weghe, P. *Org. Lett.* **2007**, *9*, 3623–3625.

(33) Wu, J.; Yang, X.; He, Z.; Mao, X.; Hatton, T. A.; Jamison, T. F. *Angew. Chem., Int. Ed.* **2014**, *53*, 8416–8420.

(34) Gonzalez-de-Castro, A.; Xiao, J. *J. Am. Chem. Soc.* **2015**, *137*, 8206–8218.

(35) Bechara, W. S.; Pelletier, G.; Charette, A. B. *Nat. Chem.* **2012**, *4*, 228–234.

CHAPTER TWO

Nickel-Catalyzed Reduction of Secondary and Tertiary Amides

Bryan J. Simmons, Marie Hoffmann, Jaeyeon Hwang, Moritz K. Jackl, and Neil K. Garg.

Org. Lett. **2017**, *19*, 1910–1913.

2.1 Abstract

The nickel-catalyzed reduction of secondary and tertiary amides to give amine products is reported. The transformation is tolerant of extensive variation with respect to the amide substrate, proceeds in the presence of esters and epimerizable stereocenters, and can be used to achieve the reduction of lactams. Moreover, this methodology provides a simple tactic for accessing medicinally relevant α-deuterated amines.

2.2 Introduction

The ability to manipulate amides using nickel catalysis represents a rapidly growing area of research.[1,2,3,4] Interest in this field has been driven in part by the stability of amides, and their consequential promise for applications in multistep synthesis.[5,6] The high abundance, low cost, and minimal CO_2 footprint associated with nickel also render these transformations highly attractive.[7] In the last year alone, several nickel-catalyzed reactions of amides have been developed (Figure 1), including esterification,[1a] transamidation,[1c] Suzuki–Miyaura couplings,[1b] Negishi couplings,[1d,2c,2d] and decarbonylative processes.[2a,2b]

With the aim of expanding the scope of base metal-catalyzed reactions of amides, we became interested in the nickel-catalyzed reduction of amides (Figure 2.1, **2.1**→**2.2**). Amide

reduction is a powerful synthetic tool and has been the topic of recent investigation,[8] with notable breakthroughs including contributions by Beller (Fe or Ru, 2° or 3° amides; Zn, 3° amides; Cu, 2° amides)[8a,8b,8e,8g] Nagashima (Pt or Fe, 3° amides),[8c,8k] and Adolfsson (Mo, 3° amides).[8d] Beller's Fe-catalyzed amide reduction[8a] is the most general of those methodologies that utilize non-precious metal catalysis, and provides a particularly impressive means to reduce tertiary amides.[9] Surprisingly, however, only scattered reports of nickel-catalyzed amide reduction have been reported over the past century, with no general methodologies having been disclosed. Most known examples of nickel-catalyzed amide reduction require the use of Raney nickel, high temperatures, and high pressures of H_2 gas.[10,11] Only one exception exists, which is the double reduction of α-ketoanilides to the corresponding α-hydroxylamines.[12] A general catalytic platform to achieve the Ni-catalyzed reduction of amides has remained elusive.

Herein, we report a simple catalyst system that enables the reduction of both secondary and tertiary amide substrates. The transformation is tolerant of extensive variation with respect to the amide C- and N-substituents. Furthermore, the nickel-catalyzed amide reduction can be performed in the presence of esters and epimerizable stereocenters. Finally, the methodology provides a simple tactic for the synthesis of α-deuterated amines, which are important motifs in medicinal chemistry.[13]

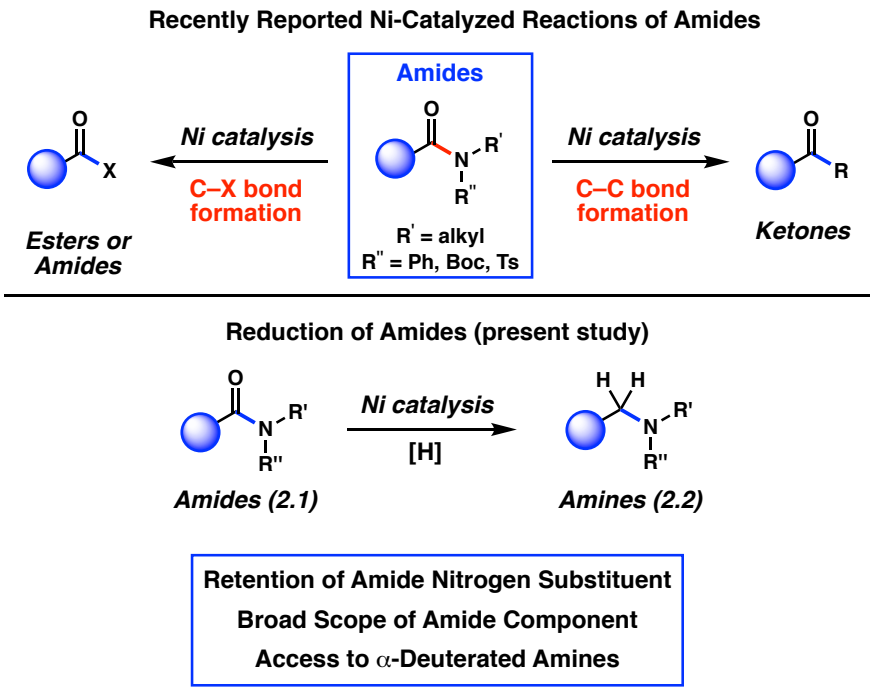

Figure 2.1. Nickel-catalyzed reactions of amides (prior studies) and nickel-catalyzed reduction of amides (present study).

2.3 Development of the Reduction Using Various Amide Substrates

To initiate our studies, we examined the nickel-catalyzed reduction of several classes of amide substrates (Table 2.1).[14] *N*-Methyl-*N*-phenylbenzamide (**2.3**), the substrate used in our initial amide coupling studies,[1a] was tested under a variety of reaction conditions.[15] Ultimately, we found that **2.3** underwent efficient reduction to amine **2.4** in the presence of $PhSiH_3$[16] and a catalytic amount of the air-stable Ni(II) precatalyst $NiCl_2$(dme) [17] (entry 1). An external ligand was not required. With this exciting result in hand, we directed our attention to assessing other amide substrate classes, especially those that did not undergo coupling in our prior studies.[1] Amide **2.5**, a substrate bearing two aliphatic nitrogen substituents, was reduced to give amine **2.6** in 92% yield (entry 2). Moreover, the use of secondary amide **2.7** as a substrate furnished amine **2.8** in excellent yield (entry 3). In the final example shown, we evaluated amide **2.9**, a substrate

derived from an aliphatic carboxylic acid (entry 4). This reduction delivered amine **2.10** in 93% yield. Given that most reported nickel-catalyzed reactions of amides require the use of benzamide-type substrates and activating groups on the nitrogen,[18] the examples shown in entries 2–4 were especially encouraging.[19]

Table 2.1. Evaluation of amide substrates.[a]

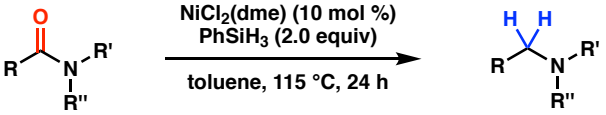

entry	*amide*	*amine*	*yield*[b]
1	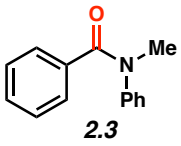 ***2.3***	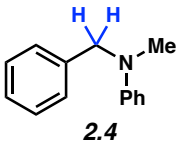 ***2.4***	86%
2	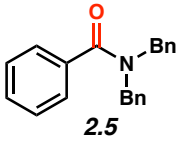 ***2.5***	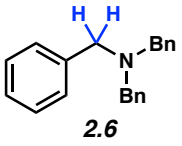 ***2.6***	92%
3	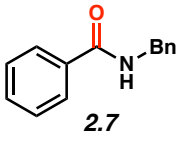 ***2.7***	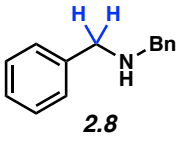 ***2.8***	95%
4	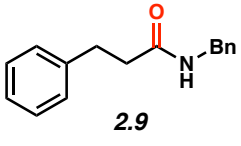 ***2.9***	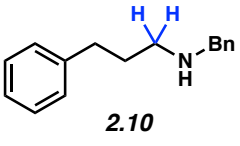 ***2.10***	93%

[a] Conditions unless otherwise stated: $NiCl_2$(dme) (10 mol %), substrate (1.0 equiv, 0.2 mmol), $PhSiH_3$ (2.0 equiv), and toluene (1.0 M) at 115 °C for 24 h in a sealed vial. [b] Yields determined by ^1H NMR analysis using hexamethylbenzene as an internal standard.

2.4 Scope of the Reduction with Respect to the Amide Substrate

Having identified conditions to effect the nickel-catalyzed reduction of secondary and tertiary amides, the scope of this methodology was evaluated.[20] We first tested substituent effects with regard to the carbon-component of the amide carbonyl using secondary amides derived

from benzylamine (Table 2.2). Reduction of the parent benzamide **2.7** gave **2.8** in 94% isolated yield. Electron-donating groups on the aromatic ring were tolerated, as exemplified by the formation of amines **2.11**–**2.13** in high yield. From the latter two cases, it should be emphasized that a tertiary amine and a phenol, respectively, did not hinder catalytic reduction. As suggested by products **2.14** and **2.15**, the electron-withdrawing groups $–CF_3$ and –F also withstood the reaction conditions. Several heteroaromatic substrates were also examined. To our delight, a free indole and a pyrazole were tolerated, as shown by the formation of amines **2.16** and **2.17** in 75 and 67% yield, respectively. In addition to nitrogen-based heterocycles, sulfur- and oxygen-containing heterocycles could be utilized to give thiophene **2.18** and furan **2.19**, both in synthetically useful yields.

As noted earlier, one of the key limitations of most nickel-catalyzed reactions of amides is the necessity to employ benzamide-type substrates. Thus, we were eager to probe a range of amides derived from aliphatic carboxylic acid substrates (Table 2.2). A secondary amide derived from decanoic acid underwent reduction to give product **2.20** in 75% isolated yield. α-Branched substrates could also be reduced in excellent yields, as shown by products **2.21** and **2.22**. It is noteworthy that significant steric bulk did not hinder the transformation. Olefin-containing compounds were also probed under our reaction conditions. Although all tests were not successful, product **2.23** was obtained in high yield, without competitive reduction of the alkene. Finally, heterocyclic amides derived from aliphatic carboxylic acids were found to undergo smooth reduction, as seen by the formation of **2.24**–**2.27**. The tolerance of this methodology to oxygen- and nitrogen-containing heterocycles, including free NHs and carbamates, bodes well for future synthetic applications.

Table 2.2. Reduction of secondary amides with varying C-substituents.[a]

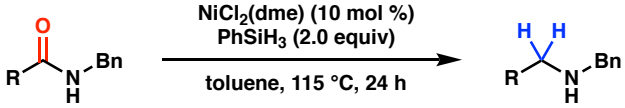

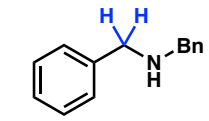

2.8
94% yield

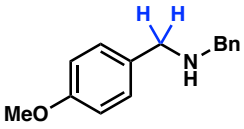

2.11
77% yield

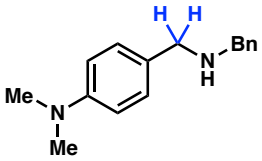

2.12
70% yield

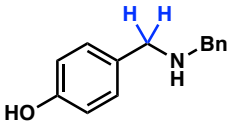

2.13
71% yield

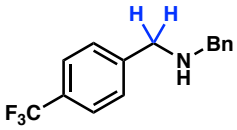

2.14
80% yield

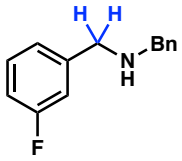

2.15
78% yield

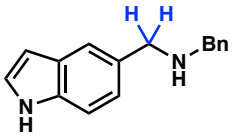

2.16
75% yield[b]

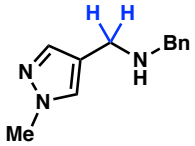

2.17
67% yield[b]

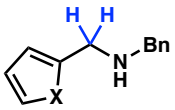

2.18 (X = S); 62% yield[b]
2.19 (X = O); 96% yield[b]

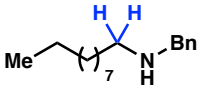

2.20
75% yield

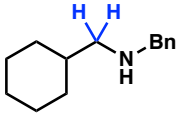

2.21
81% yield

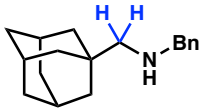

2.22
91% yield

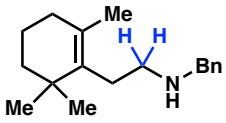

2.23
63% yield[b]

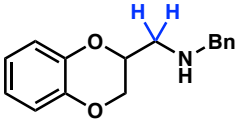

2.24
90% yield[b]

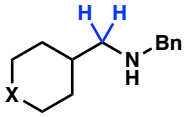

2.25 (X = O); 84% yield
2.26 (X = NBoc); 73% yield
2.27 (X = NH); 73% yield[c]

[a] Conditions unless otherwise stated: $NiCl_2$(dme) (10 mol %), substrate (1.0 equiv, 0.2 mmol), $PhSiH_3$ (2.0 equiv), and toluene (1.0 M) at 115 °C for 24 h in a sealed vial. Yields shown reflect the average of two isolation experiments. [b] $PhSiH_3$ (4.0 equiv) was used. [c] Yields determined by ^1H NMR analysis using hexamethylbenzene as an internal standard.

2.5 Scope of the Reduction with Respect to the *N*-Substituent

As shown in Table 2.3, the scope of the methodology is broad with respect to the amide nitrogen-substituents. Secondary amides beyond *N*-Bn,H-amides can be utilized as shown by the formation of **2.28** and **2.29**. The latter example also suggests that large groups on the amide nitrogen are tolerated. A series of tertiary amides were evaluated, which led to the smooth formation of reduced products **2.30**–**2.36**. These results collectively demonstrate that acyclic, cyclic, branched, and heterocyclic fragments can be utilized in this methodology.

Table 2.3. Reduction of aliphatic substrates.[a]

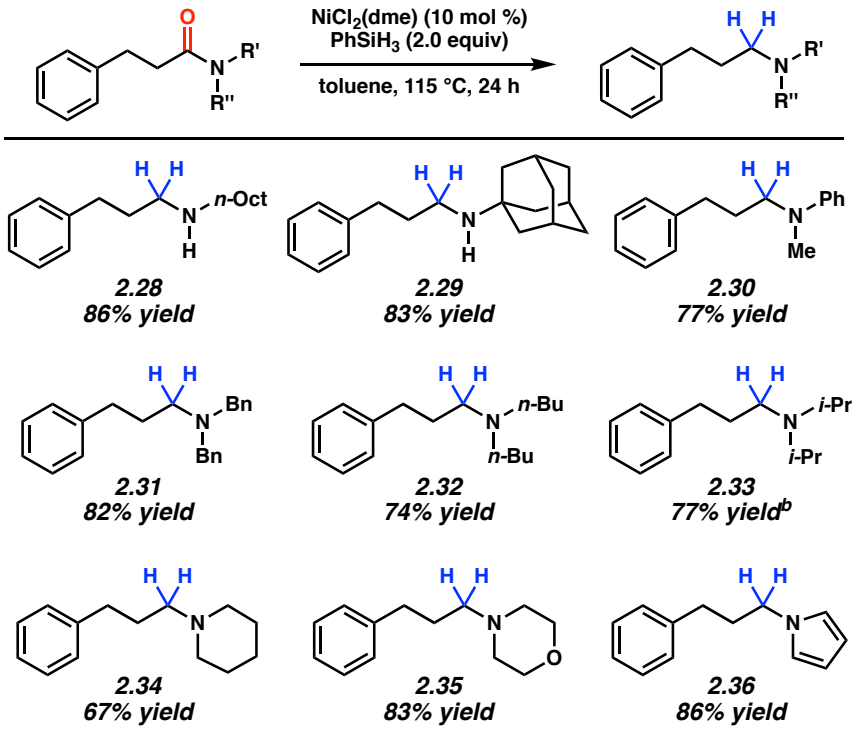

[a] Conditions unless otherwise stated: $NiCl_2$(dme) (10 mol %), substrate (1.0 equiv, 0.2 mmol), $PhSiH_3$ (2.0 equiv), and toluene (1.0 M) at 115 °C for 24 h in a sealed vial. Yields shown reflect the average of two isolation experiments. [b] Yield determined by ^{1}H NMR analysis using hexamethylbenzene as an internal standard.

2.6 Preparation of Cyclic Amines from the Corresponding Lactams

Having demonstrated the broad scope of this methodology for the reduction of acyclic amides, we sought to test its applicability to the reduction of lactam substrates. Lactam reduction is most often performed using $LiAlH_4$, Red-Al, or two-step protocols.[21] As shown in Table 2.4, we found that a 4-membered lactam underwent reduction to give azetidine **2.37** in 64% yield. Additionally, 6- and 7-membered ring substrates could be reduced to give piperidine (**2.38**) and azepane (**2.39**), respectively. Finally, reduction of a 13-membered ring substrate delivered macrocyclic amine **2.40** in quantitative yield. Thus, our nickel-based approach offers a simple and relatively mild alternative to conventional lactam reduction methods and can be used to access cyclic amines of varying ring sizes.

Table 2.4. Cyclic amines prepared by reduction of the corresponding lactams.[a]

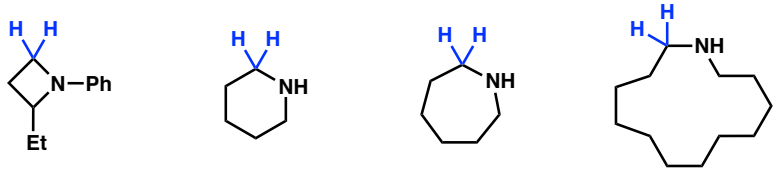

2.37	***2.38***	***2.39***	***2.40***
64% yield[b]	***58% yield***	***83% yield***	***99% yield***

[a] Conditions unless otherwise stated: $NiCl_2$(dme) (10 mol %), substrate (1.0 equiv, 0.2 mmol), $PhSiH_3$ (2.0 equiv), and toluene (1.0 M) at 115 °C for 24 h in a sealed vial. Yield determined by ^1H NMR analysis using hexamethylbenzene as an internal standard due to product volatility. [b] Yield shown reflects the average of two isolation experiments.

2.7 Reduction of Amino Acid Derivatives for the Synthesis of α-Deuteroamines

As a final test of this methodology, a variety of optically enriched amino acid derivatives were reduced using $PhSiD_3$ to give the corresponding α-deuteroamines (Table 2.5).[22] α-Deuteroamines are less prone to undergo metabolism compared to their non-deutero counterparts and are therefore sought after in drug discovery.[13,23] We found that a valine-derived amide

bearing a methyl ester could be reduced to give deuteroamine **2.41**. Similarly, reduction of a tyrosine derivative proceeded in the presence of the free alcohol to furnish **2.42**. In both cases, the ester remained intact and no epimerization was observed. The same features were noted upon reduction of a proline-derived substrate, which gave deuterated aminoester **2.43**. In the last two examples, we examined the reduction of two prolinol derivatives, one bearing a free alcohol and the other bearing an acetoxy group. In both cases, reduction proceeded smoothly to give the corresponding amines **2.44** and **2.45**, respectively. Thus, these results not only underscore the utility of our methodology for the preparation of α-deuteroamines, but also re-emphasize the relatively mild nature of the reaction conditions.

Table 2.5. Reduction of amino acid derivatives for the synthesis of α-deuteroamines.[a]

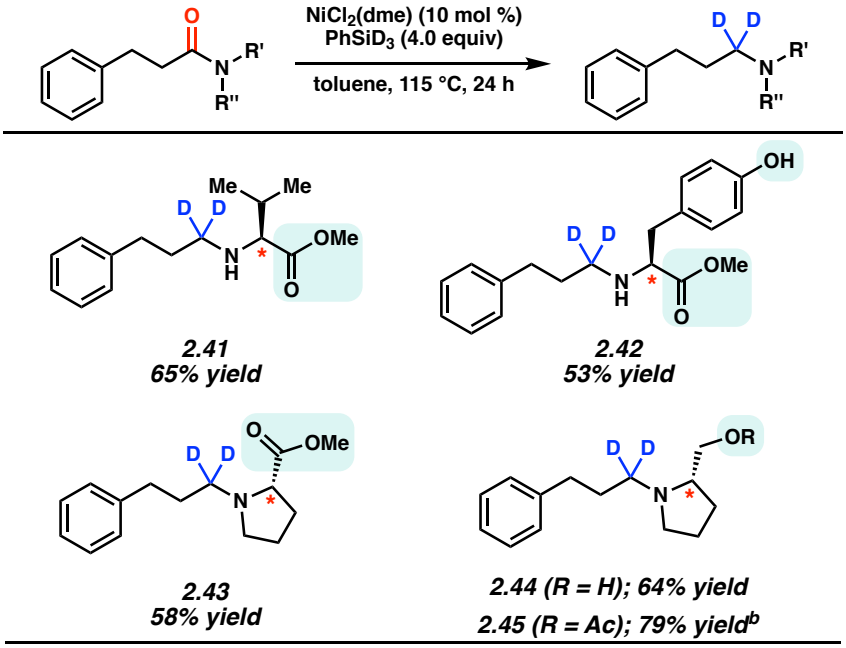

[a] Conditions unless otherwise stated: $NiCl_2$(dme) (10 mol %), substrate (1.0 equiv, 0.1 mmol), $PhSiD_3$ (4.0 equiv), and toluene (1.0 M) at 115 °C for 24 h in a sealed vial. Yields shown reflect the average of two isolation experiments.
[b] $PhSiD_3$ (2.0 equiv) was used.

2.8 Conclusion

We have developed a facile means to achieve the reduction of secondary and tertiary amides using non-precious metal catalysis. The transformation is tolerant of extensive variation with respect to the amide substrate, proceeds in the presence of esters and epimerizable stereocenters, and can be used to reduce lactams. Moreover, by employing α-deuterated silane as the reducing agent, this methodology provides a simple tactic for the synthesis of medicinally relevant α-deuterated amines. Our discovery complements the most general solutions available to the problem of amide reduction known to date.

2.9 Experimental Section

2.9.1 Materials and Methods

Unless stated otherwise, reactions were conducted in flame-dried glassware under an atmosphere of nitrogen and commercially obtained reagents were used as received. Non-commercially available substrates were synthesized following protocols specified in Section 2.9.2.1 of the Experimental Procedures. Prior to use, toluene was purified by distillation and taken through five freeze-pump-thaw cycles. $NiCl_2$(dme) and $LiAlD_4$ was obtained from Strem Chemicals. Hexamethylbenzene and $PhSiH_3$ were obtained from Alfa Aesar and used as received. Carboxylic acids **2.46**, **2.48**, **2.53**, amines **2.51**, **2.57**, **rac-2.51**, **rac-2.90**, **rac-2.91**, and lactam **2.82** were obtained from Combi-Blocks. Carboxylic acid **2.50** was obtained from Eastman Organic. Lactams **2.83**, **2.84**, and $PhSiCl_3$ (**2.85**) were obtained from Sigma–Aldrich and used as received. Benzylamine was obtained from Acros Organics and used as received. Reaction temperatures were controlled using an IKAmag temperature modulator, and unless stated otherwise, reactions were performed at elevated temperatures (approximately 115 °C).

Thin-layer chromatography (TLC) was conducted with EMD gel 60 F254 pre-coated plates (0.25 mm for analytical chromatography and 0.50 mm for preparative chromatography) and visualized using a combination of UV, anisaldehyde, iodine, and potassium permanganate staining techniques. Silicycle Siliaflash P60 (particle size 0.040–0.063 mm) was used for flash column chromatography. ^{1}H NMR spectra were recorded on Bruker spectrometers (at 300, 400 and 500 MHz) and are reported relative to residual solvent signals. Data for ^{1}H NMR spectra are reported as follows: chemical shift (δ ppm), multiplicity, coupling constant (Hz), integration. Data for ^{2}H NMR spectra are reported in terms of chemical shift (at 76 MHz). Data for ^{13}C NMR are reported in terms of chemical shift (at 75 and 125 MHz). IR spectra were recorded on a Perkin-Elmer UATR Two FT-IR spectrometer and are reported in terms of frequency absorption (cm^{-1}). High-resolution mass spectra were obtained on Thermo Scientific™ Exactive Mass Spectrometer with DART ID-CUBE. Determination of enantiopurity was carried out on a Mettler Toledo SFC (supercritical fluid chromatography) using a Daicel ChiralPak column.

2.9.2 Experimental Procedures

2.9.2.1 Syntheses of Amide Substrates

Representative Procedure A for the synthesis of amide substrates from Table 2.2. (2.47 is used as an example).

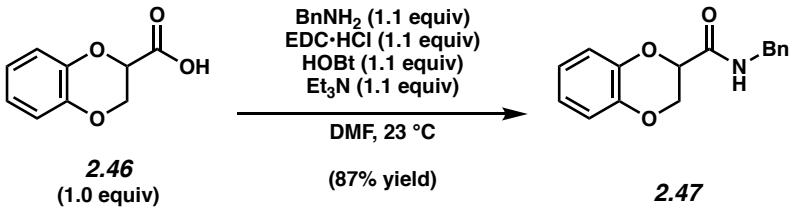

Amide 2.47. To a solution of carboxylic acid **2.46** (2.00 g, 11.1 mmol, 1.0 equiv), HOBt (1.87 g, 12.2 mmol, 1.1 equiv), and triethylamine (1.70 mL, 12.2 mmol, 1.1 equiv) in DMF (111.0 mL,

0.1 M) at 23 °C was added EDC•HCl (1.89 g, 12.2 mmol, 1.1 equiv) followed by benzylamine (1.3 mL, 12.2 mmol, 1.1 equiv) dropwise over 1 min under a N_2 atmosphere. After stirring at 23 °C for 18 h, the reaction was diluted with deionized water (100 mL) and transferred to a separatory funnel with EtOAc (75 mL). The layers were separated and the aqueous layer was extracted with EtOAc (3 x 75 mL). The organic layers were combined and washed with water (3 x 75 mL), dried over Na_2SO_4, and the volatiles were removed under reduced pressure. The resulting crude residue was purified by flash chromatography (10:1 Hexanes:EtOAc → 2:1 Hexanes:EtOAc) to yield amide **2.47** (2.6 g, 87% yield) as a white solid. Amide **2.47**: mp: 130–131 ºC; R_f 0.30 (3:1 Hexanes:EtOAc); ^{1}H NMR (500 MHz, $CDCl_3$): δ 7.35–7.27 (m, 3H), 7.25–7.23 (m, 2H), 6.94–6.85 (m, 5H), 4.75 (dd, *J* = 7.3, 2.7, 1H), 4.58 (dd, *J* = 11.4, 2.7, 1H), 4.52 (d, *J* = 6.0, 2H), 4.23 (dd, *J* = 11.4, 7.3, 1H); ^{13}C NMR (125 MHz, $CDCl_3$): δ 167.3, 143.5, 141.7, 137.6, 128.9, 127.9, 127.8, 122.6, 122.1, 117.8, 117.3, 73.4, 65.6, 43.3; IR (film): 3029, 2924, 2876, 1670, 1493 cm^{-1}; HRMS-ESI (*m/z*) $[M + H]^+$ calcd for $C_{16}H_{16}NO_3$, 270.11247; found 270.11082.

Representative Procedure B for the synthesis of amide substrates from Table 2.2. (2.49 is used as an example).

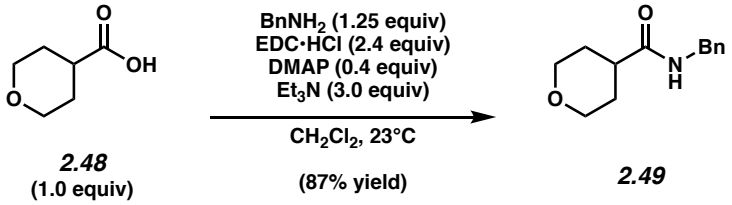

Amide 2.49. To a solution of carboxylic acid **2.48** (500.0 mg, 3.84 mmol, 1.0 equiv), EDC•HCl (1.77 g, 9.22 mmol, 2.4 equiv), and DMAP (188.0 mg, 1.54 mmol, 0.4 equiv) in CH_2Cl_2 (12 mL, 0.35 M) was added Et_3N (1.6 mL, 11.52 mmol, 3.0 equiv) followed by benzylamine **(**525.0 µL,

4.80 mmol,1.25 equiv) dropwise over 1 min under a N_2 atmosphere. After stirring at 23 °C for 18 h, the reaction mixture was transferred to a separatory funnel with EtOAc (30 mL) and washed with 1.0 M aqueous HCl (2 x 10 mL), followed by 1.0 M aqueous NaOH (2 x 10 mL), and deionized water (10 mL). The organic layer was dried over Na_2SO_4, and the volatiles were removed under reduced pressure. The resulting crude residue was purified by flash chromatography (1:15 Hexanes:EtOAc) to yield amide **2.49** (775.5 mg, 87% yield) as a white solid. Amide **2.49**: mp: 116–117 ºC; R_f 0.46 (1:4 Hexanes:EtOAc); ^{1}H NMR (500 MHz, $CDCl_3$): δ 7.35–7.33 (m, 2H), 7.30–7.27 (m, 3H), 5.71 (br. s, 1H), 4.46 (d, J = 5.7, 2H), 4.04–4.00 (m, 2H), 3.41 (td, J = 11.5, 2.8, 2H), 2.40–2.34 (m, 1H), 1.88–1.82 (m, 2H), 1.81–1.77 (m, 2H); ^{13}C NMR (125 MHz, $CDCl_3$): 174.1, 138.3, 128.9, 127.9, 127.8, 67.4, 43.7, 42.4, 29.4; IR (film): 3064, 2951, 2842, 1635, 1541 cm^{-1}; HRMS-ESI (*m/z*) $[M + H]^+$ calcd for $C_{13}H_{18}NO_2$, 220.13321; found 220.13214.

Representative Procedure C for the synthesis of amide substrates from Table 2.5. (2.52 is used as an example).

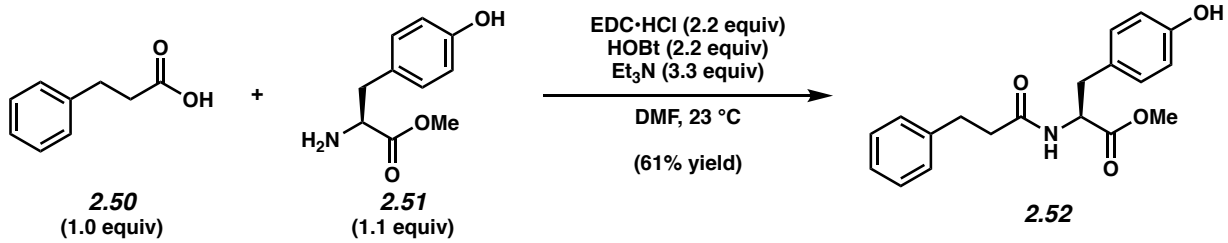

2.50 **(1.0 equiv)** ***2.51*** **(1.1 equiv)** ***2.52***

Amide 2.52. To a solution of carboxylic acid **2.50** (500.0 mg, 3.33 mmol, 1.0 equiv), HOBt (988.9 mg, 7.33 mmol, 2.2 equiv), and EDC•HCl (1.41 g, 7.33 mmol, 2.2 equiv) in DMF (16.6 mL, 0.2 M) at 23 °C was added amine **2.51** (714.9 mg, 3.66 mmol, 1.1 equiv), followed by triethylamine (1.50 mL, 10.9 mmol, 3.3 equiv) under a N_2 atmosphere. After stirring at 23 °C for

18 h, the reaction was diluted with deionized water (50 mL) and transferred to a separatory funnel with EtOAc (40 mL). The layers were separated and the aqueous layer was extracted with EtOAc (3 x 40 mL). The organic layers were combined and washed with water (3 x 40 mL), dried over Na_2SO_4, and the volatiles were removed under reduced pressure. The resulting crude residue was purified by flash chromatography (3:1 Hexanes:EtOAc → 1:1 Hexanes:EtOAc) to yield amide **2.52** (662.1 mg, 61% yield) as a white solid. Amide **2.52**: mp: 89–92 ºC; R_f 0.25 (1:1 Hexanes:EtOAc); ^{1}H NMR (500 MHz, CD_2Cl_2): δ 7.29–7.26 (m, 2H), 7.20–7.17 (m, 3H), 6.83–6.82 (m, 2H), 6.71–6.68 (m, 2H), 5.94 (br. d, *J* = 7.8, 1H), 4.79 (dt, *J* = 7.8, 5.9, 1H), 3.69 (s, 3H), 2.99 (dd, *J* = 13.8, 5.6, 1H), 2.93 (dd, *J* = 13.8, 5.6, 1H), 2.91–2.88 (m, 2H), 2.53–2.42 (m, 2H); ^{13}C NMR (125 MHz, $CDCl_3$): δ 172.1, 171.7, 154.9, 140.8, 130.4, 128.6, 128.4, 127.5, 126.3, 115.5, 53.1, 52.4, 38.2, 37.1, 31.4; IR (film): 3287, 3026, 2951, 1736, 1647 cm^{-1}; HRMS-ESI (*m/z*) $[M + H]^+$ calcd for $C_{19}H_{20}NO_4$, 326.13937, found 326.13868. $[\alpha]^{27.6}_D$ +60.00° (c = 0.10, CH_2Cl_2).

Note: Experimental procedures for the syntheses of some amides used in Tables 2.1, 2.2, 2.3, and 2.4 have previously been reported: **2.7**,[24] **2.59**,[25] **2.60**,[26] **2.61**,[27] **2.62**,[28] **2.63**,[29] **2.64**,[30] **2.65**,[25] **2.66**,[26] **2.67**,[31] **2.68**,[24] **2.69**,[32] **2.70**,[33] **2.71**,[33] **2.72**,[34] **2.73**,[35] **2.74**,[36] **2.75**,[37] **2.76**,[38] **2.77**,[39] **2.78**,[40] **2.79**,[41] **2.80**,[42] **2.81**,[43] **2.87**,[44] **2.88**,[45] **2.89**.[46] Syntheses for the remaining substrates shown in Tables 2.2 and 2.5 are as follows:

Any modifications of the conditions shown in the representative procedures above are specified in the following schemes.

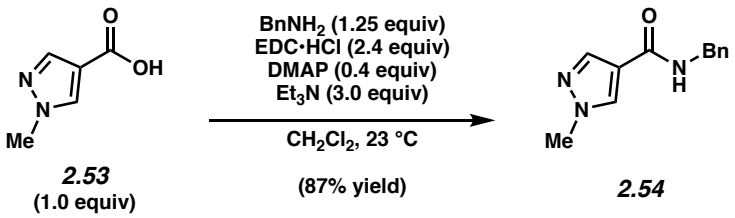

Amide 2.54. Following representative procedure B. Purification by flash chromatography (9:1 EtOAc:$CHCl_3$) yielded amide **2.54** (810.2 mg, 87% yield) as a white solid. Amide **2.54**: mp: 157–158 °C; R_f 0.27 (1:4 Hexanes:EtOAc); ^{1}H NMR (500 MHz, $CDCl_3$): δ 7.83 (s, 1H), 7.70 (s, 1H), 7.36–7.32 (m, 4H), 7.30–7.27 (m, 1H), 6.06 (s, 1H), 4.59 (d, J = 5.6, 2H), 3.91 (s, 3H); ^{13}C NMR (125 MHz, $CDCl_3$): δ 162.4, 138.4, 137.8, 131.9, 128.9, 128.0, 127.7, 118.8, 43.6, 39.4; IR (film): 3111, 3064, 2941, 1630, 1566 cm^{-1}; HRMS-ESI (*m/z*) $[M + H]^+$ calcd for $C_{12}H_{14}N_3O$, 216.11314; found 216.11201.

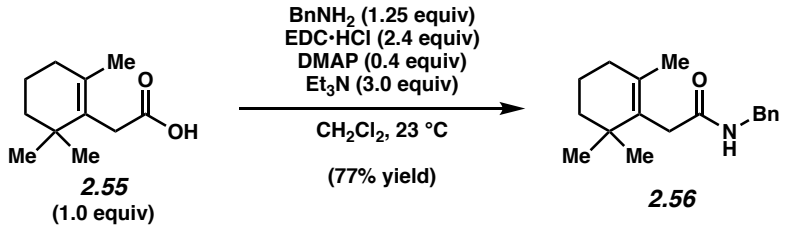

Amide 2.56. Following representative procedure B. Purification by flash chromatography (4:1 Hexanes:EtOAc) yielded amide **2.56** (230.0 mg, 77% yield) as a white solid. Amide **2.56**: mp: 78–80 °C; R_f 0.32 (3:1 Hexanes:EtOAc); ^{1}H NMR (500 MHz, C_6D_6): δ 7.13–7.09 (m, 4H), 7.05–7.02 (m, 1H), 5.62 (br. s, 1H), 4.33 (d, J = 5.9, 2H), 2.99 (s, 2H), 1.69 (t, J = 6.4, 2H), 1.42 (s, 3H), 1.41–1.38 (m, 2H), 1.31–1.28 (m, 2H), 0.90 (s, 6H); ^{13}C NMR (125 MHz, $CDCl_3$): δ 171.3, 138.4, 132.9, 132.5, 128.7, 127.5, 127.4, 43.5, 39.4, 36.7, 34.9, 32.6, 28.1, 20.5, 19.1; IR (film): 3299, 2926, 2865, 1640, 1516 cm^{-1}; HRMS-ESI (*m/z*) $[M + H]^+$ calcd for $C_{18}H_{26}NO$, 272.19901; found 272.20089.

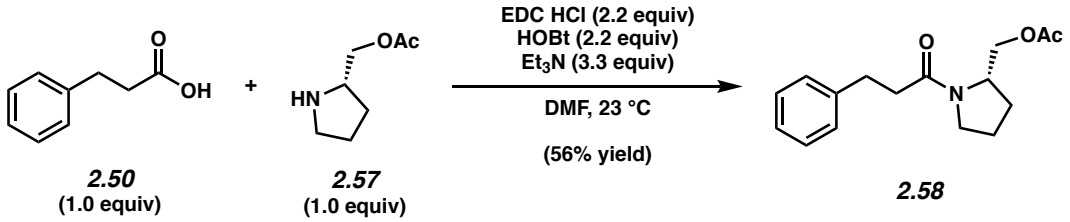

Amide 2.58. Following representative procedure C. Purification by flash chromatography (1:1 Hexanes:EtOAc) yielded amide **2.58** (234.0 mg, 56% yield) as a colorless oil. Amide **2.58** was observed as a 2.9:1 mixture of rotational isomers in $CDCl_3$. Amide **2.58**: R_f 0.29 (1:1 Hexanes:EtOAc); ^{1}H NMR (500 MHz, $CDCl_3$, **Major rotational isomer**): δ 7.26–7.23 (m, 2H), 7.20–7.14 (m, 3H), 4.34–4.31 (m, 1H), 4.14 (dd, *J* = 10.7, 3.8, 1H), 4.06 (dd, *J* = 10.7, 6.9, 1H), 3.35–3.31 (m, 1H), 3.28–3.23 (m, 1H), 2.99–2.92 (m, 2H), 2.53 (t, *J* = 7.7, 2H), 2.01 (s, 3H), 1.95–1.77 (m, 4H); ^{1}H NMR (500 MHz, $CDCl_3$, **Minor rotational isomer**): δ 7.26–7.26 (m, 2H), 7.20–7.14 (m, 3H), 3.94 (dd, *J* = 10.7, 5.5, 1H), 3.91–3.86 (m, 1H), 3.76 (dd, *J* = 10.7, 7.4, 1H), 3.51 (dt, *J* = 12.3, 8.5, 1H), 3.43–3.38 (m, 1H), 2.99–2.92 (m, 2H), 2.66 (t, *J* = 7.7, 2H), 1.99 (s, 3H), 1.95–1.77 (m, 4H); ^{13}C NMR (100 MHz, $CDCl_3$, **Major rotational isomer**): δ 171.4, 170.9, 141.5, 128.6, 128.6, 126.2, 64.0, 55.5, 47.2, 36.9, 31.2, 27.4, 24.1, 21.0; ^{13}C NMR (100 MHz, $CDCl_3$, **Minor rotational isomer**): δ 171.6, 170.7, 141.4, 128.6, 128.6, 126.2, 64.7, 55.8, 45.7, 36.2, 31.8, 28.7, 21.8, 20.9; IR (film): 3474, 2955, 2878, 1737, 1636 cm^{-1}; HRMS-ESI (*m/z*) $[M + H]^+$ calcd for $C_{16}H_{22}NO_3$, 276.15906; found 276.15942. $[\alpha]^{29.6}_D$ –29.33° (c = 0.10, CH_2Cl_2).

2.9.2.2 Initial Survey of Amide Substrates with Phenylsilane

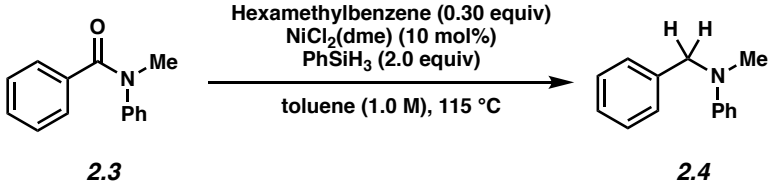

Representative Procedure for the reduction of amides from Table 2.1 and Table 2.6 (reduction of amide 2.3 is used as an example). A 1-dram vial was charged with a magnetic stir bar, flame-dried under reduced pressure, and allowed to cool under a N_2 atmosphere. Amide substrate **2.3** (42.3 mg, 0.200 mmol, 1.0 equiv), $NiCl_2$(dme) (4.4 mg, 0.0200 mmol, 10 mol%), and hexamethylbenzene (9.7 mg, 0.0600 mmol, 0.30 equiv) were added, and the vial was flushed with N_2 for 5 min. $PhSiH_3$ (49.4 μL, 0.400 mmol, 2.0 equiv) was added under a N_2 atmosphere via syringe followed by toluene (200 μL, 1.0 M). The vial was then capped with a Teflon-lined screw cap under a flow of N_2. The reaction mixture was then placed in a pre-heated aluminum block and allowed to stir at 115 °C for 24 h. After cooling to room temperature, the reaction mixture was transferred to a separatory funnel with EtOAc (3 mL) and basified with 1.0 M aqueous NaOH (4 mL). The layers were separated and the aqueous layer was extracted with EtOAc (3 x 5 mL). The combined organic layers were washed with saturated aqueous NaCl (5 mL). The volatiles were removed under reduced pressure, and the yield was determined by ^1H NMR analysis with hexamethylbenzene as an internal standard.

Table 2.6. Initial survey of amide substrates with Phenylsilane

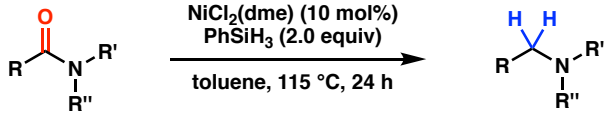

Entry	*Amide*	*Amine*	*Yield*[b]
1	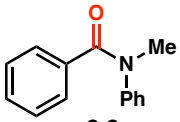 *2.3*	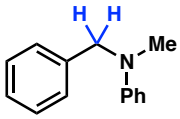 *2.4*	*86%*
2	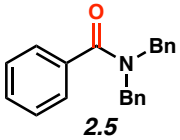 *2.5*	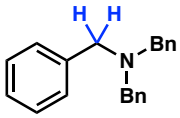 *2.6*	*92%*
3	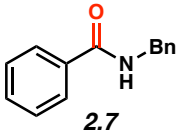 *2.7*	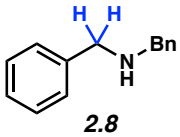 *2.8*	*95%*
4	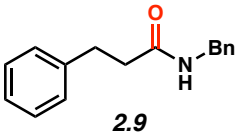 *2.9*	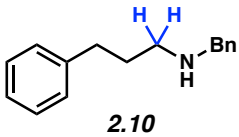 *2.10*	*93%*

[a] Conditions unless otherwise stated: $NiCl_2$(dme) (10 mol%), substrate (1.0 equiv, 0.2 mmol), $PhSiH_3$ (2.0 equiv), and toluene (1.0 M) at 115 °C for 24 h in a sealed vial. [b] Yields determined by ^1H NMR analysis using hexamethylbenzene as an internal standard.

2.9.2.3 Relevant Control Experiments for the Reduction of Amide 2.7

Table 2.7. Relevant control experiments in the reduction of amide **2.7**.[a]

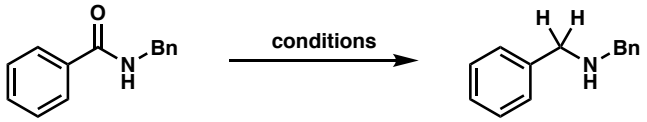

2.7 *2.8*

Reaction Conditions	*Experimental Results* *2.7*	*2.8*
$NiCl_2$(dme) (10 mol%), $PhSiH_3$ (2.0 equiv), toluene (1.0 M), 115 °C, 24 h	0%	95%
Control Experiments:		
$PhSiH_3$ (2.0 equiv), toluene (1.0 M), 115 °C, 24 h	98%	0%
$NiCl_2$(dme) (10 mol%), toluene (1.0 M), 115 °C, 24 h	100%	0%

[a] Yields were determined by ^{1}H NMR analysis using hexamethylbenzene as an internal standard.

2.9.2.4 Scope of Methodology

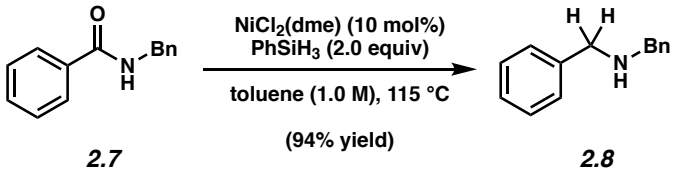

2.7 *2.8*

Representative Procedure (reduction of amide 2.7 is used as an example). Amine 2.8. A 1-dram vial was charged with a magnetic stir bar, flame-dried under reduced pressure, and allowed to cool under a N_2 atmosphere. Amide substrate **2.7** (42.3 mg, 0.200 mmol, 1.0 equiv) and $NiCl_2$(dme) (4.4 mg, 0.0200 mmol, 10 mol%) was added, and the vial was flushed with N_2. $PhSiH_3$ (49.4 μL, 0.4000 mmol, 2.0 equiv) was added under a N_2 atmosphere via syringe followed by toluene (200 μL, 1.0 M). The vial was then capped with a Teflon-lined screw cap under a flow of N_2. The reaction mixture was then placed in a pre-heated aluminum block and allowed to stir at 115 °C for 24 h. After cooling to room temperature, the reaction mixture was

transferred to a separatory funnel with EtOAc (3 mL) and basified with 1.0 M aqueous NaOH (4 mL). The layers were separated and the aqueous layer was extracted with EtOAc (3 x 5 mL). The combined organic layers were washed with saturated aqueous NaCl (5 mL). The volatiles were removed under reduced pressure, and the crude residue was purified by flash chromatography (1:1 Hexanes:EtOAc) to yield amine **2.8** (94% yield, average of two experiments) as a colorless oil. Amine **2.8**: R_f 0.36 (1:1 Hexanes:EtOAc). Spectral data match those previously reported.[47]

Any modifications of the conditions shown in the representative procedure above are specified in the following schemes, which depict all of the results shown in Tables 2.1, 2.2, and 2.3.

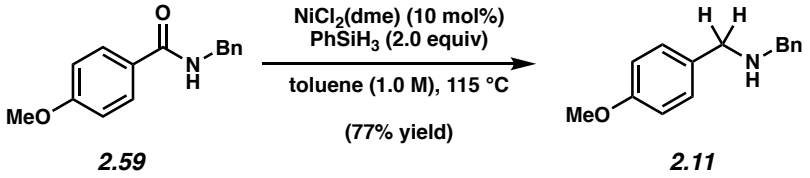

Amine 2.11. Purification by flash chromatography (3:1 Hexanes:EtOAc, 2% Et_3N) yielded amine **2.11** (77% yield, average of two experiments) as a colorless oil. Amine **2.11**: R_f 0.41 (4:1 Hexanes:EtOAc, 2% Et_3N). Spectral data match those previously reported.[48]

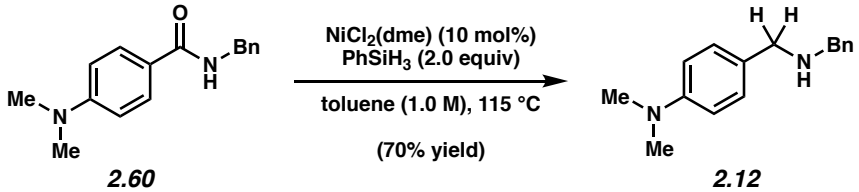

Amine 2.12. Purification by flash chromatography (1:1 CH_2Cl_2:CH_3CN, 2% Et_3N) yielded amine **2.12** (70% yield, average of two experiments) as a colorless oil. Amine **2.12**: R_f 0.50 (1:1 CH_2Cl_2:CH_3CN, 2% Et_3N). Spectral data match those previously reported.[49]

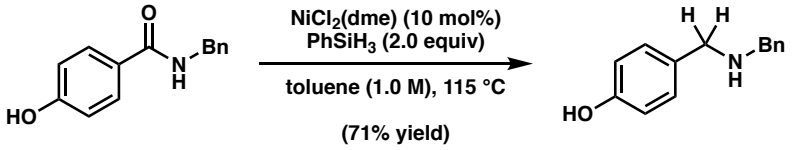

2.61 *2.13*

Amine 2.13. Purification by flash chromatography (EtOAc, 2% Et_3N) yielded amine **2.13** (71% yield, average of two experiments) as a white solid. Amine **2.13**: R_f 0.52 (EtOAc, 2% Et_3N). Spectral data match those previously reported.[50]

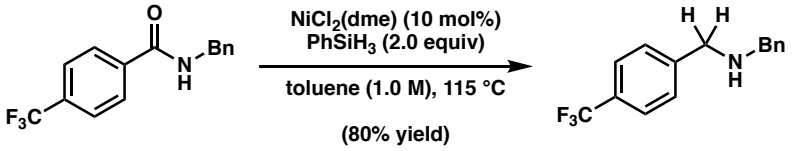

2.62 *2.14*

Amine 2.14. Purification by flash chromatography (1:1 Hexanes:EtOAc) yielded amine **2.14** (80% yield, average of two experiments) as a colorless oil. Amine **2.14**: R_f 0.60 (1:1 Hexanes:EtOAc). Spectral data match those previously reported.[51]

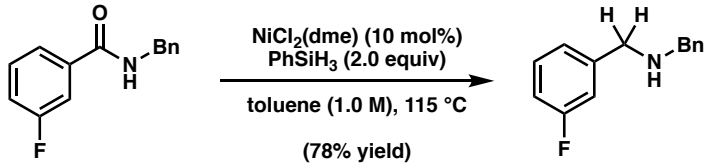

2.63 *2.15*

Amine 2.15. Purification by flash chromatography (1:1 Hexanes:EtOAc) yielded amine **2.15** (78% yield, average of two experiments) as a colorless oil. Amine **2.15**: R_f 0.59 (1:1 Hexanes:EtOAc). ^{1}H NMR (500 MHz, $CDCl_3$): δ 7.35 (d, J = 4.4, 4H), 7.31–7.26 (m, 2H), 7.12–7.09 (m, 2H), 6.95 (td, J = 8.6, 2.3, 1H), 3.81 (s, 4H), 1.77 (br. s, 1H); ^{13}C NMR (125 MHz, $CDCl_3$): δ 164.0, 162.1, 143.0 (d, $J_{C–F}$ = 6.9), 140.1, 129.8 (d, $J_{C–F}$ = 8.1), 128.3 (d, $J_{C–F}$ = 37.6), 127.1, 123.6 (d, $J_{C–F}$ = 2.9), 114.9 ($J_{C–F}$ = 21.1), 113.8 ($J_{C–F}$ = 21.1), 53.1, 52.6; IR (film): 3064,

3028, 2831, 1615, 1588 cm^{-1}; HRMS-ESI (*m/z*) $[M + H]^+$ calcd for $C_{14}H_{15}FN$, 216.11830; found 216.11803.

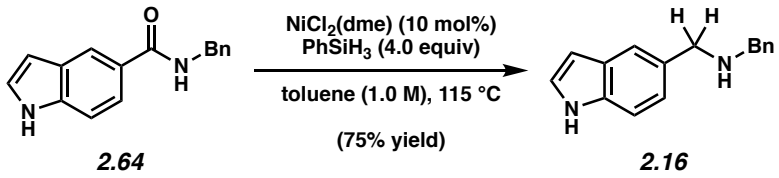

Amine 2.16. Purification by flash chromatography (4:1 Hexanes:EtOAc, 2% Et_3N → 1:1 Hexanes:EtOAc, 2% Et_3N) yielded amine **2.16** (75% yield, average of two experiments) as a colorless solid. Amine **2.16**: mp: 51–54 °C; R_f 0.36 (1:1 Hexanes:EtOAc, 2% Et_3N). ^1H NMR (500 MHz, $CDCl_3$): δ 8.34 (br. s, 1H), 7.60 (s, 1H), 7.39–7.33 (m, 5H), 7.23–7.26 (m, 1H), 7.21–7.18 (m, 2H), 6.53 (d, *J* = 3.1, 1H), 3.93 (s, 2H), 3.85 (s, 2H), 2.44 (br. s, 1H); ^{13}C NMR (125 MHz, $CDCl_3$): δ 140.0, 135.3, 131.1, 128.5, 128.4, 128.1, 127.1, 124.7, 122.9, 120.5, 111.2, 102.5, 53.5, 52.9; IR (film): 3410, 3026, 2919, 1623, 1452 cm^{-1}; HRMS-ESI (*m/z*) $[M + H]^+$ calcd for $C_{16}H_{17}N$, 237.13863; found 237.13806.

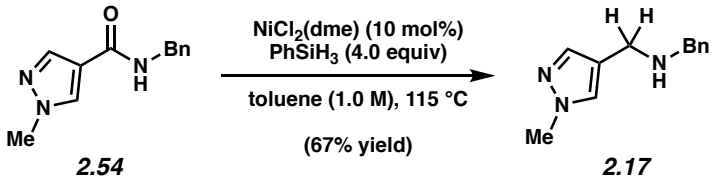

Amine 2.17. Purification by flash chromatography (EtOAc, 2% Et_3N) yielded amine **2.17** (67% yield, average of two experiments) as a colorless oil. Amine **2.17**: R_f 0.26 (EtOAc, 2% Et_3N). ^1H NMR (500 MHz, $CDCl_3$): δ 7.43 (s, 1H), 7.35–7.32 (m, 4H), 7.31–7.30 (m, 1H), 7.28–7.24 (m, 2H), 3.87 (s, 3H), 3.81 (s, 2H), 3.69 (s, 2H); ^{13}C NMR (125 MHz, $CDCl_3$): δ 140.3, 138.9, 129.1,

128.6, 128.3, 127.1, 120.6, 53.3, 43.3, 39.0; IR (film): 3303, 2936, 2849, 1642, 1453 cm^{-1}; HRMS-ESI (*m/z*) $[M + H]^+$ calcd for $C_{12}H_{16}N_3$, 202.13387; found 202.13355.

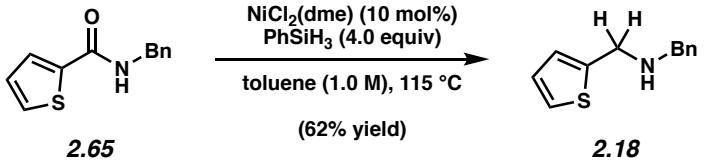

Amine 2.18. Purification by flash chromatography (10:1 Hexanes:EtOAc, 2% Et_3N) yielded amine **2.18** (62% yield, average of two experiments) as a colorless oil. Amine **2.18**: R_f 0.34 (4:1 Hexanes:EtOAc, 2% Et_3N). Spectral data match those previously reported.[49]

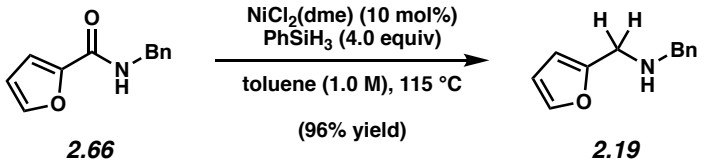

Amine 2.19. Purification by flash chromatography (4:1 Hexanes:EtOAc, 2% Et_3N) yielded amine **2.19** (96% yield, average of two experiments) as a colorless oil. Amine **2.19**: R_f 0.49 (4:1 Hexanes:EtOAc, 2% Et_3N). Spectral data match those previously reported.[48]

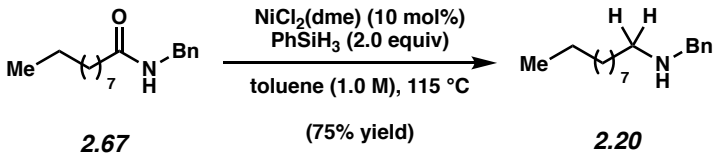

Amine 2.20. Purification by flash chromatography (10:1 Hexanes:EtOAc, 2% Et_3N) yielded amine **2.20** (75% yield, average of two experiments) as a colorless oil. Amine **2.20**: R_f 0.38 (10:1 Hexanes:EtOAc, 2% Et_3N). Spectral data match those previously reported.[52]

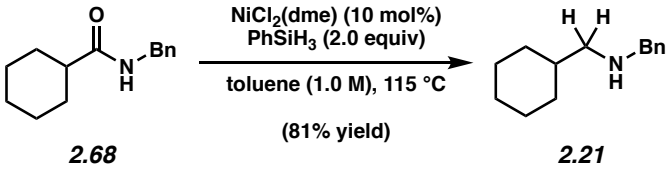

2.68 *2.21*

Amine 2.21. Purification by flash chromatography (10:1 Hexanes:EtOAc, 2% Et_3N) yielded amine **2.21** (81% yield, average of two experiments) as a colorless oil. Amine **2.21**: R_f 0.40 (10:1 Hexanes:EtOAc, 2% Et_3N). Spectral data match those previously reported.[53]

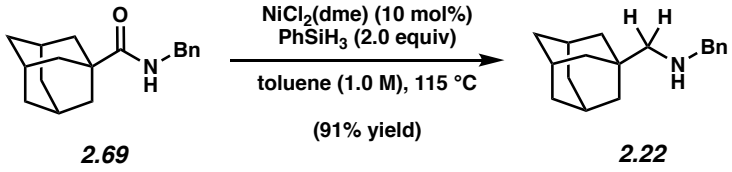

2.69 *2.22*

Amine 2.22. Purification by flash chromatography (4:1 Hexanes:EtOAc, 2% Et_3N) yielded amine **2.22** (91% yield, average of two experiments) as a colorless oil. Amine **2.22**: R_f 0.52 (4:1 Hexanes:EtOAc, 2% Et_3N). Spectral data match those previously reported.[54]

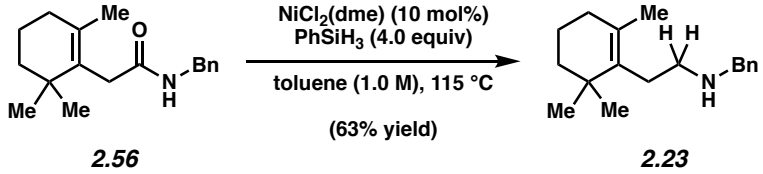

2.56 *2.23*

Amine 2.23. Purification by preparative thin-layer chromatography (10:1 Hexanes:EtOAc, 2% Et_3N) yielded amine **2.23** (63% yield, average of two experiments) as a colorless oil. Amine **2.23**: R_f 0.40 (10:1 Hexanes:EtOAc, 2% Et_3N). ^1H NMR (500 MHz, $CDCl_3$): δ 7.32–7.30 (m, 4H), 7.27–7.21 (m, 1H), 3.82 (s, 2H), 2.67–2.63 (m, 2H), 2.23 (t, J = 8.5, 2H), 1.89 (t, J = 6.4, 2H), 1.59 (s, 3H), 1.57–1.53 (m, 2H), 1.41–1.39 (m, 2H), 0.97 (s, 6H); ^{13}C NMR (125 MHz, $CDCl_3$): δ 140.7, 134.9, 128.5, 128.4, 128.1, 127.0, 54.1, 49.7, 39.9, 34.9, 32.9, 29.8, 28.9, 20.1,

19.6; IR (film): 3026, 2926, 2864, 1873, 1452 cm^{-1}; HRMS-ESI (*m/z*) $[M + H]^+$ calcd for $C_{18}H_{28}N$, 258.22074; found 258.22163.

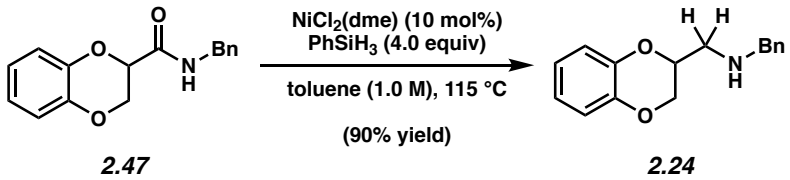

Amine 2.24. Purification by flash chromatography (10:1 Hexanes:EtOAc, 2% Et_3N → 4:1 Hexanes:EtOAc, 2% Et_3N) yielded amine **2.24** (90% yield, average of two experiments) as a colorless oil. Amine **2.24**: R_f 0.38 (4:1 Hexanes:EtOAc, 2% Et_3N). ^1H NMR (500 MHz, $CDCl_3$): δ 7.36–7.35 (m, 4H), 7.30–7.27 (m, 1H), 6.90–6.84 (m, 4H), 4.33–4.30 (m, 1H), 4.28 (dd, *J* = 11.0, 2.4, 1H), 4.05 (dd, *J* = 11.0, 7.3, 1H), 3.87 (s, 2H), 2.94 (dd, *J* = 12.4, 6.6, 1H), 2.88 (dd, *J* = 12.4, 4.6, 1H), 2.00 (br. s, 1H); ^{13}C NMR (125 MHz, $CDCl_3$): δ 143.4, 143.3, 139.9, 128.6, 128.2, 127.2, 121.6, 121.5, 117.4, 117.2, 72.7, 66.7, 54.0, 49.3; IR (film): 3027, 2919, 2831, 1592, 1492 cm^{-1}; HRMS-ESI (*m/z*) $[M + H]^+$ calcd for $C_{16}H_{18}NO_2$, 256.13321; found 256.13258.

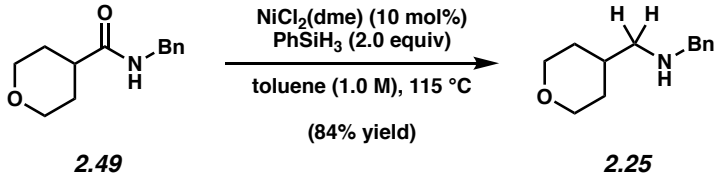

Amine 2.25. Purification by flash chromatography (1:1 Hexanes:EtOAc, 2% Et_3N) yielded amine **2.25** (84% yield, average of two experiments) as a colorless oil. Amine **2.25**: R_f 0.54 (1:1 Hexanes:EtOAc, 2% Et_3N). ^1H NMR (500 MHz, $CDCl_3$): δ 7.43–7.31 (m, 4H), 7.27–7.24 (m, 1H), 3.97–3.94 (m, 2H), 3.78 (s, 2H), 3.37 (ddd, *J* = 11.8, 11.8, 1.9, 2H), 2.52 (d, *J* = 6.6, 2H), 1.79 (br. s, 1H), 1.72 (ttt, *J* = 11.8, 6.9, 3.8, 1H), 1.65 (m, 2H), 1.29 (dddd, *J* = 11.8, 11.8, 11.8,

4.4, 2H); ^{13}C NMR (125 MHz, $CDCl_3$): δ 140.6, 128.5, 128.1, 127.0, 67.9, 55.6, 54.2, 35.6, 31.4; IR (film): 3026, 2916, 2838, 1603, 1453 cm^{-1}; HRMS-ESI (*m/z*) $[M + H]^+$ calcd for $C_{13}H_{20}NO$, 206.15394; found 206.15352.

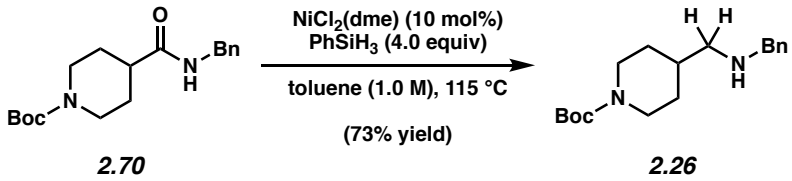

Amine 2.26. Purification by flash chromatography (4:1 Hexanes:EtOAc, 2% Et_3N) yielded amine **2.26** (73% yield, average of two experiments) as an amorphous solid. Amine **2.26**: R_f 0.52 (4:1 Hexanes:EtOAc, 2% Et_3N). ^{1}H NMR (500 MHz, $CDCl_3$, 60 °C): δ 7.32–7.27 (m, 4H), 7.22–7.18 (m, 1H), 4.03 (d, *J* = 12.7, 2H), 3.75 (s, 2H), 2.67 (t, *J* = 12.5, 2H), 2.49 (br. s, 2H) 1.67 (d, *J* = 12.4, 2H), 1.61–1.55 (m, 2H) 1.42 (s, 9H), 1.13–1.06 (m, 2H); ^{13}C NMR (125 MHz, $CDCl_3$, 60 °C): δ 154.7, 140.5, 128.2, 127.8, 126.7, 78.9, 54.9, 54.0, 43.8, 36.6, 30.3, 28.3; IR (film): 2975, 2921, 2849, 1685, 1452 cm^{-1}; HRMS-ESI (*m/z*) $[M + H]^+$ calcd for $C_{18}H_{29}N_2O_2$, 305.22235; found 305.22153.

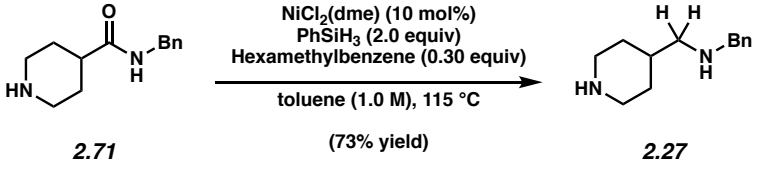

Amine 2.27. ^{1}H NMR analysis of the crude reaction mixture indicated a 73% yield (average of two experiments) of amine **2.27** relative to hexamethylbenzene internal standard. Amine **2.27**: R_f 0.11 (CH_2Cl_2, 2% MeOH). ^{1}H NMR (500 MHz, $CDCl_3$): δ 7.33–7.29 (m, 4H), 7.25–7.22 (m, 1H), 3.77 (s, 2H), 3.05 (ddd, *J* = 12.1, 2.7, 2.7, 2H), 2.58 (ddd, *J* = 12.1, 12.1, 2.4, 2H), 2.49 (d, *J* = 6.7, 2H), 1.77 (br. s, 1H), 1.72–1.69 (m, 2H), 1.59 (ttt, *J* = 12.1, 6.8, 2.5, 1H), 1.11 (dddd, *J* =

12.1, 12.1, 12.1, 3.9, 2H); ^{13}C NMR (125 MHz, $CDCl_3$): δ 140.6, 128.5, 128.2, 126.9, 55.9, 54.3, 46.6, 36.8, 31.9; IR (film): 3308, 3026, 2921, 1633, 1542 cm^{-1}; HRMS-ESI (*m/z*) $[M + H]^+$ calcd for $C_{13}H_{21}N_2$, 205.16993; found 205.16948.

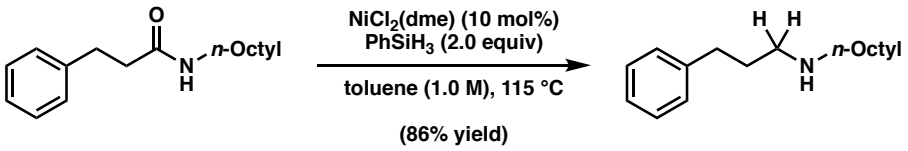

2.72 ***2.28***

Amine 2.28. Purification by preparative thin-layer chromatography (EtOAc, 2% Et_3N) yielded amine **2.28** (86% yield, average of two experiments) as a colorless oil. Amine **2.28**: R_f 0.25 (EtOAc, 2% Et_3N). Spectral data match those previously reported.[55]

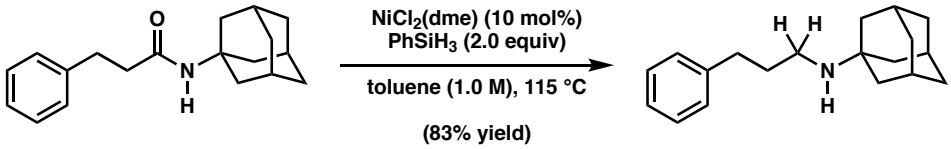

2.73 ***2.29***

Amine 2.29. Purification by preparative thin-layer chromatography (1:1 Hexanes:EtOAc, 2% Et_3N) yielded amine **2.29** (83% yield, average of two experiments) as a colorless oil. Amine **2.29**: R_f 0.34 (1:1 Hexanes:EtOAc, 2% Et_3N). Spectral data match those previously reported.[55]

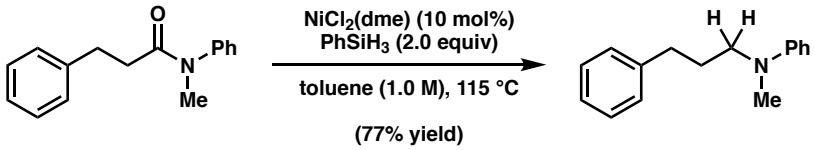

2.74 ***2.30***

Amine 2.30. Purification by flash chromatography (20:1 Hexanes:EtOAc, 2% Et_3N) yielded amine **2.30** (77% yield, average of two experiments) as a colorless oil. Amine **2.30**: R_f 0.57 (10:1 Hexanes:EtOAc, 2% Et_3N). Spectral data match those previously reported.[56]

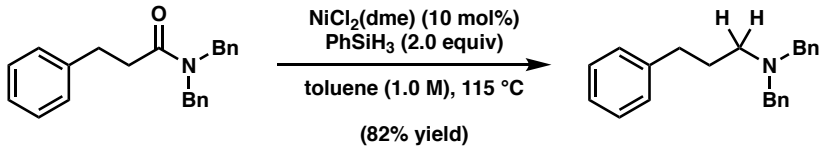

2.75 *2.31*

Amine 2.31. Purification by flash chromatography (20:1 Hexanes:EtOAc, 2% Et_3N) yielded amine **2.31** (82% yield, average of two experiments) as a colorless oil. Amine **2.31**: R_f 0.63 (10:1 Hexanes:EtOAc, 2% Et_3N). Spectral data match those previously reported.[57]

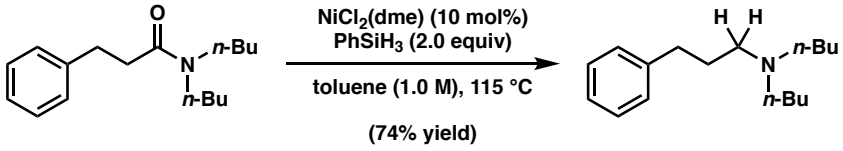

2.76 *2.32*

Amine 2.32. Purification by flash chromatography (7:3 Hexanes:EtOAc, 2% Et_3N) followed by preparative thin-layer chromatography (7:3 Hexanes:EtOAc, 2% Et_3N) yielded amine **2.32** (74% yield, average of two experiments) as a colorless oil. Amine **2.32**: R_f 0.35 (7:3 Hexanes:EtOAc, 2% Et_3N). Spectral data match those previously reported.[58]

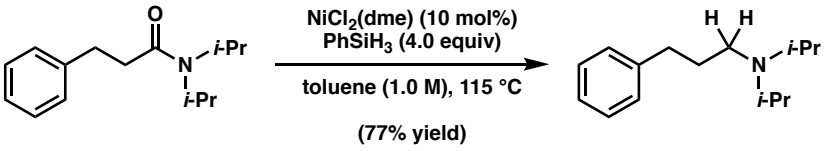

2.77 *2.33*

Amine 2.33. ^1H NMR analysis of the crude reaction mixture indicated a 77% yield (average of two experiments) of amine **2.33** relative to hexamethylbenzene internal standard. Amine **2.33**: R_f 0.23 (3:1 Hexanes:EtOAc, 2% Et_3N). Spectral data match those previously reported.[58]

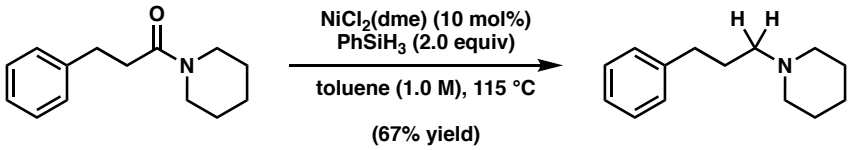

2.78 *2.34*

Amine 2.34. Purification by preparative thin-layer chromatography (1:4 Hexanes:EtOAc, 2% Et_3N) yielded amine **2.34** (67% yield, average of two experiments) as a colorless oil. Amine **2.34**: R_f 0.23 (1:4 Hexanes:EtOAc, 2% Et_3N). Spectral data match those previously reported.[59]

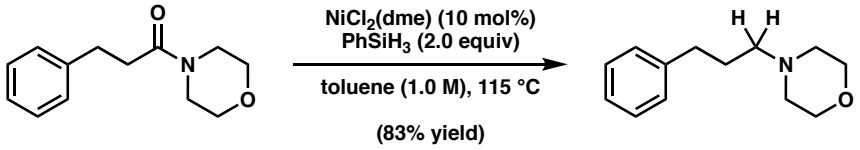

2.79 *2.35*

Amine 2.35. Purification by preparative thin-layer chromatography (1:4 Hexanes:EtOAc, 2% Et_3N) yielded amine **2.35** (83% yield, average of two experiments) as a colorless oil. Amine **2.35**: R_f 0.26 (1:4 Hexanes:EtOAc, 2% Et_3N). Spectral data match those previously reported.[60]

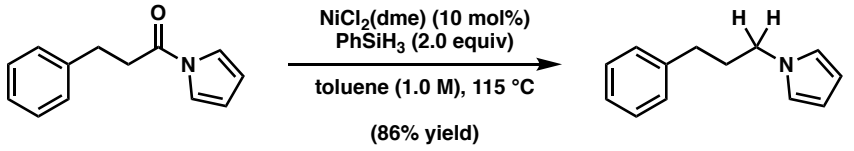

2.80 *2.36*

Amine 2.36. Purification by flash chromatography (9:1 Hexanes:EtOAc) yielded amine **2.36** (86% yield, average of two experiments) as a colorless oil. Amine **2.36**: R_f 0.55 (4:1 Hexanes:EtOAc). Spectral data match those previously reported.[61]

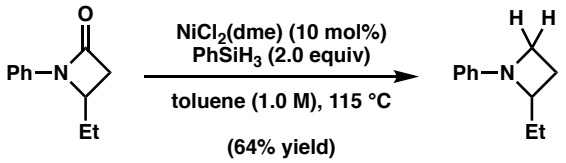

2.81 *2.37*

Amine 2.37. Purification by flash chromatography (39:1 Pentane:Et_2O) yielded amine **2.37** (64% yield, average of two experiments) as a colorless oil. Amine **2.37**: R_f 0.23 (39:1 Pentane:Et_2O). Spectral data match those previously reported.[43]

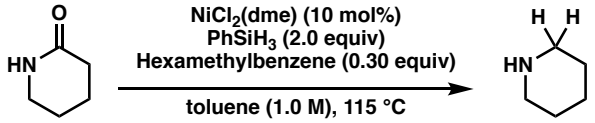

2.82 *2.38*

Amine 2.38. ^{1}H NMR analysis of the crude reaction mixture indicated a 58% yield (average of two experiments) of amine **2.38** relative to hexamethylbenzene internal standard. Spectral data match those previously reported.[62]

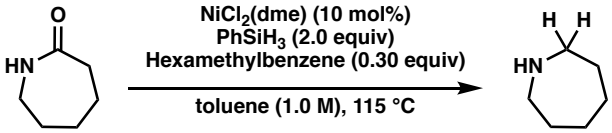

2.83 *2.39*

Amine 2.39. ^{1}H NMR analysis of the crude reaction mixture indicated an 83% yield (average of two experiments) of amine **2.39** relative to hexamethylbenzene internal standard. Spectral data match those previously reported.[62]

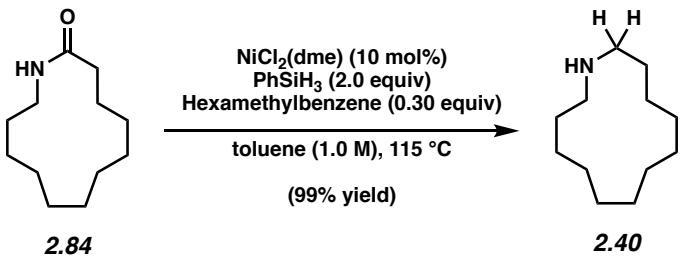

2.84 *2.40*

Amine 2.40. ^{1}H NMR analysis of the crude reaction mixture indicated a 99% yield (average of two experiments) of amine **2.40** relative to hexamethylbenzene internal standard. Amine **2.40**: R_f 0.39 (Hexanes). Spectral data match those previously reported.[63]

2.9.2.5 Synthesis of $PhSiD_3$

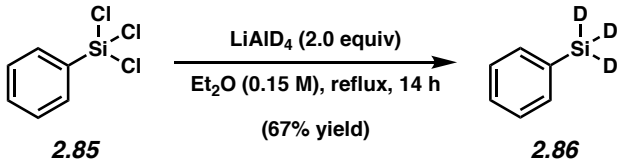

2.85 *2.86*

A round bottom flask equipped with a reflux condenser and a magnetic stir bar was flame-dried under reduced pressure, and then cooled under a N_2 atmosphere. $LiAlD_4$ (1.14 g, 27.21 mmol, 2 equiv) was added, and the flask was flushed with N_2 for 10 min. After cooling to 0 °C, Et_2O (90 mL) was added, followed by $PhSiCl_3$ (**2.85**) (2.18 mL, 13.61 mmol, 1 equiv) dropwise over 2 min. The resulting grey suspension was refluxed for 14 h. After cooling to room temperature, the resulting suspension was filtered through celite and cooled to 0 °C. The filtrate was then quenched by the dropwise addition of chilled H_2O (50 mL, 0 °C) with vigorous stirring. The reaction mixture was transferred to a separatory funnel and the aqueous layer was extracted with Et_2O (2 x 30 mL). The organic layers were combined, dried over $MgSO_4$, and filtered. Using a rotary evaporator, with a bath cooled to 0 °C, the solution was evaporated at 220 mbar for 2 h until minimal solvent remained. $MgSO_4$ was added and the mixture was filtered through cotton. Using a rotary evaporator, with a bath cooled to 0 °C, the solution was evaporated at 130 mbar

for 1 h, and then warmed to 23 °C and evaporated at 20 mbar for 10 min. Desired compound **2.86** (1.02 g, 67% yield) was obtained as a colorless oil. Spectral data match those previously reported.[64]

2.9.2.6 Reduction of Amino Acid Derivatives using $PhSiD_3$

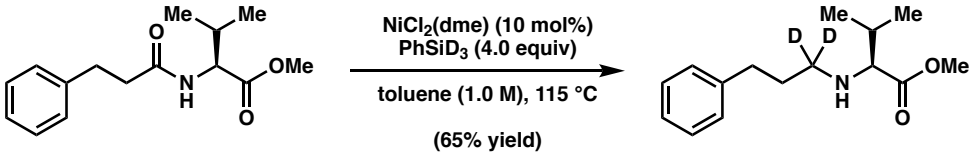

2.87 *2.41*

Representative Procedure (reduction of amide 2.87 is used as an example). Amine 2.41. A 1-dram vial was charged with a magnetic stir bar, flame-dried under reduced pressure, and allowed to cool under a N_2 atmosphere. Amide substrate **2.87** (26.3 mg, 0.100 mmol, 1.0 equiv) and $NiCl_2$(dme) (2.2 mg, 0.0100 mmol, 10 mol%) were added, and the vial was flushed with N_2 for 5 min. $PhSiD_3$ (49.4 μL, 0.4000 mmol, 4.0 equiv) was added under a N_2 atmosphere via syringe followed by toluene (100 μL, 1.0 M). The vial was then capped with a Teflon-lined screw cap under a flow of N_2. The reaction mixture was then placed in a pre-heated aluminum block and allowed to stir at 115 °C for 24 h. After cooling to room temperature, the reaction mixture was transferred to a separatory funnel with EtOAc (3 mL) and basified with 1.0 M aqueous NaOH (4 mL). The layers were separated and the aqueous layer was extracted with EtOAc (3 x 5mL). The combined organic layers were washed with saturated aqueous NaCl (5 mL). The volatiles were removed under reduced pressure, and the crude residue was purified by preparative thin-layer chromatography (4:1 Hexanes:EtOAc) to yield amine **2.41** (65% yield, average of two experiments) as a colorless oil. Amine **2.41**: R_f 0.52 (4:1 Hexanes:EtOAc). ^{1}H NMR (500 MHz, $CDCl_3$): δ 7.28–7.26 (m, 2H), 7.18–7.16 (m, 3H), 3.71 (s, 3H), 2.97 (d, J = 6.2,

1H), 2.70–2.59 (m, 2H), 1.88 (dsept, J = 6.8, 6.8, 1H), 1.81–1.71 (m, 2H), 0.95 (d, J = 6.8, 3H), 0.93 (d, J = 6.8, 3H); ^{2}H NMR (76 MHz, $CDCl_3$): δ 2.6, 2.4; ^{13}C NMR (125 MHz, $CDCl_3$): δ 176.0, 142.4, 128.6, 128.4, 125.8, 67.5, 51.5, 47.42 (m), 33.5, 31.8, 31.7, 19.4, 18.9; IR (film): 3336, 3026, 2927, 1732, 1453 cm^{-1}; HRMS-ESI (*m/z*) $[M + H]^+$ calcd for $C_{15}H_{22}D_2NO_2$, 252.19235; found 252.19381; $[\alpha]^{30.4}_D$ –7.33° (c = 0.10, CH_2Cl_2).

Any modifications of the conditions shown in the representative procedure above are specified in the following schemes, which depict all of the results shown in Table 2.5.

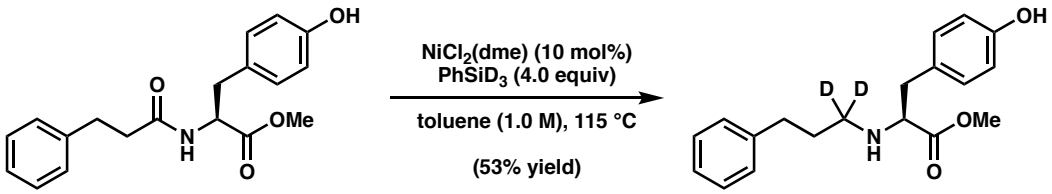

2.52 ***2.42***

Amine 2.42. Purification by preparative thin-layer chromatography (1:1 Hexanes:EtOAc) yielded amine **2.42** (53% yield, average of two experiments) as a colorless oil. Amine **2.42**: R_f 0.39 (1:1 Hexanes:EtOAc). ^{1}H NMR (500 MHz, CD_2Cl_2): δ 7.25 (t, J = 7.4, 2H), 7.17–7.12 (m, 3H), 7.02 (d, J = 8.4, 2H), 6.72 (d, J = 8.4, 2H), 3.62 (s, 3H), 3.44 (t, J = 6.6, 1H), 2.89–2.82 (m, 2H), 2.60–2.57 (m, 2H), 1.77–1.67 (m, 2H); ^{2}H NMR (76 MHz, CD_2Cl_2): δ 2.59, 2.45; ^{13}C NMR (125 MHz, CD_2Cl_2): (14 of 15 signals observed) δ 175.2, 155.0, 142.6, 130.8, 129.8, 128.8, 128.6, 126.1, 115.5, 63.4, 51.9, 38.9, 35.6, 31.8; IR (film): 3291, 3025, 2927, 1734, 1515 cm^{-1}; HRMS-ESI (*m/z*) $[M + H]^+$ calcd for $C_{19}H_{22}D_2NO_3$, 316.18762; found 316.18708; $[\alpha]^{29.7}_D$ +5.33° (c = 0.10, CH_2Cl_2).

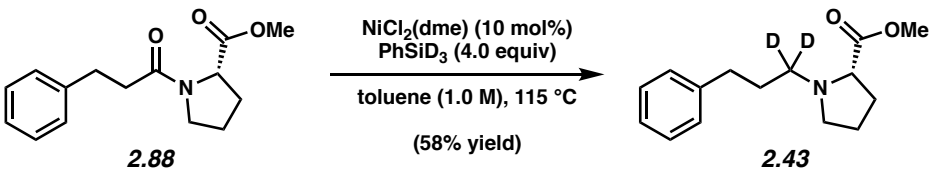

Amine 2.43. Purification by preparative thin-layer chromatography (1:1 Hexanes:EtOAc) yielded amine **2.43** (58% yield, average of two experiments) as a colorless oil. Amine **2.43**: R_f 0.52 (1:1 Hexanes:EtOAc). ^{1}H NMR (500 MHz, CD_2Cl_2): δ 7.27–7.25 (m, 2H), 7.20 –7.14 (m, 3H), 3.65 (s, 3H), 3.16–3.09 (m, 2H), 2.68–2.57 (m, 2H), 2.37–2.32 (m, 1H), 2.10–2.01 (m, 1H), 1.91–1.84 (m, 2H), 1.82–1.74 (m, 3H); ^{2}H NMR (76 MHz, $CDCl_3$): δ 2.68, 2.39; ^{13}C NMR (125 MHz, $CDCl_3$): δ 174.9, 142.2, 128.5, 128.4, 125.9, 66.2, 54.0 (m), 53.6, 52.0, 33.8, 30.1, 29.5, 23.3; IR (film): 3059, 2947, 2860, 1731, 1453 cm^{-1}; HRMS-ESI (*m/z*) $[M + H]^+$ calcd for $C_{15}H_{20}D_2NO_2$, 250.17587; found 250.17816; $[\alpha]^{30.8}_D$ –57.33° (c = 0.10, CH_2Cl_2).

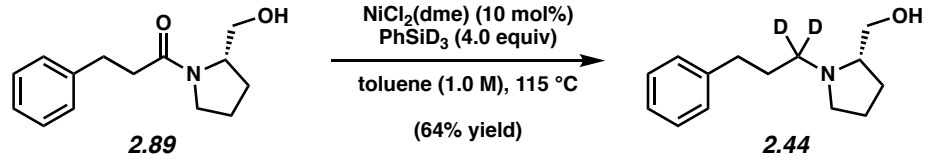

Amine 2.44. Purification by preparative thin-layer chromatography (EtOAc, 2% Et_3N) yielded amine **2.44** (64% yield, average of two experiments) as a colorless oil. Amine **2.44**: R_f 0.45 (EtOAc. 2% Et_3N). ^{1}H NMR (500 MHz, $CDCl_3$): δ 7.29–7.26 (m, 2H), 7.19–7.17 (m, 3H), 3.59 (dd, *J* = 10.6, 3.9, 1H), 3.37 (dd, *J* = 10.6, 2.2, 1H), 3.20–3.16 (m, 1H), 2.73–2.67 (m, 1H), 2.61–2.54 (m, 2H), 2.27–2.21 (m, 1H), 1.90–1.69 (m, 6H); ^{2}H NMR (76 MHz, $CDCl_3$): δ 2.73, 2.29; ^{13}C NMR (125 MHz, $CDCl_3$): δ 142.3, 128.5, 128.4, 125.9, 64.9, 61.9, 54.2, 53.5 (m), 33.7, 30.5, 27.8, 23.8; IR (film): 3362, 3084, 2936, 2800, 1602 cm^{-1}; HRMS-ESI (*m/z*) $[M + H]^+$ calcd for $C_{14}H_{20}D_2NO$, 222.18170; found 222.18214; $[\alpha]^{31.0}_D$ –44.66° (c = 0.10, CH_2Cl_2).

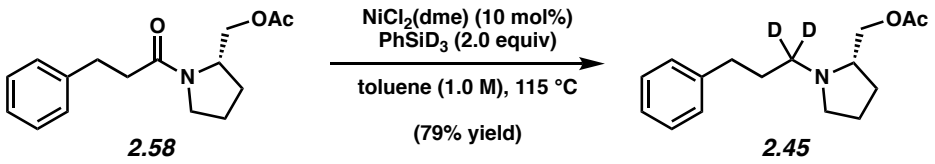

Amine 2.45. Purification by preparative thin-layer chromatography (1:1 Hexanes:EtOAc, 2% Et_3N) yielded amine **2.45** (79% yield, average of two experiments) as a colorless oil. Amine **2.45**: R_f 0.35 (1:1 Hexanes:EtOAc, 2% Et_3N). ^{1}H NMR (500 MHz, $CDCl_3$): δ 7.28–7.26 (m, 2H), 7.19–7.16 (m, 3H), 4.04 (dd, *J* = 10.9, 5.1, 1H), 3.92 (dd, *J* = 10.9, 6.1, 1H), 3.15–3.12 (m, 1H), 2.70–2.57 (m, 3H), 2.23–2.18 (m, 1H), 2.01 (s, 3H), 1.92–1.86 (m, 1H), 1.85–1.79 (m, 2H), 1.78–1.71 (m, 2H), 1.62–1.56 (m, 1H); ^{2}H NMR (76 MHz, $CDCl_3$): δ 2.79, 2.33; ^{13}C NMR (125 MHz, $CDCl_3$): δ 171.3, 142.4, 128.5, 128.4, 125.8, 67.4, 62.4, 54.8 (m), 54.4, 33.8, 30.3, 28.4, 23.2, 21.1; IR (film): 3062, 2940, 2785, 1738, 1603 cm^{-1}; HRMS-ESI (*m/z*) $[M + H]^+$ calcd for $C_{16}H_{22}D_2NO_2$, 264.19221; found 264.19271; $[\alpha]^{29.9}_D$ –54.66° (c = 0.10, CH_2Cl_2).

2.9.2.7 Verification of Enantiopurity – Racemic Compound Synthesis

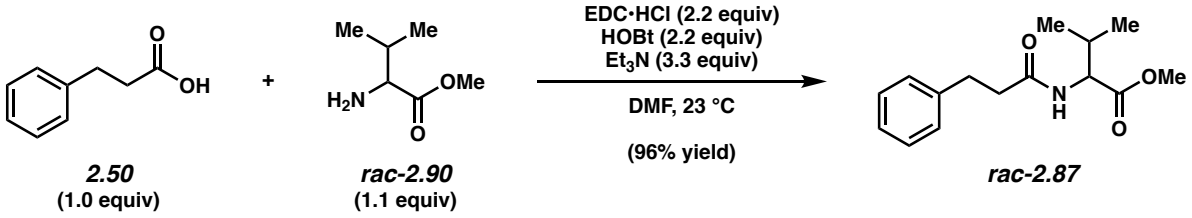

Representative Procedure for the synthesis of racemic amide substrates (synthesis of amide rac-2.87 is used as an example). Amide rac-2.87. To a solution of carboxylic acid **2.50** (300.0 mg, 1.99 mmol, 1.0 equiv), HOBt (594.0 mg, 4.39 mmol, 2.2 equiv), and EDC•HCl (848.0 mg, 4.39 mmol, 2.2 equiv) in DMF (10.0 mL, 0.2 M) at 23 °C was added amine **rac-2.90** (376.0 mg, 2.19 mmol, 1.1 equiv) followed by triethylamine (0.92 mL, 6.59 mmol, 1.1 equiv) under a N_2 atmosphere. The reaction mixture stirred at 23 °C for 18 h. The reaction was diluted with

deionized water (50 mL) and transferred to a separatory funnel with EtOAc (40 mL). The layers were separated and the aqueous layer was extracted with EtOAc (3 x 40 mL). The organic layers were combined and washed with water (3 x 40 mL), dried over Na_2SO_4, and the volatiles were removed under reduced pressure. The resulting crude residue was purified by flash chromatography (3:1 Hexanes:EtOAc) to yield amide **rac-2.87** (506.0 mg, 96% yield) as an off-white solid.

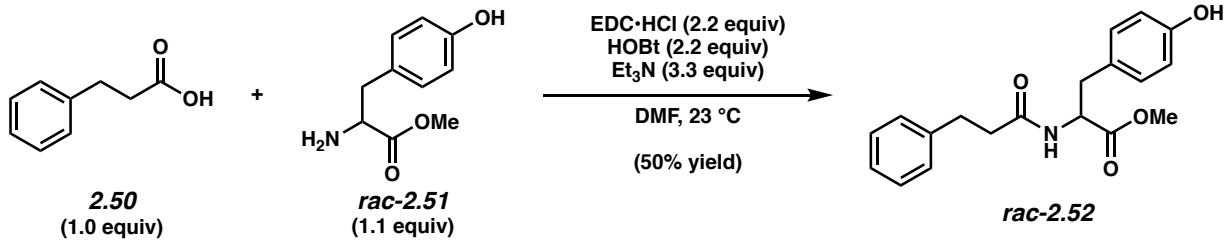

Amide rac-2.52. Following representative procedure. Purification by flash chromatography (3:1 Hexanes:EtOAc → 1:1 Hexanes:EtOAc) to yield amide **rac-2.52** (269.3 mg, 50% yield) as a white solid.

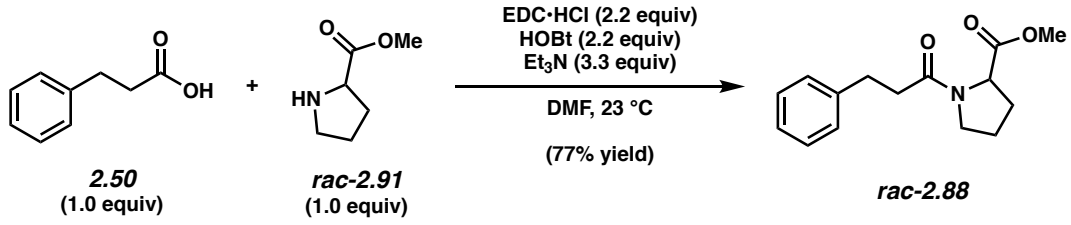

Amide rac-2.88. Following representative procedure. Purification by flash chromatography (1:1 Hexanes:EtOAc → 1:3 Hexanes:EtOAc) to yield amide **rac-2.88** (221.1 mg, 77% yield) as a colorless oil.

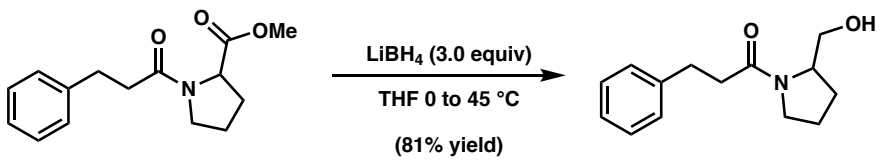

rac-2.88 *rac-2.89*

Amide rac-2.89. To a solution of amide **rac-2.88** (100.0 mg, 0.383 mmol, 1 equiv) in THF (8.0 mL, 0.05 M) at 0 °C under a N_2 atmosphere, was added $LiBH_4$ (25.0 mg, 1.15 mmol, 3 equiv) in one portion. The vial was then capped with a Teflon-lined screw cap under a flow of N_2 and placed in a pre-heated aluminum block and allowed to stir at 45 °C for 15 h. After cooling to room temperature, deionized H_2O was added (2 mL) and the reaction mixture was transferred to a separatory funnel with CH_2Cl_2 (3 mL) and extracted with CH_2Cl_2 (3 x 3mL). The combined organic layers were washed with saturated aqueous NaCl (5 mL). The volatiles were removed under reduced pressure, and the resulting crude residue was purified by flash chromatography (1:3 Hexanes:EtOAc → EtOAc) to yield amide **rac-2.89** (72.0 mg, 81% yield) as a colorless oil.

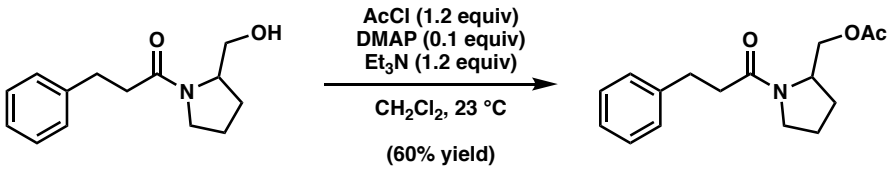

rac-2.89 *rac-2.58*

Amide rac-2.58. A 1-dram vial was charged with a magnetic stir bar, flame-dried under reduced pressure, and allowed to cool under a N_2 atmosphere. Amide substrate **rac-2.89** (25.6 mg, 0.110 mmol, 1 equiv) and DMAP (1.3 mg, 0.010 mmol, 0.1 equiv) were added and the vial flushed with N_2 for 5 min. CH_2Cl_2 (2.0 mL, 0.05 M), AcCl (9.4 μL, 0.132 mmol, 1.2 equiv), and Et_3N (18.3 μL, 0.132 mmol, 1.2 equiv) were added under a N_2 atmosphere and the reaction was left to stir for 3 h at 23 °C. NH_4Cl (2 mL) was added and the reaction mixture was transferred to separatory funnel with CH_2Cl_2 (3 mL). The layers were separated and the aqueous layer was

extracted with CH_2Cl_2 (3 x 3 mL). The combined organic layers were washed with saturated aqueous NaCl (5 mL). The volatiles were removed under reduced pressure, and the resulting crude residue was purified by preparative thin-layer chromatography (1:3 Hexanes:EtOAc → EtOAc) to yield amide **rac-2.58** (16.0 mg, 60% yield) as a colorless oil.

2.9.2.7.1 Representative Procedure for the Deuterium Reduction of Racemic Amino Acid Derivatives

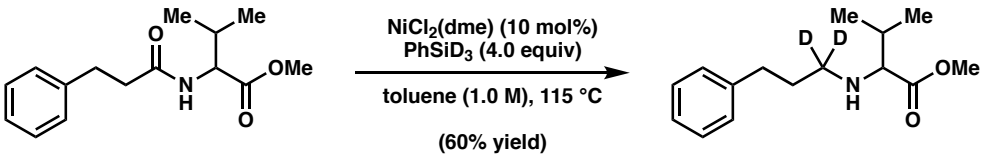

rac-2.87 *rac-2.41*

Representative Procedure (reduction of amide rac-2.87 is used as an example). Amine rac-2.41. A 1-dram vial was charged with a magnetic stir bar, flame-dried under reduced pressure, and allowed to cool under a N_2 atmosphere. Amide substrate **rac-2.87** (26.3 mg, 0.100 mmol, 1.0 equiv) and $NiCl_2$(dme) (2.2 mg, 0.0100 mmol, 10 mol%) was added, and the vial was flushed with N_2. $PhSiD_3$ (49.4 μL, 0.4000 mmol, 4.0 equiv) was added under a N_2 atmosphere via syringe followed by toluene (100 μL, 1.0 M). The vial was then capped with a Teflon-lined screw cap under a flow of N_2. The reaction mixture was then placed in a pre-heated aluminum block and allowed to stir at 115 °C for 24 h. After cooling to room temperature, the reaction mixture was transferred to a separatory funnel with EtOAc (3 mL) and basified with 1.0 M aqueous NaOH (4 mL). The layers were separated and the aqueous layer was extracted with EtOAc (3 x 5mL). The combined organics were washed with saturated aqueous NaCl (5 mL). The volatiles were removed under reduced pressure, and the crude residue was purified by preparative thin-layer

chromatography (4:1 Hexanes:EtOAc) to yield amine **rac-2.41** (15.0 mg, 60% yield) as a colorless oil.

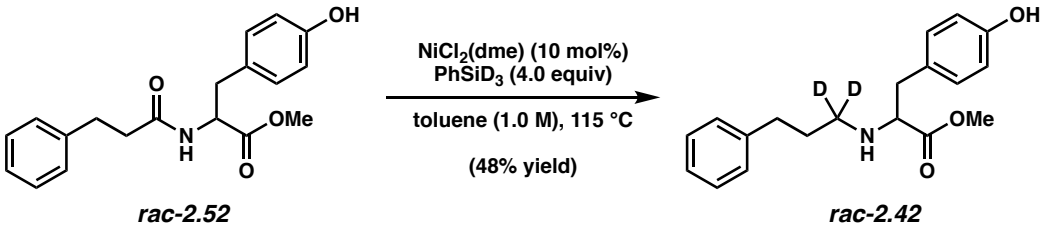

rac-2.52 *rac-2.42*

Amine rac-2.42. Purification by preparative thin-layer chromatography (1:1 Hexanes:EtOAc) yielded amine **rac-2.42** (15.0 mg, 48% yield) as a colorless oil.

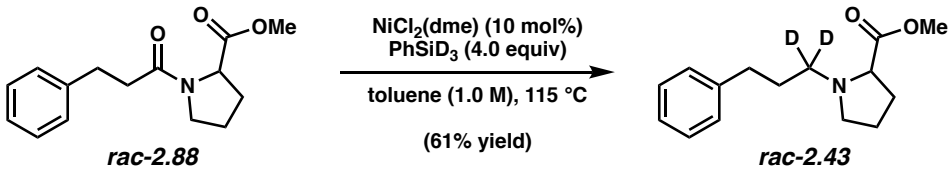

rac-2.88 *rac-2.43*

Amine rac-2.43. Purification by preparative thin-layer chromatography (1:1 Hexanes:EtOAc) yielded amine **rac-2.43** (15.2 mg, 61% yield) as a colorless oil.

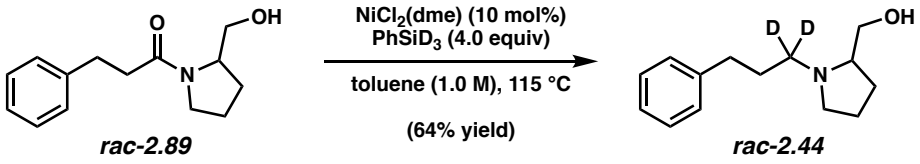

rac-2.89 *rac-2.44*

Amine rac-2.44. Purification by preparative thin-layer chromatography (EtOAc, 2% Et_3N) yielded amine **rac-2.44** (14.1 mg, 64% yield) as a colorless oil.

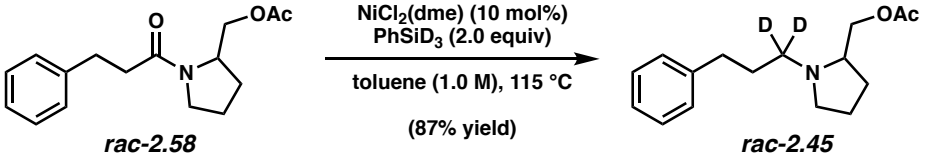

rac-2.58 *rac-2.45*

Amine rac-2.45. Purification by preparative thin-layer chromatography (1:1 Hexanes:EtOAc, 2% Et_3N) yielded amine **rac-2.45** (22.2 mg, 87% yield) as a colorless oil.

2.9.2.8 Verification of Enantiopurity – er and dr Determination

The enantiomeric ratio of **2.41** was determined by chiral SFC analysis.

Compound	Method Column /Temp	Polar Cosolvent	Method Flow Rate	Retention Times	Enantiomeric Ratio (er)
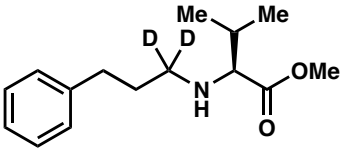 *2.41*	Daicel ChiralPak OB-H / 35 °C	1% iPrOH	0.60 mL/min	16.36/21.20 min	0:100
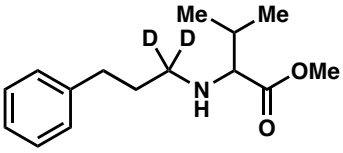 *rac-2.41*	Daicel ChiralPak OB-H / 35 °C	1% iPrOH	0.60 mL/min	14.34/17.31 min 17.42/21.53 min	51:49

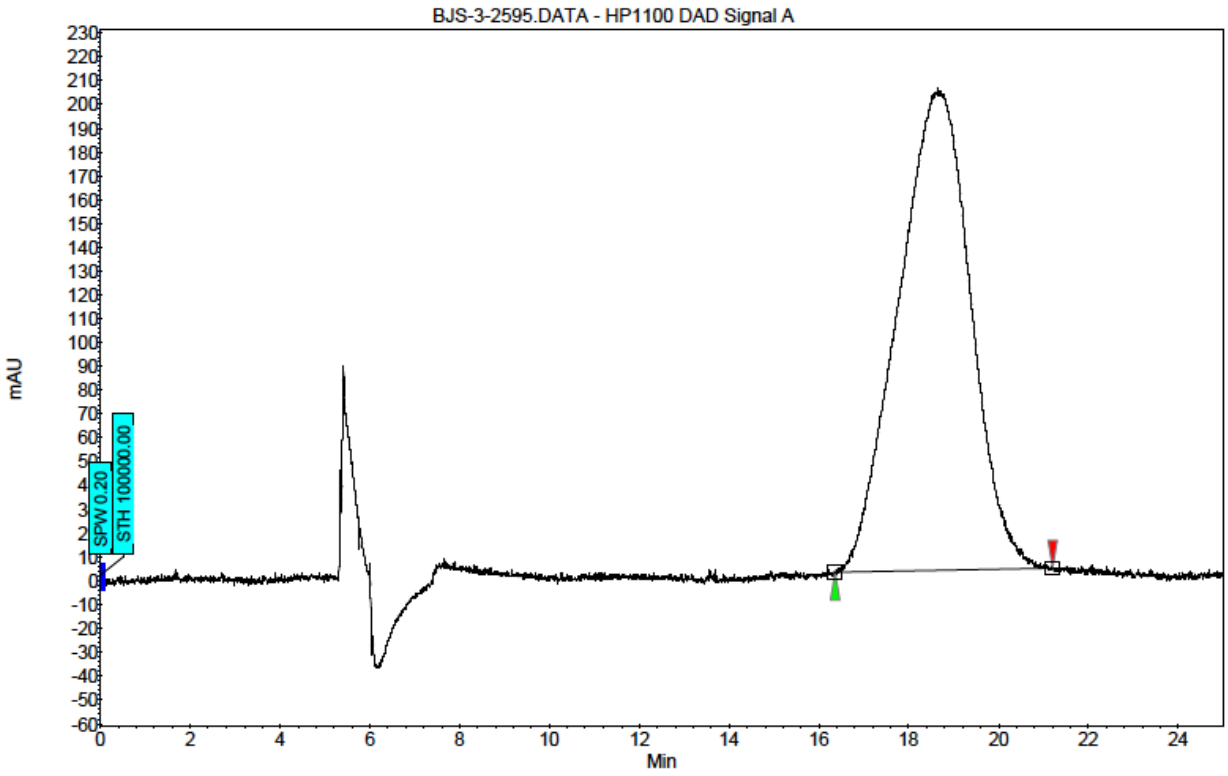

Index	Name	Start	Time	End	RT Offset	Quantity	Height	Area	Area
		[Min]	[Min]	[Min]	[Min]	[% Area]	[µV]	[µV.Min]	[%]
1	UNKNOWN	16.36	18.64	21.20	0.00	100.00	202.4	375.6	100.000
Total						100.00	202.4	375.6	100.000

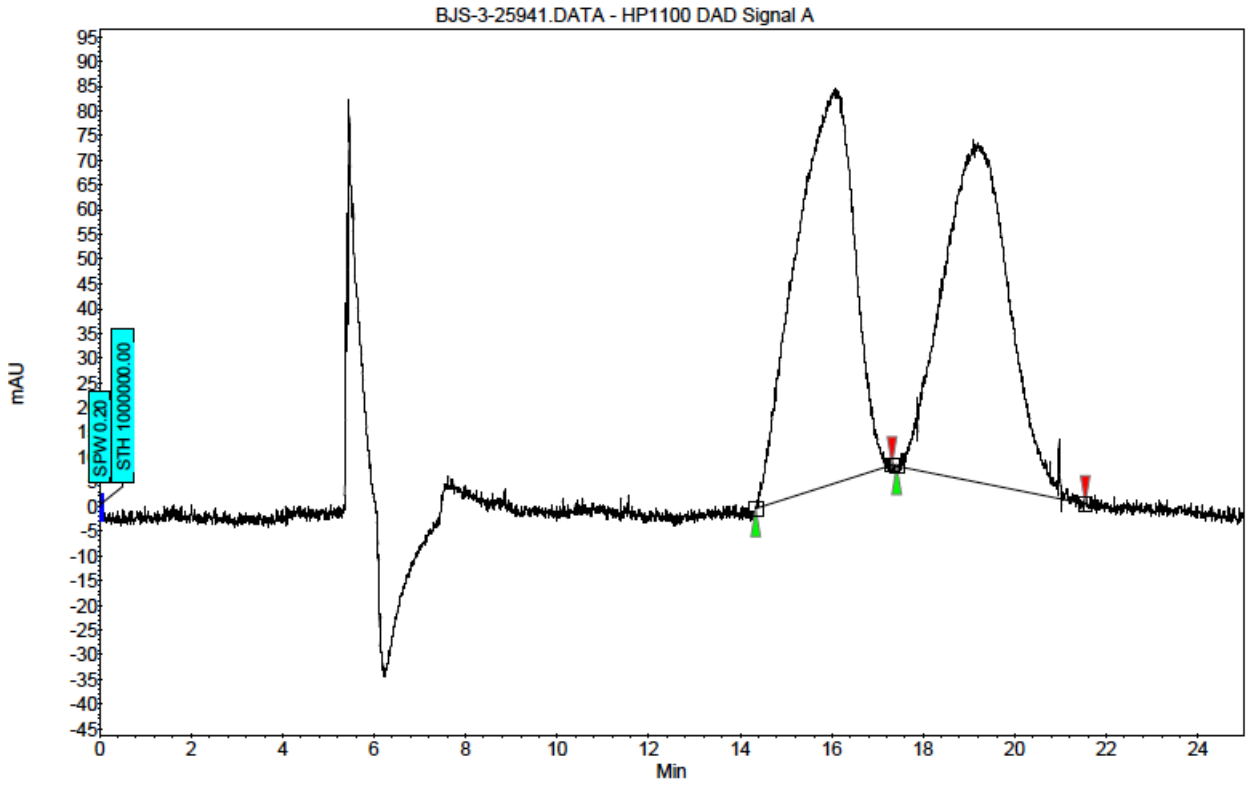

Index	Name	Start	Time	End	RT Offset	Quantity	Height	Area	Area
		[Min]	[Min]	[Min]	[Min]	[% Area]	[µV]	[µV.Min]	[%]
1	UNKNOWN	14.34	16.07	17.31	0.00	50.91	79.8	118.9	50.910
2	UNKNOWN	17.42	19.10	21.53	0.00	49.09	69.1	114.7	49.090
Total						100.00	148.9	233.6	100.000

Chiral SFC analysis of **rac-2.42** did not lead to separation of the enantiomers. The diastereomeric ratio of **2.42** was then determined by coupling with enantiopure carboxylic acid **2.92**.

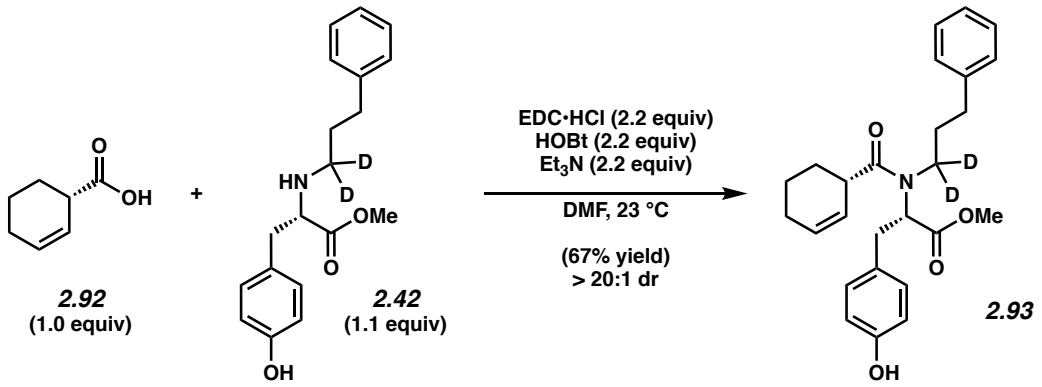

Amide 2.93. To a solution of carboxylic acid **2.92** (7.3 mg, 0.058 mmol, 1.0 equiv), HOBt (17.3 mg, 0.128 mmol, 2.2 equiv), and EDC•HCl (24.5 mg, 0.128 mmol, 2.2 equiv) in DMF (582 μL, 0.1 M) at 23 °C was added amine **2.42** (20.2 mg, 0.064 mmol, 1.1 equiv), followed by triethylamine (17.8 μL, 0.128 mmol, 2.2 equiv) under a N_2 atmosphere. The reaction mixture stirred at 23 °C for 18 h. The reaction was diluted with deionized water (2 mL) and transferred to a separatory funnel with EtOAc (3 mL). The layers were separated and the aqueous layer was extracted with EtOAc (3 x 3 mL). The organic layers were combined and washed with water (3 x 3 mL), dried over Na_2SO_4, and the volatiles were removed under reduced pressure. The resulting crude residue was purified by preparative thin-layer chromatography (3:1 Hexanes:EtOAc) to yield amide **2.93** (16.6 mg, 67% yield, > 20:1 dr) as a colorless oil. Amide **2.93**: R_f 0.50 (2:1 Hexanes:EtOAc); ^{1}H NMR (500 MHz, $CDCl_3$): δ 7.27–7.24 (m, 2H), 7.19–7.17 (m, 3H), 7.14–7.12 (m, 2H), 7.00–6.99 (m, 2H), 5.74–5.73 (m, 2H), 3.63 (s, 3H), 3.47 (t, J = 6.9, 1H), 2.92 (d, J = 6.9, 2H), 2.83–2.78 (m, 1H), 2.59 (t, J = 7.7, 2H), 2.40–2.38 (m, 2H), 2.19–2.14 (m, 3H), 1.87–1.81 (m, 1H), 1.80–1.70 (m, 2H); ^{2}H NMR (76 MHz, CD_2Cl_2): δ 2.61, 2.45; ^{13}C NMR (125 MHz, $CDCl_3$): δ 175.2, 174.5, 149.8, 142.1, 134.9, 130.2, 128.5, 128.4, 126.9, 125.9, 125.1, 121.6, 63.1, 51.8, 47.3 (m), 39.5, 39.3, 33.4, 31.5, 27.5, 25.2, 24.5 IR (film): 3331, 3025, 2925, 1752, 1507 cm^{-1}; HRMS-ESI (*m/z*) $[M + H]^+$ calcd for $C_{26}H_{30}D_2NO_4$, 424.24514; found 424.24403; $[\alpha]^{31.3}_D$ –34.00° (c = 0.10, CH_2Cl_2).

The enantiomeric ratio of **2.43** was determined by chiral SFC analysis.

Compound	Method Column /Temp	Polar Cosolvent	Method Flow Rate	Retention Times	Enantiomeric Ratio (er)
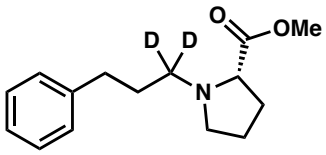 *2.43*	Daicel ChiralPak OB-H / 35 °C	3% iPrOH	3.00 mL/min	4.50/5.10 min	0:100
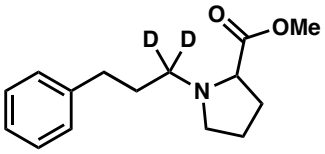 *rac-2.43*	Daicel ChiralPak OB-H / 35 °C	3% iPrOH	3.00 mL/min	3.92/4.43 min 4.44/5.06 min	50:50

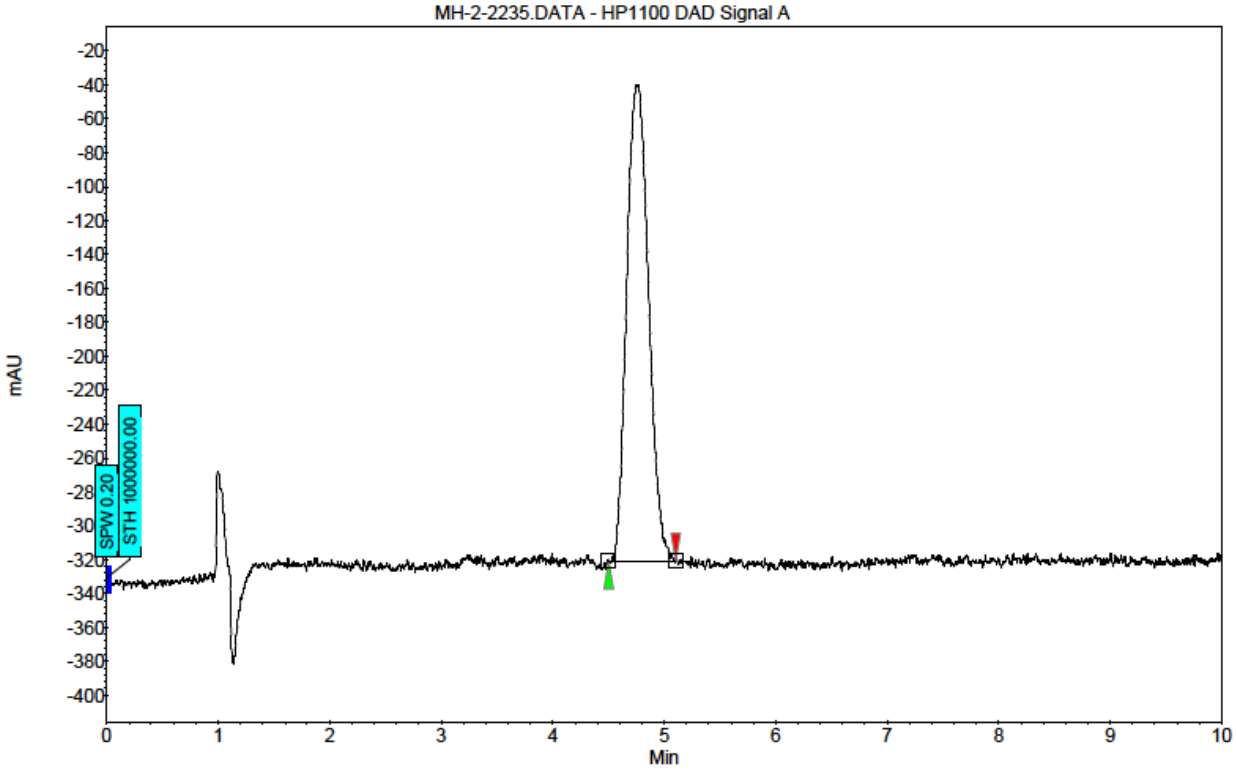

Index	Name	Start	Time	End	RT Offset	Quantity	Height	Area	Area
		[Min]	[Min]	[Min]	[Min]	[% Area]	[µV]	[µV.Min]	[%]
1	UNKNOWN	4.50	4.75	5.10	0.00	100.00	280.7	63.7	100.000
Total						100.00	280.7	63.7	100.000

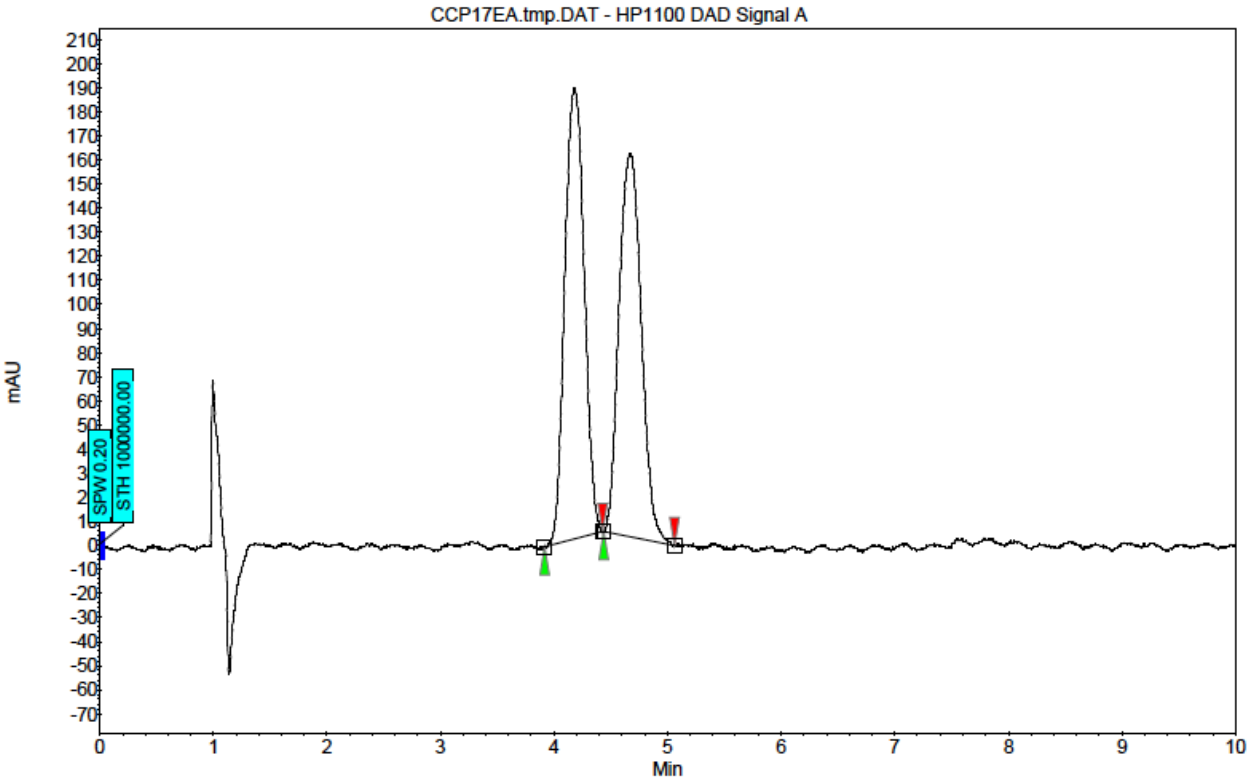

Index	Name	Start	Time	End	RT Offset	Quantity	Height	Area	Area
		[Min]	[Min]	[Min]	[Min]	[% Area]	[µV]	[µV.Min]	[%]
1	UNKNOWN	3.92	4.18	4.43	0.00	50.60	187.4	37.1	50.602
2	UNKNOWN	4.44	4.67	5.06	0.00	49.40	159.2	36.3	49.398
Total						100.00	346.7	73.4	100.000

The enantiomeric ratio of **2.44** was determined by chiral SFC analysis.

Compound	Method Column /Temp	Polar Cosolvent	Method Flow Rate	Retention Times	Enantiomeric Ratio (er)
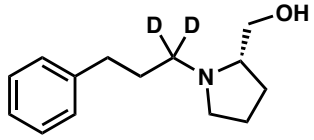 *2.44*	Daicel ChiralPak OD-H / 35 °C	15% MeOH, 2.00 min 10%/min, 25% MeOH	4.00 mL/min	2.09/2.65 min	0:100
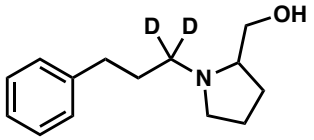 *rac-2.44*	Daicel ChiralPak OD-H / 35 °C	15% MeOH, 2.00 min 10%/min, 25% MeOH	4.00 mL/min	1.78/2.03 min 2.10/2.56 min	43:57

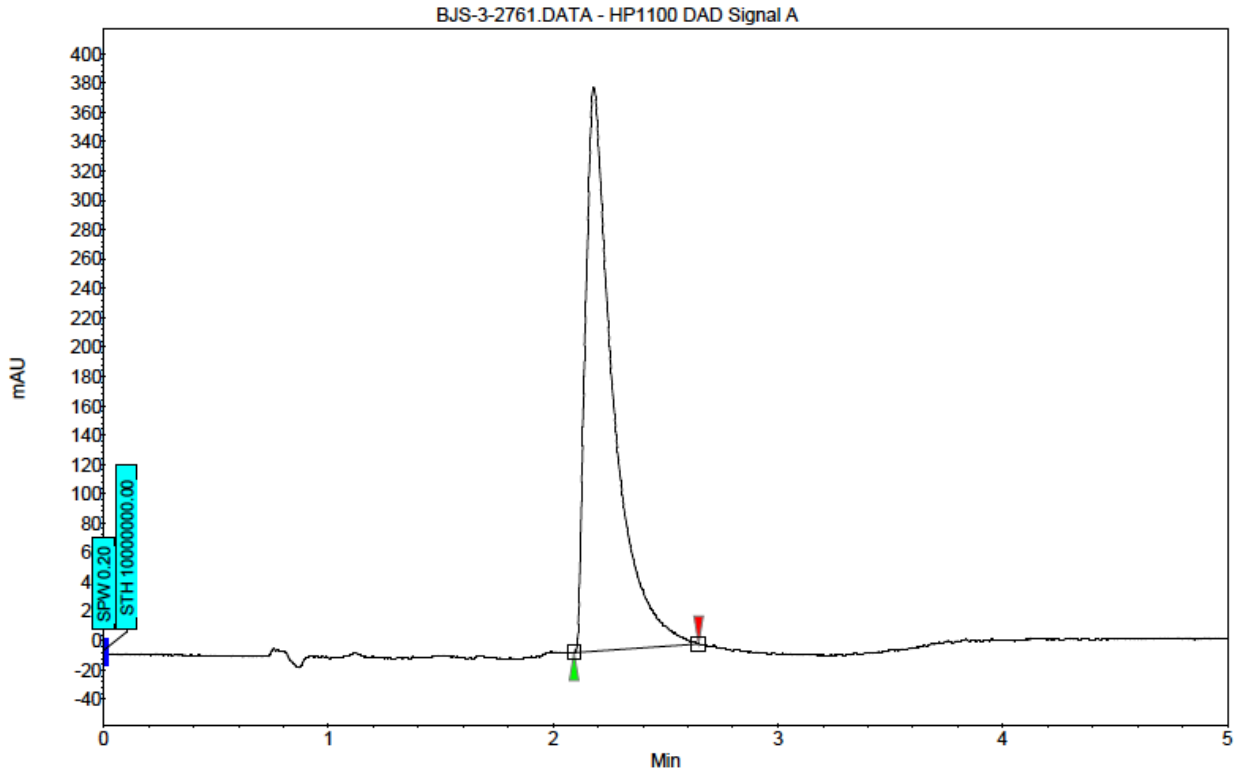

Index	Name	Start	Time	End	RT Offset	Quantity	Height	Area	Area
		[Min]	[Min]	[Min]	[Min]	[% Area]	[µV]	[µV.Min]	[%]
1	UNKNOWN	2.09	2.18	2.65	0.00	100.00	384.5	54.9	100.000
Total						100.00	384.5	54.9	100.000

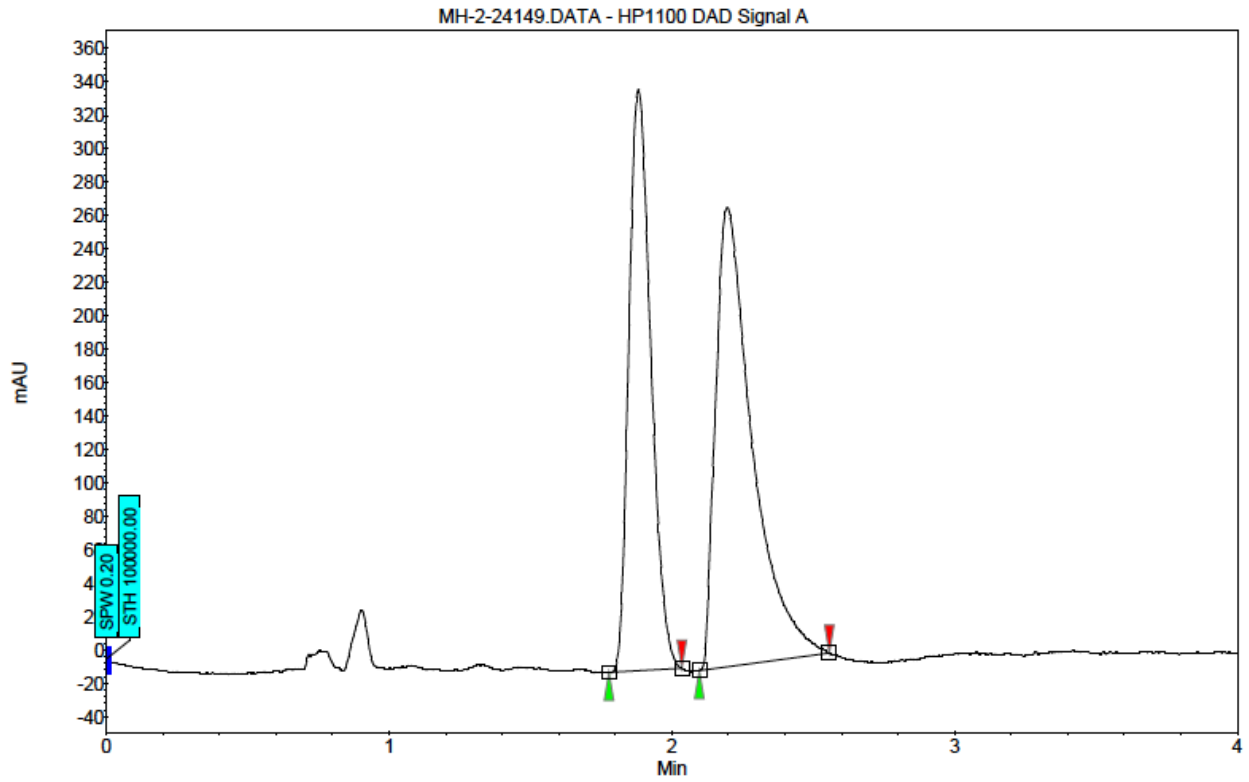

Index	Name	Start	Time	End	RT Offset	Quantity	Height	Area	Area
		[Min]	[Min]	[Min]	[Min]	[% Area]	[µV]	[µV.Min]	[%]
1	UNKNOWN	1.78	1.88	2.03	0.00	43.15	347.9	31.4	43.149
2	UNKNOWN	2.10	2.20	2.56	0.00	56.85	275.2	41.4	56.851
Total						100.00	623.1	72.8	100.000

Chiral SFC analysis of **rac-2.45** did not lead to separation of the enantiomers. For this reason, acetate **2.45** was converted to alcohol **2.44** and the enantiomeric ratio was determined by chiral SFC analysis in comparison to **rac-2.44**.

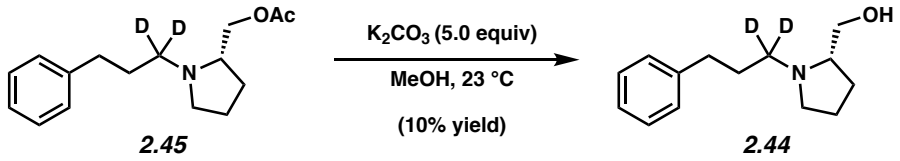

2.45 *2.44*

Amine 2.44. To a solution of amine **2.45** (20.0 mg, 0.073 mmol, 1 equiv) in MeOH (726 µL, 0.1 M) at 23 °C was added K_2CO_3 (50.2 mg, 0.363 mmol, 5 equiv) in one portion. The reaction was

stirred vigorously for 1 h. The reaction mixture was diluted with EtOAc (10 mL) and transferred to a seperatory funnel. Deionized H_2O (10 mL) was added, the layers separated, and the aqueous layer was extracted with EtOAc (3 x 10 mL). The combined organics were washed with saturated aqueous NaCl (5 mL) and dried over Na_2SO_4. The volatiles were removed under reduced pressure, and the resulting crude residue was purified by preparative thin-layer chromotagraphy (EtOAc, 2% Et_3N) to yield amine **2.44** (1.6 mg, 10% yield) as a colorless oil.

Compound	Method Column /Temp	Polar Cosolvent	Method Flow Rate	Retention Times	Enantiomeric Ratio (er)
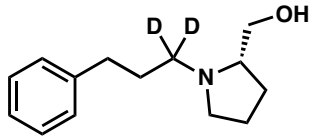 *2.44*	Daicel ChiralPak OD-H / 35 °C	15% MeOH, 2.00 min 10%/min, 25% MeOH	4.00 mL/min	2.10/2.76 min	0:100
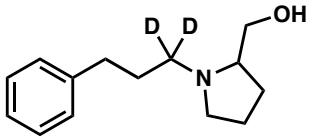 *rac-2.44*	Daicel ChiralPak OD-H / 35 °C	15% MeOH, 2.00 min 10%/min, 25% MeOH	4.00 mL/min	1.78/2.03 min 2.10/2.56 min	43:57

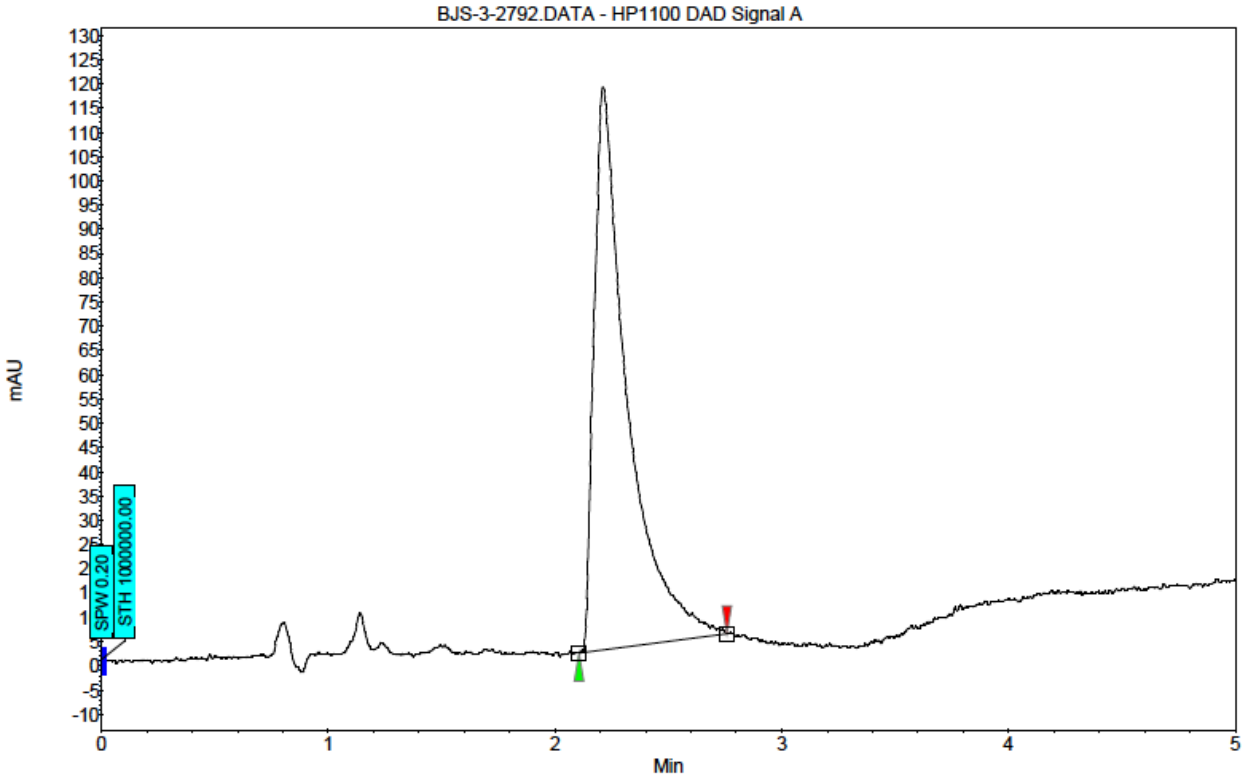

Index	Name	Start	Time	End	RT Offset	Quantity	Height	Area	Area
		[Min]	[Min]	[Min]	[Min]	[% Area]	[µV]	[µV.Min]	[%]
1	UNKNOWN	2.10	2.21	2.76	0.00	100.00	116.0	19.7	100.000
Total						100.00	116.0	19.7	100.000

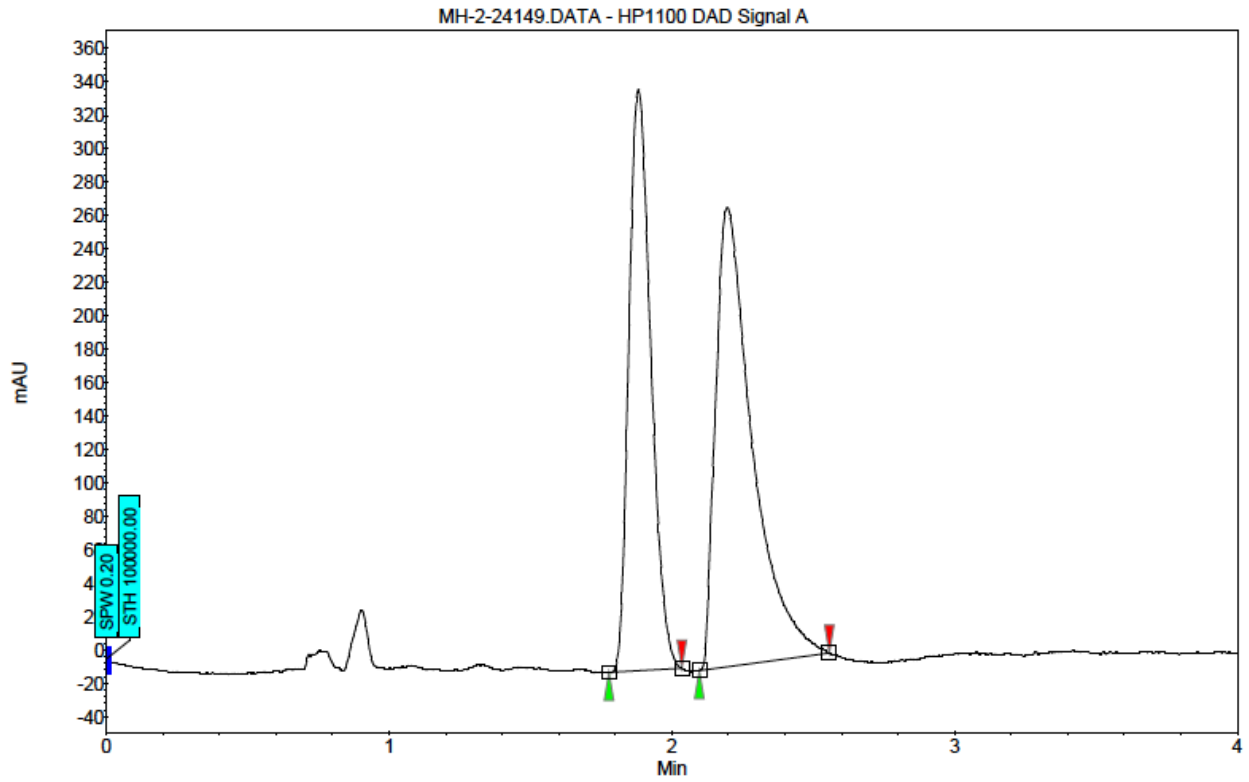

Index	Name	Start	Time	End	RT Offset	Quantity	Height	Area	Area
		[Min]	[Min]	[Min]	[Min]	[% Area]	[µV]	[µV.Min]	[%]
1	UNKNOWN	1.78	1.88	2.03	0.00	43.15	347.9	31.4	43.149
2	UNKNOWN	2.10	2.20	2.56	0.00	56.85	275.2	41.4	56.851
Total						100.00	623.1	72.8	100.000

2.9.2.9 Procedure for Reduction Performed on 1.0 mmol Scale

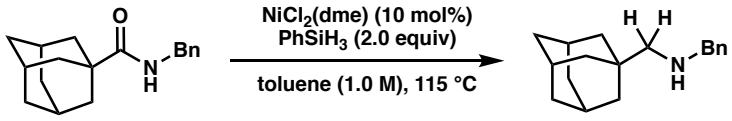

2.69 *2.22*

Representative procedure for the 1.0 mmol scale reduction of amide 2.69. Amine 2.22. A 20-scintillation vial was charged with a magnetic stir bar, flame-dried under reduced pressure, and allowed to cool under a N_2 atmosphere. Amide substrate **2.69** (269.2 mg, 1.000 mmol, 1.0 equiv) and $NiCl_2$(dme) (21.9 mg, 0.1000 mmol, 10 mol %) was added, and the vial was flushed with N_2 for 10 min. $PhSiH_3$ (246.7 µL, 2.000 mmol, 2.0 equiv) was added under a N_2 atmosphere

via syringe followed by toluene (1.0 mL, 1.0 M). The vial was then capped with a Teflon-lined screw cap under a flow of N_2. The reaction mixture was then placed in a pre-heated aluminum block and allowed to stir at 115 °C for 24 h. After cooling to room temperature, the reaction mixture was transferred to a separatory funnel with EtOAc (10 mL) and basified with 1.0 M aqueous NaOH (10 mL). The layers were separated and the aqueous layer was extracted with EtOAc (3 x 30 mL). The combined organic layers were washed with saturated aqueous NaCl (45 mL). The volatiles were removed under reduced pressure, and the crude residue was purified by flash chromatography (4:1 Hexanes:EtOAc, 2% Et_3N) to yield amine **2.22** (92% yield) as a colorless oil. Amine **2.22**: R_f 0.52 (4:1 Hexanes:EtOAc, 2% Et_3N). Spectral data match those previously reported.[54]

2.10 Spectra Relevant to Chapter Two

Nickel-Catalyzed Reduction of Secondary and Tertiary Amides

Bryan J. Simmons, Marie Hoffmann, Jaeyeon Hwang, Moritz K. Jackl, and Neil K. Garg.

Org. Lett. **2017**, *19*, 1910–1913.

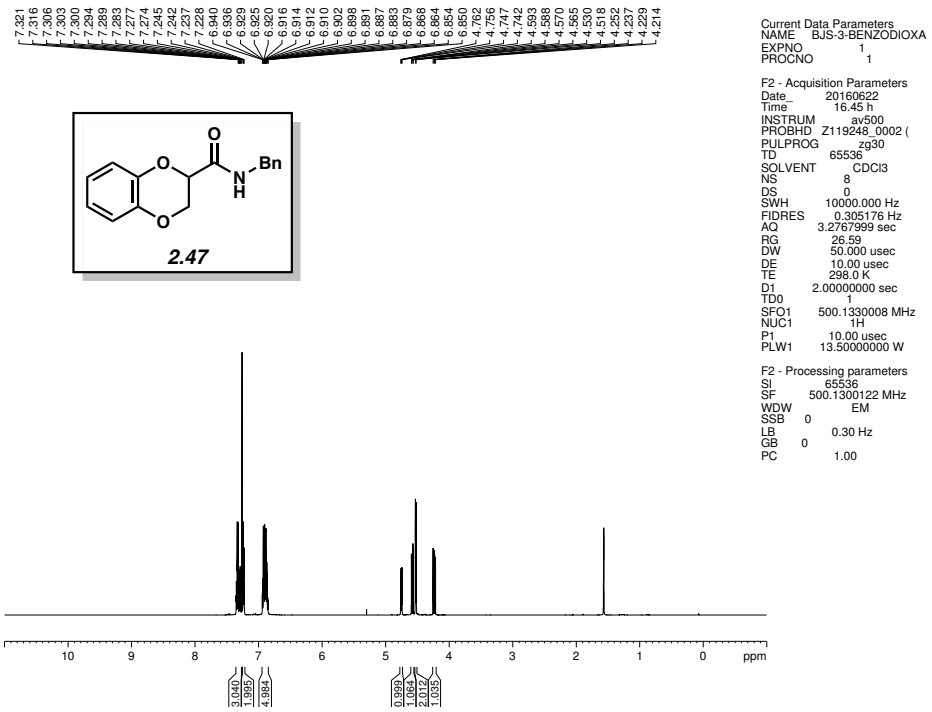

Figure 2.2 ^{1}H NMR (500 MHz, $CDCl_3$) of compound **2.47**.

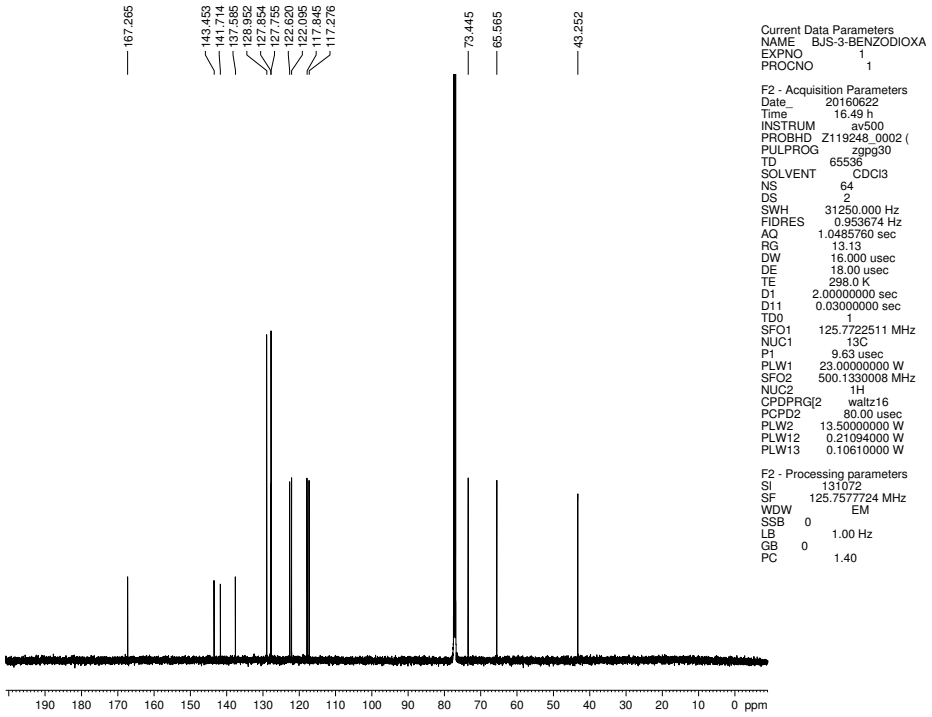

Figure 2.3 ^{13}C NMR (125 MHz, $CDCl_3$) of compound **2.47**.

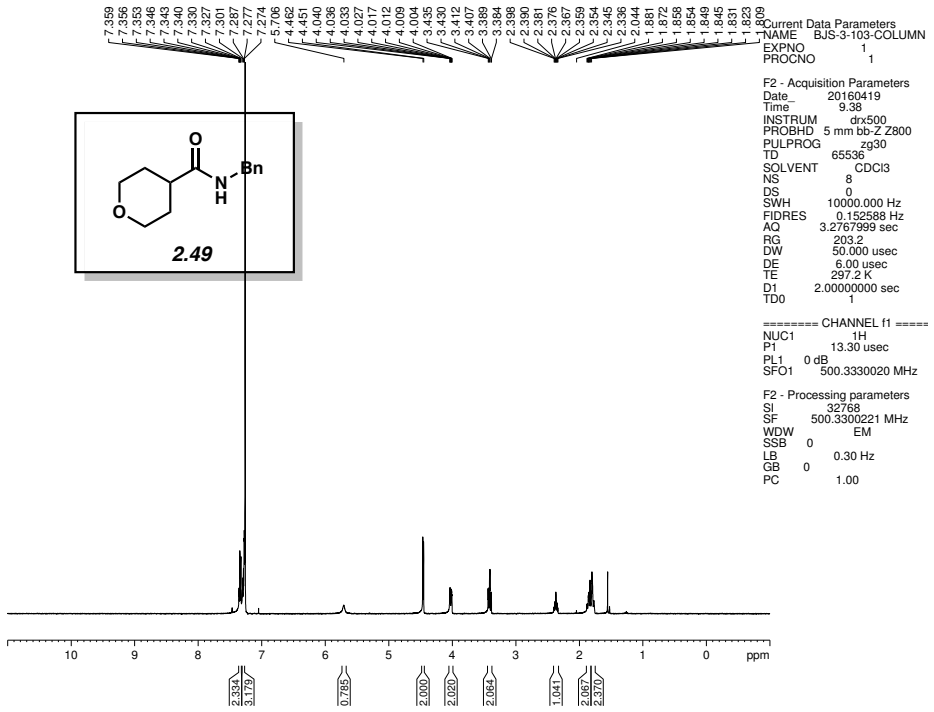

Figure 2.4 ^{1}H NMR (500 MHz, $CDCl_3$) of compound **2.49**.

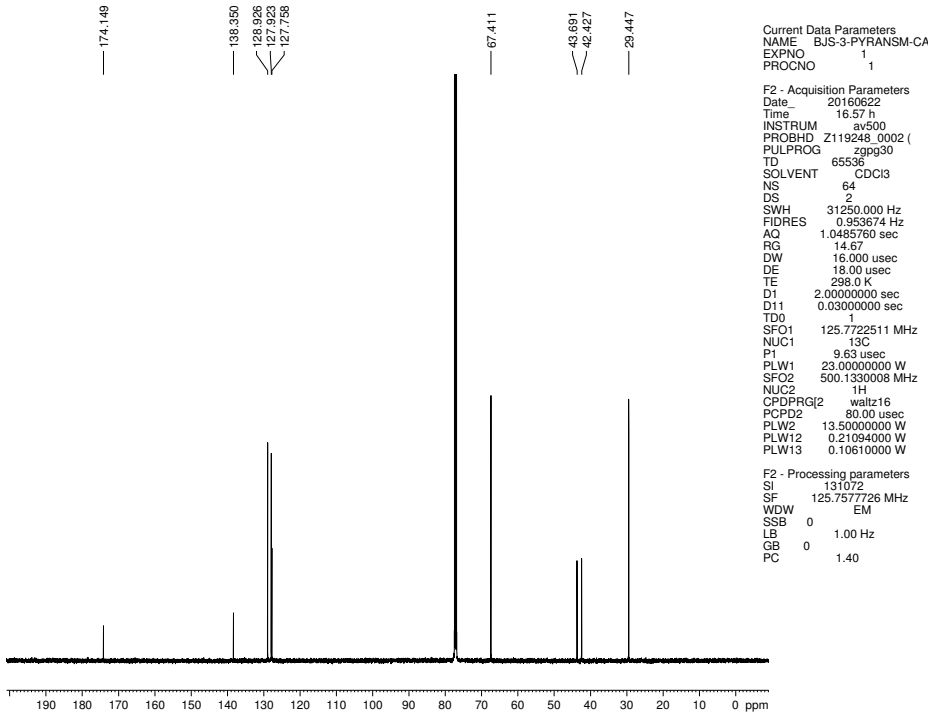

Figure 2.5 ^{13}C NMR (125 MHz, $CDCl_3$) of compound **2.49**.

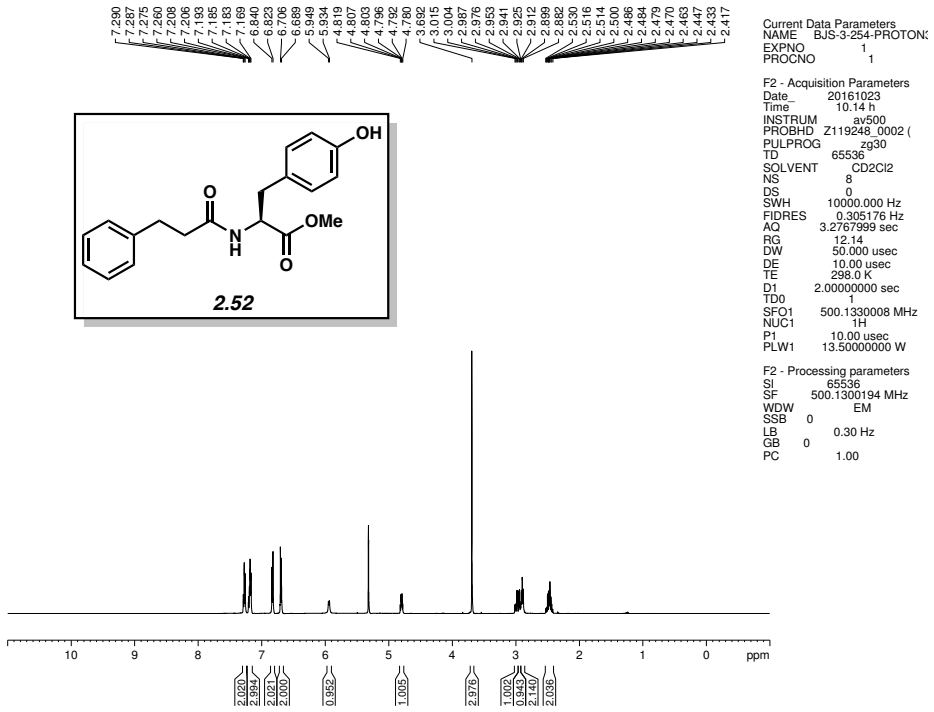

Figure 2.6 ^{1}H NMR (500 MHz, CD_2Cl_2) of compound **2.52**.

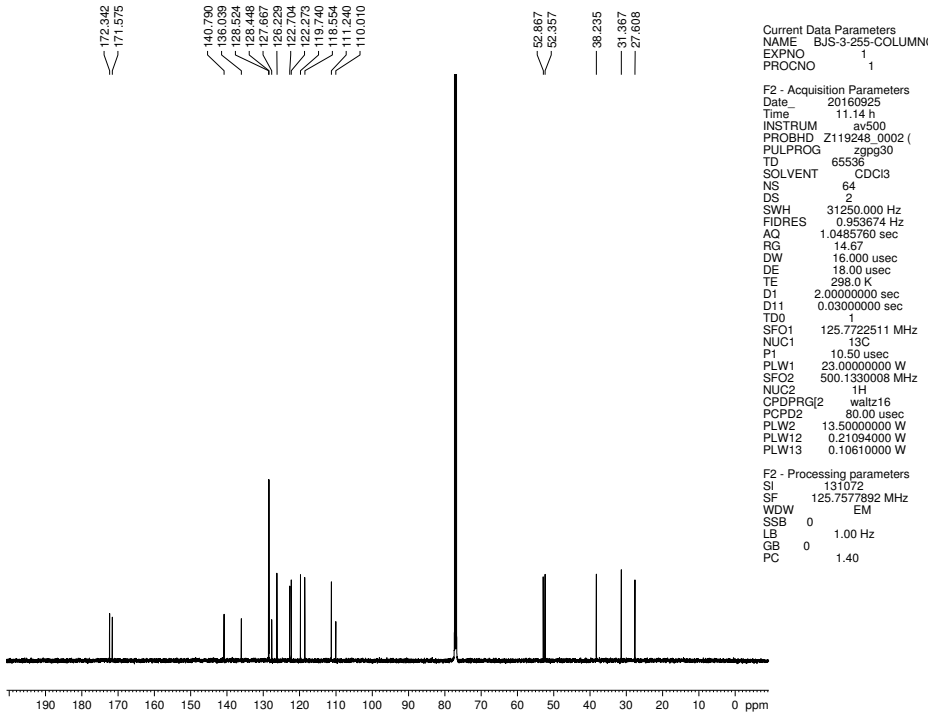

Figure 2.7 ^{13}C NMR (125 MHz, $CDCl_3$) of compound **2.52**.

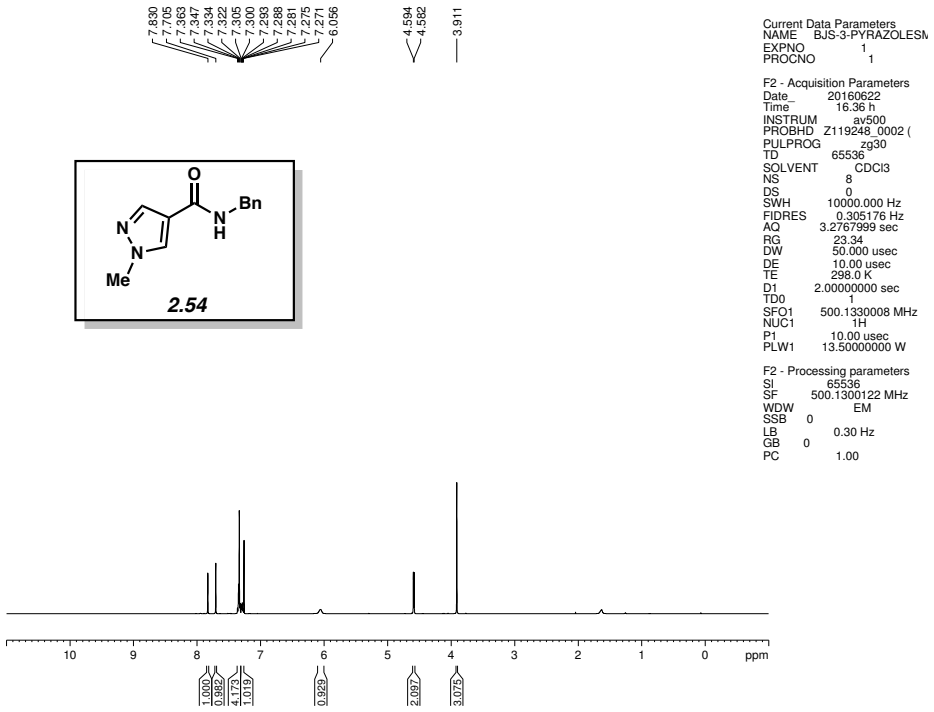

Figure 2.8 ^{1}H NMR (500 MHz, $CDCl_3$) of compound **2.54**.

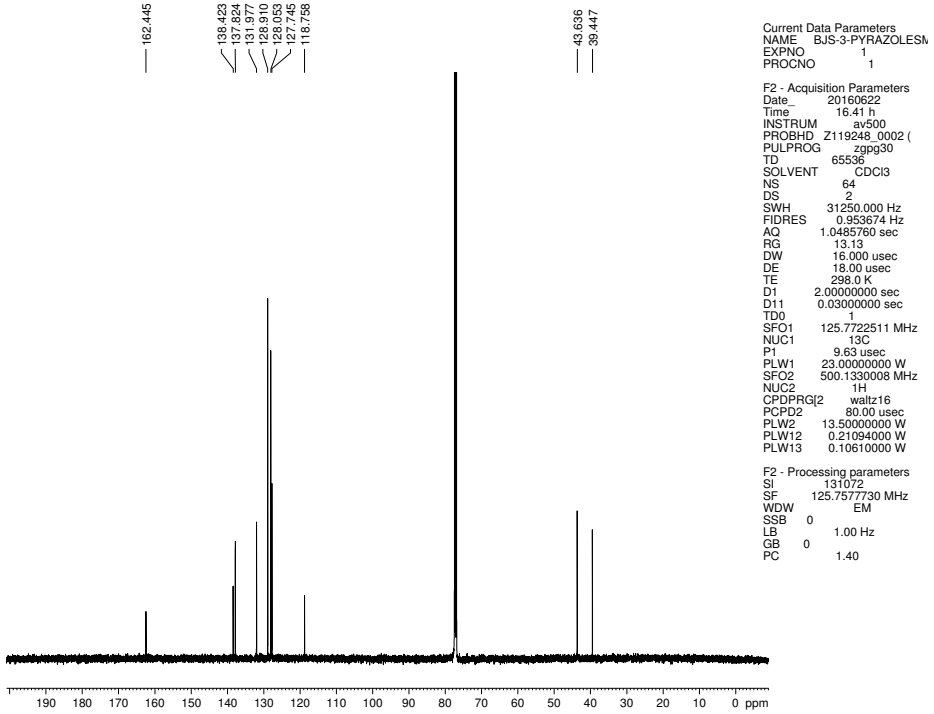

Figure 2.9 ^{13}C NMR (125 MHz, $CDCl_3$) of compound **2.54**.

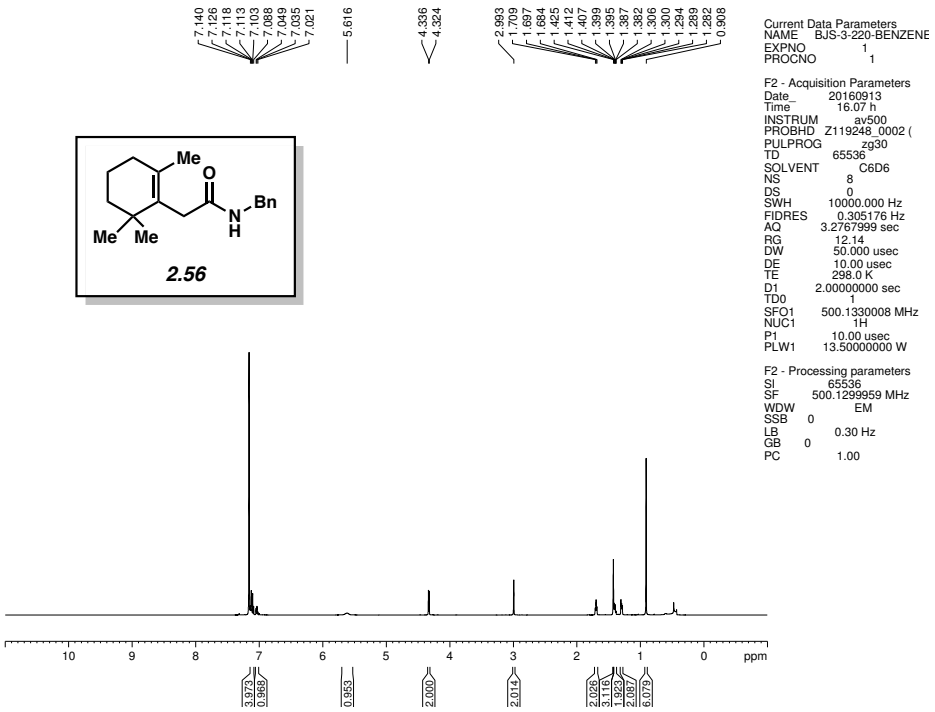

Figure 2.10 ^{1}H NMR (500 MHz, C_6D_6) of compound **2.56**.

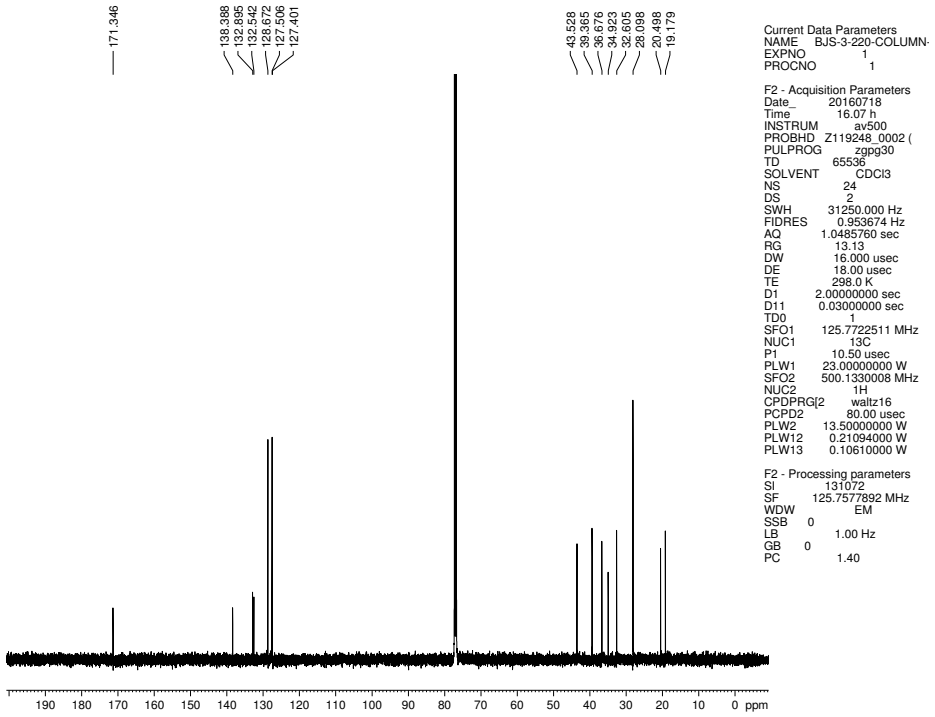

Figure 2.11 ^{13}C NMR (125 MHz, $CDCl_3$) of compound **2.56**.

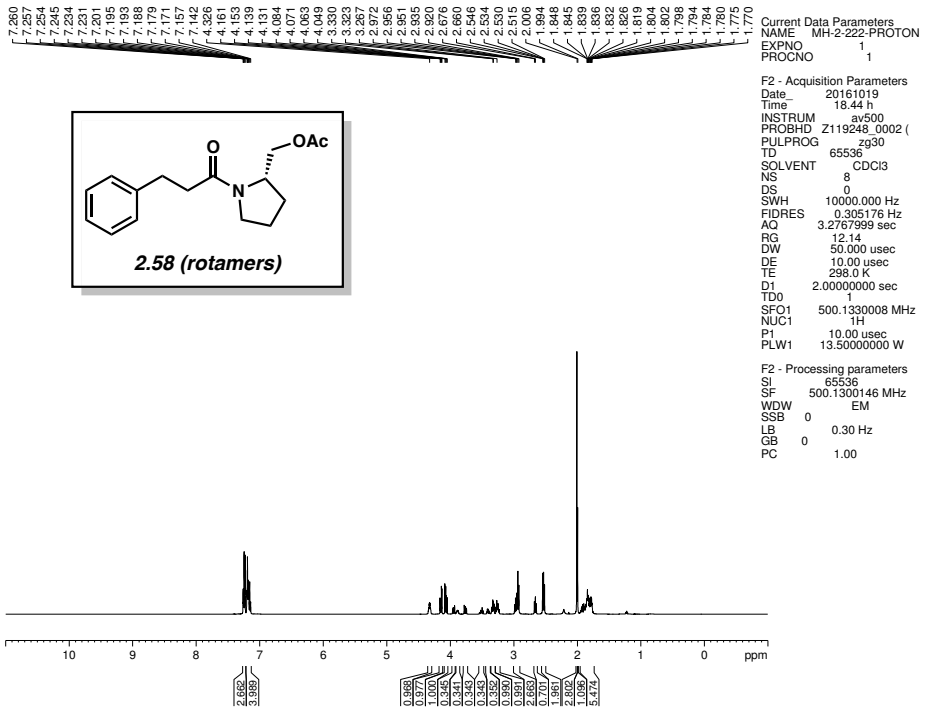

Figure 2.12 ^{1}H NMR (500 MHz, $CDCl_3$) of compound **2.58**.

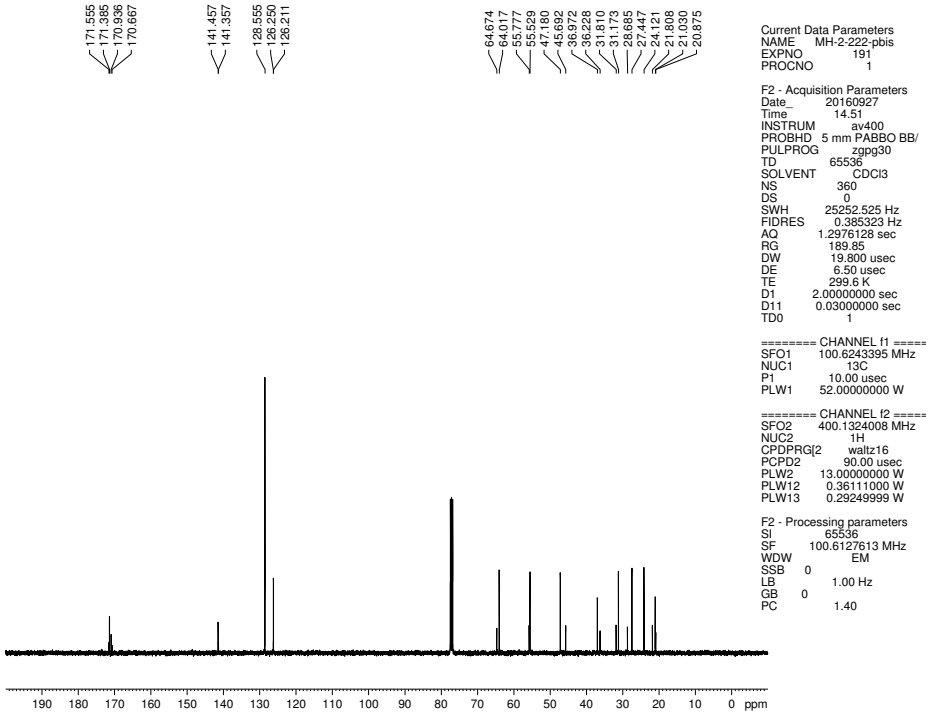

Figure 2.13 ^{13}C NMR (125 MHz, $CDCl_3$) of compound **2.58**.

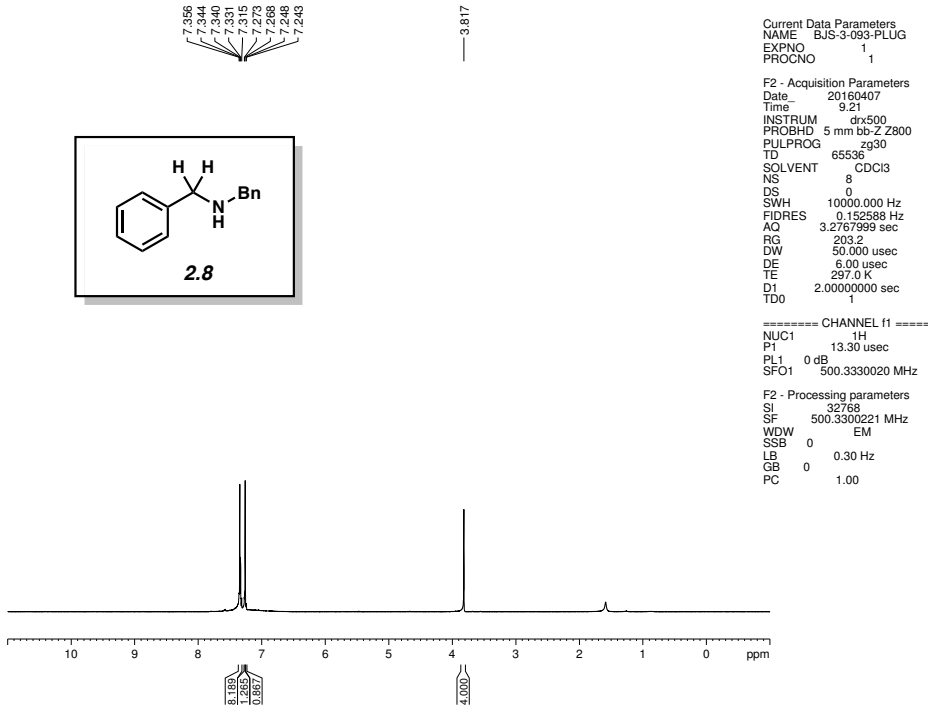

Figure 2.14 ^{1}H NMR (500 MHz, $CDCl_3$) of compound **2.8**.

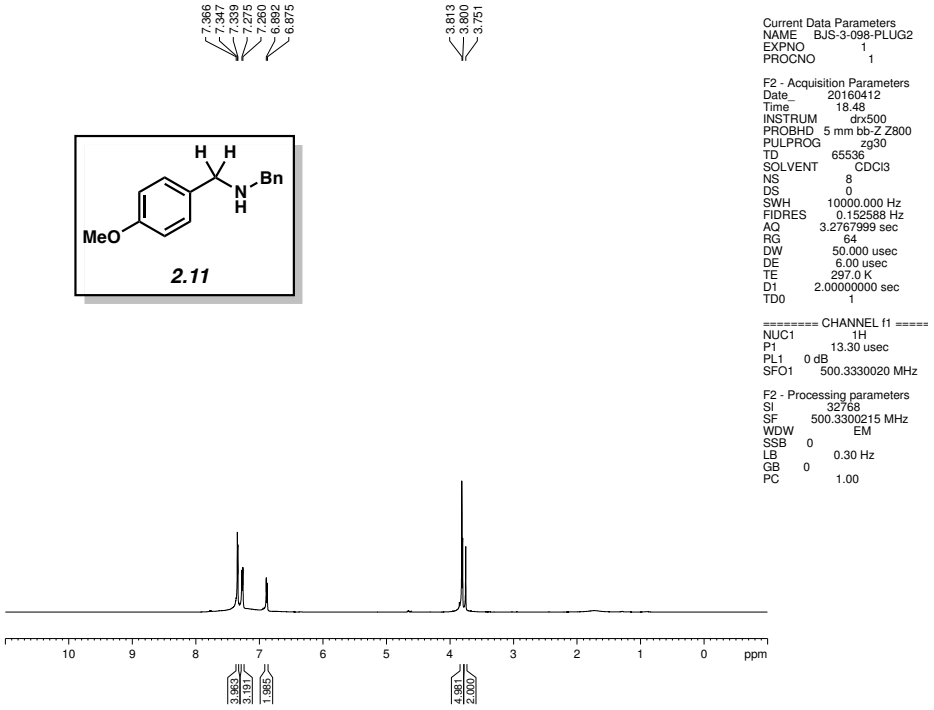

Figure 2.15 ^{1}H NMR (500 MHz, $CDCl_3$) of compound **2.11**.

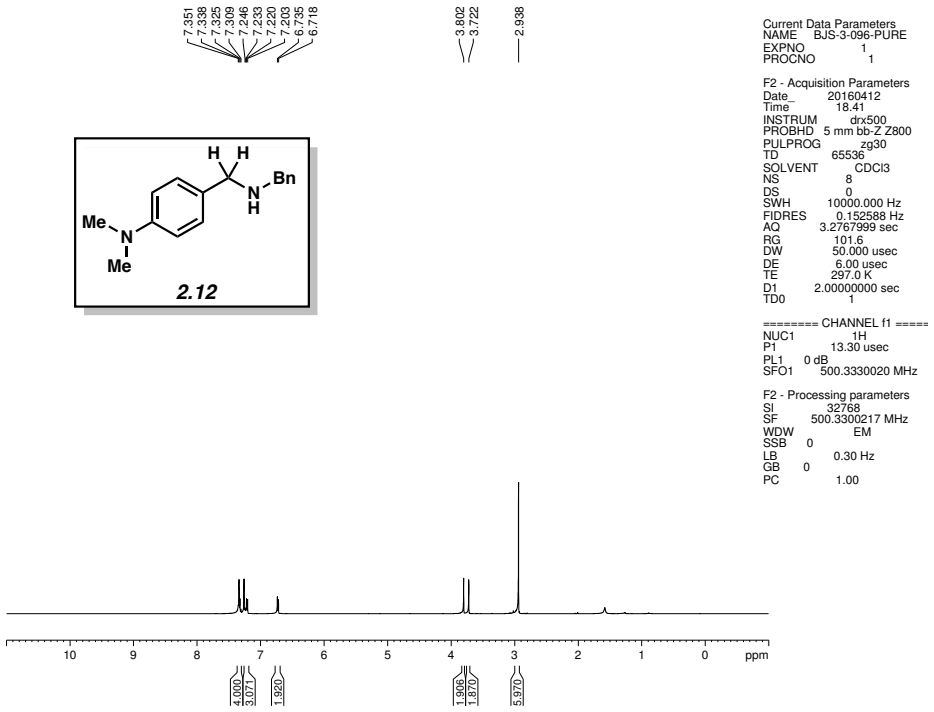

Figure 2.16 ^{1}H NMR (500 MHz, $CDCl_3$) of compound **2.12**.

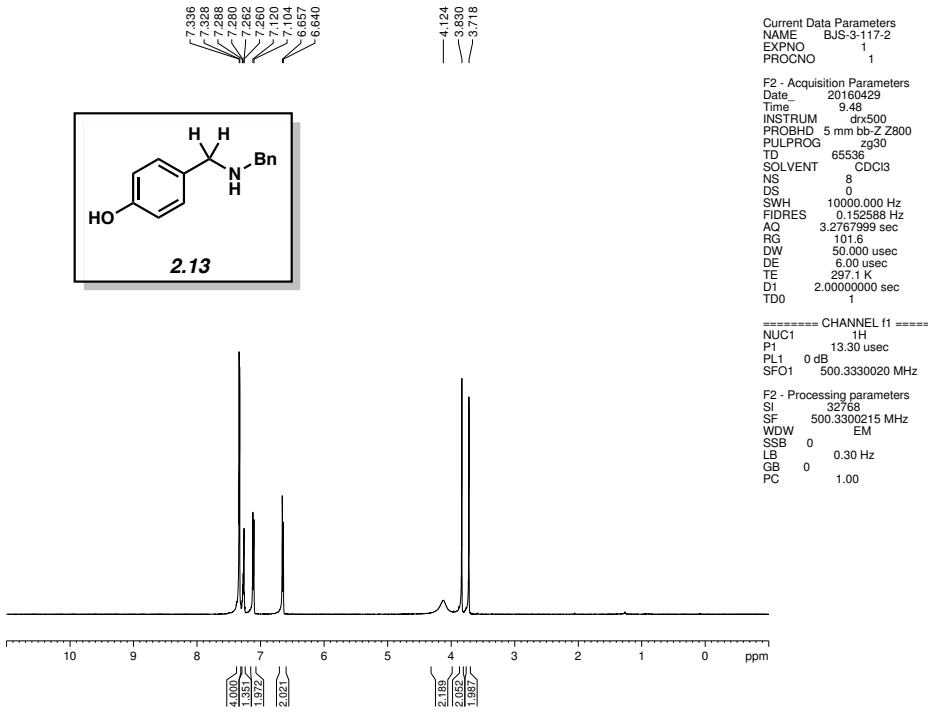

Figure 2.17 ^{1}H NMR (500 MHz, $CDCl_3$) of compound **2.13**.

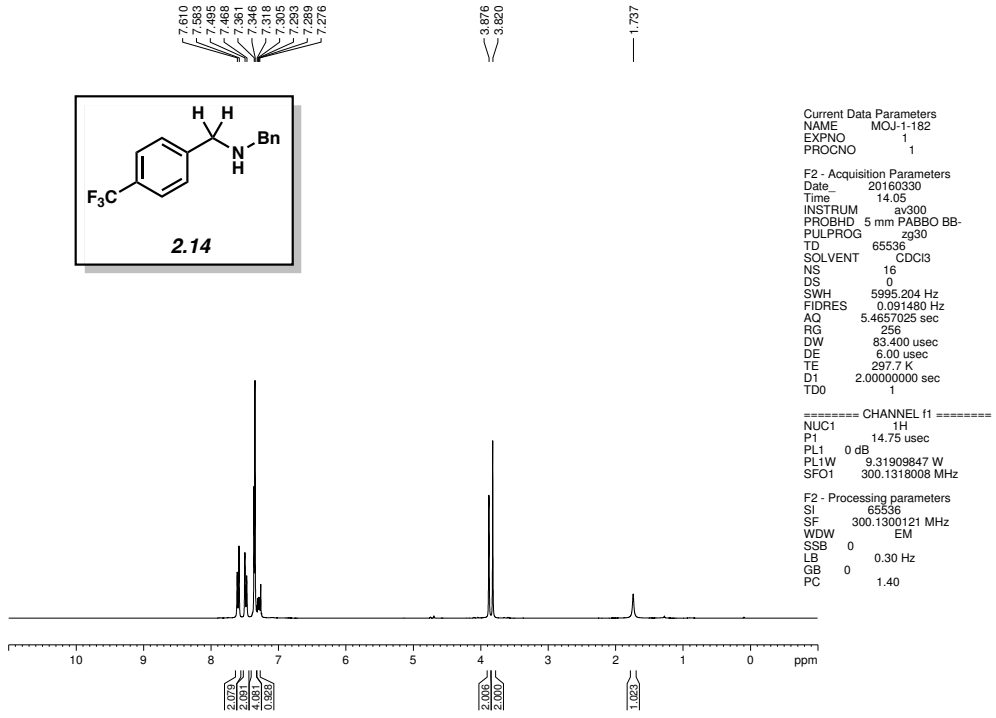

Figure 2.18 ^{1}H NMR (500 MHz, $CDCl_3$) of compound **2.14**.

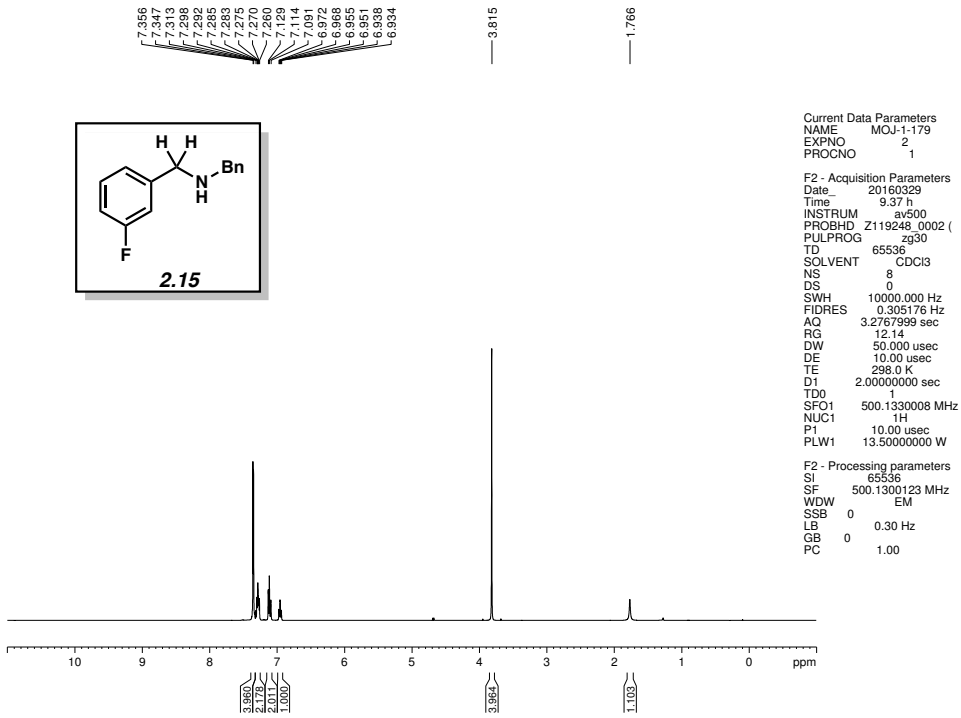

Figure 2.19 ^{1}H NMR (500 MHz, $CDCl_3$) of compound **2.15**.

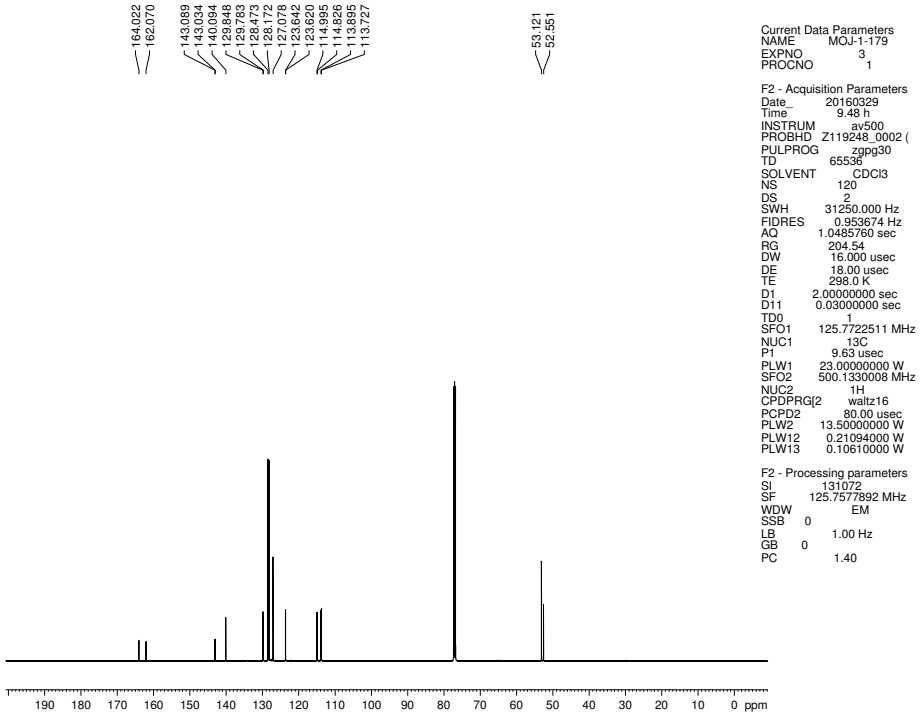

Figure 2.20 ^{13}C NMR (125 MHz, $CDCl_3$) of compound **2.15**.

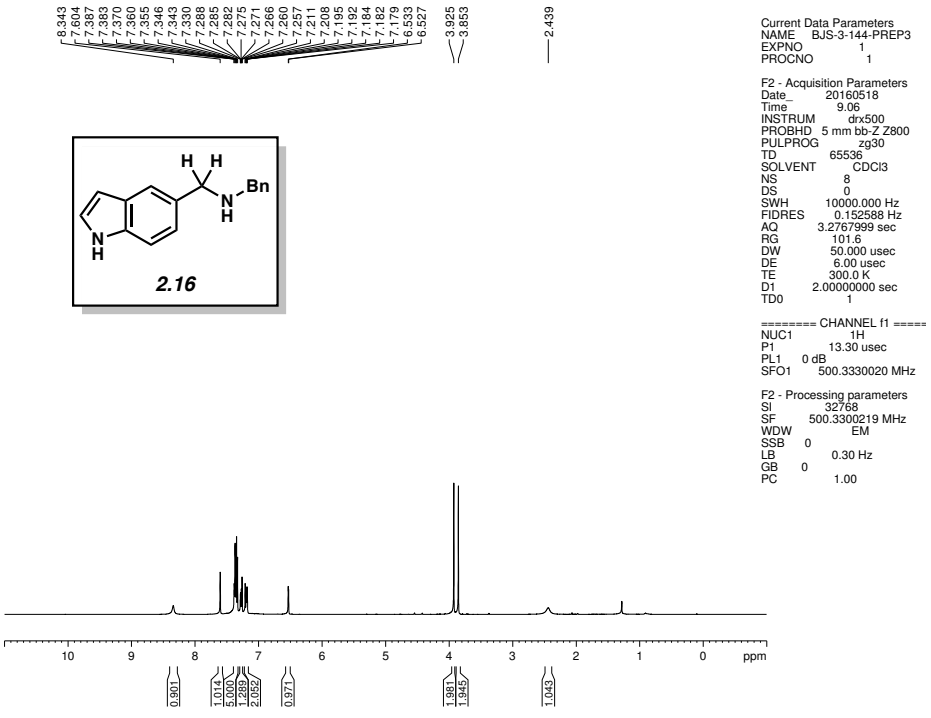

Figure 2.21 ^{1}H NMR (500 MHz, $CDCl_3$) of compound **2.16**.

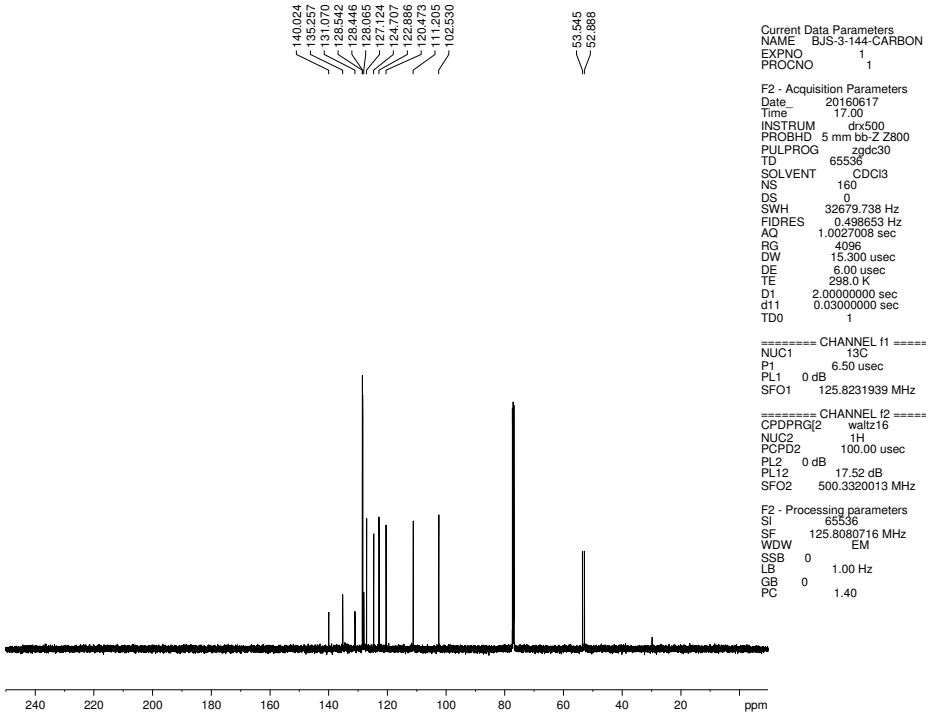

Figure 2.22 ^{13}C NMR (125 MHz, $CDCl_3$) of compound **2.16**.

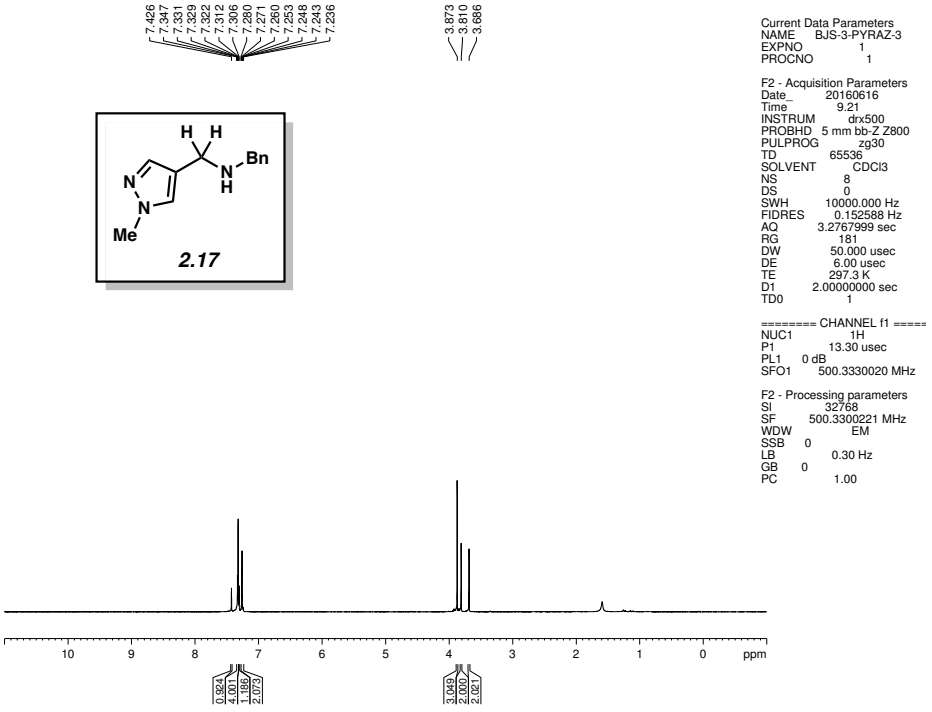

Figure 2.23 ^{1}H NMR (500 MHz, $CDCl_3$) of compound **2.17**.

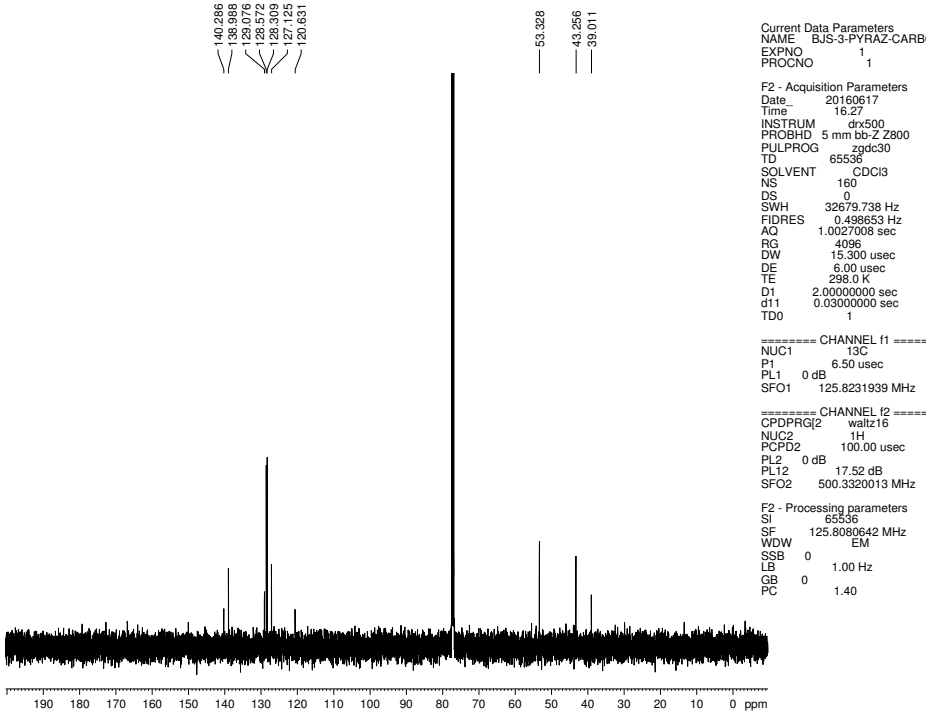

Figure 2.24 ^{13}C NMR (125 MHz, $CDCl_3$) of compound **2.17**.

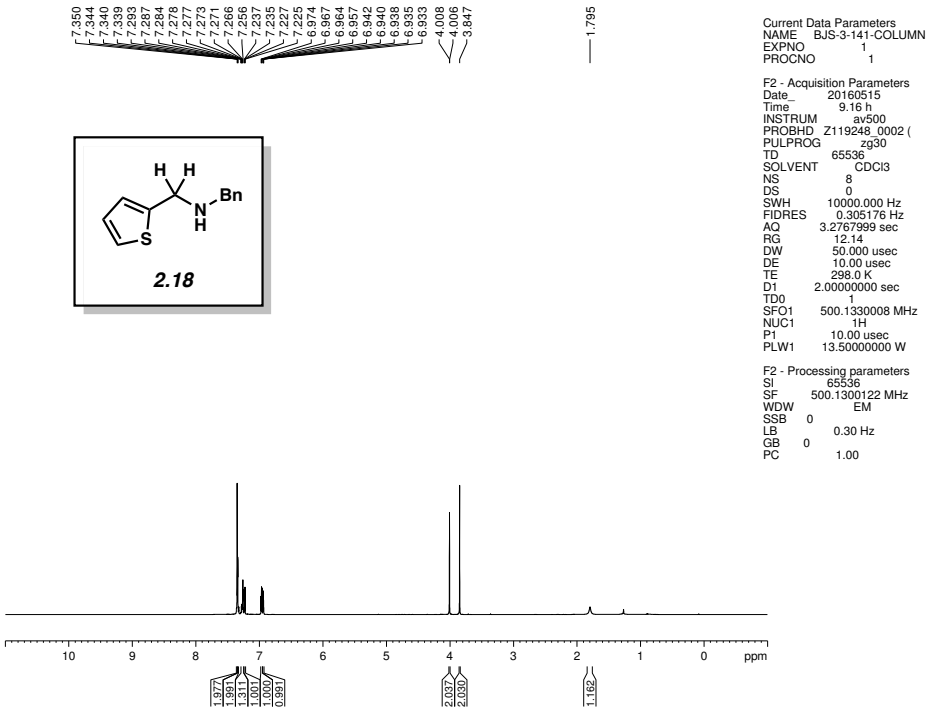

Figure 2.25 ^{1}H NMR (500 MHz, $CDCl_3$) of compound **2.18**.

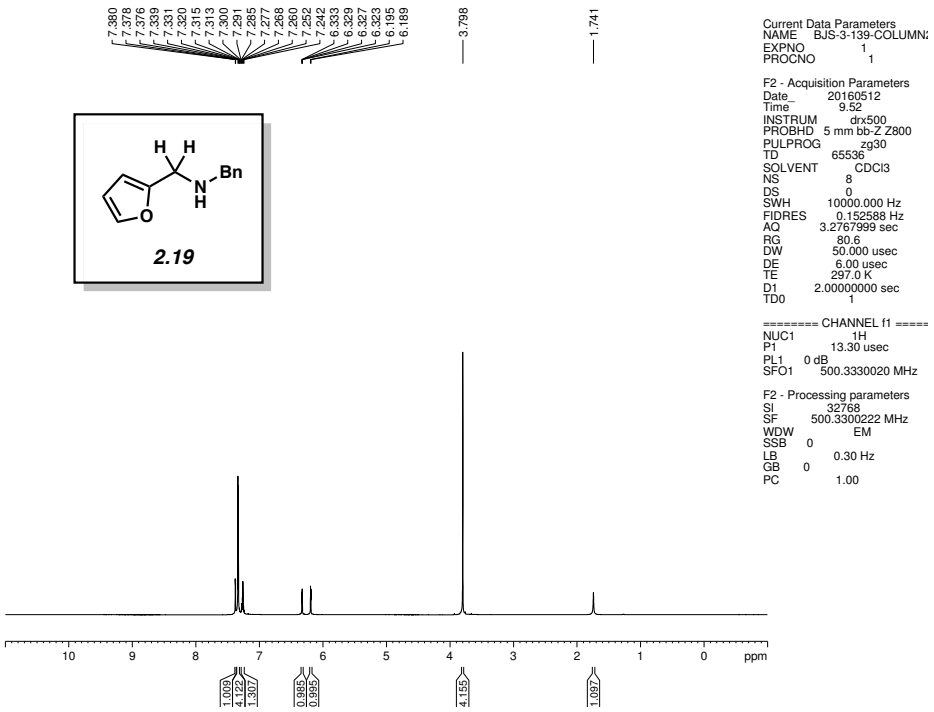

Figure 2.26 ^{1}H NMR (500 MHz, $CDCl_3$) of compound **2.19**.

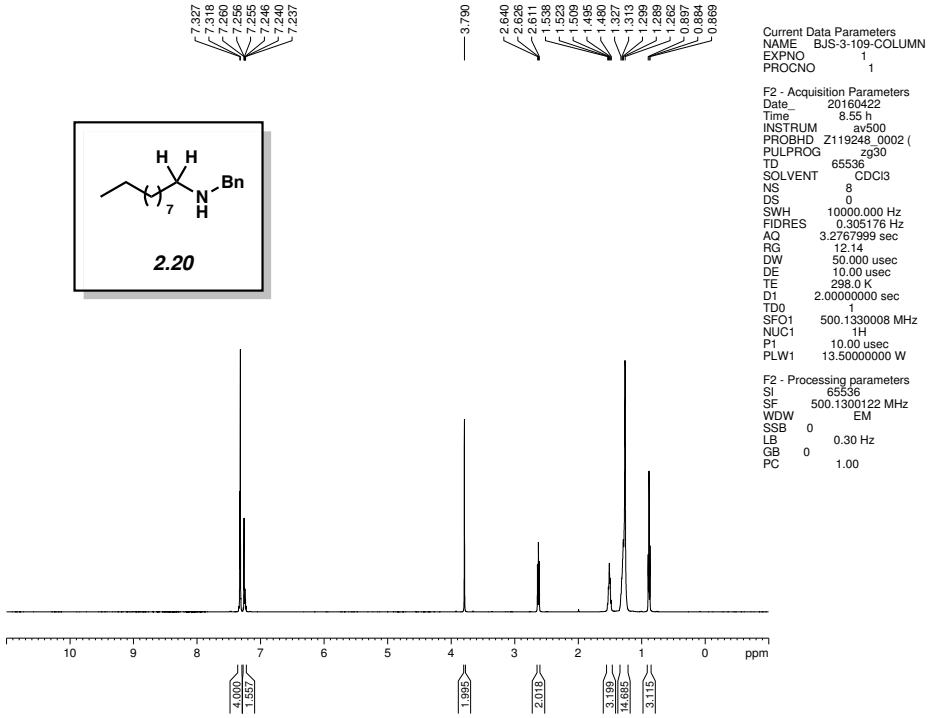

Figure 2.27 ^{1}H NMR (500 MHz, $CDCl_3$) of compound **2.20**.

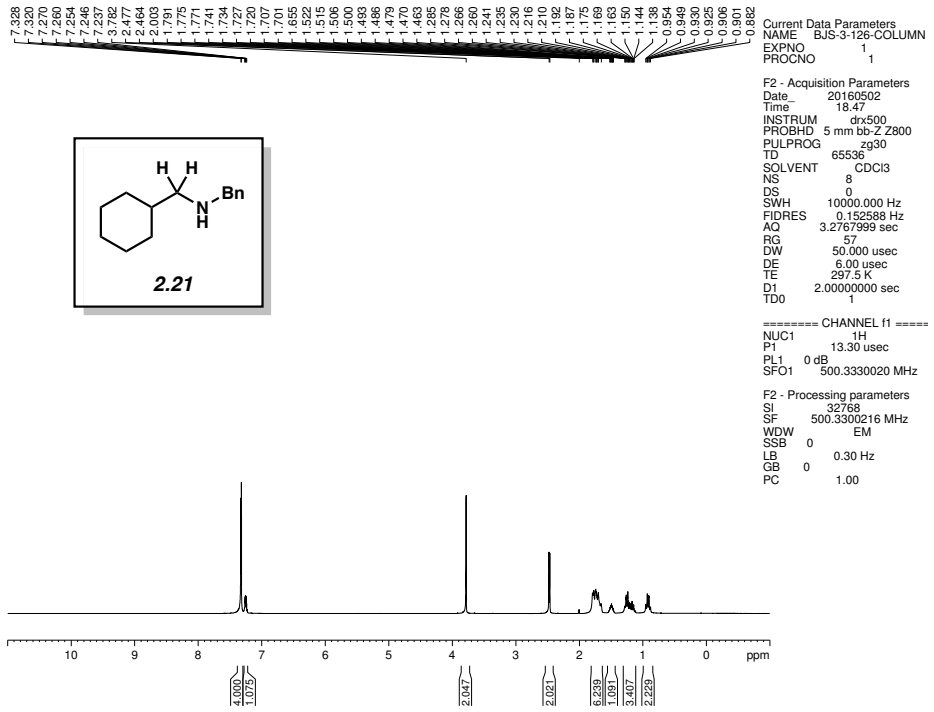

Figure 2.28 ^{1}H NMR (500 MHz, $CDCl_3$) of compound **2.21**.

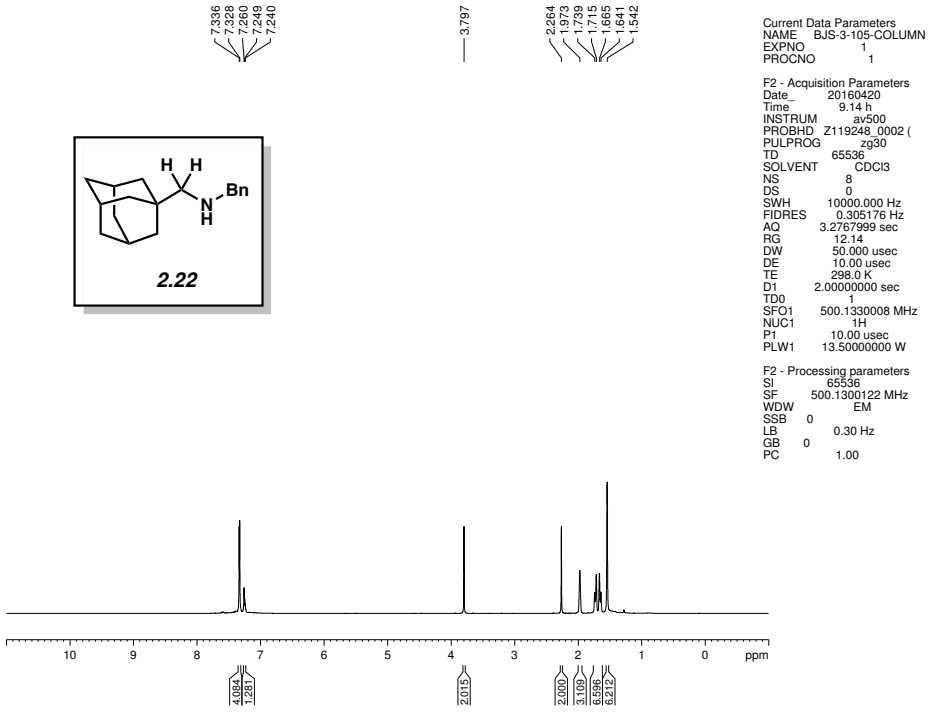

Figure 2.29 ^{1}H NMR (500 MHz, $CDCl_3$) of compound **2.22**.

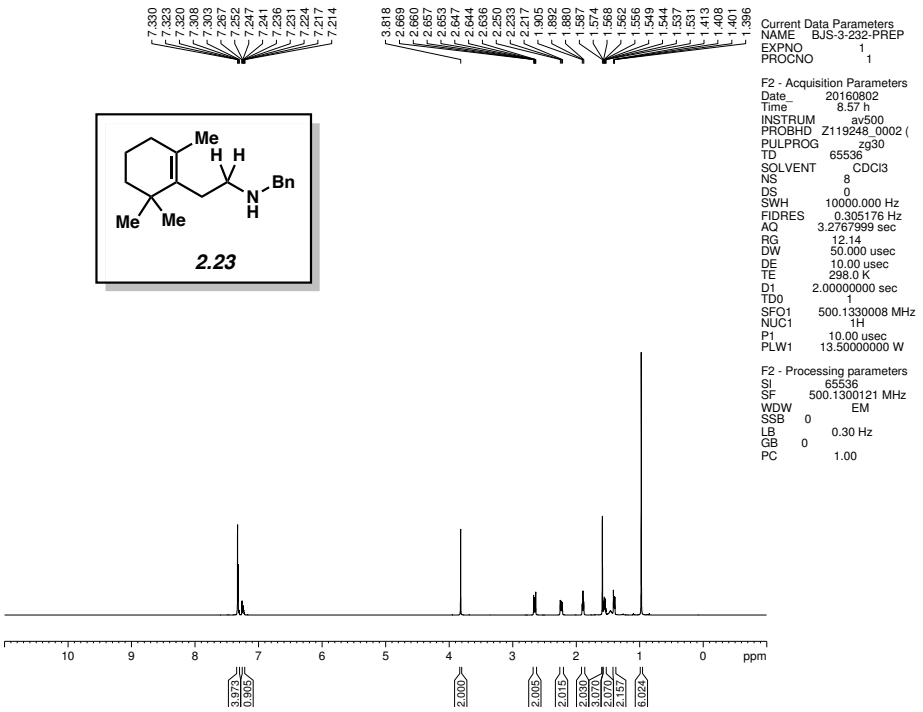

Figure 2.30 ^{1}H NMR (500 MHz, $CDCl_3$) of compound **2.23**.

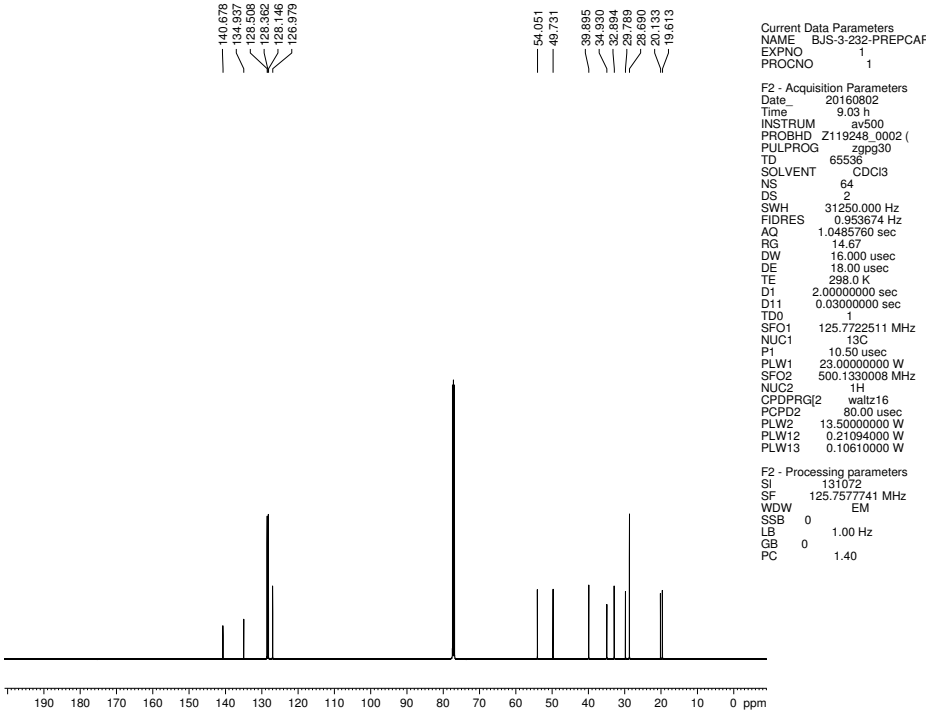

Figure 2.31 ^{13}C NMR (125 MHz, $CDCl_3$) of compound **2.23**.

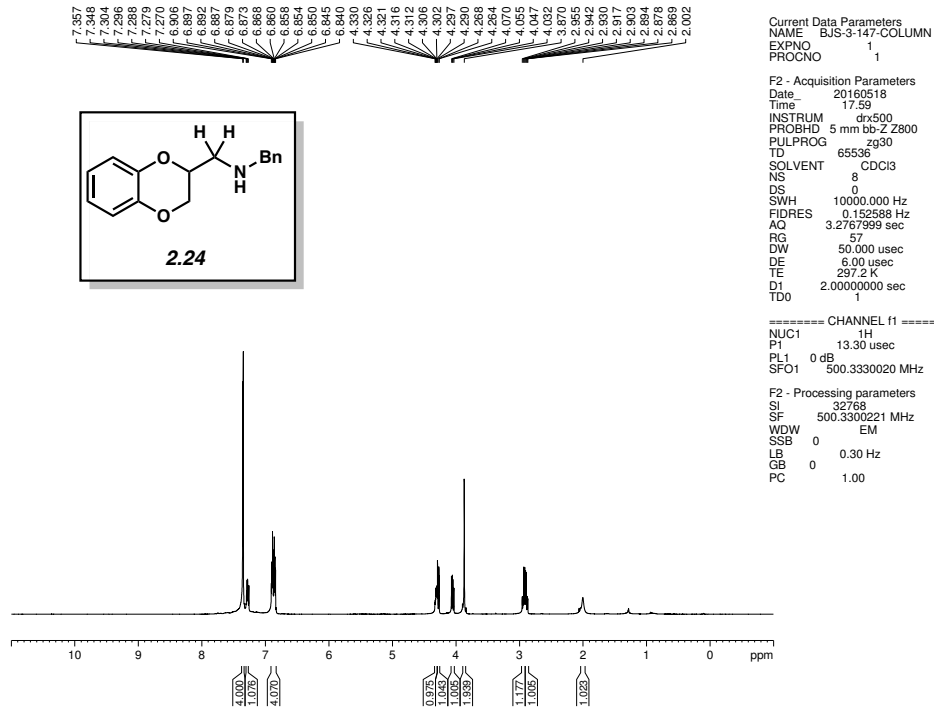

Figure 2.32 ^{1}H NMR (500 MHz, $CDCl_3$) of compound **2.24**.

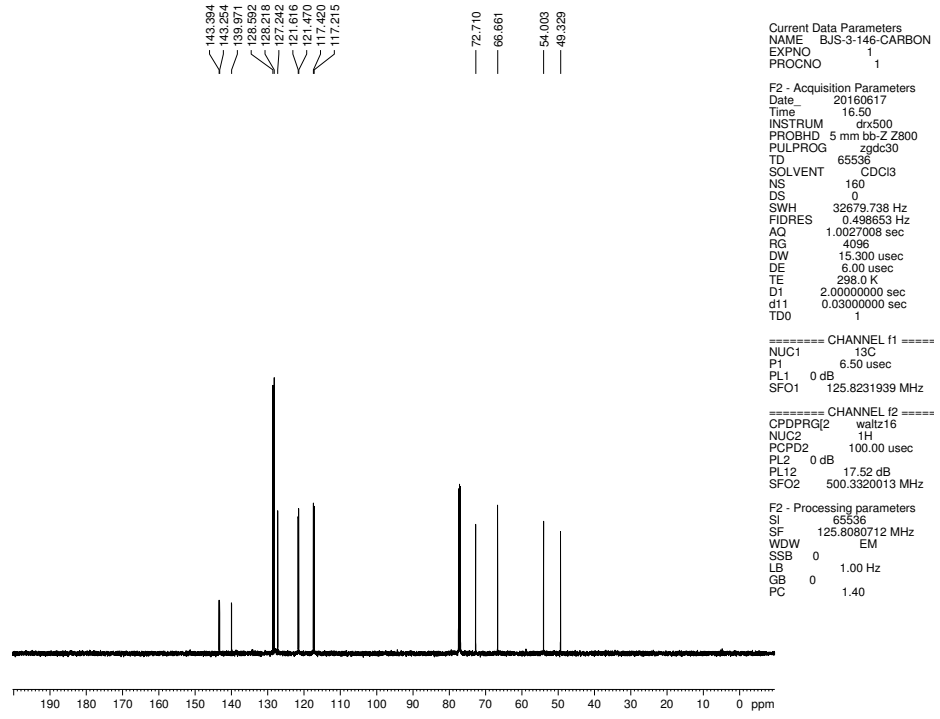

Figure 2.33 ^{13}C NMR (125 MHz, $CDCl_3$) of compound **2.24**.

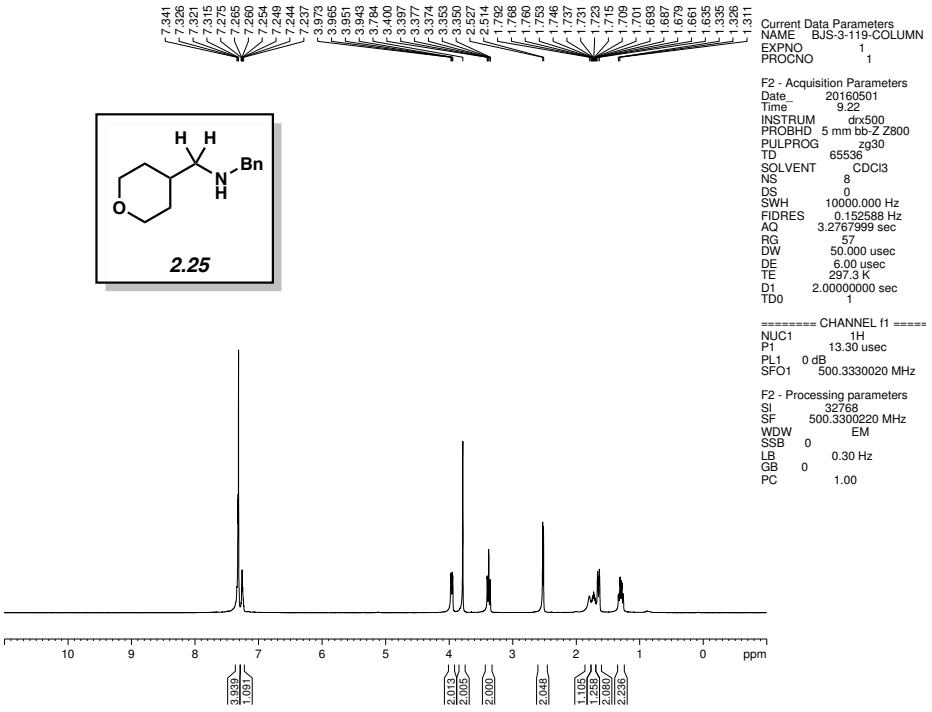

Figure 2.34 ^{1}H NMR (500 MHz, $CDCl_3$) of compound **2.25**.

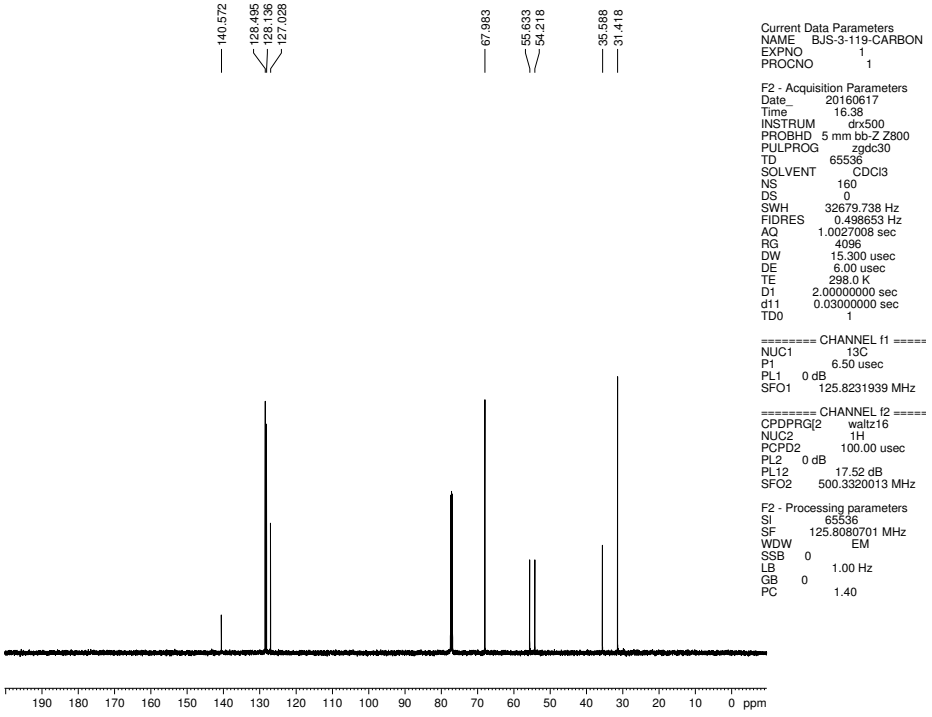

Figure 2.35 ^{13}C NMR (125 MHz, $CDCl_3$) of compound **2.25**.

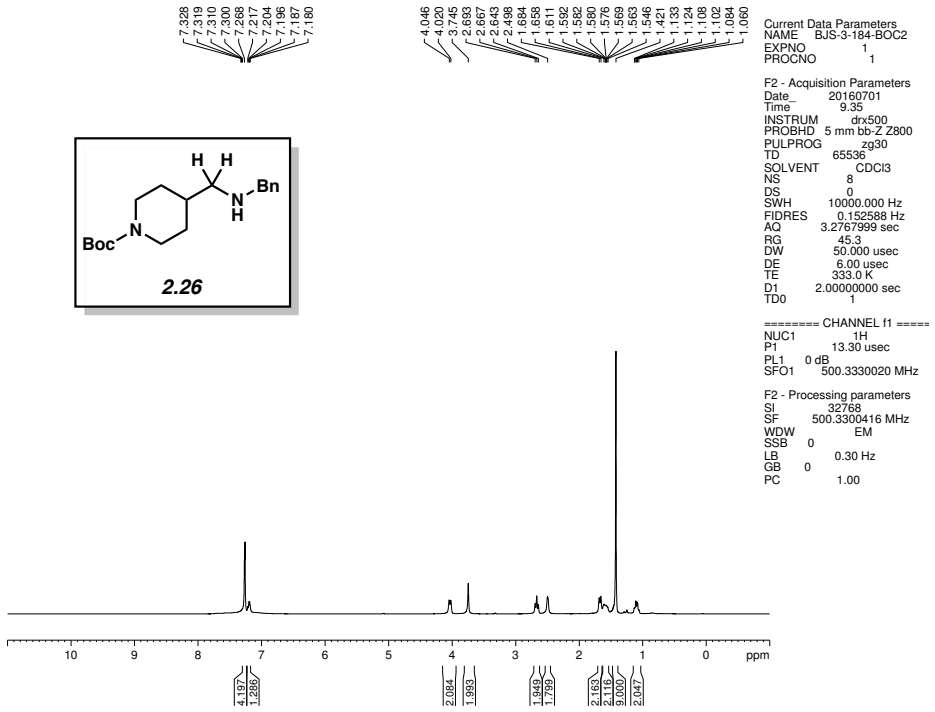

Figure 2.36 ^{1}H NMR (500 MHz, $CDCl_3$) of compound **2.26**.

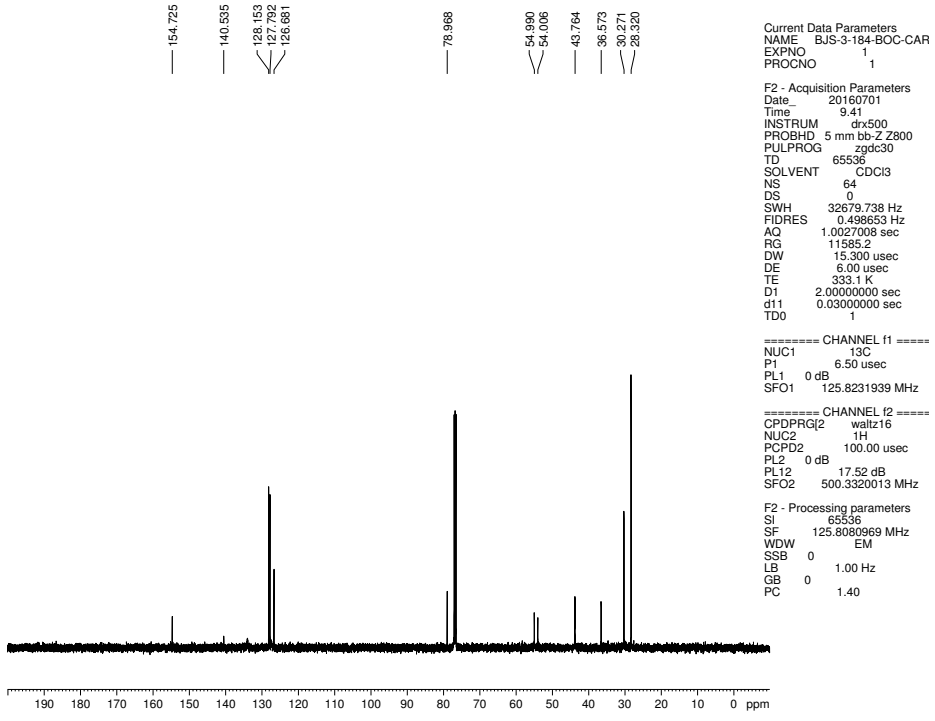

Figure 2.37 ^{13}C NMR (125 MHz, $CDCl_3$) of compound **2.26**.

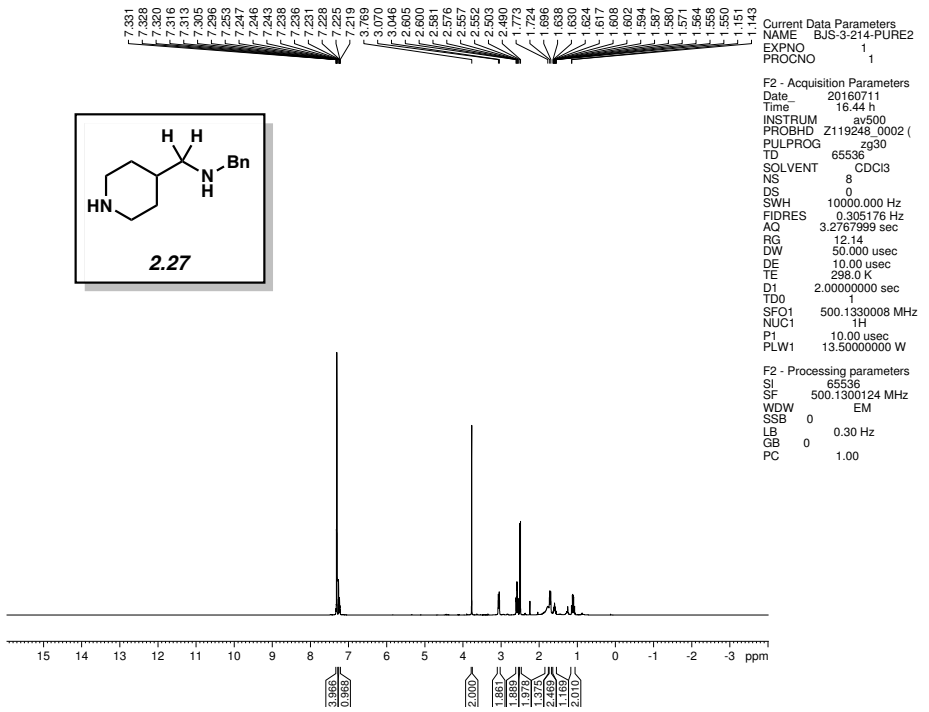

Figure 2.38 ^{1}H NMR (500 MHz, $CDCl_3$) of compound **2.27**.

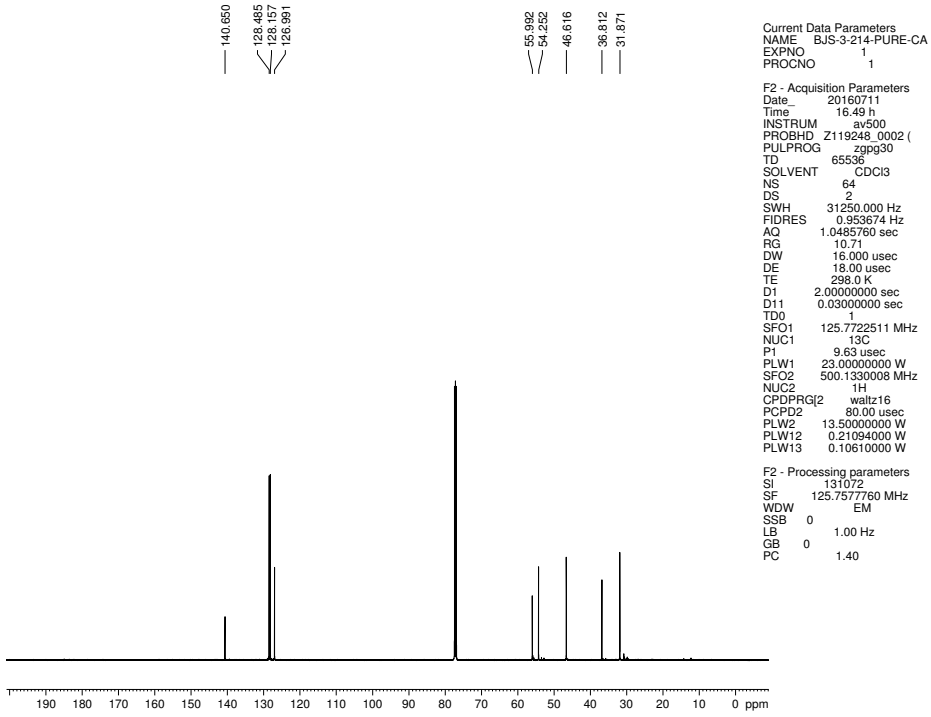

Figure 2.39 ^{13}C NMR (125 MHz, $CDCl_3$) of compound **2.27**.

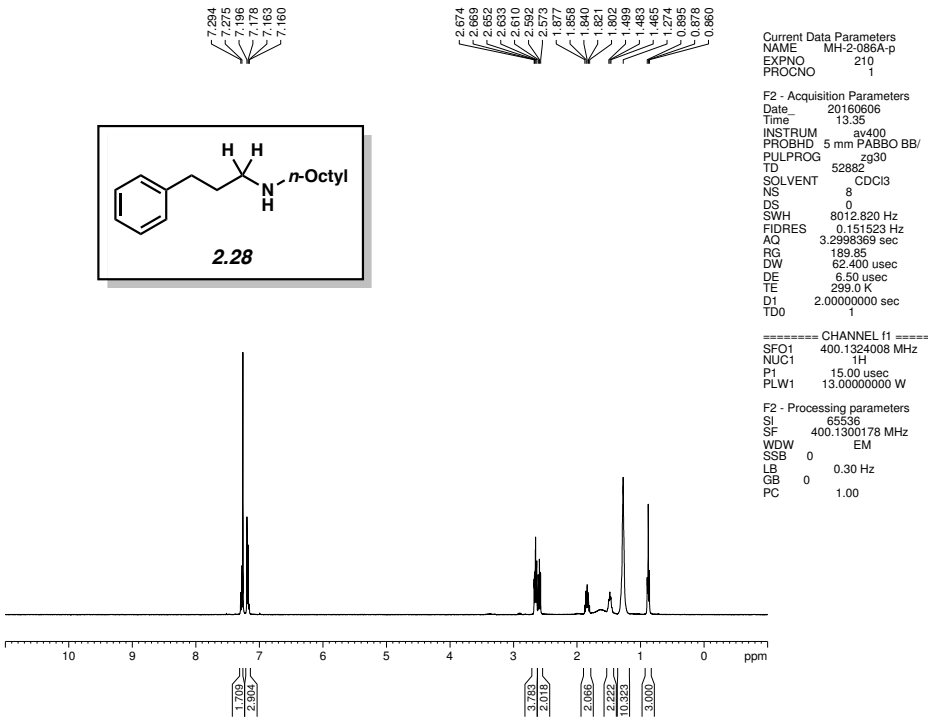

Figure 2.40 ^{1}H NMR (500 MHz, $CDCl_3$) of compound **2.28**.

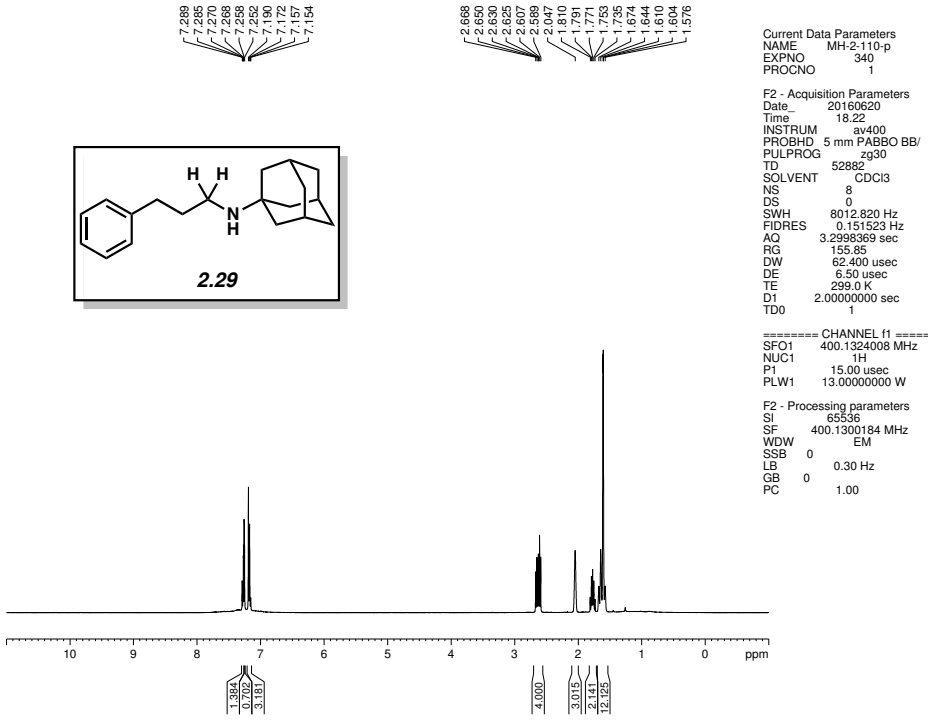

Figure 2.41 ^{1}H NMR (500 MHz, $CDCl_3$) of compound **2.29**.

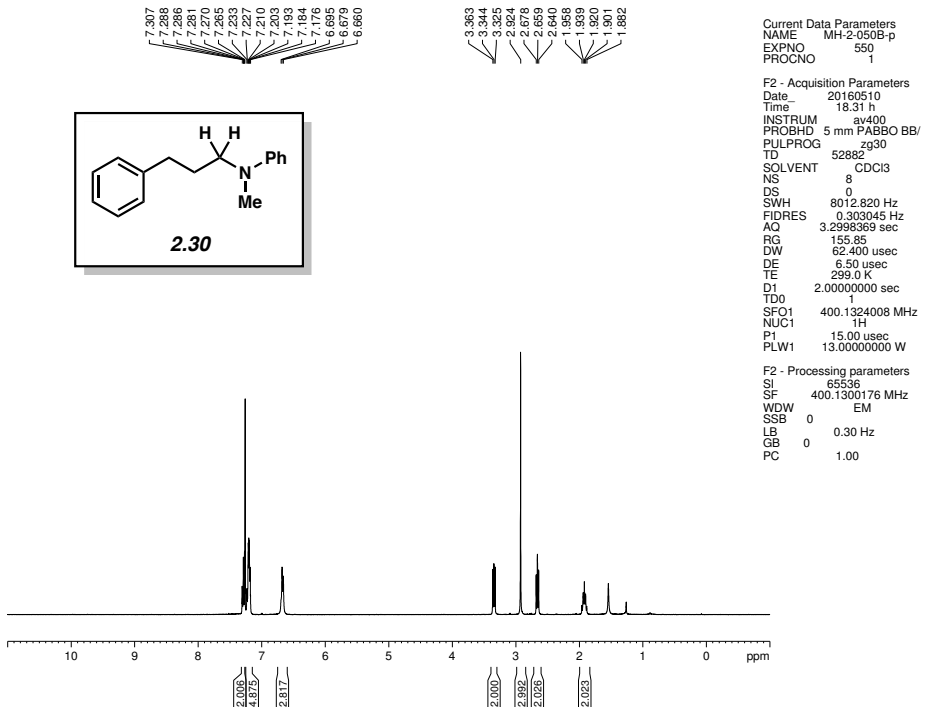

Figure 2.42 ^{1}H NMR (500 MHz, $CDCl_3$) of compound **2.30**.

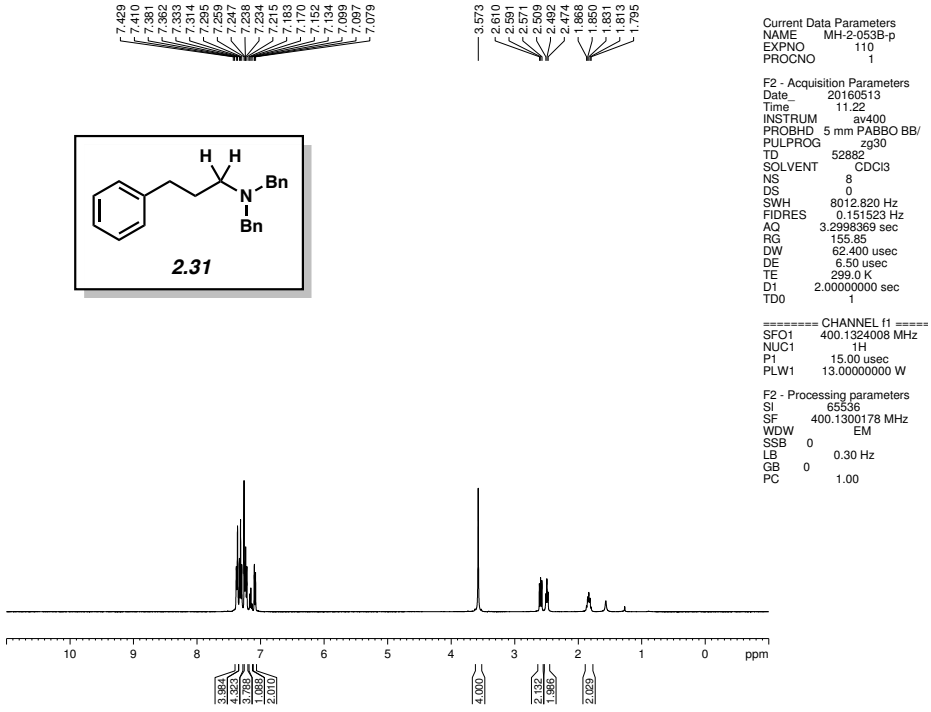

Figure 2.43 ^{1}H NMR (500 MHz, $CDCl_3$) of compound **2.31**.

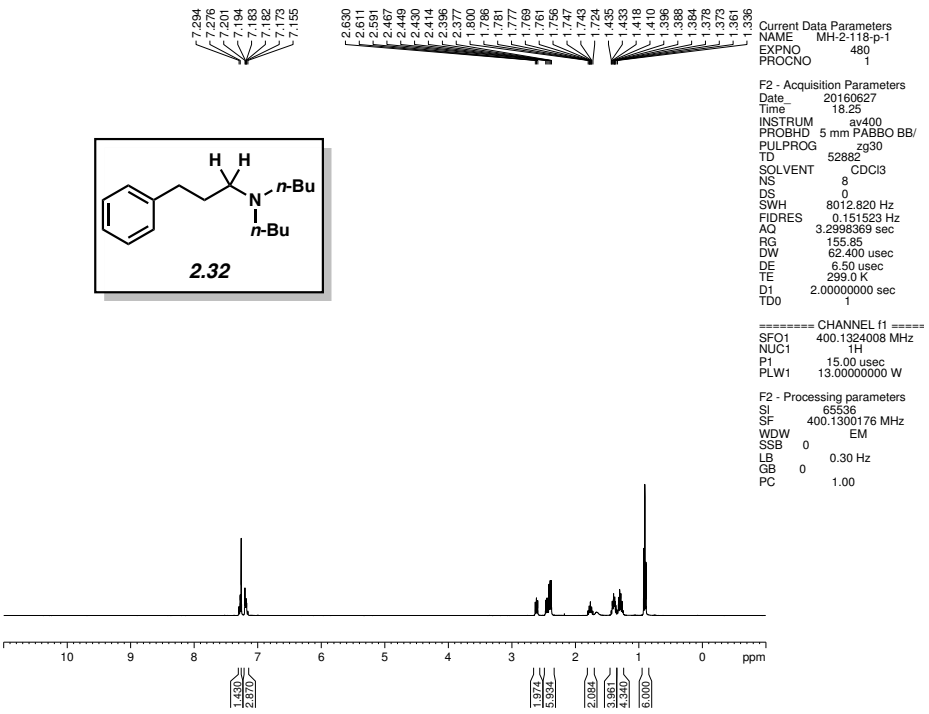

Figure 2.44 ^{1}H NMR (500 MHz, $CDCl_3$) of compound **2.32**.

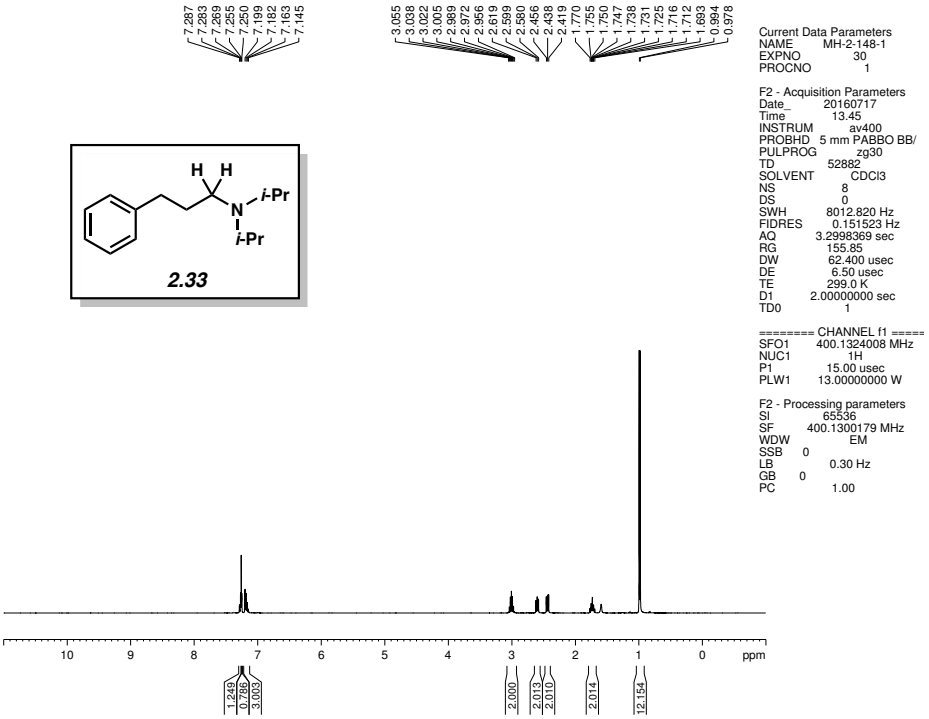

Figure 2.45 ^{1}H NMR (500 MHz, $CDCl_3$) of compound **2.33**.

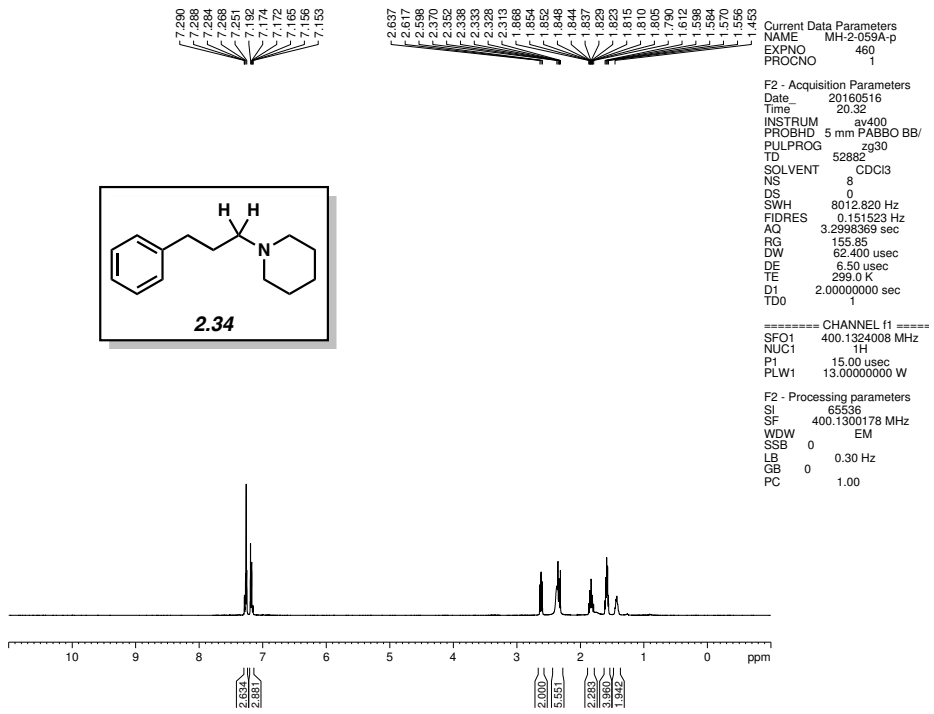

Figure 2.46 ^{1}H NMR (500 MHz, $CDCl_3$) of compound **2.34**.

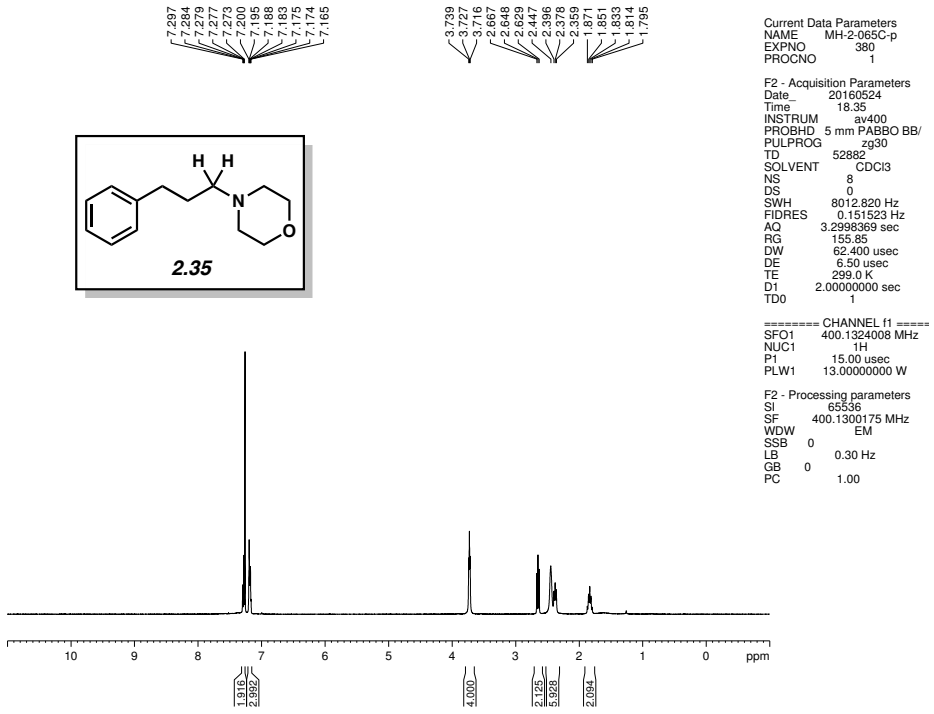

Figure 2.47 ^{1}H NMR (500 MHz, $CDCl_3$) of compound **2.35**.

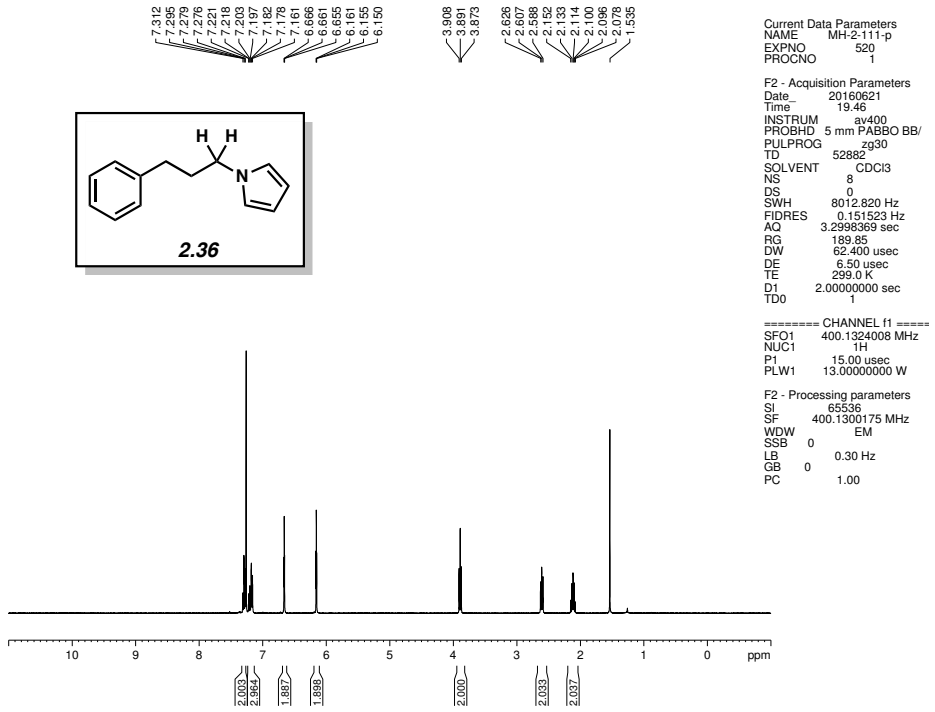

Figure 2.48 ^{1}H NMR (500 MHz, $CDCl_3$) of compound **2.36**.

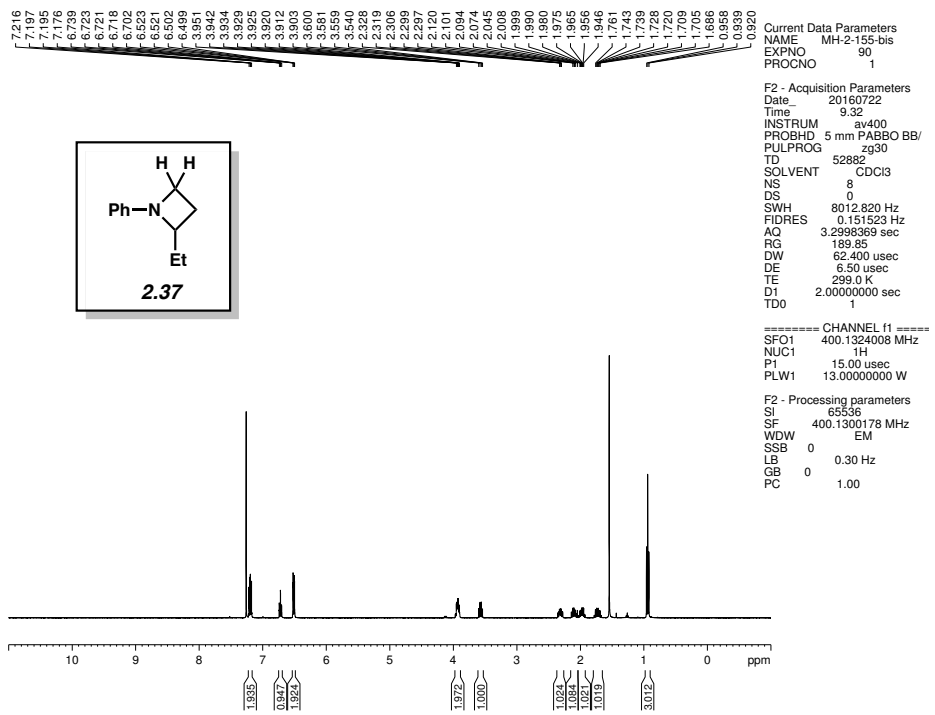

Figure 2.49 ^{1}H NMR (500 MHz, $CDCl_3$) of compound **2.37**.

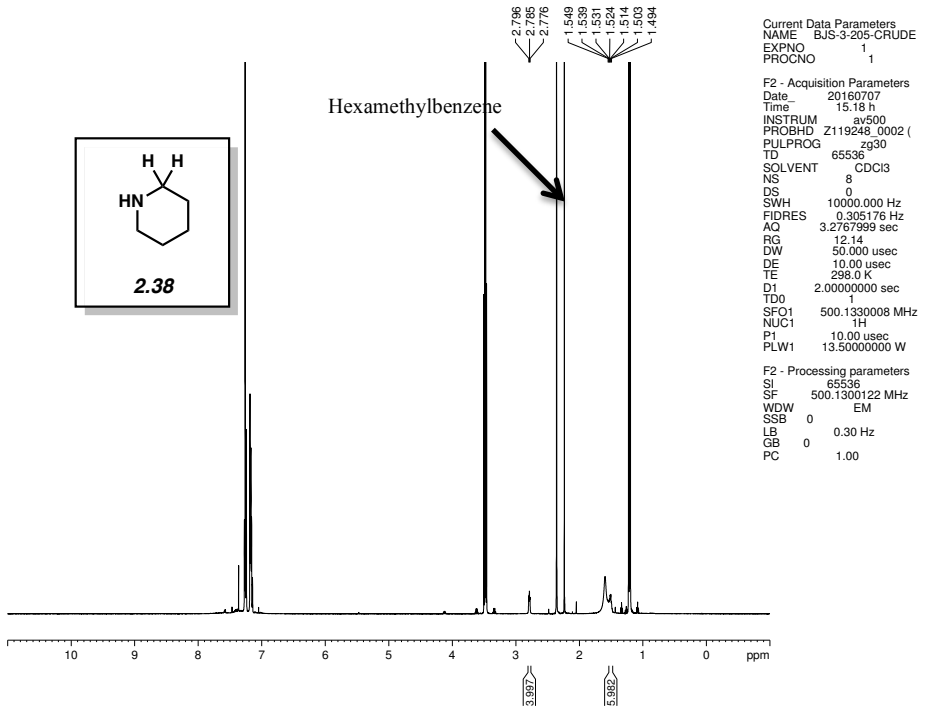

Figure 2.50 ^{1}H NMR (500 MHz, $CDCl_3$) of compound **2.38**.

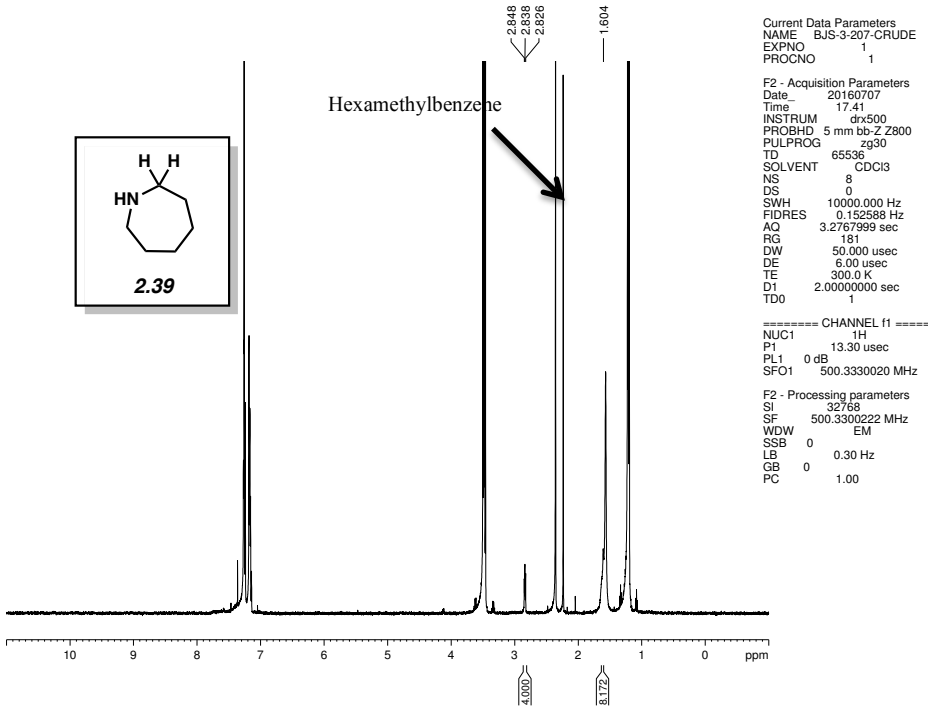

Figure 2.51 ^{1}H NMR (500 MHz, $CDCl_3$) of compound **2.39**.

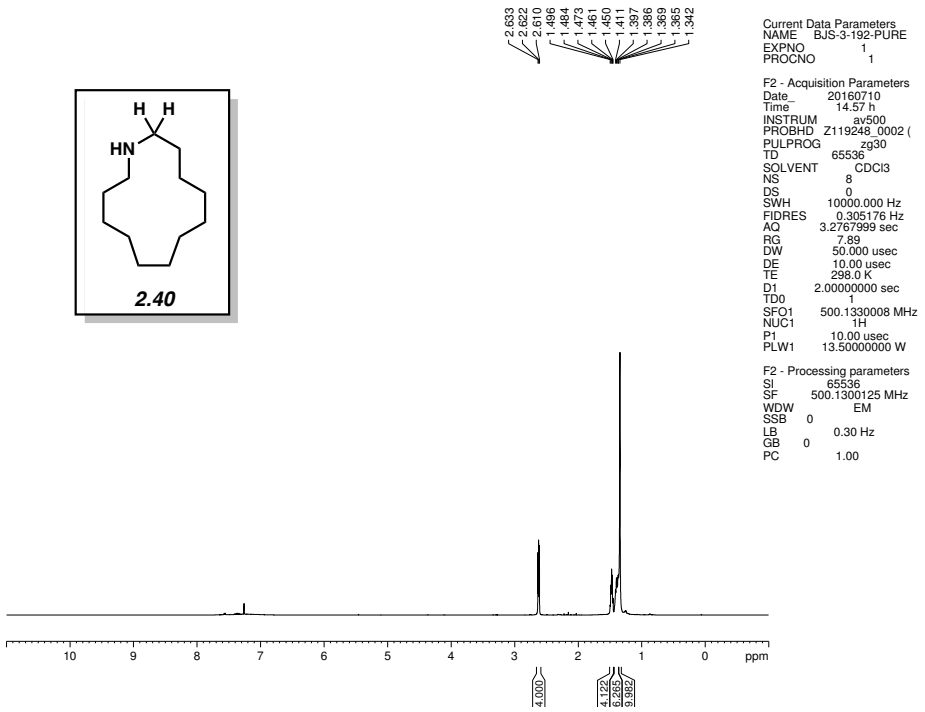

Figure 2.52 ^{1}H NMR (500 MHz, $CDCl_3$) of compound **2.40**.

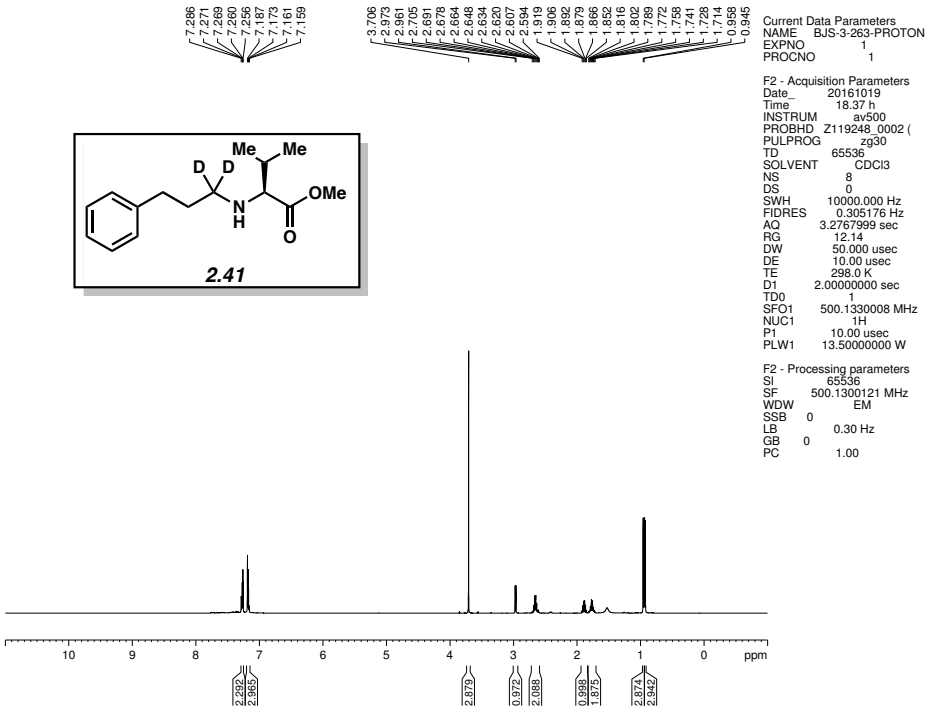

Figure 2.53 ^{1}H NMR (500 MHz, $CDCl_3$) of compound **2.41**.

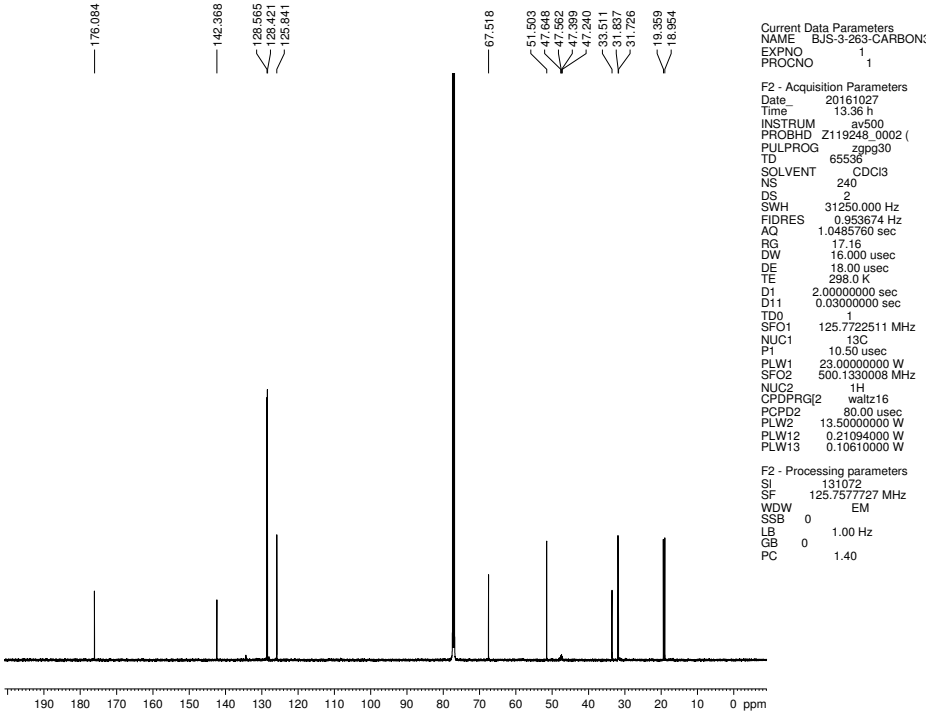

Figure 2.54 ^{13}C NMR (125 MHz, $CDCl_3$) of compound **2.41**.

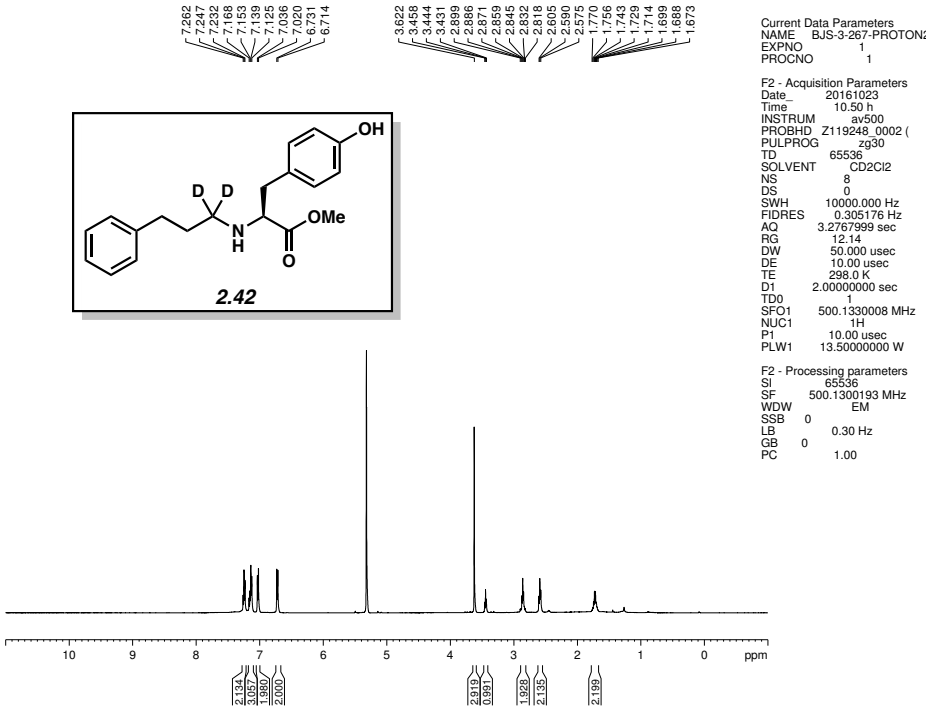

Figure 2.55 ^{1}H NMR (500 MHz, CD_2Cl_2) of compound **2.42**.

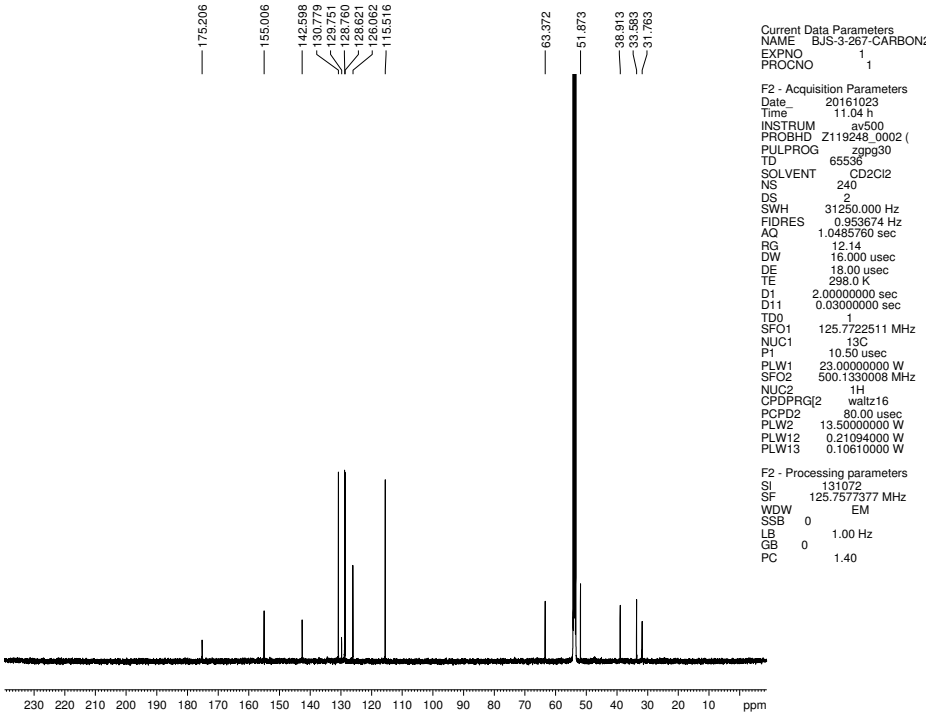

Figure 2.56 ^{13}C NMR (125 MHz, CD_2Cl_2) of compound **2.42**.

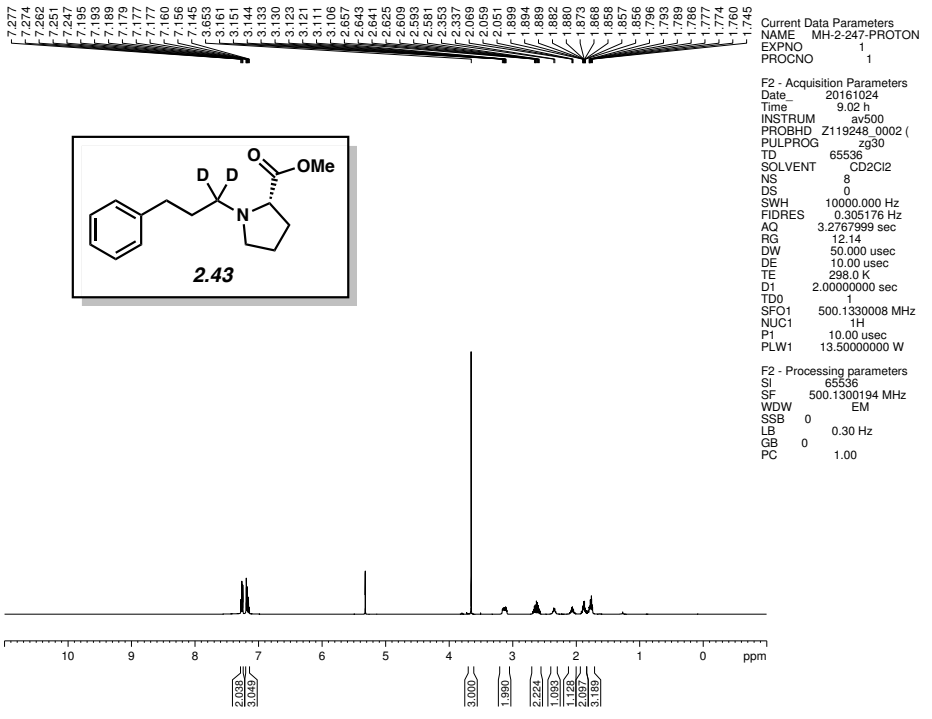

Figure 2.57 ^{1}H NMR (500 MHz, CD_2Cl_2) of compound **2.43**.

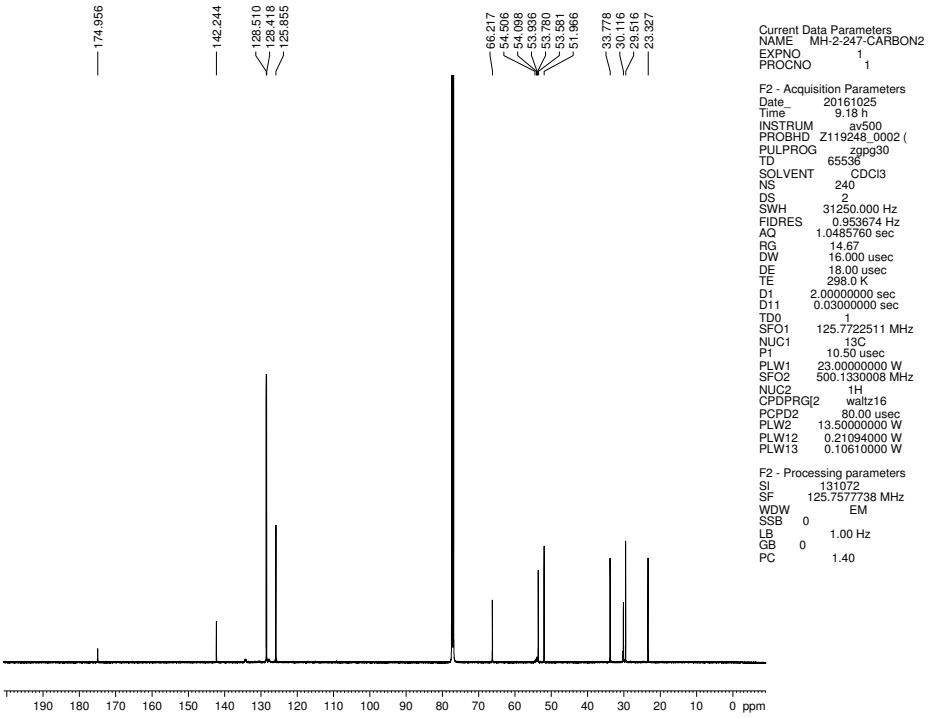

Figure 2.58 ^{13}C NMR (125 MHz, $CDCl_3$) of compound **2.43**.

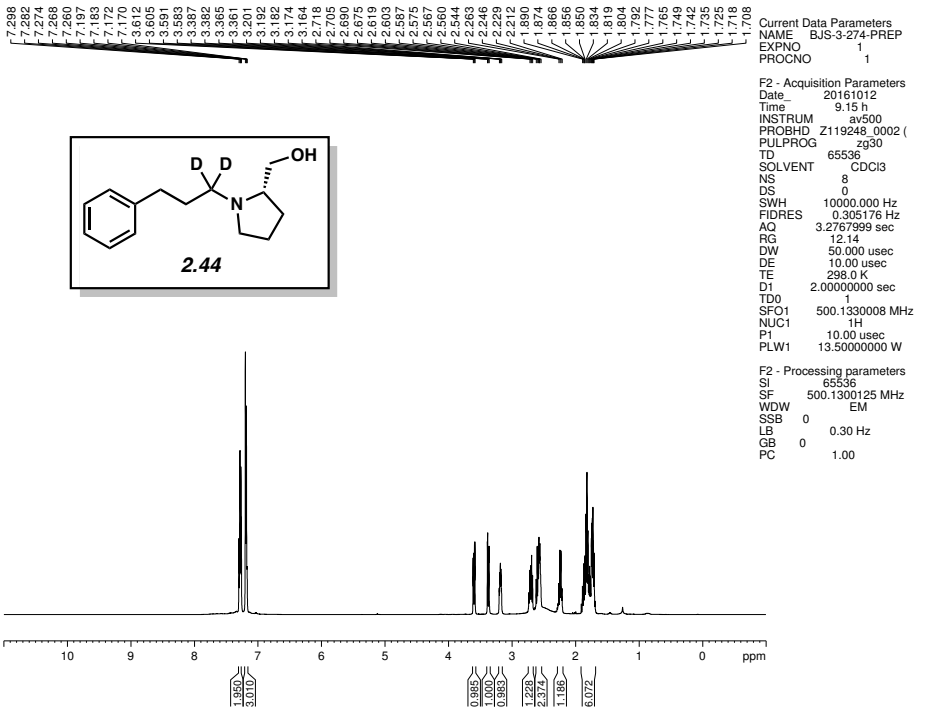

Figure 2.59 ^{1}H NMR (500 MHz, $CDCl_3$) of compound **2.44**.

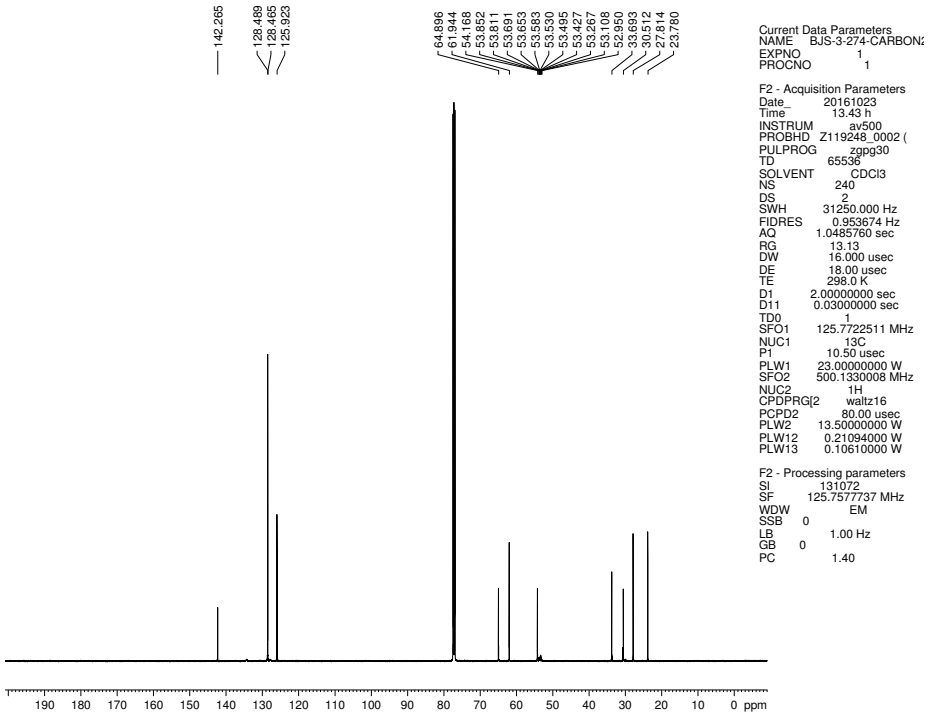

Figure 2.60 ^{13}C NMR (125 MHz, $CDCl_3$) of compound **2.44**.

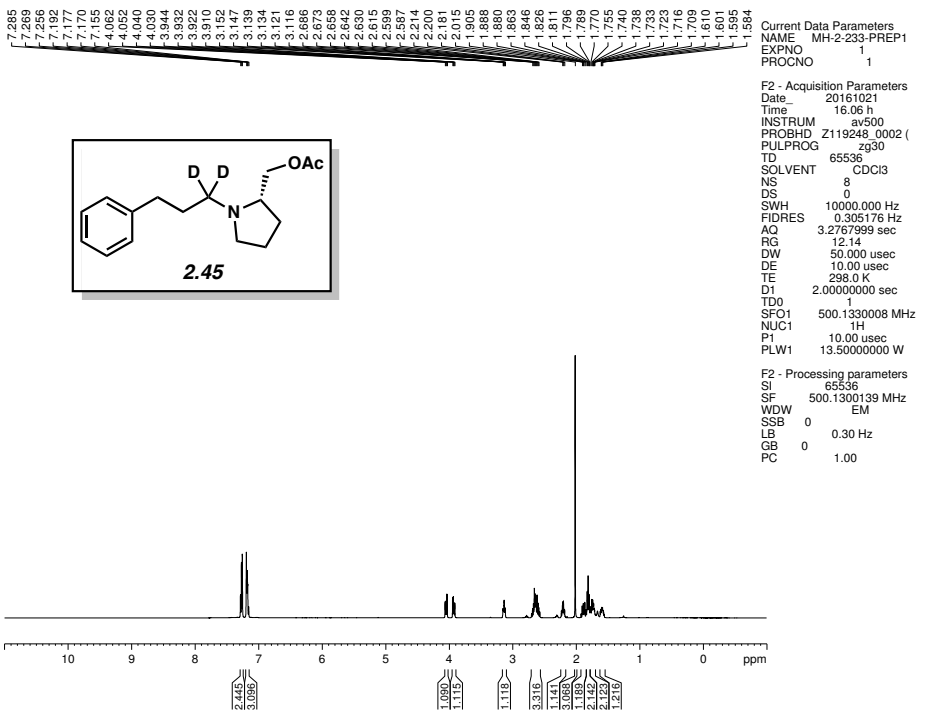

Figure 2.61 ^{1}H NMR (500 MHz, $CDCl_3$) of compound **2.45**.

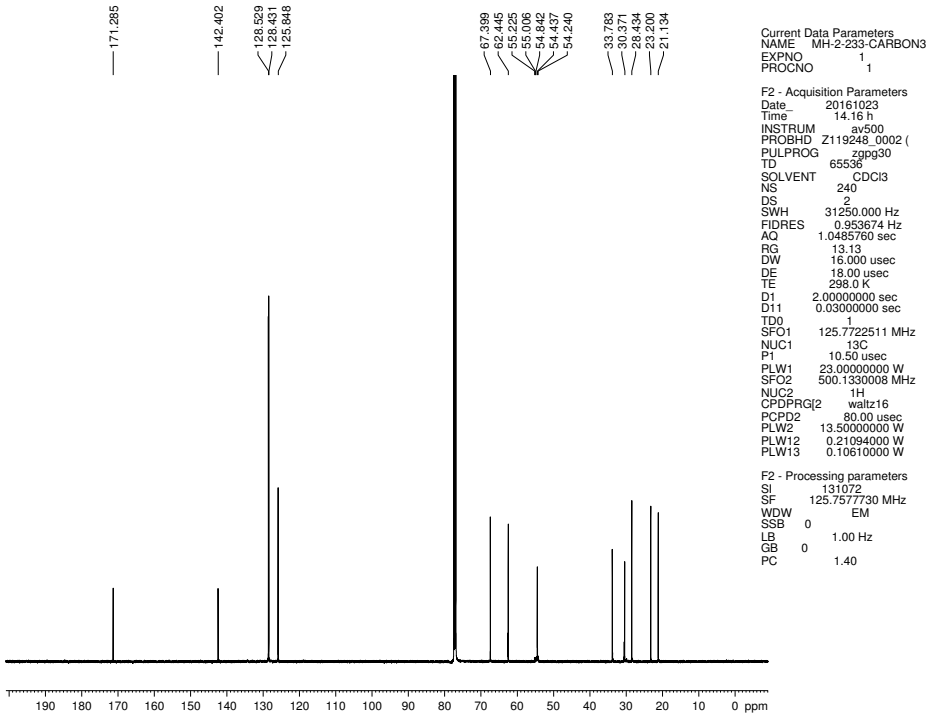

Figure 2.62 ^{13}C NMR (125 MHz, $CDCl_3$) of compound **2.45**.

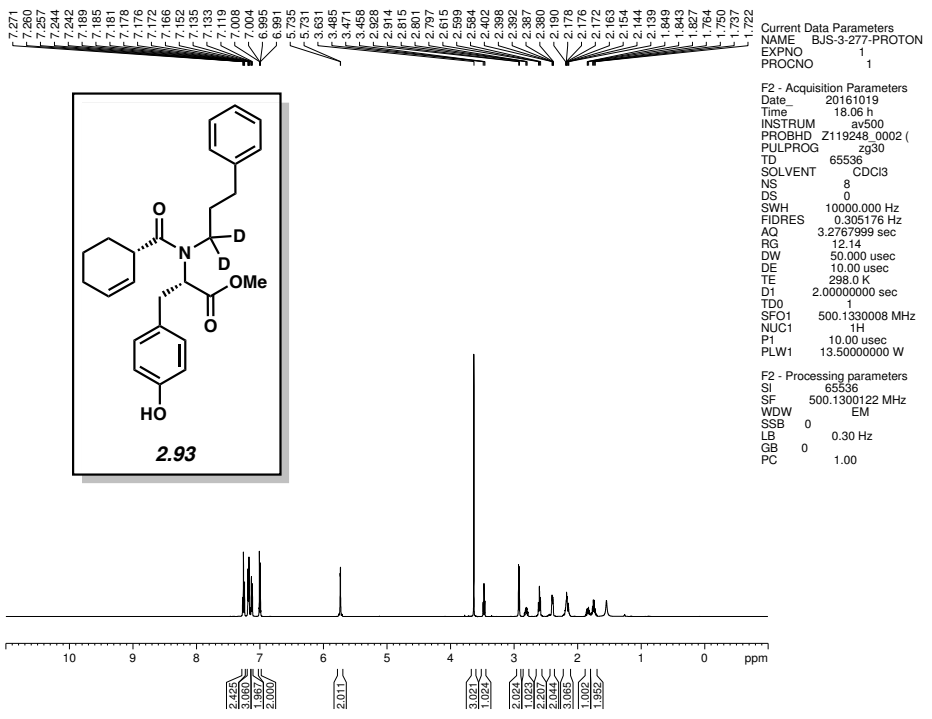

Figure 2.63 ^{1}H NMR (500 MHz, $CDCl_3$) of compound **2.93**.

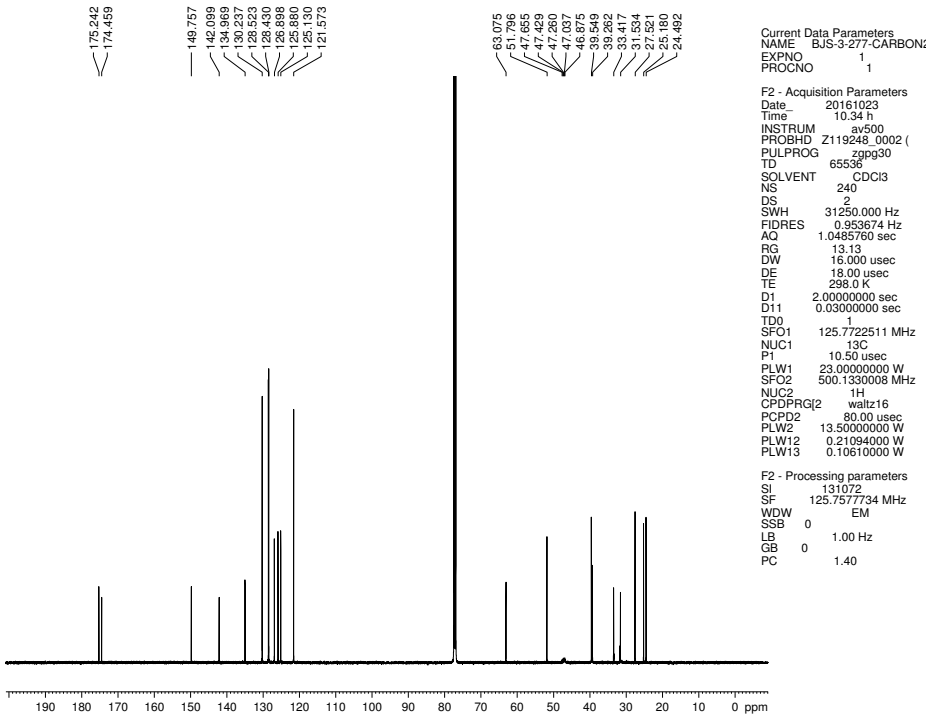

Figure 2.64 ^{13}C NMR (125 MHz, $CDCl_3$) of compound **2.93**.

2.11 Notes and References

(1) (a) Hie, L.; Fine Nathel, N. F.; Shah, T.; Baker, E. L.; Hong, X.; Yang, Y.-F.; Liu, P.; Houk, K. N.; Garg, N. K. *Nature* **2015**, *524*, 79–83. (b) Weires, N. A.; Baker, E. L.; Garg, N. K. *Nat. Chem*. **2016**, *8*, 75–79. (c) Baker, E. L.; Yamano, M. M.; Zhou, Y.; Anthony, S. M.; Garg, N. K. *Nat. Commun*. **2016**, *7*, 11554. (d) Simmons, B. J.; Weires, N. A.; Dander, J. E.; Garg, N. K. *ACS Catal*. **2016**, *6*, 3176–3179. (e) Dander, J. E.; Weires, N. A.; Garg, N. K. *Org. Lett*. **2016**, *18*, 3934–3936. (f) Hie, L.; Baker, E. L.; Anthony, S. M.; Desrosiers, J.-N.; Senanayake, C.; Garg, N. K. *Angew. Chem., Int. Ed.* **2016**, *55*, 15129–15132.

(2) For nickel-catalyzed amide C–N bond activation studies from other labs, see: (a) Hu, J.; Zhao, Y.; Zhang, Y.; Shi, Z. *Angew. Chem., Int. Ed.* **2016**, *55*, 8718–8722. (b) Shi, S.; Meng, G.; Szostak, M. *Angew. Chem., Int. Ed.* **2016**, *55*, 6959–6963. (c) Shi, S.; Szostak, M. *Chem. Eur. J.* **2016**, *22*, 10420–10424. (d) Shi, S.; Szostak, M. *Org. Lett.* **2016**, *18*, 5872–5875. (e) Liu, L.; Chen, P.; Sun, Y.; Wu, Y.; Chen, S.; Zhu, J.; Zhao, Y. *J. Org. Chem.* **2016**, *81*, 11686–11696. (f) Dey, A.; Sasmal, S.; Seth, K.; Lahiri, G. K.; Maiti, D. *ACS Catal.* **2017**, *7*, 433–437.

(3) For palladium-catalyzed amide C–N bond activation, see: (a) Meng, G.; Szostak, M. *Org. Lett.* **2015**, *17*, 4364–4367. (b) Meng, G.; Szostak, M. *Org. Biomol. Chem.* **2016**, *14*, 5690–5705. (c) Liu, C.; Meng, G.; Liu, Y.; Liu, R.; Lalancette, R.; Szostak, R.; Szostak, M. *Org. Lett.* **2016**, *18*, 4194–4197. (d) Meng, G.; Szostak, M. *Angew. Chem., Int. Ed.* **2015**, *54*, 14518–14522. (e) Meng, G.; Shi, S.; Szostak, M. *ACS Catal.* **2016**, *6*, 7335–7339. (f) Liu, C.; Meng, G.; Szostak, M. *J. Org. Chem.* **2016**, *81*, 12023–12030. (g) Li, X.; Zou, G. *Chem. Commun.* **2015**, *51*, 5089–5092. (h) Li, X.; Zou, G. *J. Organomet. Chem.* **2015**, *794*, 136–145. (i) Yada, A.; Okajima, S.; Murakami, M. *J. Am. Chem. Soc.* **2015**, *137*, 8708–8711. (j) Lei, P.; Meng, G.; Szostak, M. *ACS*

Catal. **2017**, *7*, 1960–1965. (k) Cui, M.; Wu, H.; Jian, J.; Wang, H.; Liu, C.; Daniel, S.; Zeng, Z. *Chem. Commun.* **2016**, *52*, 12076–12079. (l) Liu, C.; Liu, Y.; Liu, R.; Lalancette, R.; Szostak, R.; Szostak, M. *Org. Lett.* **2017**, *19*, 1434–1437.

(4) (a) Meng, G.; Shi, S.; Szostak, M. *Synlett* **2016**, *27*, 2530–2540. (b) Dander, J. E.; Garg, N. K. *ACS Catal.* **2017**, *7*, 1413–1423.

(5) Amides are considered to be ideally suited for use as synthons in chemical synthesis. For select recent examples involving amide directing groups in transition metal-catalyzed methodologies, see: (a) Topczewski, J. J.; Cabrera, P. J.; Saper, N. I.; Sanford, M. S. *Nature* **2016**, *531*, 220–224. (b) He, J.; Jiang, H.; Takise, R.; Zhu, R.-Y.; Chen, G.; Dai, H.-X.; Murali Dhar, T. G.; Shi, J.; Zhang, H.; Cheng, P. T. W.; Yu, J.-Q. *Angew. Chem., Int. Ed*. **2016**, *55*, 785–789. (c) Gurak Jr., J. A.; Yang, K. S.; Liu, Z.; Engle, K. M. *J. Am. Chem. Soc.* **2016**, *138*, 5805–5808. (d) Zhang, X.-G.; Dai, H.-X.; Wasa, M.; Yu, J.-Q. *J. Am. Chem. Soc*. **2012**, *134*, 11948–11951. (e) Shang, R.; Ilies, L.; Nakamura, E. *J. Am. Chem. Soc.* **2015**, *137*, 7660–7663. (f) Matsubara, T.; Ilies, L.; Nakamura, E. *Chem. Asian J.* **2016**, *11*, 380–384. (g) Yokota, A.; Aihara, Y.; Chatani, N. *J. Org. Chem*. **2014**, *79*, 11922–11932. (h) Fruchey, E. R.; Monks, B. M.; Cook, S. P. *J. Am. Chem. Soc*. **2014**, *136*, 13130–13133. (h) Roane, J.; Daugulis, O. *Org. Lett.* **2013**, *15*, 5842–5845. (i) Nishino, M.; Hirano, K.; Satoh, T.; Miura, M. *Angew. Chem., Int. Ed. **2013, 52,*** 4457–4461.

(6) For reviews on amides as directing groups in ortho-metalation, see: (a) Whisler, M. C.; MacNeil, S.; Snieckus, V.; Beak, P. *Angew. Chem., Int. Ed*. **2004**, *43*, 2206–2225. (b) Snieckus, V. *Chem. Rev*. **1990**, *90*, 879–933. (c) Beak, P.; Snieckus, V. *Acc. Chem. Res*. **1982**, *15*, 306–312.

(7) (a) Rosen, B. M.; Quasdorf, K. W.; Wilson, D. A.; Zhang, N.; Resmerita, A.-M.; Garg, N. K.; Percec, V. *Chem. Rev*. **2011**, *111*, 1346−1416. (b) Tasker, S. Z.; Standley, E. A.; Jamison, T. F. *Nature* **2014**, *509*, 299−309. (c) Mesganaw, T.; Garg, N. K. *Org. Process Res. Dev.* **2013**, *17*, 29−39. (d) Ananikov, V. P. *ACS Catal*. **2015**, *5*, 1964−1971.

(8) For recent breakthroughs (non-nickel), see the following and references therein: (a) Zhou, S.; Junge, K.; Addis, D.; Das, S.; Beller, M. *Angew. Chem., Int. Ed.* **2009**, *48*, 9507–9510. (b) Das, S.; Addis, D.; Zhou, S.; Junge, K.; Beller, M. *J. Am. Chem. Soc.* **2010**, *132*, 1770–1771. (c) Nakatani, N.; Hasegawa, J.-Y., Sunada, Y.; Nagashima, H. *Dalton Trans.* **2015**, *44*, 19344–19356. (d) Tennis, F.; Volkov, A.; Slagbrand, T.; Adolfsson, H. *Angew. Chem., Int. Ed.* **2016**, *55*, 4562–4566. (e) Das S.; Join B.; Junge, K.; Beller, M. *Chem. Commun.* **2012**, *48*, 2683–2685.; (f) Das S.; Addis D.; Junge K.; Beller M. *Chem. Eur. J.* **2011**, *17*, 12186–12191. (g) Cabrero-Antonino, J.R.; Alberico, E.; Junge, K.; Junge, H.; Beller, M. *Chem. Sci.* **2016**, *7*, 3432-3442. (h) Reeves, J. T.; Tan, Z.; Marsini, M. A.; Han, Z. S.; Xu, Y.; Reeves, D. C.; Lee, H.; Lu, B. Z.; Senanayake, C. H. *Adv. Synth. Catal.* **2013**, *355*, 47–52. (i) Xie, W.; Zhao, M.; Cui, C. *Organometallics* **2013**, *32*, 7440–7444. (j) Pelletier, G.; Bechara, W. S.; Charette, A. B. *J. Am. Chem. Soc.* **2010**, *132*, 12817–12819. (k) Sunada, Y.; Kawakami, H.; Imaoka, T.; Motoyama, Y.; Nagashima, H. *Angew. Chem., Int. Ed.* **2009**, *48*, 9511–9514. (l) Fernandes A. C.; Romão, C. C. *J. Mol. Catal. A: Chem.* **2007**, *272*, 60–63. (m) Zhang, T.; Zhang, Y.; Zhang, W.; Luo, M. *Adv. Synth. Catal.* **2013**, *355*, 2775–2780.

(9) Beller's report includes one example pertaining to the reduction of a secondary amide (*N*-Me-benzamide).

(10) (a) Smith, M. E.; Adkins, H. *J. Am. Chem. Soc.* **1938**, *60*, 407–409. (b) Ovakimian, G.; Christman, C. C.; Kuna, M.; Levene, P. A. *J. Biol. Chem.* **1940**, *134*, 151–161. (c) Witkop, B. *J. Am. Chem. Soc.* **1949**, *71*, 2559–2566. (d) Riebsomer, J. L. *J. Org. Chem.* **1950**, *15*, 68–73. (e) Rault, S.; Sevricourt, C. D.; Robba, M. *Heterocycles* **1979**, *12*, 1009–1011.

(11) For the reduction of imides using Raney nickel and H_2, see: (a) Adkins, H.; Cramer, H. I. *J. Am. Chem. Soc.* **1930**, *52*, 4349–4358. (b) Paden, J. H.; Adkins, H. *J. Am. Chem. Soc.* **1936**, *58*, 2487–2499. (c) Arévalo, A.; Ovando-Segovia, S.; Flores-Alamo, M.; García, J. J. *Organometallics* **2013**, *32*, 2939–2943.

(12) Mamillapalli, N. C.; Sekar, G. *Chem. Commun.* **2014**, *50*, 7881–7884.

(13) For a discussion regarding deuterated drugs, see: Mullard, A. *Nature Reviews Drug Discovery* **2016**, *15*, 219–221.

(14) Attempts to reduce primary amides, such as benzamide, led to decomposition of the starting material.

(15) Performing the reaction at lower temperature and in solvents other than toluene led to decreased yield of the reduced product.

(16) Two equivalents of $PhSiH_3$ enabled the reduction of most substrates and was therefore used in most experiments. Altering the silane (e.g., Ph_2SiH_2, Ph_3SiH, PHMDS, Et_3SiH) proved detrimental to the yield of amine **2.4**.

(17) Numerous nickel(II) pre-catalyst (e.g., $NiBr_2$, $NiCl_2$, $Ni(acac)_2$, $NiCl_2{\bullet}H_2O$, $NiCl_2(PPh_3)_2$) were screened in the reduction of **2.3** with no appreciable decrease in yield seen.

(18) We recently reported the Ni-catalyzed esterification of amides using non-benzamide substrates, albeit with *N*-Boc groups for activation (ref 1f).

(19) The reduction of **2.3** was performed in the presence of galvinoxyl (1.0 equiv). The formation of the corresponding amine **2.4** was observed in 70% yield, which may indicate that a radical mechanism is not operative. Any further mechanistic conjecture would be premature at this stage.

(20) Nitriles were deemed incompatible with our methodology. Attempts to employ nitriles led to nonspecific decomposition.

(21) For select examples of lactam reduction in total synthesis, see: (a) Bonazzi, S.; Cheng, B.; Wzorek, J. S.; Evans, D. A. *J. Am. Chem. Soc.* **2013**, *135*, 9338–9341. (b) Petronijevic, F. R.; Wipf, P. *J. Am. Chem. Soc.* **2011**, *133*, 7704–7707. (c) Mewald, M.; Medley, J. W.; Movassaghi, M. *Angew. Chem., Int. Ed.* **2014**, *53*, 11634–11639. (d) Mercado-Marin, E. V.; Sarpong, R. *Chem. Sci.* **2015**, *6*, 5048–5052. (e) Beadle, J. D.; Powell, N. H.; Raubo, P.; Clarkson, G. J.; Shipman, M. *Synlett* **2016**, *27*, 169–172.

(22) The reduction of amino acid derivatives has previously been achieved using lithium aluminum deuteride, which led to global reduction and the formation of a-deutero aminoalcohols; see: Franchi, P.; Lucarini, M.; Mezzina, E.; Pedulli, G. F. *J. Am. Chem. Soc.* **2004**, *126*, 4343–4354.

(23) For examples of deuterium in pharmaceuticals, see: (a) Foster, A. B. *Trends Pharmacol. Sci.* **1984**, 524–527. (b) Kushner, D. J.; Baker, A.; Dunstal, T. G. *Can. J. Physiol. Pharmacol.* **1999**, *77*, 79–88. (c) Nelson, S. D.; Trager, W. F. *Drug Metab. Dispos.* **2003**, *31*, 1481–1498. (d) Sharma, R.; Strelevitz, T. J.; Gao, H.; Clark, A. J.; Schildknegt, K.; Obach, R. S.; Ripp, S. L.; Spracklin, D. K.; Tremaine, L. M.; Vaz, A. D. N. *Drug Metab. Dispos.* **2012**, *40*, 625–634. See also references therein.

(24) Fu, R.; Yang, Y.; Ma, Y.; Yang, F.; Li, J.; Chai, W.; Wang, Q.; Yuan, R. *Tetrahedron Lett.* **2015**, *56*, 4527–4531.

(25) Kosal, A. D.; Wilson, E. E.; Ashfeld, B. L. *Angew. Chem., Int. Ed.* **2012**, *51*, 12036–12040.

(26) Kulkami, S. S.; Hu, X.; Manetsch, R. *Chem. Commun.* **2013**, *49*, 1193–1195.

(27) Bavetsias, V.; Faisal, A.; Crumpler, S. et. al. *J. Med. Chem.* **2013**, *56*, 9122–9135.

(28) Caldwell, N.; Jamieson, C.; Simpson, I.; Watson, A. J. B. *Chem. Commun.* **2015**, *51*, 9495–9498.

(29) Chen. C.; Hong, S. K. *Org. Lett.* **2012**, *14*, 2992–2995.

(30) Lawrence, N.; Sebtl, S.; Pireddu, R. *Novel Rho Kinase Inhibitors and Methods of use*. U.S. Patent 20140179689A1, Oct. 4, 2012.

(31) Henry, C.; Bolien, D.; Ibanescu, B.; Bloodworth, S.; Harrowven, D. C.; Zhang, X.; Craven, A.; Sneddon, H. F.; Whitby, R. J. *Eur. J. Org. Chem.* **2015**, *7*, 1491–1499.

(32) Maki, T.; Ishihara, K.; Yamamoto, H. *Org. Lett.* **2006**, *8*, 1431–1434.

(33) Zampler, D.; Mamolo, M. G.; Laurin, E.; Florio, C.; Zanette, C.; Fermeglia, M.; Poscocco, P.; Paneni, M. S.; Prici, S.; Vio, L. *J. Med. Chem.* **2009**, *52*, 5380–5393.

(34) Soulé, J.-F.; Miyamura, H.; Kobayashi, S. *Chem. Asian J.* **2013**, *8*, 2614–2626.

(35) Lamar, A. A.; Liebeskind, L. S. *Tetrahedron Lett.* **2015**, *56*, 6034–6037.

(36) Yang, C.-C.; Tai, H.-M.; Sun, P.-J. *Synlett* **1997**, *7*, 812–814.

(37) Zhou, S.; Junge, K.; Addis, D.; Das, S.; Beller, M. *Angew. Chem., Int. Ed.* **2009**, *48*, 9507–9510.

(38) Xia, J.-J.; Li, X.-Y.; Zhang, S.-Z.; Liu, J.-Q.; Zhang, W.-M.; Yan, Y.-X.; Ding, Z.-T.; Qiu, M.-H. *Tetrahedron Lett.* **2014**, *55*, 2104–2106.

(39) Saito, Y.; Ouchi, H.; Takahata, H. *Tetrahedron* **2008**, *64*, 11129–11135.

(40) Toledo, H.; Pisarevsky, E.; Abramovich, A.; Szpilman, A. M. *Chem. Commun.* **2013**, *49*, 4367–4369.

(41) Watson, A. J. A.; Maxwell, A. C.; Williams, J. M. J. *Org. Lett.* **2009**, *11*, 2667–2670.

(42) Evans, D. A.; Borg, G.; Scheidt, K. A. *Angew. Chem., Int. Ed.* **2002**, *41*, 3188–3191.

(43) Kern, N.; Hoffmann, M.; Weibel, J.-M.; Pale, P.; Blanc, A. *Tetrahedron* **2014**, *70*, 5519–5531.

(44) Wheeler, P.; Vora, H. U.; Rovis, T. *Chem. Sci.* **2013**, *4*, 1674–1679.

(45) Bartuschat, A. L.; Wicht, K.; Heinrich, M. R. *Angew. Chem., Int. Ed.* **2015**, *54*, 10294–10298.

(46) Takaharu, T.; Naoki, H.; Masayuki, S.; Masaki, H. *Novel Biologically Active Compound Having Anti-Prolyl Endopeptidase Activity.* U.S. Patent 19864743616, Feb. 26, 1986.

(47) Dang, T. T.; Ramalingam, B.; Shan, S. P.; Seayad, A. M. *ACS Catalysis* **2013**, *3*, 2356–2540.

(48) Lee, O.-Y.; Law, K.-L.; Yang, D. *Org. Lett.* **2009**, *11*, 3302–3305.

(49) Cheng, C.; Brookhart, M. *J. Am. Chem. Soc.* **2012**, *134*, 11304–11307.

(50) Silvers, M. A.; Robertson, G. T.; Taylor, C. M.; Waldrop, G. L. *J. Med. Chem.* **2014**, *57*, 8947–8959.

(51) Das, S.; Join, B.; Junge, K.; Beller, M. *Chem. Commun.* **2012**, *48*, 2683–2685.

(52) Parks, B. W.; Gilbertson, R. D.; Domaille, D. W.; Hutchison, J. E. *J. Org. Chem.* **2006**, *71*, 9622–9627.

(53) Chao, B. T.; Kang, S. K. *Tetrahedron* **2005**, *61*, 5725–5734.

(54) Popov, Y. V.; Mokhov, V. M.; Tankabekyan, N. A. *Russ. J. Gen. Chem.* **2014**, *84*, 826–830.

(55) Salvatore, R. N.; Nagle, A. S.; Jung, K. W. *J. Org. Chem.* **2002**, *67*, 674–683.

(56) Moriya, T.; Yoneda, S.; Kawana, K.; Ikeda, R.; Konakahara, T.; Sakai, N. *J. Org. Chem.* **2013**, *78*, 10642–10650.

(57) Bélanger, G.; Doré, M.; Ménard, F.; Darsigny, V. *J. Org. Chem.* **2006**, *71*, 7481–7484.

(58) Li, S.; Huang, K.; Zhang, J.; Wu, W.; Zhang, X. *Org. Lett.* **2013**, *15*, 3078–3081.

(59) Jeong, J.; Lee, D.; Chang, S. *Chem. Commun.* **2015**, *51*, 7035–7038.

(60) Gooodman, C. A.; Janci, E. M.; Onwodi, O.; Simpson, C. C.; Hamaker, C. G.; Hitchcock, S. R. *Tetrahedron Lett.* **2015**, *56*, 4468–4471.

(61) Jorapur, Y. R.; Jeong, J. M.; Chi, D. Y. *Tetrahedron Lett.* **2006**, *47*, 2435–2438.

(62) Meuresch, M.; Westhues, S.; Leitner, W.; Klankermayer, J. *Angew. Chem., Int. Ed.* **2016**, *55*, 1392–1395.

(63) Egorov, M.; Delpech, B.; Aubert, G.; Cresteil, T.; Garcia-Alvarez, M. C.; Collin, P.; Marazano, C. *Org. Biomol. Chem.* **2014**, *12*, 1518–1524.

(64) Kumar, A.; Pandiakumar, A. K.; Samuelson, A. G. *Tetrahedron* **2014**, *70*, 3185–3190.

CHAPTER THREE

Computationally Assisted Mechanistic Investigation and Development of Pd-Catalyzed Asymmetric Suzuki–Miyaura and Negishi Cross-Coupling Reactions for Tetra-*ortho*-Substituted Biaryl Synthesis

Nitinchandra Dahyabhai Patel, Joshua D. Sieber, Sergei Tcyrulnikov, Bryan J. Simmons, Daniel Rivalti, Krishnaja Duvvuri, Yongda Zhang, Donghong A. Gao, Keith R. Fandrick, Nizar Haddad, Kendricks So Lao, Hari Prasad Reddy Mangunuru, Soumik Biswas, Bo Qu, Nelu Grinberg, Scott Pennino, Heewon Lee, Jinhua J. Song, B. Frank Gupton, Neil K. Garg, Marisa C. Kozlowski, and Chris H. Senanayake

ACS Catal. **2018**, *8*, 10190–10209.

3.1 Abstract

Metal-catalyzed cross-coupling reactions are extensively employed in both academia and industry for the synthesis of biaryl derivatives for applications to both medicine and material science. Application of these methods to prepare tetra-*ortho*-substituted biaryls leads to chiral atropisomeric products that introduces the opportunity to use catalyst-control to develop asymmetric cross-coupling procedures to access these important compounds. Asymmetric Pd-catalyzed Suzuki–Miyaura and Negishi cross-coupling reactions to form tetra-*ortho*-substituted biaryls were studied employing a collection of *P*-chiral dihydrobenzooxaphosphole (BOP) and dihydrobenzoazaphosphole (BAP) ligands. Enantioselectivities of up to 95:5 and 85:15 er were identified for the Suzuki–Miyaura and Negishi cross-coupling reactions, respectively. Unique ligands for the Suzuki–Miyaura reaction and the Negishi reaction were identified. A computational study on these Suzuki–Miyaura and Negishi cross-coupling reactions enabled an

understanding of the differences between the enantiodiscriminating events between these two cross-coupling reactions. These results support that enantioselectivity in the Negishi reaction results from the reductive elimination step, whereas all steps in the Suzuki–Miyaura catalytic cycle contribute to the overall enantioselection with transmetalation and reductive elimination providing the most contribution to the observed selectivities.

3.2 Introduction

Transition metal catalyzed sp^2–sp^2 cross-coupling is one of the most powerful and extensively utilized reactions in organic synthesis and materials science to access biaryl compounds.[1] Of these methods, the Pd-catalyzed Suzuki–Miyaura[2] and Negishi[3] cross-coupling have received considerable development over the past 40 years.[1,4] Significant advances in the development of highly active Pd-catalysts[5] to achieve efficient processes have even allowed for these reactions to be employed on industrial scale.[6] In general, bulky electron-rich phosphines[7] and *N*-heterocyclic carbenes[8,9] have been the ligands of choice to enable these cross-coupling reactions. Despite these advances, cross-coupling catalysts for the formation of sterically demanding biaryls, such as tetra-*ortho*-substituted systems, remains limited.[9] Additionally, because appropriately substituted tri- and tetra-*ortho*-substituted biaryls exist as chiral atropisomers about the biaryl axis, methods to forge this bond in an enantioselective fashion are important since many biologically active natural products[10] and potential pharmaceuticals[11] contain single atropisomeric biaryl groups within their structure (Figure 3.1). Therefore, one desirable strategy to access the biaryl functionality in these compounds is to utilize a catalyst-controlled asymmetric Suzuki–Miyaura or Negishi sp^2–sp^2 cross-coupling.[12] While transition metal catalyzed asymmetric Suzuki–Miyaura[13] and Negishi[14] sp^2–sp^2 cross-coupling reactions

have been developed, significantly fewer methods are available for the asymmetric construction of tetra-*ortho*-substituted biaryls.[13c,d,p-t,14,15]

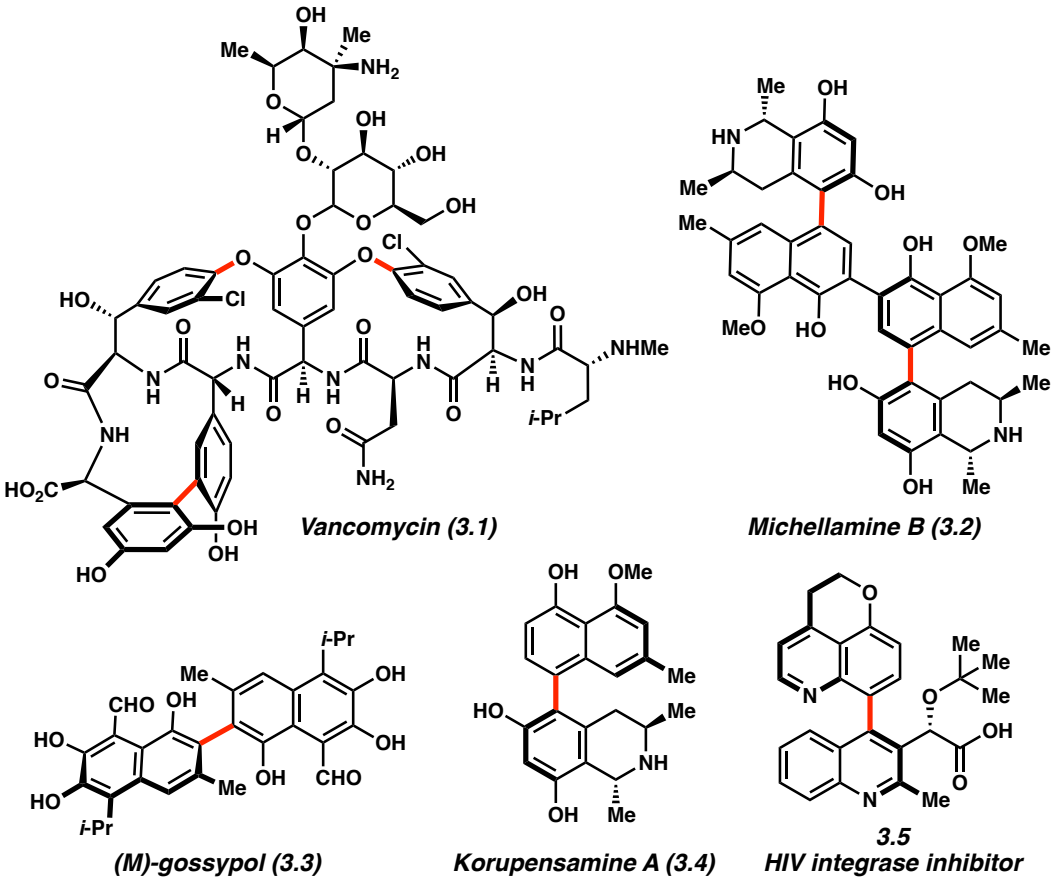

Figure 3.1 Natural products and bioactive atropisomeric compounds

The first highly enantioselective sp^2–sp^2 cross-coupling reaction was reported in 1988 by Hayashi and coworkers[15] to afford atopisomeric binaphthalenes in up to 95% ee using a Kumada–Corriu[16] coupling. It was not until the year 2000 that the first reports of Pd-catalyzed asymmetric Suzuki–Miyaura cross-coupling reactions were disclosed by the groups of Cammidge[13c,d] and Buchwald.[13a,b] Cammidge applied Hayashi's[15] chiral ferrocene ligand (PFNMe) to access tri-*ortho*-substituted biaryl **3.8a** with modest enantioselection (82:18 er, Table 3.1). At the same time, Buchwald discovered that KenPhos could be employed as the

chiral ligand affording high enantioselectivities in the cross-coupling if the R-substituent of the aryl halide coupling partner contained a Lewis basic donating group at the *ortho*-position (**3.8b-d**). Mechanistic studies on this class of cross-coupling by Buchwald[13b] and others[11b,13n,x] typically consider reductive elimination as the enantiodetermining event in the catalytic cycle and have shown that these Lewis basic *ortho*-substituents aid in the stabilization of the dominating transition state. However, restricted rotation of the intermediate Pd-complexes as a function of the *ortho*-substitution pattern of the aryl halide coupling partner can lead to scenarios where oxidative addition[13f] and transmetalation[13d,f] may be involved in enantioselection.[17] After these initial reports, intense research into the area of catalyst-controlled asymmetric biaryl synthesis by a variety of groups has led to the introduction of multiple chiral ligands that affect this transformation (Table 3.1).[11,13] The majority of these studies have focused on the investigation of the formation of tri-*ortho*-substituted binaphthalene derivatives.[11,13a,b,e-o,u-bb] Of these, asymmetric synthesis of the aryl phosphonate products (**3.8b**–**3.8d**) by asymmetric cross-coupling have been one of the more common systems studied between different chiral catalysts with variable results. [13a,b,j,n,u-y] For example, our group[11,13n,o] introduced the *P*-chiral dihydrobenzooxaphosphole (BOP) class of ligands (BIDIME, **3.9**, **3.10**) that are effective in asymmetric cross-coupling reactions and are highly tunable to enable ligand modification for enhancement of stereoselectivities. Suzuki–Miyaura cross-coupling to afford **3.8c** employing BOP ligand **3.9b**[13n] gave improved enantioselectivity to that of KenPhos;[13a] however, in the coupling to produce **3.8b**, KenPhos resulted in improved selectivity over ligand **3.9b**. These results highlight the fact that asymmetric cross-coupling reactions are typically very substrate dependent. Synthesis of **3.8b**–**3.8d** has also been acheived by asymmetric cross-coupling employing the atropisomeric, hemi-labile ligands Cy-MOP,[13w] **3.11**,[13u,x] and **3.12**,[13v] and using a

helically-chiral polymeric phosphine ligand (PQXPhos). [13i] Other ligand classes including chiral dienes (**3.13**),[13h] bis(hydrazones) (**3.14**),[13f] and a resin-supported chiral ligand (**3.15**)[13p] have all been shown to afford high enantioselectivities in certain asymmetric Suzuki–Miyaura cross-coupling reactions. Despite these significant advances in asymmetric cross-coupling methodologies, a general catalyst for a wide-array of substitution patterns is still an unsolved problem. However, these technologies have found utility in natural product[13k,o] and API synthesis (*e.g.* **3.5** *via* **3.8**).[11]

Table 3.1 Asymmetric Suzuki–Miyaura cross-coupling reactions to prepare tri-*ortho*-substituted biaryls.

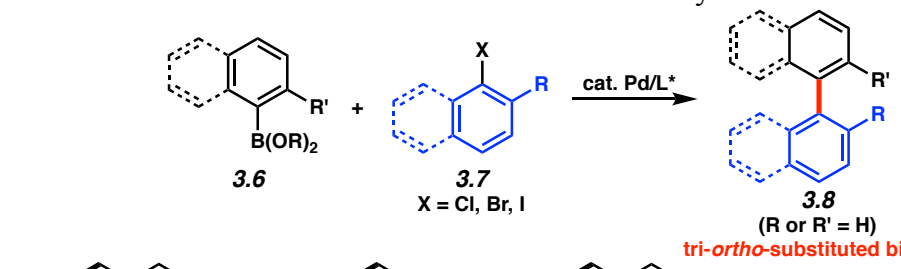

3.6 ***3.7*** X = Cl, Br, I ***3.8*** (R or R' = H) tri-*ortho*-substituted biaryls

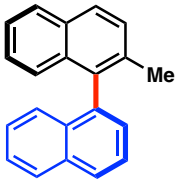

3.8a
(*S*,*R*)-PFNMe: 82:18 er
3.13: 5:95 er
3.14: 5:95 er

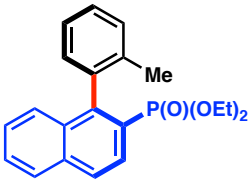

3.8b
(*R*)-KenPhos: 94:6 er
3.9b: 90:10 er
PQXPhos: 97:3 er
3.12a: 90:10 er

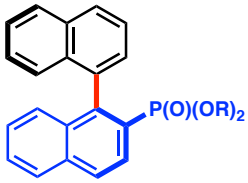

3.8c
(*R*)-KenPhos: 79:21 er
3.9b: 95:5 er
PQXPhos: 95:5 er
3.11: 94:6 er
3.12b: 84:16 er

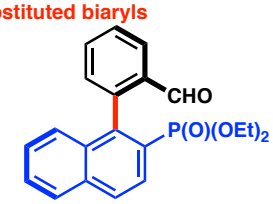

3.8d
(*R*)-Cy-MOP: 98:2 er

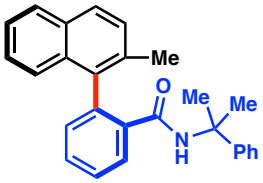

3.8e
(*S*)-KenPhos: 97:3 er

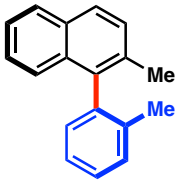

3.8f
3.13: 92:8 er
3.15: 96:4 er

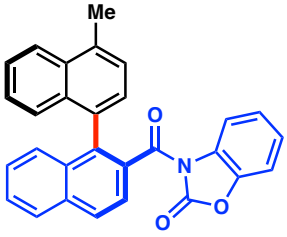

3.8g
3.9a: 98:2 er

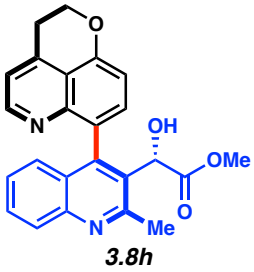

3.8h
(*S*)-BIDIME: 83:17 dr
(*R*)-BIDIME: 17:83 dr
(*S*)-***3.10***: 94:6 dr

Ligands:

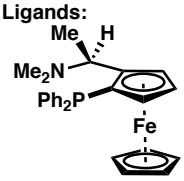

(*S*,*R*)-PFNMe

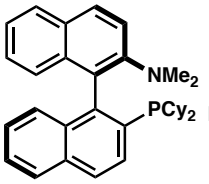

(*R*)-KenPhos

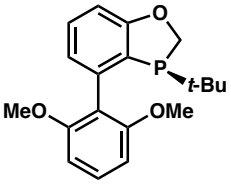

(*S*)-BIDIME

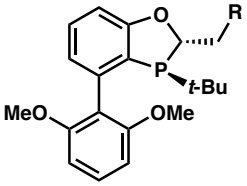

3.9a, R = H
3.9b, R = 1-napthyl

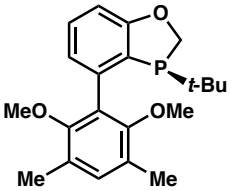

(*S*)-***3.10***

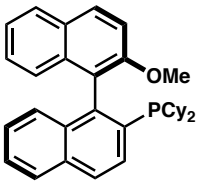

(*R*)-Cy-MOP

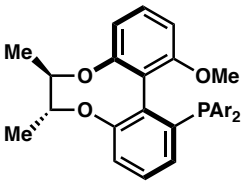

3.11
Ar = 3,5-di-t-BuPh

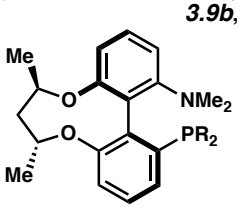

R = Cy: ***3.12a***
R = Ph: ***3.12b***

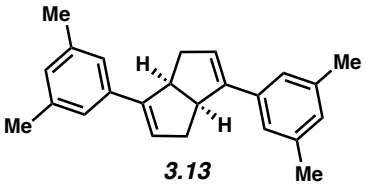

3.13

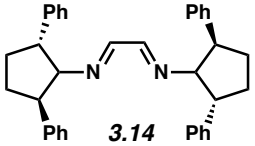

3.14

PQXPhos: helical chiral polymer

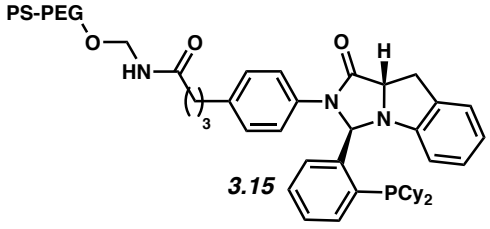

3.15

While asymmetric Suzuki–Miyaura cross-coupling to generate tri-*ortho*-substituted biaryls (Table 3.1) has been successful with a variety of chiral ligand types, [13a,b,e-o,u-bb] the synthesis of tetra-*ortho*-substituted biaryls by the same means has proven more difficult. [13c,d,p-t] Tetra-*ortho*-substituted biaryl product **3.18** (Table 3.2)[13c,d,p-q] has typically been the standard cross-coupling reaction analyzed when developing new catalysts for this challenging coupling.[12c] While the Ni-catalyzed Kumada–Corriu[16] coupling to prepare **3.18** was reported by Hayashi[15] with good enantioselectivity, the analogous Suzuki–Miyaura coupling has proven more challenging.[13c,d,p-t] Cammidge's initial report[13c,d] demonstrated that the PFNMe ligand gave good enantioselectivity (93:7 er) in this reaction; however, long reaction time (6 days) was required affording only modest yield (Table 3.2). Espinet[13r] was able to optimize this result to reduce the reaction time to 3 days at 5 mol % Pd loading by using $Pd_2(dba)_3$•$CHCl_3$ as the Pd-source in the presence of excess ligand (20 mol %) to improve the yield to 85%. The catalyst loading could be reduced to employ 3 mol % Pd and 12 mol % ligand by utilizing $Pd(MeCN)_4(BF_4)_2$ in place of $Pd_2(dba)_3$•$CHCl_3$ as the precatalyst with an improvement in enantioselectivity of up to 95:5 er. However, only 55% yield was obtained after 4 day reaction time. While these conditions can be applied to the synthesis of **3.18**, reaction times are still quite long (days), and the scope of the reaction to other substrates is limited or has not been further investigated. Of the catalytic systems reported for the synthesis of **3.16** by Suzuki–Miyaura cross-coupling, Uozumi's[13p] conditions employing resin-supported phosphine ligand **3.15** are performed in water under heterogeneous conditions that allow for recycling of the catalyst and show the most generality in terms of reaction scope and enantioselectivity; however, only simple substituted naphthalenes have been disclosed in the coupling. Recently there has been increased focus on the development of Suzuki–Miyaura cross-coupling reactions performed using water[18,19] as the solvent due to the

potential "greenness" of replacing typical organic solvents by water.[20,21] However, none of these methods have been extended to enantioselective cross-coupling. Uozumi's[13p] report represents the only known catalytic asymmetric cross-coupling carried out in neat water.[22] Future studies are needed in this area to determine if improvements in catalytic asymmetric coupling reactions can be achieved using water as solvent.

Table 3.2 Asymmetric Suzuki–Miyaura cross-coupling reactions to prepare tetra-*ortho*-substituted biaryls.

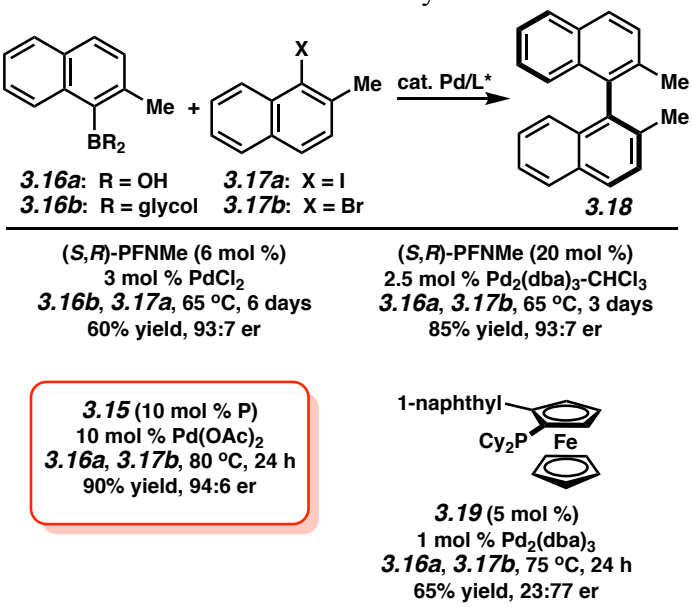

As noted above (Table 3.1), previous work in our laboratories identified the *P*-chiral dihydrobenzooxaphosphole (BOP) ligand class (BIDIME, **3.9**, **3.10**) as a highly tunable scaffold for applications in many different types of asymmetric transformations by modulating the substituents of ligand structure **3.23** (Scheme 3.1). By variation of the oxaphosphole C-2 R-substituent and the bis(alkoxy)phenyl aryl-group of ligand **3.23**, catalysts for Suzuki–Miyaura[7p-t,9a,19a,23] and asymmetric Suzuki–Miyaura[11,13n-o] cross-coupling, Buchwald–Hartwig amination,[24] borylation,[25] asymmetric propargylation of aldehydes[26] and imines,[27] asymmetric conjugate addition,[28] asymmetric addition of boronic acids to imines,[29] asymmetric allenylation of imines,[30]

asymmetric hydrogenation of polar[31] and unfunctionalized[32] alkenes, asymmetric hydrogenation of heterocycles,[33] asymmetric hydroformylation,[34] and asymmetric hydrogenation of ketones[35] have all been developed. Due to the lack of a general solution for the asymmetric synthesis of tetra-*ortho*-substituted biaryls using the Suzuki–Miyaura cross-coupling reaction, we sought to investigate application of ligand family **3.23** as a potential solution to this problem because of the modular nature of **3.23** and because of its good activity in the asymmetric cross-coupling to furnish tri-*ortho*-substituted biaryls.[11,13n,o] We disclose our studies towards the application of the dihydrobenzooxaphosphole (**3.23**, X = O, BOP) and dihydrobenzoazaphosphole (**3.23**, X = NR, BAP) ligand scaffold for both the asymmetric Pd-catalyzed Suzuki–Miyaura and Negishi cross-coupling reaction to form tetra-*ortho*-substituted biaryls (Scheme 3.1). The differences in the enantiodiscrimination mechanism between these two processes were probed computationally and are also disclosed herein.

Scheme 3.1 Tunable *P*-chiral phosphine ligands for asymmetric Pd-catalyzed cross-couplings.

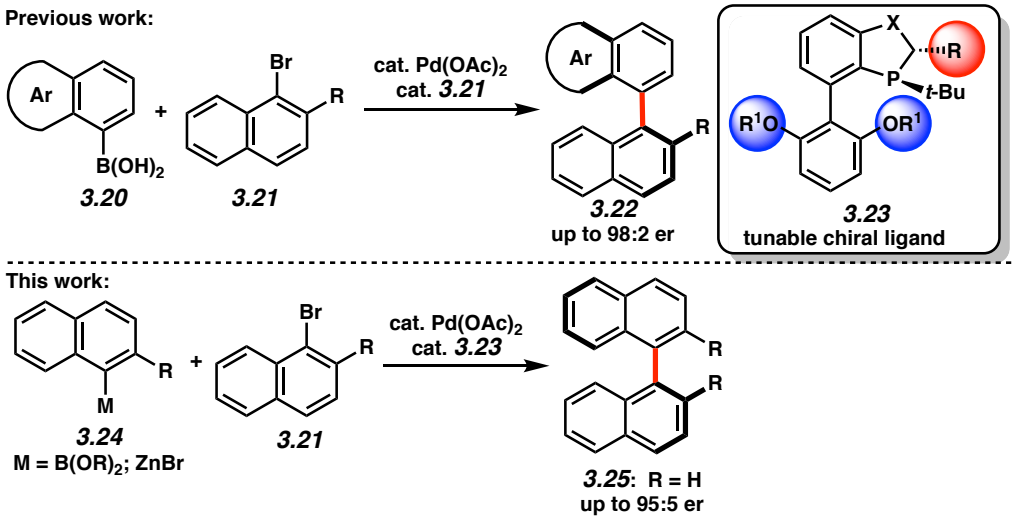

3.3 Ligand Synthesis

The ligands employed in the current study were prepared by the general strategy outlined in Scheme 3.2. Starting from the known *P*-chiral triflates (**3.26**, **3.27**),[13n,35b] Negishi[7t] or Suzuki–Miyaura cross-coupling was used to install the lower aryl ring of the ligand biaryl axis affording oxides **3.29** or **3.30**. Deprotonation of **3.29** or **3.30** with LDA followed by electrophilic trapping allowed for substitution of the C-2 position of the oxaphosphole or azaphosphole ring providing **3.31** or **3.32**, respectively. Oxide reduction then provided the final BOP (X = O) or BAP (X = NR) ligands (**3.33**). Additionally, the 3,5-positions of the lower aryl ring of the biaryl group of **3.34** can be functionalized by bromination[11b] to afford **3.35** followed by cross-coupling and alkylation to afford ligand family **3.36**. These procedures have enabled the synthesis of a tunable family of *P*-chiral phosphine ligands. The ligands prepared and used in this study are shown in Figure 3.2.

Scheme 3.2 Ligand synthesis.

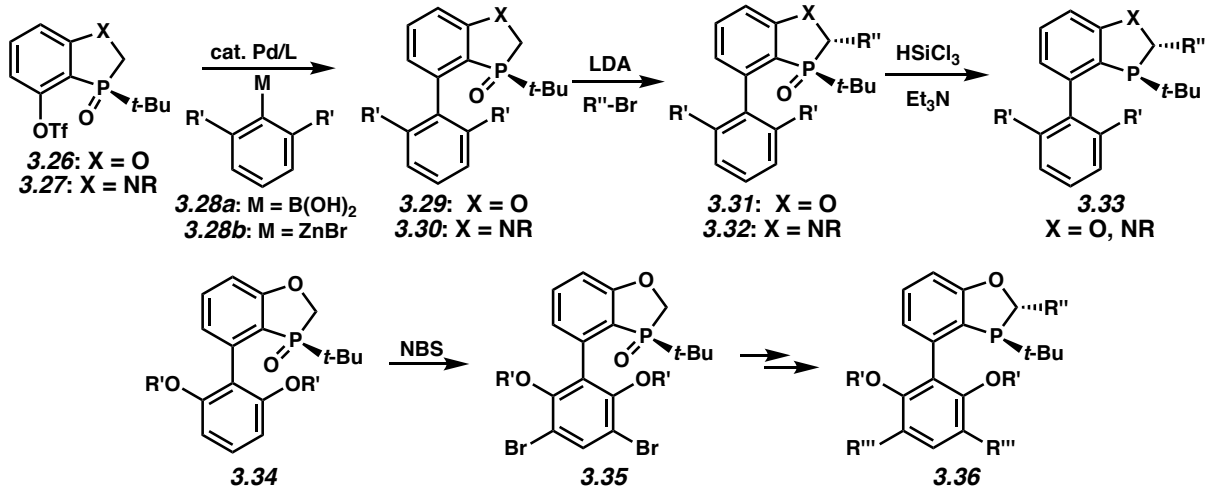

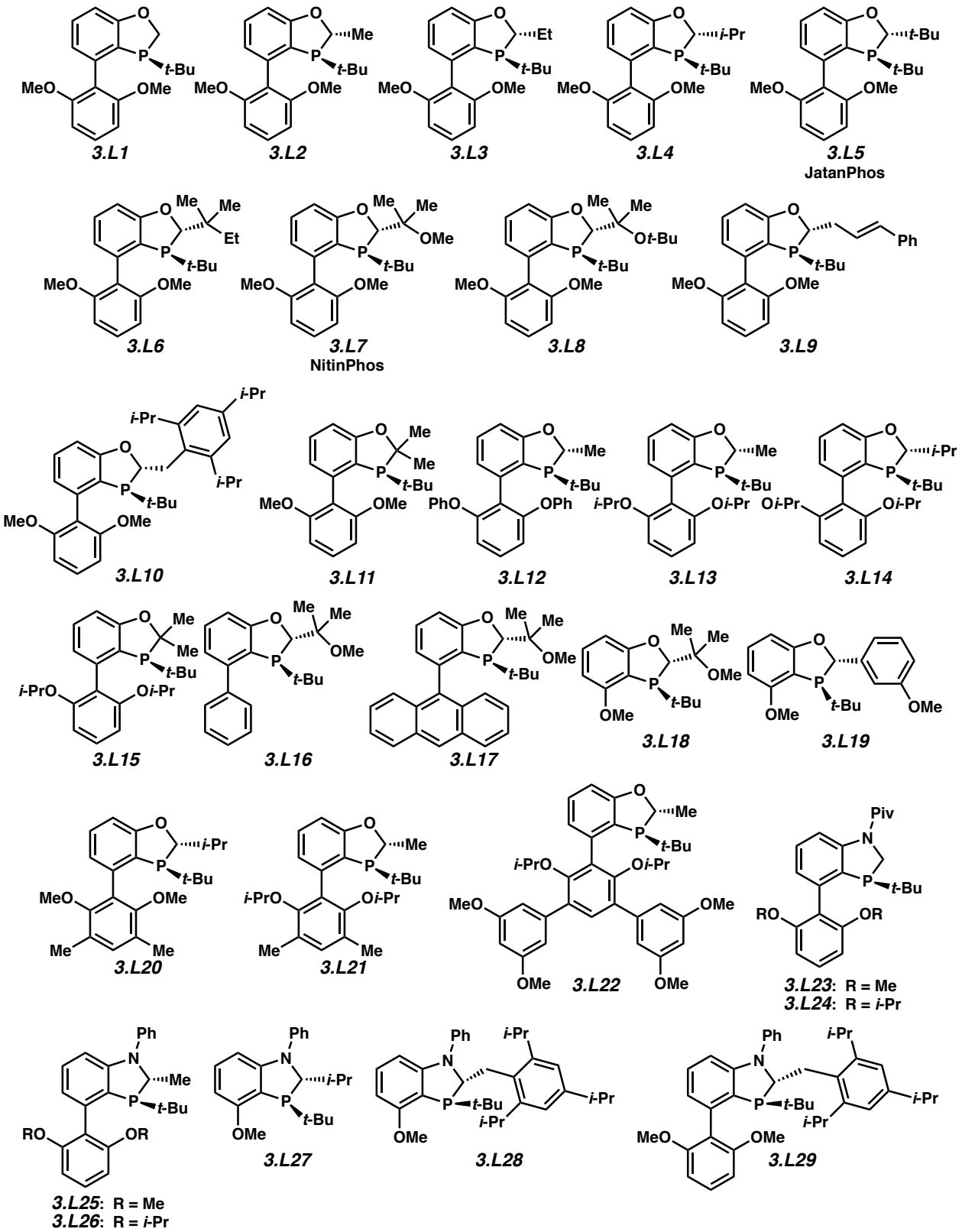

Figure 3.2 Ligands used in this study.

3.4 Asymmetric Suzuki–Miyaura Cross-Coupling

To investigate the Suzuki–Miyaura cross-coupling to prepare tetra-*ortho*-substituted biaryls, we initially examined the "benchmark"[12c] cross-coupling reaction to form tetra-*ortho*-substituted biaryl compound **3.18** (Table 3.3) employing 1-bromo-2-methylnaphthalene (**3.17b**) and (2-methylnaphthalen-1-yl)boronic acid (**3.16a**) as the coupling partners. Initial experiments probed conditions that previously were shown to be suitable for hindered cross-coupling reactions (Entries 1 – 3). These consisted of the use of K_3PO_4 as base and employing BIDIME (**3.L1**), AntPhos, or C2-*i*-Pr-BIDIME (**3.L4**) as the ligand. Gratifyingly, under these conditions, product **3.18** was observed. While almost no enantioinduction was observed using BIDIME (**3.L1**) or AntPhos, which lack substitution at the C-2 position of the oxaphosphole ring (entries 1 and 2), C2-*i*-Pr-BIDIME (**3.L4**) afforded modest enantioselectivity and yield in the reaction (entry 3). As has been previously noted for reactions forming tetra-*ortho*-substituted biaryls,[13d,r] protodeboronation was a significant side-reaction that prevented the coupling from proceeding to full conversion. To circumvent this issue, alternate bases were examined in an effort to reduce protodeboronation; however, no improvements over the use of K_3PO_4 were identified (entries 3 – 8). Additionally, solvents such as toluene and 1,4-dioxane were found to be equally effective in the coupling and did not improve enantioselectivity or yield (entries 9 and 10). Finally, to achieve full reaction conversion, the effect of catalyst loading was examined (entries 11 – 14). Use of 5 mol% Pd was needed to achieve full conversion and allowed for high yield in the desired reaction (entry 13). Addition of water as a co-solvent to these reactions when employing THF or *n*-BuOH as solvent afforded < 10% yield of product due to significant amounts of protodeboronation (data not shown) that is not uncommon considering that the addition of excess water is often avoided in sterically demanding and asymmetric cross-coupling reactions.[9,13]

Table 3.3 Asymmetric Suzuki–Miyaura cross-coupling towards tetra-*ortho*-substituted biaryls: base and solvent survey.

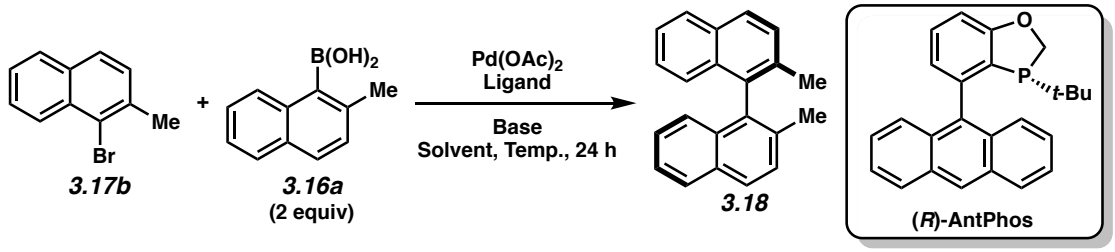

Entry	Mol % Pd	Ligand (mol%)	Base (3 equiv)	Solvent	%Yield[a]	er[b]
1	1	**3.L1** (2)	K_3PO_4	THF	40	55:44
2	1	(*R*)-AntPhos (2)	K_3PO_4	THF	30	50:50
3	1	**3.L4** (2)	K_3PO_4	THF	50	86:14
4	1	**3.L4** (2)	CsF	THF	18	ND
5	1	**3.L4** (2)	KF	THF	< 5	ND
6	1	**3.L4** (2)	K_2CO_3	THF	9	ND
7	1	**3.L4** (2)	Na_2CO_3	THF	< 2	ND
8	1	**3.L4** (2)	NaO*t*-Bu	THF	< 3	ND
9	1	**3.L4** (2)	K_3PO_4	Toluene	48	85:15
10	1	**3.L4** (2)	K_3PO_4	1,4-dioxane	50	85.5: 14.5
11	3	**3.L4** (6)	K_3PO_4	THF	64	86:14
12	3	**3.L4** (6)	K_3PO_4	Toluene	56	85:15
13	**5**	**3.L4 (10)**	**K_3PO_4**	**THF**	**90**	**86:14**
14	5	**3.L4** (10)	K_3PO_4	Toluene	85	85:15

[a]Isolated yield. [b]Determined by chiral HPLC analysis with Chiralpak OD-H column.

With moderate conditions in hand for the Suzuki–Miyaura cross-coupling reaction (Table 3.3, entry 13), we next attempted to modify the ligand structure to improve enantioselection (Table 3.4). The substitution at the C-2 position of the oxaphosphole ring of the ligand was first examined (entries 1–6). This enabled the identification of a ligand that provided enantioselectivities of up to 95:5 er when a dimethylmethoxy (DMM) substituent was at the C-2 position of the oxaphosphole ring (**3.L7**, NitinPhos, entry 4). Furthermore, it was critical that the ligand contained a dimethoxyphenyl ring as part of the biaryl axis of the ligand. When this group was replaced with phenyl, anthracene, or methoxy, inferior yields and selectivities were obtained (entry 4 *vs* entries 9–11). The importance of the lower dimethoxyphenyl ring in enhancing

enantioselectivities through an interaction between one methoxy-group and Pd has been postulated previously,[11b,13n] and is further supported by DFT modeling of this system (*vide infra*). Replacement of the methoxy-groups on this lower aryl ring with *iso*-propoxy groups afforded no improvement (entry 1 *vs* entries 7–8).

Table 3.4 Ligand survey in the asymmetric Suzuki–Miyaura cross-coupling towards tetra-*ortho*-substituted biaryls.

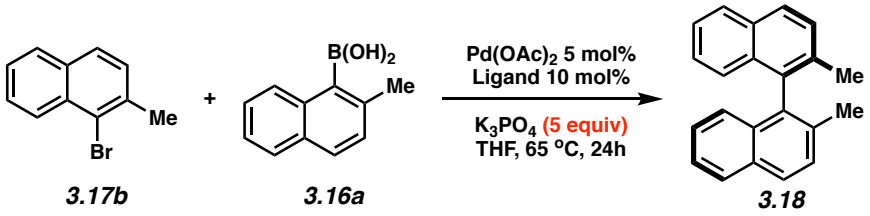

3.17b ***3.16a*** (5 equiv) ***3.18***

	Ligand	% yield[a]	er[b]
1	**3.L4**	92	86:14
2	**3.L5**	80	90:10
3	**3.L6**	75	86:14
4	**3.L7**	**97**	**94.5:5.5**
5	**3.L8**	45	81.5:18.5
6	**3.L10**	91	83:17
7	**3.L13**	73	84.5:15.5
8	**3.L14**	75	83:17
9	**3.L16**	75	73:27
10	**3.L17**	35	88:12
11	**3.L18**	50	64:36
12	**3.L20**	89	78:22

[a]Isolated yield. [b]Determined by chiral HPLC analysis with Chiralpak OD-H column.

The effect of Pd-precatalyst and Pd:ligand loading was next examined (Table 3.5). The use of excess ligand enabled the highest reaction yield (entry 1 *vs* 2). Additionally, $Pd(OAc)_2$ gave less side-product formation than compared to the use of $Pd_2(dba)_3$ or $[PdCl(allyl)]_2$ (entry 2 *vs* entries 3–4).

Table 3.5 Effect of Pd-precatalyst and Pd:ligand loading.

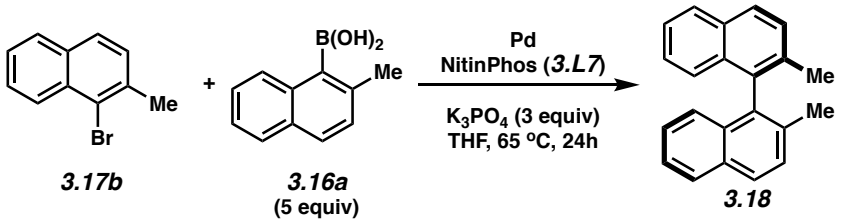

3.17b ***3.16a*** (5 equiv) ***3.18***

	Pd Source (mol %)	Mol % **L7**	% yield[a]	er[b]
1	$Pd(OAc)_2$ (5)	10	97%	94.5:5.5
2	$Pd(OAc)_2$ (5)	5	75%[c]	94.5:5.5
3	$Pd_2(dba)_3$ (2.5)	5	64%[d]	94:6
4	$[PdCl(allyl)]_2$ (5)	5	55%[e]	93.7:6.3

[a]Isolated yield. [b]Determined by chiral HPLC analysis with Chiralpak OD-H column. [c]1-2% side products were observed with 23 % of bromide substrate remaining, [d]5-7% side products were observed with 29% of bromide substrate, [e]8-9% side products were observed with 35% of bromide substrate.

In an effort to further reduce the loading of the boron coupling partner, we next examined other boron derivatives in the coupling reaction in an effort to reduce protodeboronation side-reactions (Table 3.6). Use of the glycol ester (**3.16b**) that was optimal in Cammidge's system[13d] and has been recently shown to give improved transmetalation rates in Suzuki–Miyaura cross-coupling reactions[30] gave similar enantioselectivities as that observed with boronic acid **3.16a** but did not afford full conversion in the reaction, even at prolonged reaction times. Use of the pinacol ester **3.16c** allowed for reduction of the boron coupling partner to 2 equiv; however, long reaction times were required and a slight loss in enantiopurity was obtained. The change in enantioselectivity based off of the nature of the boronate[36] employed has been observed previously[13d] and hints that the transmetalation step in the catalytic cycle for this reaction may be involved in the enantiodeterming event (*vide infra*). Finally, use of the potassium trifluoroborate salt (**3.16d**), which are known for their resistance to protodeboronation,[37] was not effective in the cross-coupling reaction.

Table 3.6 Effect of boronate coupling partner.

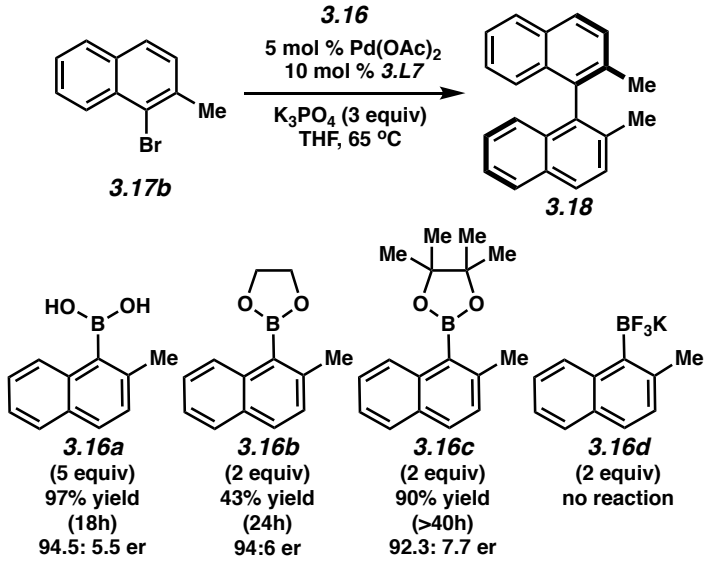

With identification of a reactive catalytic system to form tetra-*ortho*-substituted biaryl product **3.18** with good enantioselectivities, the scope of this catalytic system was then briefly examined (Table 3.7). Unfortunately, it was quickly determined that the present system did not show good generality, as has been a common problem in asymmetric Pd-catalyzed Suzuki–Miyaura reactions providing tetra-*ortho*-substituted biaryls. Even subtle modification to the coupling partners led to decreased reaction efficiency due to increased amounts of protodeboronation.

Table 3.7 Asymmetric Suzuki–Miyaura cross-coupling reaction scope.

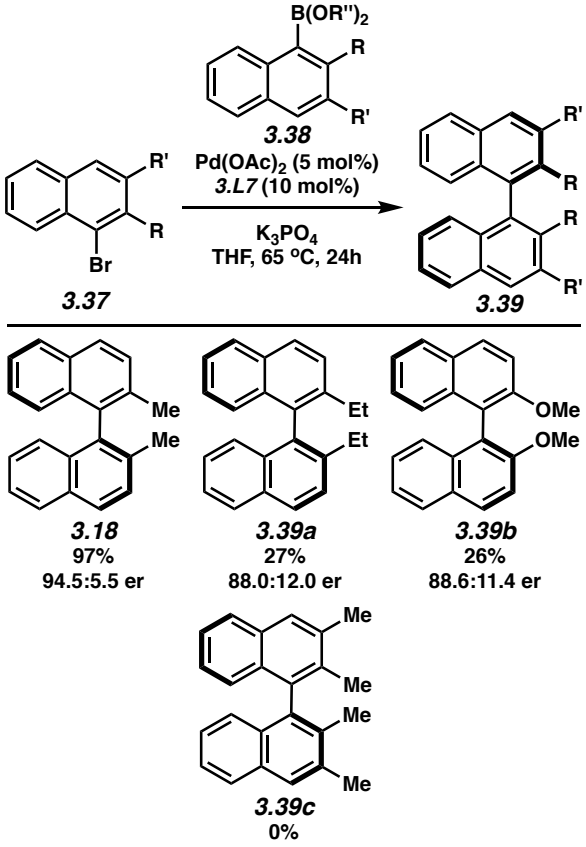

3.5 Asymmetric Negishi Cross-Coupling

Because of the issues identified with the Suzuki–Miyaura cross-coupling reaction (poor generality, high boronate loading), we decided to investigate the analogous reaction employing Negishi cross-coupling with aryl-zinc reagent **3.40** prepared by lithium-halogen exchange of **3.17b** with *t*-BuLi followed by addition of a THF solution of anhydrous $ZnBr_2$. $ZnBr_2$ was our preferred choice over $ZnCl_2$ due to its higher solubility in THF. Towards this end, we surveyed our family of *P*-chiral oxaphosphole and azaphosphole ligands in the Negishi cross-coupling reaction (Table 3.8). The highest yield and selectivity was obtained with **3.L13** having *iso*-propoxy groups on the lower aryl-ring of the ligand biaryl axis (entry 10). Surprisingly, the optimal ligand for the asymmetric Suzuki–Miyaura reaction (NitinPhos, **3.L7**, entry 5) gave poor

yield and selectivity in the Negishi coupling considering that the presumed enantiodetermining step of reductive elimination should be identical for the Negishi and Suzuki–Miyaura reactions. This difference in selectivity was something we wanted to understand further (*vide infra*). In general, C2-substituion on the oxaphosphole or azaphosphole ring of the ligand was required for good selectivity (entry 1 *vs* entries 2–10, and entries 15–16 *vs* entries 17–21). Further increasing the steric bulk at this C2-position by introducing a second methyl group enabled similar selectivities but led to a reduction in yield (entries 8 & 12). Additionally, a trend was observed where increasing the electron-donating ability of the lower aryl-ring bearing the alkoxy-substituents led to improved enantioselection (compare entries 2, 9, and 10). Lastly, the azaphosphole series of ligands were extremely efficient in terms of reaction yield; however, enantioselectivities were lower with this series (entries 15, 17, 18, 19).

Table 3.8 Ligand survey in the asymmetric Negishi cross-coupling towards tetra-*ortho*-substituted biaryls.

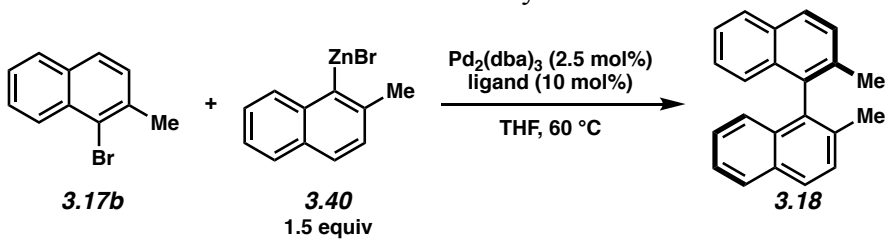

Entry	**Ligand**	% yield[a]	er[b]
1	**3.L1**	69	52.5:47.5
2	**3.L2**	49	78.5:21.5
3	**3.L3**	ND	81.5:18.5
4	**3.L4**	38	82.5:17.5
5	**3.L7**	44	72.5:27.5
6	**3.L9**	82	76.5:23.5
7	**3.L10**	89	83.0:17.0
8	**3.L11**	69	85.5:14.5
9	**3.L12**	81	71.3:28.7
10	**3.L13**	**93**	**85.0:15.0**
11	**3.L14**	45	82.0:18.0
12	**3.L15**	24	83.0:17.0
13	**3.L21**	67	77.0:23.0
14	**3.L22**	36	65.0:35.0
15	**3.L23**	91	60.5:39.5
16	**3.L24**	68	61.0:39.0
17	**3.L25**	96	82.5:17.5
18	**3.L26**	89	79.0:21.0
19	**3.L27**	99	53.0:47.0
20	**3.L28**	76	60.0:40.0
21	**3.L29**	82	78.0:22.0

[a]Isolated yield. [b]Determined by chiral HPLC analysis with Chiralpak OD-H column.

With identification of **3.L13** as the best ligand out of the ligand survey in Table 3.8, we further optimized parameters for the Negishi coupling reaction with ligand **3.L13** in an effort to improve enantioselection (Table 3.9). The Pd-precatalyst, metal-ligand ratio, Zn-source, and solvent were examined in the reaction (Table 3.9). The choice of Pd-precatalyst had little impact on the reaction enantioselectivity, but the yield varied from 70–80% (entries 1, 4, 5, 7). The

metal-ligand ratio also had no impact on selectivity; however, the yield improved if a 1:1.5 Pd:**3.L13** ratio was employed (entries 8–10). Finally, use of other Zn-salt precursors or other solvents did not lead to improvements in reaction efficiency (entries 2, 3, 6, 7).

Table 3.9 Survey of Pd-precatalyst, Pd:**3.L13** ratio, Zn-source, and solvent in the Negishi cross-coupling reaction.

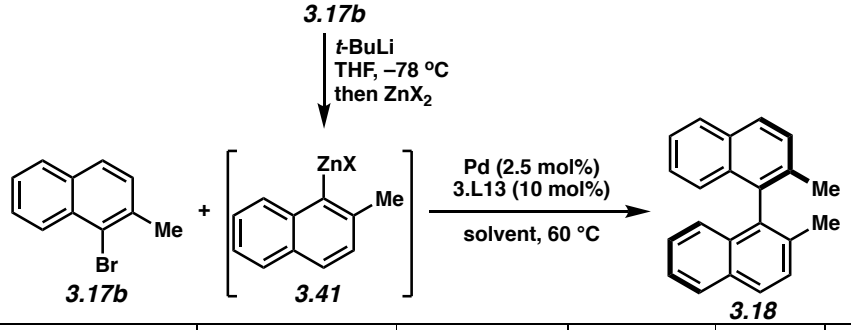

Entry	Pd	Metal:**3.L13** ratio	ZnX_2	Solvent	Yield %[a]	er[b]
1	$Pd(OAc)_2$	1:2	$ZnBr_2$	THF	81	85.0:15.0
2	$Pd_2(dba)_3$	1:2	$ZnBr_2$	Toluene	80	85.0:15.0
3	$Pd_2(dba)_3$	1:2	$ZnBr_2$	Dioxane	90	85.0:15.0
4	$PdCl_2(PhCN)_2$	1:2	$ZnBr_2$	THF	71	82.0:18.0
5	$[crotylPdCl]_2$	1:2	$ZnBr_2$	THF	73	83.0:17.0
6	$Pd_2(dba)_3$	1:2	$Zn(OAc)_2$	THF	56	78.0:22.0
7[c]	$Pd_2(dba)_3$	1:2	$Zn(OPiv)_2$	THF	77	84.0:16.0
8	$Pd_2(dba)_3$	1:2	$ZnBr_2$	THF	80	85.0:15.0
9	**$Pd_2(dba)_3$**	**1:1.5**	**$ZnBr_2$**	**THF**	**93**	**85.0:15.0**
10	$Pd_2(dba)_3$	1:1	$ZnBr_2$	THF	76	85.0:15.0

[a]Isolated yield. [b]Determined by chiral HPLC. [c]The zinc reagent was prepared from the Grignard according to Knochel's protocol (ref 38a).

To determine if enantioselection in the reaction was variable with reaction progress, the enantioselectivity was monitored over time at both 40 and 60 ^{o}C (Figure 3.3). Enantioselection

was independent of conversion implying that the active catalyst was not changing over time. Reduction of the reaction temperature led to slight improvements in enantioselectivity, but incomplete conversion was obtained at 40 °C.

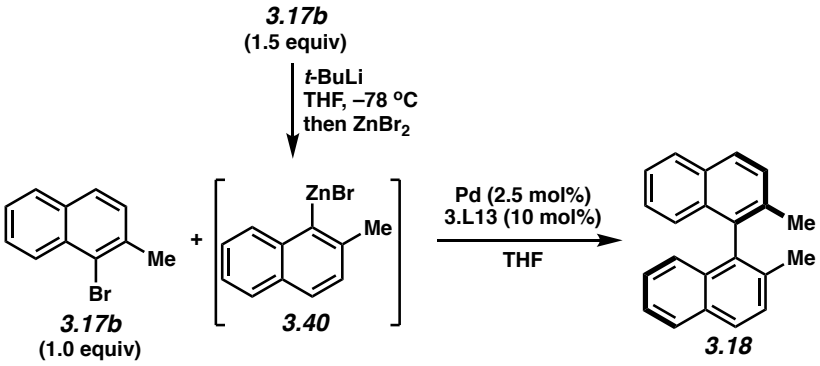

(a) 60 °C

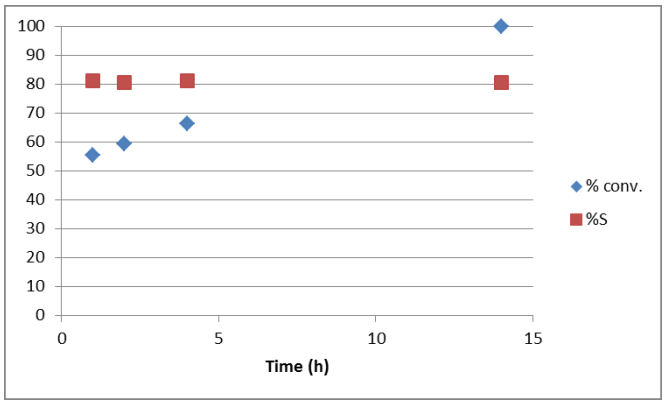

(b) 40 °C

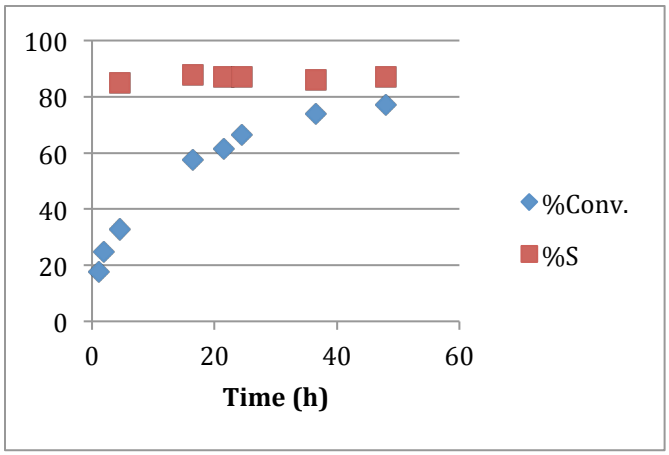

Figure 3.3 Enantioselectivity vs time at 40 and 60 °C

The most efficient catalyst conditions identified in our studies (Table 3.9, entry 9) were next utilized to examine the scope of the Negishi cross-coupling to afford other tetra-*ortho*-substitued biaryls (Table 3.10). Notably, the Negishi reaction showed much better scope in terms of reaction yield relative to the Suzuki–Miyaura reaction albeit with lower enantioselection. For the first time, a variety of R-alkyl substituents other than R = Me or OMe have been analyzed in an asymmetric cross-coupling reaction to provide tetra-*ortho*-substituted products (**3.39d-f**). In general, the cross-coupling employing **3.35** with R = *n*-alkyl afforded comparable results (**3.18**, **3.39a,c-f**). Methoxy-substitution (**3.39b**) was not well tolerated and afforded reduced yield due to significant amounts of reduction of the aryl bromide as a byproduct. Adding an additional methyl-substituent on the naphthalene ring also led to decreased reaction efficiency and enantioselectivity (**3.39c**); however, product formation was observed whereas the corresponding Suzuki–Miyaura coupling afforded no reaction with this substrate class (Table 3.7). Finally, the present system was specific to coupling naphthalene derivatives. Cross-coupling to afford **3.43** proceeded in moderate to good yields, but almost no enantioselection was observed despite the nature of the alkoxy-substituent.

Table 3.10 Asymmetric Negishi cross-coupling reaction scope.

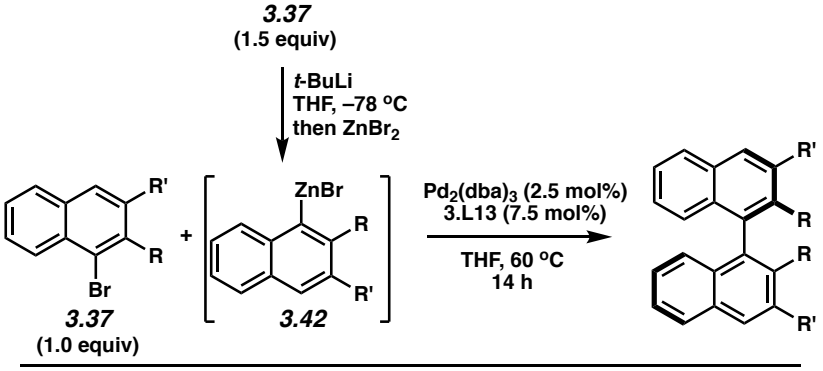

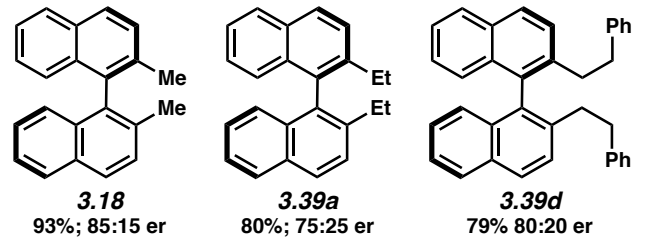

3.18
93%; 85:15 er

3.39a
80%; 75:25 er

3.39d
79% 80:20 er

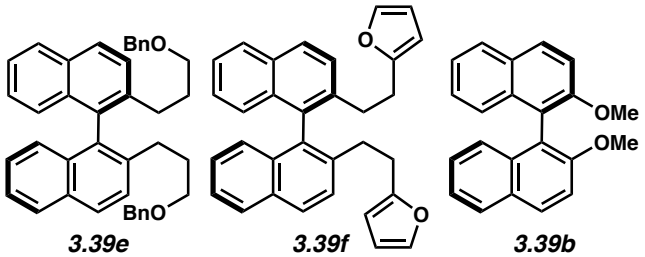

3.39e
81%; 83:17 er

3.39f
61%; 81:19 er

3.39b
31%; 75:25 er

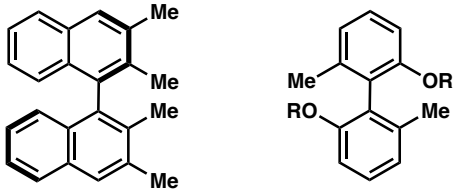

3.39c
29%; 67:33 er

3.43a: R = Me
52%; 58:42 er
3.43b: R = *i*-Pr
81%; 60:40 er
3.43c: R = *t*-Bu
67%; 54:46 er

3.6 Mechanistic Modeling by DFT Analysis.

The results of our combined studies of the asymmetric Suzuki–Miyaura and Negishi cross-coupling reactions employing ligand series **3.33** and **3.36** prompted us to investigate the mechanistic differences between these two reactions in terms of the enantiodiscrimination steps. Specifically, these ligands gave very different results in the coupling reaction when employed in a Suzuki–Miyaura *vs* a Negishi type protocol, yet mechanistically, the final step in the catalytic

cycle for both processes would presumably proceed through the same reductive elimination intermediate (*vide supra*). To help understand these differences and to aid in the development of new ligand structures to improve enantioselectivity, we modeled the cross-coupling process using density functional theory (DFT) calculations.[39]

3.6.1 Negishi Cross-Coupling

Most analyses of the stereoselectivity in cross-couplings regard the final step as stereodetermining.[11b,13b,n,x] Such an approach assumes equal accessibility to all of the different conformers of the transition state precursors. The percentage of product that forms via each of the possible reductive elimination transitions states can then be determined by Boltzmann analysis of their relative energies.

For the system in question here, a defining feature of the Pd biaryl intermediates preceding reductive elimination is the hindered rotation along the aryl-Pd bonds due to the large size of the aryl groups employed. As such, direct interconversion[13f,15a] of the different conformations of these intermediates does not occur. However, we hypothesize that all the conformers will be equally accessible due to the reversibility of transmetalation and oxidative addition in the Negishi coupling.[40] In such a scenario, a classical analysis of just the reductive elimination transition states pertains. Thus, all four of the possible biaryl palladium isomers need to be considered, each giving rise to two reductive elimination transition states, pro-*S* and pro-*R* (Figure 3.4).

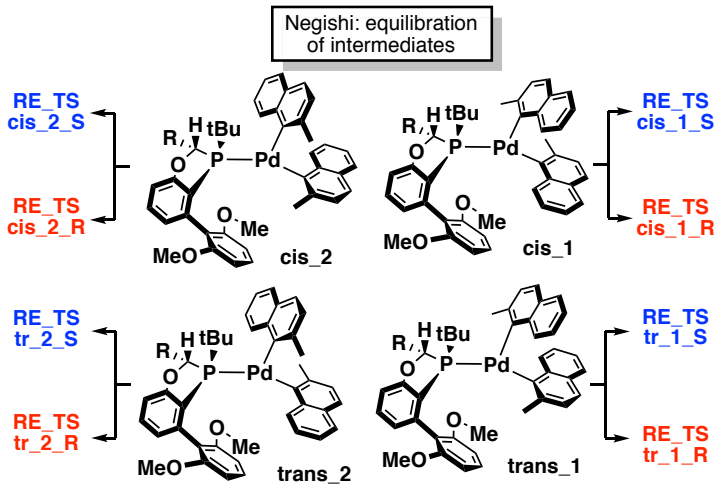

Figure 3.4. Stereoselection in Negishi coupling

Analyzing reductive eliminations for the Me-BOP ligand **3.L2** in such a fashion, we found that there is one dominant transition state for each of pro-*S* and pro-*R* sets, controlling the overall selectivity (Figure 3.5).

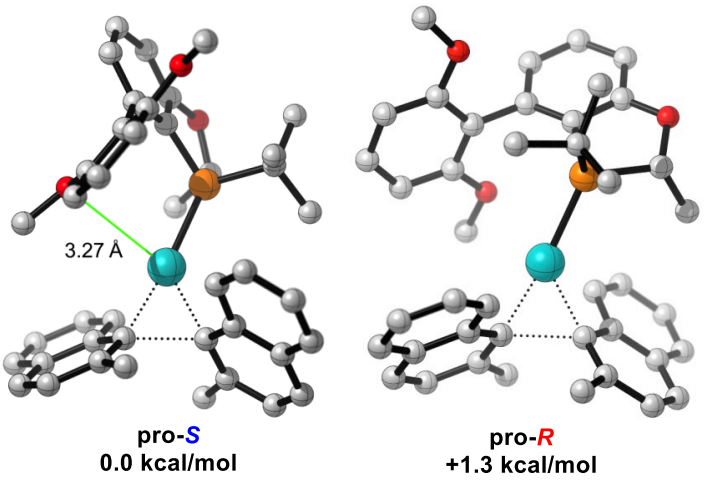

Figure 3.5 Lowest energy pro-*S* and pro-*R* reductive elimination transition states for Me-BOP ligand **3.L2**. Total of 8 transition states were located and analyzed. Free energies were computed using M06/6-311+G(d,p)-LANL2DZ(Pd)-SMD-THF//B3LYP/6-31G(d)-LANL2DZ(Pd); values are in kcal/mol.

Coordination of Pd to the methoxy-group of the lower aryl ring of the Me-BOP ligand provides extra stabilization for the pro-*S* transition state, resulting in highly *S*-selective reaction.

For the pro-*R* transition state, such an arrangement is not favorable due to the steric interactions with the ligand. A correlation between the electron-donating properties of the lower ring substituent (s_p) and the experimental *er* of the product supports the contribution of this specific substituent to the enantioselection mechanism (Figure 3.6).

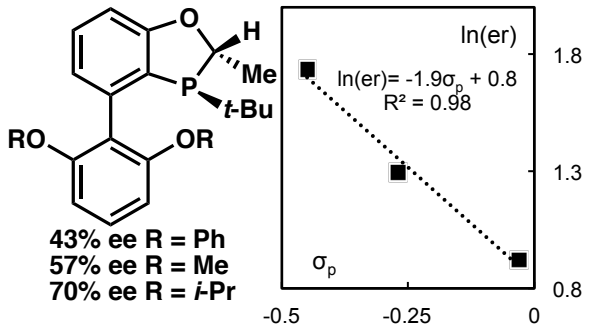

Figure 3.6 Efficiency of the chiral Me-BOP ligand vs electron donating property of the lower aryl-ring substituent

When the Negishi coupling is performed with the alternate DMM-substituted BOP ligand (NitinPhos, **3.L7**), enantioselectivity drops. This result can be rationalized using the same approach. Analysis of the selectivity-determining transition states revealed that the additional coordinating group of the DMM-substituent of NitinPhos ligand **3.L7** allows selective stabilization of the higher energy pro-*R* transition state (Figure 3.7), which diminishes the pro-*R* – pro-*S* energy gap and hence the selectivity of the overall process.

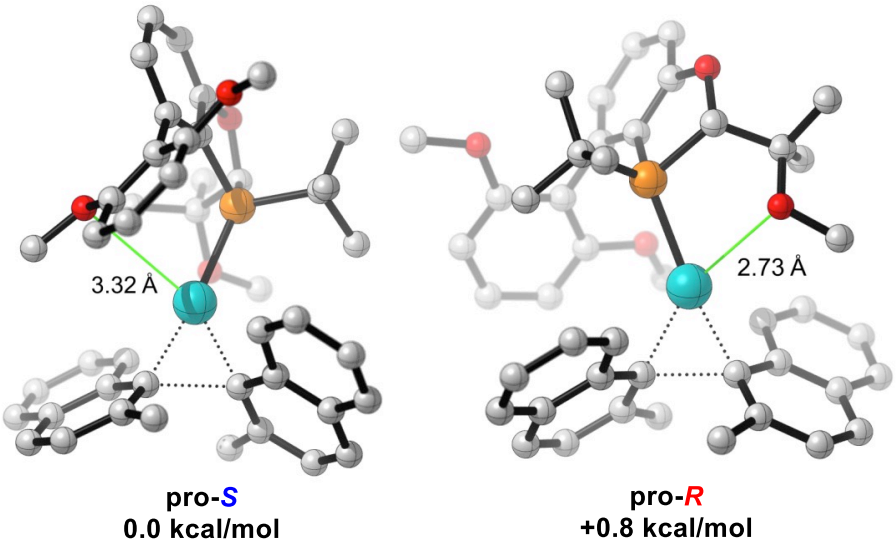

Figure 3.7 Lowest energy pro-*S* and pro-*R* reductive elimination transition states for the DMM-BOP ligand (NitinPhos, **3.L7**). Total of 32 transition states were located and analyzed. Free energies were computed using M06/6-311+G(d,p)-LANL2DZ(Pd)-SMD-THF//B3LYP/6-31G(d)-LANL2DZ(Pd); values are in kcal/mol.

This analysis of the reductive elimination transition states for the Negishi reaction rationalizes the experimentally observed enantioselectivities and highlights the key interactions (Figure 3.8).

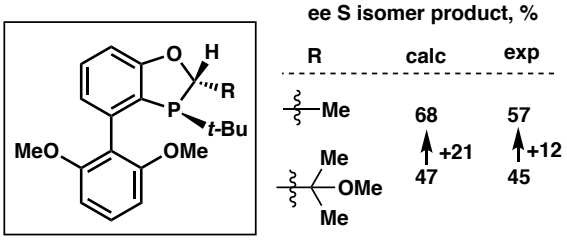

Figure 3.8 Comparison of the experimental and calculated efficiencies of the ligands in the Negishi coupling.

3.6.2 Suzuki–Miyaura Cross-Coupling

The different performance of the DMM-BOP ligand (NitinPhos, **3.L7**) in the Suzuki–Miyaura coupling requires a different enantioselection mechanism. Irreversible transmetalation[41] in Suzuki–Miyaura coupling would prevent pre-equilibration of pre-reductive elimination Pd(II)

species. As such, enantioselectivity of the overall process would be determined not only by the energetics of reductive elimination, but also by the relative population of the pre-reductive elimination Pd(II) intermediates. Thus, it is necessary to consider the relative rates of formation of corresponding species by modeling the transmetalation step. Based on the proposed structures of the pre-transmetalation intermediates,[42] the same hindered rotation issues are expected as for the pre-reductive elimination intermediates. Therefore, pre-transmetalation intermediates partition into two groups that react via independent pathways. In turn, the population of the pre-transmetalation intermediates is controlled by the energetics of oxidative addition. Therefore, all three major steps of the cross-coupling mechanism contribute to the overall selectivity of the reaction (Figure 3.9). Earlier computational studies of the stereoselectivity in Suzuki–Miyaura cross-coupling suggest that oxidative addition is the stereodetermining step.[43] We further develop this idea of early enantioinduction by employing the experimental findings of Denmark,[42a,b] Hartwig, [42c] and others[42d,e] that point to the mechanism of the transmetalation step proceeding through a Pd-OH complex.[17] The exact mechanism for the transmetalation step in Suzuki–Miyaura cross-coupling is still somewhat controversial[39] as there are some reports[44] that support the alternate "boronate"-transmetalation pathway.[45] The studies reported herein are calculated using the Pd-OH transmetalation pathway;[42] however, we would like to stress that the model proposed herein is also compatible with the "boronate"-transmetalation[44,45] mechanism: both possibilities ultimately lead to the same transmetalation transition states. The nature of the incoming boron species (boronate *vs* boronic acid) is not crucial for the selection of the productive oxidative addition step (discussed later) as the same steric interactions are present.

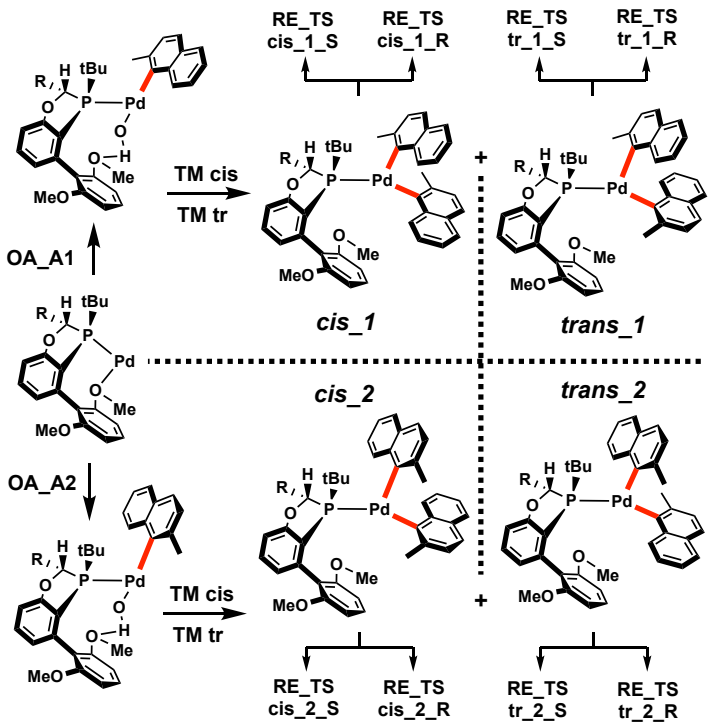

Figure 3.9 Proposed stereoselection mechanism in Suzuki coupling. Species separated by dashed lines cannot equilibrate. Rotation around the bonds marked in red is hindered.

Hence, detailed computational analysis of all the steps of the coupling is required. The resultant three-layer selectivity mechanism is shown in Figure 3.9. This important difference between the Suzuki–Miyaura and Negishi couplings is the result of the irreversible nature of transmetalation in Suzuki–Miyaura coupling. As such, the difference in the energetics of transmetalation significantly complicates the stereoselection process, which explains the well-known challenges in the design of stereoselective Suzuki–Miyaura couplings.

This analysis of the Suzuki–Miyaura coupling focuses two very similar ligands, DMM- and DME-BOP (**3.L7** *vs* **3.L6**, respectively). Despite minor differences in structure, these ligands provide substantially different selectivity levels. The following study rationalizes these selectivity differences within the proposed multi-level selectivity framework. To begin, a detailed analysis of the DME-BOP (**3.L6**) ligand is outlined.

3.6.2.1 Oxidative Addition

Oxidative addition to Pd(0) can occur via two pathways, A and B (Figure 3.10). Exchange of the bromide ultimately leads to several isomers of the PdOH species (Figure 3.11).

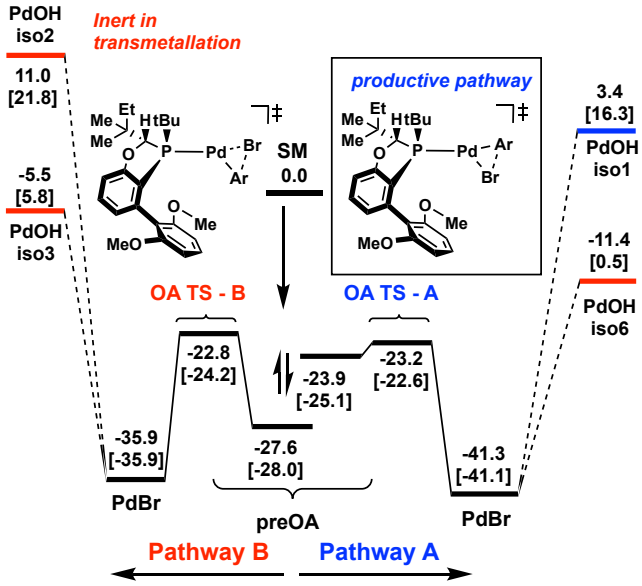

Figure 3.10 Oxidative addition pathways in Suzuki coupling. Intermediates marked in red are inert in transmetallation step. Enthalpies and free energies (in brackets) were computed using B3LYP-d3/6-31G(d)-lanl2dz(Pd, Br); values are in kcal/mol. Reactions are balanced using water as the OH source and HBr as the by-product of the exchange.

In considering the PdOH isomers (Figure 3.11), only **iso1** is ultimately relevant to the next step, transmetalation. For transmetalation to take place, the hydroxyl group and the vacant orbital in PdOH species must be positioned *cis* on the metal center, which rules out **iso2** and **iso3**. Isomers **iso4** and **iso5** gave severe destabilizing steric interactions between ligand and the naphthyl group, making them unlikely to be formed. Furthermore, **iso6** is not active in transmetalation as the vacant orbital is blocked by the ligand, so the approach of incoming boronic acid is problematic. As a consequence, only **iso1**, which arises from oxidative addition pathway A, needs to be analyzed. Given the activity of **iso1** PdOH in transmetalation, we theorize that the other species may eventually convert to **iso1**.

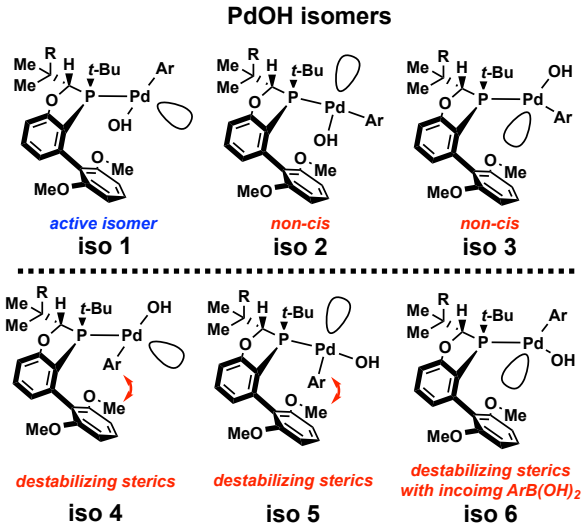

Figure 3.11 Isomeric PdOH intermediates.

Pathway A oxidative addition can occur via two conformations, corresponding to different orientations of the aryl group ('up' and 'down', see Figure 3.12). The relative energies of these conformations ultimately translate to the ratio of the PdOH species after exchange of the bromide. Based on the energies of oxidative addition transition states, 85% of the formed PdOH arises from **OA A1** where the methyl of the naphthyl unit is pointing 'away'. This selectivity is attributed to an unfavorable methyl-ligand interaction in the transition state **OA A2** (red arrow, Figure 3.12 insert). This differentiation sets up the first layer in the enantioselection mechanism.

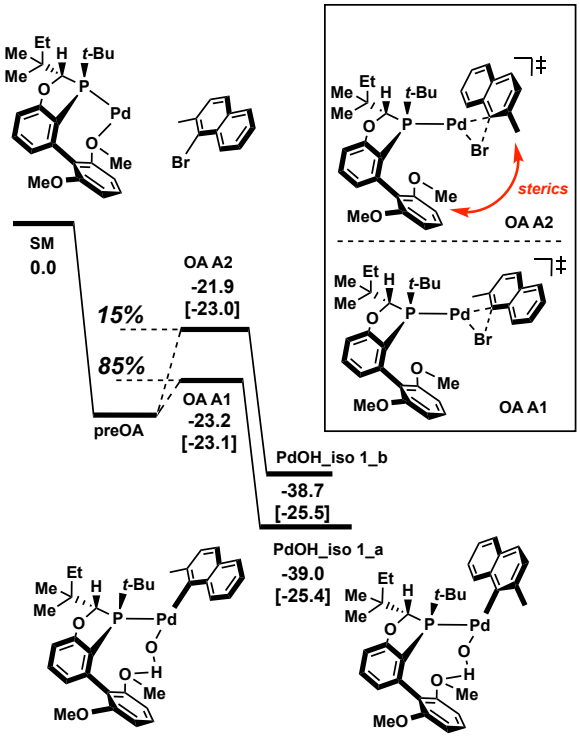

Figure 3.12 Energetics and selectivity of the productive oxidative addition pathway in Suzuki coupling. Total of 8 oxidative addition transition states were located and analyzed. Enthalpies and free energies (in brackets) were computed using B3LYP-d3/6-31G(d)-LANL2DZ (Pd, Br); values are in kcal/mol. From here on the reactions are balanced using KOH as the OH source and KBr as the by-product of PdOH formation.

3.6.2.2 Transmetalation

The resultant PdOH intermediates form a pre-transmetalation complex with the boronic acid (preTM, insert in Figure 3.13). The incoming boronic acid can coordinate such that the methyl substituents on the naphthyl rings are *cis* or *trans*. Starting from the major PdOH adduct (**PdOH_iso 1_a**, Figure 3.12), the *trans* adduct is more favorable due to the lack of Me-Me repulsion. This interaction also controls the energies of the concomitant transmetalation transition states (**TM TS** *cis* and *trans*, Figure 3.13). The energy gap between transition states results in 85% of the **pre-RE-*trans*** product vs 15% of the **pre-RE-*cis*** product. For the minor PdOH adduct (**PdOH_iso 1_b**, Figure 3.12), these trends are reversed (see Figure 3.14) due to the greater spacing between the naphthyl units. As a result, the *cis* adduct (**pre-RE-*cis***, figure

3.14) predomominates over the *trans* (**pre-RE-*trans***, Figure 3.14) adduct (76% vs 24%). During the transmetalation process, an equivalent of boronic acid is released that exists as the borate under the basic reaction conditions.[46]

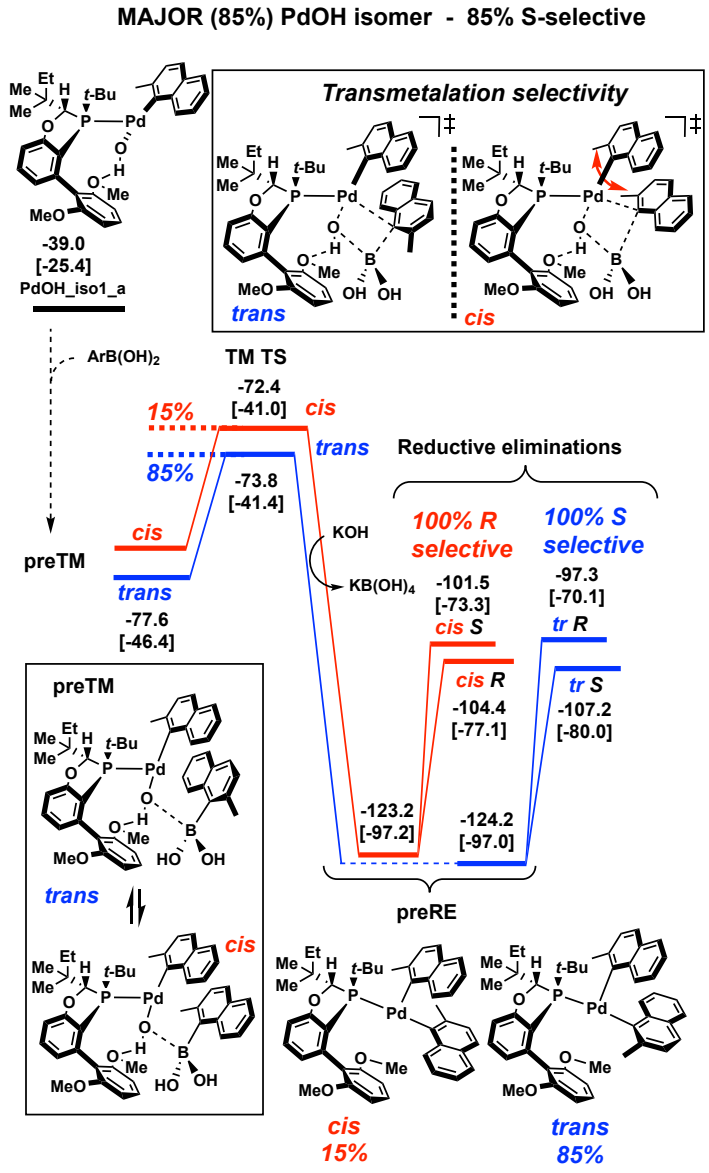

Figure 3.13 Energetics and selectivities of the transmetalation and reductive eliminations arising from the major PdOH isomer. Total of 8 transmetalation transition states and 16 reductive elimination transition states were located and analyzed. Enthalpies and free energies (in brackets) were computed using B3LYP-d3/6-31G(d)-LANL2DZ (Pd, Br); values are in kcal/mol.

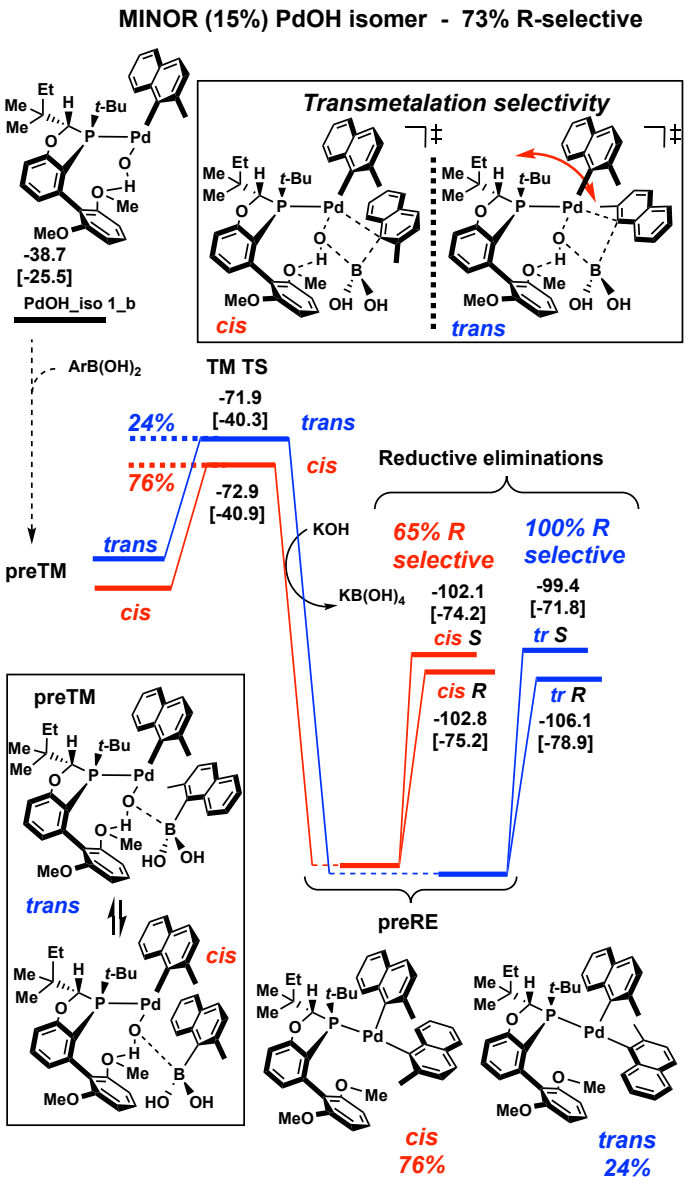

Figure 3.14 Energetics and selectivities of the transmetalation and reductive eliminations arising from the minor PdOH isomer. Total of 10 transmetalation transition states and 16 reductive elimination transition states were located and analyzed. Enthalpies and free energies (in brackets) were computed using B3LYP-d3/6-31G(d)-lanl2dz (Pd, Br); values are in kcal/mol.

3.6.2.3 Reductive Elimination

Both the *cis* and *trans* isomers of the diaryl Pd species (**preRE** intermediates in Figures 3.13 and 3.14) can reductively eliminate to form either the *S* or *R* binaphthyl. Analyzing the energetics of reductive eliminations resulting from the major PdOH isomer, we found that *cis*

pre-reductive elimination intermediate affords the *R*-isomer with excellent selectivity, while the *trans* isomer furnishes exclusively the *S*-product (reductive eliminations, Figure 3.13).

The extremely high selectivity of the individual reductive eliminations is due to the compact nature of the transition states. Even minor deviations from the optimal arrangement result in significant energetic penalties. For example, the reductive elimination transition states from the major PdOH isomer depicted in Figure 3.13, illustrate these phenomena (Figure 3.15). For the pre-RE-*trans* isomer, ***tr S*** transition state (100%) is much more favorable than ***tr R***, in which interactions of the methyl of the upper naphthyl unit (arising from the aryl bromide) and the back side of the ligand destabilize the structure. Similarly, ***cis R*** (100%) is more stable than ***cis S*** for the pre-RE-*cis* isomer.

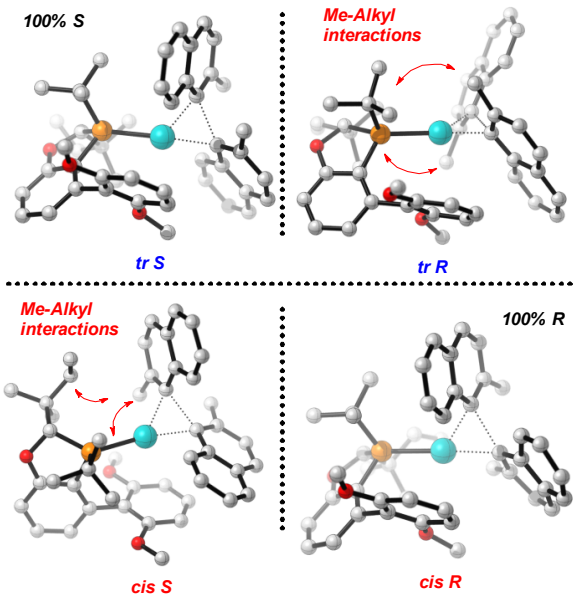

Figure 3.15 Lowest energy pro-*S* and pro-*R* reductive elimination transition states from the major *trans* and *cis* isomers of diaryl Pd.

As the orientation of the naphthyl fragment is important for the high stereoselectivity of reductive elimination, one might expect lower selectivities for the case of reductive elimination

from the minor PdOH isomer (Figure 3.14), where the upper naphthyl unit is rotated in the opposite direction. Indeed, the pre-RE-*cis* is only moderately selective towards reductive elimination *vs* ***cis R*** (65%). Reductive elimination from **pre-RE-*trans*** remains highly selective (100% ***tr R***) because the methyl group on the lower ring is pointing toward a sterically crowded portion of the transition state.

However, the relative energies of the reductive elimination transition states do not tell the whole story as the intermediates needed for this step form at different rates with both oxidative addition and transmetalation contributing to the partitioning. Figure 3.16 illustrates a simplified version where different conformational isomers are not shown for each of the branches. Oxidative addition leads to two branches (left = minor, right = major), which again bifurcate at transmetalation and reductive elimination. The pathway highlighted with blue arrows is the only *S*-selective channel on the diagram. Even though there are more pathways to the *R*-enantiomer, the *S*-selective channel is lower in energy and is the main route responsible for formation of the product.

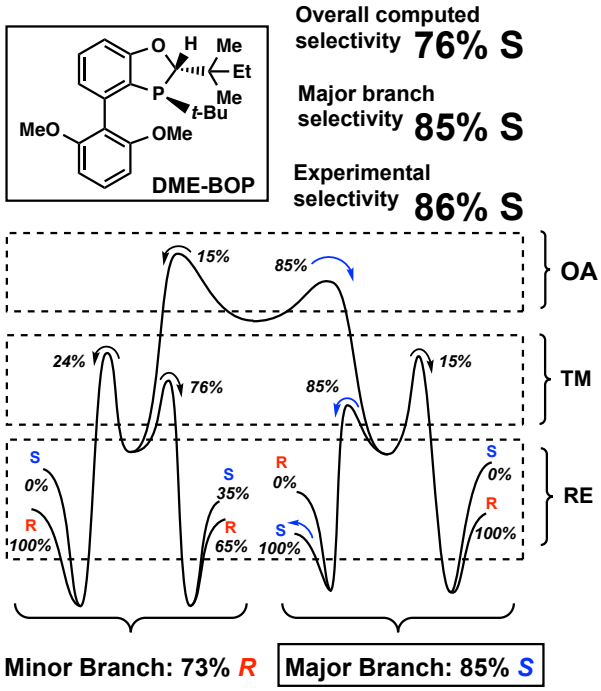

Figure 3.16 Simplified energy diagram for Suzuki coupling with DME-BOP (**3.L6**) ligand. Selectivities of each step were calculated based on the Boltzmann distribution of the energies of corresponding transition states. (Alternatively, such multi-level processes can be analyzed using a system of rate equations, *i.e.* microkinetic modeling.[47])

Analysis of the DMM-BOP (NitinPhos, **3.L7**) ligand generates a similar outcome (Figure 3.17). The entire transformation is still *S*-selective and just like in a previous case, there is only one pathway responsible for the production of the major product. However, this pathway is more favorable than it is in the DME-BOP (**3.L6**) case. For the DMM ligand (NitinPhos, **3.L7**) transmetalation selectivity in the 'major branch' (Figure 3.17) is 90:10, whereas for the DME ligand it is at a slightly smaller 85:15. This difference causes selectivity levels to be higher for DMM (NitinPhos, **3.L7**).

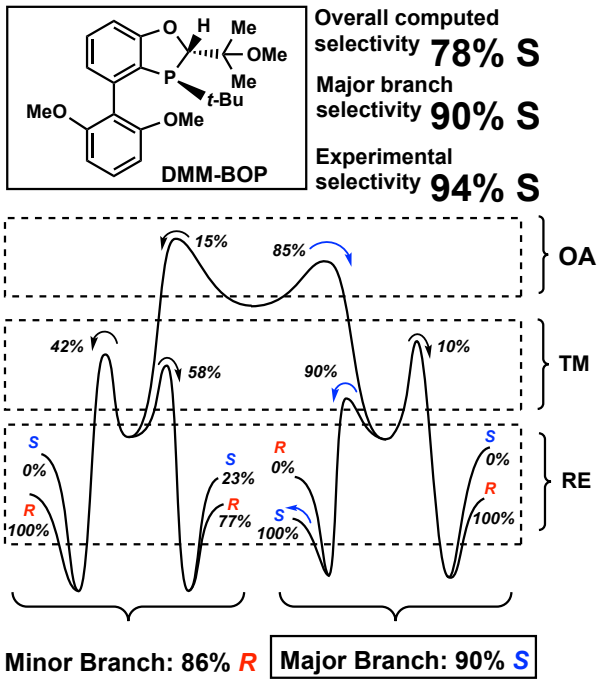

Figure 3.17 Simplified energy diagram for Suzuki coupling with DMM-BOP (NitinPhos, **L7**) ligand.

If one assumes that the entire reaction is controlled only by the selectivity of the major branch, then the difference in the transmetalation energetics would predict the experimentally observed selectivities with improved accuracy (see 'major branch' selectivities on each of the diagrams). Thus, our model would predict 85% *S* selectivity for DME-BOP (**3.L6**) ligand vs 86% experimental and 90% *S* selectivity for DMM-BOP (NitinPhos, **3.L7**) ligand vs 94% experimental. Given the complex nature of the selectivity mechanism and the large number of transition states that contribute to the finalized percentages (26 transition states conformers were analyzed and utilized in Boltzmann distributions), this result may indicate that the major branch is indeed the only controlling channel. Such a situation would occur if our estimates of the pre-transmetalation intermediates are not entirely accurate. In our work we tested five computational methods (different combinations of various optimization and single-point calculations) with 36-56 transition state conformations depending on the method. These analyses did not improve the

quality of the predictions. This high sensitivity of the selectivity estimates to the type of method used may indicate that our method of choice is not optimal and leads to incorrect estimates of the energetics of major/minor branch splitting. It might also point to the existence of other selectivity-contributing steps (for example, Br exchange) that were not considered.

Since the transmetalation selectivity in the major branch seems to account for the observed difference in the performance of the ligands, we undertook further study of the transmetalation step. As discussed earlier, each of the energy levels shown on the diagrams represents only the lowest energy structure out of a set of calculated conformational isomers. Importantly, molecules traversing the reaction coordinate proceed through a distribution of available conformational transition states rather than through the single lowest energy pathway;[48] therefore, the calculated selectivities given in this study were determined using the energies of all the available conformations identified by calculation. This consideration accounts for the computationally observed different transmetalation selectivities of the DMM-BOP (NitinPhos, **3.L7**) and DME-BOP (**3.L6**) ligands (Figure 3.18). For the DMM-BOP (NitinPhos, **3.L7**) ligand, the transmetalation pathways leading to *S*-selective reductive elimination are more populated than that for the DME (**3.L6**) ligand (90% vs 85%), while the other pathways are less populated (10% vs 15%). This result arises from the greater partitioning to the *S*-selective transition states for the DMM-BOP ligand which are clustered close together relative to those for the DME-BOP ligand which cover a larger range and are less populated overall relative to the R-selective transition state. This phenomenon accounts for the improved transmetalation selectivity obtained with the DMM-BOP ligand (**3.L7**) *vs* the DME-BOP ligand (**3.L6**), and can be explained structurally by the presence of hydrogen bonding interactions between weak C–H hydrogen bond donors of the methylnaphthalene coupling partners with the methoxy-group of the DMM-BOP

ligand that is not possible in the DME-BOP ligand case (*i.e.* **3.42** *vs* **3.45**). Hydrogen bond contacts between the methoxy-group of NitinPhos (**3.L7**) and C–H bonds of the methylnaphthalene coupling partners are present in transmetalation transition states (**3.42**, **3.43**). The bond distances for these O–H interactions are within the distance and angles typical of weak C–H–O hydrogen bonds (2.2–2.8 A; **3.42**: C_{sp2}–H–O = 119°, C_{sp3}–H–O = 157°; **3.43**: C_{sp3}–H–O = 158°, 135°).[13b,49] These stabilizing interactions cause fewer accessible low-energy transmetalation transition state conformations to be available in the DMM-BOP ligand case because rotation of the DMM-group results in loss of these interactions which creates a higher energy gap between these conformations such that they cannot contribute to product formation. In contrast, the DME-BOP ligand does not have these interactions, and therefore, the energy splitting between conformers is less severe and leads to several accessible pathways of various energy levels with slight differences in steric interactions due to the orientation of the ethyl-group of the DME-substituent. Finally, it is worth noting that direct coordination of the methoxy-substituent of the DMM-BOP ligand (**3.L7**) to the metal center was not found in any of the relevant transition states.

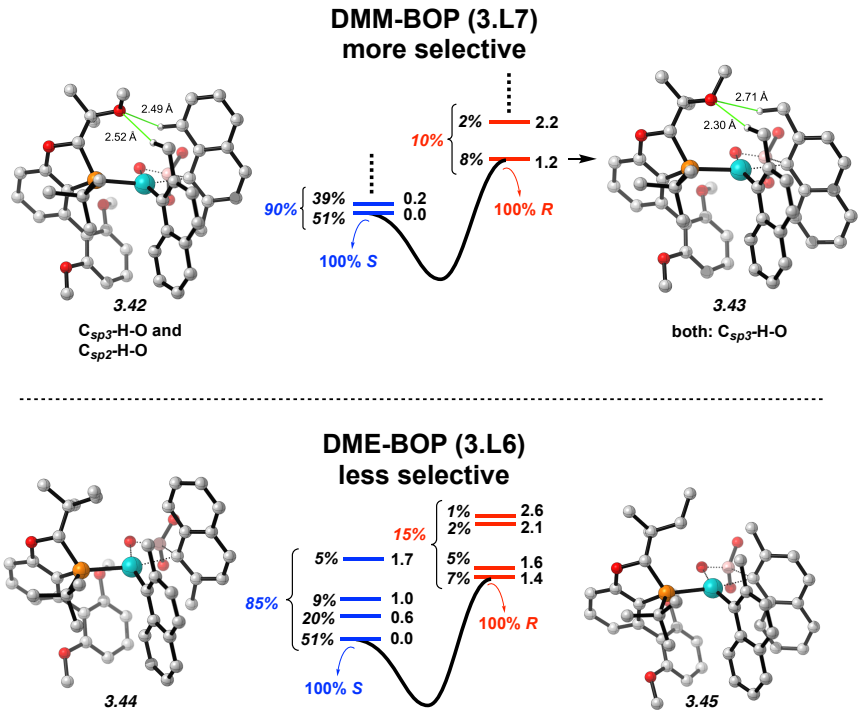

Figure 3.18 Relative energies (in bold), and relative populations of the major branch transmetalation transition states for DMM-BOP (NitinPhos, **3.L7**) and DME-BOP (**3.L6**) ligands. Green lines represent C–H---O hydrogen bonding interactions. Dashed lines indicate additional high-energy conformations that do not significantly contribute to the population distribution.

This DFT study of the stereoselectivity of Suzuki–Miyaura coupling allowed us to propose a multi-step stereoselection framework. This mechanism is likely to operate in the coupling of sterically hindered substrates, where isomeric organometallic intermediates do not readily interconvert.

3.7 Conclusion

In conclusion, Pd-catalyzed asymmetric Suzuki–Miyaura and Negishi cross-coupling reactions to form tetra-*ortho*-substituted biaryls were developed. Higher enantioselectivities were obtained for the Suzuki–Miyaura reaction; however, better substrate generality was obtained for the Negishi coupling. For each coupling reaction, a unique ligand was identified to be optimal

for the Suzuki–Miyaura *vs* the Negishi reaction in terms of providing maximum enantioselection. Detailed DFT calculations of these two processes offered an explanation for the differences in the enantiodiscrimination mechanism between the Suzuki–Miyaura and Negishi cross-coupling reactions that likely proceed through the same Pd-intermediate for reductive elimination.

Analysis of only the reductive elimination step in the Negishi cross-coupling reaction by DFT provided good correlation with the experimental enantioselectivity, implying that reductive elimination was enantiodetermining. In contrast, this same analysis for the Suzuki–Miyaura coupling did not accurately predict the observed experimental selectivities. A complete analysis of the oxidative addition, transmetalation, and reductive elimination steps in the Suzuki–Miyaura reaction using DFT revealed that the selectivity in the Suzuki–Miyaura reaction was influenced by all three steps in the catalytic cycle. The delicate interplay of oxidative addition, transmetalation, and reductive elimination calculated for stereocontrol in the Suzuki–Miyaura cross-coupling reaction for the formation of tetra-*ortho*-substituted biaryls may be the reason why the Suzuki–Miyaura reaction was less tolerant to substrate modifications relative to the analogous Negishi reaction. These findings may aid in the design and development of new catalysts to improve reactivity and selectivity in asymmetric cross-coupling reactions to furnish tetra-*ortho*-substituted biaryls.

3.8 Experimental Section

3.8.1 Materials and Methods

^{1}H NMR spectra were recorded on Bruker 400 MHz or 500 MHz spectrometers. Chemical shifts are reported in ppm from tetramethylsilane with the solvent resonance as an internal standard ($CDCl_3$: 7.26 ppm, CD_2Cl_2: 5.32 ppm). Data are reported as follows: chemical

shift, integration, multiplicity (s = singlet, d = doublet, t = triplet, q = quartet, p = pentet, h = hextet, hept = heptet, br = broad, m = multiplet), and coupling constants (Hz). ^{13}C NMR was recorded on a Bruker 500 MHz (125 MHz) or 400 MHz (100 MHz) instrument with complete proton decoupling. Chemical shifts are reported in ppm from tetramethylsilane with the solvent as the internal standard ($CDCl_3$: 77.0 ppm, CD_2Cl_2: 54 ppm). ^{31}P shifts were referenced to 85% H_3PO_4 in D_2O at 0.0 ppm as external standard and obtained with ^{1}H decoupling. Liquid chromatography was performed using forced flow (flash chromatography) on silica gel using a Biotage system. Thin layer chromatography (TLC) was performed on EMD silica gel F_{254} 2.5x7.5 cm plates. Visualization was achieved using UV light or potassium permanganate in water followed by heating. HRMS was collected using Thermo LTQ FT Ultra mass spectrometer at 100,000 resolving power using DART source ionization. All reactions were conducted in oven or flame dried glassware under an inert atmosphere of nitrogen or argon with magnetic stirring unless otherwise noted. THF (<0.02% water content), CH_2Cl_2, EtOH, EtOAc, IPAc, Diglyme, MeOH, DMF, hexane and toluene were purchased from Sigma Aldrich and used directly without further purifications. PMHS (polymethylhydrosiloxane) and TMDS (1,1,3,3-tetramethyldisiloxane) were purchased from Aldrich and used without further purifications. Solvents were degassed by Ar sparge. Ligand **3.L1**,[13n] **3.L2**,[13n,24] **3.L4**,[13o] **3.L9**,[29] **3.L10**,[23] **3.L19**,[24] **3.L20,**[11b] and **3.L23**[7v,35b] were prepared according to our previously published procedures. 1-Bromo-2-ethylnaphthalene and 1-bromo-2,3-dimethylnaphthalene were prepared according to the literature.[9] All other reagents were purchased from either Fisher or Aldrich Chemical Companies and used directly.

3.8.2 Experimental Procedures

3.8.2.1 Synthetic Route to Ligands

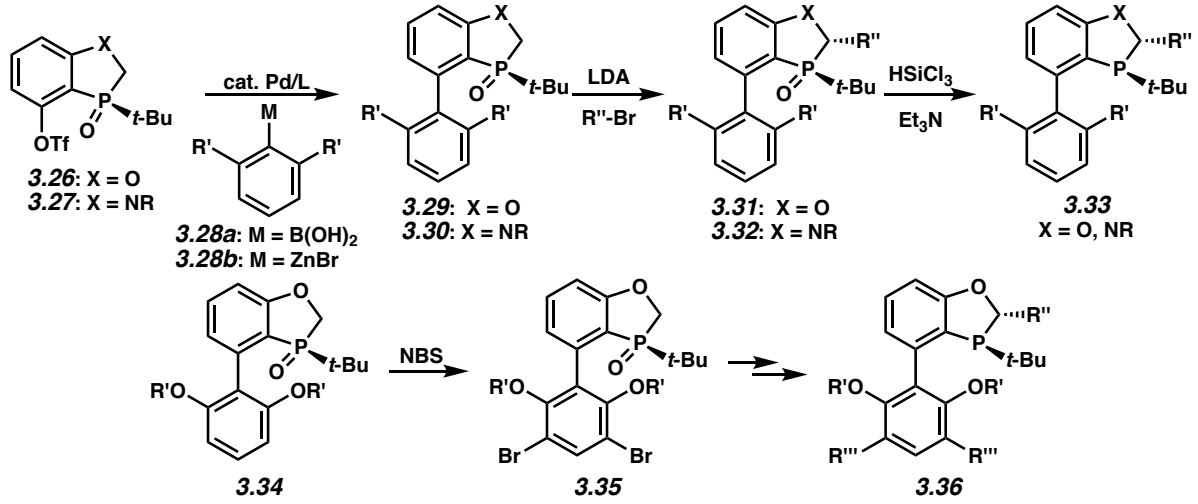

Figure 3.19 General synthetic route to various ligand scaffolds.

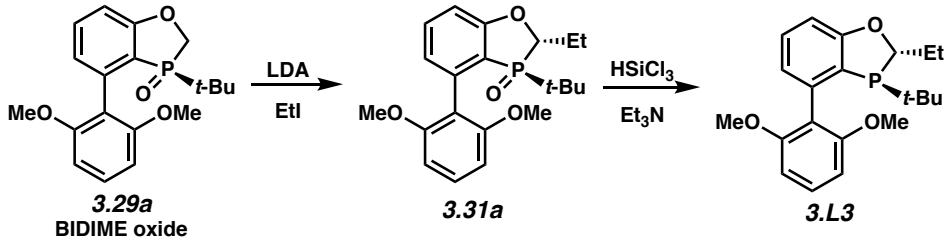

To a solution of 3.84 g (11.1 mmol) of BIDIME oxide (**3.29a**) in 20 mL of THF at –78 °C was slowly added a solution of LDA in THF (2M, 20 mL, 40 mmol). The mixture was allowed to sitr at –78 °C for 1 h. Iodoethane (3.26 mL, 40.5 mmol) was then added dropwise at –78 °C. The resultant mixture was allowed to stir at –78 °C for 2 h and then allowed to warm to 23 °C overnight. Water was then added, and the mixture was extracted with CH_2Cl_2. The combined organic layers were washed with brine, dried with anhydrous Na_2SO_4, and concentrated *in vacuo*. The crude residue was purified by flash chromatography (gradient, 20 – 70% EtOAc/hexanes) to afford 2.3 g (55%) of oxide **3.31a** as a white solid. $[\alpha]_D^{22}$ = – 20.4 (*c* 0.69, $CHCl_3$); ^{1}H NMR (500 MHz, $CDCl_3$): δ 7.47 (t, *J* = 7.9 Hz, 1H), 7.29 (t, *J* = 8.4 Hz, 1H),

6.87–6.89 (m, 2H), 6.64 (d, J = 8.4 Hz, 1H), 6.56 (d, J = 8.4, 1H), 4.28–4.31 (m, 1H), 3.77 (s, 3H), 3.72 (s, 3H), 1.97 (q, J = 7.5 Hz, 2H), 1.16 (t, J = 7.4, 3H), 0.84 (d, J = 16, 9H); $^{31}P\{^{1}H\}$NMR (162 MHz, $CDCl_3$): δ 59 ppm; $^{13}C\{^{1}H\}$NMR (100 MHz, $CDCl_3$): δ 163.9 (d, J_{CP} = 19 Hz), 158.8, 157.3, 138.4 (d, J_{CP} = 5.0 Hz), 133.9 (d, J_{CP} = 1.7 Hz), 129.8, 124.7 (d, J_{CP} = 8.2 Hz), 117.5, 114.4 (d, J_{CP} = 90 Hz), 112.2 (d, J_{CP} = 5.5 Hz), 104.5, 103.0, 75.1 (d, J_{CP} = 62 Hz), 56.1, 55.4, 33.3 (d, J_{CP} = 71 Hz), 23.7, 23.4, 10.4 (d, J_{CP} = 7.3 Hz); HRMS (DART) *m*/*z* calculated for $C_{21}H_{28}O_4P$ $[M + H]^+$: 375.1720; found: 375.1722.

To a 200 mL two-neck round bottom flask with magnetic stir-bar was charged 2.0 g (5.3 mmol) of oxide **3.31a**. A reflux condenser was added, and the reaction was inerted with Ar using vacuum-purge cycles (3x). Toluene (25 mL) was charged followed by triethylamine (3.44 mL, 25 mmol) and $HSiCl_3$ (1.88 mL, 18.8 mmol). The mixture was then immersed in an oil bath at 65 °C and monitored by ^{31}P NMR spectroscopy. After 12 h, the reaction was cooled to 23 °C and quenched with 20 mL of degassed (Ar sparge) 30% NaOH (aq.). The mixture was then allowed to vigorously stir at 23 °C for 1 h. The flask was transferred in the glove box. The aqueous layer was removed and subsequently extracted with MTBE (2 × 15 mL). The combined organics were dried with Na_2SO_4, filtered quickly through a pad of basic alumina, and immediately concentrated *in vacuo* to afford 1.7 g (92%) of **3.L3** as a white solid. $[\alpha]_D^{22}$ = – 125 (*c* 0.51, $CHCl_3$); ^{1}H NMR (400 MHz, $CDCl_3$): δ 7.26–7.32 (m, 2H), 6.82–6.86 (m, 2H), 6.64 (d, J = 8.3, 1H), 6.58 (d, J = 8.3 Hz, 1H), 4.76 (t, J = 6.8, 1H), 3.73 (s, 3H), 3.71 (s, 3H), 1.69–1.82 (m, 2H), 1.01 (t, J = 7.2, 3H), 0.73 (d, J = 12, 9H); $^{31}P\{^{1}H\}$NMR (202 MHz, $CDCl_3$): δ 3.9 ppm; $^{13}C\{^{1}H\}$NMR (100 MHz, $CDCl_3$): δ 163.2, 157.8, 157.1, 138.5 (d, J_{CP} = 17 Hz), 130.4, 128.9, 124.3 (d, $J_{C\text{-}P}$ = 13 Hz), 123.4 (d, $J_{C\text{-}P}$ = 4.0 Hz), 119.8, 109.4, 104.4, 103.6, 84.7 (d, $J_{C\text{-}P}$ = 22

Hz), 55.8, 55.4, 30.8 (d, $J_{C\text{-}P}$ = 18 Hz), 28.5 (d, J_{CP} = 26 Hz), 26.7 (d, J_{CP} = 14 Hz), 10.2 (d, J_{CP} = 13 Hz); HRMS (DART) *m*/*z* calculated for $C_{21}H_{28}O_3P$ $[M + H]^+$: 359.1771; found: 359.1770.

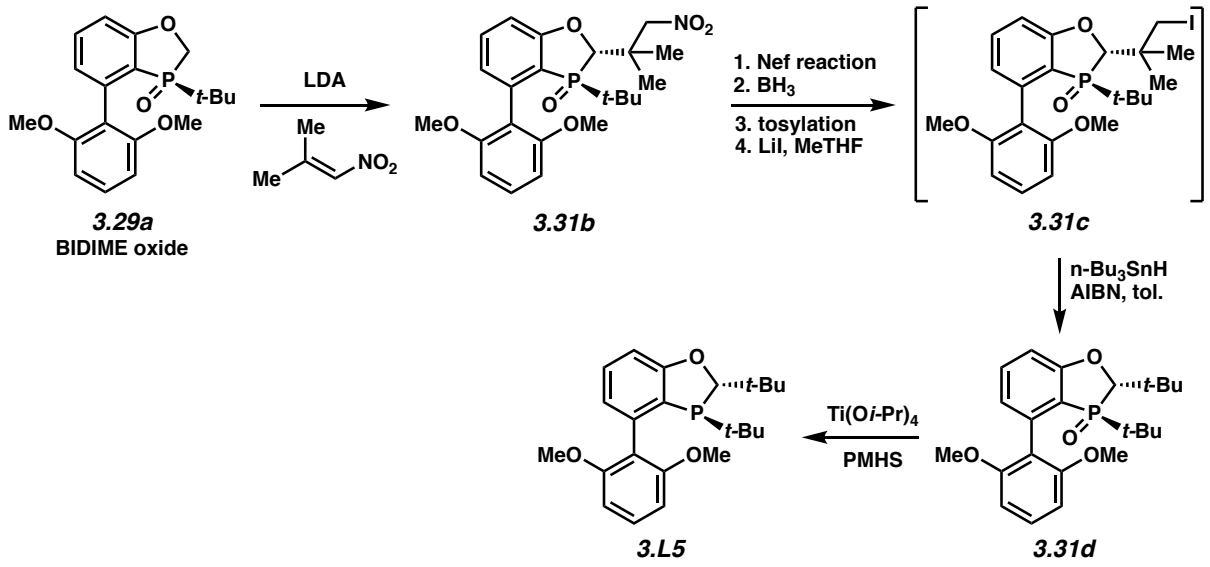

To a solution of BIDIME oxide (**3.29a**, 6.0 g, 17.5 mmol, 1 equiv) in THF (60 mL) at –78 °C was added LDA (10.5 mL, 2.0 M in heptane/THF/chlorobenzene, 21.0 mmol, 1.2 equiv). The mixture was stirred at –78 °C for 30 min before dropwise addition of 2-methyl-1-nitroprop-1-ene (2.05g, 19.2 mmol, 1.1 equiv, 95% purity). The resulting mixture was kept at –78 °C for 1 h before it was warmed to 23 °C over 1 h. After stirring at 23 °C for 1h, saturated aqueous NH_4Cl and EtOAc were added to the mixture. The aqueous layer was further extracted with EtOAc. The combined EtOAc solution was washed with brine, dried over $MgSO_4$, concentrated to give the crude product (**3.31b**, 2.34 g, crude product was used in the next step without any purification). ^{1}H NMR (500 MHz, $CDCl_3$): δ 7.51 (t, *J* = 8.0 Hz, 1H), 7.29 (t, *J* = 8.4 Hz, 1H), 6.94 (ddd, *J* = 13.0, 7.3, 3.5 Hz, 2H), 6.62 (d, *J* = 8.4 Hz, 1H), 6.55 (d, *J* = 8.4 Hz, 1H), 4.85 (d, *J* = 11.3 Hz, 1H), 4.56 (d, *J* = 11.3 Hz, 1H), 4.42 (d, *J* = 2 Hz, 1H), 3.72 (d, *J* = 1 Hz, 6H), 1.33 (s, 3H), 1.32 (s, 3H), 0.9 (d, *J* = 15.8 Hz, 9H); ^{31}P NMR (202 MHz, $CDCl_3$): δ 61.18 ppm; ^{13}C NMR

(125 MHz, $CDCl_3$): δ 163.4 (d, *J* = 19.2 Hz), 158.5, 157.1, 138.6 (d, *J* = 5.3 Hz), 134.5 (d, *J* = 2.0 Hz), 129.9, 125.4 (d, *J* = 8.6 Hz), 116.3 (d, *J* = 2.2 Hz), 113.1 (d, *J* = 92.0 Hz), 111.5 (d, *J* = 5.8 Hz), 104.0, 103.0, 82.2 (d, *J* = 4.4 Hz), 75.5 (d, *J* = 57.0 Hz), 55.5, 55.3, 40.6 (d, *J* = 1.0 Hz), 34.2 (d, *J* = 71.0 Hz), 23.1 (d, *J* = 1.0 Hz), 21.2 (dd, *J* = 10.4, 3.7 Hz). HRMS (DART) *m*/*z* calculated for $C_{23}H_{31}O_6NP$ $[M+H]^+$: 448.1884; found: 448.1885.

To a solution of **3.31b** (0.3 g, 0.67 mmol, 1 equiv) in methanol (5 mL) was charged a mixture of 0.5M disodium phosphate, Na_2HPO_4 (12.07 mL, 6.03 mmol, 9.0 equiv) and 1M sodium hydroxide, NaOH (12.07 mL, 12.07 mmol, 18.0 equiv) and stirred for 1 h. To the resulting suspension was charged a solution of Oxone (1.23g, 2.01 mmol, 3.0 equiv) in water (2.0 mL) and stirred at 23 °C for 24h. Upon reaction completion by HPLC, the reaction mixture was acidified with 4N aqueous HCl (3.0 mL, 12.07 mmol, 18.0 equiv) to maintain pH ~ 1-2. The mixture was extracted with isopropyl acetate, IpOAc (2 x 5 mL). The combined organic layer was washed with water, brine and then dried over sodium sulfate before solvent evaporation to afford the desired carboxylic acid product (0.261 g) that was used directly in the next step.

To a solution of the carboxylic acid (0.261 g, 0.604 mmol, 1 equiv) in THF (5 mL) at 0 °C was charged 1 M solution of BH_3•THF (1.21 mL, 1.21 mmol, 2 equiv) under nitrogen atmosphere. The resulting mixture was allowed to warm to 23 °C and stirred overnight. Upon reaction completion (HPLC), the reaction mixture was quenched with methanol (0.5 mL) and water (0.5 mL) and stirred for 30 min. The volatiles (THF, MeOH) were removed by Rotavap and the residue was diluted with EtOAc (5 mL) and washed with water (2 mL). The organics were concentrated to afford desired primary alcohol product (0.253 g) that was used directly in the next step.

To the solution of the primary alcohol (0.250 g, 0.6 mmol, 1 equiv) was charged dry pyridine (1.25 mL) and *p*-toluenesulfonyl chloride (0.24 g, 1.26 mmol, 2.1 equiv) under nitrogen. The resulting mixture was stirred at 23 °C for 24 h, after which the reaction mixture was diluted with EtOAc (5 mL) and sat. ammonium chloride (3 mL). The top organic layer was concentrated to afford the desired tosylate product (0.37 g) that was used directly in the next step without any purification.

To a solution of the tosylate (200 mg, 0.28 mmol, ~ 1 equiv) in 2-MeTHF (4 mL) was charged anhydrous lithium iodide (510 mg, 3.81 mmol, 13.7 equiv) under nitrogen, heated to 80 °C (reflux) and stirred for 15 h and cooled to 23 °C The reaction mixture was quenched with 10% sodium thiosulfate solution (0.5 mL) and water (1 mL) and extracted with EtOAc (2 x 2 mL). The organics were combined and concentrated under reduced pressure to give crude residue which was then purified using silica gel chromatography (0-100% EtOAc) to afford the desired iodide product (**3.31c**, 152 mg, 0.264 mmol, 95% crude yield with 92 area% purity) as an oily residue.

To the solution of iodide **3.31c** (153 mg, 1 equiv) in toluene (5 mL) were charged tributyltin hydride (180 mg, 0.612 mmol, 2.10 equiv) and AIBN (28.0 mg, 0.18 mmol, 60 mol%) under nitrogen and then heated to 80 °C for 2 h. The reaction mixture was cooled to 23 °C and quenched with methanol (2 mL) and sat. ammonium chloride (4 mL). The resulting mixture was extracted with toluene (5 mL). The organic layer was dried over sodium sulfate and concentrated under reduced pressure to afford crude residue, which was purified using silica gel chromatography (R_f: 0.52 in 1:1 EtOAc in hexanes) using 0-90% EtOAc in hexanes to afford **3.31d** (104 mg, 89%) as a white solid. ^{1}H NMR (400 MHz, $CDCl_3$): δ 7.47 (t, J = 8.0 Hz, 1H), 7.27 (t, J = 8.4 Hz, 1H), 6.89–6.85 (m, 2H), 6.63 (d, J = 8.3 Hz, 1H), 6.55 (d, J = 8.3 Hz, 1H),

3.99 (d, *J* = 3.0 Hz, 1H), 3.74 (s, 3H), 3.72 (s, 3H), 1.17 (s, 9H), 0.89 (d, *J* = 15.4 Hz, 9H); ^{31}P NMR (162 MHz, $CDCl_3$): δ 59.80 ppm; ^{13}C NMR (100 MHz, CDCl3): δ 163.9 (d, *J* = 20.0 Hz), 158.7, 157.1, 138.5 (d, *J* = 5.0 Hz), 134.0 (d, *J* = 1.7 Hz), 129.6, 124.6 (d, *J* = 8.4 Hz), 116.7 (d, *J* = 2.0 Hz), 114.0 (d, *J* = 91.0 Hz), 111.4 (d, *J* = 5.6 Hz), 104.0, 102.8, 80.4 (d, *J* = 59.3 Hz), 55.6, 55.3, 36.4, 33.9 (d, *J* = 71.5 Hz), 25.9 (d, *J* = 3.8 Hz), 23.2. HRMS (DART) *m*/*z* calculated for $C_{23}H_{32}O_4P$ $[M+H]^+$: 403.2033; found: 403.2033.

To a solution of **3.31d** (61 mg, 0.151 mmol, 1.0 equiv) in THF (2.3 mL) at 23 °C was added PMHS (0.15 g) and Ti(O*i*-Pr)$_4$ (0.150 mL, 0.52 mmol, 3.4 equiv). The mixture was stirred at reflux for 12 h, and then concentrated under vacuum to remove most THF. 30% aqueous NaOH solution (3 mL) was carefully added to the residue. Gas was generated during addition. The resulting mixture was further stirred at 60 °C for 0.5 h. To the mixture at 23 °C was added MTBE (5 mL). The MTBE layer was separated and the aqueous layer was washed with MTBE (2 x 5 mL) under nitrogen. The MTBE solution was dried, concentrated, and purified by passing through a neutral alumina plug to afford **3.L5** (20 mg, 35%) as a white crystalline solid. ^{1}H NMR (400 MHz, $CDCl_3$): δ 7.23–7.18 (m, 2H), 6.77 (d, *J* = 8.09 Hz, 1H), 6.71 (dd, *J* = 7.3, 3.0 Hz, 1H), 6.56 (d, *J* = 8.5 Hz, 1H), 6.50 (d, *J* = 8.3 Hz, 1H), 4.38 (s, 1H), 3.65 (s, 3H), 3.64 (s, 3H), 0.93 (s, 3H), 0.65 (d, *J* = 12.0, 9H); ^{31}P NMR (202 MHz, $CDCl_3$): δ -3.36 ppm; ^{13}C NMR (100 MHz, $CDCl_3$): δ 163.6, 156.8, 156.0, 137.0 (d, *J* = 17.8 Hz), 129.2, 127.8, 123.3 (d, *J* = 14.2 Hz), 122.2 (d, *J* = 4.1 Hz), 118.7, 107.6, 103.2, 102.5, 92.0 (d, J = 30.5 Hz), 54.6, 54.4, 35.1 (d, *J* = 16.4 Hz), 29.7 (d, *J* = 18.0 Hz), 25.5 (d, *J* = 14.5 Hz), 25.1 (d, *J* = 8.6 Hz). HRMS (DART) *m*/*z* calculated for $C_{23}H_{32}O_3P$ $[M+H]^+$: 387.2084; found: 387.2083.

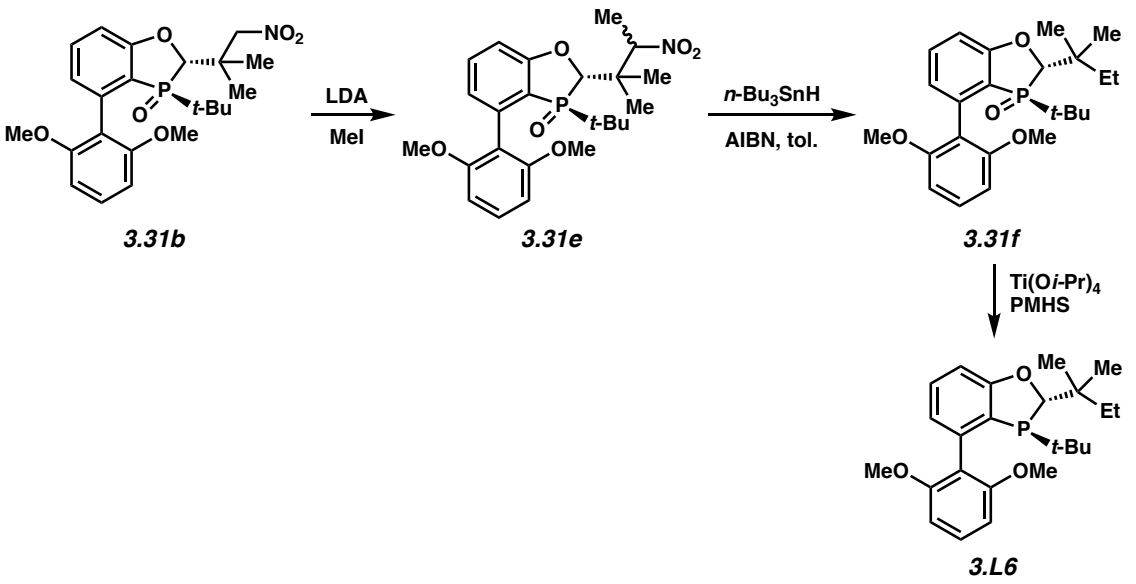

To a solution of **3.31b** (0.7 g, 1.56 mmol, 1.0 equiv) in THF (8.0 mL) was added 2.0 M LDA/THF/EtPh/heptane (2.4 mL, 4.7 mmol, 3.0 equiv) at –78 °C under argon atmosphere. The resulting mixture was aged at –78 °C for additional 30 min before it was warmed to –30 °C for a brief hold of 30 min and then was cooled back to –78 °C using a dry ice/acetone bath. To the resulting solution, was charged iodomethane (1.1 g, 7.82 mmol, 5.0 equiv) and then allowed to age for 12 h while warming up to 23 °C. The reaction mixture was quenched with saturated ammonium chloride (5 mL) and extracted with EtOAc (2 x 20 mL). The organics were combined and washed with water (15 mL). The resulting organics were dried over magnesium sulfate and concentrated under reduced pressure to afford oily residue. The crude residue was purified by silica gel column chromatography using 0-60% EtOAc in hexanes to afford 0.68 g of crude **31e** as a foam in a 2:1 diastereromeric mixture (from methylation) along with the unreacted starting material in 25-30 area%. R_f 0.256 (30% EtOAc in hexanes). This crude mixture was used directly in the next step. HRMS (DART) *m*/*z* calculated for $C_{24}H_{33}O_6NP$ $[M+H]^+$: 462.2040; found: 462.2042.

To the solution of **3.31e** (0.68 g, 1.06 mmol, 1.0 equiv, 70% purity) in degassed toluene (13 mL) were charged tributyltin hydride (3.09 g, 10.6 mmol, 10.0 equiv) and AIBN (2,2'-Azobis(2-methylpropionitrile) (122 mg, 0.74 mmol, 0.75 equiv) under argon. The resulting mixture was heated to 110 °C (reflux) for 12 h and then cooled to 0 °C using an ice/salt bath. The reaction mixture was quenched with 1M NaOH (10.6 mL, 10.6 mmol, 10.0 equiv) and stirred for additional 2 h at 23 °C. The resulting milky white biphasic layers were passed through a short Celite pad and the filtrate was diluted with water (5 mL). The layers were separated and an aqueous layer was extracted with toluene (15 mL). The organics were combined and washed with saturated ammonium chloride (10 mL). The resulting organics were dried over magnesium sulfate and concentrated to afford crude product, which was purified using silica gel column chromatography using 0-100% EtOAc in hexanes to afford 0.260 g of **3.31f** as an off-white solid (59%). R_f = 0.38 in 30% EtOAc in hexanes. ^{1}H NMR (400 MHz, $CDCl_3$): δ 7.48-7.45 (m, 1H), 7.26 (t, *J* = 8.4 Hz, 1H), 6.89–6.83 (m, 1H), 6.62 (d, *J* = 8.3 Hz, 1H), 6.53 (d, *J* = 8.3 Hz, 1H), 4.07 (d, *J* = 2.5 Hz, 1H), 3.73 (s, 3H), 3.71 (s, 3H), 1.73–1.52 (m, 2H), 1.11 (s, 6H), 0.94–0.87 (m, 3H), 0.87 (d, *J* = 15.3 Hz, 9H); ^{31}P NMR (162 MHz, $CDCl_3$): δ 60.08 ppm; ^{13}C NMR (100 MHz, $CDCl_3$): δ 163.9 (d, *J* = 20.0 Hz), 158.8, 157.1, 138.4 (d, *J* = 5.0 Hz), 133.9 (d, *J* = 1.7 Hz), 129.6, 124.5 (d, *J* = 8.4 Hz), 116.7 (d, *J* = 2.0 Hz), 113.7 (d, *J* = 91.0 Hz), 111.3 (d, *J* = 5.6 Hz), 104.0, 102.8, 79.4 (d, *J* = 59.2 Hz), 55.6, 55.3, 39.1, 34.0 (d, *J* = 71.0 Hz), 30.9 (d, *J* = 4.7 Hz), 23.2, 22.4 (d, *J* = 3.9 Hz), 21.6 (d, *J* = 2.7 Hz), 7.97. HRMS (DART) *m*/*z* calculated for $C_{24}H_{34}O_4P$ $[M+H]^+$: 417.2189; found: 417.2193. *Note: Isolated solids of **3.31f** were contaminated with ~5-10% of the tributyltin byproducts.*

To a solution of **3.31f** (0.2 g, 0.48 mmol, 1.0 equiv) in THF (3.0 mL) at 23 °C was added PMHS (0.3 g) and Ti(O*i*Pr)$_4$ (0.36 mL, 1.2 mmol, 2.5 equiv). The mixture was stirred at reflux

for 12 h, and then concentrated under vacuum to remove most THF. 30% aqueous NaOH solution (4 mL) was carefully added to the residue. Gas was generated during addition. The resulting mixture was further stirred at 60 °C for 0.5 h. To the mixture at 23 °C was added MTBE (5 mL). The MTBE layer was separated and the aqueous layer was washed with MTBE (2 x 8 mL) under nitrogen. The MTBE solution was dried, concentrated, and purified by passing through a neutral alumina plug affording the desired product (2*S*,3*S*)-3-(tert-butyl)-4-(2,6-dimethoxyphenyl)-2-(tert-pentyl)-2,3-dihydrobenzo[d][1,3]oxaphosphole (**3.L6**) as white solid (164 mg, 85%). ^{1}H NMR (500 MHz, $CDCl_3$): δ 7.21–7.18 (m, 2H), 6.77 (d, *J* = 7.9 Hz, 1H), 6.71 (dd, *J* = 7.5, 3.2 Hz, 1H), 6.56 (d, *J* = 8.3 Hz, 1H), 6.50 (d, *J* = 8.4 Hz, 1H), 4.47 (s, 1H), 3.65 (s, 3H), 3.64 (s, 3H), 1.46–1.30 (m, 2H), 0.85 (d, *J* = 2.5 Hz, 6H), 0.81 (t, *J* = 7.5 Hz, 3H), 0.66 (d, *J* = 12.0, 9H); ^{31}P NMR (202 MHz, $CDCl_3$): δ -3.83 ppm; ^{13}C NMR (125 MHz, $CDCl_3$): δ 163.7, 156.7, 156.0, 137.0 (d, *J* = 17.4 Hz), 129.2 (d, *J* = 0.7 Hz), 127.8, 123.4 (d, *J* = 14.0 Hz), 122.2 (d, *J* = 4.2 Hz), 118.7 (d, *J* = 1.2 Hz), 107.6 (d, *J* = 0.8 Hz), 103.1, 102.5, 91.1 (d, *J* = 30.6 Hz), 54.6 (d, *J* = 1.2 Hz), 54.4, 37.7 (d, *J* = 14.7 Hz), 29.8 (d, *J* = 7.6 Hz), 29.6, 25.6 (d, *J* = 14.5 Hz), 21.7 (d, *J* = 8.4 Hz), 21.5 (d, *J* = 9.7 Hz), 7.2 (d, *J* = 0.7 Hz). HRMS (DART) *m*/*z* calculated for $C_{24}H_{34}O_3P$ $[M+H]^+$: 401.2240; found: 401.2243.

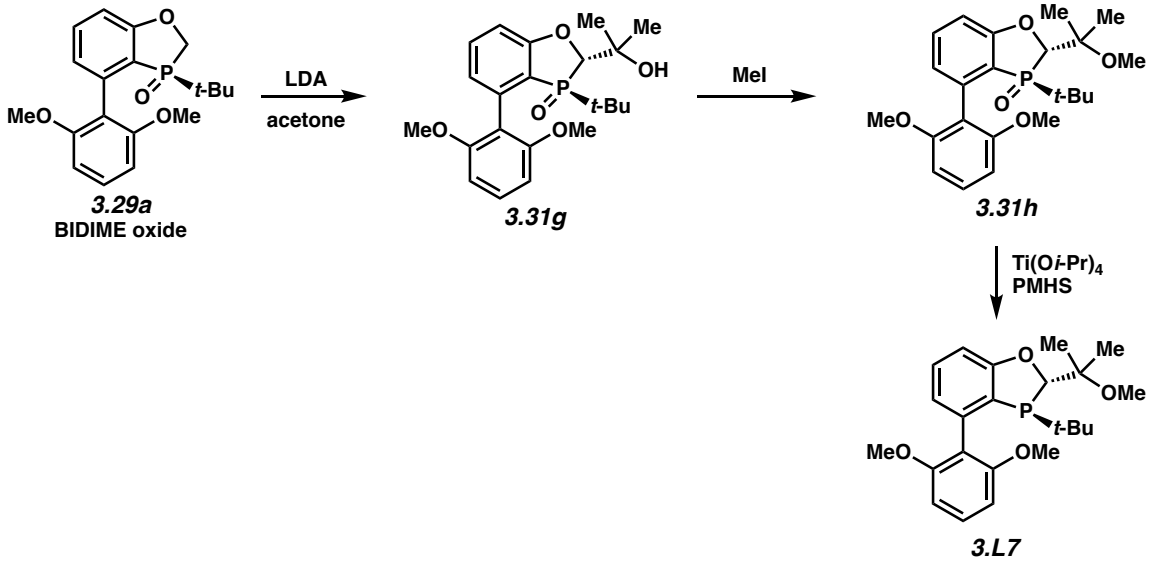

To a solution of BIDIME oxide (**3.29a**, 0.50 g, 1.444 mmol, 1 equiv) in THF (5 mL) at –78 °C was added LDA (0.938 mL, 2.0 M in heptane/THF/chlorobenzene, 1.877 mmol, 1.3 equiv). The mixture was stirred at –78 °C for 30 min before addition of dry acetone (0.4 mL, 5.5 mmol, 3.8 equiv). The resulting mixture was kept at –78 °C for 2 h before it was warmed to 23 °C over 1 h. After stirring at 23 °C overnight, saturated aqueous NH_4Cl and EtOAc were added to the mixture. The aqueous layer was further extracted with EtOAc. The combined EtOAc solution was washed with brine, dried over magnesium sulfate and concentrated to afford 0.565 g (97%) of **3.31g** as an off-white solid that was used without further purification. ^{1}H NMR (500 MHz, $CDCl_3$): δ 7.50 (t, *J* = 7.9 Hz, 1H), 7.29 (t, *J* = 8.4 Hz, 1H), 6.90 (ddd, *J* = 10.8, 7.0, 3.0 Hz, 2H), 6.63 (d, *J* = 8.4 Hz, 1H), 6.55 (d, *J* = 8.3 Hz, 1H), 4.38 (s, 1H), 4.18 (d, *J* = 2.5 Hz, 1H), 3.73 (s, 6H), 1.43 (s, 3H), 1.40 (s, 3H), 0.91 (d, *J* = 16 Hz, 9H); ^{31}P NMR (202 MHz, $CDCl_3$): δ 65.7 ppm; ^{13}C NMR (125 MHz, $CDCl_3$): δ 164.3 (d, *J* = 20.0 Hz), 158.5 (d, *J* = 164.0 Hz), 138.4 (d, *J* = 5.2 Hz), 134.5 (d, *J* = 2H), 130.0, 125.1 (d, *J* = 8.4 Hz), 116.6 (d, *J* = 2.0 Hz), 113.5 (d, *J* = 91.0 Hz), 111.9 (d, *J* = 5.8 Hz), 103. 9 (d, *J* = 124.2 Hz), 77.7 (d, *J* = 60.7 Hz), 73.4 (d, *J* = 2.0 Hz), 55.5 (d, *J* = 17.1 Hz), 34.2 (d, *J* = 71.0 Hz), 28.5 (d, *J* = 6.6 Hz), 24.4 (d, *J* = 2.5 Hz), 23.1

(d, J = 1 Hz). HRMS (DART) *m/z* calculated for $C_{22}H_{30}O_5P$ $[M+H]^+$: 405.1825; found: 405.1824.

To a solution of **3.31g** (0.50 g, 1.24 mmol, 1 equiv) in THF (5 mL) at 0 °C was added NaH (0.34 g, 60% dispersion in mineral oil, 1.5 mmol, 1.2 equiv). The mixture was stirred at 10 °C for 2 h before addition of iodomethane (0.38 g, 2.64 mmol, 2.1 equiv). The resulting mixture was warmed to 23 °C over 1 h. After stirring at 23 °C overnight, saturated aqueous NH_4Cl and EtOAc were added to the mixture. The aqueous layer was further extracted with EtOAc. The combined organic solution was washed with brine, dried over magnesium sulfate, concentrated, and purified by silica gel column chromatography (0-100% EtOAc in hexanes) to afford 0.50 g (97%) of **3.31h** as a white solid. R_f = 0.45 in 100% EtOAc. ^{1}H NMR (500 MHz, $CDCl_3$): δ 7.49 (t, J = 8.0 Hz, 1 H), 7.28 (t, J = 8.3 Hz, 1H), 6.99 (dd, J = 8.3, 3.5 Hz, 1H), 6.91 (dd, J = 7.3, 3.2 Hz, 1H), 6.62 (d, J = 8.4 Hz, 1H), 6.54 (d, J = 8.4 Hz, 1H), 4.39 (s, 1H), 3.72 (d, J = 6.4 Hz, 6H), 3.36 (s, 3H), 1.43 (s, 3H), 1.36 (s, 3H), 0.88 (d, J = 15.6 Hz, 9H); ^{31}P NMR (202 MHz, $CDCl_3$): δ 58.8 ppm; ^{13}C NMR (125 MHz, $CDCl_3$): δ 163.8 (d, J = 19.5 Hz), 158.8, 157.2, 138.5 (d, J = 5.5 Hz), 134.2 (d, J = 1.9 Hz), 129.7, 124.9 (d, J = 8.6 Hz), 116.7 (d, J = 2.2 Hz), 113.6, 112.8, 111.8 (d, J = 5.8 Hz), 104.0, 102.9, 77.5, 77.2 (d, J = 3.0 Hz), 55.5 (d, J = 35.0 Hz), 49.3 (d, J = 1.0 Hz), 34.1 (d, J = 72.7 Hz), 23.3 (d, J = 1.0 Hz), 20.3, 19.9 (d, J = 1.6 Hz). HRMS (DART) *m/z* calculated for $C_{23}H_{32}O_5P$ $[M+H]^+$: 419.1982; found: 419.1984.

To a solution of **3.31h** (0.44 g, 1.04 mmol) in THF (7 mL) at 23 °C was added PMHS (0.45 g) and Ti(O*i*-Pr)$_4$ (0.62 mL, 2.08 mmol, 2.0 equiv). The mixture was stirred at reflux for 12 h, and then concentrated under vacuum to remove most THF. 30% aqueous NaOH solution (5 mL) was carefully added to the residue. Gas was generated during addition. The resulting mixture was further stirred at 60 °C for 0.5 h. To the mixture at 23 °C was added MTBE (5 mL).

The MTBE layer was separated and the aqueous layer was washed with MTBE under nitrogen. The MTBE solution was dried, concentrated, and purified by passing through a neutral alumina plug to afford 0.416 g (99%) of **3.L7** as a white crystalline solid. ^{1}H NMR (400 MHz, $CDCl_3$) δ 7.31–7.26 (m, 2H), 6.91 (d, *J* = 7.9 Hz, 1H), 6.80 (d, *J* = 4.6 Hz), 6.60 (dd, *J* = 19.8, 8.2 Hz, 2H), 4.77 (s, 1H), 3.72 (d, *J* = 3.0 Hz, 6H), 3.34 (s, 3H), 1.22 (s, 3H), 1.18 (s, 3H), 0.74 (d, *J* = 12.0, 9H); ^{31}P NMR (162 MHz, $CDCl_3$) δ 1.8 ppm; ^{13}C NMR (100 MHz, $CDCl_3$) δ 164.6, 157.4 (d, J = 85.0 Hz), 138.0 (d, *J* = 17.7 Hz), 130.4, 128.9, 124.2 (d, *J* = 14.0 Hz), 123.5 (d, *J* = 4.0 Hz), 119.6, 109.1, 103.9 (d, *J* = 57.6 Hz), 89.1 (d, *J* = 31.0 Hz), 77.8 (d, *J* = 19.0 Hz), 55.5 (d, *J* = 18.6 Hz), 49.9, 31.1 (d, *J* = 18.2 Hz), 26.6 (d, *J* = 14.5 Hz), 21.3 (d, *J* = 11.9 Hz), 20.8 (d, *J* = 5.0 Hz). HRMS (DART) *m/z* calculated for $C_{23}H_{32}O_4P$ $[M+H]^+$: 403.2033; found: 403.2037.

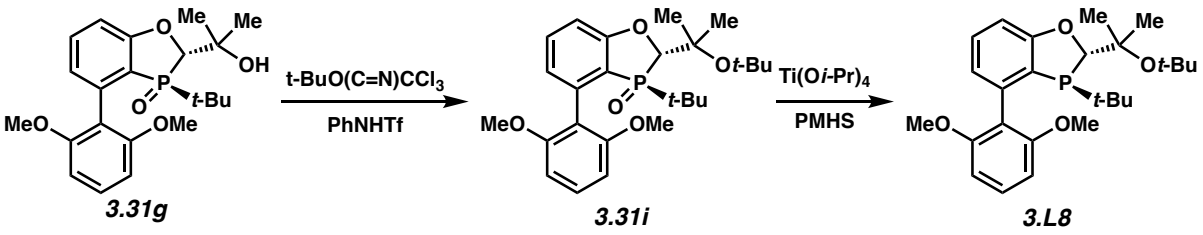

Synthesis of **3.31i** was performed using a modification of our literature procedure.[11o] To a solution of oxide **3.31g** (0.5 g, 1.23 mmol, 1.0 equiv) in fluorobenzene (12.5 mL) was charged a premixed catalyst solution prepared in the glovebox of 1,1,1-trifluoro-*N*-phenylmethanesulfonamide (18.2 mg, 0.062 mmol, 5 mol%) and 2,6-lutidine (66.2 mg, 0.618 mmol, 50 mol%). To the resulting mixture was added *tert*-butyl 2,2,2-trichloroacetimidate (4.05 g, 18.55 mmo, 15.0 equiv), and the mixture was allowed to stir at 23 °C for 24 h (*Note:* white slurry was formed gradually). The reaction mixture was concentrated under reduced pressure and diluted with hexanes (20 mL). The insoluble solids of 2,2,2-trichloroacetamide were collected by filtration, and the resulting filtrate was concentrated under reduced pressure and purified using

silica gel column chromatography (0-100% EtOAc in hexanes) to afford 0.55 g (97%) of oxide **3.31i** as a glossy solid. R_f = 0.68 in 1:1 EtOAc/hexanes. ^{1}H NMR (400 MHz, $CDCl_3$) δ 7.48–7.45 (m, 1 H), 7.28 (t, *J* = 8.4 Hz, 1H), 6.90 (ddd, *J* = 8.3, 3.4, 1.0 Hz, 1H), 6.86 (ddd, *J* = 7.4, 3.3, 1.0 Hz, 1H), 6.62 (d, *J* = 8.0 Hz, 1H), 6.54 (d, *J* = 8.3 Hz, 1H), 4.13 (d, *J* = 3.0 Hz, 1H), 3.72 (s, 3H), 3.71 (s, 3H), 1.52 (s, 3H), 1.48 (s, 3H), 1.32 (s, 9H), 0.88 (d, *J* = 15.4 Hz, 9H); ^{31}P NMR (162 MHz, $CDCl_3$) δ 58.65 ppm; ^{13}C NMR (100 MHz, $CDCl_3$) δ 163.8 (d, *J* = 20.0 Hz), 158.7, 157.2, 138.5 (d, *J* = 5.3 Hz), 133.9 (d, *J* = 1.6 Hz), 129.6, 124.6 (d, *J* = 8.4 Hz), 116.9 (d, *J* = 2.0 Hz), 113.7 (d, *J* = 92.0 Hz), 111.6 (d, *J* = 5.6 Hz), 104.0, 102.9, 79.3 (d, *J* = 59.6 Hz), 78.0, 75.2, 55.6, 55.3, 34.0 (d, *J* = 73.2 Hz), 31.7, 26.2 (d, *J* = 4.0 Hz), 23.8, 23.3. HRMS (DART) *m/z* calculated for $C_{26}H_{38}O_5P$ $[M+H]^+$: 461.2451; found: 461.2449.

To a solution of **3.31i** (0.117 g, 0.253 mmol) in THF (2 mL) at 23 °C was added PMHS (0.121 g) and Ti(O*i*-Pr)$_4$ (0.15 mL, 0.51 mmol, 2.0 equiv). The mixture was stirred at reflux for 12 h, and then concentrated under vacuum to remove most THF. 30% aqueous NaOH solution (5 mL) was carefully added to the residue. Gas was generated during addition. The resulting mixture was further stirred at 60 °C for 0.5 h. To the mixture at 23 °C was added MTBE (5 mL). The MTBE layer was separated and the aqueous layer was washed with MTBE (5 mL x 3) under nitrogen. The MTBE solution was dried, concentrated, and purified by passing through a neutral alumina plug to afford 95 mg (85%) of **3.L8** as a thick pale orange oil. ^{1}H NMR (400 MHz, CD_2Cl_2) δ 7.18 (t, *J* = 8.4 Hz, 1H), 7.12 (t, *J* = 7.9 Hz, 1H), 6.70 (d, *J* = 8.0 Hz, 1H), 6.62 (dd, *J* = 7.5, 3.2 Hz, 1H), 6.54 (dd, *J* = 15.1, 8.4 Hz, 2H), 4.37 (s, 1H), 3.61 (d, *J* = 2.0 Hz, 6H), 1.28 (s, 3H), 1.19 (s, 9H), 1.16 (s, 3H), 0.60 (d, *J* = 11.8, 9H). ^{31}P NMR (162 MHz, CD_2Cl_2) δ 1.25 ppm; ^{13}C NMR (100 MHz, CD_2Cl_2) δ 164.8, 157.9, 156.9, 138.3 (d, *J* = 17.5 Hz), 129.7, 128.8, 125.3 (d, *J* = 16.8 Hz), 123.4 (d, *J* = 3.8 Hz), 119.6, 103.8 (d, *J* = 25.5 Hz), 91.7 (d, *J* = 29.1 Hz), 77.6

(d, J = 15.2 Hz), 74.6, 55.4, 55.3, 31.3, 26.6 (d, J = 3.7 Hz), 26.4 (d, J = 14.8 Hz), 23.3 (d, J = 11.4 Hz). HRMS (DART) *m/z* calculated for $C_{26}H_{38}O_4P$ $[M+H]^+$: 445.2502; found: 445.2501.

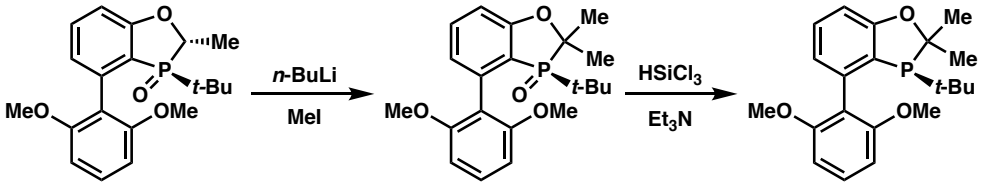

3.31j ***3.31k*** ***3.L11***

To a solution of oxide **3.31j** (400 mg, 1.11 mmol, 1.0 eq) in THF (8 mL) cooled to –78 °C was added a 2.55M solution of *n*-BuLi (520 µL, 1.33 mmol, 1.2 eq). The dark red solution was allowed to stir for 1 hour at –78 °C. Methyl iodide (100 µL, 1.67 mmol, 1.5 eq) was then added dropwise and the reaction mixture was stirred at –78 °C for 30 min then slowly warmed to 23 °C. After 30 min, the reaction was quenched with sat NH_4Cl, and extracted with CH_2Cl_2 (3x). The combined organic layers were washed with water, then brine, dried with $MgSO_4$, and concentrated *in vacuo*. The crude residue was purified by flash chromatography (0.5% to 7% MeOH in CH_2Cl_2) to afford **3.31k** as a white solid (260 mg) in 63% yield. ^{1}HNMR (400 MHz, $CDCl_3$): δ 7.45 (td, J = 7.9 Hz, J = 0.7 Hz, 1H), 7.28 (t, J = 8.4 Hz, 1H), 6.93 (ddd, J = 7.5 Hz, J = 3.0 Hz, J = 0.8 Hz, 1H), 6.79 (ddd, J = 8.2 Hz, J = 3.8 Hz, J = 0.8 Hz, 1H), 6.63 (d, J = 8.4 Hz, 1H), 6.55 (d, J = 8.1 Hz, 1H), 3.77 (s, 3H), 3.73 (s, 3H), 1.75 (d, J = 11 Hz, 3H), 1.61 (d, J = 10 Hz, 3H), 0.96 (d, J = 15 Hz, 9H); ^{31}P{^{1}H}NMR (162 MHz, $CDCl_3$): δ 62 ppm; ^{13}C{^{1}H}NMR (100 MHz, $CDCl_3$): δ 161.8 (d, $J_{C\text{-}P}$ = 17 Hz), 158.7, 157.0, 139.0 (d, $J_{C\text{-}P}$ = 3.8 Hz), 133.4 (d, $J_{C\text{-}P}$ = 1.6 Hz), 129.7, 125.3 (d, J_{CP} = 7.9 Hz), 116.6 (d, J_{CP} = 2.0 Hz), 115.7 (d, J_{CP} = 88 Hz), 112.4 (d, J_{CP} = 4.9 Hz), 104.2, 102.9, 81.8 (d, $J_{C\text{-}P}$ = 67 Hz), 55.9, 55.3, 34.8 (d, $J_{C\text{-}P}$ = 65 Hz), 24.3 (d, $J_{C\text{-}P}$ = 3.4 Hz), 24.0, 22.2 (d, $J_{C\text{-}P}$ = 4.2 Hz); HRMS (DART) *m/z* calculated for $C_{21}H_{28}O_4P$ $[M + H]^+$: 375.1720; found: 375.1720.

To a 10 mL Schlenk flask with magnetic stir bar was charged oxide **3.31k** (206 mg, 0.55 mmol, 1.0 eq). A reflux condenser was added, and the reaction was inerted with Ar using vacuum-purge cycles. PhMe (2.0 mL) was as added followed by triethylamine (155 μL, 1.10 mmol, 2.0 eq) and $HSiCl_3$ (83 μL, 0.83 mmol, 1.5 eq). The mixture was then immersed in an oil bath at 60 °C and monitored by ^{31}P NMR spectroscopy. After 3 h, the reaction was cooled to 23 °C and quenched with 10 mL of degassed (Ar sparge) 30% NaOH (aq.). The mixture was then allowed to vigorously stir at 23 °C for 1 h. The aqueous layer was removed and subsequently extracted under Ar with MTBE (3 × 5 mL). The combined organics were dried with $MgSO_4$, filtered quickly through a pad of Celite, and immediately concentrated *in vacuo*. The crude residue was chromatographed on the bench by dissolving the crude solid in CH_2Cl_2 and loading the mixture onto a short pad of silica gel and eluting with degassed (Ar sparge) 20% EtOAc in hexanes using Ar to pressurize the flash column. The product fractions were immediately collected and concentrated *in vacuo* to afford 98.2 mg (50%) of **3.L11** as a white solid. $[\alpha]_D^{25}$ = – 160 (*c* 0.32, $CHCl_3$); ^1H NMR (400 MHz, $CDCl_3$) δ 7.23–7.17 (m, 2H), 6.79–6.75 (m, 2H), 6.55 (d, *J* = 8.4, 1H), 6.51 (d, J = 8.4 Hz, 1H), 3.65 (d, *J* = 2.9 Hz, 6H), 1.73 (d, *J* = 7.25 Hz, 3H), 1.35 (d, *J* = 16.2 Hz, 3H), 0.72 (d, *J* = 11.6Hz, 9H); $^{31}P\{1\ H\}$NMR (202 MHz, $CDCl_3$) δ 12.5 ppm; $^{13}C\{^1H\}$NMR (100 MHz, $CDCl_3$) δ 161.4 (d, $J_{C–P}$ = 0.8 Hz), 156.5, 156.0, 137.8 (d, $J_{C–P}$ = 16.2 Hz), 129.0 (d, $J_{C–P}$ = 1.0 Hz), 127.9, 126.4 (d, $J_{C–P}$ = 13.4 Hz), 122.7 (d, $J_{C–P}$ = 4.3 Hz), 118.8 (d, $J_{C–P}$ = 1.35 Hz), 108.9 (d, $J_{C–P}$ = 1.0 Hz), 103.4, 102.6, 87.2 (d, $J_{C–P}$ = 26.6 Hz), 54.7 (d, $J_{C–P}$ = 1.7 Hz), 54.4, 31.3 (d, $J_{C–P}$ = 22.3 Hz), 28.1 (d, $J_{C–P}$ = 32.2 Hz), 26.1 (d, $J_{C–P}$ = 14.1 Hz), 22.7 (d, $J_{C–P}$ = 4.2 Hz). HRMS (DART) *m*/*z* calculated for $C_{21}H_{28}O_3P$ $[M + H]^+$: 359.1771; found: 359.1770.

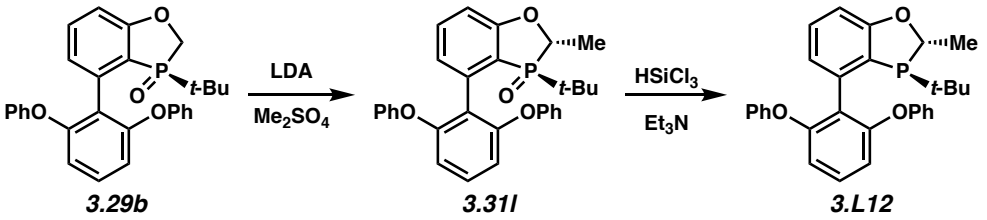

To a solution oxide **3.29b** (0.289 g, 0.614 mmol) in THF (1 mL) cooled to –78 °C was added a freshly prepared solution of LDA in THF (0.48 mL (1.2 mmol, 2.0 eq) of 2.55 M solution of *n*-BuLi was added to a solution of di-*iso*propylamine (180 µL, 1.29 mmol, 2.1 eq) in THF (2 mL) at –78 °C and stirred for 25 min before use). The dark red solution was allowed to stir for 1 h at –78 °C. Dimethyl sulfate (0.87 mL, 0.92 mol) was then added dropwise, and the reaction mixture was stirred at –78 °C for 30 min and then slowly warmed to 23 °C. After 30 min, the reaction was quenched with sat NH_4Cl, and extracted with CH_2Cl_2 (3x). The combined organic layers were washed with water, then brine, dried with $MgSO_4$, and concentrated *in vacuo*. The crude residue was purified by flash chromatography (20% to 80% EtOAc in hexanes) to afford **3.31l** as a white solid (214 mg) in 72% yield. ^{1}H NMR (400 MHz, $CDCl_3$) δ 7.38 (t, J = 8.1 Hz, 1H), 7.29–7.36 (m, 6H), 7.07–7.15 (m, 3H), 6.98 (d, J = 7.6 Hz, 2H), 6.93 (dd, *J* = 7.1 Hz, *J* = 2.7 Hz 1H), 6.86 (dd, *J* = 8.2 Hz, *J* = 3.4 Hz, 1H), 6.51 (d, *J* = 8.2 Hz, 1H), 6.41 (d, *J* = 8.4 Hz, 1H), 4.58 (p, *J* = 6.4 Hz, 1H), 1.62 (dd, *J* = 12 Hz, *J* = 7.1 Hz, 3H), 1.06 (d, *J* = 16 Hz, 9H); ^{31}P{^{1}H}NMR (162 MHz, $CDCl_3$) δ 60 ppm; ^{13}C{^{1}H}NMR (100 MHz, $CDCl_3$) δ 163.9 (d, J_{C-P} = 18 Hz), 158.6, 156.6, 155.8, 155.5, 137.2 (d, J_{CP} = 5.0 Hz), 134.0 (d, J_{CP} = 1.6 Hz), 129.8, 129.6, 129.4, 124.6, 124.5, 124.4, 123.6, 122.2, 119.4, 114.7 (d, J_{CP} = 88 Hz), 113.0 (d, J_{CP} = 5.3 Hz), 110.4, 109.5, 70.5 (d, J_{CP} = 6.3 Hz), 33.3 (d, J_{CP} = 7.1 Hz), 24.2, 15.1. HRMS (DART) *m*/*z* calculated for $C_{30}H_{30}O_4P$ $[M + H]^+$: 485.1876; found: 485.1880.

To a Schlenk flask with magnetic stir bar was charged oxide **3.31l** (205 mg, 0.423 mmol, 1.0 eq). A reflux condenser was added, and the reaction was inerted with Ar using vacuum-purge

cycles. PhMe (2.0 mL) was as added followed by triethylamine (120 μL, 0.846 mmol, 2.0 eq) and $HSiCl_3$ (65 μL, 0.635 mmol, 1.5 eq). The mixture was then immersed in an oil bath at 60 °C and monitored by ^{31}P NMR spectroscopy. After 3.5 h, the reaction was cooled to 23 °C and quenched with 8 mL of degassed (Ar sparge) 30% NaOH (aq.). The mixture was then allowed to vigorously stir at for 1 h. The aqueous layer was removed and subsequently extracted under Ar with MTBE (3 × 6 mL). The combined organics were dried with MgSO4, filtered quickly through a pad of Celite, and immediately concentrated *in vacuo*. The crude residue was chromatographed on the bench by dissolving the crude solid in CH_2Cl_2 and loading the mixture onto a short pad of silica gel and eluting with degassed (Ar sparge) 20% EtOAc in hexanes using Ar to pressurize the flash column. The product fractions were immediately collected and concentrated *in vacuo* to afford 186 mg (93%) of **3.L12** as a white solid. $[\alpha]_D^{25}$ = + 50.8 (*c* 0.19, $CHCl_3$); ^1H NMR (400 MHz, $CDCl_3$) δ 7.37–7.33 (m, 2H), 7.25–7.21 (m, 2H), 7.18–7.11 (m, 3H), 7.04–6.98 (m, 5H), 6.87–6.84 (m, 1H), 6.80 (dd, *J* = 8.0 Hz, *J* = 0.8 Hz, 1H), 6.67 (dd, *J* = 8.3 Hz, *J* = 0.9 Hz, 1H), 6.58 (dd, *J* = 8.3 Hz, J = 0.9 Hz, 1H), 5.02 (m, 1H), 1.40 (dd, *J* = 16.4 Hz, *J* = 7.12 Hz, 3H), 0.88 (d, *J* = 12.0 Hz, 9H); $^{31}P\{^1H\}$NMR (202 MHz, $CDCl_3$) δ 8.8 ppm; $^{13}C\{^1H\}$NMR (100 MHz, $CDCl_3$) δ 162.6, 156.8, 156.6, 156.4, 155.2, 137.4 (d, J_{CP} = 16.9 Hz), 130.5, 129.8, 129.3, 128.8, 123.7, 123.4, 123.3, 123.0, 119.8, 119.2, 119.2, 122.9, 111.7, 110.2, 78.9 (d, J_{CP} = 23.9 Hz), 31.1 (d, J_{CP} = 17.9 Hz), 27.0 (d, J_{CP} = 14.2 Hz), 21.3 (d, J_{CP} = 28.9 Hz). HRMS (DART *m*/*z* calculated for $C_{30}H_{30}O_3P$ $[M + H]^+$: 469.1927; found: 469.1926.

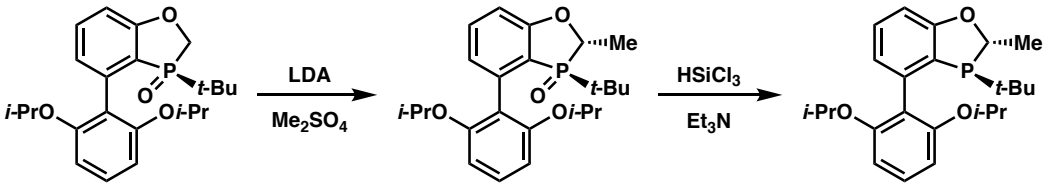

3.29c *3.31m* *(S_P)-3.L13*

To a solution oxide **3.29c** (1.2 g, 2.98 mmol, 1.0 eq) in THF (5 mL) cooled to –78 °C was added a freshly prepared solution of LDA in THF (2.28 mL (5.82 mmol, 1.95 eq) of 2.55M solution of *n*-BuLi was added to a solution of diisopropylamine (890 µL, 6.26 mmol, 2.1 eq) in THF (2 mL) at –78 °C and stirred for 25 min before use). The dark red solution was allowed to stir for 1 hour at –78 °C. Dimethyl sulfate was then added dropwise and the reaction mixture was stirred at –78 °C for 30 min then slowly warmed to 23 °C. After 30 min, the reaction was quenched with sat NH_4Cl, and extracted with CH_2Cl_2 (3x). The combined organic layers were washed with water, then brine, dried with MgSO4, and concentrated in vacuo. The crude residue was purified by flash chromatography (0% to 8% MeOH in CH_2Cl_2) to afford **3.31m** as a semi-solid (1.12 g) in 90% yield. $[\alpha]_D^{22}$ = – 82.1 (*c* 0.33, $CHCl_3$); ^{1}H NMR (400 MHz, $CDCl_3$) δ 7.43 (t, *J* = 7.7 Hz, 1H), 7.21 (t, *J* = 8.4 Hz, 1H), 6.83–6.79 (m, 2H), 6.54 (d, *J* = 8.4 Hz, 1H), 6.46 (d, *J* = 8.4 Hz, 1H), 4.54–4.44 (m, 3H), 1.54 (dd, *J* = 11.6 Hz, *J* = 7.2 Hz, 3H), 1.31 (d, *J* = 6.0 Hz, 3H), 1.22 (d, *J* = 6.0 Hz, 3H), 1.17 (d, *J* = 3.6 Hz, 3H), 1.15 (d, *J* = 3.6 Hz, 3H), 1.31 (d, *J* = 6.0 Hz, 3H), 0.87 (d, *J* = 15.4 Hz, 9H); ^{31}P{1 H}NMR (202 MHz, $CDCl_3$) δ 59.5 ppm; ^{13}C{1 H}NMR (100 MHz, $CDCl_3$) δ 162.1 (d, J_{C-P} = 19.2 Hz), 157.7, 155.9, 139.7 (d, J_{C-P} = 5.34 Hz), 133.5 (d, J_{C-P} = 1.7 Hz), 129.2(d, J_{C-P} = 12.2 Hz), 125.1 (d, J_{C-P} = 8.4 Hz), 118.4 (d, J_{C-P} = 2.0 Hz), 114.5, 113.6, 111.6 (d, J_{C-P} = 5.6 Hz), 104.9, 103.6, 70.5, 70.3, 69.6, 69.3, 33.7, 32.9, 24.3, 23.8, 22.3, 22.1, 22.0, 21.9, 15.5. HRMS (DART) *m/z* calculated for $C_{24}H_{34}O_4P$ $[M + H]^+$: 417.2189; found: 417.2188.

To a 10 mL Schlenk flask with magnetic stir bar was charged oxide **3.31m** (0.99 g, 2.38 mmol, 1.0 eq). A reflux condenser was added, and the reaction was inerted with Ar using vacuum-purge cycles. PhMe (8.0 mL) was added followed by triethylamine (0.67 mL, 4.76 mmol, 2.0 eq) and $HSiCl_3$ (0.36 mL, 3.6 mmol, 1.5 eq). The mixture was then immersed in an oil bath at 60 °C and monitored by ^{31}P NMR spectroscopy. After 3 h, the reaction was cooled to 23 °C and quenched with 10 mL of degassed (Ar sparge) 30% NaOH (aq.). The mixture was then allowed to vigorously stir at 23 °C for 1 h. The aqueous layer was removed and subsequently extracted under Ar with MTBE (3 × 10 mL). The combined organics were dried with $MgSO_4$, filtered quickly through a pad of Celite, and immediately concentrated *in vacuo*. The crude residue was chromatographed on the bench by dissolving the crude solid in CH_2Cl_2 and loading the mixture onto a short pad of silica gel and eluting with degassed (Ar sparge) 20% EtOAc in hexanes using Ar to pressurize the flash column. The product fractions were immediately collected and concentrated *in vacuo* to afford 865 mg (91%) of **3.L13** as a white solid. $[\alpha]_D^{22}$ = –111 (*c* 0.28, $CHCl_3$); ^1H NMR (500 MHz, $CDCl_3$) δ 7.24 (t, *J* = 7.8 Hz, 1H), 7.18 (t, *J* = 8.3 Hz, 1H), 6.82 (d, *J* = 8.0 Hz, 1H), 6.77 (dd, *J* = 7.5 Hz, *J* = 3.1Hz, 1H), 6.60 (d, *J* = 8.25 Hz, 1H), 6.52 (d, *J* = 8.35 Hz, 1H), 4.98 (q, *J* = 7.1 Hz, 1H), 4.47 (p, *J* = 6.1 Hz, 1H), 4.29 (p, *J* = 6.1 Hz, 1H), 1.44 (dd, *J* = 12.1 Hz, *J* = 7.2 Hz, 3H), 1.26 (d, *J* = 6.0 Hz, 3H), 1.24 (d, *J* = 6.0 Hz, 3H), 1.14 (d, *J* = 6.1 Hz, 3H), 1.00 (d, *J* = 6.1 Hz, 3H), 0.74 (d, *J* = 11.9 Hz, 3H); $^{31}P\{1\ H\}$NMR (202 MHz, $CDCl_3$) δ 9.6 ppm; $^{13}C\{1\ H\}$NMR (100 MHz, $CDCl_3$) δ 162.3, 156.4, 155.7, 139.5 (d, J_{C-P} = 13.5 Hz), 129.7 (d, J_{C-P} = 0.7 Hz), 128.4, 124.3, 124.2 (d, J_{C-P} = 3.4 Hz), 122.4 (d, J_{C-P} = 0.9 Hz), 109.1 (d, J_{C-P} = 0.7 Hz), 108.3, 104.9, 78.8, 78.6, 71.5, 69.1, 31.0 (d, J_{C-P} = 14.7 Hz), 26.9 (d, J_{C-P} = 11.4 Hz), 22.5 (d, J_{C-P} = 2.1 Hz), 22.2, 22.1, 22.0, 21.8, 21.6. HRMS (DART) *m*/*z* calculated for $C_{24}H_{34}O_3P$ $[M + H]^+$: 401.2240; found: 401.2242.

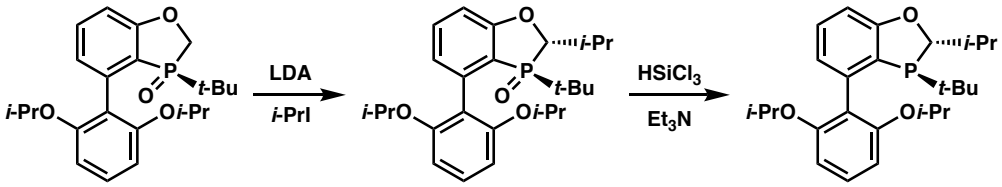

To a solution oxide **3.29c** (1.00 g, 2.48 mmol) in THF (3 mL) cooled to –78 °C was added a freshly prepared solution of LDA in THF (1.95 mL (4.97 mmol, 2.0 eq) of 2.55 M solution of *n*-BuLi was added to a solution of di-*iso*propylamine (730 µL, 5.21 mmol, 2.1 eq) in THF (8 mL) at –78 °C and stirred for 30 min before use). The dark red solution was allowed to stir for 1 h at –78 °C. 2-Iodopropane (0.57 mL, 3.7 mol) was then added dropwise, and the reaction mixture was stirred at –78 °C for 30 min and then slowly warmed to 23 °C. After 30 min, the reaction was quenched with sat NH_4Cl, and extracted with CH_2Cl_2 (3x). The combined organic layers were washed with water, then brine, dried with $MgSO_4$, and concentrated *in vacuo*. The crude residue was purified by flash chromatography (20% to 70% EtOAc in hexanes) to afford **3.31n** as a white solid (852 mg) in 78% yield. ^{1}H NMR (400 MHz, $CDCl_3$) δ 7.40 (td, J = 7.8 Hz, J = 0.7 Hz, 1H), 7.18 (t, J = 8.4 Hz, 1H), 6.82 (d, J = 8.2 Hz, J = 3.5 Hz, 1H), 6.77 (ddd, J = 7.4 Hz, J = 3.2 Hz, J = 0.6 Hz, 1H), 6.53 (d, J = 8.4 Hz, 1H), 6.46 (d, J = 8.3 Hz, 1H), 4.40–4.55 (m, 2H), 4.10 (dd, J = 6.2 Hz, J = 3.5 Hz, 1H), 2.25–2.41 (m, 1H), 1.30 (d, J = 6.1 Hz, 3H), 1.21 (d, J = 6.0 Hz, 3H), 1.16 (d, J = 6.4 Hz, 6H), 1.12 (d, J = 6.0 Hz, 3H), 1.11 (d, J = 6.7 Hz, 3H), 0.90 (d, J = 16 Hz, 9H); ^{31}P{^{1}H}NMR (162 MHz, $CDCl_3$) δ 59 ppm; ^{13}C{^{1}H}NMR (100 MHz, $CDCl_3$) δ 163.7 (d, J_{CP} = 20 Hz), 157.6, 156.0, 139.5 (d, J_{CP} = 5.1 Hz), 133.4 (d, J_{CP} = 1.7 Hz), 129.1, 124.9 (d, J_{CP} = 8.4 Hz), 118.5 (d, J_{CP} = 2.1 Hz), 114.3 (d, J_{CP} = 90 Hz), 111.1 (d, J_{CP} = 5.6 Hz), 105.0, 103.6, 78.0 (d, J_{CP} = 61 Hz), 70.3, 69.3, 33.6 (d, J_{CP} = 71 Hz), 29.8, 23.6, 22.3, 22.1, 22.0, 21.9, 19.7 (d, J_{CP} = 5.2 Hz), 18.1 (d, J_{CP} = 4.6 Hz). HRMS (DART) *m*/*z* calculated for $C_{26}H_{38}O_4P$ $[M + H]^+$: 445.2502; found: 445.2503.

To a Schlenk flask with magnetic stir bar was charged oxide **3.31n** (806 mg, 1.81 mmol, 1.0 eq). A reflux condenser was added, and the reaction was inerted with Ar using vacuum-purge cycles. PhMe (8.0 mL) was added followed by triethylamine (504 µL, 3.63 mmol, 2.0 eq) and $HSiCl_3$ (275 µL, 2.72 mmol, 1.5 eq). The mixture was then immersed in an oil bath at 60 °C and monitored by 31P NMR spectroscopy. After 3 h, the reaction was cooled to 23 °C and quenched with 10 mL of degassed (Ar sparge) 30% NaOH (aq.). The mixture was then allowed to vigorously stir at 23 °C for 1 h. The aqueous layer was removed and subsequently extracted under Ar with MTBE (3 × 12 mL). The combined organics were dried with $MgSO_4$, filtered quickly through a pad of Celite, and immediately concentrated *in vacuo*. The crude residue was chromatographed on the bench by dissolving the crude solid in CH_2Cl_2 and loading the mixture onto a short pad of silica gel and eluting with degassed (Ar sparge) 20% EtOAc in hexanes using Ar to pressurize the flash column. The product fractions were immediately collected and concentrated in vacuo to afford 659 mg (85%) of **3.L14** as a white solid. $[a]_D^{25}$ = – 94.8 (*c* 0.33, $CHCl_3$); ^{1}H NMR (400 MHz, $CDCl_3$) δ 7.22–7.15 (m, 2H), 6.80 (dd, *J* = 8.0 Hz, *J* = 0.8 Hz, 1H), 6.80–6.70 (m, 1H), 6.60 (d, *J* = 8.2 Hz, 1H), 6.51 (d, *J* = 8.2 Hz, 1H), 4.54 (d, *J* = 7.2 Hz, 1H), 4.46 (p, *J* = 6.0 Hz, 1H), 4.33 (p, *J* = 6.0 Hz, 1H), 2.00–1.93 (m, 1H), 1.25 (t, *J* = 6.6 Hz, 3H), 1.44 (d, *J* = 16.0 Hz, 3H), 1.28 (d, *J* = 6.0 Hz, 3H), 1.25 (d, J = 6.0 Hz, 3H), 1.14 (d, J = 6.0 Hz, 6H), 1.14 (d, J = 6.1 Hz, 3H), 1.03 (d, J = 6.1 Hz, 3H), 1.00 (d, *J* = 6.1 Hz, 3H), 0.97 (d, *J* = 6.1 Hz, 3H), 0.76 (d, *J* = 11.9 Hz, 9H); ^{31}P{1 H}NMR (202 MHz, $CDCl_3$) δ –0.2 ppm; ^{13}C{1 H}NMR (100 MHz, $CDCl_3$) δ 163.7, 156.5, 155.9, 139.1 (d, $J_{C–P}$ = 17.4 Hz), 129.5, 128.4, 124.0 (d, $J_{C–P}$ = 4.3 Hz), 108.3, 107.9, 104.8, 89.3 (d, $J_{C–P}$ = 27.9 Hz), 71.5, 69.1, 33.1 (d, $J_{C–P}$ = 21.6 Hz), 30.7 (d, $J_{C–P}$ = 18.4 Hz), 26.9 (d, $J_{C–P}$ = 14.4 Hz), 22.3 (d, $J_{C–P}$ = 2.1 Hz), 22.2, 22.1, 21.9,

19.2, 19.1, 19.0, 18.9. HRMS (DART) *m*/*z* calculated for $C_{26}H_{38}O_3P$ $[M + H]^+$: 429.2553; found: 429.2552.

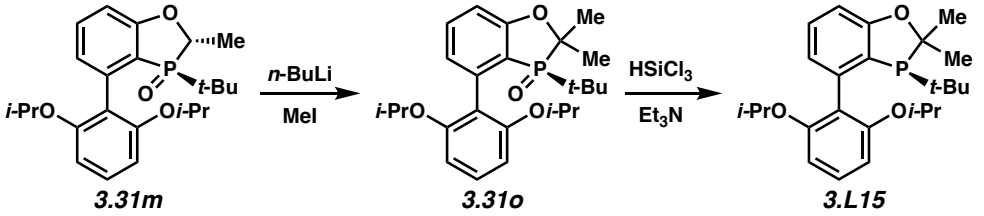

To a solution of oxide **3.31m** (840 mg, 2.01 mmol, 1.0 eq) in THF (12 mL) cooled to –78 °C was added a 2.55M solution of *n*-BuLi (960 μL, 2.42 mmol, 1.2 eq). The dark red solution was allowed to stir for 45 minutes at –78 °C. Methyl iodide (200 μL, 3.02 mmol, 1.5 eq) was then added dropwise and the reaction mixture was stirred at –78 °C for 30 min then slowly warmed to 23 °C. After 30 min, the reaction was quenched with sat NH_4Cl, and extracted with CH_2Cl_2 (3x). The combined organic layers were washed with water, then brine, dried with $MgSO_4$, and concentrated *in vacuo*. The crude residue was purified by flash chromatography (0% to 8% MeOH in CH_2Cl_2) to afford **3.31o** as a white solid (489 mg) in 52% yield. $[a]_D^{25}$ = –54.0 (*c* 0.19, $CHCl_3$); ^{1}H NMR (400 MHz, $CDCl_3$) δ 7.38 (t, *J* = 8.1 Hz, 1H), 7.19 (t, *J* = 8.4 Hz, 1H), 6.83–6.73 (m, 2H), 6.53 (d, *J* = 8.3 Hz, 1H), 6.44 (d, *J* = 8.3 Hz, 1H), 4.51–4.44 (m, 2H), 1.74 (d, *J* = 10.7 Hz, 3H), 1.60 (d, *J* = 10.0 Hz, 3H), 1.35 (d, *J* = 6.0 Hz, 3H), 1.24 (d, *J* = 6.0 Hz, 3H), 1.15 (d, *J* = 6.0 Hz, 3H), 1.11 (d, *J* = 6.0 Hz, 3H), 1.00 (d, *J* = 14.8 Hz, 9H); ^{31}P{1 H}NMR (202 MHz, $CDCl_3$) δ 61.6 ppm; ^{13}C{1 H}NMR (100 MHz, $CDCl_3$) δ 161.7 (d, $J_{C–P}$ = 16.9 Hz), 157.4, 155.8, 140.1 (d, $J_{C–P}$ = 4.0Hz), 132.8 (d, $J_{C–P}$ = 1.5 Hz), 129.1 (d, $J_{C–P}$ = 5.0 Hz), 125.9 (d, $J_{C–P}$ = 8.1 Hz), 117.9, 116.3, 115.4, 111.8 (d, $J_{C–P}$ = 4.9 Hz), 104.7, 103.3, 81.9. 81.2, 35.2, 34.6, 25.1 (d, $J_{C–P}$ = 3.5 Hz), 24.3, 22.7 (d, $J_{C–P}$ = 4.2 Hz), 22.2 (d, $J_{C–P}$ = 13.8 Hz), 22.0 (d, $J_{C–P}$ = 13.8 Hz). HRMS (DART) *m*/*z* calculated for $C_{25}H_{36}O_4P$ $[M + H]^+$: 431.2346; found: 431.2344.

To a Schlenk flask with magnetic stir bar was charged oxide **3.31o** (448 mg, 1.04 mmol, 1.0 eq). A reflux condenser was added, and the reaction was inerted with Ar using vacuum-purge cycles. PhMe (4.0 mL) was added followed by triethylamine (290 µL, 2.08 mmol, 2.0 eq) and $HSiCl_3$ (160 µL, 1.56 mmol, 1.5 eq). The mixture was then immersed in an oil bath at 60 °C and monitored by ^{31}P NMR spectroscopy. After 3 h, the reaction was cooled to 23 °C and quenched with 8 mL of degassed (Ar sparge) 30% NaOH (aq.). The mixture was then allowed to vigorously stir at 23 °C for 1 h. The aqueous layer was removed and subsequently extracted under Ar with MTBE (3 × 8 mL). The combined organics were dried with $MgSO_4$, filtered quickly through a pad of Celite, and immediately concentrated *in vacuo*. The crude residue was chromatographed on the bench by dissolving the crude solid in CH_2Cl_2 and loading the mixture onto a short pad of silica gel and eluting with degassed (Ar sparge) 20% EtOAc in hexanes using Ar to pressurize the flash column. The product fractions were immediately collected and concentrated *in vacuo* to afford 865 mg (91%) of **3.L15** as a white solid. $[a]_D^{25}$ = – 104 (*c* 0.36, $CHCl_3$); ^1H NMR (400 MHz, $CDCl_3$) δ 7.24–7.16 (m, 3H), 6.81–6.76 (m, 2H), 6.61 (d, *J* = 8.1 Hz, 1H), 6.50 (d, *J* = 8.2 Hz, 1H), 4.45 (p, *J* = 6.1 Hz, 1H), 4.36 (p, *J* = 6.1 Hz, 1H), 1.79 (d, *J* = 7.8 Hz, 3H), 1.44 (d, *J* = 16.0 Hz, 3H), 1.28 (d, *J* = 6.0 Hz, 3H), 1.25 (d, *J* = 6.0 Hz, 3H), 1.14 (d, *J* = 6.0 Hz, 3H), 0.96 (d, *J* = 6.0 Hz, 3H), 0.81 (d, *J* = 11.5 Hz, 9H); $^{31}P\{1\ H\}$NMR (202 MHz, $CDCl_3$) δ 12.6 ppm; $^{13}C\{1\ H\}$NMR (100 MHz, $CDCl_3$) δ 162.2, 156.2, 155.8, 139.7 (d, $J_{C–P}$ = 16.4 Hz), 129.3, 128.4, 124.5 (d, $J_{C–P}$ = 4.4 Hz), 109.3, 108.1, 104.6, 88.3, 88.0, 71.5, 69.1, 32.5 (d, $J_{C–P}$ = 22.7 Hz), 29.7 (d, $J_{C–P}$ = 32.2 Hz), 27.4 (d, $J_{C–P}$ = 14.1 Hz), 24.1 (d, $J_{C–P}$ = 3.9 Hz), 22.6 (d, $J_{C–P}$ = 1.9 Hz), 22.1 (d, $J_{C–P}$ = 7.2 Hz). HRMS (DART) *m*/*z* calculated for $C_{25}H_{36}O_3P$ $[M + H]^+$: 415.2397; found: 415.2397.

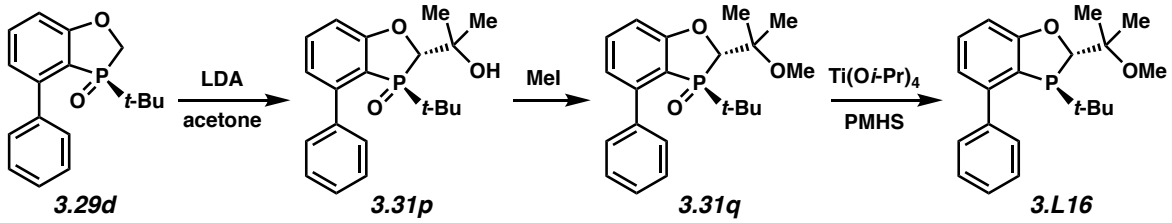

To a solution of oxide **3.29d** (1.0 g, 3.5 mmol, 1 equiv) in THF (13 mL) at –78 °C was added LDA (2.27 mL, 2.0 M in heptane/THF/chlorobenzene, 4.54 mmol, 1.3 equiv). The mixture was stirred at –78 °C for 30 min before addition of dry acetone (3.5 mL, 47.7 mmol, 13.7 equiv). The resulting mixture was kept at –78 °C for 2 h before it was warmed to 23 °C over 1 h. After stirring at 23 °C overnight, saturated aqueous NH_4Cl and EtOAc were added to the mixture. The aqueous layer was further extracted with EtOAc. The combined EtOAc solution was washed with brine, dried over magnesium sulfate, concentrated to give 1.13 g (94%) of **3.31p** as a beige solid that was used directly in the next step without further purification. HRMS (DART) *m/z* calculated for $C_{20}H_{26}O_3P$ $[M+H]^+$: 345.1614; found: 345.1614.

To a solution of oxide **3.31p** (1.0 g, ~2.90 mmol, 1 equiv) in THF (10 mL) at 0 °C was added NaH (1.0 g, 60% dispersion in mineral oil, 4.4 mmol, 1.5 equiv). The mixture was stirred at 10 °C for 2 h before addition of iodomethane (1.5 g, 10.6 mmol, 3.65 equiv). The resulting mixture was warmed to 23 °C over 1 h. After stirring at 23 °C overnight, saturated aqueous NH_4Cl and EtOAc were added to the mixture. The aqueous layer was further extracted with EtOAc. The combined organic solution was washed with brine, dried over magnesium sulfate, concentrated, and purified by silica gel column chromatography (0-100% EtOAc in hexanes) to give afford 0.78 g (75%) of **3.31q** as a white solid. R_f = 0.45 100% EtOAc. ^{1}H NMR (400 MHz, $CDCl_3$): δ 7.76–7.74 (m, 2H), 7.52–7.48 (m, 1H), 7.44–7.40 (m, 2H), 7.37–7.33 (m, 1H), 7.02 (dddd, J = 13.8, 7.5, 3.8, 0.8 Hz, 2H), 4.4 (d, J = 1.3 Hz, 1H), 3.36 (s, 3H), 1.49 (s, 3H), 1.44 (s,

3H), 0.77 (d, J = 15.8 Hz, 9H); ^{31}P NMR (162 MHz, $CDCl_3$): δ 60.41 ppm; ^{13}C NMR (100 MHz, $CDCl_3$): δ 164.4 (d, J = 18.8 Hz), 146.8 (d, 5.9 Hz), 140.3 (d, J = 2.0 Hz), 134.8 (d, J = 1.7 Hz), 130.0, 128.3, 128.2, 123.4 (d, J = 8.2 Hz), 112.2 (d, J = 5.5 Hz), 111.9 (d, J = 89.0 Hz), 77.4, 76.8, 49.4, 34.4 (d, J = 72.0 Hz), 23.8, 20.3, 20.1 (d, J = 1.4 Hz). HRMS (DART) *m/z* calculated for $C_{21}H_{28}O_3P$ $[M+H]^+$: 359.1771; found: 359.1771.

To a solution of oxide **3.31q** (0.2 g, 0.56 mmol) in THF (3.5 mL) at 23 °C was added PMHS (0.40 g) and Ti(O*i*-Pr)$_4$ (0.33 mL, 1.12 mmol, 2.0 equiv). The mixture was stirred at reflux for 12 h, and then concentrated under vacuum to remove most THF. 30% aqueous NaOH solution (3 mL) was carefully added to the residue. Gas was generated during addition. The resulting mixture was further stirred at 60 °C for 0.5 h. To the mixture at 23 °C was added MTBE (5 mL). The MTBE layer was separated and the aqueous layer was washed with MTBE (5 mL x 2) under nitrogen. The MTBE solution was dried, concentrated, and purified by passing through a neutral alumina plug to afford 0.185 g (97%) of **3.L16** as a white crystalline solid. ^{1}H NMR (400 MHz, $CDCl_3$): δ 7.60–7.58 (m, 2H), 7.34–7.30 (m, 2H), 7.25–7.21 (m, 2H), 6.88–6.84 (m, 2H), 4.68 (d, J = 1.5 Hz, 1H), 3.27 (s, 1H), 1.21 (s, 3H), 1.18 (s, 3H), 0.58 (d, J = 12.0 Hz, 9H); ^{31}P NMR (162 MHz, $CDCl_3$): δ -2.31 ppm; ^{13}C NMR (100 MHz, $CDCl_3$): δ 165.1, 145.5 (d, J = 13.3 Hz), 142.5, 131.2, 129.1 (d, J = 5.2 Hz), 128.3, 127.3, 121.7 (d, J = 3.0 Hz), 121.2 (d, J = 18.1 Hz), 109.6, 89.0 (d, J = 30.6 Hz), 77.5 (d, J = 18.1 Hz), 49.9, 31.8 (d, J = 19.6 Hz), 26.7 (d, J = 13.4 Hz), 21.3, 21.1 (d, J = 15.0 Hz). HRMS (DART) *m/z* calculated for $C_{21}H_{28}O_2P$ $[M+H]^+$: 343.1821; found: 343.1821.

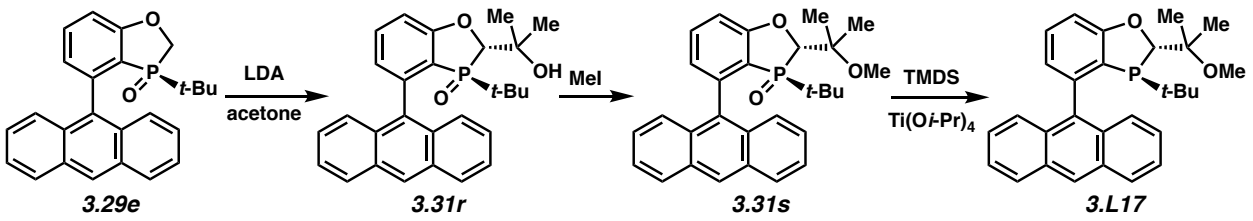

To a solution of oxide **3.29e** (0.22 g, 0.57 mmol, 1 equiv) in THF (2.5 mL) at –78 °C was added LDA (0.37 mL, 2.0 M in heptane/THF/chlorobenzene, 0.74 mmol, 1.3 equiv). The mixture was stirred at –78 °C for 30 min before addition of dry acetone (1.0 mL, 13.6 mmol, 24 equiv). The resulting mixture was kept at –78 °C for 1 h before it was warmed to 23 °C over 1 h. After stirring at 23 °C overnight, saturated aqueous NH_4Cl and EtOAc were added to the mixture. The aqueous layer was further extracted with EtOAc. The combined EtOAc solution was washed with brine, dried over magnesium sulfate, concentrated to give 0.266 g) of oxide **3.31r** that was used directly in the next step without further purification.

To a solution of oxide **3.31r** (0.266 g, 0.598 mmol, 1 equiv) in THF (2.5 mL) at 0 °C was added NaH (0.165 g, 60% dispersion in mineral oil, 0.72 mmol, 1.2 equiv). The mixture was stirred at 10 °C for 2 h before addition of iodomethane (0.2 g, 1.40 mmol, 2.35 equiv). The resulting mixture was warmed to 23 °C over 1 h. After stirring at 23 °C overnight, saturated aqueous NH_4Cl and EtOAc were added to the mixture. The aqueous layer was further extracted with EtOAc. The combined organic solution was washed with brine, dried over magnesium sulfate, concentrated, and purified by silica gel column chromatography (0–50% EtOAc in hexanes) to afford 0.270 g (98%) of oxide **3.31s** as an off-white solid. R_f: 0.8 in 1:1 EtOAc in hexanes. ^{1}H NMR (400 MHz, $CDCl_3$): δ 8.48 (s, 1H), 7.99 (dd, J = 24.0, 8.5 Hz, 2H), 7.66–7.62 (m, 3H), 7.46–7.32 (m, 4H), 7.24 (ddd, *J* = 9.0, 3.8, 0.7 Hz, 1H), 7.07 (ddd, *J* = 8.0, 4.1, 0.7 Hz, 1H), 4.41 (d, J = 2.2 Hz, 1H), 3.37 (s, 3H), 1.46 (s, 3H), 1.37 (s, 3H), 0.52 (d, J = 15.8 Hz, 9H); ^{31}P NMR (162 MHz, $CDCl_3$): δ 58.3 ppm; ^{13}C NMR (100 MHz, $CDCl_3$): δ 164.6 (d, *J* = 19.0

Hz), 142.2 (d, J = 6.1 Hz), 134.5 (d, J = 1.6 Hz), 133.5 (d, J = 1.9 Hz), 131.1, 131.0, 130.7, 130.4, 128.8, 128.2, 127.6, 127.5, 126.2, 126.0, 125.9, 125.6, 124.9, 124.6, 115.2 (d, J = 90.0 Hz), 112.9 (d, J = 5.3 Hz), 78.0 (d, J = 56.1 Hz), 77.4 (d, J = 2.7 Hz), 49.3, 33.8 (d, J = 72.3 Hz), 23.4, 20.4, 19.9.

To a solution of **3.31s** (0.270 g, 0.589 mmol) in THF (0.6 mL) at 23 °C was added 1,1,3,3-tetramethyldisiloxane (TMDS, 0.158 g, 1.18 mmol, 2 equiv) and Ti(O*i*-Pr)$_4$ (0.227 mL, 0.765 mmol, 1,3 equiv). The mixture was stirred at reflux for 12 h, and then concentrated under vacuum to remove most THF. 30% aqueous NaOH solution (3 mL) was carefully added to the residue. Gas was generated during addition. The resulting mixture was further stirred at 60 °C for 0.5 h. To the mixture at 23 °C was added MTBE (5 mL). The MTBE layer was separated and the aqueous layer was washed with MTBE (3 mL x 3) under nitrogen. The MTBE solution was dried, concentrated, and purified by passing through a neutral alumina plug to afford 0.173 g (67%) of **3.L17** as a beige solid. ^{1}H NMR (500 MHz, $CDCl_3$): δ 8.47 (s, 1H), 8.01 (t, J = 7.2 Hz, 2H), 7.89 (d, J = 8.7 Hz, 1H), 7.66 (d, J = 8.8 Hz, 1H), 7.47–7.42 (m, 3H), 7.39–7.32 (m, 2H), 7.12 (d, J = 8.0 Hz, 1H), 6.98 (dd, J = 7.3, 3.2 Hz, 1H), 4.75 (s, 1H), 3.33 (s, 3H), 1.27 (s, 3H), 1.25 (s, 3H), 0.45 (d, J = 12.2 Hz, 9H); ^{31}P NMR (202 MHz, $CDCl_3$): δ 0.138 ppm; ^{13}C NMR (125 MHz, $CDCl_3$): δ 165.3, 141.7 (d, J = 17.1 Hz), 136.4, 131.4 (d, J = 12.5 Hz), 130.8 (d, J = 5.9 Hz), 129.0, 128.5, 128.3, 127.4 (d, J = 3.6 Hz), 127.0 (d, J = 10.7 Hz), 125.4, 125.2 (d, J = 9.8 Hz), 124.8, 124.7 (d, J = 3.8 Hz), 110.0, 89.8 (d, J = 30.9 Hz), 77.8 (d, J = 18.6 Hz), 49.9 (d, J = 0.9 Hz), 30.7 (d, J = 19.6 Hz), 26.9 (d, J = 14.5 Hz), 21.0 (d, J = 3.8 Hz), 20.9 (d, J = 1.1 Hz). HRMS (DART) *m/z* calculated for $C_{29}H_{32}O_2P$ $[M+H]^+$: 443.2134; found: 443.2133.

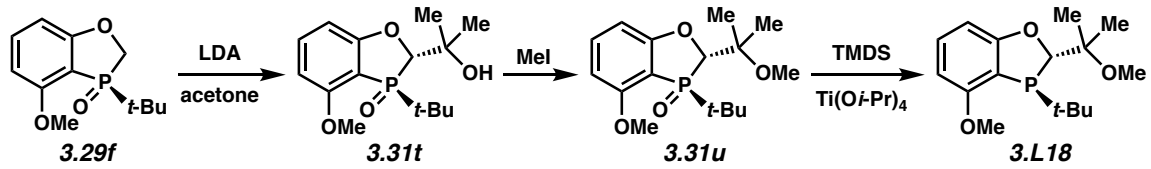

To a solution of oxide **3.29f** (3.0 g, 12.5 mmol, 1 equiv) in THF (30.0 mL) at –78 °C was added LDA (8.2 mL, 2.0 M in heptane/THF/chlorobenzene, 16.2 mmol, 1.3 equiv). The mixture was stirred at –78 °C for 30 min before addition of dry acetone (3.7 mL, 50.0 mmol, 4 equiv). The resulting mixture was kept at –78 °C for 1 h before it was warmed to 23 °C over 1 h. After stirring at 23 °C overnight, saturated aqueous NH_4Cl and EtOAc were added to the mixture. The aqueous layer was further extracted with EtOAc. The combined EtOAc solution was washed with brine, dried over $MgSO_4$, concentrated and purified using silica gel column chromatography (0-70% EtOAc in hexanes) to afford 2.7 g (73%) of oxide **3.31t** as an off-white solid. ^{1}H NMR (400 MHz, $CDCl_3$): δ 7.38 (t, *J* = 8.3 Hz, 1H), 6.53 (dd, *J* = 8.0, 3.0 Hz, 1H), 6.45 (dd, *J* = 8.1 Hz, 4.2 Hz, 1H), 4.19 (d, *J* = 3.7 Hz, 1H), 3.85 (s, 3H), 1.44 (s, 3H), 1.37 (s, 3H), 1.23 (d, *J* = 16.3 Hz, 9H); ^{31}P NMR (162 MHz, $CDCl_3$): δ 66.5 ppm; ^{13}C NMR (100 MHz, $CDCl_3$): δ 165.8 (d, *J* = 16.7 Hz), 161.3 (d, *J* = 1.8 Hz), 136.7, 106.0 (d, *J* = 5.4 Hz), 103.1 (d, *J* = 5.7 Hz), 101.8 (d, *J* = 91.3 Hz), 78.8 (d, *J* = 59.4 Hz), 73.2 (d, *J* = 2.0 Hz), 55.6, 34.0 (d, *J* = 72.6 Hz), 28.5 (d, J = 5.6 Hz), 24.7 (d, *J* = 2.8 Hz), 24.3.

To a solution of oxide **3.31t** (1.9 g, 6.4 mmol, 1 equiv) in THF (15 mL) at 0 °C was added NaH (0.73 g, 60% dispersion in mineral oil, 18.3 mmol, 2.8 equiv). The mixture was stirred at 10 °C for 2 h before addition of iodomethane (1.81 g, 12.74 mmol, 2.0 equiv). The resulting mixture was warmed to 23 °C over 1 h. After stirring at 23 °C overnight, saturated aqueous NH_4Cl and EtOAc were added to the mixture. The aqueous layer was further extracted with EtOAc. The combined organic solution was washed with brine, dried over magnesium sulfate, concentrated, and purified by silica gel column chromatography (0-100% EtOAc in

hexanes) to afford 1.8 g (91%) of oxide **3.31u** as a clear oil. R_f: 0.42 (100% EtOAc). ^{1}H NMR (400 MHz, $CDCl_3$): δ 7.38 (t, *J* = 8.3 Hz, 1H), 6.60 (dd, *J* = 8.2, 3.0 Hz, 1H), 6.45 (dd, *J* = 8.2 Hz, 4.2 Hz, 1H), 4.38 (d, *J* = 3.0 Hz, 1H), 3.86 (s, 3H), 3.33 (s, 3H), 1.46 (s, 3H), 1.35 (s, 3H), 1.23 (d, *J* = 16.0 Hz, 9H); ^{31}P NMR (162 MHz, $CDCl_3$): δ 60.74 ppm; ^{13}C NMR (100 MHz, $CDCl_3$): δ 165.2 (d, *J* = 16.5 Hz), 161.4 (d, *J* = 1.9 Hz), 136.4, 105.9 (d, *J* = 5.4 Hz), 102.9 (d, *J* = 5.7 Hz), 102.2 (d, *J* = 92.6 Hz), 78.6 (d, *J* = 55.3 Hz), 77.2 (d, *J* = 2.0 Hz), 55.5, 49.3, 34.2 (d, *J* = 74.6 Hz), 24.6, 20.4, 20.2 (d, *J* = 1.8 Hz).

To a solution of oxide **3.31u** (0.78 g, 2.5 mmol) in THF (1.2 mL) at 23 °C was added 1,1,3,3-tetramethyldisiloxane (TMDS, 0.67 g, 5.0 mmol, 2.0 equiv) and Ti(O*i*-Pr)$_4$ (0.96 mL, 3.3 mmol, 1.3 equiv). The mixture was stirred at reflux for 12 h, and then concentrated under vacuum to remove most THF. 30% aqueous NaOH solution (8 mL) was carefully added to the residue. Gas was generated during addition. The resulting mixture was further stirred at 60 °C for 0.5 h. To the mixture at 23 °C was added MTBE (5 mL). The MTBE layer was separated and the aqueous layer was washed with MTBE (3 mL x 3) under nitrogen. The MTBE solution was dried, concentrated, and purified by passing through a neutral alumina plug to afford 0.700 g (95%) of **3.L18** as a thick light yellow oil. ^{1}H NMR (400 MHz, $CDCl_3$): δ 7.13 (t, *J* = 8.1 Hz, 1H), 6.53 (dd, *J* = 8.0, 0.5 Hz, 1H), 6.34 (dd, *J* = 8.0 Hz, 3.8 Hz, 1H), 4.74 (d, *J* = 1.8 Hz, 1H), 3.75 (s, 3H), 3.23 (s, 3H), 1.17 (s, 3H), 1.04 (s, 3H), 0.93 (d, *J* = 12.4 Hz, 9H); ^{31}P NMR (162 MHz, $CDCl_3$): δ -3.55 ppm; ^{13}C NMR (100 MHz, $CDCl_3$): δ 166.0, 161.4 (d, *J* = 12.2 Hz), 132.1, 109.8 (d, *J* = 12.5 Hz), 104.0, 102.3 (d, *J* = 2.0 Hz), 89.8 (d, *J* = 30.0 Hz), 77.7 (d, *J* = 19.3 Hz), 55.3, 49.9 (d, *J* = 1.0 Hz), 31.5 (d, *J* = 18.8 Hz), 27.1 (d, *J* = 14.0 Hz), 21.0 (d, *J* = 11.0 Hz), 20.5 (d, *J* = 6.0 Hz). HRMS (DART) *m/z* calculated for $C_{16}H_{26}O_3P$ $[M+H]^+$: 297.1614; found: 297.1614.

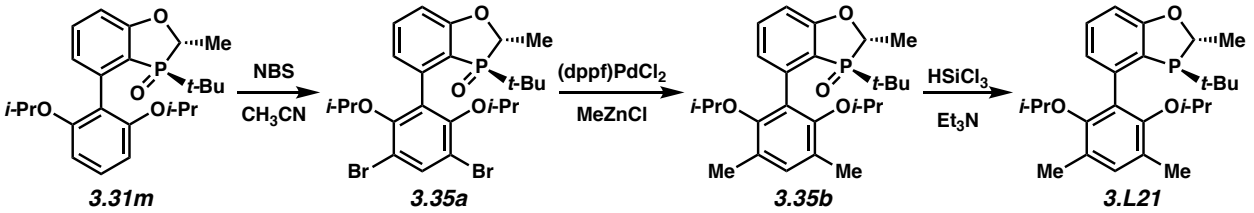

To a solution of oxide **3.31m** (544 mg, 1.31 mmol) in 2.0 mL of MeCN was charged 581 mg (3.27 mmol) of NBS in three portions over 5 min. The resultant mixture was then stirred at 23 °C for 6 h. Water (5 mL) and EtOAc (10 mL) was then charged, and the mixture agitated for 10 min. The layers were then separated, and the aqueous layer was extracted 1x with 10 mL of EtOAc. The combined organics were washed with 10 mL of 1 M HCl, dried with anhydrous Na_2SO_4, and concentrated *in vacuo*. The crude residue was purified by flash chromatography (gradient, 20–50% EtOAc/hexanes) to afford 732 mg of **3.35a** as a white solid that was contaminated with a small amount of NBS and succinimide. Purity assay of this material by quantitative ^{1}HNMR spectroscopy using dimethylfumarate as the standard showed the material was 95 wt% purity (93% yield). This material was used directly in the next step. ^{1}H NMR (500 MHz, $CDCl_3$): δ 7.77 (s, 1H), 7.46 (t, J = 7.8 Hz, 1H), 6.96 (dd, J = 8.3 Hz, J = 3.1 Hz, 1H), 6.91 (dd, J = 7.5 Hz, J = 3.1 Hz, 1H), 4.67 (p, J = 6.8 Hz, 1H), 4.38 (sept, J = 6.1 Hz, 1H), 4.36 (sept, J = 6.1 Hz, 1H), 1.47 (dd, J = 12 Hz, J = 7.2 Hz, 3H), 1.16 (d, J = 6.1 Hz, 3H), 1.14 (d, J = 6.1 Hz, 3H), 1.13 (d, J = 16 Hz, 9H), 0.91 (d, J = 6.1 Hz, 3H), 0.82 (d, J = 6.1 Hz, 3H); ^{31}P{^{1}H}NMR (202 MHz, $CDCl_3$): δ 62 ppm; ^{13}C{^{1}H}NMR (100 MHz, $CDCl_3$): δ 164.3 (d, J_{CP} = 18 Hz), 154.2, 152.7, 138.2 (d, J_{CP} = 4.9 Hz), 136.0, 133.4 (d, J_{CP} = 1.7 Hz), 132.0, 125.5 (d, J_{CP} = 7.7 Hz), 115.5 (d, J_{CP} = 85 Hz), 114.1 (d, J_{CP} = 5.1 Hz), 113.5, 112.2, 77.8, 76.5, 71.3 (d, J_{CP} = 62 Hz), 33.8 (d, J_{CP} = 70 Hz), 23.8, 23.0, 22.7, 22.5, 15.4; HRMS (DART) *m*/*z* calculated for $C_{24}H_{32}O_4Br_2P$ $[M + H]^+$: 573.0399; found: 573.0400.

To a crimp-cap vial was charged 82.3 mg (0.112 mmol) of (dppf)$PdCl_2$ and 680 mg (95 wt%, 1.13 mmol) of oxide **3.35a**. The vial was sealed and inerted with Ar using vac-purge cycles (3x). 2-MeTHF (1.9 mL) was then charged and the resultant mixture was stirred at 23 °C for 5 min. A THF solution of MeZnCl (2.0 M, 1.7 mL, 3.4 mmol) was then charged, and the mixture was allowed to stir for 10 min (gas evolution). The mixture was then heated at 65 °C in an oil bath for 22 h. The reaction was cooled to 23 °C and quenched with 10 mL of 1 M HCl. The mixture was then extracted with CH_2Cl_2 (3x), and the combined organics were washed with 5% citric acid (2 x 10mL), dried with anhydrous Na_2SO_4, and concentrated *in vacuo*. The crude residue was purified by flash chromatography (gradient, 20–60% EtOAc/hexanes) to afford an orange solid that was further purified by preparatory reverse phase HPLC (Agilent Prep-C18 column, 0.1% formic acid/MeCN, 68% MeCN) to afford 311 mg (58%) of pure **3.35b** as a white solid. $[a]_D^{24}$ = + 29.5 (*c* 0.27, $CHCl_3$); ^{1}H NMR (500 MHz, $CDCl_3$): δ 7.43 (t, *J* = 7.9 Hz, 1H), 6.97 (dd, *J* = 7.2 Hz, *J* = 3.3 Hz, 1H), 6.96 (s, 1H), 6.91 (dd, *J* = 8.3 Hz, *J* = 3.3 Hz, 1H), 4.62 (p, *J* = 6.8 Hz, 1H), 4.18 (sept, *J* = 6.2 Hz, 1H), 4.00 (sept, *J* = 6.2 Hz, 1H), 2.24 (s, 3H), 2.17 (s, 3H), 1.48 (dd, *J* = 12 Hz, *J* = 7.1 Hz, 3H), 1.09 (d, *J* = 16 Hz, 9H), 1.07 (d, *J* = 6.2 Hz, 3H), 1.00 (d, *J* = 6.2 Hz, 3H), 0.84 (d, *J* = 6.2 Hz, 3H), 0.78 (d, *J* = 6.2 Hz, 3H); ^{31}P{^{1}H}NMR (202 MHz, $CDCl_3$): δ 62 ppm; ^{13}C{^{1}H}NMR (100 MHz, $CDCl_3$): δ 164.1 (d, $J_{C\text{-}P}$ = 19 Hz), 153.5, 152.2, 140.7 (d, $J_{C\text{-}P}$ = 5.2 Hz), 133.0 (d, $J_{C\text{-}P}$ = 1.7 Hz), 132.4, 128.7 (d, $J_{C\text{-}P}$ = 1.9 Hz), 126.7, 125.9 (d, $J_{C\text{-}P}$ = 8.0 Hz), 125.8, 115.6 (d, $J_{C\text{-}P}$ = 86 Hz), 112.9 (d, $J_{C\text{-}P}$ = 5.2 Hz), 75.25 (d, $J_{C\text{-}P}$ = 71 Hz), 71.30, 70.67, 33.64 (d, $J_{C\text{-}P}$ = 70 Hz), 23.78, 22.77, 22.66, 22.51, 22.40, 16.89, 16.86, 15.39; HRMS (DART) *m*/*z* calculated for $C_{26}H_{38}O_4P$ $[M + H]^+$: 445.2502; found: 445.2501.

To a 25 mL Schlenk flask with magnetic stir bar was charged 289 mg (0.650 mmol) of oxide **3.35b**. A reflux condenser was added, and the reaction was inerted with Ar using vacuum-

purge cycles. Toluene (3.0 mL) was charged followed by triethylamine (0.27 mL, 2.0 mmol) and $HSiCl_3$ (0.16 mL, 1.6 mmol). The mixture was then immersed in an oil bath at 60 °C and monitored by ^{31}P NMR spectroscopy. After 3 h, the reaction was cooled to 23 °C and quenched with 3 mL of degassed (Ar sparge) 30% NaOH (aq.) at 0 °C. The mixture was then allowed to vigorously stir at 23 °C for 1 h. The aqueous layer was removed and subsequently extracted under Ar with MTBE (3 x 3 mL). The combined organics were dried with $MgSO_4$, filtered quickly through a pad of celite, and immediately concentrated *in vacuo*. The crude residue was chromatographed on the bench by dissolving the crude in hexanes and loading the mixture onto a short pad of silica gel and eluting with degassed (Ar sparge) hexanes/EtOAc (gradient, neat hexanes to 10% EtOAc/hexanes) using Ar to pressurize the flash column. The product fractions were immediately collected and concentrated *in vacuo* to afford 251 mg (90%) of **3.L21** as a white solid. $[a]_D^{25} = -198$ (*c* 0.46, $CHCl_3$); ^1H NMR (400 MHz, $CDCl_3$): δ 7.28 (t, *J* = 7.8 Hz, 1H), 7.10 (ddd, *J* = 7.6 Hz, *J* = 4.0 Hz, *J* = 0.9 Hz, 1H), 6.95 (s, 1H), 6.87 (dd, *J* = 8.0 Hz, *J* = 0.9 Hz, 1H), 5.01 (q, *J* = 7.0 Hz, 1H), 3.86 (sept, *J* = 6.0 Hz, 1H), 3.70 (sept, *J* = 6.1 Hz, 1H), 2.26 (s, 3H), 2.20 (s, 3H), 1.48 (dd, *J* = 16 Hz, *J* = 7.1 Hz, 3H), 1.04 (d, *J* = 6.1 Hz, 3H), 1.00 (d, *J* = 6.0 Hz, 3H), 0.98 (d, *J* = 6.1 Hz, 3H), 0.84 (d, *J* = 6.0 Hz, 3H), 0.77 (d, *J* = 12 Hz, 9H); $^{31}P\{^1H\}$NMR (202 MHz, $CDCl_3$): δ 14 ppm; $^{13}C\{^1H\}$NMR (100 MHz, $CDCl_3$): δ 163.2, 152.2, 151.7, 140.5 (d, J_{CP} = 16 Hz), 131.9, 130.0, 129.4, 127.3, 126.6, 124.5 (d, $J_{C\text{-}P}$ = 4.1 Hz), 124.0 (d, $J_{C\text{-}P}$ = 21 Hz), 110.2, 78.5 (d, $J_{C\text{-}P}$ = 23 Hz), 75.0, 73.8, 31.1 (d, J_{CP} = 20 Hz), 27.1 (d, J_{CP} = 14 Hz), 22.7, 22.4, 22.2 (d, J_{CP} = 31 Hz), 22.1, 17.2, 16.9; HRMS (DART) *m*/*z* calculated for $C_{26}H_{38}O_3P$ $[M + H]^+$: 429.2553; found: 429.2553.

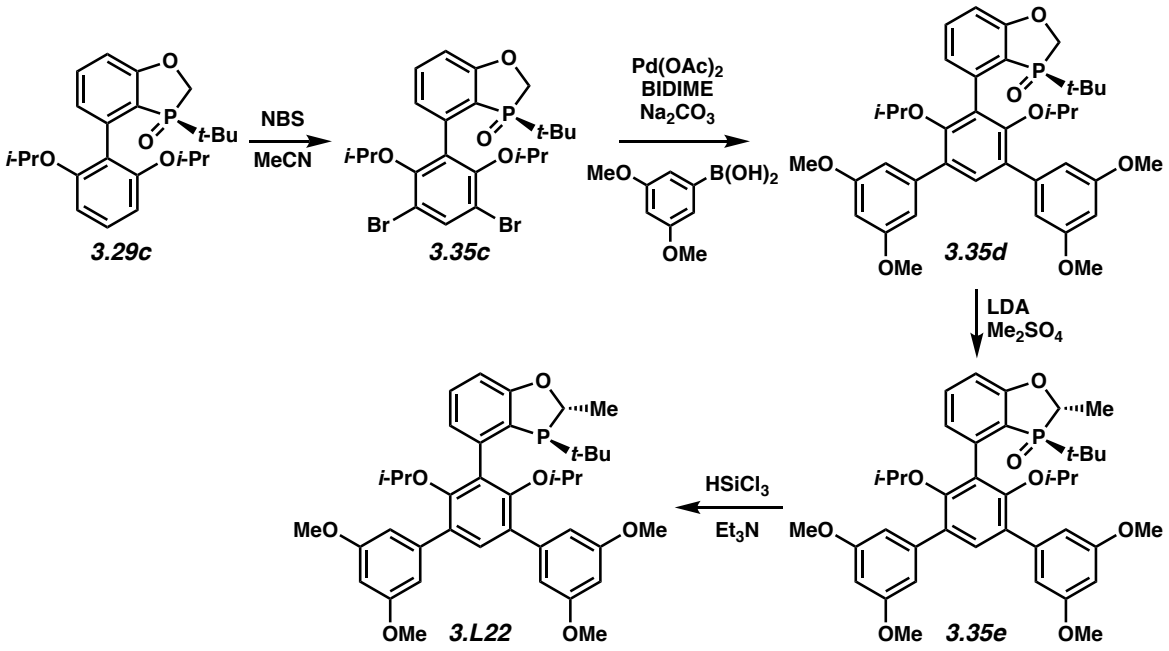

To a solution of oxide **3.29c** (871 mg, 2.16 mmol) in 4.0 mL of MeCN was charged 963 mg (5.41 mmol) of NBS in three portions over 5 min. The resultant mixture was then stirred at 23 °C. After 4 h, a slurry had formed, and an additional 2 mL of MeCN was charged. The slurry was stirred for an additional 4 h, and then the solid was isolated by filtration to afford 740 mg (61%) of **3.35c** as a white solid. ^{1}H NMR (500 MHz, $CDCl_3$): δ 7.78 (s, 1H), 7.49 (t, J = 7.8 Hz, 1H), 7.00 (dd, J = 8.4 Hz, J = 3.1 Hz, 1H), 6.95 (dd, J = 7.3 Hz, J = 3.3 Hz, 1H), 4.59 (dd, J = 14 Hz, J = 2.8 Hz, 1H), 4.40 (sept, J = 6.2 Hz, 1H), 4.28 – 4.36 (m, 2H), 1.16 (d, J = 5.5 Hz, 3H), 1.15 (d, J = 17 Hz, 9H), 1.14 (d, J = 5.2 Hz, 3H), 0.92 (d, J = 6.2 Hz, 3H), 0.86 (d, J = 6.2 Hz, 3H); ^{31}P{^{1}H}NMR (202 MHz, $CDCl_3$): δ 63 ppm; ^{13}C{^{1}H}NMR (100 MHz, $CDCl_3$): δ 165.8 (d, J_{CP} = 19 Hz), 154.2, 152.7, 137.7 (d, J_{CP} = 5.6 Hz), 136.1, 133.5 (d, J_{CP} = 1.6 Hz), 131.9 (d, J_{CP} = 2.0 Hz), 125.7 (d, J_{CP} = 7.8 Hz), 116.0 (d, J_{CP} = 87 Hz), 113.9 (d, J_{CP} = 5.1 Hz), 113.6, 112.2, 77.9, 76.6, 66.5 (d, J_{CP} = 60 Hz), 34.2 (d, J_{CP} = 70 Hz), 23.9, 22.9, 22.6, 22.48, 22.47; HRMS (DART) m/z calculated for $C_{23}H_{30}O_4Br_2P$ $[M + H]^+$: 559.0243; found: 559.0246.

To a crimp-cap vial was charged 8.7 mg (0.039 mmol) of $Pd(OAc)_2$, 12.8 mg (0.0387 mmol) of *rac*-BIDIME, 410 mg (3.87 mmol) of Na_2CO_3, 587 mg (3.23 mmol) of dimethoxyphenyl boronic acid, and 723 mg (1.29 mmol) of oxide **3.35c**. The vial was sealed and inerted with Ar using vac-purge cycles (3x). 2-MeTHF (3.2 mL) and water (1.1 mL) was then charged and the resultant mixture was heated at 70 °C in an oil bath for 18 h. The reaction was cooled to 23 °C and water was added. The layers were separated, and the aqueous layer was then extracted with EtOAc (1x). The combined organics were washed with water (1x), dried with anhydrous Na_2SO_4, and concentrated *in vacuo*. The crude residue was purified by flash chromatography (gradient, 50–100% EtOAc/hexanes) to afford 852 mg (97%) of **3.35d** as a tan solid. $[a]_D^{25}$ = + 43.2 (*c* 0.30, $CHCl_3$); ^{1}H NMR (500 MHz, $CDCl_3$): δ 7.47 (t, *J* = 7.9 Hz, 1H), 7.31 (s, 1H), 6.98 (dd, *J* = 7.4 Hz, *J* = 3.3 Hz, 1H), 6.96 (dd, *J* = 8.3 Hz, *J* = 3.3 Hz, 1H), 6.87 (d, *J* = 2.2 Hz, 2H), 6.68 (d, *J* = 2.2 Hz, 2H), 6.43 (t, *J* = 2.2 Hz, 1H), 6.40 (t, *J* = 2.2 Hz, 1H), 4.56 (dd, *J* = 14 Hz, *J* = 2.1 Hz, 1H), 4.37 (dd, *J* = 14 Hz, *J* = 11 Hz, 1H), 4.03 (sept, *J* = 6.1 Hz, 1H), 3.94 (sept, *J* = 6.1 Hz, 1H), 3.82 (s, 6H), 3.81 (s, 6H), 1.19 (d, *J* = 16 Hz, 9H), 0.87 (d, *J* = 6.1 Hz, 3H), 0.81 (d, *J* = 6.1 Hz, 3H), 0.69 (d, *J* = 6.1 Hz, 3H), 0.66 (d, *J* = 6.1 Hz, 3H); ^{31}P{^{1}H}NMR (202 MHz, $CDCl_3$): δ 62 ppm; ^{13}C{^{1}H}NMR (100 MHz, $CDCl_3$): δ 165.4 (d, J_{CP} = 19 Hz), 160.5, 160.3, 154.4, 152.2, 141.8, 141.4, 139.8 (d, J_{CP} = 5.6 Hz), 133.1, 133.0 (d, J_{CP} = 1.4 Hz), 131.4, 130.1 (d, J_{CP} = 2.0 Hz), 129.7, 126.0 (d, J_{CP} = 8.2 Hz), 116.0 (d, J_{CP} = 89 Hz), 112.7 (d, J_{CP} = 5.3 Hz), 107.7, 106.9, 99.4, 99.3, 76.0, 74.2, 66.0 (d, J_{CP} = 61 Hz), 55.5, 55.4, 34.0 (d, J_{CP} = 71 Hz), 24.2, 22.52, 22.50, 22.4, 22.2. HRMS (DART) *m*/*z* calculated for $C_{39}H_{48}O_8P$ $[M + H]^+$: 675.3081; found: 675.3083.

To a solution of oxide **3.35d** (0.500 g, 0.741 mmol) in 2.3 mL of THF at –78 °C was slowly charged a freshly prepared solution of LDA in THF (LDA prep: dropwise addition of

0.40 mL, 0.89 mmol of 2.2 M *n*-BuLi in hexanes to 0.14 mL, 0.96 mmol of di-*iso*-propylamine in 0.55 mL of THF at 0 °C followed by stirring at 0 °C for 20 min) by canula. The resultant red-orange solution was stirred at –78 °C for 40 min. Dimethyl sulfate (0.091 mL, 0.96 mmol) was then charged by syringe, and the mixture was stirred at –78 °C for 30 min. The reaction was then quenched by the addition of 3 mL of 10% aqueous NH_4Cl. The mixture was warmed to 23 °C, extracted with CH_2Cl_2, and the combined organic layers were dried with anhydrous Na_2SO_4 and concentrated *in vacuo*. The crude residue was then purified by flash chromatography (gradient, 50–80% EtOAc/hexanes) to afford 418 mg (82%) of **3.35e** as a white solid. $[a]_D^{25}$ = + 81.8 (*c* 0.14, $CHCl_3$); ^{1}H NMR (500 MHz, $CDCl_3$): δ 7.46 (t, *J* = 7.9 Hz, 1H), 7.31 (s, 1H), 6.96 (dd, *J* = 7.3 Hz, *J* = 3.3 Hz, 1H), 6.92 (dd, *J* = 8.2 Hz, *J* = 3.3 Hz, 1H), 6.87 (d, *J* = 2.2 Hz, 2H), 6.68 (d, *J* = 2.2 Hz, 2H), 6.43 (t, *J* = 2.2 Hz, 1H), 6.40 (t, *J* = 2.2 Hz, 1H), 4.63 (dq, *J* = 6.0 Hz, *J* = 7.0 Hz, 1H), 4.06 (sept, *J* = 6.1 Hz, 1H), 3.93 (sept, *J* = 6.1 Hz, 1H), 3.81 (s, 6H), 3.80 (s, 6H), 1.54 (dd, *J* = 12 Hz, *J* = 7.2 Hz, 3H), 1.19 (d, *J* = 16 Hz, 9H), 0.86 (d, *J* = 6.1 Hz, 3H), 0.81 (d, *J* = 6.1 Hz, 3H), 0.67 (d, *J* = 6.1 Hz, 3H), 0.63 (d, *J* = 6.1 Hz, 3H); ^{31}P{^{1}H}NMR (162 MHz, $CDCl_3$): δ 61 ppm; ^{13}C{^{1}H}NMR (100 MHz, $CDCl_3$): δ 163.7 (d, J_{CP} = 19 Hz), 160.5, 160.2, 154.4, 152.2, 141.8, 141.4, 140.4 (d, J_{CP} = 5.0 Hz), 133.0 (d, $J_{C\text{-}P}$ = 1.7 Hz), 132.9, 131.4, 130.1 (d, J_{CP} = 1.9 Hz), 129.6, 126.0 (d, J_{CP} = 8.0 Hz), 115.5 (d, J_{CP} = 87 Hz), 112.8 (d, J_{CP} = 5.3 Hz), 107.9, 106.8, 99.4, 99.3, 75.9, 74.3, 70.8 (d, J_{CP} = 63 Hz), 55.5, 55.4, 33.6 (d, J_{CP} = 70 Hz), 21.1, 22.6, 22.5, 22.4, 22.1, 15.2; HRMS (DART) *m*/*z* calculated for $C_{40}H_{50}O_8P$ $[M + H]^+$: 689.3238; found: 689.3241.

To a 25 mL Schlenk flask with magnetic stir-bar was charged 382 mg (0.555 mmol) of oxide **3.35e**. A reflux condenser was added, and the reaction was inerted with Ar using vacuum-purge cycles. Toluene (2.5 mL) was charged followed by triethylamine (0.23 mL, 1.7 mmol) and

$HSiCl_3$ (0.14 mL, 1.4 mmol). The mixture was then immersed in an oil bath at 60 °C and monitored by ^{31}P NMR spectroscopy. After 5 h, the reaction was cooled to 23 °C and quenched with 3 mL of degassed (Ar sparge) 30% NaOH (aq.) at 0 °C. The mixture was then allowed to vigorously stir at 23 °C for 1 h. The aqueous layer was removed and subsequently extracted under Ar with MTBE (3x3 mL). The combined organics were dried with $MgSO_4$, filtered quickly through a pad of celite, and immediately concentrated *in vacuo*. The crude residue was chromatographed on the bench by dissolving the crude in hexanes and loading the mixture onto a short pad of silica gel and eluting with degassed (Ar sparge) hexanes/EtOAc (gradient, neat hexanes to 30% EtOAc/hexanes) using Ar to pressurize the flash column. The product fractions were immediately collected and concentrated *in vacuo* to afford 283 mg (76%) of **3.L22** as a white solid. $[a]_D^{25} = -65.4$ (*c* 0.66, $CHCl_3$); ^1H NMR (500 MHz, $CDCl_3$): δ 7.288 (s, 1H), 7.287 (t, *J* = 7.9 Hz, 1H), 7.04 (dd, *J* = 7.9 Hz, *J* = 3.4 Hz, 1H), 6.89 (d, *J* = 2.3 Hz, 2H), 6.87 – 6.91 (m, 1H), 6.68 (d, *J* = 2.3 Hz, 2H), 6.42 (t, *J* = 2.2 Hz, 2H), 5.03 (q, *J* = 7.2 Hz, 1H), 3.94 (sept, *J* = 6.1 Hz, 1H), 3.83 (s, 6H), 3.80 (s, 3H), 3.65 (sept, *J* = 6.1 Hz, 1H), 1.43 (dd, *J* = 16 Hz, *J* = 7.1 Hz, 3H), 0.90 (d, *J* = 6.1 Hz, 3H), 0.89 (d, *J* = 6.1 Hz, 3H), 0.87 (d, *J* = 12 Hz, 9H), 0.71 (d, *J* = 6.1 Hz, 3H), 0.61 (d, *J* = 6.1 Hz, 3H); $^{31}P\{^1H\}$NMR (202 MHz, $CDCl_3$): δ 12.1 ppm; $^{13}C\{^1H\}$NMR (100 MHz, $CDCl_3$): δ 162.7, 160.4, 160.2, 152.9, 152.6, 142.2, 141.5, 140.6, 140.4, 131.9, 131.2, 130.5, 129.6, 125.6 (d, J_{CP} = 19 Hz), 124.0 (d, J_{CP} = 3.8 Hz), 110.0, 107.6, 107.2, 99.2, 99.1, 79.1 (d, J_{CP} = 25 Hz), 75.5, 73.8, 55.4, 30.9 (d, J_{CP} = 20 Hz), 27.2 (d, J_{CP} = 15 Hz), 22.5, 22.4, 22.2, 22.1, 21.6 (d, J_{CP} = 30 Hz); HRMS (DART) *m*/*z* calculated for $C_{40}H_{50}O_7P$ $[M + H]^+$: 673.3289; found: 673.3290.

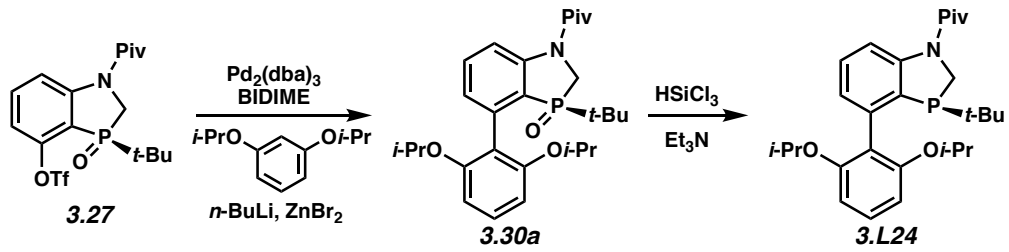

A crimp-cap vial with a magnetic stir bar was sealed with a crimp-cap septum and inerted with Ar using vacuum-purge cycles. To the vial was charged 1,3-diisopropoxybenzene (0.62 mL, 3.07 mmol, 2.2 eq) followed by hexanes (1.5 mL). A 2.55 M solution of *n*-BuLi (1.1 mL. 2.75 mmol, 2.0 eq) was charged dropwise. The mixture was then stirred at 70 °C for 2 h. In a second crimp-cap vial was prepared a slurry of $ZnBr_2$ (754 mg, 3.34 mmol, 2.38 eq) in THF (2.2 mL). To the $ZnBr_2$ mixture cooled in an ice-bath was charged the aryllithium solution by syringe. The resulting mixture was then warmed to 23 °C and allowed to stir for 15 min before use. In a third crimp-cap vial with stir bar were charged triflate **3.27**[8] (835 mg, 1.40 mmol, 1 eq), $Pd(OAc)_2$ (9.4 mg, 0.042 mmol, 3 mol%), and BI-DIME (21 mg, 0.063 mmol, 4.5 mol%). The mixture was inerted with Ar using vacuum-purge cycles. THF (2 mL) was then added, and the mixture was allowed to stir for 10 min. The zincate solution was then transferred to the catalyst/triflate solution by syringe. The final mixture was then immersed in an oil bath at 70 °C. After 12 h, the reaction was cooled to 23 °C and quenched with 2 M HCl (10 mL). CH_2Cl_2 (80 mL) was then added. The layers were separated, and the aqueous phase was extracted with CH_2Cl_2 (1 x 50 mL). Combined organics were washed with 20% citric acid (50 mL), dried with $MgSO_4$, and concentrated *in vacuo*. Purification of the crude mixture by flash chromatography (gradient, 40-100% EtOAc in hexanes then 0-5% MeOH in CH_2Cl_2) afforded 602 mg (89%) of **3.30a** as a white solid. ^{1}H NMR (500 MHz, $CDCl_3$) δ 8.18 (dd, J = 8.5 Hz, J = 3.2 Hz, 1H), 7.48 (t, J = 7.5 Hz, 1H), 7.21 (t, J = 8.4 Hz, 1H), 6.97–6.94 (m, 1H), 6.55 (d, J = 8.4 Hz, 1H), 6.46 (d, J = 8.4 Hz, 1H), 4.48 (sext, J = 6.0 Hz, 1H), 4.34 (dd, J = 13.5 Hz, J = 7.6 Hz, 1H), 3.93 (t, J = 13.9 Hz,

1H), 1.44 (s, 9H), 1.28 (d, J = 6.0 Hz, 3H), 1.21 (d, J = 6.0 Hz, 3H), 1.17–1.14 (m, 6H), 0.94 (d, J = 15.6 Hz, 9H); ^{31}P{1 H}NMR (202 MHz, $CDCl_3$) δ 56.96 ppm; ^{13}C NMR (100 MHz, CDCl3) δ 176.9 (d, $J_{C–P}$ = 3.5 Hz), 157.8, 156.1, 148.8 (d, $J_{C–P}$ = 15.6 Hz), 139.3 (d, $J_{C–P}$ = 5.0 Hz), 132.5 (d, $J_{C–P}$ = 1.9 Hz), 128.2 (d, $J_{C–P}$ = 9.3 Hz),119.3, 119.0 (d, $J_{C–P}$ = 8.7 Hz), 118.5, 118.0, 117.9, 104.9, 103.7, 70.6, 69.4, 46.6, 46.0, 41.0, 34.3, 33.6, 28.3, 23.9, 22.4, 23.6, 22.1, 21.9. HRMS (DART) *m*/*z* calculated for $C_{28}H_{41}O_4NP$ $[M + H]^+$: 486.2768; found: 486.2766.

To a Schlenk flask with magnetic stir bar was charged **3.30a** (362 mg, 0.754 mmol, 1.0 eq). A reflux condenser was added, and the reaction was inerted with Ar using vacuum-purge cycles. PhMe (3.0 mL) was as added followed by triethylamine (1.2 mL, 9.05 mmol, 12.0 eq) and $HSiCl_3$ (600 µL, 5.96 mmol, 8.0 eq). The mixture was then immersed in an oil bath at 107 °C and monitored by ^{31}P NMR spectroscopy. After 3 h, the reaction was cooled to 23 °C and quenched with 10 mL of degassed (Ar sparge) 30% NaOH (aq.). The mixture was then allowed to vigorously stir at 23 °C for 1 h. The aqueous layer was removed and subsequently extracted under Ar with MTBE (3 × 10 mL). The combined organics were dried with $MgSO_4$, filtered quickly through a pad of Celite, and immediately concentrated *in vacuo*. The crude residue was chromatographed on the bench by dissolving the crude solid in CH_2Cl_2 and loading the mixture onto a short pad of silica gel and eluting with degassed (Ar sparge) 20% EtOAc in hexanes using Ar to pressurize the flash column. The product fractions were immediately collected and concentrated *in vacuo* to afford 257 mg (74%) of **3.L24** as a white solid. $[a]_D^{25}$ = – 155 (*c* 0.28, $CHCl_3$); ^{1}H NMR (400 MHz, $CDCl_3$) δ 8.09 (dd, J = 8.32 Hz, J = 0.88 Hz, 1H), 7.32 (t, J = 8.08 Hz, 1H), 7.19 (t, J = 8.32 Hz, 1H), 6.95–6.92 (m, 1H), 6.58 (d, J = 8.04 Hz, 1H), 6.53 (d, J = 8.24 Hz, 1H), 4.47 (p, J = 6.1 Hz, 1H), 4.41–4.37 (m, 1H), 4.22 (p, J = 6.12 Hz, 1H), 3.93–3.85 (m, 1H), 1.45 (s, 9H), 1.26 (d, J = 6.0 Hz, 3H), 1.20 (d, J = 6.0 Hz, 3H), 1.12 (d, J = 6.0 Hz, 3H),

0.99 (d, J = 6.0 Hz, 3H), 0.75 (d, J = 12.0 Hz, 9H); $^{31}P\{^{1}H\}$NMR (202 MHz, $CDCl_3$) δ – 11.1 ppm; ^{13}C NMR (100 MHz, $CDCl_3$) δ 176.6, 156.6, 155.8, 148.5, 138.8 (d, $J_{C–P}$ = 19.8 Hz), 129.1, 128.6, 127.3, 127.2, 122.0, 118.4, 108.2, 104.9, 71.6, 69.2, 46.9, 46.7, 40.7, 31.4, 31.2, 27.0 (d, $J_{C–P}$ = 14.7 Hz), 22.4, 22.2, 22.1, 21.9. HRMS (DART) m/z calculated for $C_{28}H_{41}O_3NP$ $[M + H]^+$: 470.2819; found: 470.2818.

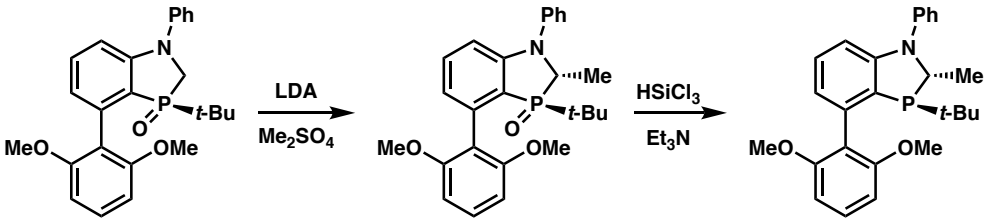

3.30b ***3.32a*** ***3.L25***

To a solution of oxide **3.30b**[7,8] (0.400 g, 0.949 mmol) in 10 mL of THF at –78 °C was charged a solution of LDA in THF (2.0 M, 1.42 mL, 2.8 mmol). The mixture was stirred for 5 min and then dimethyl sulfate (0.13 mL, 1.4 mmol) was charged dropwise. The mixture was stirred at –78 °C for 1 h and then quenched by the addition of 10% NH_4Cl. The mixture was warmed to 23 °C and extracted with EtOAc. The combined organics were dried with anhydrous Na_2SO_4 and concentrated *in vacuo*. The crude residue was purified by flash chromatography (gradient, 25 to 100% EtOAc in hexanes) to afford 343 mg (83%) of oxide **3.32a** as a light brown solid. ^{1}HNMR (400 MHz, $CDCl_3$) δ 7.40 (t, J = 8.2 Hz, 2H), 7.25–7.33 (m, 4H), 7.19 (t, J = 7.3 Hz, 1H), 6.72 (dd, J = 8.3 Hz, J = 3.5 Hz, 1H), 6.68 (dd, J = 7.34 Hz, J = 3.5 Hz, 1H), 6.66 (d, J = 8.0 Hz, 1H), 6.57 (d, J = 8.2 Hz, 1H), 3.83 (s, 3H), 3.77–3.85 (m, 1H), 3.74 (m, 3H), 1.48 (dd, J = 12 Hz, J = 7.0 Hz, 3H), 0.89 (d, J = 15 Hz, 9H); $^{31}P\{^{1}H\}$NMR (162 MHz, $CDCl_3$) δ 59 ppm; ^{13}CNMR (100 MHz, $CDCl_3$) δ 159.0, 157.4, 152.8 (d, J_{CP} = 16 Hz), 142.7 (d, J_{CP} = 6.5 Hz), 139.1 (d, J_{CP} = 4.4 Hz), 133.0 (d, J_{CP} = 1.7 Hz), 129.64, 129.57, 125.0, 124.6, 122.4 (d, J_{CP} = 9.1 Hz), 117.9 (d, J_{CP} = 2.7 Hz), 114.5 (d, J_{CP} = 87 Hz), 110.6 (d, J_{CP} = 8.1 Hz), 104.5, 103.0,

56.1, 55.4, 52.9 (d, J_{CP} = 67 Hz), 33.4 (d, J_{CP} = 70 Hz), 23.9, 14.1 (d, J_{CP} = 2.0 Hz). HRMS (DART) *m*/*z* calculated for $C_{26}H_{31}O_3NP$ $[M + H]^+$: 436.2036; found: 436.2038.

To a Schlenk flask with magnetic stir bar was charged **3.32a** (250 mg, 0.574 mmol). A reflux condenser was added, and the reaction was inerted with Ar using vacuum-purge cycles. PhMe (6.0 mL) was as added followed by triethylamine (0.23 mL, 1.7 mmol) and $HSiCl_3$ (144 µL, 1.44 mmol). The mixture was then immersed in an oil bath at 65 °C and monitored by ^{31}P NMR spectroscopy. After 3 h, the reaction was cooled to 23 °C and quenched with 15 mL of degassed (Ar sparge) 30% NaOH (aq.). The mixture was then allowed to vigorously stir at 23 °C for 1 h. The aqueous layer was removed and subsequently extracted under Ar with MTBE (3 × 10 mL). The combined organics were dried with $MgSO_4$, filtered quickly through a pad of Celite, and immediately concentrated *in vacuo*. The crude residue was chromatographed on the bench by dissolving the crude in 10% EtOAc in hexanes and loading the mixture onto a short pad of silica gel and eluting with degassed (Ar sparge) hexanes/EtOAc (gradient, neat hexanes to 15% EtOAc/hexanes) using Ar to pressurize the flash column. The product fractions were immediately collected and concentrated *in vacuo* to afford 149 mg (62%) of **3.L25** as a white solid that was contaminated with a small amount of impurities that could not be removed by further purification and therefore was used directly in subsequent experiments. We cannot rule out that low enantioselectivity in the subsequent cross-coupling reactions using this ligand was a result of the present impurities. $[a]_D^{25}$ = – 108 (*c* 0.65, $CHCl_3$); ^1H NMR (400 MHz, $CDCl_3$) δ 7.14–7.30 (m, 6H), 6.98 (dd, *J* = 8.1 Hz, J = 0.8 Hz, 1H), 6.90 (tt, *J* = 7.1 Hz, *J* = 1.2 Hz, 1H), 6.66 (dd, *J* = 3.2 Hz, *J* = 0.8 Hz, 1H), 6.58 (d, *J* = 8.2 Hz, 1H), 6.52 (d, *J* = 8.3 Hz, 1H), 3.99 (q, *J* = 7.0 Hz, 1H), 3.70 (s, 3H), 3.67 (s, 3H), 1.38 (dd, *J* = 17 Hz, *J* = 7.0 Hz, 3H), 0.64 (d, *J* = 12 Hz, 9H); $^{31}P\{^1H\}$NMR (162 MHz, $CDCl_3$) δ 7.6 ppm; ^{13}C NMR (100 MHz, $CDCl_3$) δ 157.9,

157.1, 149.1, 144.7, 139.8 (d, J_{CP} = 18 Hz), 129.6, 129.2, 128.8, 122.3 (d, J_{CP} = 4.4 Hz), 121.5, 119.9, 119.1, 112.7, 111.3, 104.4, 103.6, 58.5 (d, J_{CP} = 18 Hz), 55.8 (d, J_{CP} = 1.8 Hz), 55.4, 30.5 (d, J_{CP} = 19 Hz), 26.9 (d, J_{CP} = 14 Hz), 20.8 (d, J_{CP} = 33 Hz). HRMS (DART) *m*/*z* calculated for $C_{26}H_{31}O_2NP$ $[M + H]^+$: 420.2087; found: 420.2089.

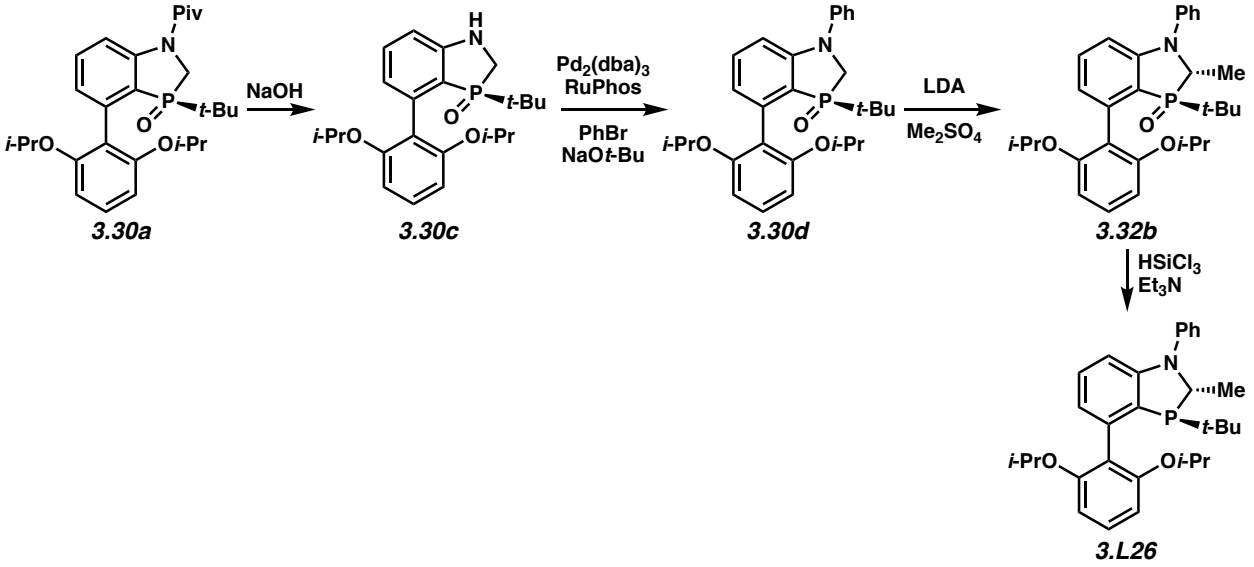

A crimp-cap vial with a magnetic stir bar was charged oxide **3.30a** (1.27 g, 2.62 mmol, 1.0 eq) followed by methanol (13 mL). A 1.0 M solution of NaOH (3.9 mL, 3.93 mmol, 1.5 eq) was charged. The mixture was then stirred at 50 °C for 1 h. The reaction mixture was cooled to 23 °C then concentrated *in vacuo*. Purification of the crude mixture by flash chromatography (gradient, 50–100% EtOAc in hexanes then 0–10% MeOH in CH_2Cl_2) afforded 1.04 g (99%) of **3.30c** as a white semi-solid. ^{1}H NMR (500 MHz, $CDCl_3$) δ 7.29–7.26 (m, 1H), 7.17 (t, *J* = 8.4 Hz, 1H), 6.63–6.58 (m, 2H), 6.55 (t, *J* = 8.4 Hz, 1H), 6.46 (t, *J* = 8.3 Hz, 1H), 4.51–4.41 (m, 2H), 3.61–3.48 (m, 2H), 1.30–1.14 (m, 12H), 0.92 (d, *J* = 15.6 Hz, 9H); ^{31}P{^{1}H}NMR (202 MHz, $CDCl_3$) δ 64.95 ppm.

A crimp-cap vial with a magnetic stir bar was charged with $Pd_2(dba)_3$ (48 mg, 0.052 mmol, 2 mol%), RuPhos (70 mg, 0.157 mmol, 6 mol%), NaO*t*-Bu (302 mg, 3.14 mmol, 1.2 eq) and the reaction vessel was inerted with Ar using vacuum-purge cycles. A solution of oxide **3.30c** (1.04 g, 2.62 mmol, 1.0 eq) in THF (10 mL) was added followed by PhBr (414 µL, 3.93, 1.5 eq). The mixture was then stirred at 70 °C for 4.5 h. The reaction was cooled to 23 °C, quenched with 1M HCl, and extracted with CH_2Cl_2, washed with water and brine, dried with $MgSO_4$, filtered and concentrated *in vacuo*. Purification of the crude mixture by flash chromatography (gradient, 40–100% EtOAc in hexanes) afforded 791 mg (63% - over 2 steps) of **3.30d** as a white solid. ^{1}H NMR (500 MHz, $CDCl_3$) δ 7.38 (t, *J* = 7.3 Hz, 2H), 7.31–7.10 (m, 4H), 6.91 (dd, *J* = 8.3 Hz, *J* = 3.6 Hz, 1H), 6.63 (dd, *J* = 8.2 Hz, *J* = 2.8 Hz, 1H), 6.57 (d, *J* = 8.4 Hz, 1H), 6.47 (d, *J* = 8.4 Hz, 1H), 4.53–4.48 (m, 2H), 4.00 (t, *J* = 13.6 Hz, 1H), 3.76 (dd, *J* = 13.5 Hz, *J* = 6.1 Hz, 1H), 1.35 (d, *J* = 6.0 Hz, 3H), 1.26–1.19 (m, 9H), 0.96 (d, *J* = 15.4 Hz, 9H); ^{31}P{^{1}H}NMR (202 MHz, $CDCl_3$) δ 57.98. ppm; ^{13}C NMR (100 MHz, $CDCl_3$) δ 158.0, 156.0, 152.8 (d, $J_{C\text{-}P}$ = 15.5 Hz), 144.2 (d, $J_{C\text{-}P}$ = 6.5 Hz), 140.2 (d, $J_{C\text{-}P}$ = 4.8 Hz), 132.4 (d, $J_{C\text{-}P}$ = 1.8 Hz), 129.5, 129.2, 123.9, 123.3, 123.2, 122.4, 118.8, 116.4, 115.5, 109.4 (d, $J_{C\text{-}P}$ = 8.3 Hz), 105.2, 103.7, 70.8, 69.3, 50.4, 49.8, 34.2, 33.5, 23.1 (d, $J_{C\text{-}P}$ = 27.6 Hz) 22.4, 22.1, 21.9.

A crimp-cap vial with a magnetic stir-bar was charged oxide **3.30d** (450 mg, 0.943 mmol, 1.0 eq) followed by dimethyl sulfate (135 µL, 1.42 mmol, 1.5 eq) and the reaction vessel was inerted with Ar using vacuum-purge cycles. THF (5 mL) was charged and the reaction mixture was cooled to –78 °C. A 1.0 M solution of freshly made LDA (1.91 mL, 1.88 mmol, 2.0 eq) was charged dropwise. The mixture was then stirred at –78 °C for 30 min and then allowed to reach 23 °C. The reaction mixture quenched with sat NH_4Cl, and extracted with CH_2Cl_2, washed with water and brine, dried with $MgSO_4$, filtered and concentrated *in vacuo*. Purification of the crude

mixture by flash chromatography (gradient, 40-100% EtOAc in hexanes) afforded 453 mg (98%) of **3.32b** as a white solid. ^{1}H NMR (500 MHz, $CDCl_3$) δ 7.40–7.30 (m, 4H), 7.26–7.13 (m, 4H), 6.76–6.73 (m, 1H), 6.63–6.61 (m, 1H), 6.55 (d, J = 8.4 Hz, 1H), 6.46 (d, J = 8.3 Hz, 1H), 4.53–4.47 (m, 2H), 3.84–3.78 (m, 1H), 1.51–1.46 (m, 3H), 1.37 (d, J = 6.1 Hz, 3H), 1.25–1.19 (m, 9H), 0.93 (d, J = 15.0 Hz, 9H); ^{31}P{^{1}H}NMR (202 MHz, $CDCl_3$) δ 59.5 ppm; ^{13}C NMR (100 MHz, $CDCl_3$) δ 157.9, 156.0, 151.7 (d, $J_{C\text{-}P}$ = 16.4 Hz), 143.4 (d, $J_{C\text{-}P}$ = 6.2 Hz), 140.4 (d, $J_{C\text{-}P}$ = 4.5 Hz), 132.3 (d, $J_{C\text{-}P}$ = 1.8 Hz), 129.5, 129.0, 124.4, 123.6, 123.2, 123.1, 118.7 (d, $J_{C\text{-}P}$ = 2.9 Hz), 115.3, 114.4, 110.2 (d, $J_{C\text{-}P}$ = 8.2 Hz), 104.9, 103.6, 70.5, 69.2, 53.5, 52.8, 33.9, 33.2, 23.9, 22.4, 22.3, 22.1, 22.0, 14.8 (d, $J_{C\text{-}P}$ = 1.5 Hz). HRMS (DART) *m*/*z* calculated for $C_{30}H_{39}O_3NP$ [M + H]$^{+}$: 492.2662; found: 492.2660.

To a Schlenk flask with magnetic stir bar was charged azaphosphole **3.32b** (360 mg, 0.727 mmol, 1.0 eq). A reflux condenser was added, and the reaction was inerted with Ar using vacuum-purge cycles. PhMe (3.0 mL) was as added followed by triethylamine (1.2 mL, 8.72 mmol, 12.0 eq) and $HSiCl_3$ (590 µL, 5.82 mmol, 8.0 eq). The mixture was then immersed in an oil bath at 107 °C and monitored by ^{31}P NMR spectroscopy. After 3 h, the reaction was cooled to 23 °C and quenched with 10 mL of degassed (Ar sparge) 30% NaOH (aq.). The mixture was then allowed to vigorously stir at 23 °C for 1 h. The aqueous layer was removed and subsequently extracted under Ar with MTBE (3 × 10 mL). The combined organics were dried with $MgSO_4$, filtered quickly through a pad of Celite, and immediately concentrated *in vacuo*. The crude residue was chromatographed on the bench by dissolving the crude solid in CH_2Cl_2 and loading the mixture onto a short pad of silica gel and eluting with degassed (Ar sparge) 10% EtOAc in hexanes using Ar to pressurize the flash column. The product fractions were immediately collected and concentrated *in vacuo* to afford 304 mg (88%) of **3.L26** as a white

solid. $[\alpha]_D^{25}$ = – 107 (*c* 0.24, $CHCl_3$); ^1H NMR (400 MHz, $CDCl_3$) δ 7.37-7.27 (m, 4H), 7.20-7.15 (m, 2H), 7.03-7.00 (m, 1H), 6.97-6.93 (m, 1H), 6.67-6.64 (m, 1H), 6.62 (d, *J* = 8.1 Hz, 1H), 6.53 (d, *J* = 8.3 Hz, 1H), 4.49 (p, *J* = 6.0 Hz, 1H), 4.31 (p, *J* = 6.0 Hz, 1H), 4.06 (q, *J* = 7.0 Hz, 1H), 1.51-1.44 (m, 3H), 1.29-1.24 (m, 9H), 1.18 (d, *J* = 6.1 Hz, 3H), 1.00 (d, *J* = 6.1 Hz, 3H), 0.71 (d, *J* = 11.7 Hz, 9H); $^{31}P\{^1H\}$NMR (202 MHz, $CDCl_3$) δ 7.5 ppm; ^{13}C NMR (100 MHz, $CDCl_3$) δ 156.7, 155.7, 148.8, 145.1 (d, J_{C-P} = 1.5 Hz), 140.5 (d, J_{C-P} = 18.6 Hz), 129.1, 128.7, 128.2, 123.2 (d, J_{C-P} = 4.6 Hz), 121.3, 119.0, 110.8, 108.7, 105.0, 71.7, 69.2, 58.6 (d, J_{C-P} = 18.6 Hz), 30.7, 30.5, 29.7, 27.3 (d, J_{C-P} = 14.5 Hz), 22.5 (d, J_{C-P} = 2.0 Hz), 22.2, 22.1, 22.0. HRMS (DART) *m*/*z* calculated for $C_{30}H_{39}O_2NP$ $[M + H]^+$: 476.2713; found: 476.2714.

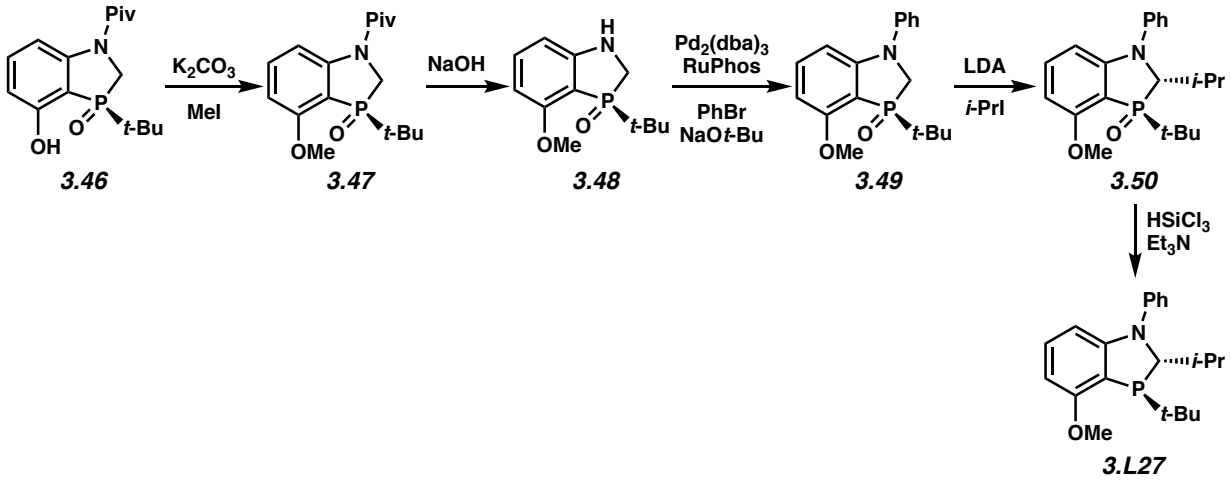

To a slurry of phenol **3.46**[8] (8.00 g, 25.9 mmol) and 3.88 g (64.7 mmol) of K_2CO_3 in 16 mL of DMF and 80 mL of 2-MeTHF was charged 4.0 mL (65 mmol) of iodomethane, and the resultant mixture was allowed to stir at 23 °C for 15 h. Water was then charged, and the layers were separated. The aqueous layer was extracted with 2-MeTHF (2x10 mL), and the combined organic layers were washed with brine, dried with anhydrous Na_2SO_4, and concentrated *in vacuo* to afford 7.42 g (89%) of **3.47** as a white solid that was used directly in the next step without

further purification. $[\alpha]_D^{25}$ = – 44.0 (*c* 0.42, $CHCl_3$); ^{1}H NMR (500 MHz, $CDCl_3$) δ 7.88 (dd, *J* = 8.5 Hz, *J* = 2.8 Hz, 1H), 7.45 (t, *J* = 8.4 Hz, 1H), 6.65 (dd, *J* = 8.2 Hz, *J* = 4.4 Hz, 1H), 4.29 (dd, *J* = 14 Hz, *J* = 6.3 Hz, 1H), 4.08 (dd, *J* = 15 Hz, *J* = 14 Hz, 1H), 3.90 (s, 3H),1.41 (s, 9H), 1.24 (d, *J* = 16 Hz, 9H); ^{13}C NMR (125 MHz, $CDCl_3$) δ 177.3 (d, J_{CP} = 4.1 Hz), 161.0 (d, J_{CP} = 1.2 Hz), 151.0 (d, J_{CP} = 12 Hz), 135.7 (d, J_{CP} = 1.4 Hz), 113.5 (d, J_{CP} = 0.7 Hz), 106.3 (d, J_{CP} = 88 Hz), 106.0 (d, J_{CP} = 6.1 Hz), 55.62, 46.47 (d, J_{CP} = 62 Hz), 41.11, 34.05 (d, J_{CP} = 73 Hz), 28.24, 24.46 (d, J_{CP} = 1.1 Hz); ^{31}P NMR (202 MHz, $CDCl_3$) δ 59. HRMS (DART) *m*/*z* calculated for $C_{17}H_{27}O_3NP$ $[M + H]^+$: 324.1723; found: 324.1723.

A mixture of **3.47** (7.00 g, 21.6 mmol), 32 mL of 1M NaOH (32 mmol), and 70 mL of MeOH was agitated at 50 °C for 22 h. The reaction was then cooled to 23 °C and concentrated *in vacuo* to crystallize a white solid. The resultant slurry was agitated at 23 °C for 1 h, and the solid was then isolated by filtration and washed with water. The solid was dried *in vacuo* overnight to provide 4.01 g (77%) of **3.48** as a white solid. $[\alpha]_D^{25}$ = + 9.5 (*c* 0.38, $CHCl_3$); ^{1}H NMR (500 MHz, $CDCl_3$) δ 7.24 (t, *J* = 8.1 Hz, 1H), 6.28 (dd, *J* = 8.1 Hz, *J* = 3.1 Hz, 1H), 6.24 (dd, *J* = 8.1 Hz, *J* = 4.5 Hz, 1H), 4.19 (d, *J* = 19 Hz, 1H), 3.85 (s, 3H), 3.60 (d, *J* = 3.7 Hz, 1H), 3.58 (ddd, *J* = 19 Hz, *J* = 14 Hz, *J* = 3.7 Hz, 1H), 1.24 (d, *J* = 16 Hz, 9H); ^{13}C NMR (125 MHz, $CDCl_3$) δ 161.9 (d, J_{CP} = 1.9 Hz), 157.5 (d, J_{CP} = 17 Hz), 135.9 (d, J_{CP} = 1.3 Hz), 105.1 (d, J_{CP} = 7.3 Hz), 101.2 (d, J_{CP} = 91 Hz), 100.2 (d, J_{CP} = 5.9 Hz), 55.26, 43.45 (d, J_{CP} = 64 Hz), 33.95 (d, J_{CP} = 74 Hz), 24.42; ^{31}P NMR (202 MHz, $CDCl_3$) δ 67; HRMS (DART) *m*/*z* calculated for $C_{12}H_{19}O_2NP$ $[M + H]^+$: 240.1148; found: 240.1149.

Oxide **3.48** (1.00 g, 4.18 mmol), $Pd_2(dba)_3$ (0.0962 g, 0.105 mmol), RuPhos (0.1951 g, 0.418 mmol), and sodium *tert*-butoxide (0.482 g, 5.01 mmol) were added to a flask under N_2. The flask was backfilled with N_2 three times. Phenyl bromide (0.51 mL, 5.0 mmol) and THF (10

mL) were added, followed by backfilling with N_2 three times. The reaction mixture was stirred at 23 °C for 5 min and heated at 67 °C overnight. The reaction mixture was passed through a pad of celite, which was then washed with THF (3 × 50 mL). The crude product was concentrated and purified by column chromatography on silica gel (CH_2Cl_2/MeOH, 94:6) to obtain **3.49** as a yellow solid (1.29 g, 98% yield). $[\alpha]_D^{25}$ = + 68.9 (*c* 0.52, $CHCl_3$); ^{1}H NMR (400 MHz, $CDCl_3$) δ 7.41−7.35 (m, 2H), 7.27−7.14 (m, 4H), 6.48 (dd, *J* = 8.3, 3.0 Hz, 1H), 6.29 (dd, *J* = 8.1, 4.5 Hz, 1H), 4.03 (t, *J* = 14.5 Hz, 1H), 3.88 (s, 3H), 3.85 (dd, *J* = 14.0, 4.27 Hz, 1H), 1.29 (d, *J* = 16.0 Hz, 9H); ^{13}C NMR (100 MHz, $CDCl_3$) δ 143.6, 135.7, 129.659, 125.0, 123.4, 104.3, 104.2, 100.7, 100.6, 55.4, 50.8, 50.1, 34.4, 33.6, 24.5; ^{31}P NMR (162 MHz, $CDCl_3$) δ 60.37. HRMS (DART) *m*/*z* calculated for $C_{18}H_{23}O_2NP$ $[M + H]^+$: 316.1461; found: 316.1462.

To a solution of **3.49** (0.400 g, 1.27 mmol) in 4 mL of THF under Ar was charged 2-iodopropane (0.32 g, 1.9 mmol), and the mixture was cooled to –78 °C. A solution of LDA (2.0 M in THF/heptane/ethylbenzene, 1.6 mL, 3.2 mmol) was charged dropwise. The mixture was agitated at –78 °C for 10 min and then allowed to warm to 23 °C and stirred an additional 15 min. Aqueous HCl (2.0 M, 10 mL) was then charged, and volatile organics were removed *in vacuo*. The aqueous residue was then extracted with CH_2Cl_2 (3 x 10mL). The combined organics were dried with anhydrous Na_2SO_4 and concentrated *in vacuo*. The crude residue was then purified by flash chromatography (gradient, 0 to 5% MeOH in CH_2Cl_2) to afford 304 mg (70%) of **3.50** as a yellow solid. ^{1}H NMR (500 MHz, $CDCl_3$) δ 7.41 (t, *J* = 7.8 Hz, 2H), 7.28 (d, *J* = 7.9 Hz, 2H), 7.24 (t, *J* = 7.4 Hz, 1H), 7.15 (t, *J* = 8.2 Hz, 1H), 6.18 – 6.24 (m, 2H), 3.84 (s, 3H), 3.75 (dd, *J* = 5.5 Hz, *J* = 3.7 Hz, 1H), 2.13 – 2.29 (m, 1H), 1.24 (d, *J* = 15 Hz, 9H), 1.20 (d, *J* = 7.1 Hz, 3H), 1.11 (d, *J* = 7.0 Hz, 3H); ^{13}C NMR (125 MHz, $CDCl_3$) δ 162.3 (d, J_{CP} = 0.7 Hz), 155.3 (d, J_{CP} = 14 Hz), 142.2 (d, J_{CP} = 6.7 Hz), 135.5 (d, J_{CP} = 1.2 Hz), 129.7, 126.4, 126.1,

103.1 (d, J_{CP} = 8.2 Hz), 101.3 (d, J_{CP} = 88 Hz), 100.0 (d, J_{CP} = 6.1 Hz), 61.0 (d, J_{CP} = 63 Hz), 55.2, 34.7 (d, J_{CP} = 73 Hz), 30.4 (d, J_{CP} = 2.3 Hz), 24.5 (d, J_{CP} = 0.7 Hz), 18.5 (d, J_{CP} = 0.7 Hz), 17.8 (d, J_{CP} = 5.1 Hz); ^{31}P NMR (162 MHz, $CDCl_3$) δ 61; HRMS (DART) *m*/*z* calculated for $C_{21}H_{29}O_2NP$ $[M + H]^+$: 358.1930; found: 358.1931.

To a 10 mL Schlenk flask with magnetic stir bar was charged **3.50** (260 mg, 0.727 mmol, 1.0 eq). A reflux condenser was added, and the reaction was inerted with Ar using vacuum-purge cycles. PhMe (2.0 mL) was as added followed by triethylamine (210 µL, 1.45 mmol, 2.0 eq) and $HSiCl_3$ (110 µL, 1.09 mmol, 1.5 eq). The mixture was then immersed in an oil bath at 60 °C and monitored by ^{31}P NMR spectroscopy. After 3.5 h, the reaction was cooled to 23 °C and quenched with 3 mL of degassed (Ar sparge) 30% NaOH (aq.). The mixture was then allowed to vigorously stir at 23 °C for 1 h. The aqueous layer was removed and subsequently extracted under Ar with MTBE (3 × 5 mL). The combined organics were dried with $MgSO_4$, filtered quickly through a pad of Celite, and immediately concentrated in vacuo. The crude residue was chromatographed on the bench by dissolving the crude solid in CH_2Cl_2 and loading the mixture onto a short pad of silica gel and eluting with degassed (Ar sparge) 25% EtOAc in hexanes using Ar to pressurize the flash column. The product fractions were immediately collected and concentrated *in vacuo* to afford 130 mg (52%) of **3.L27** as a white solid that was contaminated with a small impurity (93/7 by ^{31}PNMR spectroscopy). This material was used without further purification. We cannot rule out that low enantioselectivity in the subsequent cross-coupling reactions using this ligand was a result of the present impurities. $[\alpha]_D^{25}$ = + 57.5 (*c* 0.43, $CHCl_3$); ^{1}H NMR (500 MHz, $CDCl_3$) δ 7.29–7.37 (m, 4H), 7.08 (t, *J* = 7.9 Hz, 2H), 6.46 (d, *J* = 8.2 Hz, 1H), 6.28 (dd, *J* = 8.1 Hz, *J* = 2.6 Hz, 1H), 4.08 (t, *J* = 3.5 Hz, 1H), 3.83 (s, 3H), 2.10–2.22 (m, 1H), 1.00 (d, *J* = 6.7 Hz, 3H), 0.99 (d, *J* = 12 Hz, 9H), 0.81 (d, *J* = 6.7 Hz, 3H); ^{13}C

NMR (125 MHz, $CDCl_3$) δ 161.8 (d, J_{CP} = 12 Hz), 154.4 (d, J_{CP} = 1.0 Hz), 144.5 (d, J_{CP} = 1.4 Hz), 131.3, 129.3, 123.7, 123.3, 110.4 (d, J_{CP} = 11 Hz), 104.0, 100.4 (d, J_{CP} = 2.3 Hz), 70.4 (d, J_{CP} = 23 Hz), 55.1, 31.3 (d, J_{CP} = 20 Hz), 30.9 (d, J_{CP} = 19 Hz), 27.3 (d, J_{CP} = 14 Hz), 18.8 (d, J_{CP} = 11 Hz), 16.5 (d, J_{CP} = 12 Hz); ^{31}P NMR (202 MHz, $CDCl_3$) δ – 19. HRMS (DART) *m*/*z* calculated for $C_{21}H_{29}ONP$ $[M + H]^+$: 342.1981; found: 342.1981.

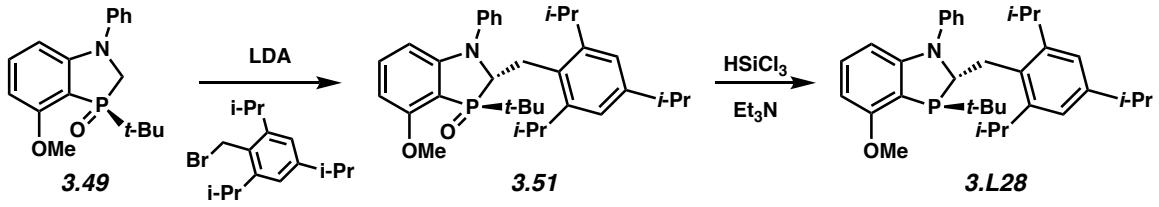

To a crimp vial was added the azaphosphole **3.49** (535 mg, 1.69 mmol, 1 eq), 2,4,6-triisopropylbenzylbromide (1.01 g, 3.40 mmol, 2.0 eq). The reaction was inerted with Ar using vacuum-purge cycles and Ar-purged THF (5.0 mL) was added. The solution was cooled to –78 °C. To a second crimp vial was added diisopropylamine (521 μL, 3.72 mmol, 2.2 eq) and THF (1 mL). The reaction mixture was cooled to –78 °C and a 2.50 M solution of *n*-BuLi was added (1.42 mL, 3.55 mmol, 2.1 eq). The reaction was stired for 20 min at –78 °C and the LDA was added via syringe to the first vial. The reaction mixture was stirred for 25 min at –78 °C then allowed to warm to 23 °C. UPLC analysis showed 100% conversion. The reaction was quenched with 1M HCl (20 mL), extracted with CH_2Cl_2 (3 x 25 mL) and washed with water and brine. The combined organic layers were dried with $MgSO_4$, filtered and concentrated *in vacuo*. Purification of the crude mixture by flash chromatography (gradient, 0–10% MeOH in CH_2Cl_2) afforded 337 mg (81%) of **3.51** as an off-white solid. ^{1}H NMR (500 MHz, $CDCl_3$) 7.31 (t, *J* = 8.2 Hz, 1H), 7.00 (br s, 2H), 6.84 (t, *J* = 6.0 Hz, 2H), 6.78 (t, *J* = 5.8 Hz, 1H), 6.59 (dd, *J* = 6.48 Hz, *J* = 2.3 Hz, 1H), 6.46 (dd, *J* = 6.6 Hz, *J* = 3.2 Hz, 1H), 6.24 (d, *J* = 7.9 Hz, 2H), 3.91 (s, 3H), 3.77–3.72

(m, 1H), 3.47–3.43 (m, 2H), 3.16–3.13 (m, 2H), 2.88 (p, J = 5.5 Hz, 1H), 1.27 (d, J = 6.9 Hz, 9H), 1.16–1.12 (m, 18H); ^{31}P NMR (202 MHz, $CDCl_3$) δ 67.0, 66.9 ppm; ^{13}C NMR (125 MHz, $CDCl_3$) δ 162.8 (d, $J_{C–P}$ = 1.2 Hz), 153.2 (d, $J_{C–P}$ = 16.0 Hz), 147.6, 145.5 (d, $J_{C–P}$ = 2.8 Hz), 135.2 (d, $J_{C–P}$ = 1.35 Hz), 130.8 (d, $J_{C–P}$ = 10.8 Hz), 128.6, 122.5, 121.4, 119.9, 110.3 (d, $J_{C–P}$ = 7.2 Hz), 106.4, 105.7, 103.4 (d, $J_{C–P}$ = 5.9 Hz), 62.9 (d, $J_{C–P}$ = 58.4 Hz), 55.5, 34.4, 32.7 (d, $J_{C–P}$ = 66.8 Hz), 29.3, 27.3, 24.6, 24.5, 24.3, 24.2. HRMS (DART) *m*/*z* calculated for $C_{34}H_{47}O_2NP$ $[M + H]^+$: 532.3339; found: 532.3337.

To a 10 mL Schlenk flask with magnetic stir bar was charged azaphosphole 3-oxide **3.51** (600 mg, 1.13 mmol, 1.0 eq). A reflux condenser was added, and the reaction was inerted with Ar using vacuum-purge cycles. PhMe (3.0 mL) was as added followed by triethylamine (315 µL, 2.26 mmol, 2.0 eq) and $HSiCl_3$ (170 µL, 1.69 mmol, 1.5 eq). The mixture was then immersed in an oil bath at 60 °C and monitored by ^{31}P NMR spectroscopy. After 3 h, the reaction was cooled to 23 °C and quenched with 4 mL of degassed (Ar sparge) 30% NaOH (aq.). The mixture was then allowed to vigorously stir at 23 °C for 1 h. The aqueous layer was removed and subsequently extracted under Ar with MTBE (3 × 5 mL). The combined organics were dried with $MgSO_4$, filtered quickly through a pad of Celite, and immediately concentrated *in vacuo*. The crude residue was chromatographed on the bench by dissolving the crude solid in CH_2Cl_2 and loading the mixture onto a short pad of silica gel and eluting with degassed (Ar sparge) 20% EtOAc in hexanes using Ar to pressurize the flash column. The product fractions were immediately collected and concentrated *in vacuo* to afford 520 mg (89%) of **3.L28** as a white solid. $[a]_D^{25}$ = + 25.4 (*c* 0.37, $CHCl_3$); ^{1}H NMR (500 MHz, $CDCl_3$) δ 7.21 (t, J = 8.1 Hz, 1H), 6.98 (s, 2H), 6.96 (t, J = 7.9 Hz, 2H), 6.79 (t, J = 7.3 Hz, 1H), 6.70 (d, J = 8.1 Hz, 1H), 6.56 (d, J = 8.1 Hz, 2H), 6.46 (dd, J = 8.1 Hz, J = 3.7 Hz, 1H), 4.08 (dd, J = 10 Hz, J = 4.0 Hz, 1H), 3.88

(s, 3H), 3.04–3.21 (m, 3H), 2.94–3.03 (m, 1H), 2.88 (sept, J = 6.9 Hz, 1H), 1.26 (d, J = 6.9 Hz, 6H), 1.11–1.89 (m, 6H), 1.10 (d, J = 6.7 Hz, 6H), 0.87 (d, J = 12 Hz, 9H); ^{13}C NMR (125 MHz, $CDCl_3$) δ 162.7 (d, J_{CP} = 13 Hz), 151.7, 147.5, 147.3, 145.8 (d, J_{CP} = 2.1 Hz), 131.4 (d, J_{CP} = 15 Hz), 131.2, 129.1, 128.5, 128.3, 121.7, 121.2, 120.1, 113.5 (d, J_{CP} = 13 Hz), 108.9, 102.3 (d, J_{CP} = 2.2 Hz), 66.9 (d, J_{CP} = 21 Hz), 55.3, 34.4, 33.9 (d, J_{CP} = 39 Hz), 30.7 (d, J_{CP} = 22 Hz), 29.4, 27.7 (d, J_{CP} = 14 Hz), 24.5, 24.3, 24.2, 24.1; ^{31}P NMR (202 MHz, $CDCl_3$) δ 2.3. HRMS (DART) m/z calculated for $C_{34}H_{47}ONP$ $[M + H]^+$: 516.3390; found: 516.3390.

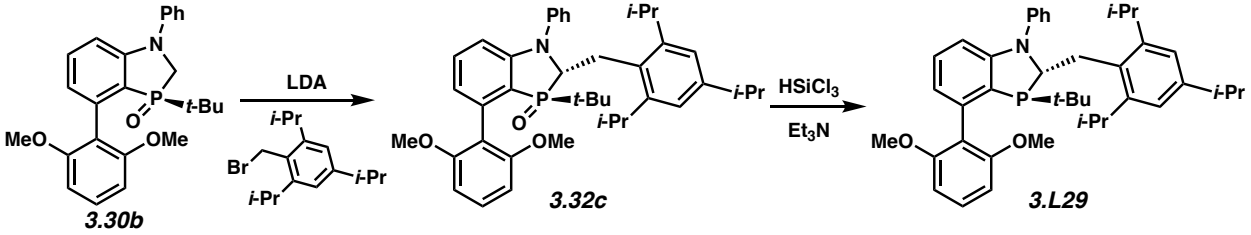

A solution of **3.30b** (0.400 g, 0.949 mmol) and the benzyl bromide derivative (0.422 g, 1.42 mmol) in 10 mL of THF was prepared under Ar, and the mixture was cooled to –78 °C. A solution of LDA (2.0 M in THF/heptane/ethylbenzene, 1.4 mL, 2.8 mmol) was charged dropwise. The mixture was agitated at –78 °C for 1 h and then allowed to warm to 23 °C and stirred an additional 1 h. Aqueous NH_4Cl (10%, 10 mL) was then charged, and volatile organics were removed *in vacuo*. The aqueous residue was then extracted with EtOAc (3 x 15 mL). The combined organics were dried with anhydrous Na_2SO_4 and concentrated *in vacuo*. The crude residue was then purified by flash chromatography (gradient, 0 to 30% EtOAc in hexanes) to afford 304 mg (70%) of **3.32c** as an off-white solid. ^{1}H NMR (400 MHz, $CDCl_3$) δ 7.44 (td, J = 7.9 Hz, J = 0.8 Hz, 1H), 7.31 (t, J = 8.4 Hz, 1H), 7.11 (dd, J = 8.1 Hz, J = 0.5 Hz, 1H), 7.03 (s, 2H), 6.89 (dd, J = 7.2 Hz, J = 0.6 Hz, 1H), 6.86 (t, J = 8.4 Hz, 2H), 6.73 (t, J = 7.0 Hz, 1H), 6.67 (d, J = 8.4 Hz, 1H), 6.57 (d, J = 8.2 Hz, 1H), 6.34 (d, J = 8.0 Hz, 2H), 3.83 (s, 3H), 3.76 (s, 3H),

3.69–3.77 (m, 1H), 3.48–3.57 (m, 1H), 3.34–3.44 (m, 1H), 3.14 (sept, J = 6.8 Hz, 2H), 2.91 (sept, J = 7.0 Hz, 1H), 1.29 (d, J = 6.9 Hz, 6H), 1.05–1.24 (m, 12 H), 0.86 (d, J = 15 Hz, 9H); ^{13}C NMR (100 MHz, $CDCl_3$) δ 159.2, 157.2, 150.5 (d, J_{CP} = 18 Hz), 147.6, 145.3 (d, J_{CP} = 2.5 Hz), 140.3 (d, J_{CP} = 4.7 Hz), 132.8 (d, J_{CP} = 1.7 Hz), 131.3 (d, J_{CP} = 11 Hz), 129.6, 128.5, 125.0 (d, J_{CP} = 8.7 Hz), 121.5, 121.4, 118.5, 118.3 (d, J_{CP} = 88 Hz), 116.7 (d, J_{CP} = 2.6 Hz), 116.1, 116.0, 104.3, 102.8, 62.7 (d, J_{CP} = 60 Hz), 56.0, 55.3, 34.4, 32.5 (d, J_{CP} = 65 Hz), 29.3, 26.6, 24.7 (br), 24.33, 24.28, 23.9; ^{31}P NMR (162 MHz, $CDCl_3$) δ 63 ppm. HRMS (DART) *m*/*z* calculated for $C_{41}H_{53}O_3NP$ $[M + H]^+$: 638.3758; found: 638.3758.

To a 10 mL Schlenk flask with magnetic stir bar was charged azaphosphole 3-oxide **3.32c** (274 mg, 0.431 mmol). A reflux condenser was added, and the reaction was inerted with Ar using vacuum-purge cycles. Toluene (6 mL) was added followed by triethylamine (172 µL, 1.29 mmol) and $HSiCl_3$ (108 µL, 1.08 mmol). The mixture was then immersed in an oil bath at 60 °C and monitored by ^{31}P NMR spectroscopy. After 3 h, the reaction was cooled to 23 °C and quenched with 15 mL of degassed (Ar sparge) 30% NaOH (aq.). The mixture was then allowed to vigorously stir at 23 °C for 0.5 h. The aqueous layer was removed and subsequently extracted under Ar with MTBE (3 × 5 mL). The combined organics were dried with $MgSO_4$, filtered quickly through a pad of Celite, and immediately concentrated *in vacuo*. The crude residue was chromatographed on the bench by dissolving the crude solid in 10% EtOAc/hexanes and loading the mixture onto a short pad of silica gel and eluting with degassed (Ar sparge) 10% EtOAc in hexanes using Ar to pressurize the flash column. The product fractions were immediately collected and concentrated *in vacuo* to afford 206 mg (77%) of **3.L29** as a white solid. $[\alpha]_D^{24}$ = –94.1 (*c* 0.25, $CHCl_3$); ^{1}H NMR (400 MHz, $CDCl_3$) δ 7.20–7.30 (m, 2H), 7.02 (d, J = 8.0 Hz, 1H), 6.93 (s, 2H), 6.84 (t, J = 7.4 Hz, 2H), 6.78 (dd, J = 7.4 Hz, J = 3.2 Hz, 1H), 6.66 (t, J = 7.0 Hz,

1H), 6.62 (d, J = 8.2 Hz, 1H), 6.55 (d, J = 8.4 Hz, 1H), 6.43 (d, J = 8.1 Hz, 2H), 3.98 (dd, J = 11 Hz, J = 2.8 Hz, 1H), 3.73 (s, 3H), 3.69 (s, 3H), 3.13–3.24 (m, 1H), 2.95–3.13 (m, 3H), 2.82 (sept, J = 6.9 Hz, 1H), 1.20 (d, J = 7.0 Hz, 6H), 1.08 (d, J = 6.6 Hz, 6H), 1.04 (d, J = 6.8 Hz, 6H), 0.61 (d, J = 12 Hz, 9H); ^{13}C NMR (100 MHz, $CDCl_3$) δ 157.9, 157.1, 149.6, 147.4, 147.3, 145.9 (d, J_{CP} = 1.9 Hz), 139.8 (d, J_{CP} = 19 Hz), 131.8 (d, J_{CP} = 17 Hz), 129.5, 128.9, 128.3, 123.5, 123.4, 121.2, 120.8, 120.2, 118.7, 114.5, 104.7, 103.6, 66.9 (d, J_{CP} = 20 Hz), 56.0, 55.4, 34.3 33.6 (d, J_{CP} = 39 Hz), 30.2 (d, J_{CP} = 20 Hz), 29.3, 27.4 (d, J_{CP} = 15 Hz), 24.6, 24.3, 24.2, 24.0; ^{31}P NMR (162 MHz, $CDCl_3$) δ 11. HRMS (DART) m/z calculated for $C_{41}H_{53}O_2NP$ $[M + H]^+$: 622.3808; found: 622.3813.

3.8.2.2 Substrate Synthesis

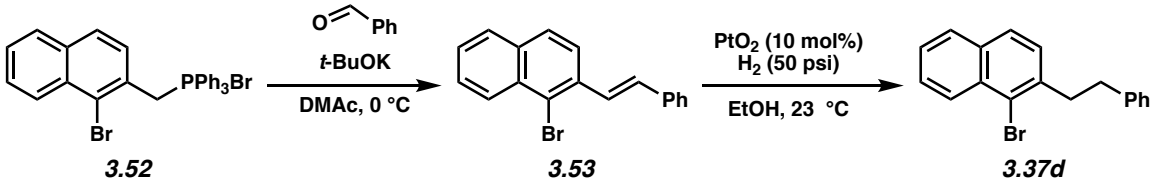

A round bottom flask equipped with a magnetic stir bar was heat-dried under reduced pressure, and then cooled under a N_2 atmosphere. Wittig reagent **3.52**[14] (5.30 g, 9.42 mmol, 1.0 equiv) was added and the flask backfilled with N_2 three times. DMAc (0.25 M, 38 mL) was added and the reaction cooled to 0 °C in an ice/water bath. *t*-BuOK (1.16 g, 10.4 mmol, 1.1 equiv) was added in one portion and the solution turned bright orange. After 1 min, freshly distilled benzaldehyde (1.0 g, 9.42 mmol, 1.0 equiv) was added dropwise over 3 min and the reaction was left to run at 0 °C for 20 min. The reaction was then quickly transferred to a separatory funnel with EtOAc (5 mL) and quenched with deionized water (20 mL). The layers were separated and the resulting aqueous layer was extracted with EtOAc (3 x 20 mL). The organic layers were combined and washed with deionized water (4 x 10 mL), brine (2 x 10 mL),

dried over Na_2SO_4, and the volatiles were removed under reduced pressure. The resulting crude residue was purified by flash chromatography (Hexanes → 9:1 Hexanes:EtOAc) to yield 2.36 g (81%) of olefin **3.53** as an *E*/*Z* mixture that was used directly in the next step.

To a 100 mL bomb was charged alkene **3.53** (2.36 g, 7.62 mmol, 1.0 equiv) and PtO_2 (173 mg, 0.76 mmol, 0.10 equiv). EtOH (51 mL) was added, and the vessel was sealed and placed under N_2 by pressurizing the vessel to ~100 psi of N_2 followed by venting. This was repeated 2x. The reactor was then placed under a H_2 atmosphere by pressurizing the reactor to 50 psi H_2 followed by venting. This process was performed 3x. The reactor was then pressurized with 50 psi of H_2 and agitated at 23 °C with mechanical stirring for 2 h. The reaction was then vented and filtered through a pad of celite with EtOAc as the eluent, and the volatiles were removed under reduced pressure. The resulting crude residue was purified by flash chromatography (Hexanes → 9:1 Hexanes:EtOAc) to yield 2.09 g (88%) of bromide **3.37d** as a colorless oil. ^{1}H NMR (500 MHz, $CDCl_3$): δ 8.35 (d, *J* = 8.5, 1H), 7.80 (d, *J* = 8.3, 1H), 7.72 (d, *J* = 8.3, 1H), 7.59 (t, *J* = 7.8, 1H), 7.50 (t, *J* = 7.8, 1H), 7.33–7.26 (m, 5H), 7.25–7.22 (m, 1H), 3.29 (t, *J* = 8.3, 2H), 3.01 (t, *J* = 8.3, 2H); ^{13}C NMR (125 MHz, $CDCl_3$): δ 141.6, 139.3, 133.4, 132.8, 128.7, 128.6, 128.3, 128.2, 127.7, 127.5, 127.4, 126.2, 126.1, 123.9, 39.8, 36.5. HRMS (DART) calculated for $C_{18}H_{15}Br$ $[M]^+$: 310.0357; found $[M]^+$: 310.0353.

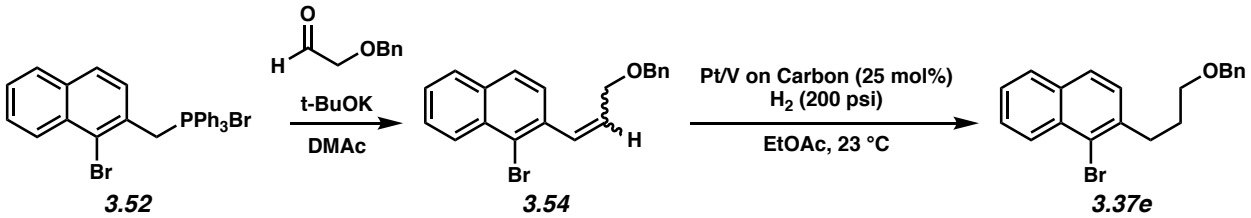

3.52 *3.54* *3.37e*

A round bottom flask equipped with a magnetic stir bar was heat-dried under reduced pressure, and then cooled under a N_2 atmosphere. Wittig reagent **3.52**[14] (1.87 g, 3.33 mmol, 1.0

equiv) was added and the flask backfilled with N_2 three times. DMAc (0.25 M, 13 mL) was added and the reaction cooled to 0 °C in an ice/water bath. *t*-BuOK (0.411g, 3.66 mmol, 1.1 equiv) was added in one portion and the solution turned bright orange. After 1 min, freshly distilled benzyloxyacetaldehyde (0.500 g, 3.33 mmol, 1.0 equiv) was added dropwise over 3 min and the reaction was left to run at 0 °C for 20 min. The reaction was then quickly transferred to a separatory funnel with EtOAc (5 mL) and quenched with deionized water (20 mL). The layers were separated and the resulting aqueous layer was extracted with EtOAc (3 x 20 mL). The organic layers were combined and washed with deionized water (4 x 10 mL), brine (2 x 10 mL), dried over Na_2SO_4, and the volatiles were removed under reduced pressure. The resulting crude residue was purified by flash chromatography (Hexanes → 20:1 Hexanes:EtOAc) to yield 1.11 g (94%) of olefin **3.54** as a light green oil (5:1 mixture Z:E). ^{1}H NMR (500 MHz, $CDCl_3$): δ 8.33 (d, *J* = 8.6, 1H), 7.80 (d, *J* = 8.6, 1H), 7.71 (d, *J* = 8.2, 1H), 7.60–7.56 (m, 1H), 7.53–7.47 (m, 1H), 7.42–7.36 (m, 1H), 7.33–7.31 (m, 1H), 7.29–7.28 (m, 3H), 7.26–7.23 (m, 1H), 6.92 (d, *J* = 11.9, 1H), 6.07 (dd, *J* = 13.8, 7.1, 1H), 4.48 (s, 2H), 4.16 (d, *J* = 6.7, 2H); ^{13}C NMR (125 MHz, $CDCl_3$): (35 of 36 signals observed) δ 138.2, 138.1, 134.9, 134.2, 133.9, 133.6, 133.0, 132.6, 132.3, 132.2, 129.9, 129.6, 128.4, 128.3, 128.0, 127.9, 127.9, 127.7, 127.7, 127.7, 127.6, 127.6, 127.6, 127.6, 127.2, 127.1, 126.6, 126.6, 126.3, 123.8, 123.7, 72.4, 72.3, 70.7, 66.6.

To an Endeavor test tube was charged alkene **3.54** (713.1 mg, 2.02 mmol, 1.0 equiv) and Pt/V on carbon (179.0 mg, 0.50 mmol, 0.25 equiv). EtOAc (7.2 mL) was added and the reaction placed in an Endeavor reactor under 200 psi H_2 gas and 23 °C for 36 h. The reaction was then filtered through a plug of celite with EtOAc as the eluent (10 mL) and the volatiles were removed under reduced pressure. The resulting crude residue was purified by flash chromatography (Hexanes → 9:1 Hexanes:EtOAc) to yield bromide **3.37e** (716.5 mg, 99%

yield) as a light brown oil. ^{1}H NMR (500 MHz, $CDCl_3$): δ 8.31 (d, *J* = 8.8, 1H), 7.78 (d, *J* = 8.4, 1H), 7.71 (d, *J* = 8.4, 1H), 7.57 (t, *J* = 7.7, 1H), 7.47 (t, *J* = 7.7, 1H), 7.37–7.33 (m, 5H), 7.30–7.27 (m, 1H), 4.54 (s, 2H), 3.56 (t, *J* = 6.5, 2H), 3.10 (t, *J* = 7.7, 2H), 2.06–2.01 (m, 2H); ^{13}C NMR (125 MHz, $CDCl_3$): δ 139.7, 138.7, 133.4, 132.8, 128.5, 128.4, 128.1, 127.8, 127.7, 127.6, 127.4, 127.4, 125.9, 123.9, 73.1, 69.6, 34.2, 30.1. HRMS (DART) calculated for $C_{20}H_{20}BrO$ [M + H]$^+$: 355.0698; found [M + H]$^+$: 355.0693.

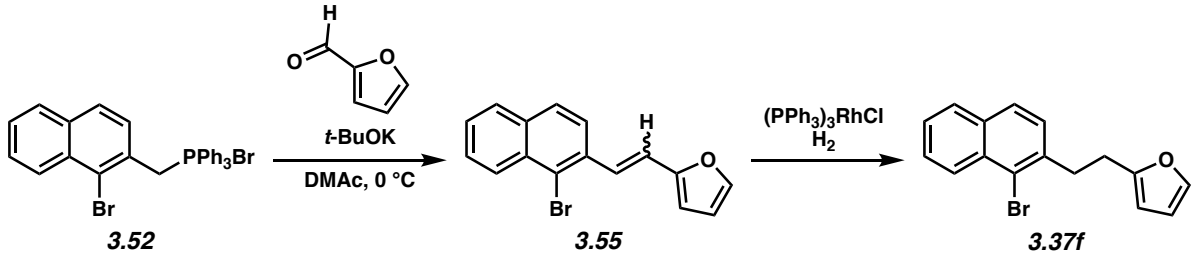

3.52 *3.55* *3.37f*

A round bottom flask equipped with a magnetic stir bar was heat-dried under reduced pressure, and then cooled under a N_2 atmosphere. Wittig reagent **3.52**[14] (1.76 g, 3.122 mmol, 1.0 equiv) was added and the flask backfilled with N_2 three times. DMAc (0.25 M, 12.5 mL) was added and the reaction cooled to 0 °C in an ice/water bath. *t*-BuOK (385.4 mg, 3.434 mmol, 1.1 equiv) was added in one portion and the solution turned bright orange. After 1 min, freshly distilled furfural (300.0 mg, 3.122 mmol, 1.0 equiv) was added dropwise over 3 min and the reaction was left to run at 0 °C for 20 min. The reaction was then quickly transferred to a separatory funnel with EtOAc (5 mL) and quenched with deionized water (20 mL). The layers were separated and the resulting aqueous layer was extracted with EtOAc (3 x 20 mL). The organic layers were combined and washed with deionized water (4 x 10 mL), brine (2 x 10 mL), dried over Na_2SO_4, and the volatiles were removed under reduced pressure. The resulting crude residue was purified by flash chromatography (Hexanes → 9:1 Hexanes:EtOAc) to yield 760 mg (82%) of olefin **3.55** as a white solid (1:1 mixture Z:E). ^{1}H NMR (500 MHz, $CDCl_3$): δ 8.35 (dd,

J = 8.5, 5.8, 2H), 7.83–7.70 (m, 6H), 7.61–7.57 (m, 2H), 7.54–7.48 (m, 4H), 7.25 (app. s, 1H), 6.98 (d, *J* = 16.2, 1H), 6.69 (d, *J* = 12.4, 1H), 6.57 (d, *J* = 12.4, 1H), 6.47 (app. s, 2H), 6.27–6.26 (m, 1H), 6.10 (d, *J* = 3.2, 1H); ^{13}C NMR (125 MHz, $CDCl_3$): (30 of 32 signals observed) δ 153.3, 151.9, 142.9, 142.2, 136.4, 134.5, 133.9, 133.9, 133.0, 132.6, 128.2, 128.2, 128.1, 128.0, 127.9, 127.8, 127.5, 127.4, 127.1, 126.9, 126.7, 126.7, 124.3, 123.6, 119.7, 119.5, 112.0, 111.5, 110.6, 109.9.

To a 100 mL bomb was charged alkene **3.55** (0.700 g, 2.35 mmol, 1.0 equiv), 163 mg (0.176 mmol) of $(PPh_3)_3RhCl$, and 17 mL of a 1:1 mixture of THF:*t*-BuOH. The vessel was sealed and placed under N_2 by pressurizing the vessel to ~100 psi of N_2 followed by venting. This was repeated 2x. The reactor was then placed under a H_2 atmosphere by pressurizing the reactor to 50 psi H_2 followed by venting. This process was performed 3x. The reactor was then pressurized with 300 psi of H_2 and agitated at 23 °C with mechanical stirring for 6 h. The reaction was then vented and filtered through a pad of celite with EtOAc as the eluent, and the volatiles were removed under reduced pressure. The resulting crude residue was purified by flash chromatography (Hexanes → 9:1 Hexanes:EtOAc) to yield 513 mg (73%) of bromide **3.37f**. ^{1}HNMR (500 MHz, $CDCl_3$): δ 8.33 (d, *J* = 8.6, 1H), 7.79 (d, *J* = 8.1, 1H), 7.71 (d, *J* = 8.3, 1H), 7.58 (t, *J* = 7.4, 1H), 7.48 (t, *J* = 7.3, 1H), 7.34 (d, *J* = 1.2 Hz, 1H), 7.27 (d, *J* = 8.4 Hz, 1H), 6.28 (dd, *J* = 3.0 Hz, *J* = 1.2 Hz, 1H), 5.99 (d, *J* = 3.0 Hz, 1H), 3.26 (t, *J* = 8.3 Hz, 2H), 3.03 (t, *J* = 8.3 Hz, 2H); ^{13}CNMR (125 MHz, $CDCl_3$): δ 155.1, 141.2, 138.8, 133.5, 132.7, 128.2, 128.1, 127.7, 127.5, 127.4, 126.1, 123.9, 110.3, 105.6, 36.3, 28.5. HRMS (DART) calculated for $C_{16}H_{14}BrO$ $[M + H]^+$: 301.0228; found $[M + H]^+$: 301.0223.

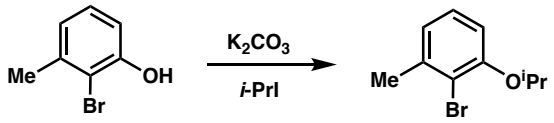

3.56 ***3.57***

To a solution of 5.0 g (26.7 mmol) of phenol **3.56** in 50 mL of acetone under N_2 was charged 8.87 g (64.2 mmol) of K_2CO_3 and 10.0 g (58.8 mmol) of *i*-PrI. The mixture was then agitated at reflux for 14 h. The reaction was then cooled to 23 °C and diluted with 60 mL of water. The layers were separated, and the aqueous layer was extracted with CH_2Cl_2 (3 x 70 mL). The combined organic layers were then washed with water, brine, and dried with anhydrous Na_2SO_4. Volatile material was then removed *in vacuo* and the crude residue purified by flash chromatography (gradient, hexanes to 2:1 hexanes:EtOAc) to afford 6.03 g (98%) of the desired bromide **3.57** as a light brown oil. ^{1}H NMR (500 MHz, $CDCl_3$): δ 7.11 (t, *J* = 7.8, 1H), 6.84 (d, *J* = 7.5, 1H), 6.75 (d, *J* = 8.2, 1H), 4.53 (sept, *J* = 6.1, 1H), 2.41 (s, 3H), 1.38 (d, *J* = 6.1, 6H); ^{13}C NMR (125 MHz, $CDCl_3$): δ 154.8, 140.0, 127.4, 123.1, 116.6, 113.1, 72.28, 23.62, 22.26. HRMS (DART) calculatedd for $C_{10}H_{14}BrO$ $[M + H]^+$: 229.0228; found $[M + H]^+$: 229.0223.

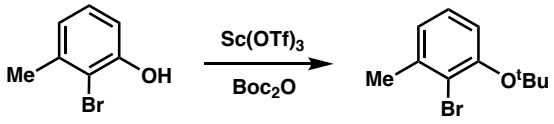

3.56 ***3.58***

To a solution of 3.08 g (16.5 mmol) of phenol **3.56** and 405 mg (0.823 mmol) of $Sc(OTf)_3$ under N_2 in 25 mL of CH_2Cl_2 was charged 8.27 g (37.9 mmol) of Boc_2O. The mixture was allowed to stir at 23 °C for 2 h. An additional 4.32 g (19.8 mmol) of Boc_2O was then charged and stirring was continued at 23 °C. After a further 5 h, another charge of 4.32 g (19.8 mmol) of Boc_2O was added, and the mixture was stirred at 23 °C for an additional 17 h. To the reaction was then charged 2 M aqueous NaOH (30 mL), and the mixture was agitated for 30 min.

The layers were then separated, and the aqueous was extracted with CH_2Cl_2 (2x). Combined organics were washed with water, brine, dried with anhydrous Na_2SO_4, and concentrated *in vacuo*. The crude residue was purified by flash chromatography (gradient, hexanes to 10% EtOAc/hexanes) to afford 3.0 g (75%) of the desired bromide **3.58** as a colorless oil. ^{1}H NMR (500 MHz, $CDCl_3$): δ 7.08 (t, *J* = 7.9, 1H), 6.94 (d, *J* = 8.2 Hz, 1H), 6.93 (d, *J* = 7.5 Hz, 1H), 2.41 (s, 3H), 1.44 (s, 9H); ^{13}C NMR (125 MHz, $CDCl_3$): δ 153.5, 139.7, 126.7, 125.1, 121.8, 120.8, 81.05, 29.06, 23.78. HRMS (DART) calculated for $C_{11}H_{16}BrO$ $[M + H]^+$: 243.0385; found $[M + H]^+$: 243.0381.

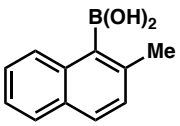

3.16a

(2-Methylnaphthalen-1-yl)boronic acid (**3.16a**) was synthesized using the literature procedure.[15] ^{1}H NMR (400 MHz, $CDCl_3$): δ 8.48 (s, 2H), 7.88 (dd, *J* = 8.0, 1.0 Hz, 1H), 7.80 (d, *J* = 8.3 Hz, 2H), 7.52-7.43 (m, 2H), 7.36 (d, *J* = 8.3 Hz, 1H), 2.52 (s, 3H); ^{13}C NMR (100 MHz, $CDCl_3$): δ 136.8, 135.2, 131.2, 128.6, 128.5, 128.2, 127.6, 125.9, 124.9, 22.7. HRMS (DART-TOF+): mass [M+H] calculated for $C_{11}H_{11}O_2B$ 186.08466, found 186.08478.

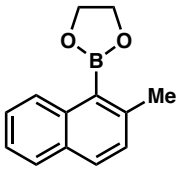

3.16b

2-(2-Methylnaphthalen-1-yl)-1,3,2-dioxaborolane (3.16b) was prepared according to a literature procedure[16] with a slight modification of the solvent. To a 10 mL dram vial equipped with a stir bar, were added (2-methylnaphthalen-1-yl)boronic acid (0.25g, 1.34 mmol, 1 equiv), molecular sieves 4Å activated powder (1 g) and *tert*-butyl methyl ether, MTBE (2 mL) under nitrogen. To the resulting mixture was added anhydrous ethylene glycol (83.42 mg, 1.34 mmol, 1.0 equiv), sealed with a lid and stirred for 12 h at 23 °C. The molecular sieves were collected by the filtration and rinsed the solids with additional MTBE (1 ml). The combined fractions were dried concentration under reduced

pressure to afford 293 mg (100%) of 2-(2-Methylnaphthalen-1-yl)-1,3,2-dioxaborolane **3.16b** as clear oil. The oil was used directly without further purification for the coupling reactions. ^{1}H NMR (400 MHz, $CDCl_3$) δ 8.12 (d, J = 8.4 Hz, 1H), 7.76 (d, J = 8.3 Hz, 2H), 7.46-7.36 (m, 2H), 7.29 (d, J = 8.5 Hz, 1H), 4.48 (s, 4H), 2.61 (s, 3H); ^{11}B NMR (128.3 MHz, $CDCl_3$) δ 33.0 ppm, ^{13}C NMR (100 MHz, $CDCl_3$) δ 142.1, 136.7, 131.4, 129.9, 128.8, 128.5, 128.1, 127.8, 126.1, 124.7, 65.9, 23.0.

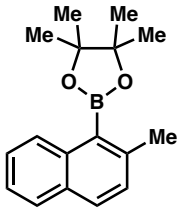

3.16c

4,4,5,5-tetramethyl-2-(2-methylnaphthalen-1-yl)-1,3,2-dioxaborolane (**3.16c**) was prepared according to the literature procedure.[17]

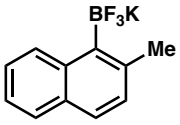

3.16d

Potassium trifluoro(2-methylnaphthalen-1-yl)borate (3.16d) was prepared according to a literature procedure.[18] White solid, ^{1}H NMR (400 MHz, CD_3CN): δ 8.69 (d, J = 8.5 Hz, 1H), 7.70 (dd, J = 7.8, 1.7 Hz, 1H), 7.56 (d, J = 8.30 Hz, 1H), 7.35-7.27 (m, 2H), 7.21 (d, J = 8.3 Hz, 1H), 2.63 (q, J = 1.9 Hz, 3H); ^{19}F NMR (376.4 MHz, CD_3CN): δ -129.0 ppm (m); ^{13}C NMR (100 MHz, CD_3CN): δ 139.1, 138.4, 132.5, 130.8 (q, J = 4.3 Hz), 130.3, 127.9, 126.2, 124.2, 123.6, 117.9, 23.3 (q, J = 3.4 Hz).

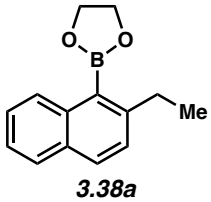

3.38a

2-(2-ethylnaphthalen-1-yl)-1,3,2-dioxaborolane (3.38a) was prepared according to the literature.[16] Clear oil (92% yield); ^{1}H NMR (400 MHz, $CDCl_3$): δ 8.04 (dd, J = 8.3, 0.7 Hz, 1H), 7.80 (d, J = 8.4 Hz, 2H), 7.78 (dd, J

= 8.0, 1.3, 2H), 7.47-7.37 (m, 2H), 7.34 (d, *J* = 8.5 Hz, 1H), 4.51 (s, 4H), 2.88 (q, *J* = 7.6 Hz, 2H), 1.29 (t, *J* = 7.6 Hz, 3H); ^{13}C NMR (100 MHz, $CDCl_3$): δ 148.1, 136.5, 131.4, 130.0, 129.1, 128.1, 127.8, 127.1, 125.9, 124.7, 65.9, 30.2, 17.0.

3.8.2.3 General Procedure for the Asymmetric Suzuki–Miyaura Cross-Coupling

To a 10 mL screw-cap threaded vial with a stir bar were charged aryl bromide (0.2 mmol, 1.0 equiv), arylboronic acid (1 mmol, 5.0 equiv), $Pd(OAc)_2$ (0.01 mmol, 5 mol%), ligand **(*S*$_P$)-3.L7** (0.02 mmol, 10 mol%, Pd/ligand ratio = 1:2) followed by potassium phosphate tribasic (1.0 mmol, 5.0 equiv). The vial was briefly inerted with argon and then charged dry THF (1 mL). The mixture was stirred at reflux (65 °C) for 24 h (unless otherwise mentioned) and then quenched with 2% ammonium chloride solution (2 mL). The resulting mixture was extracted with EtOAc (4 mL) and organics were dried over sodium sulfate, concentrated, and purified by silica gel column chromatography to provide chiral tetra-*ortho*-substituted bisnaphthalene products. Enantiomeric ratios were determined by chiral HPLC or SFC.

3.8.2.4 General Procedure for the Asymmetric Negishi Cross-Coupling

A 10-mL microwave vial equipped with a magnetic stir bar was heat-dried under reduced pressure, and then cooled under a N_2 atmosphere. The aryl bromide (1.5 equiv) was then added under N_2, followed by THF (0.42 M). The reaction was then cooled to –78 °C where a solution of *t*-BuLi in pentanes (1.7 M, 3.0 equiv) was added dropwise over 10 min while keeping the reaction at –78 °C. After 20 min, a solution of $ZnBr_2$ (2.0 equiv) in THF (0.56 M) was added dropwise to the reaction over 5 min while keeping the reaction at –78 °C. After ~2 min, the reaction was allowed to warm to 23 °C. During this time, a second 10-mL microwave vial

equipped with a magnetic stir bar was heat-dried under reduced pressure and then cooled under a N_2 atmosphere. Aryl bromide (70.0 mg, 1.0 equiv), $Pd_2(dba)_3$ (2.5 mol%), and ligand (7.5 mol%) were added, and the vial inerted with N_2 using vacuum-purge cycles (3x). The organozinc solution was then cannulated into the second vial. The combined mixture was then placed in a pre-heated 60 °C oil bath and allowed to stir for 16 h. Once at 23 °C, the reaction mixture was quenched with 2.0 M HCl (3 mL), and then transferred to a separatory funnel with EtOAc (2 mL). The layers were separated, and the aqueous layer extracted with EtOAc (3 x 4 mL). The organic layers were combined and washed brine (5 mL), and dried over $MgSO_4$. The volatiles were removed under reduced pressure. The resulting crude residue was purified by flash chromatography (Hexanes → 9:1 Hexanes:EtOAc) to yield the desired biaryl compounds.

3.8.2.5 Analytical Data of Cross-Coupling Products

3.8.2.5.1 Asymmetric Suzuki–Miyaura Reaction

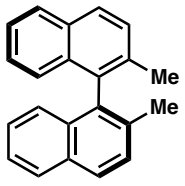

(S)-3.18

(*S*)-2,2'-Dimethyl-1,1'-binaphthalene (*S)*-**3.18**: This product was purified with silica gel chromatography (eluent: 0-15% EtOAc in hexanes). Thick oil (40.1 mg, 97% corrected yield, containing 10% regiosiomer); 89% ee; Enantiomeric excess was determined by chiral HPLC on a Chiralcel OD-H (4.6 x 250 mm, hexanes, isocratic, 0.8 mL/min, run time: 25 min, 25 ^{o}C, 11.12 min (*S*), 14.87 min (*R*)). ^{1}H NMR (400 MHz, $CDCl_3$): δ 7.89–7.85 (m, 4H), 7.49 (d, *J* = 8.4 Hz, 2H), 7.38 (m, 2H), 7.19 (m, 2H), 7.04 (d, *J* = 8.4 Hz), 2.02 (s, 6H); ^{13}C NMR (100 MHz, $CDCl_3$): δ 135.1, 134.3, 132.7, 132.2, 128.7, 127.9, 127.4, 126.0, 125.6, 124.9, 20.05. HRMS (DART): mass [M+H] calculated for $C_{22}H_{16}$ 282.14030, found 282.14042. Analytical data was in agreement with the reported literature.[19] Absolute configuration was confirmed by comparison of the optical rotation to the literature

value: $[a]_D^{25}$ = + 36.5 (*c* 0.31, $CHCl_3$, 95:5 er), lit.[19] $[a]_D^{20}$ = – 37.1 (*c* 1, $CHCl_3$, 95% ee, *R*-isomer).

*Chiral HPLC (Chiralcel OD-H,100% hexanes, 220 nm) analysis of Suzuki Reaction product (S)-**3.18**:*

Asymmetric Reaction: *Racemic Reaction:*

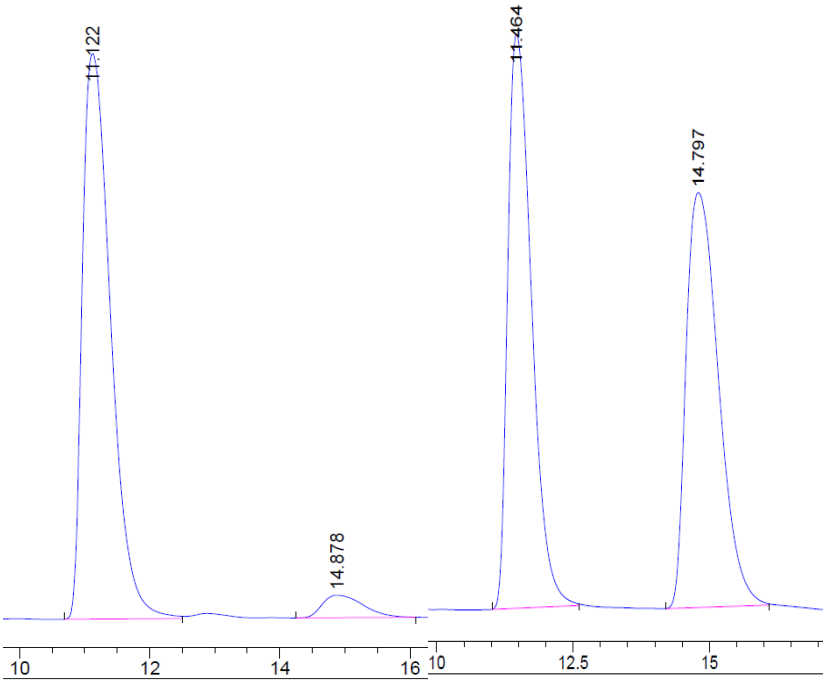

Peak #	RetTime [min]	Type	Width [min]	Area [mAU*s]	Height [mAU]	Area %
1	11.122	BB	0.4758	2.19062e4	722.41168	94.5424
2	14.878	BB	0.6918	1264.57922	28.82508	5.4576

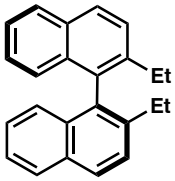

(S)-3.39a

(*S*)-2,2'-diethyl-1,1'-binaphthalene (*S*)-**3.39a**: Arylbromide (1.0 equiv), 2-(2-ethylnaphthalen-1-yl)-1,3,2-dioxaborolane, **3.38a** (2.0 equiv), K_3PO_4 (3.0 equiv) and rest as described in the general procedure using ligand (S_P)-**3.L7**. This product was purified with silica gel chromatography ((eluent: 0-10% EtOAc in hexanes). Clear

oil (27% yield); 76% ee; Enantiomeric excess was determined by chiral HPLC on a Chiralcel OD-H (4.6 x 250 mm, hexanes, isocratic, 0.8 mL/min, run time: 25 min, 25 °C, 9.73 min (*S*), 12.6 min (*R*)). R_f = 0.38 in 100% hexanes. ^{1}H NMR (500 MHz, $CDCl_3$): δ 7.90 (d, *J* = 8.5 Hz, 2H), 7.88 (d, *J* = 8.1 Hz, 2H), 7.56 (d, *J* = 8.5 Hz, 2H), 7.39-7.37 (m, 2H), 7.20-7.16 (m, 2H), 7.03 (d, *J* = 8.5 Hz), 2.40-2.28 (m, 4H), 1.01(t, *J* = 7.6 Hz, 6H); ^{13}C NMR (125 MHz, $CDCl_3$): δ 140.2, 134.1, 133.2, 132.1, 127.7 (d, *J* = 3.8 Hz), 126.8, 126.3, 125.8, 124.9, 26.7, 14.8. HRMS (DART) *m/z* calculated for $C_{24}H_{22}$ $[M]^+$: 310.1716; found $[M]^+$: 310.1719. Analytical data was in agreement with the reported literature.[20]

Asymmetric Reaction: *Racemic Reaction:*

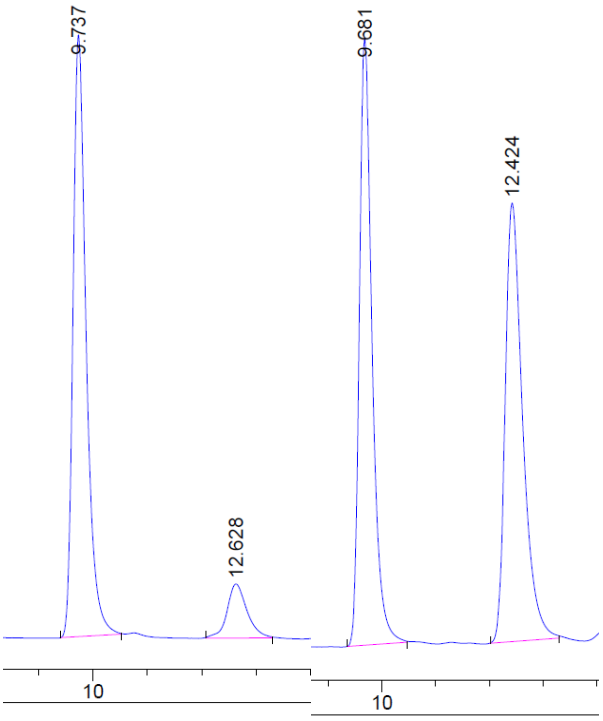

Signal 1: DAD1 B, Sig=220,8 Ref=500,100

Peak #	RetTime [min]	Type	Width [min]	Area [mAU*s]	Height [mAU]	Area %
1	9.737	BB	0.2538	3054.43945	182.04266	88.0345
2	12.628	BB	0.3781	415.15460	16.35651	11.9655

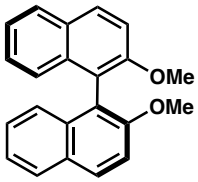

(S)-3.39b

(*S*)-2,2'-dimethoxy-1,1'-binaphthalene (*S*)-**3.39b**: This product was purified with silica gel chromatography ((eluent: 0-30% EtOAc in hexanes). White solid (18.0 mg, 26% yield); 77% ee; Enantiomeric excess was determined by chiral SFC (Lux Cel 1, MeOH, flow rate: 3 mL/min, BPR pressure: 150 bar, 10min, 35 ^{o}C, Gradient: 1 – 3% MeOH in 3 min to 50% MeOH in 5 min, then hold at 50% MeOH for 1 min, 5.10 min (*R*), 5.72 min (*S*)). ^{1}H NMR (400 MHz, $CDCl_3$): δ 7.96 (d, *J* = 9.0 Hz, 2H), 7.86 (d, *J* = 8.2 Hz, 2H), 7.50 (d, *J* = 9.0 Hz, 2H), 7.32–7.28 (m, 2H), 7.21–7.17 (m, 2H), 7.09 (d, *J* = 8.5 Hz, 2H), 3.75 (s, 6H); ^{13}C NMR (100 MHz, $CDCl_3$): δ 154.9, 134.0, 129.4, 129.2, 127.9, 126.3, 125.2, 123.5, 119.6, 114.2, 56.9. HRMS (DART) *m/z* calculated for $C_{22}H_{19}O_2$ $[M+H]^+$: 315.1380; found: 315.1380. Analytical data was in agreement with the reported literature.[50]

Chiral SFC (Lux Cel 3, gradient: 1 – 3% MeOH (3 min); 50% MeOH (5 min), 220 nm) analysis:

Asymmetric Reaction:

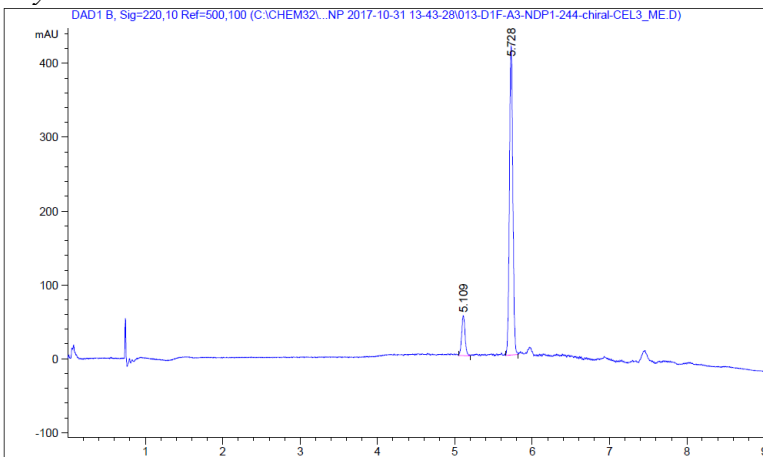


```
Signal 1: DAD1 B, Sig=220,10 Ref=500,100

Peak RetTime Type  Width     Area      Height     Area
  #   [min]        [min]    [mAU*s]     [mAU]       %
----|-------|----|-------|----------|----------|--------|
   1   5.109 BV R  0.0466  164.22279   53.78522  11.4227
   2   5.728 BB    0.0471 1273.45923  417.69534  88.5773

Totals :                   1437.68202  471.48057

---------------------------------------------------------------
```

Racemic reaction:

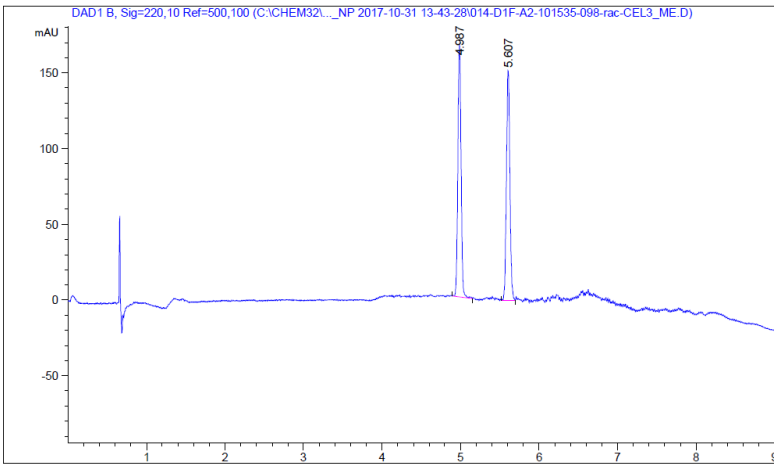

3.8.2.5.2 Asymmetric Negishi Reaction

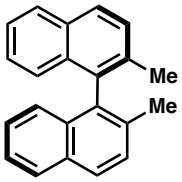

(R)-3.18

(*R*)-2,2'-dimethyl-1,1'-binaphthalene (*R*)-**3.18**: Arylzinc formation: 89.3 mg (0.43 mmol) aryl bromide, 0.52 mL (0.88 mmol) 1.7 M *t*-BuLi in pentane, 1 mL THF, 136 mg (0.604 mmol) $ZnBr_2$ in 1 mL of THF. Cross-coupling: 59.1 mg (0.267 mmol) aryl bromide, 6.1 mg (0.0067 mmol) $Pd_2(dba)_3$, 8.4 mg (0.020 mmol) ligand (R_p)-**3.L13**, and the arylzinc solution afforded 71.1 mg (94%) of biaryl (*R*)-**3.16** as a colorless oil. Spectral data was consistent with the literature.[19] Absolute configuration was confirmed by comparison of the optical rotation to the literature value: $[a]_D^{25} = -24.3$ (*c* 1, $CHCl_3$, 85:15 er), lit.[19] $[a]_D^{20} = -37.1$ (*c* 1, $CHCl_3$, 95% ee).

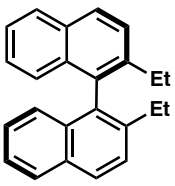

(R)-3.39a

(*R*)-2,2'-diethyl-1,1'-binaphthalene (*R*)-**3.39a**: Arylzinc formation: 105 mg (0.447 mmol) aryl bromide, 0.52 mL (0.89 mmol) 1.7 M *t*-BuLi in pentane, 1.1 mL THF, 134 mg (0.593 mmol) $ZnBr_2$ in 1.1 mL of THF. Cross-coupling: 70.0 mg (0.298 mmol) aryl bromide, 6.7 mg (0.0073 mmol) $Pd_2(dba)_3$, 8.3 mg (0.022 mmol) ligand (R_p)-**3.L13**, and the arylzinc solution afforded 74.1 mg (80%) of biaryl (*R*)-**3.39a**.

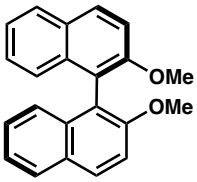

(R)-3.39b

(*R*)-2,2'-dimethoxy-1,1'-binaphthalene (*R*)-**3.39b**: Arylzinc formation: 105 mg (0.443 mmol) aryl bromide, 0.52 mL (0.89 mmol) 1.7 M *t*-BuLi in pentane, 1 mL THF, 131 mg (0.576 mmol) $ZnBr_2$ in 0.95 mL of THF. Cross-coupling: 70.0 mg (0.295 mmol) aryl bromide, 6.7 mg (0.0073 mmol) $Pd_2(dba)_3$, 8.8 mg (0.022 mmol) ligand (R_p)-**3.L13**, and the arylzinc solution afforded 28.6 mg (31%) of biaryl (*R*)-**3.39b** as a colorless oil. Spectral data was consistent with the literature. Absolute configuration was confirmed by comparison of the optical rotation to the literature value: $[\alpha]_D^{25}$ = + 48.6 (*c* 0.19, THF, 75:25 er), lit.[20] $[\alpha]_D^{20}$ = + 72.8 (*c* 1.2, THF).

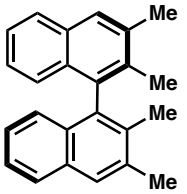

(R)-3.39c

(*R*)-2,2',3,3'-tetramethyl-1,1'-binaphthalene (*R*)-**3.39c**: Arylzinc formation: 105 mg (0.447 mmol) aryl bromide, 0.52 mL (0.89 mmol) 1.7 M *t*-BuLi in pentane, 1 mL THF, 134 mg (0.595 mmol) $ZnBr_2$ in 1 mL of THF. Cross-coupling: 70.0 mg (0.298 mmol) aryl bromide, 6.7 mg (0.0073 mmol) $Pd_2(dba)_3$, 8.9 mg (0.022 mmol) ligand (R_p)-**3.L13**, and the arylzinc solution afforded 26.4 mg (29%) of biaryl (*R*)-**3.39c** as a white solid after prep. TLC (10% CH_2Cl_2 in hexanes). ^{1}H NMR (400 MHz, $CDCl_3$): δ 7.80 (d, *J* = 8.1 Hz, 2H), 7.74 (s, 2H), 7.35 (m, 2H), 7.11 (m, 2H), 6.94 (d, *J* = 8.6 Hz, 2H), 2.54 (s, 6H), 1.94 (s, 6H); ^{13}C NMR (100 MHz, $CDCl_3$): δ 135.8, 135.5, 134.3, 132.3, 131.7, 127.2, 127.1, 126.0, 125.1, 124.9, 21.2, 16.8. HRMS (DART) *m*/*z* calculated for $C_{24}H_{23}$ $[M + H]^+$: 311.1794; found: 311.1794.

Chiral HPLC ((R,R)-Whelk-01, 100% heptane, 1.3 mL/min, 220 nm) analysis:

Asymmetric Reaction: *Racemic Reaction:*

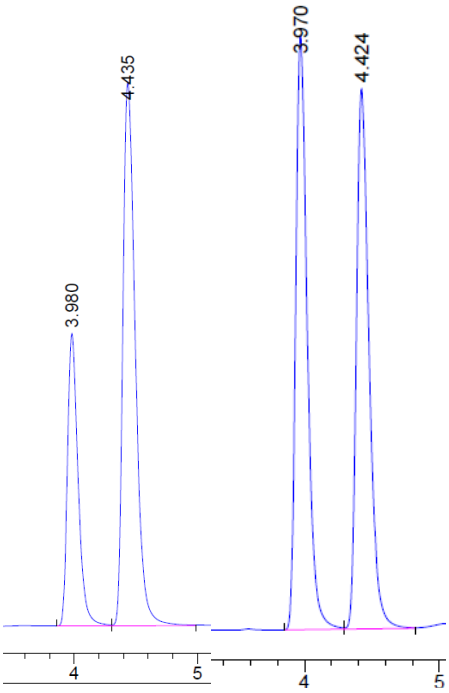

Peak #	RetTime [min]	Type	Width [min]	Area [mAU*s]	Height [mAU]	Area %
1	3.980	BV	0.0917	4383.76416	733.98224	31.5237
2	4.435	VB	0.1095	9522.47168	1363.94604	68.4763

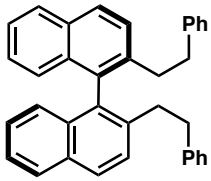

(R)-3.39d

(*R*)-2,2'-diphenethyl-1,1'-binaphthalene (*R*)-**3.39d**: Arylzinc formation: 105 mg (0.337 mmol) aryl bromide, 0.40 mL (0.68 mmol) 1.7 M *t*-BuLi in pentane, 0.8 mL THF, 101 mg (0.450 mmol) $ZnBr_2$ in 0.8 mL of THF. Cross-coupling: 70.0 mg (0.225 mmol) aryl bromide, 5.1 mg (0.0056 mmol) $Pd_2(dba)_3$, 6.7 mg (0.017 mmol) ligand (R_p)-**3.L13**, and the arylzinc solution afforded 86.0 mg (83%) of biaryl (*R*)-**3.39d** as a colorless oil. ^{1}H NMR (400 MHz, $CDCl_3$): δ 7.92 (t, *J* = 9.0, 4H), 7.56 (d, *J* = 8.6, 2H), 7.41 (t, *J* = 7.4, 2H), 7.21 (t, *J* = 7.4, 2H), 7.13–7.05 (m, 8H), 6.73 (d, *J* = 7.4, 4H), 2.74–2.51 (m, 8H); ^{13}C NMR (125 MHz, $CDCl_3$): δ 142.0, 138.2, 134.7, 133.5, 132.5, 128.3, 128.3, 128.0,

128.0, 127.7, 126.6, 126.2, 125.9, 125.4, 37.1, 36.5. HRMS (APCI) *m/z* calculated for $C_{36}H_{29}$ [M – H]: 439.2270; found: 461.2264.

Chiral SFC (Lux Cel 3, gradient: 1 – 3% IPA (3 min); 50% IPA (5 min), 220 nm) analysis:

Asymmetric Reaction: *Racemic Reaction:*

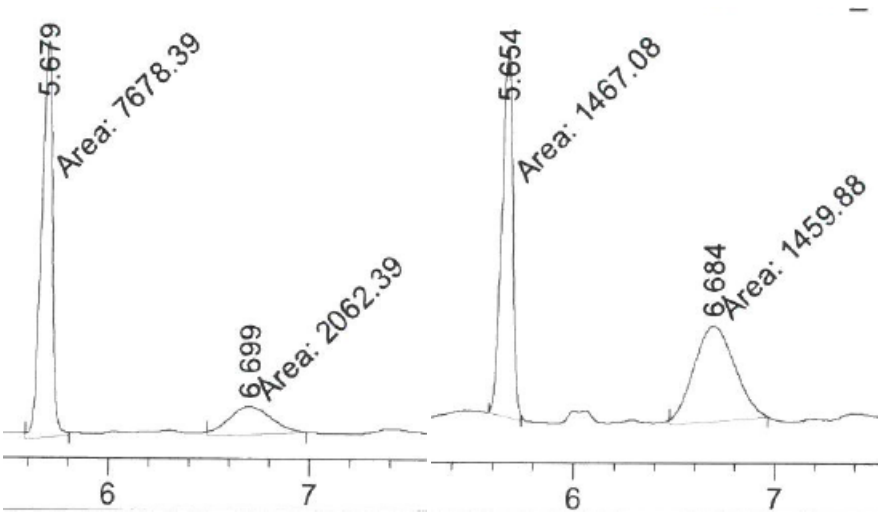

Peak #	RetTime [min]	Type	Width [min]	Area [mAU*s]	Height [mAU]	Area %
1	5.679	MM	0.0634	7678.39160	2017.69739	78.8273
2	6.699	MM	0.2437	2062.39014	141.03665	21.1727

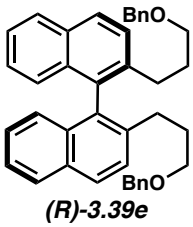

(R)-3.39e

(*R*)-2,2'-bis(3-(benzyloxy)propyl)-1,1'-binaphthalene (*R*)-**3.39e**: arylzinc formation: 105 mg (0.296 mmol) aryl bromide, 0.35 mL (0.59 mmol) 1.7 M *t*-BuLi in pentane, 0.7 mL THF, 88.7 mg (0.394 mmol) $ZnBr_2$ in 0.7 mL of THF. Cross-coupling: 70.0 mg (0.192 mmol) aryl bromide, 4.5 mg (0.0049 mmol) $Pd_2(dba)_3$, 5.9 mg (0.015 mmol) ligand (R_p)-**3.L13**, and the arylzinc solution afforded 92.2 mg (87%) of biaryl (*R*)-**3.39e** as an amorphous solid. ^{1}H NMR (500 MHz, $CDCl_3$): δ 7.89 (d, *J* = 8.6 Hz, 2H), 7.87 (d, *J* = 8.2 Hz, 2H), 7.55 (d, *J* = 8.5 Hz, 2H), 7.34 (t, *J* = 7.2 Hz, 2H), 7.20–7.29

(m, 6H), 7.17 (t, J = 7.1 Hz, 2H), 7.13 (d, J = 6.9 Hz, 4H), 7.02 (d, J = 8.5 Hz, 2H), 4.21 (d, J = 12 Hz, 2H), 4.19 (d, J = 12 Hz, 2H), 3.16–3.28 (m, 4H), 2.33–2.51 (m, 4H), 1.66–1.77 (m, 4H); ^{13}C NMR (100 MHz, $CDCl_3$): δ 138.6, 138.5, 134.6, 133.4, 132.3, 128.4, 128.0, 127.9, 127.64, 127.62, 127.5, 126.5, 126.1, 125.2, 72.4, 69.9, 30.5, 30.3. HRMS (DART) *m/z* calculated for $C_{40}H_{39}O_2$ $[M + H]^+$: 551.2950; found: 551.2946.

Chiral SFC (Lux Cel 3, gradient: 1 – 3% MeOH (3 min); 50% MeOH (5 min), 220 nm) analysis:

Asymmetric Reaction: *Racemic Reaction:*

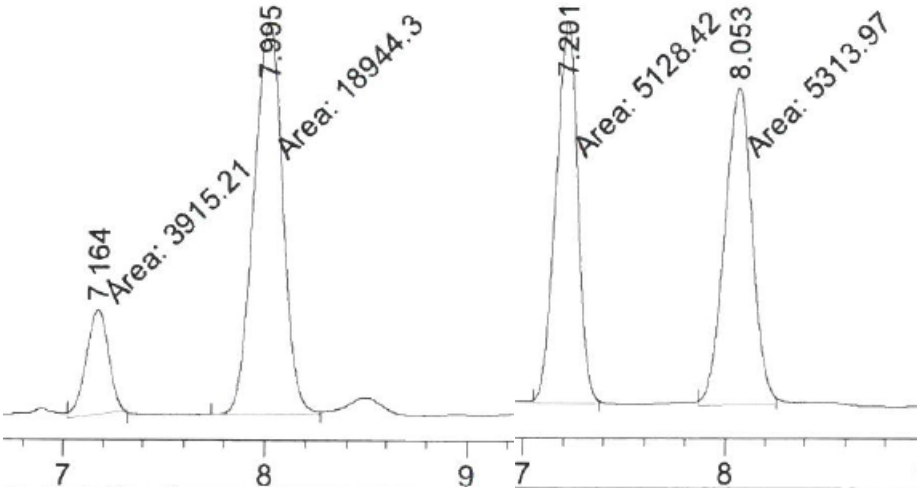

Peak #	RetTime [min]	Type	Width [min]	Area [mAU*s]	Height [mAU]	Area %
1	7.164	MM	0.1277	3915.20874	510.94980	17.1273
2	7.995	MM	0.1651	1.89443e4	1912.73413	82.8727
Totals :				2.28595e4	2423.68393	

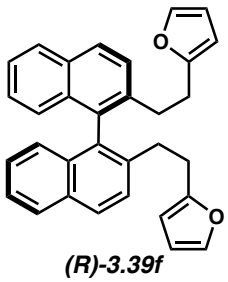

(R)-3.39f

(*R*)-2,2'-bis(2-(furan-2-yl)ethyl)-1,1'-binaphthalene (*R*)-**3.39f**: Arylzinc formation: 105 mg (0.349 mmol) aryl bromide, 0.41 mL (0.70 mmol) 1.7 M *t*-BuLi in pentane, 0.85 mL THF, 105 mg (0.465 mmol) $ZnBr_2$ in 0.85 mL of THF. Cross-coupling: 70.0 mg (0.232 mmol) aryl bromide, 5.3 mg (0.0058

mmol) $Pd_2(dba)_3$, 7.0 mg (0.017 mmol) ligand (R_p)-**3.L13**, and the arylzinc solution afforded 62.3 mg (61%) of biaryl (*R*)-**3.39f** as a yellow solid. ^{1}H NMR (500 MHz, $CDCl_3$): δ 7.89 (t, *J* = 8.3, 4H), 7.47 (d, *J* = 8.4, 2H), 7.40 (t, *J* = 7.5, 2H), 7.21–7.18 (m, 4H), 7.02 (d, *J* = 8.4, 2H), 6.14 (t, *J* = 2.4, 2H), 5.68 (d, *J* = 3.1, 2H), 2.75–2.64 (m, 8H); ^{13}C NMR (100 MHz, $CDCl_3$): δ 155.4, 140.9, 137.5, 134.7, 133.4, 132.5, 128.1, 128.0, 127.4, 126.5, 126.2, 125.4, 110.1, 105.2, 32.5, 28.7. HRMS (APCI) *m/z* calculated for $C_{32}H_{27}O_2$ $[M + H]^+$: 443.2011; found: 443.2006.

Chiral SFC (Lux Cel 3, gradient: 1 – 3% MeOH (3 min); 50% MeOH (5 min), 220 nm) analysis:

Asymmetric Reaction: *Racemic Reaction:*

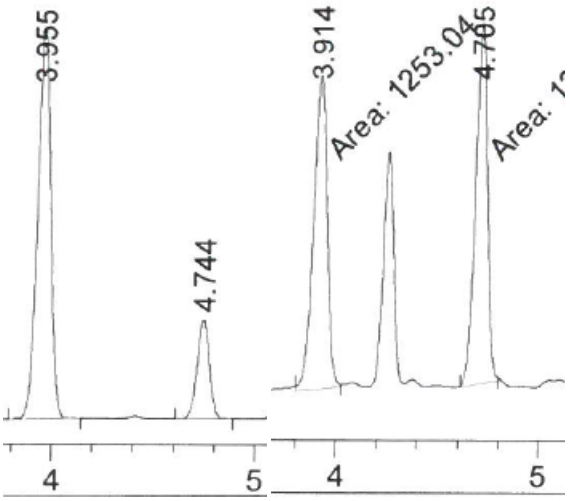

Peak #	RetTime [min]	Type	Width [min]	Area [mAU*s]	Height [mAU]	Area %
1	3.955	VV R	0.0699	3795.49463	845.15338	80.9575
2	4.744	VB R	0.0642	892.75995	213.85602	19.0425

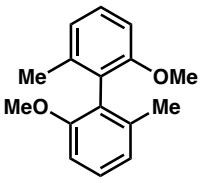

3.43a

2,2'-dimethoxy-6,6'-dimethyl-1,1'-biphenyl (**3.43a**): Arylzinc formation: 88.4 mg (0.440 mmol) aryl bromide, 0.52 mL (0.88 mmol) 1.7 M *t*-BuLi in pentane,

1.1 mL THF, 132 mg (0.586 mmol) $ZnBr_2$ in 1.1 mL of THF. Cross-coupling: 60.0 mg (0.293 mmol) aryl bromide, 6.7 mg (0.0073 mmol) $Pd_2(dba)_3$, 8.8 mg (0.022 mmol) ligand (R_p)-**3.L13**, and the arylzinc solution afforded 37.0 mg (52%) of biaryl **3.43a** as a colorless oil. Spectal data was consistent with the literature.[51]

Chiral HPLC (Chiralcel IC-3, 99:1 heptane:isopropanol, 220 nm) analysis:

Asymmetric Reaction: *Racemic Reaction:*

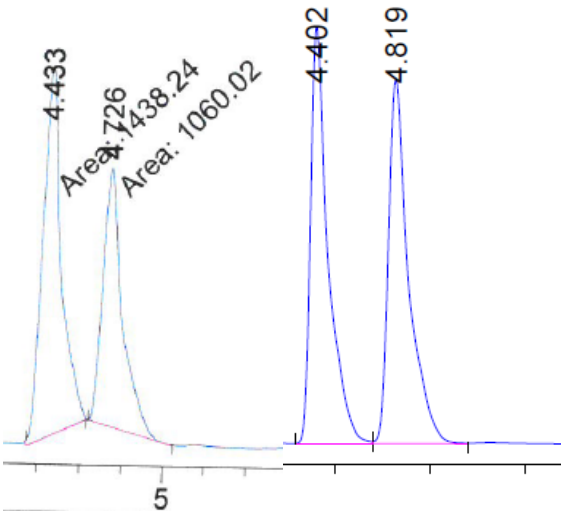

Peak #	RetTime [min]	Type	Width [min]	Area [mAU*s]	Height [mAU]	Area %
1	4.433	MM	0.1034	1438.23633	231.86115	57.5696
2	4.726	MM	0.1102	1060.02075	160.24545	42.4304
Totals :				2498.25708	392.10660	

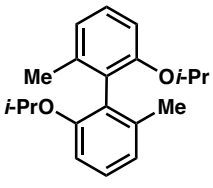

3.43b

2,2'-di-*iso*propoxy-6,6'-dimethyl-1,1'-biphenyl (**3.43b**): Arylzinc formation: 105 mg (0.459 mmol) aryl bromide, 0.54 mL (0.92 mL) 1.7 M *t*-BuLi in pentane, 1.1 mL THF, 138 mg (0.612 mmol) $ZnBr_2$ in 1.1 mL of THF. Cross-coupling: 70.0 mg (0.306 mmol) aryl bromide, 7.0 mg (0.0077 mmol) $Pd_2(dba)_3$, 9.2 mg (0.023 mmol) ligand (R_p)-**3.L13**, and the arylzinc solution afforded 70.0 mg (81%) of biaryl **3.43b** as a colorless oil. ^{1}H NMR (500 MHz, $CDCl_3$): δ 7.10 (t, J = 7.9, 2H), 6.88 (d, J = 7.9, 2H), 6.85 (d, J

= 7.9, 2H), 1.99 (s, 6H), 1.22 (s, 18H); ^{13}C NMR (125 MHz, $CDCl_3$): δ 154.0, 138.7, 131.5, 126.7, 122.5, 116.4, 77.7, 29.2, 20.3. HRMS (DART) *m/z* calculated for $C_{20}H_{27}O_2$ $[M + H]^+$: 299.2011; found: 299.2006.

Chiral HPLC (Chiral AGP, 0.1% H_3PO_4 in water/MeCN, gradient: 0 min; 10% MeCN, 5.0 min; 30% MeCN, 15 min; 50% MeCN, 220 nm) analysis:

Asymmetric Reaction: *Racemic Reaction:*

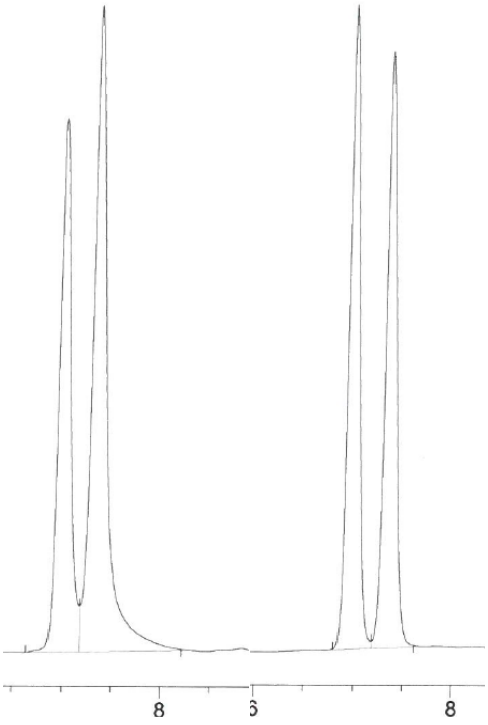

Peak #	RetTime [min]	Type	Width [min]	Area [mAU*s]	Height [mAU]	Area %
1	6.996	BV	0.1223	1451.73364	179.69226	39.7387
2	7.339	VB	0.1481	2201.46045	217.46477	60.2613

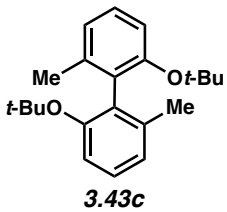

3.43c

2,2'-di-*tert*-butoxy-6,6'-dimethyl-1,1'-biphenyl (**3.43c**): Arylzinc formation: 105 mg (0.432 mmol) aryl bromide, 0.51 mL (0.86 mmol) 1.7 M *t*-BuLi in

pentane, 1 mL THF, 136 mg (0.604 mmol) $ZnBr_2$ in 1 mL of THF. Cross-coupling: 70.0 mg (0.288 mmol) aryl bromide, 6.6 mg (0.0072 mmol) $Pd_2(dba)_3$, 8.7 mg (0.022 mmol) ligand (R_p)-**3.L13**, 1 mL of THF, and the arylzinc solution afforded 60.3 mg (67%) of biaryl **3.41c** as a colorless oil. ^{1}H NMR (500 MHz, $CDCl_3$): δ 7.10 (t, J = 7.9, 2H), 6.88 (d, J = 7.9, 2H), 6.85 (d, J = 7.9, 2H), 1.99 (s, 6H), 1.22 (s, 18H); ^{13}C NMR (125 MHz, $CDCl_3$): δ 154.0, 138.7, 131.5, 126.7, 122.5, 116.4, 77.7, 29.2, 20.3. HRMS (DART) *m/z* calculated for $C_{22}H_{31}O_2$ $[M + H]^+$: 327.2324; found: 327.2320.

Chiral HPLC (Chiral AGP, 0.1% H_3PO_4 in water/MeCN, gradient: 0 min; 20% MeCN, 5.0 min; 30% MeCN, 15 min; 50% MeCN, 220 nm) analysis:

Asymmetric Reaction: *Racemic Reactions:*

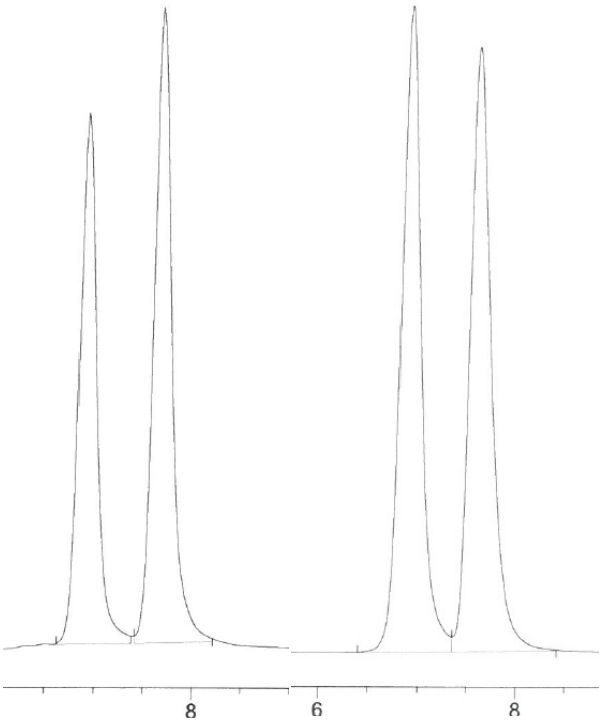

Peak #	RetTime [min]	Type	Width [min]	Area [mAU*s]	Height [mAU]	Area %
1	6.908	BB	0.1846	684.94440	56.82662	44.5270
2	7.658	BB	0.1884	853.32153	67.99604	55.4730

3.8.2.6 Details of Computational Studies

Optimizations of intermediates and transition states were performed using Gaussian 09[52] software with spin-restricted DFT using the RB3LYP[53] functional and split basis set [6-31G(d) for C, P, N, O, H, Br and LANL2DZ for Pd] in the gas phase. For Suzuki coupling, RB3LYP with Grimme dispersion correction D3[54] was used instead. The method is based on those successfully used before for description of Suzuki couplings.[55] However, unlike regular B3LYP[56], it accounts for dispersion interactions. They may be of a paramount importance for the reaction and have been considered in the recent computational studies of Suzuki couplings.[57] We have also tested other methods and their combinations. Thus, we analyzed the performance of B3LYP/6-31G(d),LANL2DZ; B3LYP-D3/6-31G(d),LANL2DZ, SMD: THF, Gaussian-2 theories M06/6-311+G(d,p),LANL2DZ, SMD:THF//B3LYP/6-31G(d),LANL2DZ and M06/6-311+G(d,p),LANL2DZ, SMD:THF//B3LYP-D3/6-31G(d),LANL2DZ. However, RB3LYP-D3/6-31G(D),LANL2DZ proved to be the best method, allowing us to obtain data that is in good standing with experimental findings. Given the massive number of intricately connected transition states that define selectivity in this model, it is highly unlikely that success of the approach is a fortuitous discovery. Rather, we attribute the suitability of the method to its ability to appropriately treat a large number of dispersion interactions, that seem to be crucial for the stereoselectivity of the reaction.

For all species, vibrational frequencies were also computed at the specified level of theory to obtain thermal Gibbs Free Energy corrections (at 298 K) and to characterize the stationary points as transition states (one and only one imaginary frequency) or minima (zero imaginary frequencies). For Negishi coupling analysis, single point energy calculations were performed on optimized geometries in THF solvent using the SMD[58]-solvation model, M06[59]

functional, and split basis set [6-311+G(d,p) for C, P, N, O, H; LANL2DZ for Pd]. The single-point energies were converted to the enthalpies and Gibbs free energies using corrections from gas-phase frequency analysis. Extensive conformational analysis of the transition states and intermediates was performed manually. For determination of the selectivities of elementary steps, we calculated the weight of each conformation using Boltzmann distribution:

$$w_i = \exp\left(-\frac{E_{i\,rel}}{RT}\right)$$

Where $E_{i\,rel}$ is the relative energy (Gibbs Free energy was used for Negishi coupling analysis and enthalpy was used for Suzuki coupling) of conformation i. The relative contribution of the given conformation to the overall step is:

$$n_i = \frac{w_i}{\sum_i w_i}$$

For each of the steps analyzed, we provide a table with the list of transition states conformations, their relative energies and Boltzmann weights w_i. Only those conformations that have high w_i values, contribute to the selectivity of the process (corresponding entries highlighted in bold). Coordinates and thermochemical data are provided for those conformations. In Table 1 we also provide relative contribution values, n_i, to show how ee values were calculated.

3.8.2.7 Coordinates and Thermochemical Data for Computed Intermediates and Transition States

Coordinates and thermochemical data for computed intermediates and transition states were reported in the literature.[60]

3.9 Spectra Relevant to Chapter Three:

Computationally Assisted Mechanistic Investigation and Development of Pd-Catalyzed Asymmetric Suzuki–Miyaura and Negishi Cross-Coupling Reactions for Tetra-*ortho*-Substituted Biaryl Synthesis

Nitinchandra Dahyabhai Patel, Joshua D. Sieber, Sergei Tcyrulnikov, Bryan J. Simmons, Daniel Rivalti, Krishnaja Duvvuri, Yongda Zhang, Donghong A. Gao, Keith R. Fandrick, Nizar Haddad, Kendricks So Lao, Hari Prasad Reddy Mangunuru, Soumik Biswas, Bo Qu, Nelu Grinberg, Scott Pennino, Heewon Lee, Jinhua J. Song, B. Frank Gupton, Neil K. Garg, Marisa C. Kozlowski, and Chris H. Senanayake

ACS Catal. **2018**, *8*, 10190–10209.

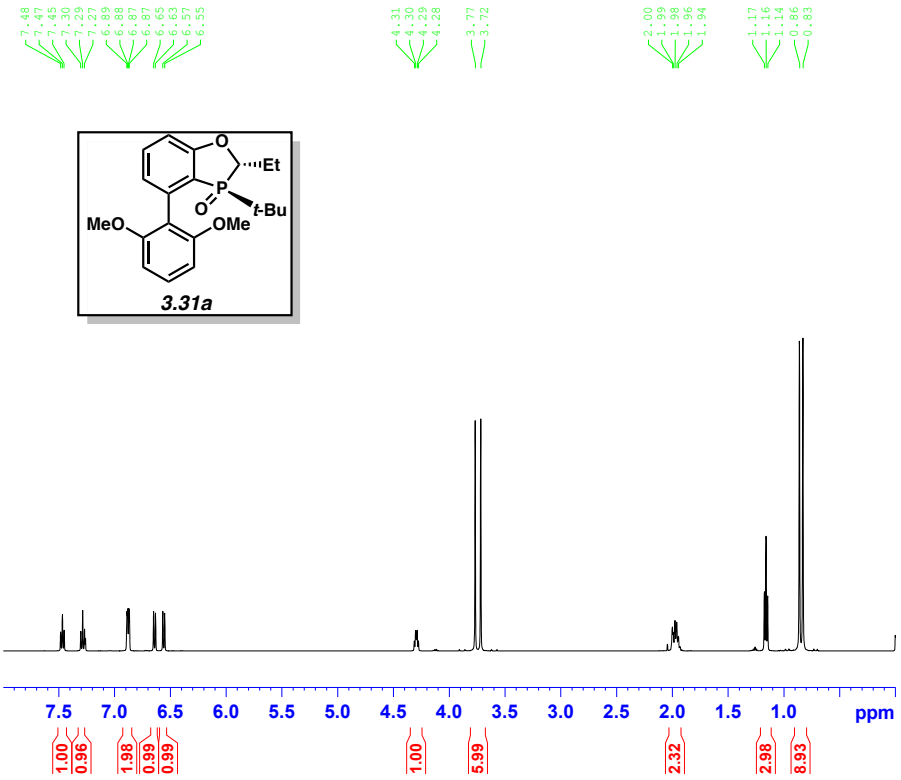

Figure 3.20 ^{1}H NMR (500 MHz, $CDCl_3$) of compound **3.31a**.

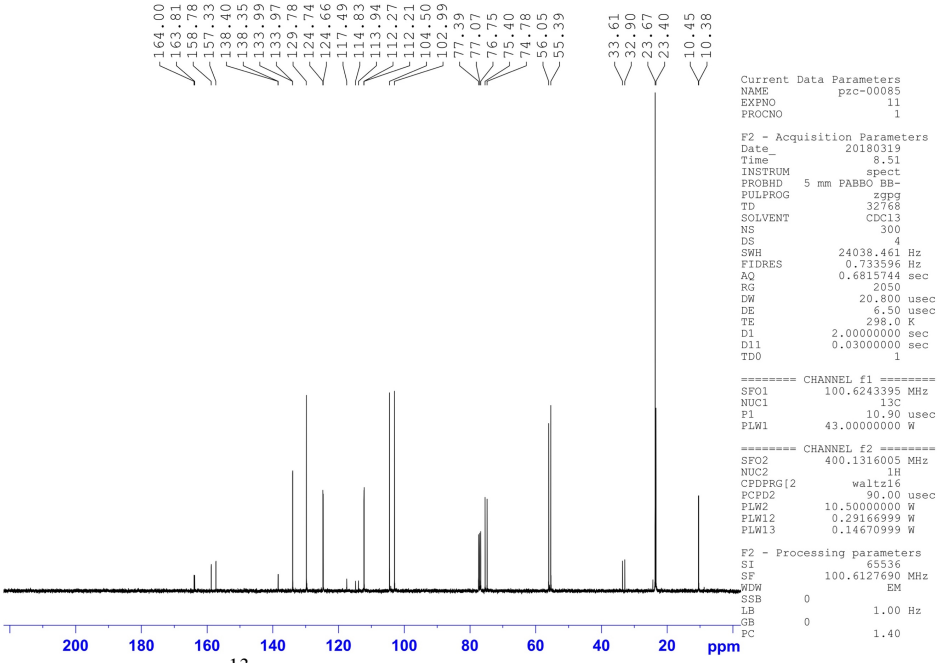

Figure 3.21 ^{13}C NMR (125 MHz, $CDCl_3$) of compound **3.31a**.

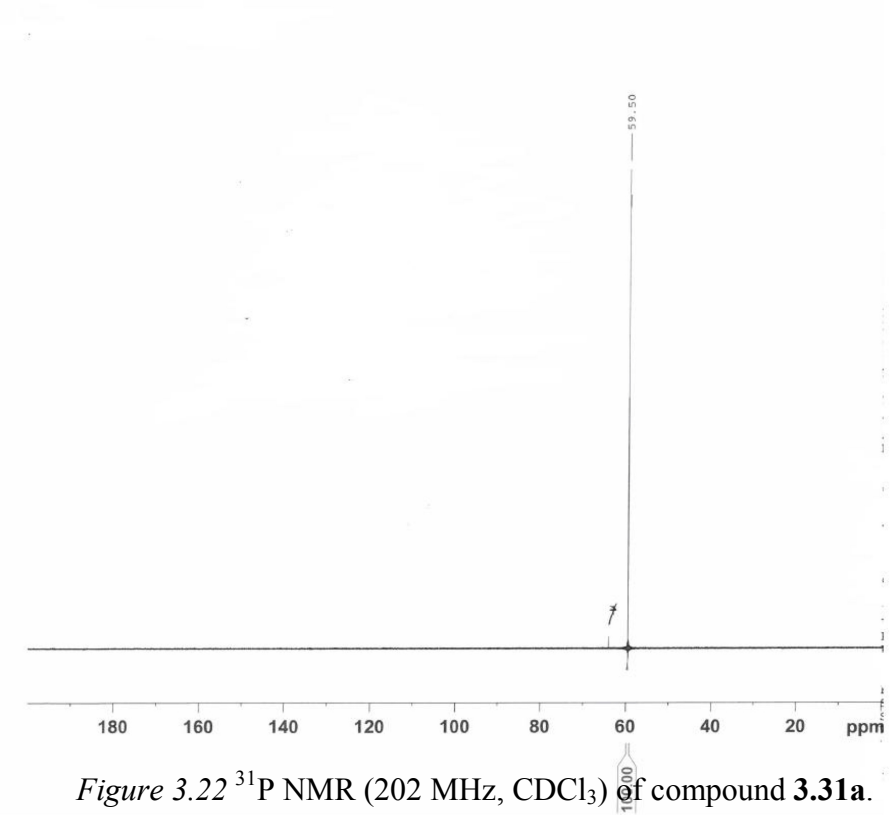

Figure 3.22 ^{31}P NMR (202 MHz, $CDCl_3$) of compound **3.31a**.

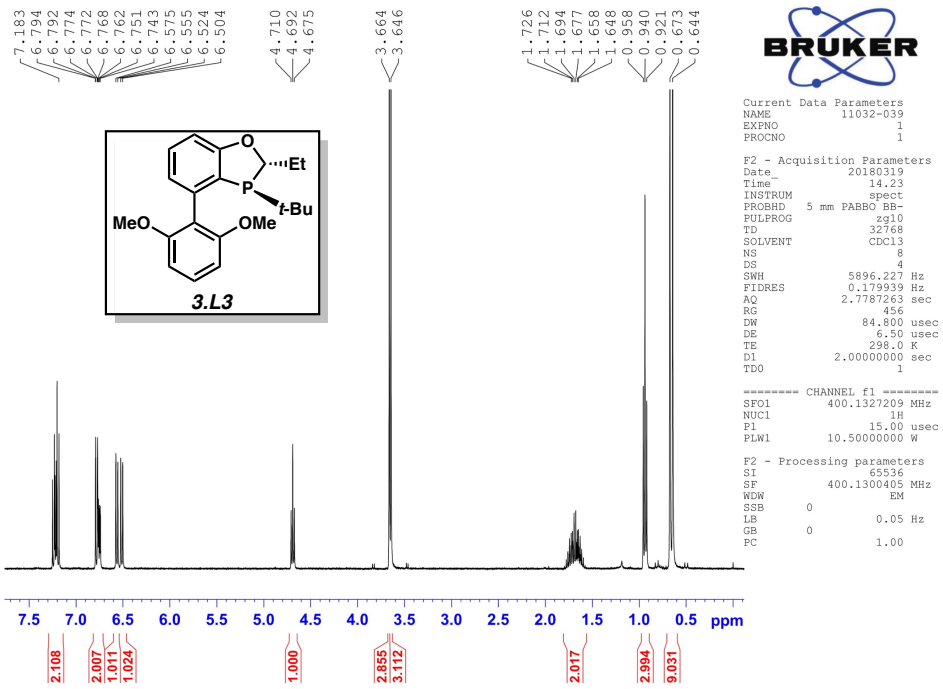

Figure 3.23 ^{1}H NMR (400 MHz, $CDCl_3$) of compound **3.L3**.

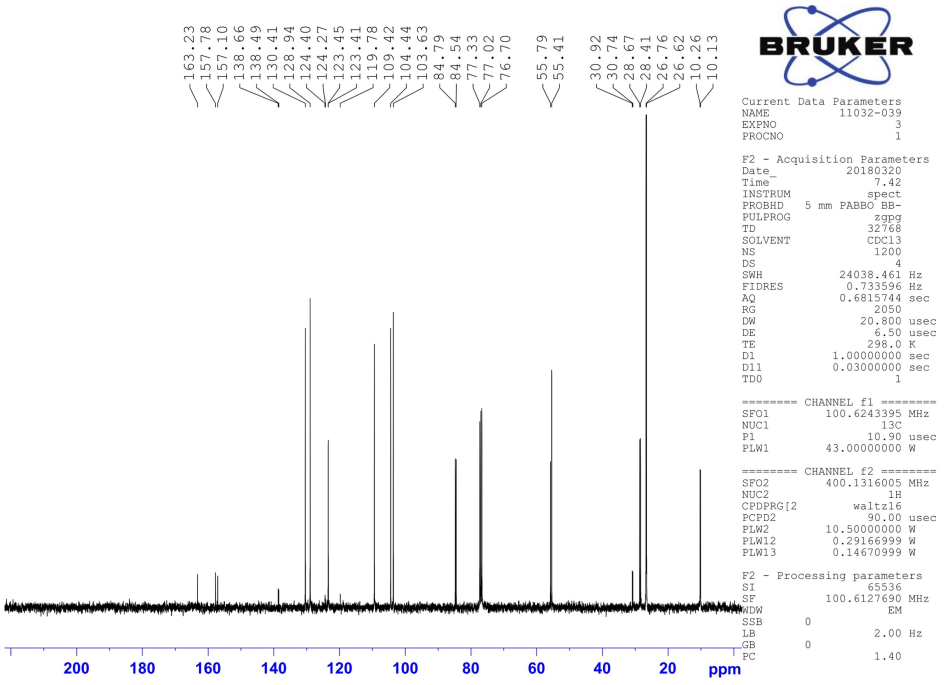

Figure 3.24 ^{13}C NMR (100 MHz, $CDCl_3$) of compound **3.L3**.

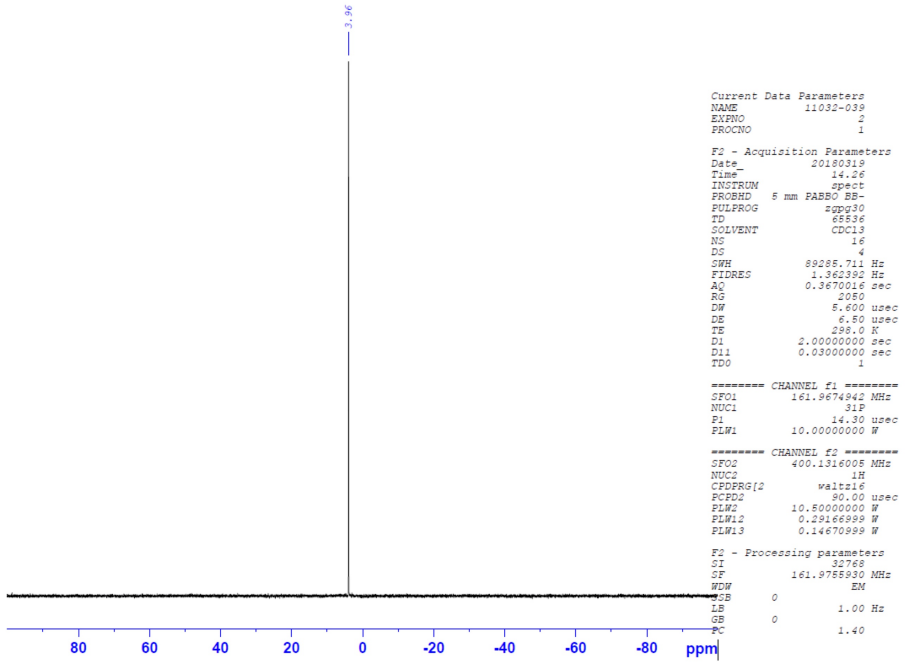

Figure 3.25 ^{31}P NMR (162 MHz, $CDCl_3$) of compound **3.L3**.

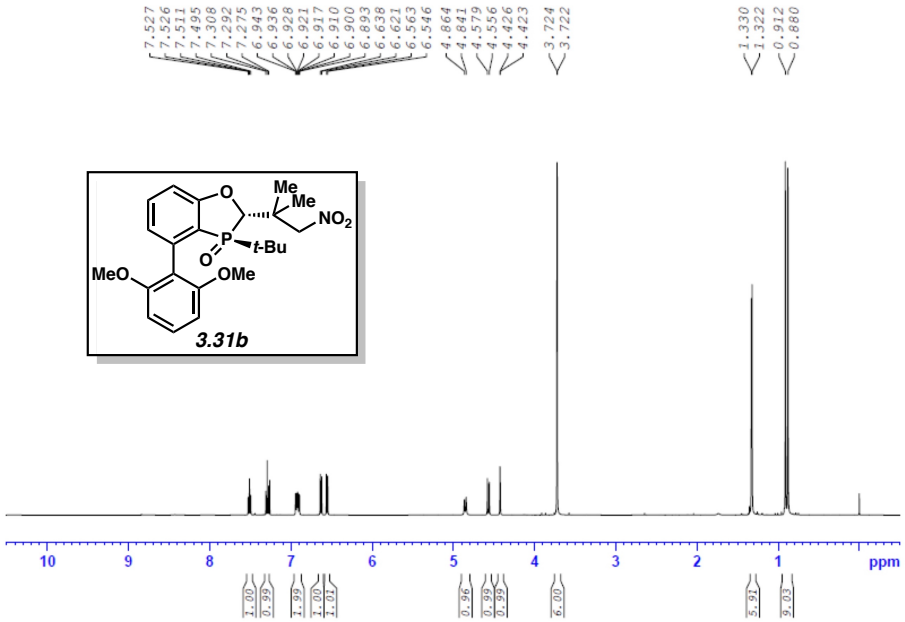

Figure 3.26 ^{1}H NMR (500 MHz, $CDCl_3$) of compound **3.31b**.

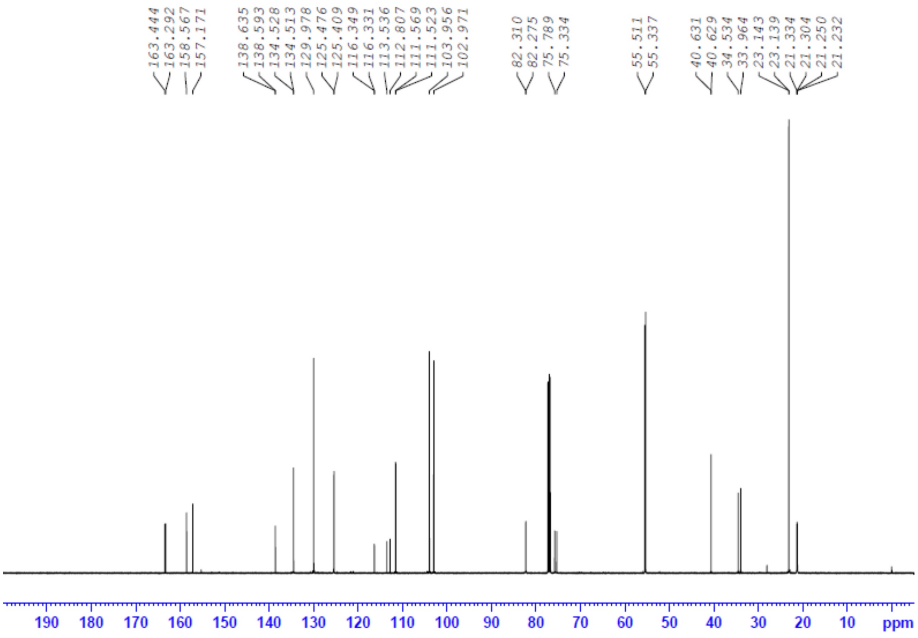

Figure 3.27 ^{13}C NMR (125 MHz, $CDCl_3$) of compound **3.31b**.

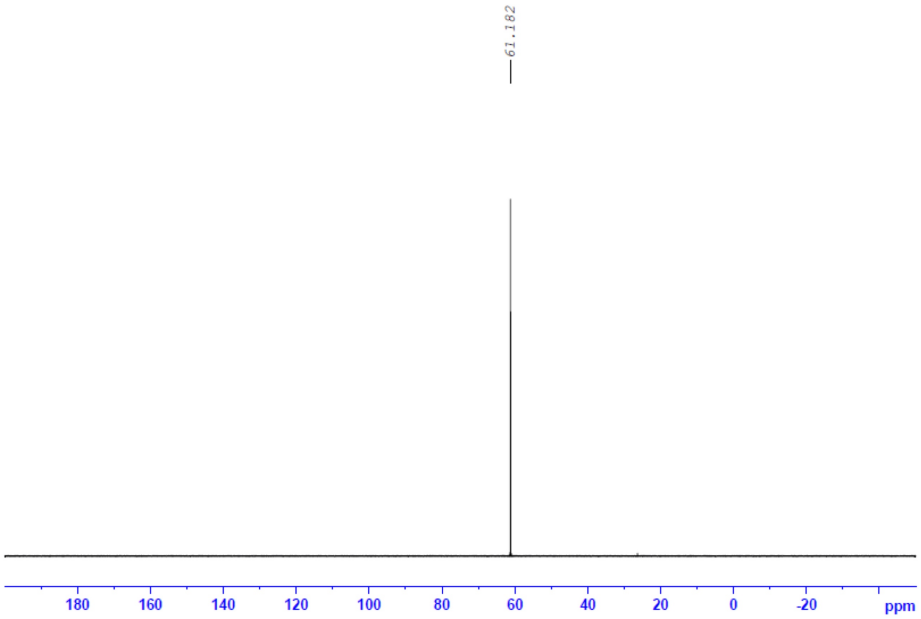

Figure 3.28 ^{31}P NMR (202 MHz, $CDCl_3$) of compound **3.31b**.

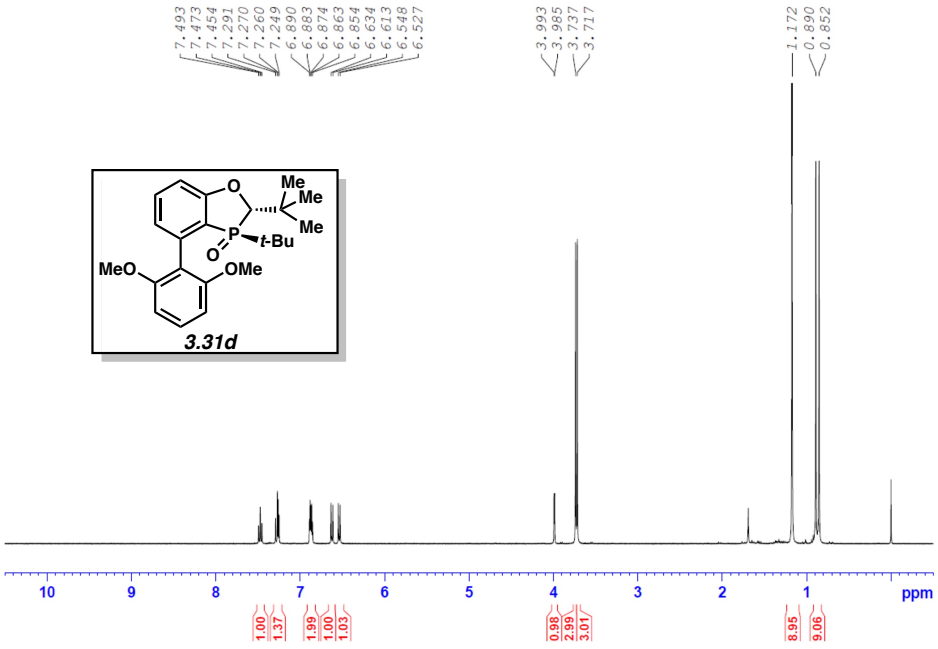

Figure 3.29 ^{1}H NMR (400 MHz, $CDCl_3$) of compound **3.31d**.

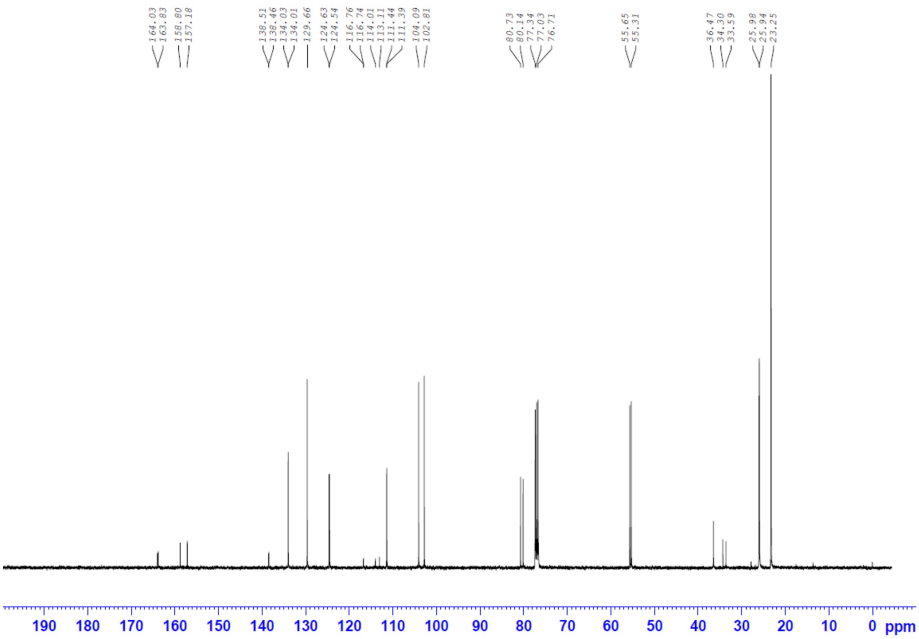

Figure 3.30 ^{13}C NMR (100 MHz, $CDCl_3$) of compound **3.31d**.

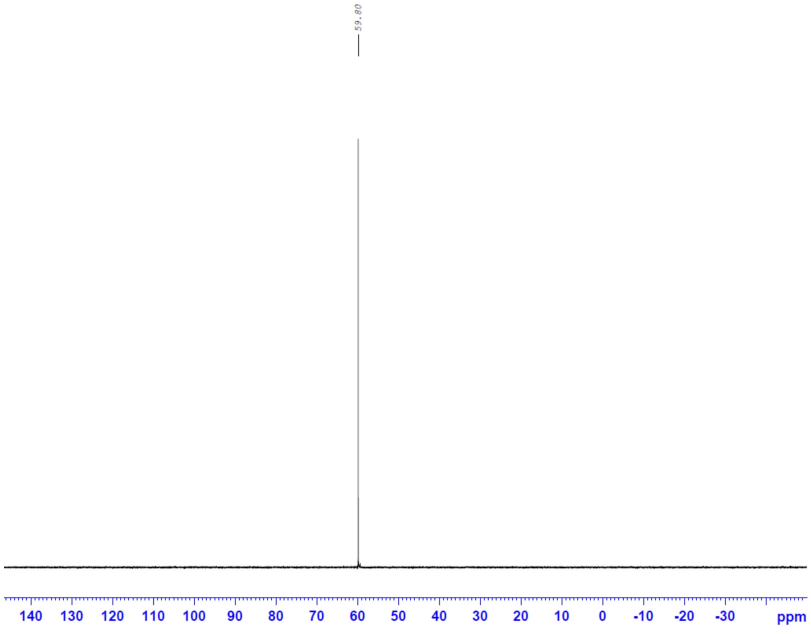

Figure 3.31 ^{31}P NMR (162 MHz, $CDCl_3$) of compound **3.31d**.

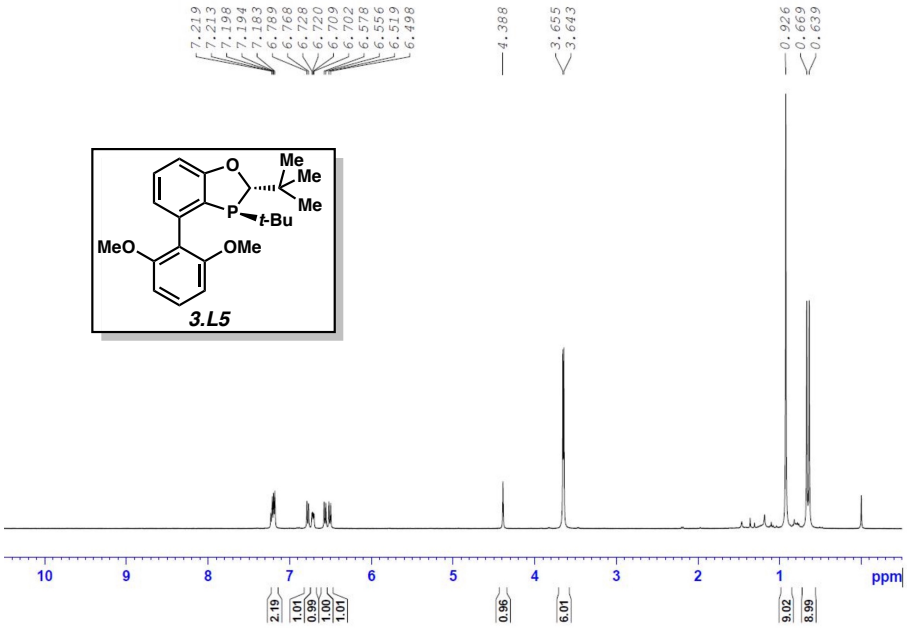

Figure 3.32 ^{1}H NMR (500 MHz, $CDCl_3$) of compound **3.L5**.

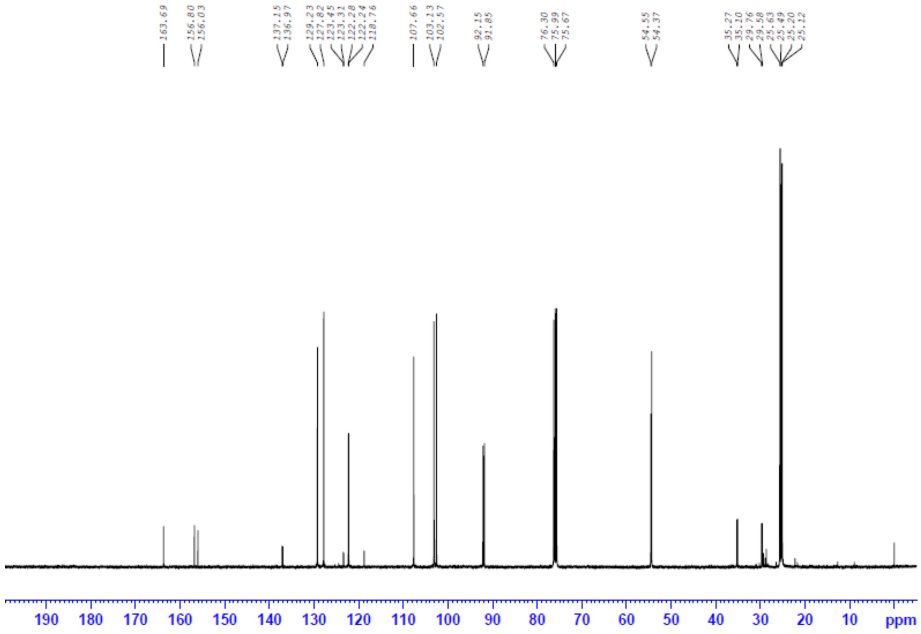

Figure 3.33 ^{13}C NMR (125 MHz, $CDCl_3$of compound **3.L5**.

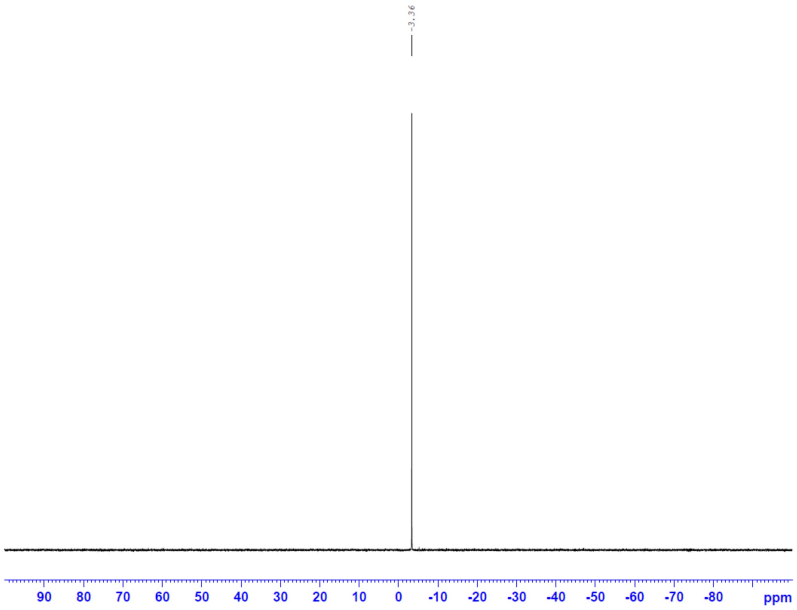

Figure 3.34 ^{31}P NMR (202 MHz, $CDCl_3$) of compound **3.L5**.

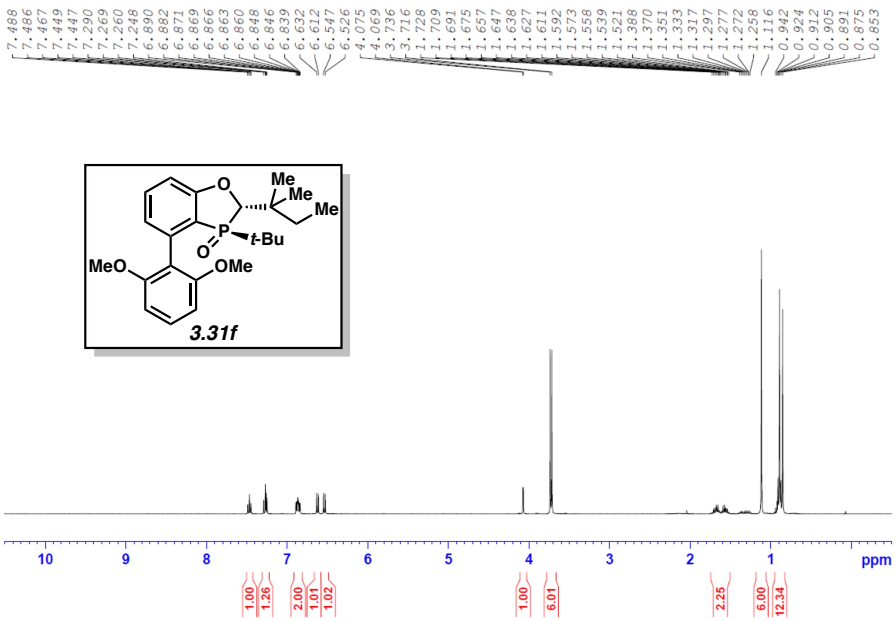

Figure 3.35 ^{1}H NMR (400 MHz, $CDCl_3$) of compound **3.31f**.

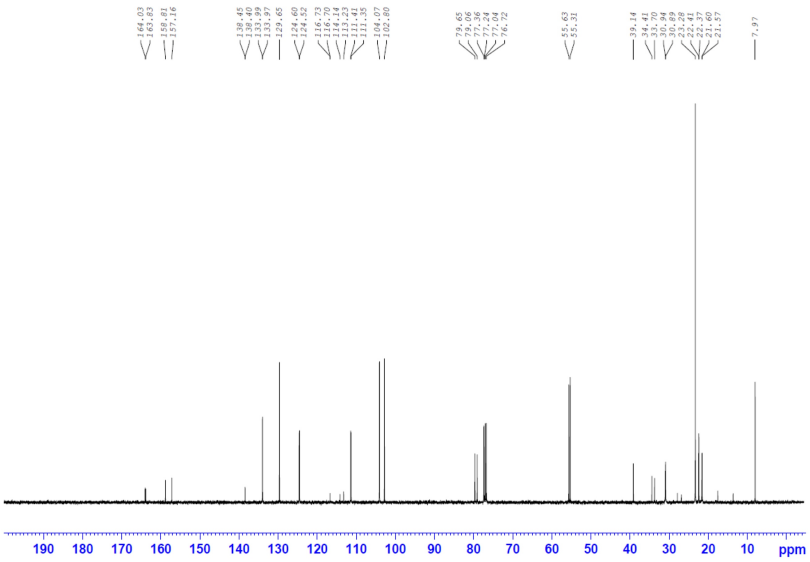

Figure 3.36 ^{13}C NMR (100 MHz, $CDCl_3$) of compound **3.31f**.

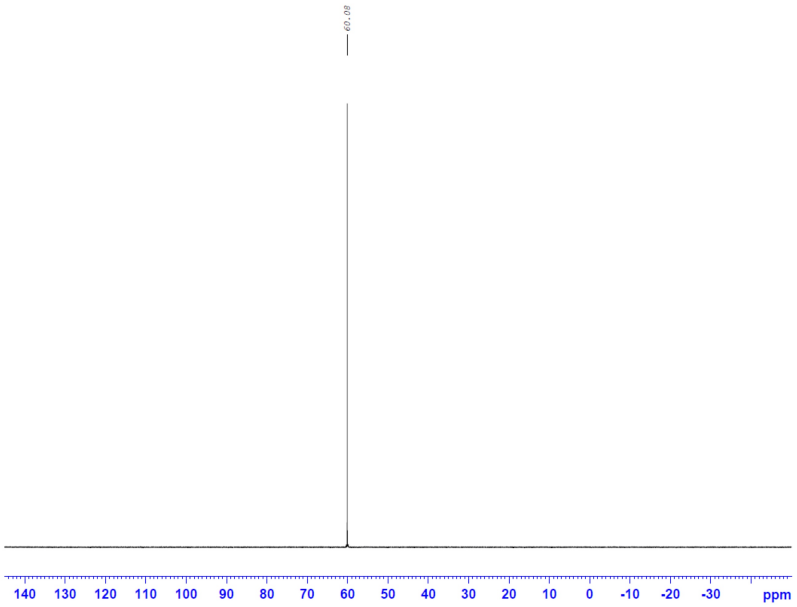

Figure 3.37 ^{31}P NMR (162 MHz, $CDCl_3$) of compound **3.31f**.

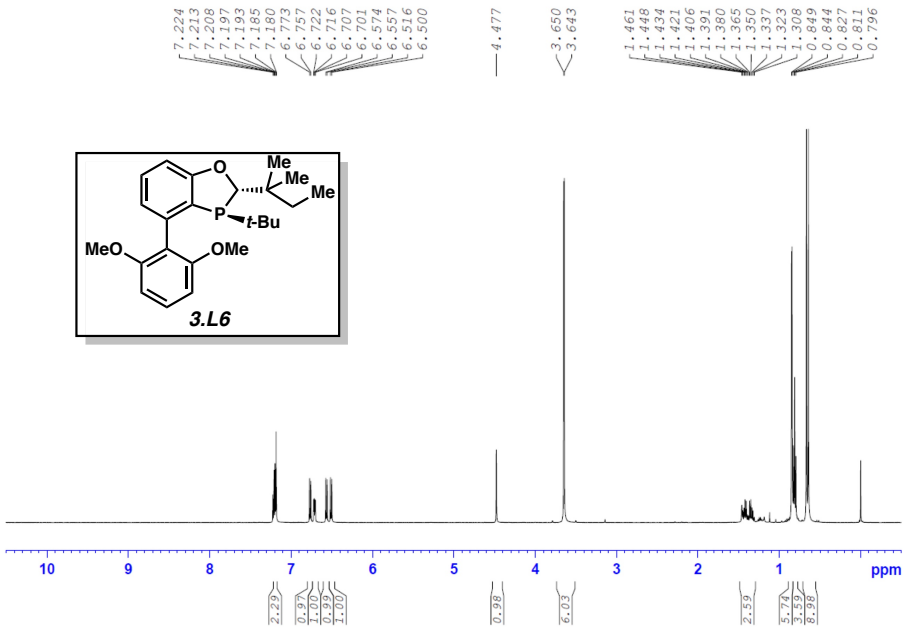

Figure 3.38 ^{1}H NMR (500 MHz, $CDCl_3$) of compound **3.L6**.

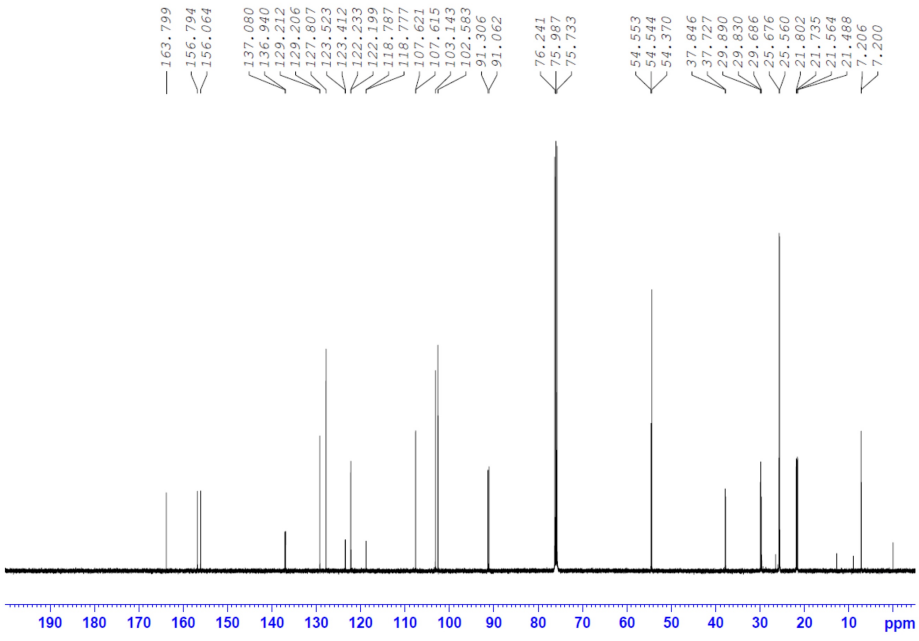

Figure 3.39 ^{13}C NMR (125 MHz, $CDCl_3$) of compound **3.L6**.

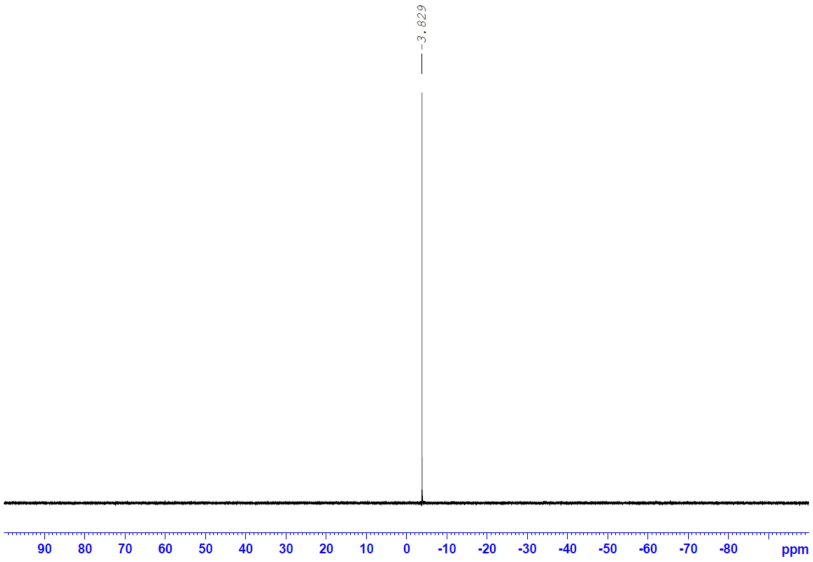

Figure 3.40 ^{31}P NMR (202 MHz, $CDCl_3$) of compound **3.L6**.

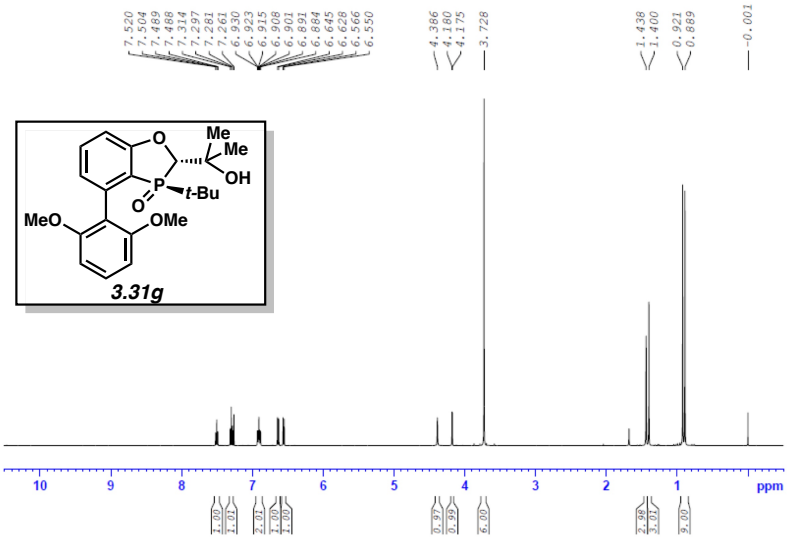

Figure 3.41 ^{1}H NMR (500 MHz, $CDCl_3$) of compound **3.31g**.

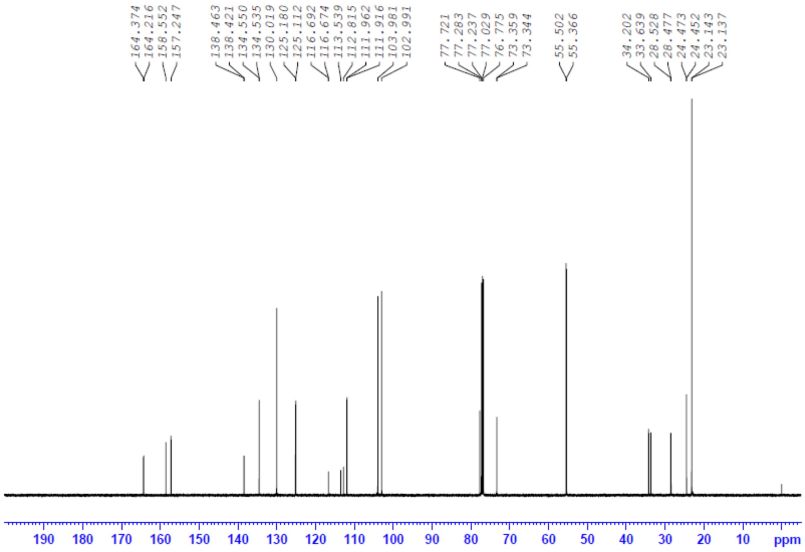

Figure 3.42 ^{13}C NMR (125 MHz, $CDCl_3$) of compound **3.31g**.

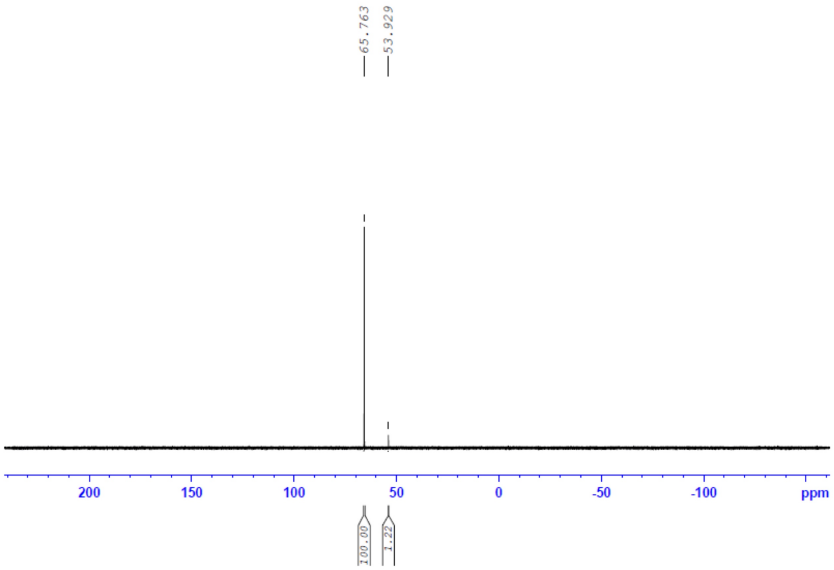

Figure 3.43 ^{31}P NMR (202 MHz, $CDCl_3$) of compound **3.31g**.

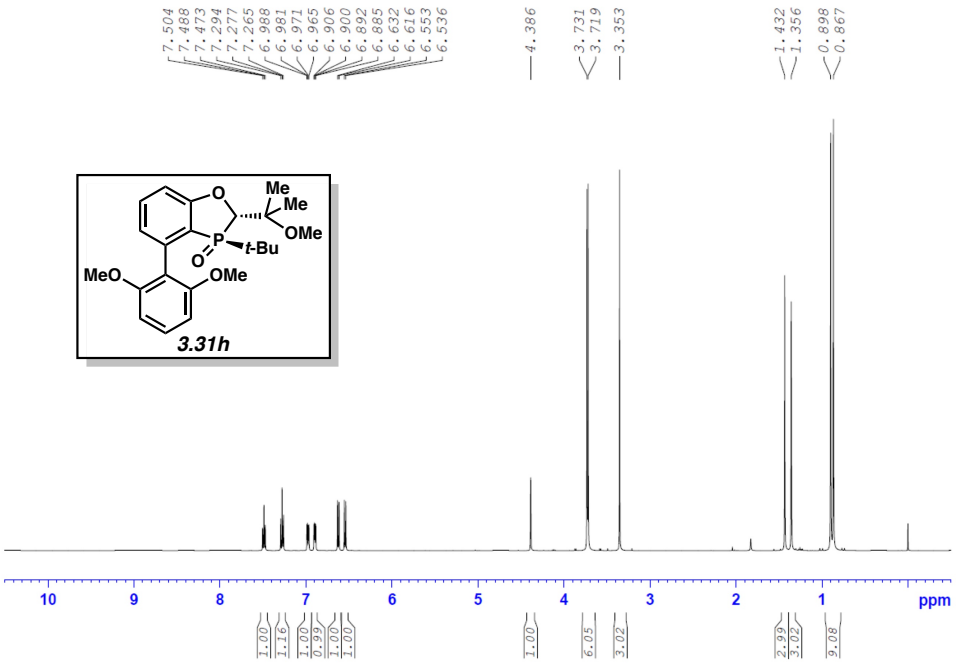

Figure 3.44 ^{1}H NMR (500 MHz, $CDCl_3$) of compound **3.31h**.

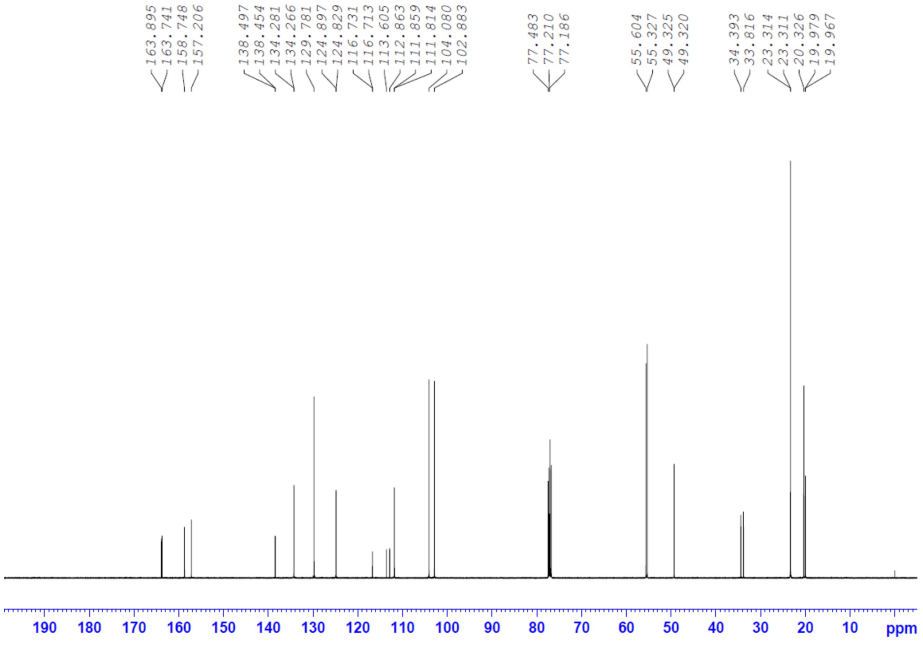

Figure 3.45 ^{13}C NMR (125 MHz, $CDCl_3$) of compound **3.31h**.

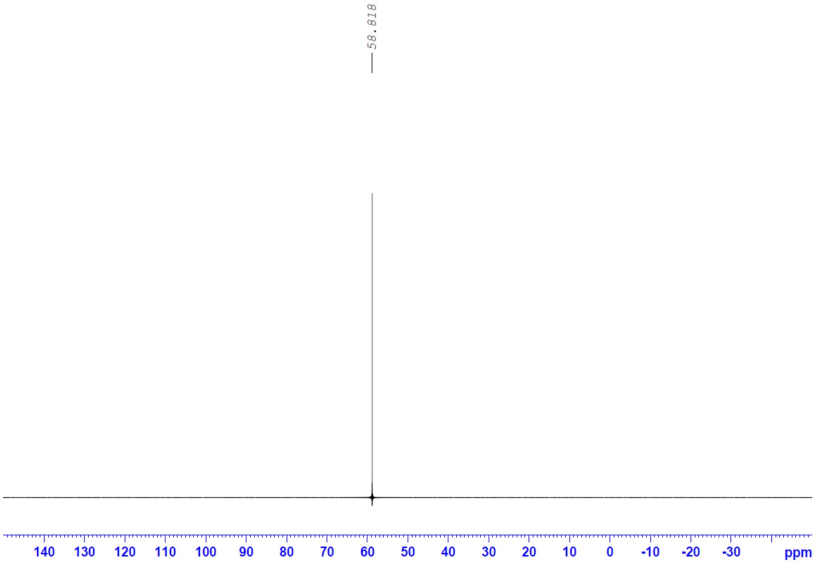

Figure 3.46 ^{31}P NMR (202 MHz, $CDCl_3$) of compound **3.31h**.

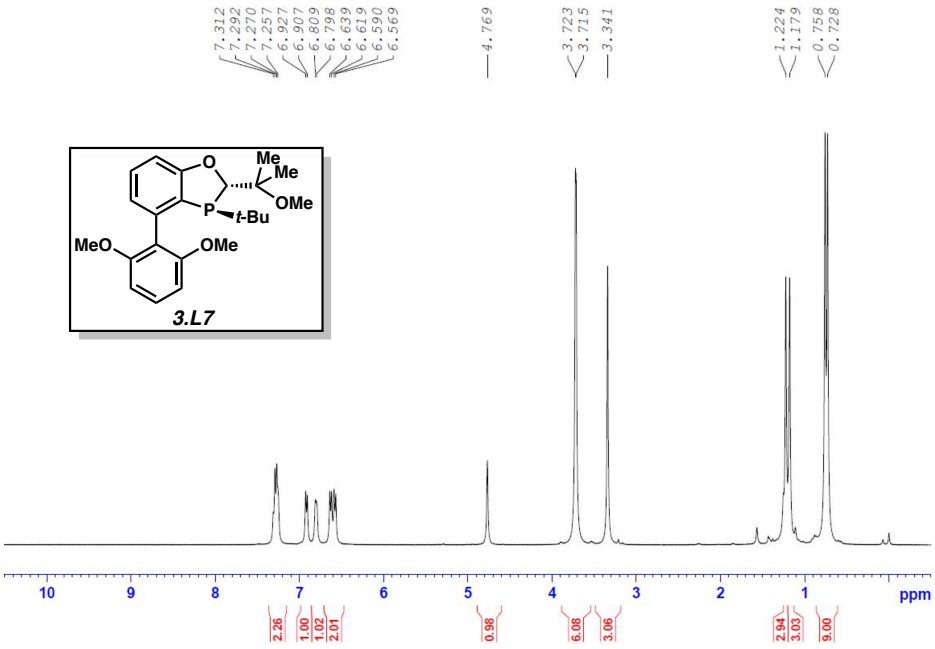

Figure 3.47 ^{1}H NMR (400 MHz, $CDCl_3$) of compound **3.L7**.

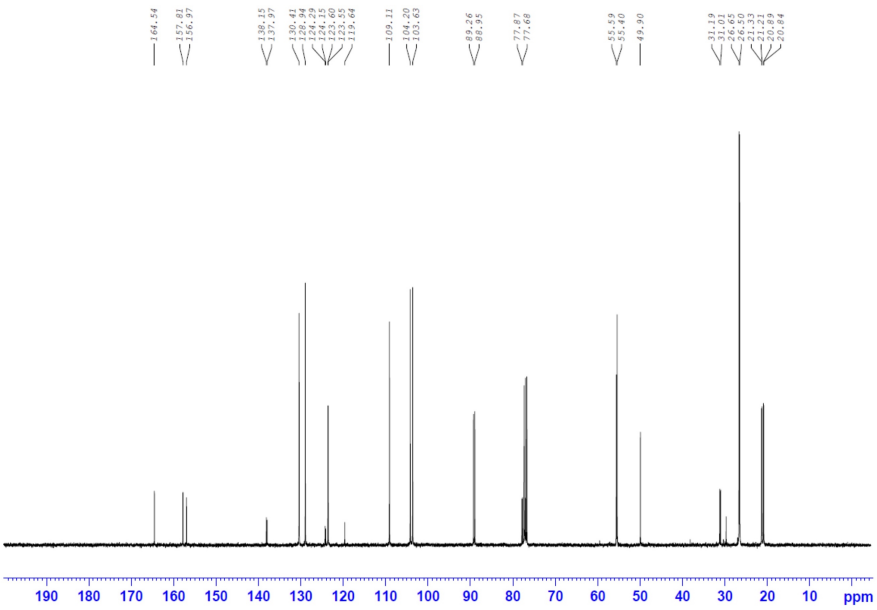

Figure 3.48 ^{13}C NMR (100 MHz, $CDCl_3$) of compound **3.L7**.

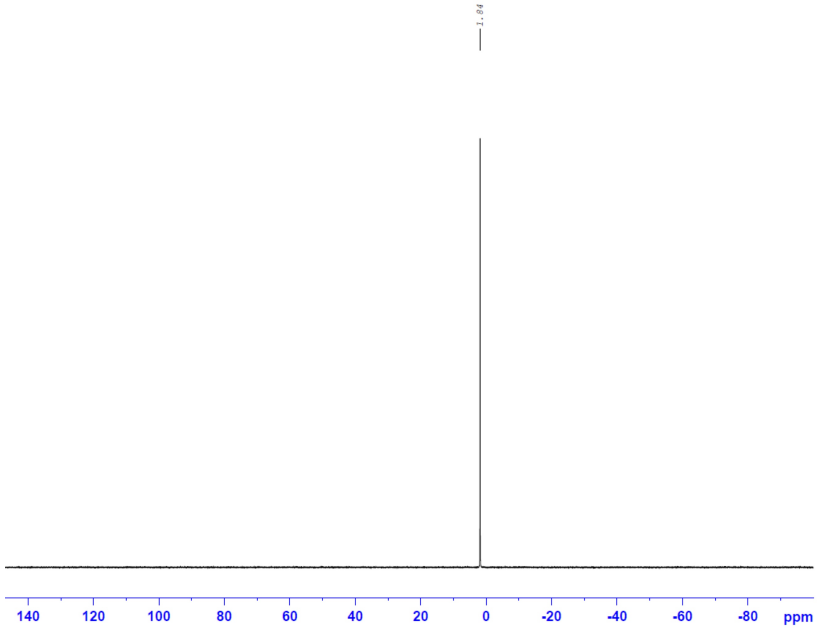

Figure 3.49 ^{31}P NMR (162 MHz, $CDCl_3$) of compound **3.L7**.

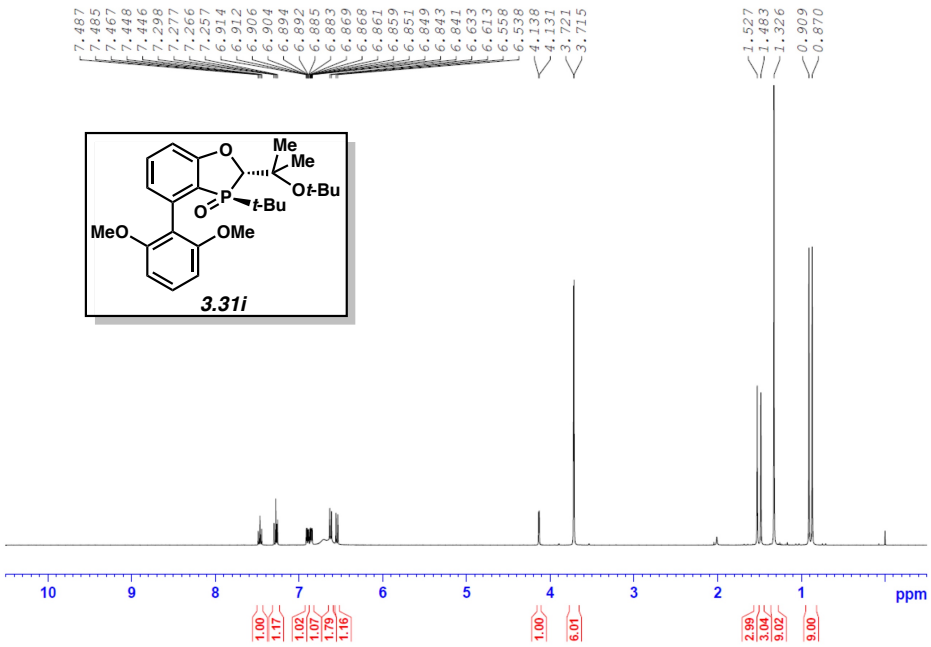

Figure 3.50 ^{1}H NMR (400 MHz, $CDCl_3$) of compound **3.31i**.

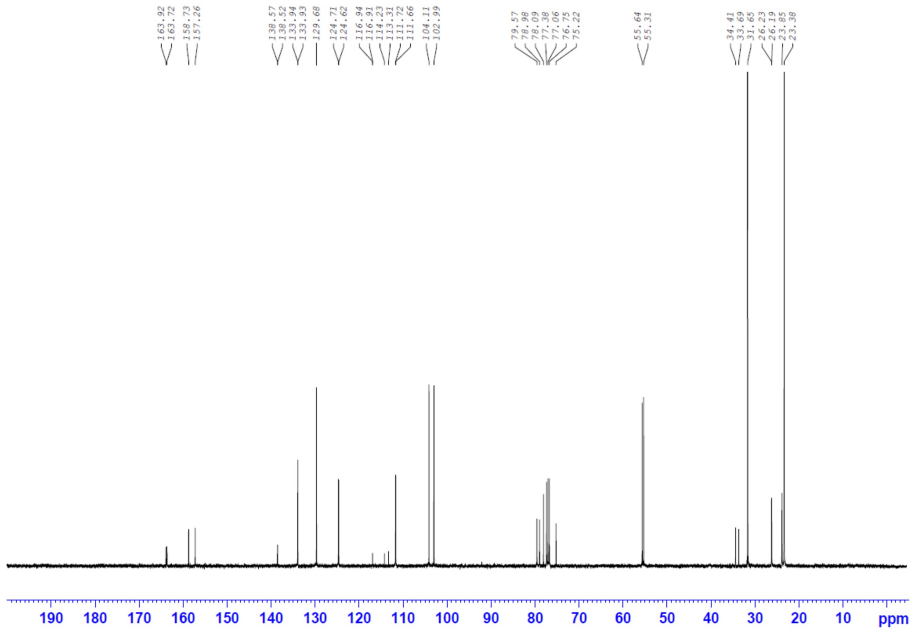

Figure 3.51 ^{13}C NMR (100 MHz, $CDCl_3$) of compound **3.31i**.

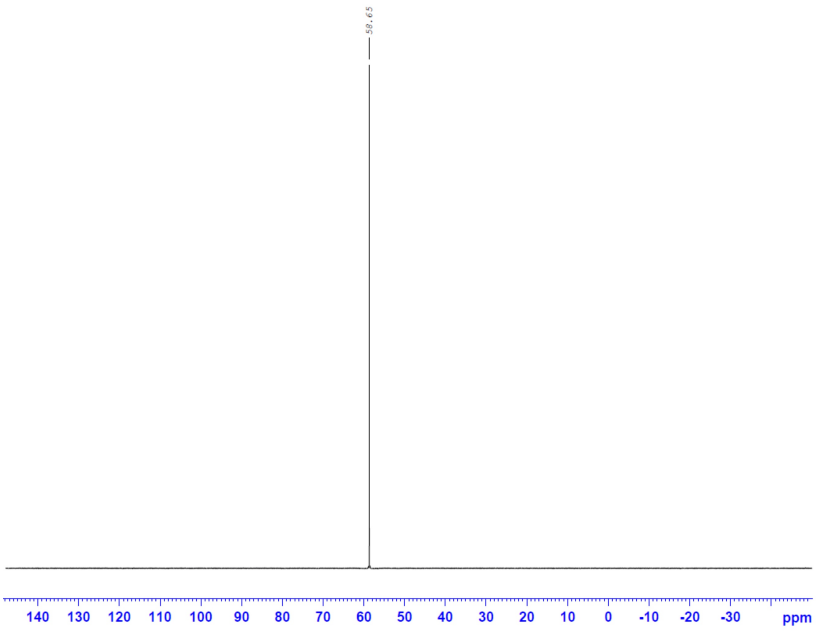

Figure 3.52 ^{31}P NMR (162 MHz, $CDCl_3$) of compound **3.31i**.

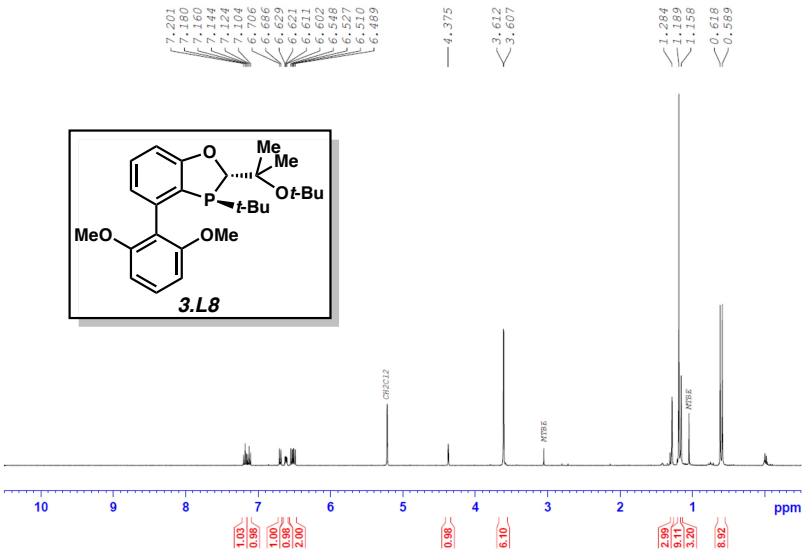

Figure 3.53 ^{1}H NMR (400 MHz, $CDCl_3$) of compound **3.L8**.

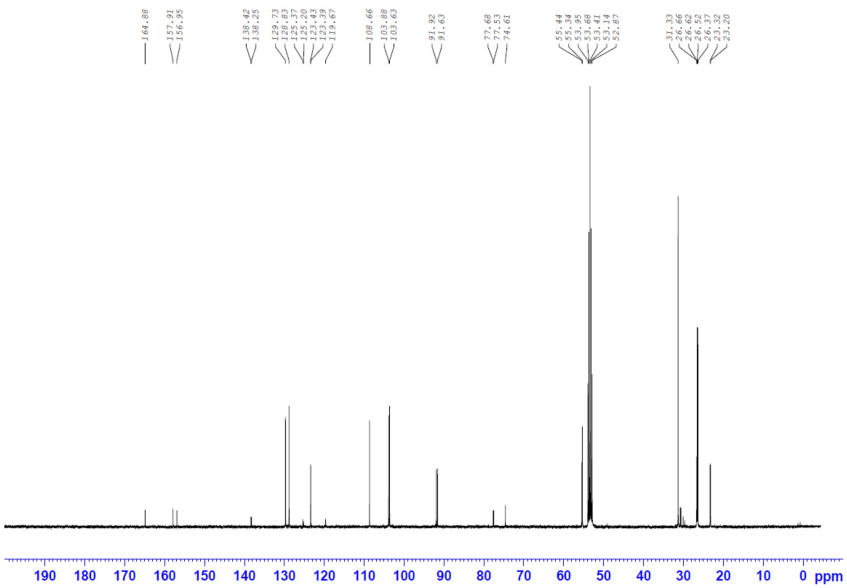

Figure 3.54 ^{13}C NMR (100 MHz, $CDCl_3$) of compound **3.L8**.

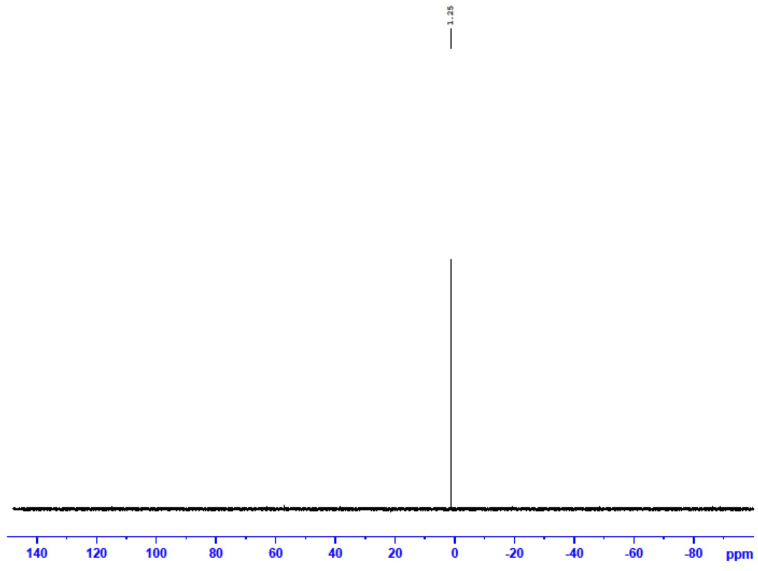

Figure 3.55 ^{31}P NMR (162 MHz, $CDCl_3$) of compound **3.L8**.

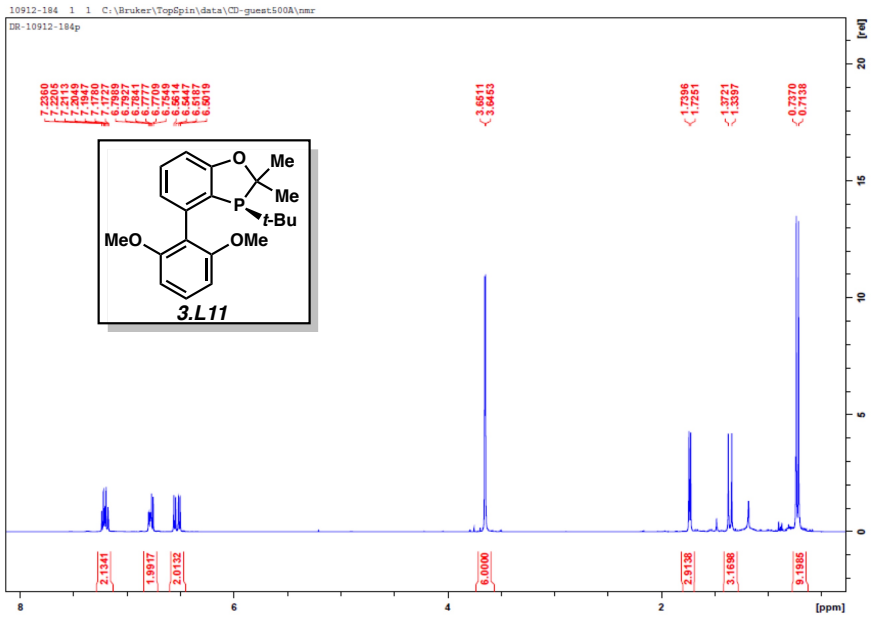

Figure 3.56 ^{1}H NMR (400 MHz, $CDCl_3$) of compound **3.L11**.

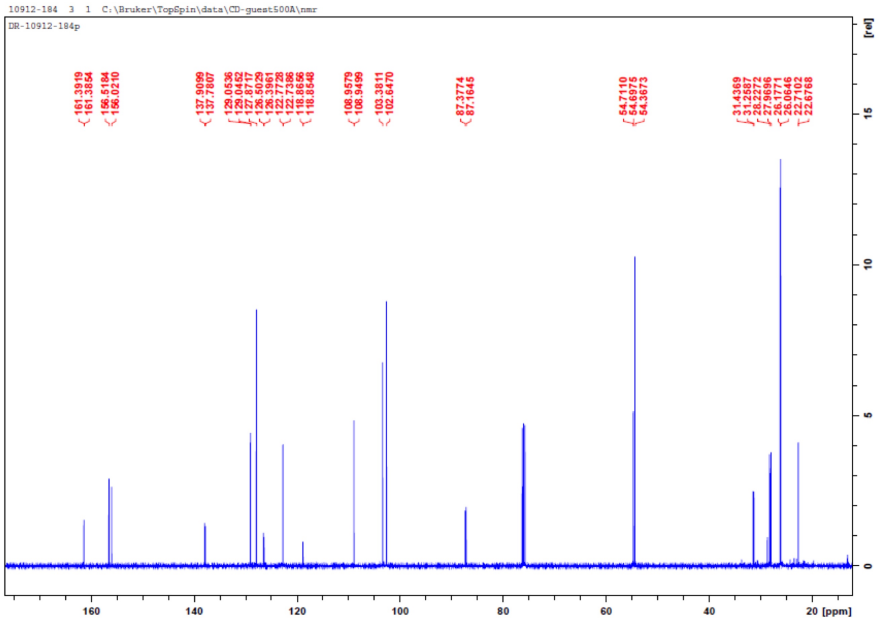

Figure 3.57 ^{13}C NMR (100 MHz, $CDCl_3$) of compound **3.L11**.

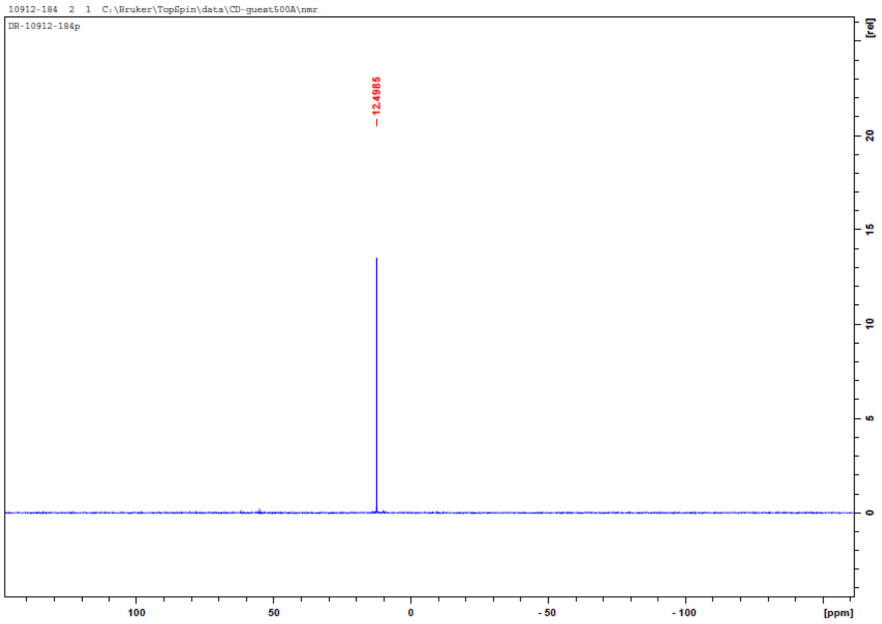

Figure 3.58 ^{31}P NMR (202 MHz, $CDCl_3$) of compound **3.L11**.

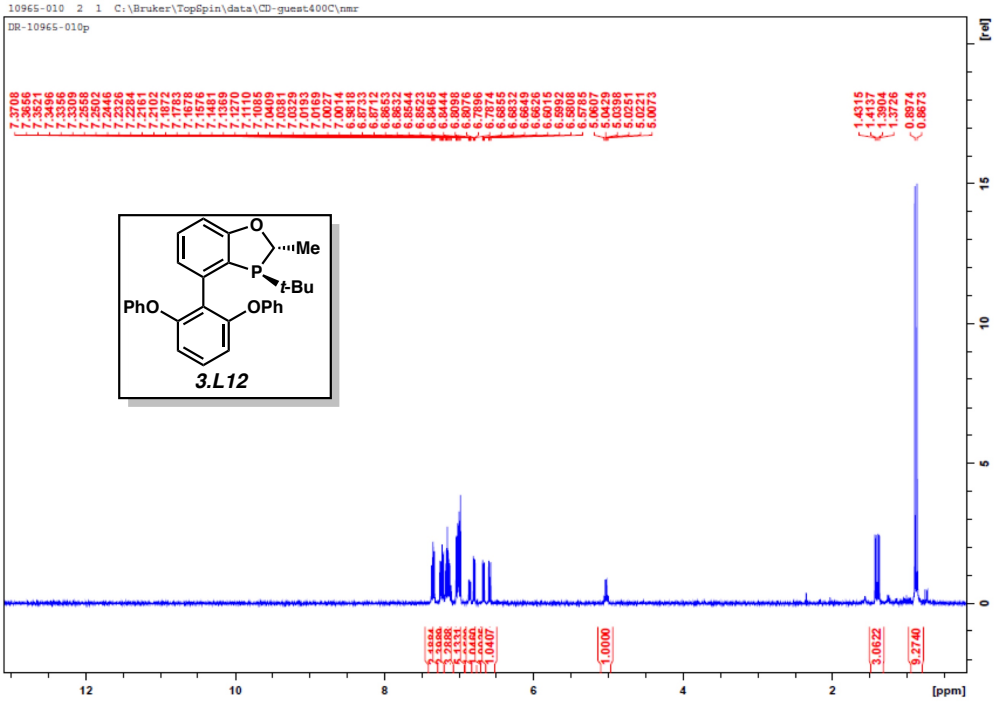

Figure 3.59 ^{1}H NMR (400 MHz, $CDCl_3$) of compound **3.L12**.

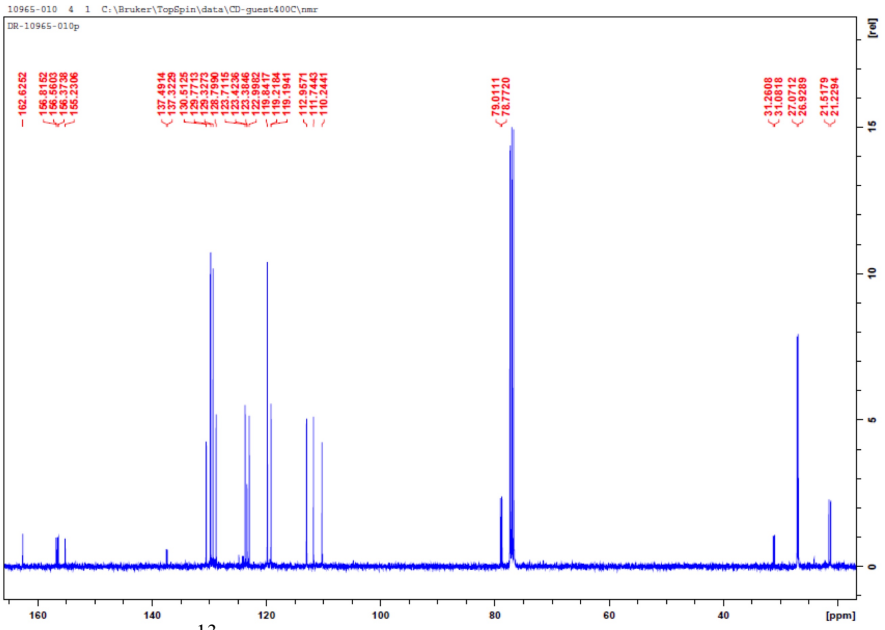

Figure 3.60 ^{13}C NMR (100 MHz, $CDCl_3$) of compound **3.L12**.

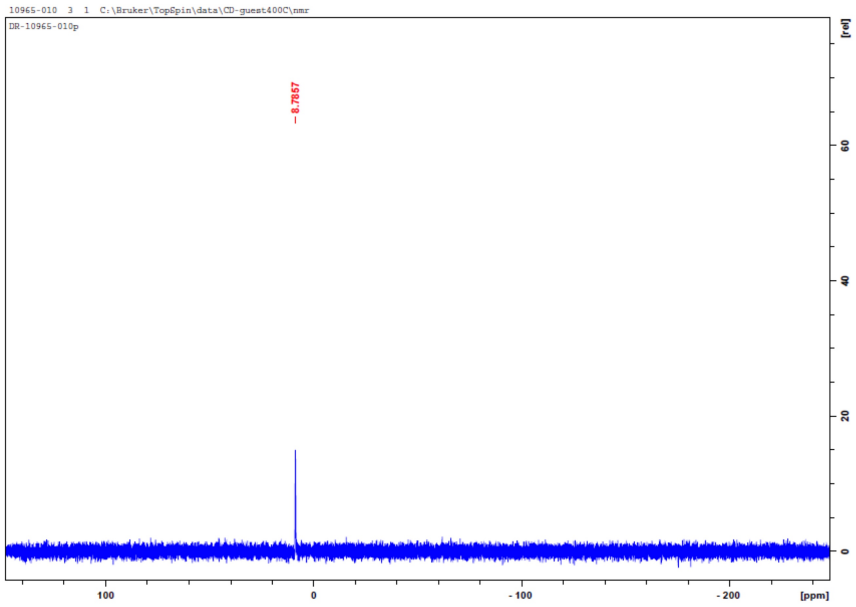

Figure 3.61 ^{31}P NMR (202 MHz, $CDCl_3$) of compound **3.L12**.

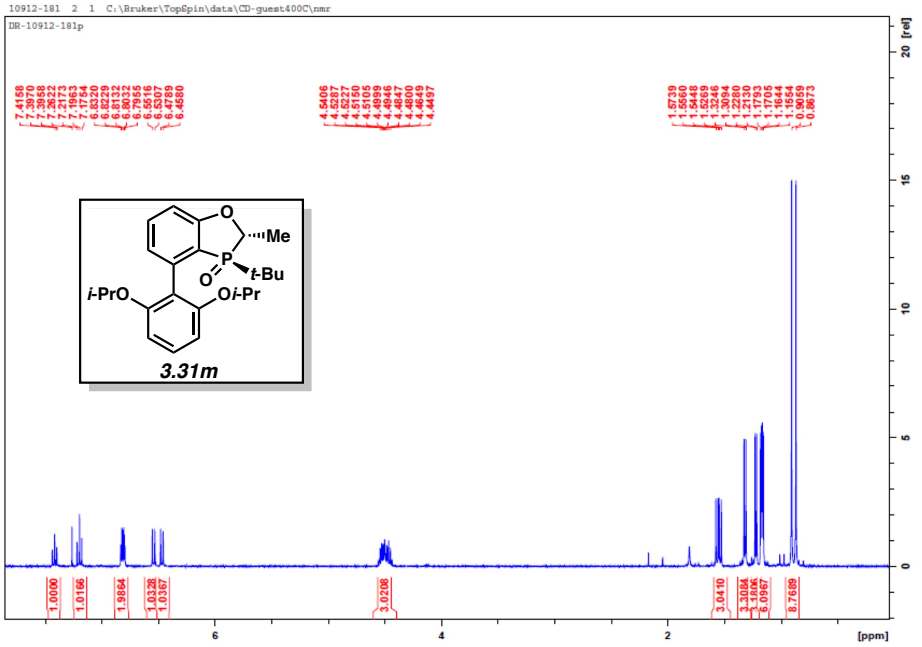

Figure 3.62 ^{1}H NMR (400 MHz, $CDCl_3$) of compound **3.31m**.

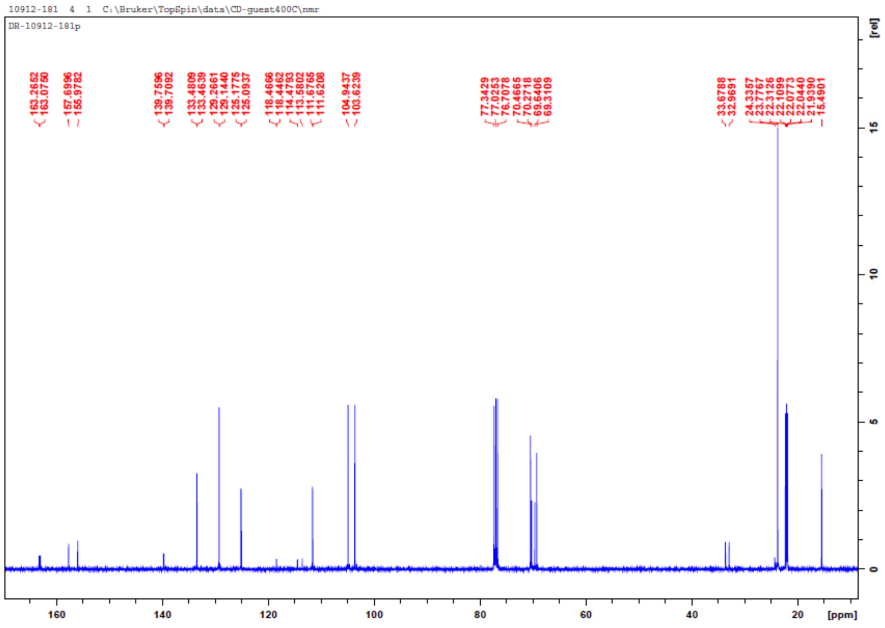

Figure 3.63 ^{13}C NMR (100 MHz, $CDCl_3$) of compound **3.31m**.

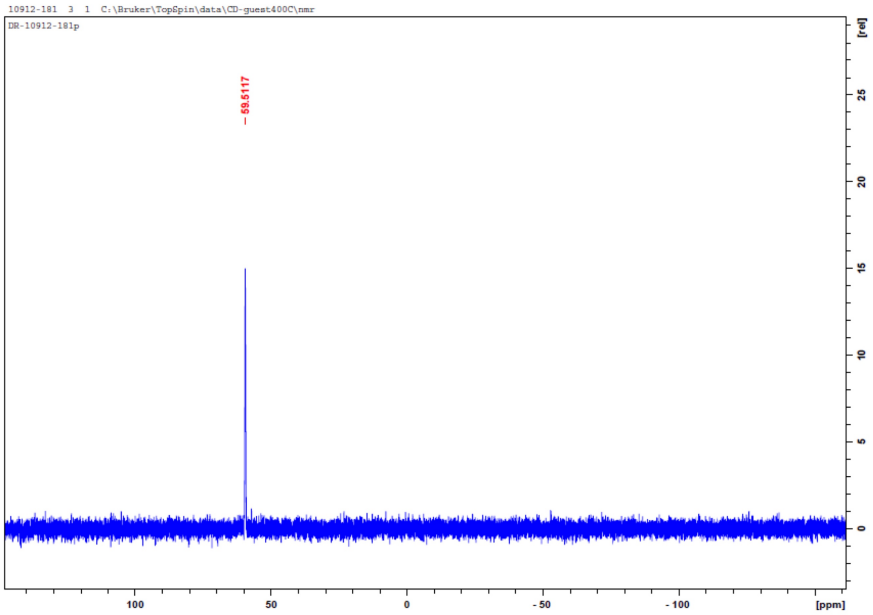

Figure 3.64 ^{31}P NMR (202 MHz, $CDCl_3$) of compound **3.31m**.

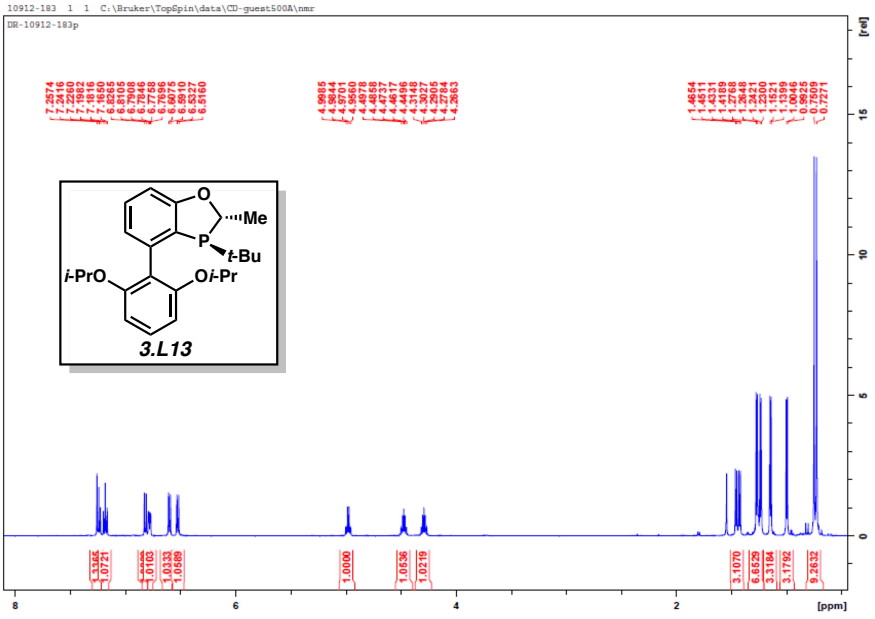

Figure 3.65 ^{1}H NMR (500 MHz, $CDCl_3$) of compound **3.L13**.

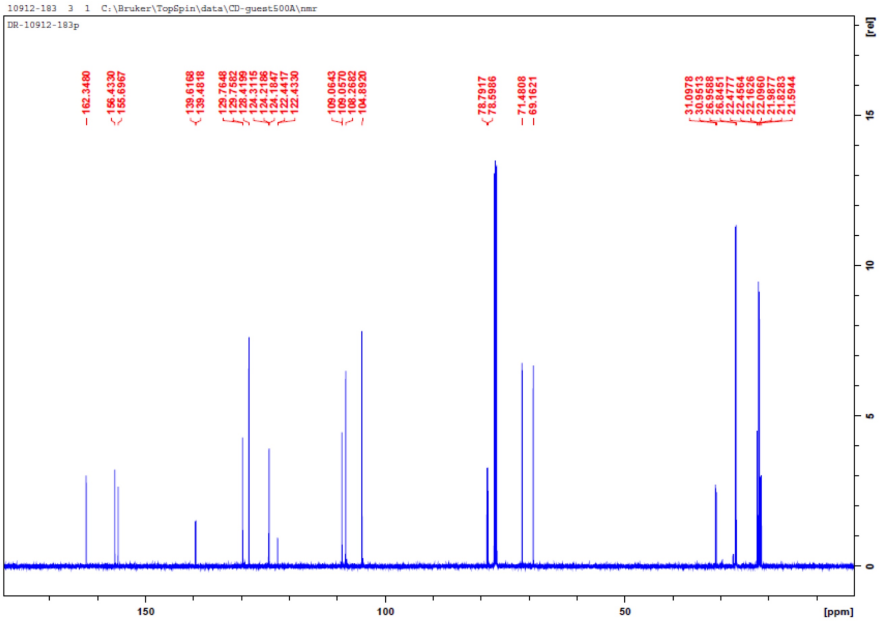

Figure 3.66 ^{13}C NMR (100 MHz, $CDCl_3$) of compound **3.L13**.

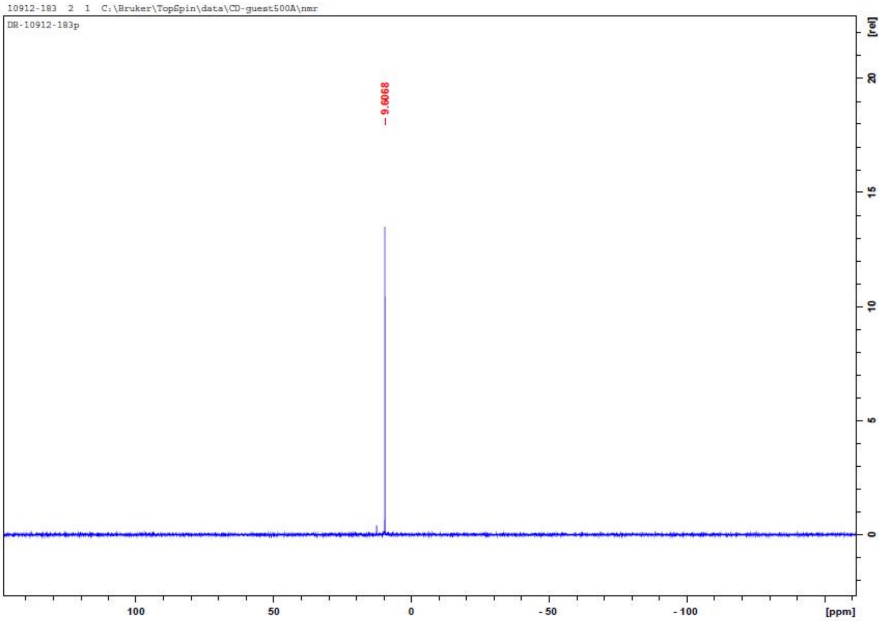

Figure 3.67 ^{31}P NMR (162 MHz, $CDCl_3$) of compound **3.L13**.

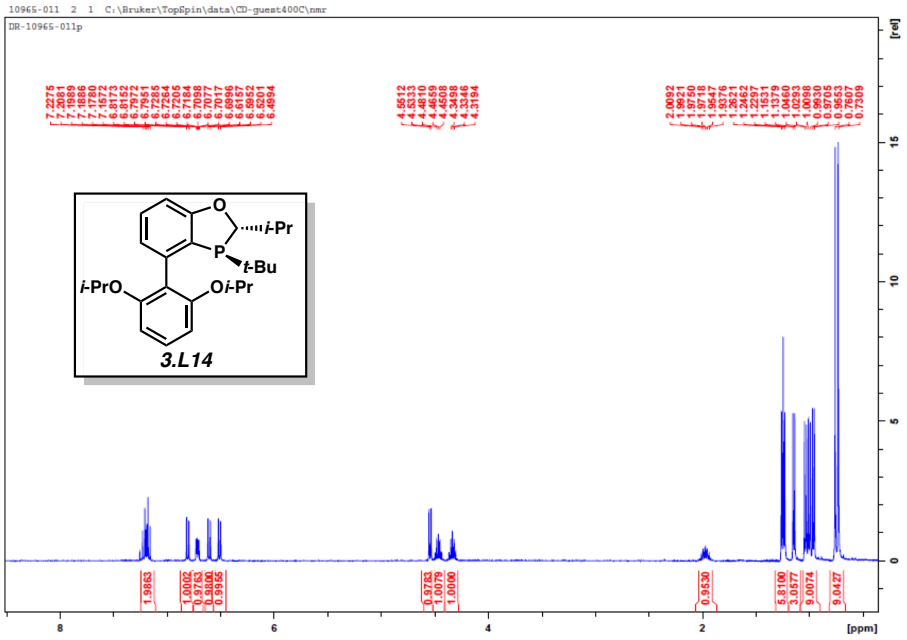

Figure 3.68 ^{1}H NMR (400 MHz, $CDCl_3$) of compound **3.L14**.

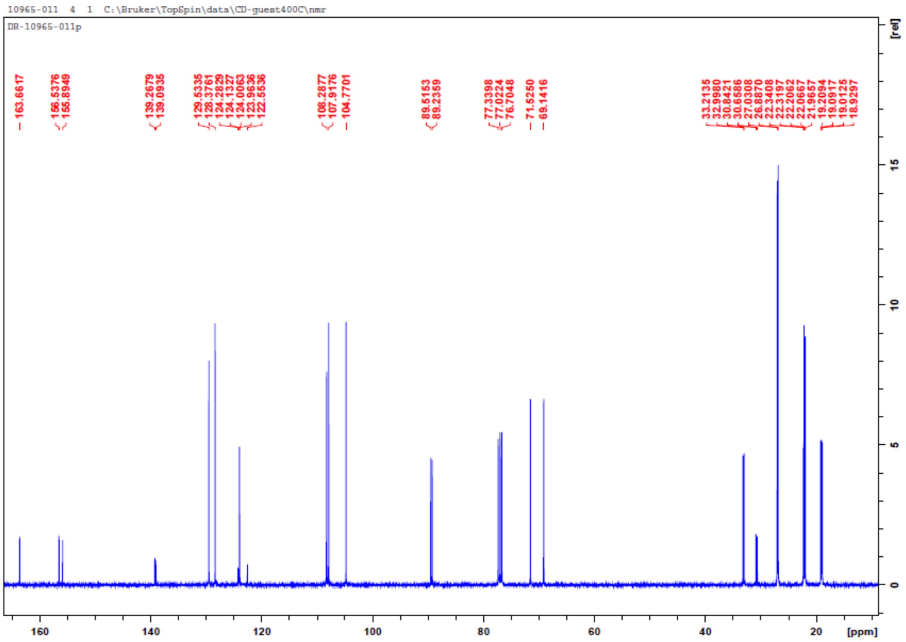

Figure 3.69 ^{13}C NMR (100 MHz, $CDCl_3$) of compound **3.L14**.

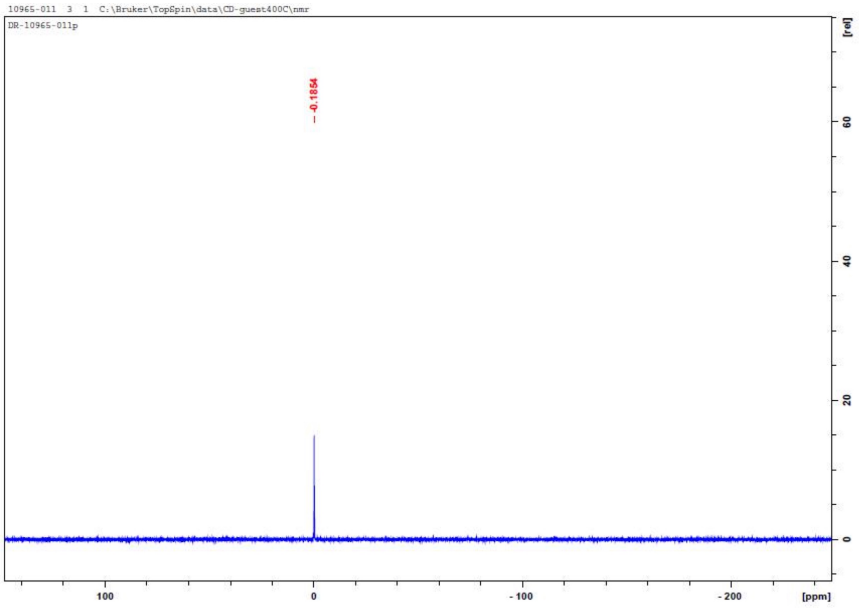

Figure 3.70 ^{31}P NMR (202 MHz, $CDCl_3$) of compound **3.L14**.

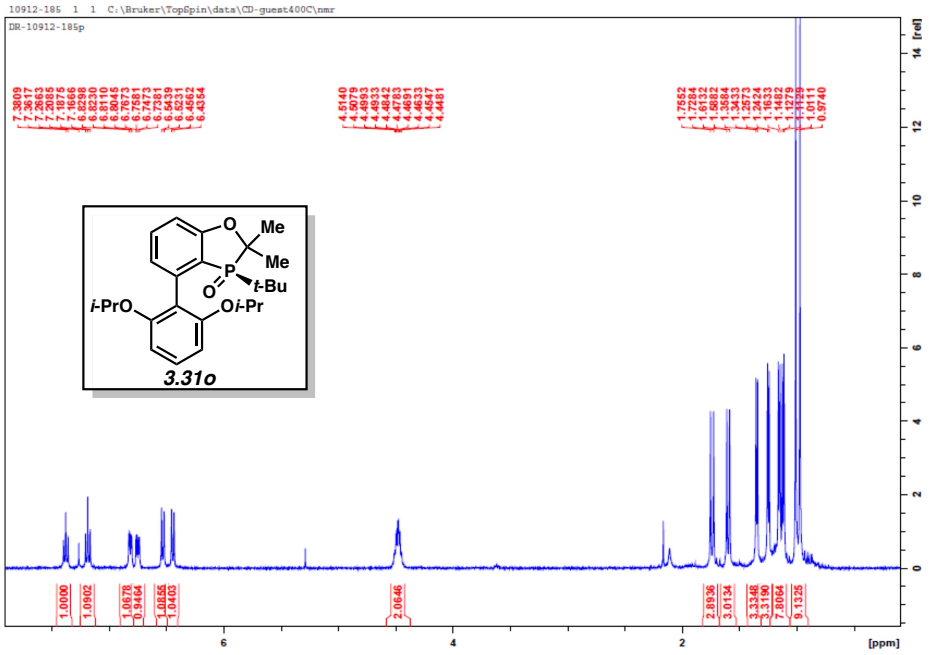

Figure 3.71 ^{1}H NMR (400 MHz, $CDCl_3$) of compound **3.31o**.

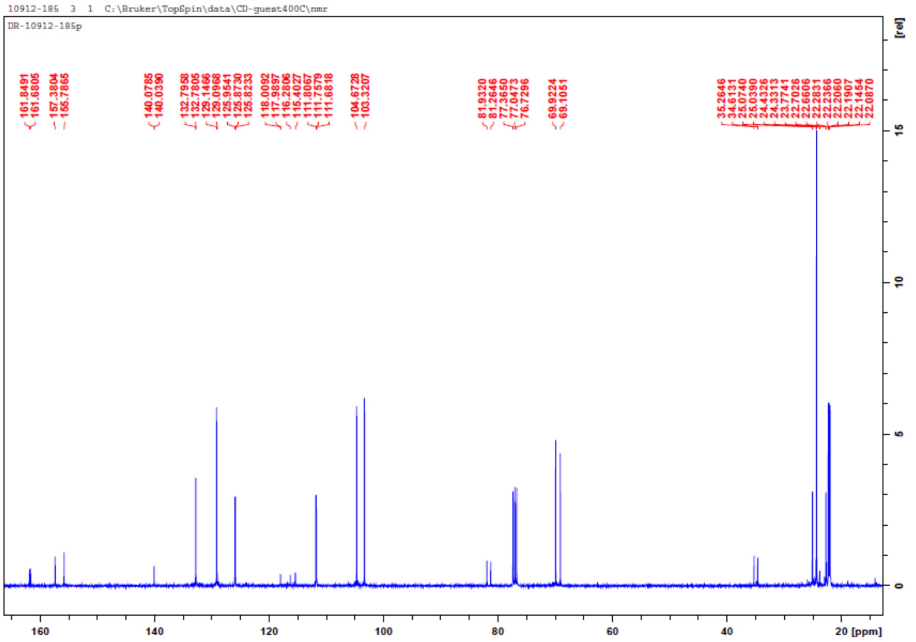

Figure 3.72 ^{13}C NMR (100 MHz, $CDCl_3$) of compound **3.31o**.

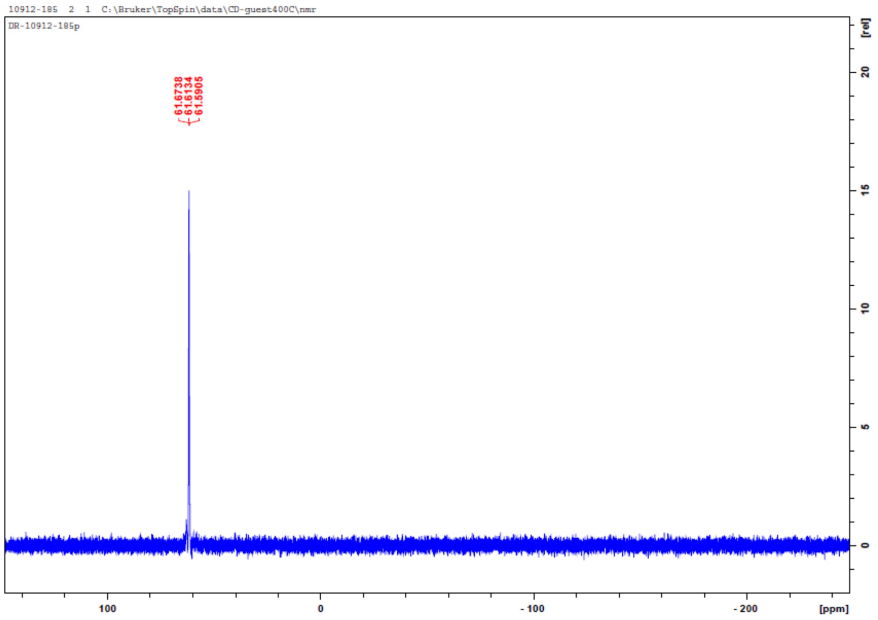

Figure 3.73 ^{31}P NMR (202 MHz, $CDCl_3$) of compound **3.31o**.

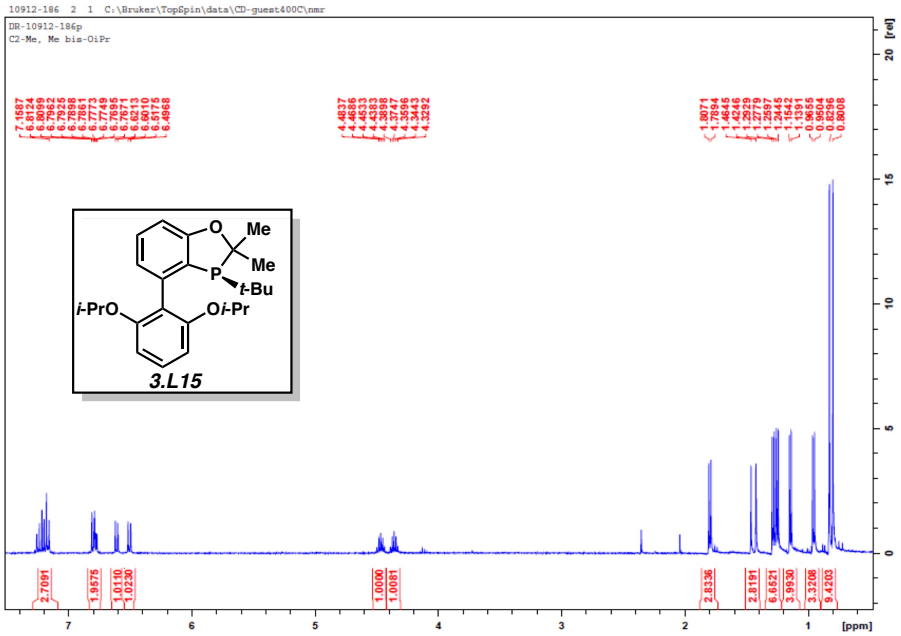

Figure 3.74 ^{1}H NMR (400 MHz, $CDCl_3$) of compound **3.L15**.

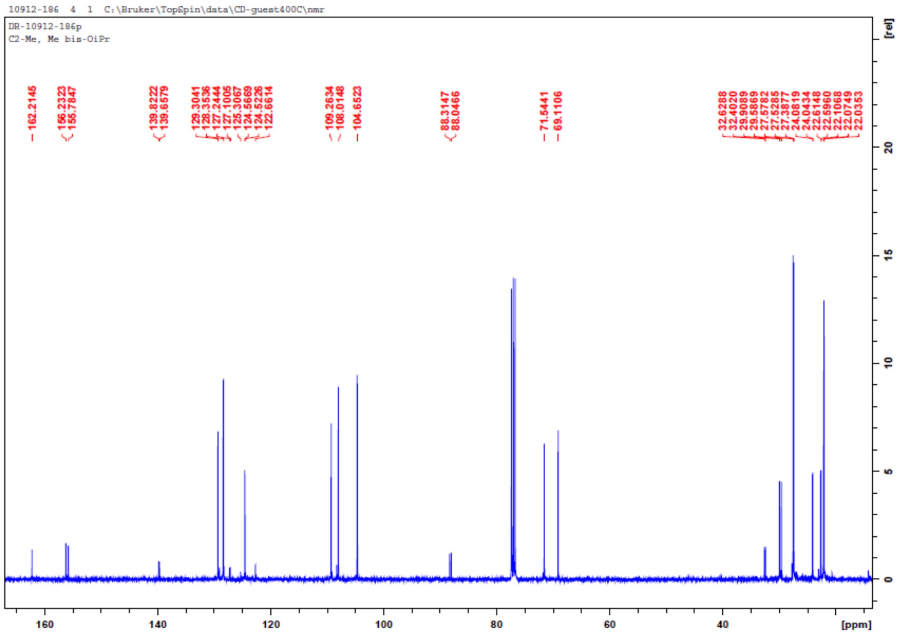

Figure 3.75 ^{13}C NMR (100 MHz, $CDCl_3$) of compound **3.L15**.

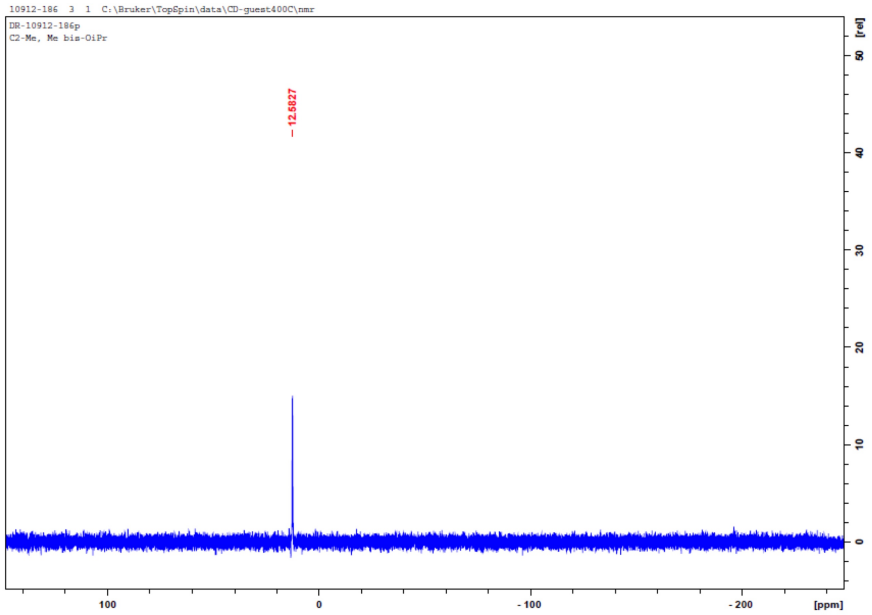

Figure 3.76 ^{31}P NMR (202 MHz, $CDCl_3$) of compound **3.L15**.

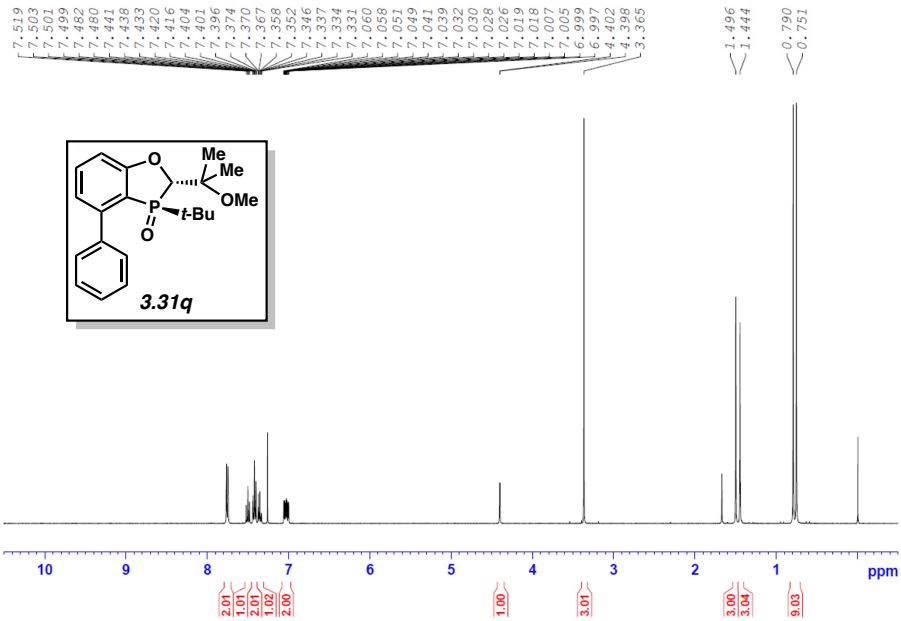

Figure 3.77 ^{1}H NMR (400 MHz, $CDCl_3$) of compound **3.31q**.

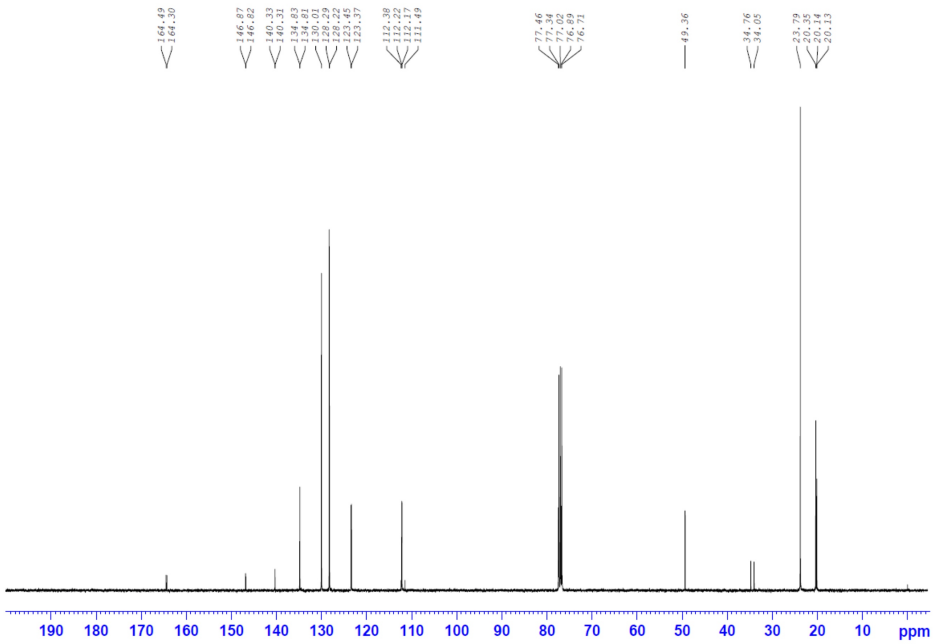

Figure 3.78 ^{13}C NMR (100 MHz, $CDCl_3$) of compound **3.31q**.

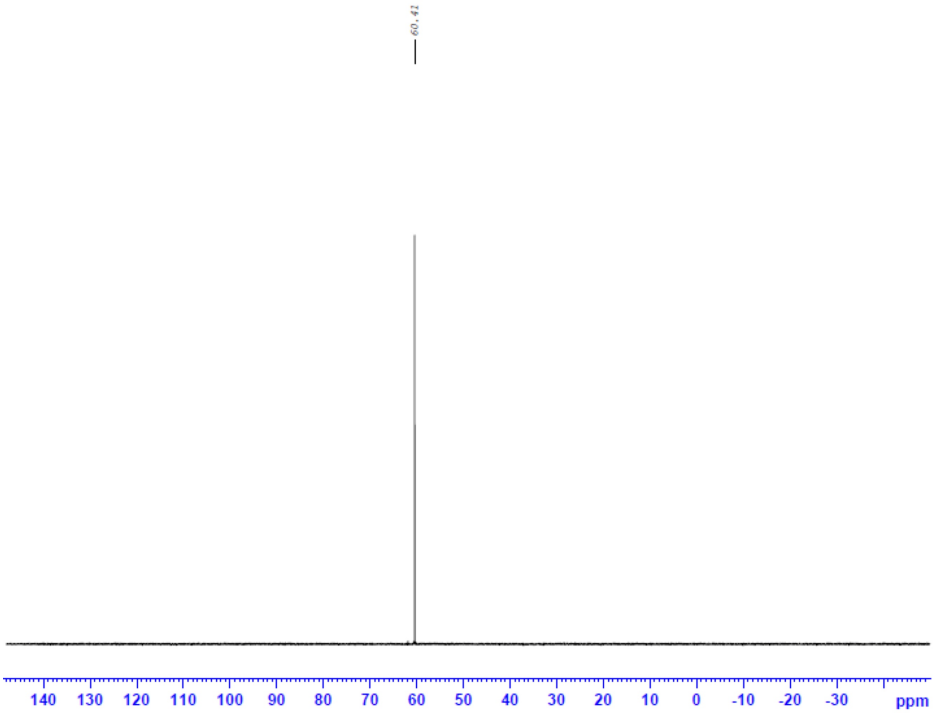

Figure 3.79 ^{31}P NMR (162 MHz, $CDCl_3$) of compound **3.31q**.

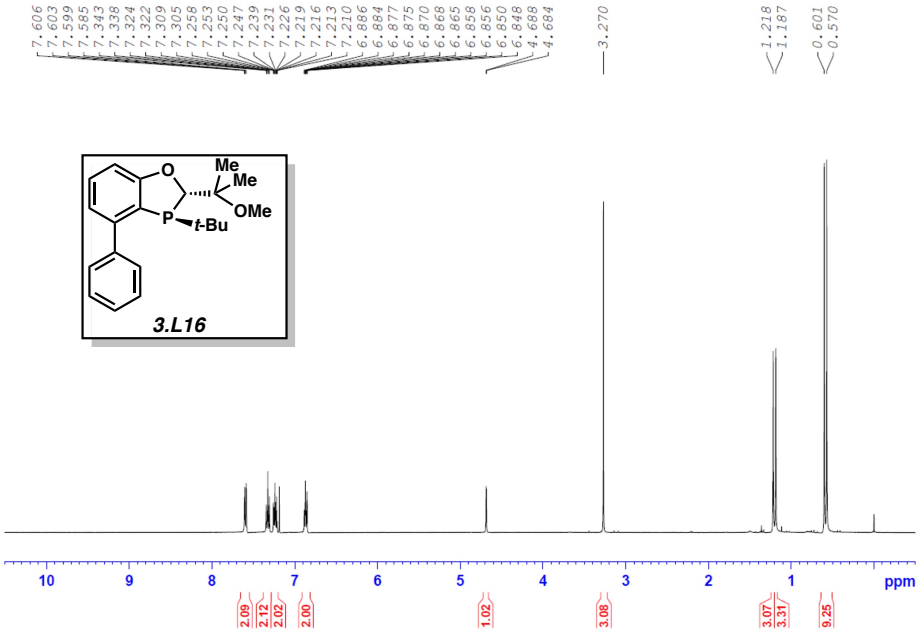

Figure 3.80 ^{1}H NMR (400 MHz, $CDCl_3$) of compound **3.L16**.

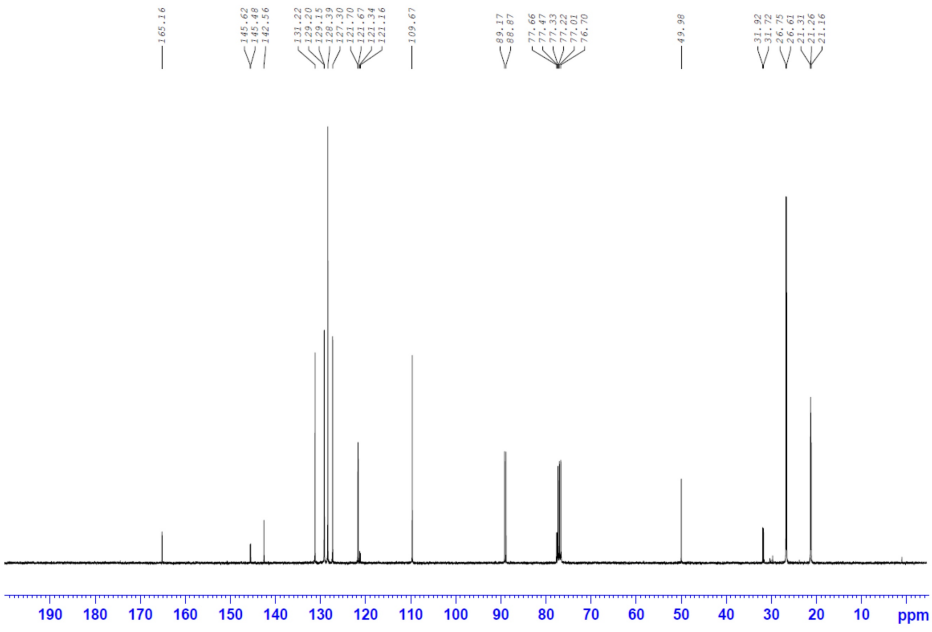

Figure 3.81 ^{13}C NMR (100 MHz, $CDCl_3$) of compound **3.L16**.

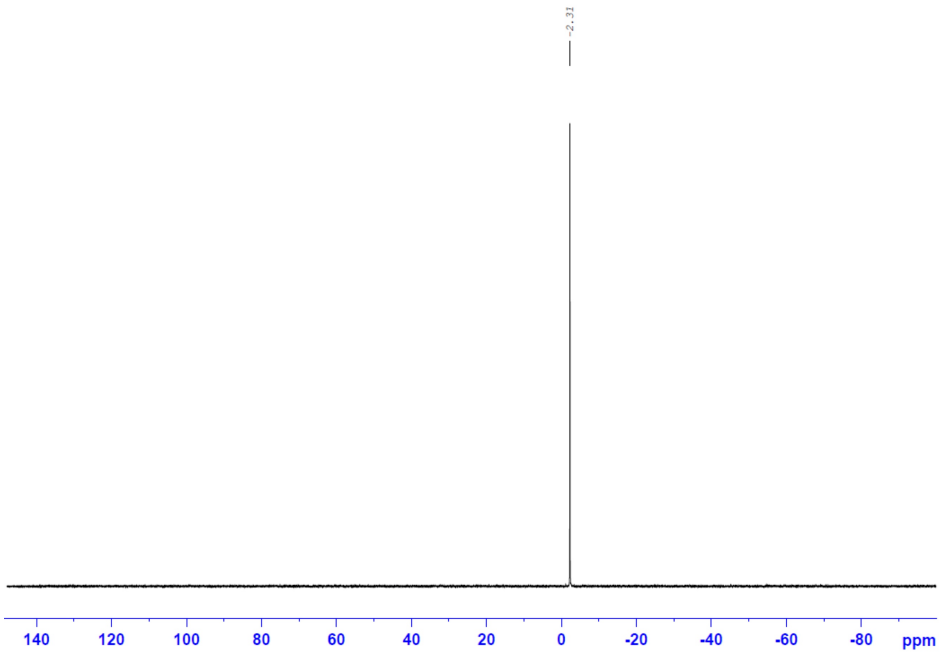

Figure 3.82 ^{31}P NMR (162 MHz, $CDCl_3$) of compound **3.L16**.

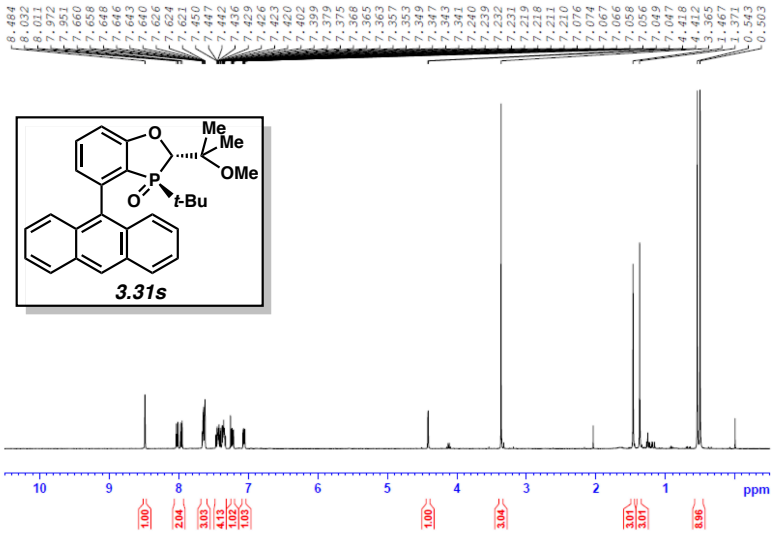

Figure 3.83 ^{1}H NMR (400 MHz, $CDCl_3$) of compound **3.31s**.

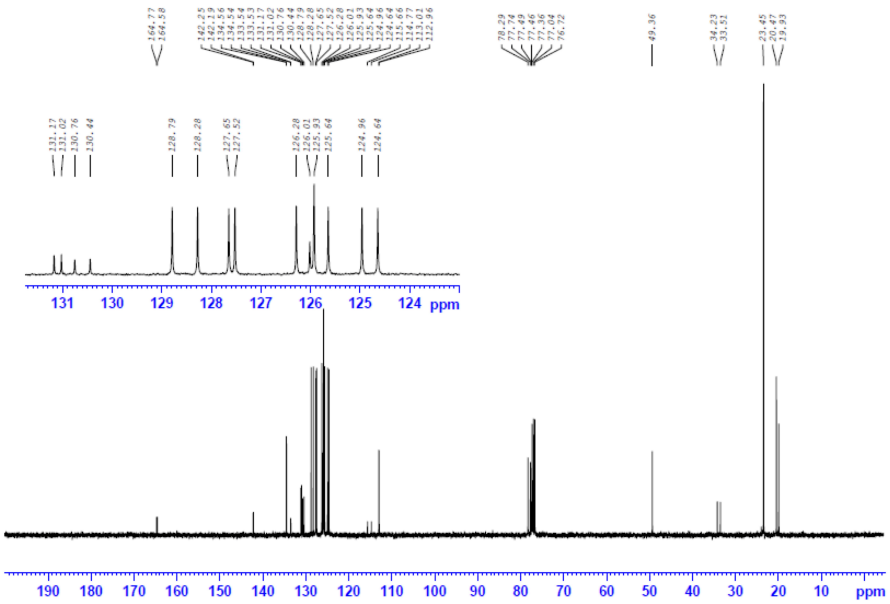

Figure 3.84 ^{13}C NMR (100 MHz, $CDCl_3$) of compound **3.31s**.

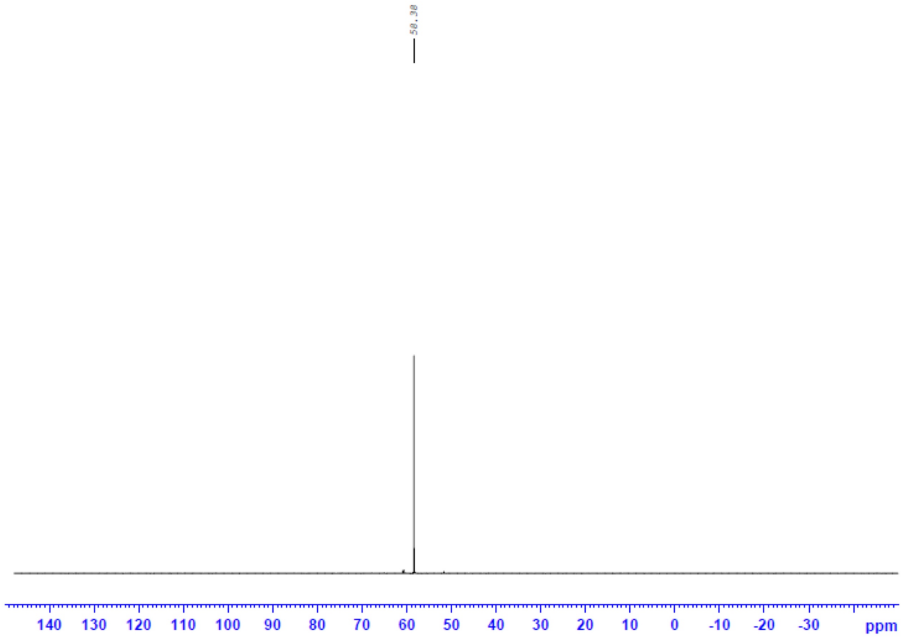

Figure 3.85 ^{31}P NMR (162 MHz, $CDCl_3$) of compound **3.31s**.

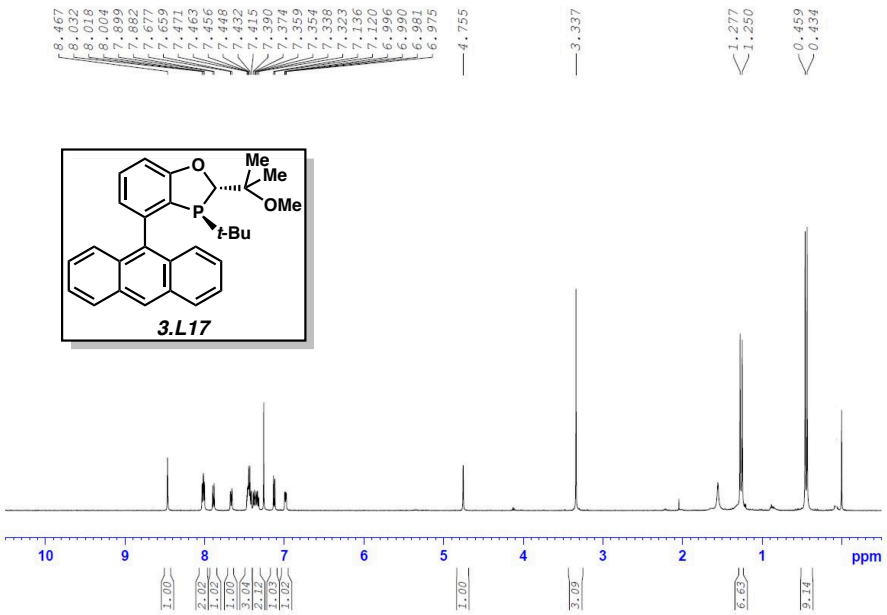

Figure 3.86 ^{1}H NMR (500 MHz, $CDCl_3$) of compound **3.L17**.

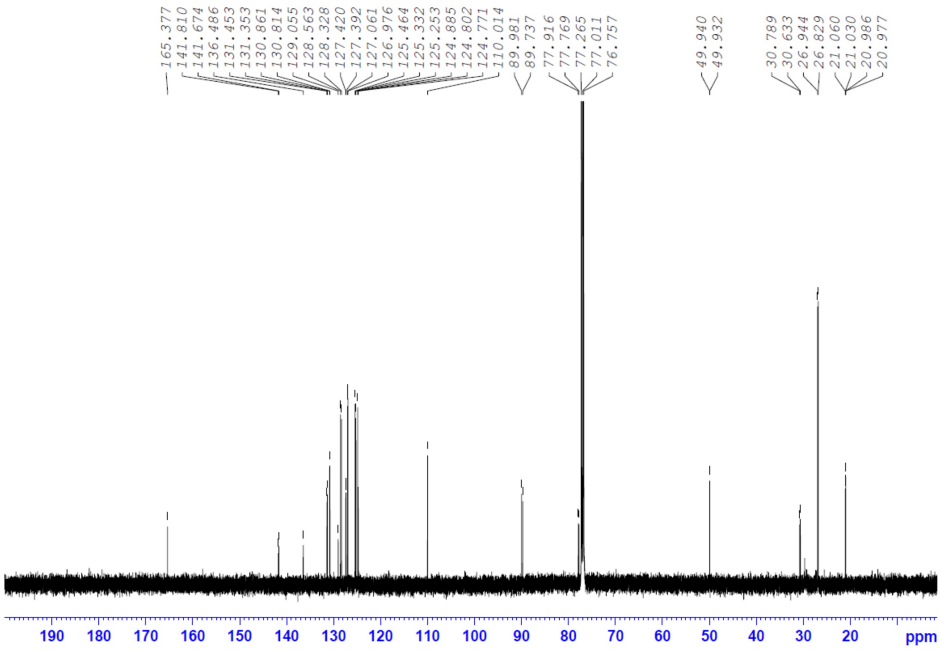

Figure 3.87 ^{13}C NMR (125 MHz, $CDCl_3$) of compound **3.L17**.

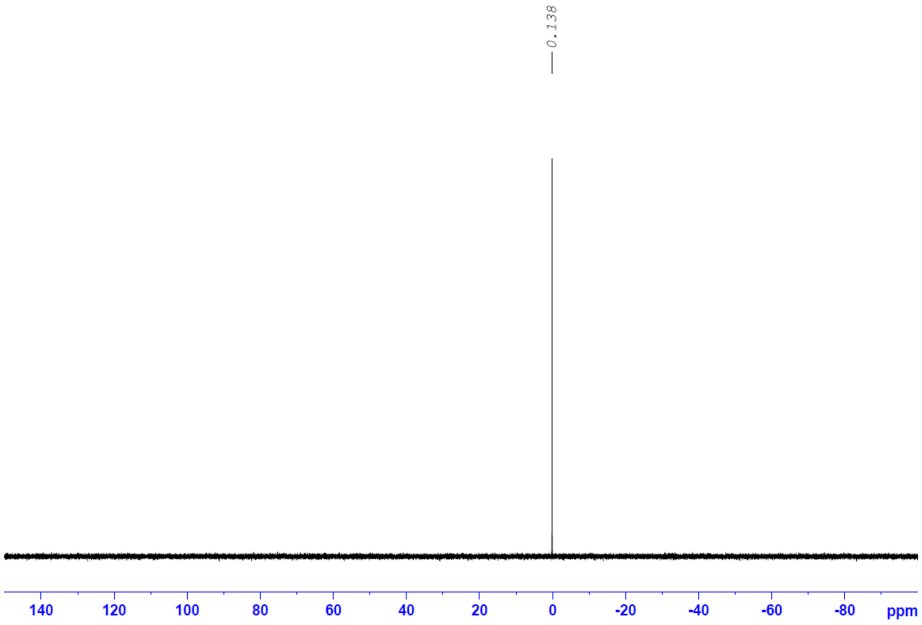

Figure 3.88 ^{31}P NMR (202 MHz, $CDCl_3$) of compound **3.L17**.

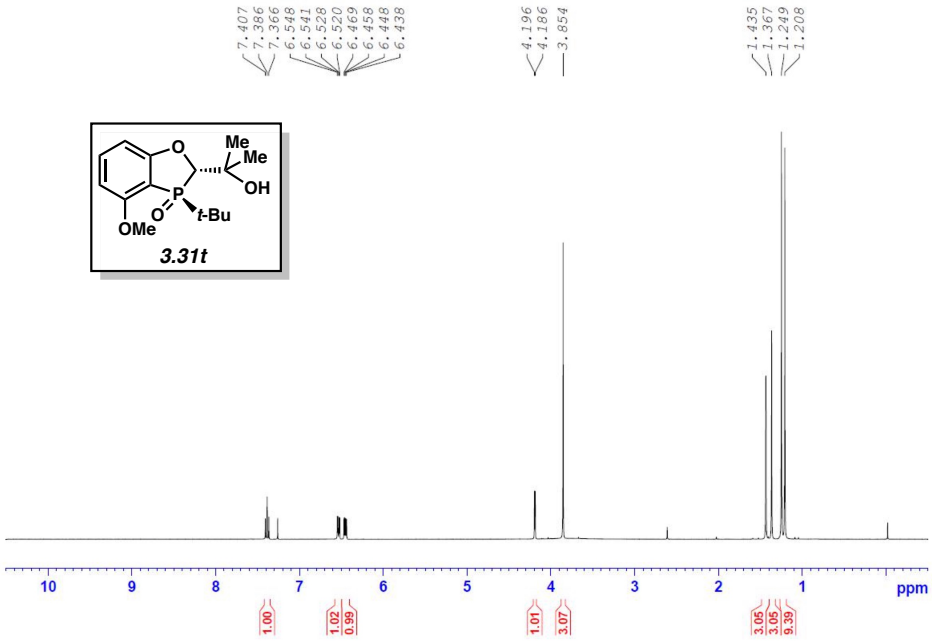

Figure 3.89 ^{1}H NMR (400 MHz, $CDCl_3$) of compound **3.31t**.

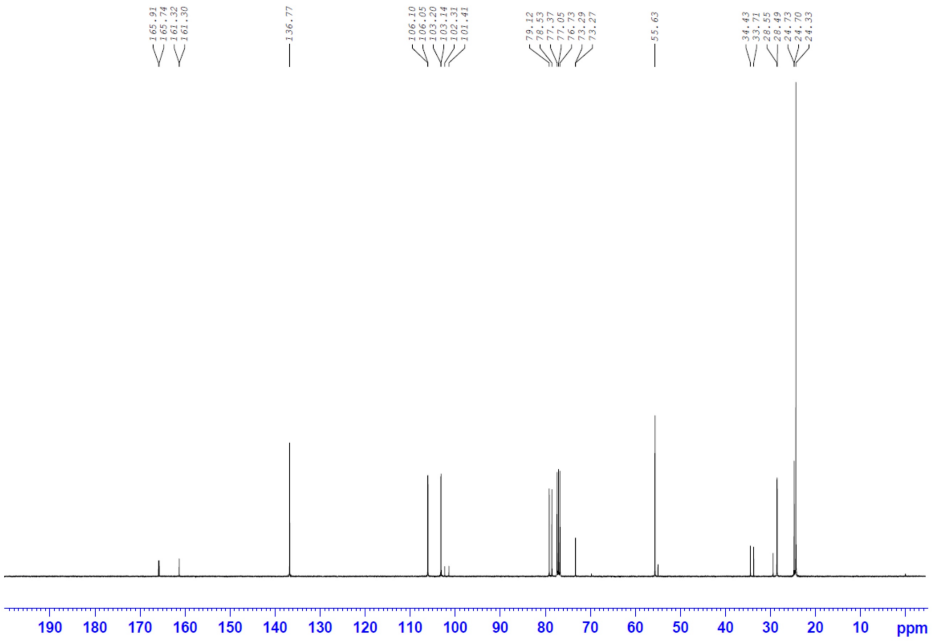

Figure 3.90 ^{13}C NMR (100 MHz, $CDCl_3$) of compound **3.31t**.

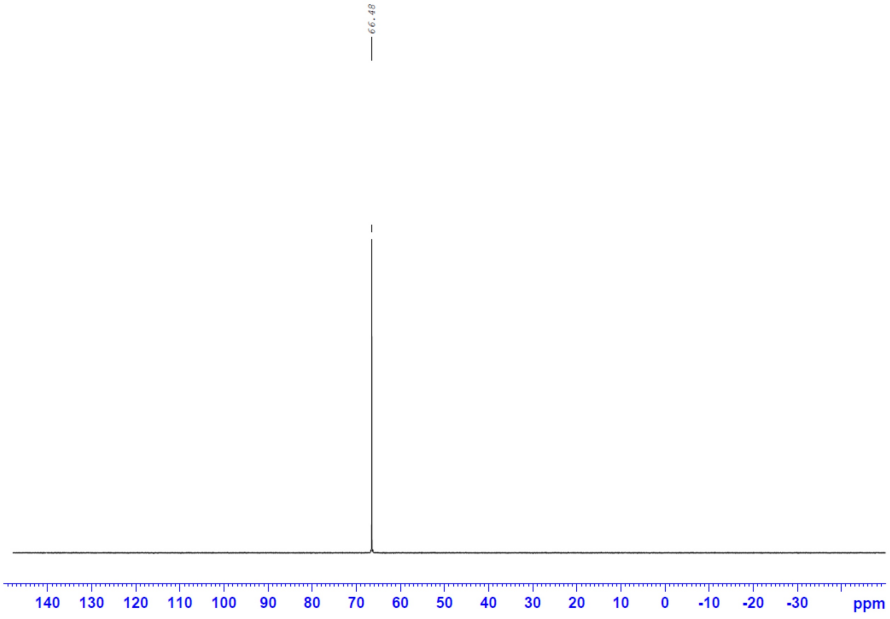

Figure 3.91 ^{31}P NMR (162 MHz, $CDCl_3$) of compound **3.31t**.

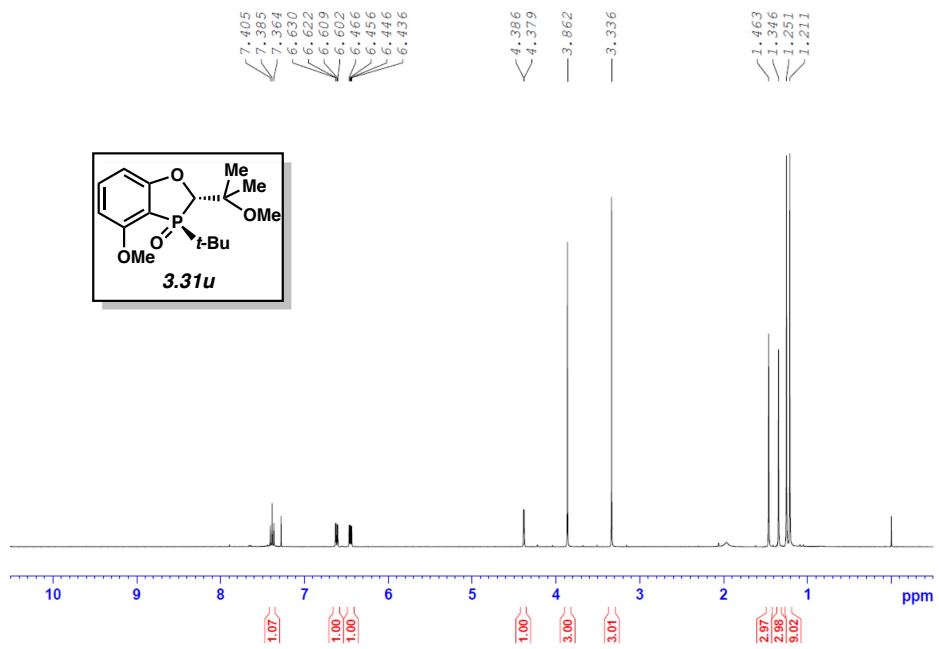

Figure 3.92 ^{1}H NMR (400 MHz, $CDCl_3$) of compound **3.31u**.

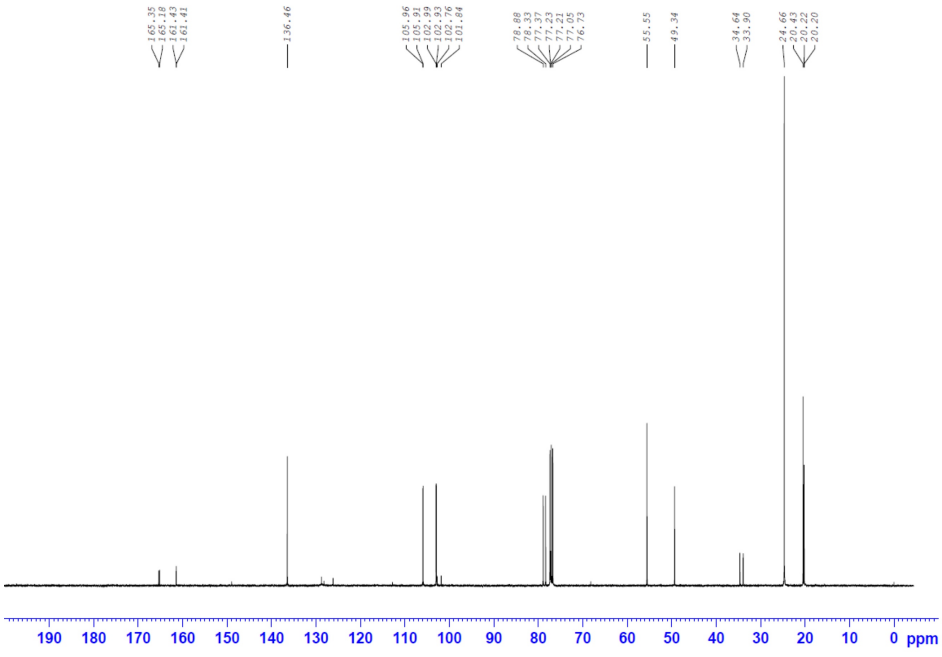

Figure 3.93 ^{13}C NMR (100 MHz, $CDCl_3$) of compound **3.31u**.

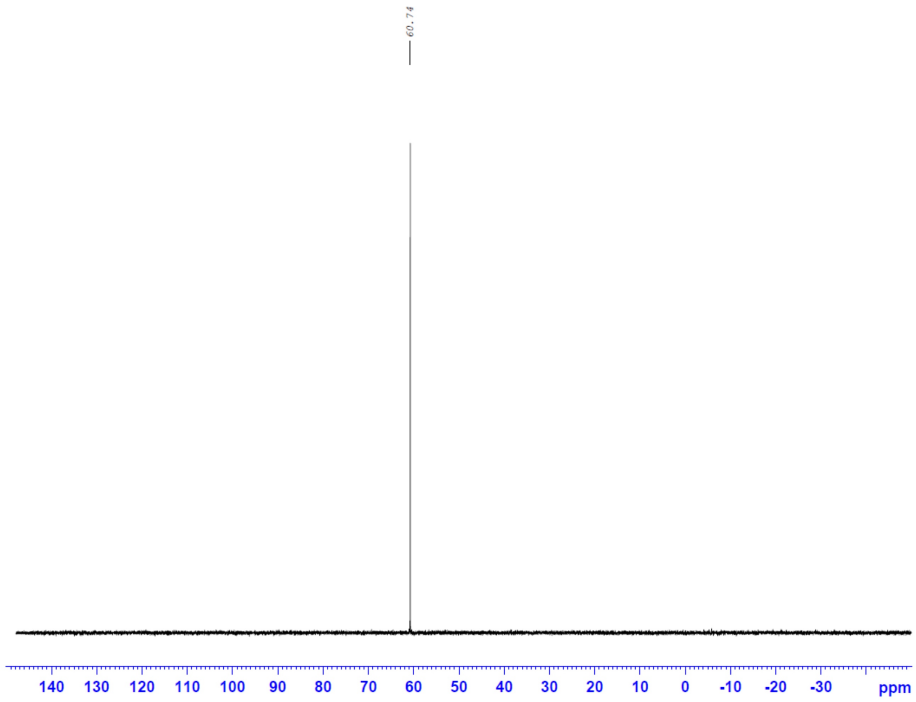

Figure 3.94 ^{31}P NMR (162 MHz, $CDCl_3$) of compound **3.31u**.

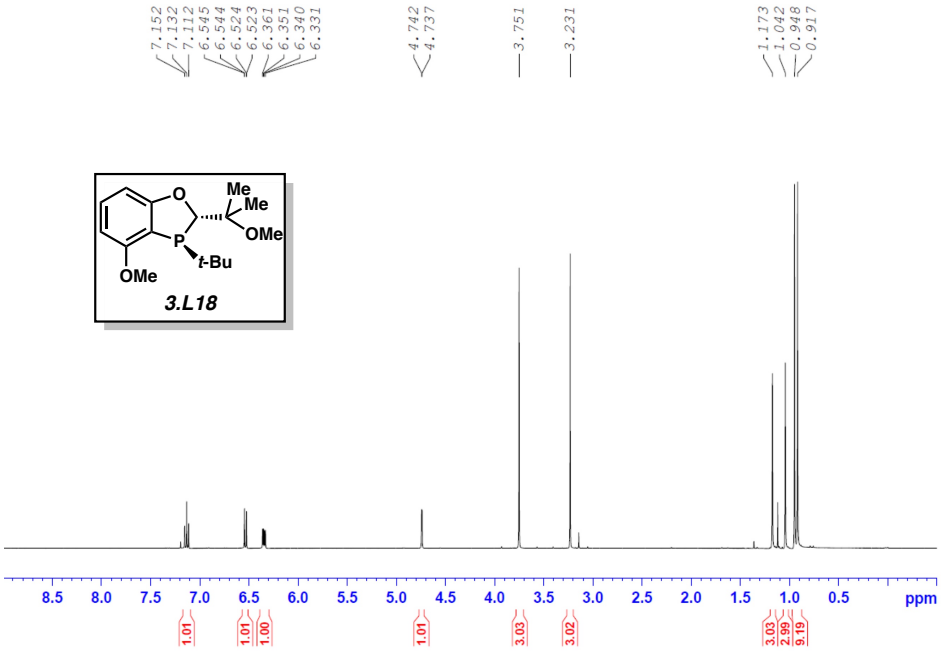

Figure 3.95 ^{1}H NMR (400 MHz, $CDCl_3$) of compound **3.L18**.

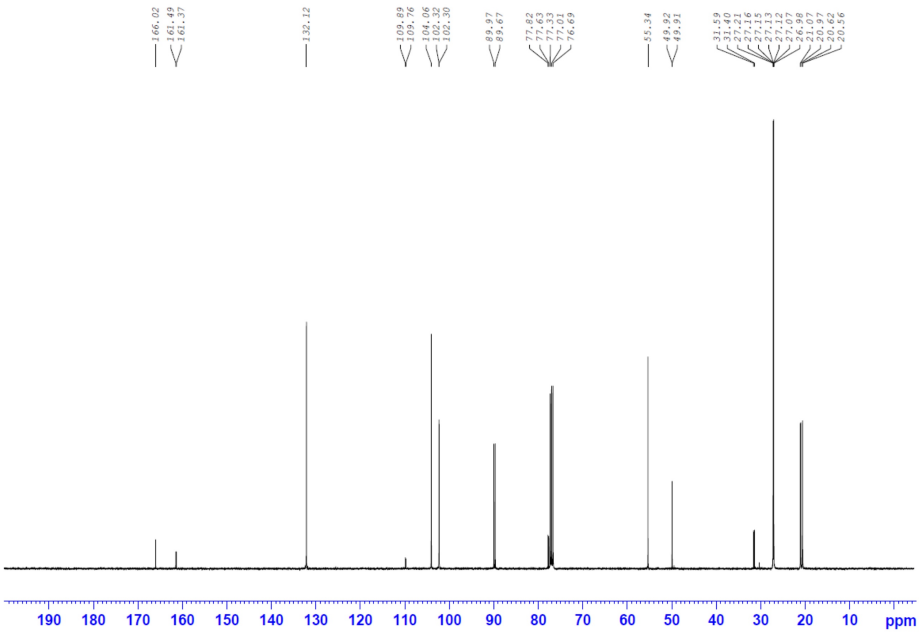

Figure 3.96 ^{13}C NMR (100 MHz, $CDCl_3$) of compound **3.L18**.

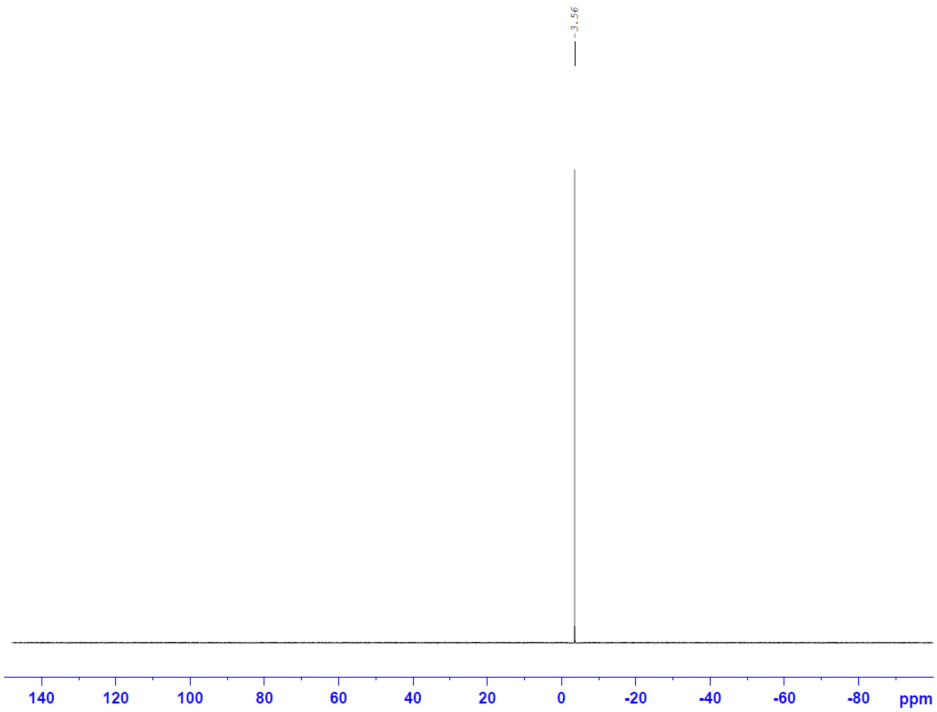

Figure 3.97 ^{31}P NMR (162 MHz, $CDCl_3$) of compound **3.L18**.

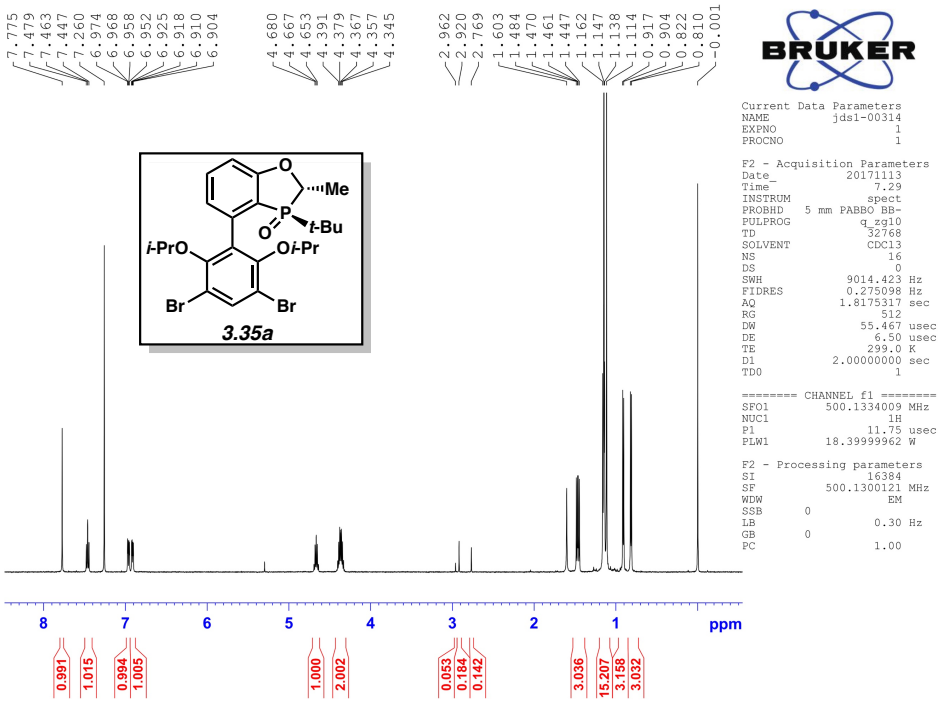

Figure 3.98 ^{1}H NMR (500 MHz, $CDCl_3$) of compound **3.35a**.

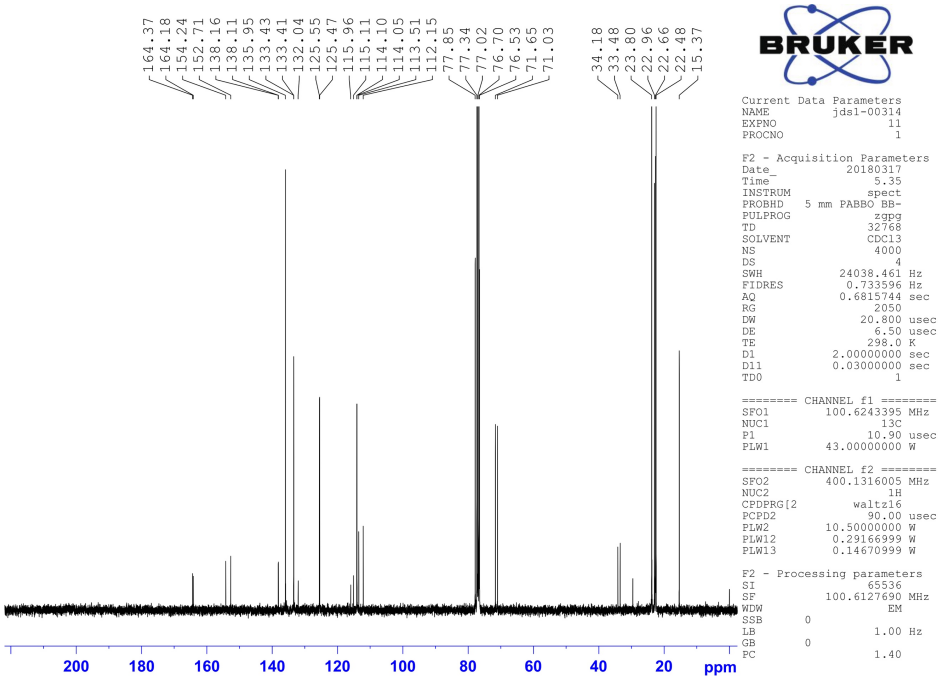

Figure 3.99 ^{13}C NMR (100 MHz, $CDCl_3$) of compound **3.35a**.

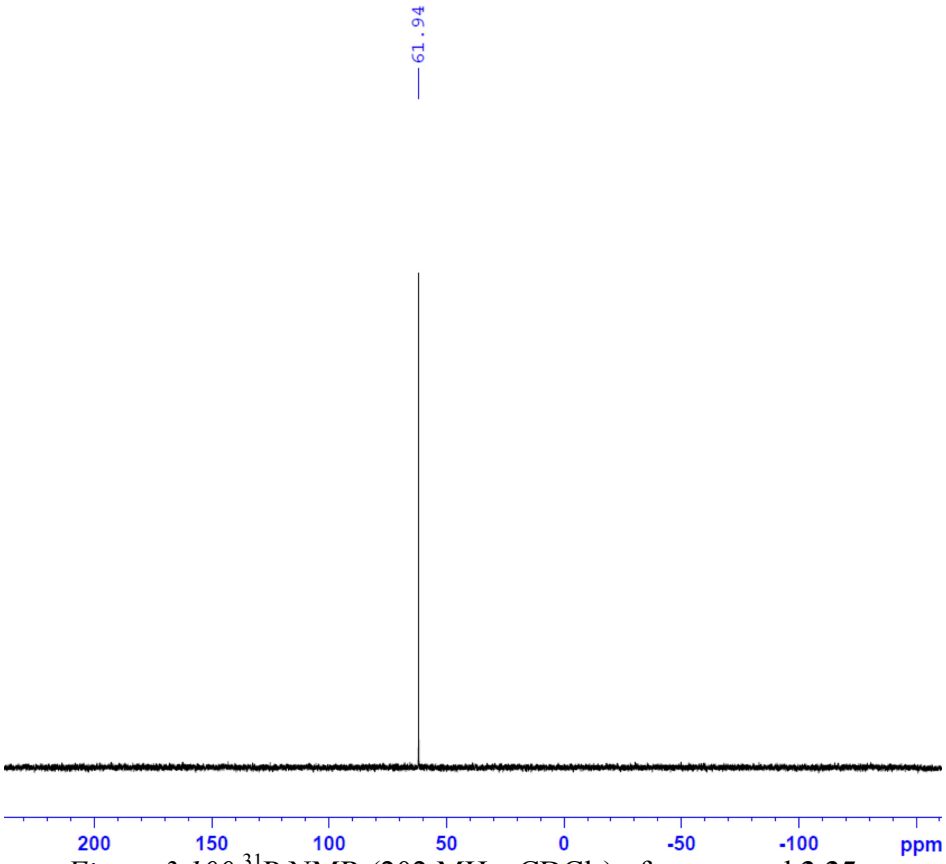

Figure 3.100 ^{31}P NMR (202 MHz, $CDCl_3$) of compound **3.35a**.

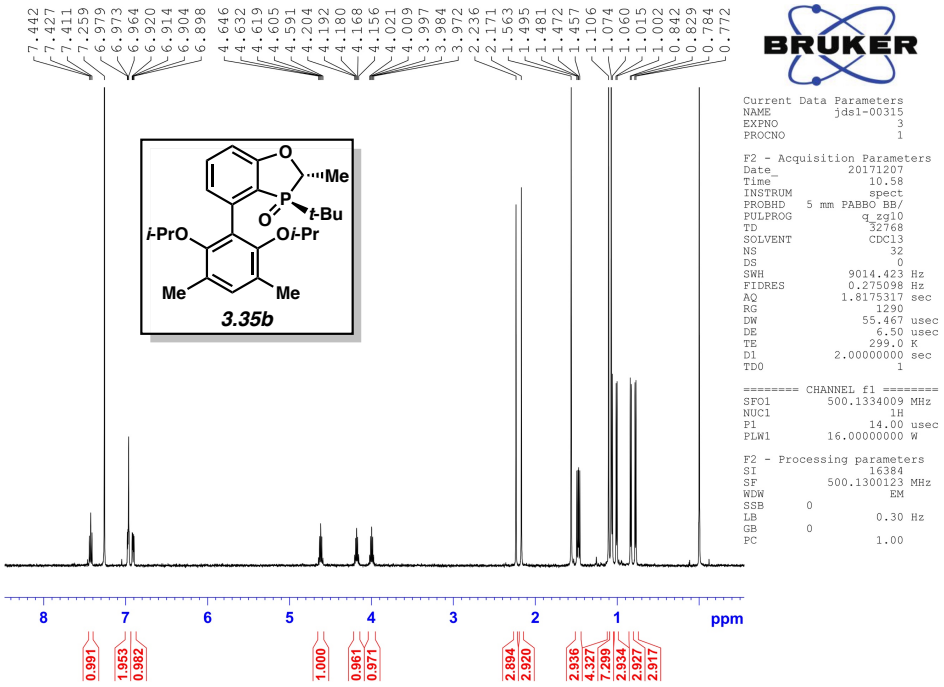

Figure 3.101 ^{1}H NMR (500 MHz, $CDCl_3$) of compound **3.35b**.

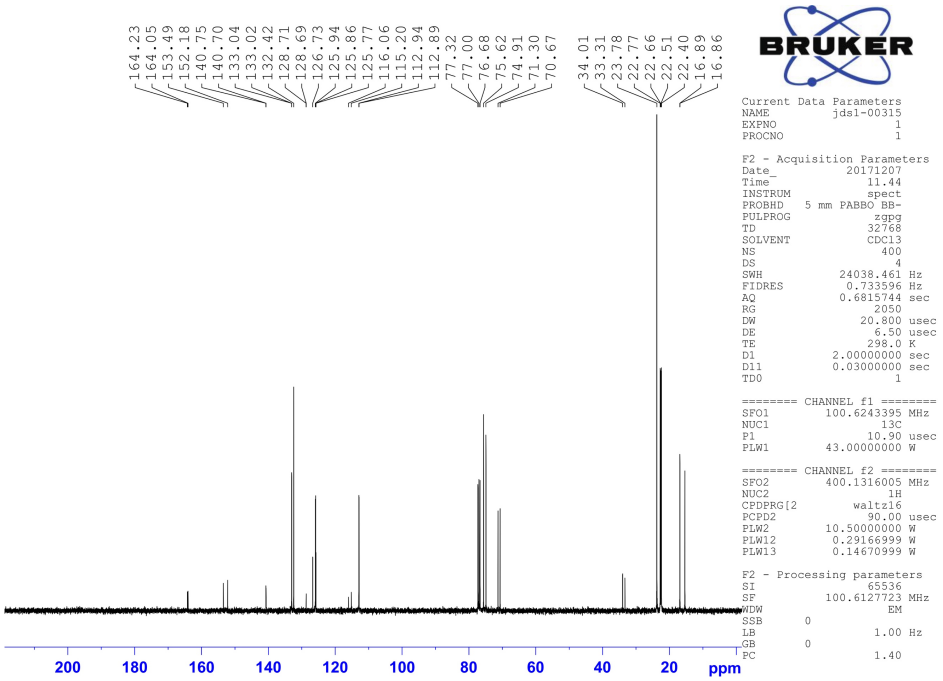

Figure 3.102 ^{13}C NMR (100 MHz, $CDCl_3$) of compound **3.35b**.

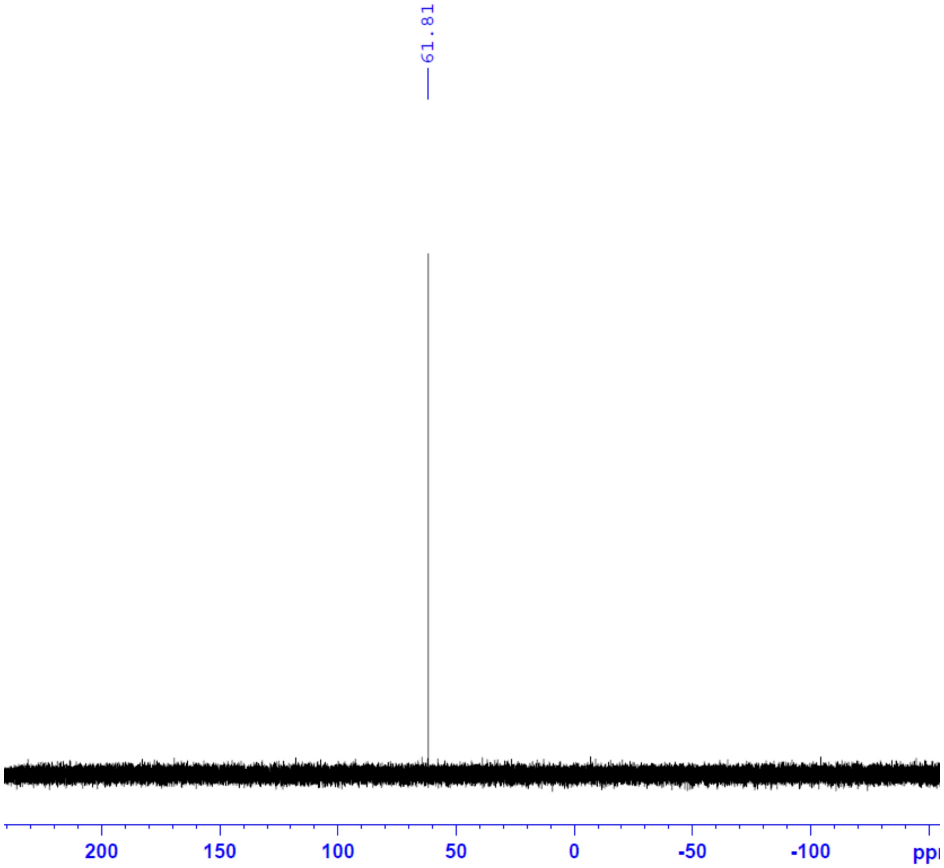

Figure 3.103 ^{31}P NMR (202 MHz, $CDCl_3$) of compound **3.35b**.

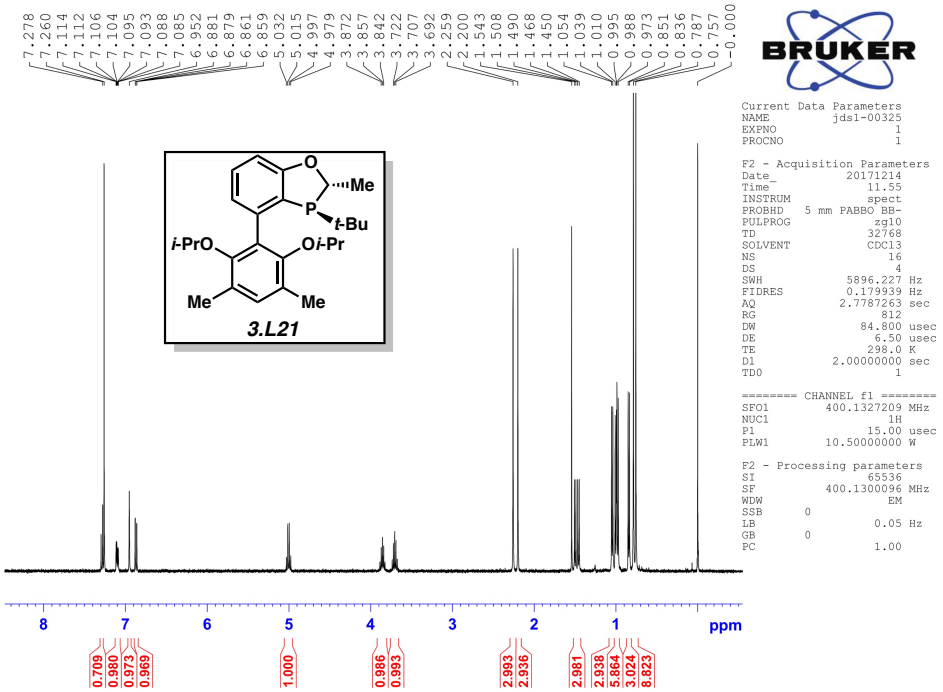

Figure 3.104 ^{1}H NMR (400 MHz, $CDCl_3$) of compound **3.L21**.

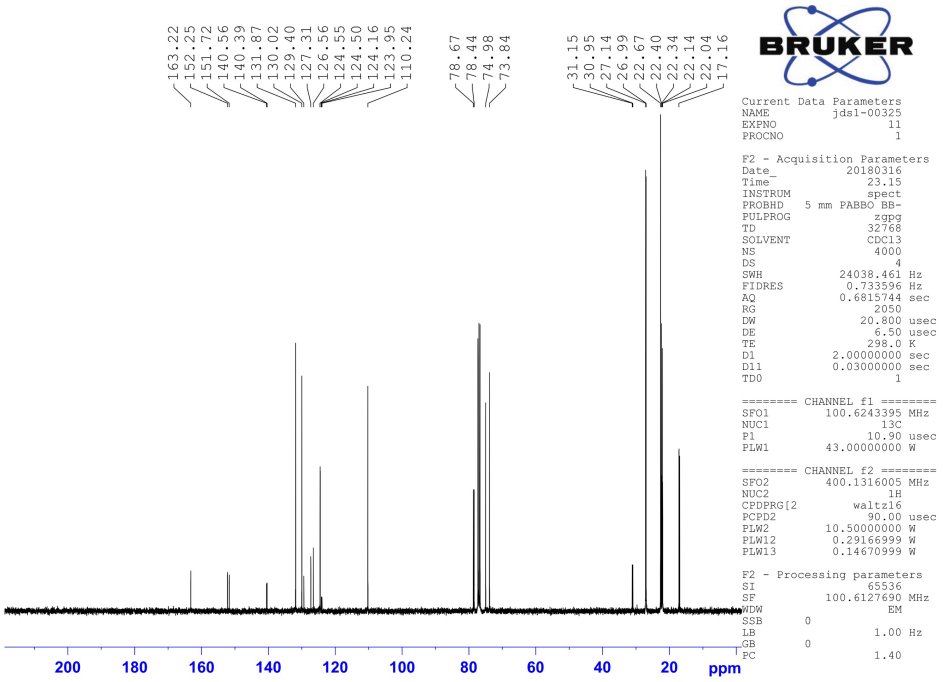

Figure 3.105 ^{13}C NMR (100 MHz, $CDCl_3$) of compound **3.L21**.

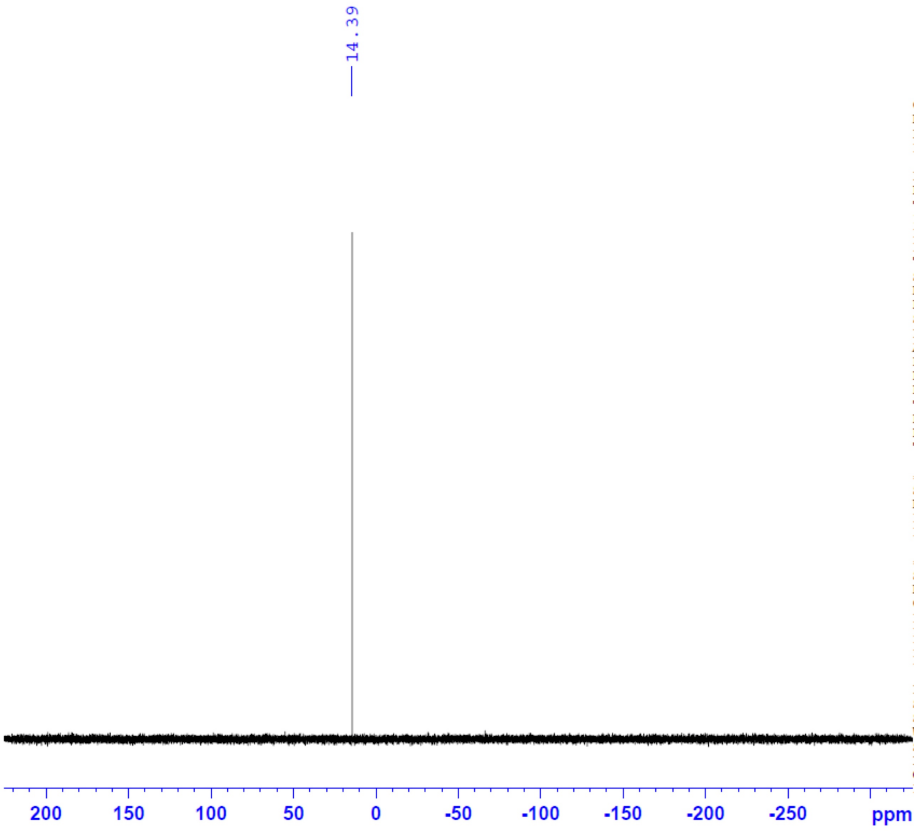

Figure 3.106 ^{31}P NMR (202 MHz, $CDCl_3$) of compound **3.L21**.

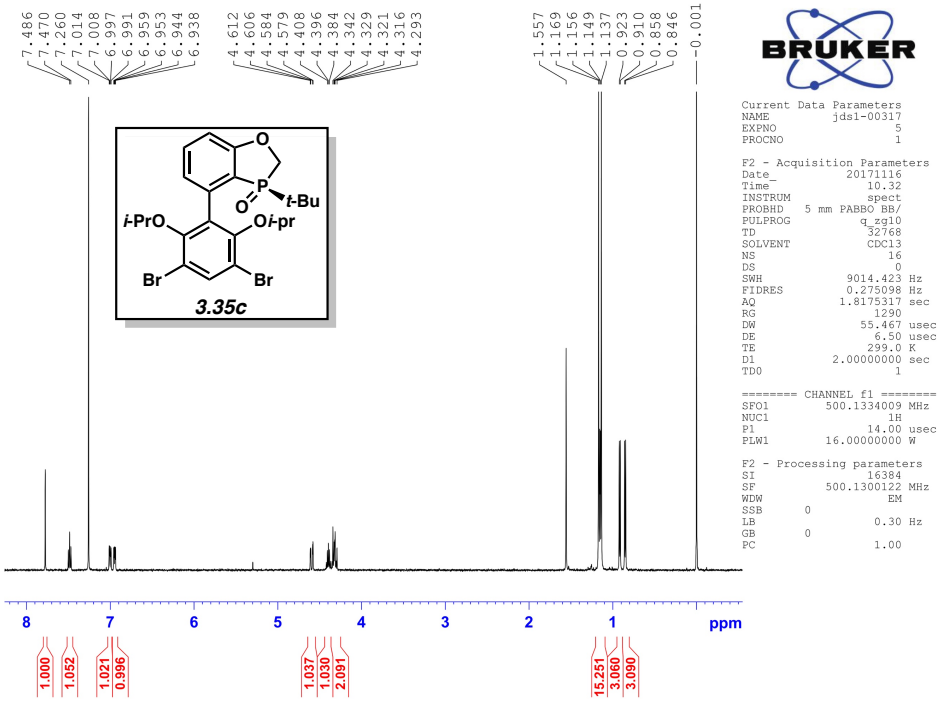

Figure 3.107 ^{1}H NMR (500 MHz, $CDCl_3$) of compound **3.35c**.

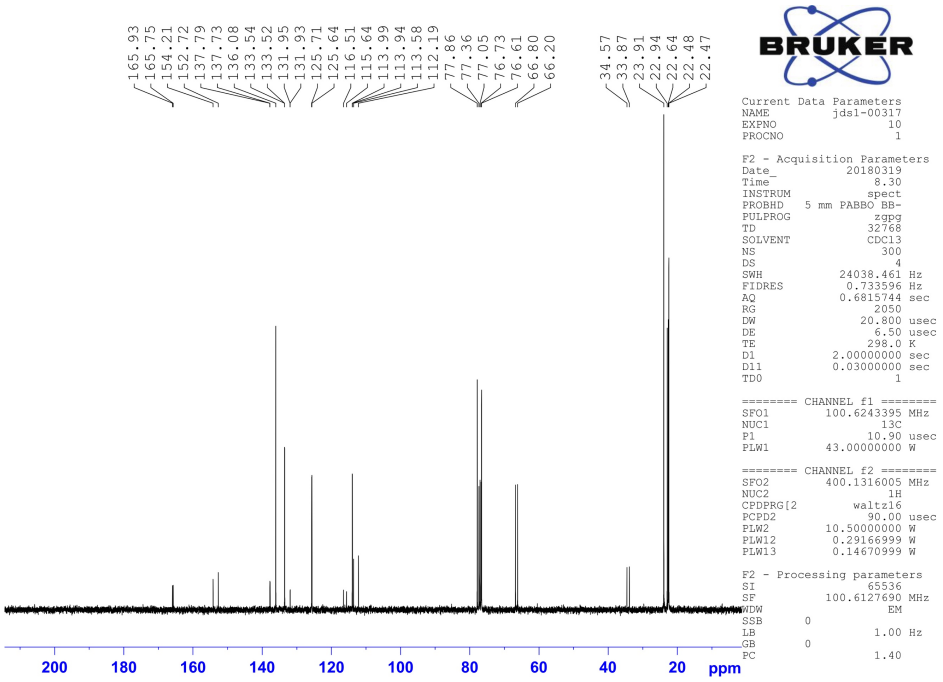

Figure 3.108 ^{13}C NMR (100 MHz, $CDCl_3$) of compound **3.35c**.

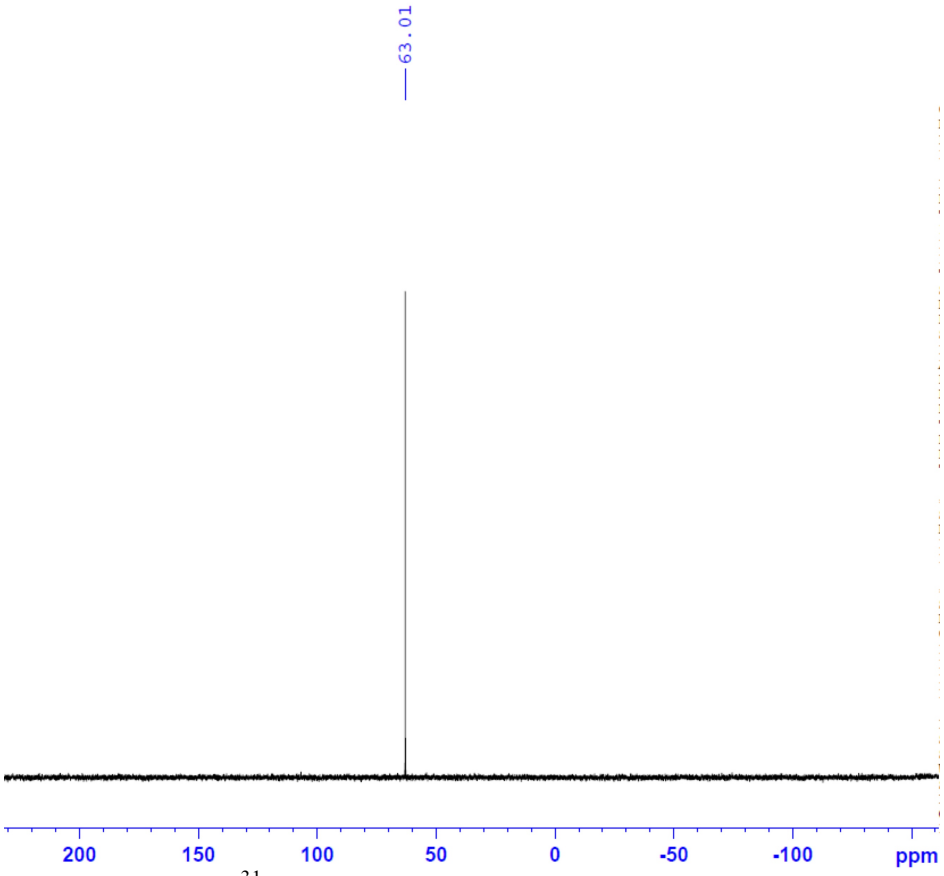

Figure 3.109 ^{31}P NMR (202 MHz, $CDCl_3$) of compound **3.35c**.

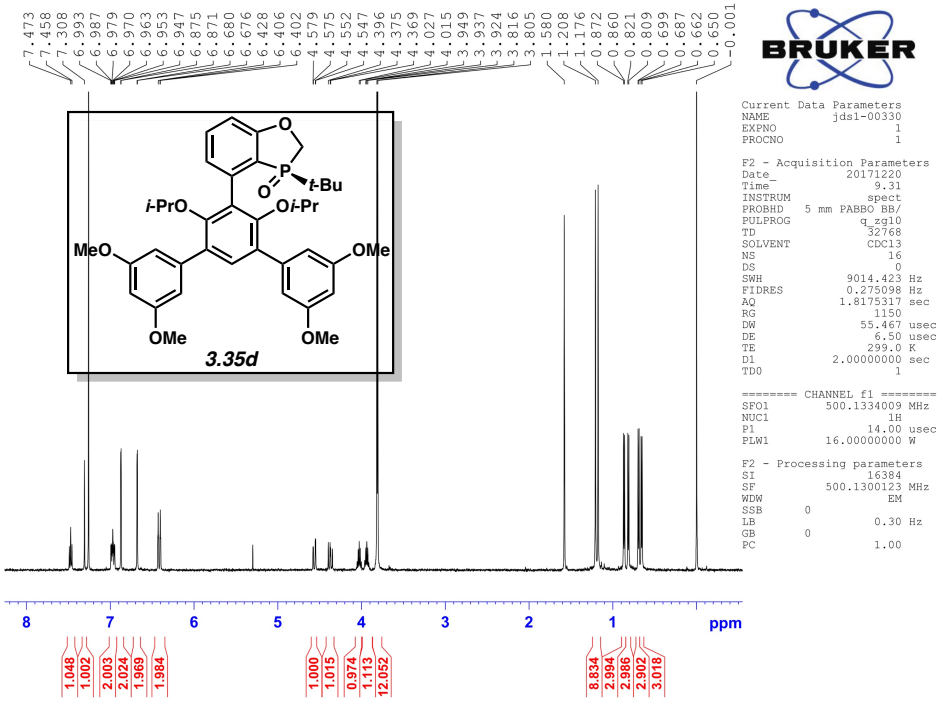

Figure 3.110 ^{1}H NMR (500 MHz, $CDCl_3$) of compound **3.35d**.

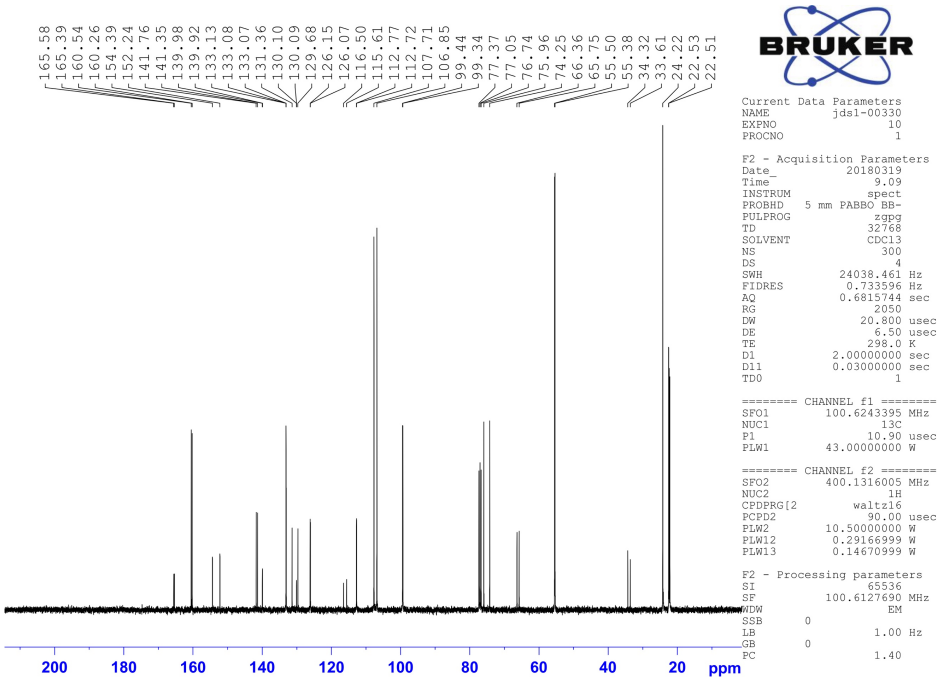

Figure 3.111 ^{13}C NMR (100 MHz, $CDCl_3$) of compound **3.35d**.

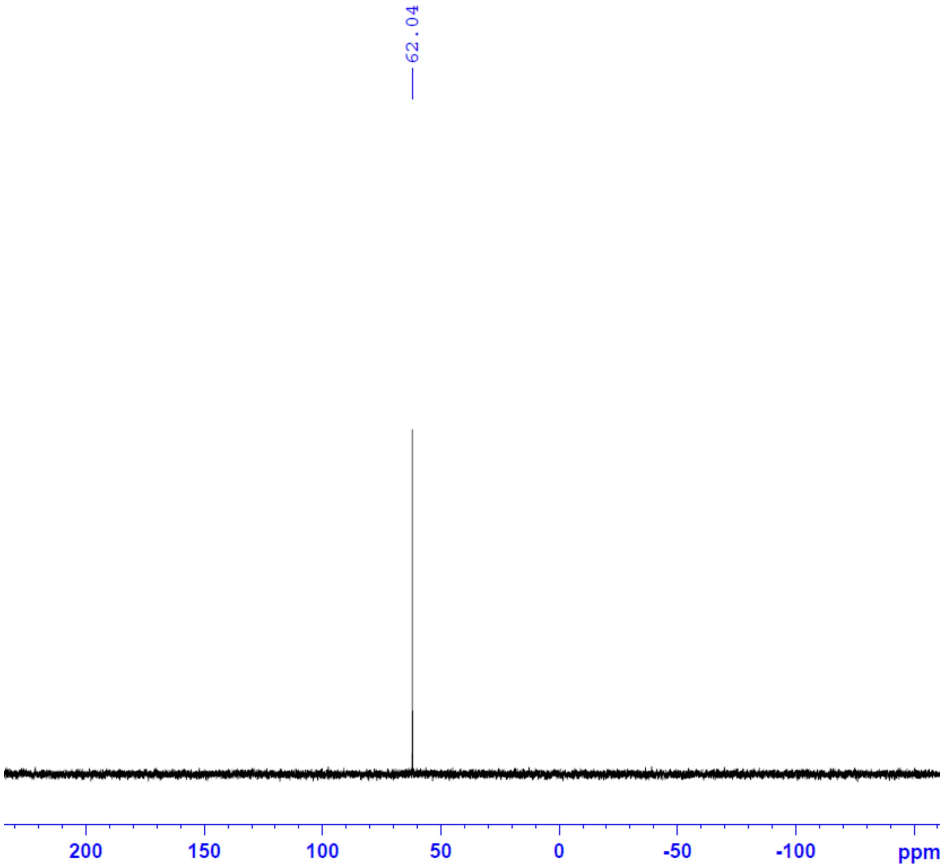

Figure 3.112 ^{31}P NMR (202 MHz, $CDCl_3$) of compound **3.35d**.

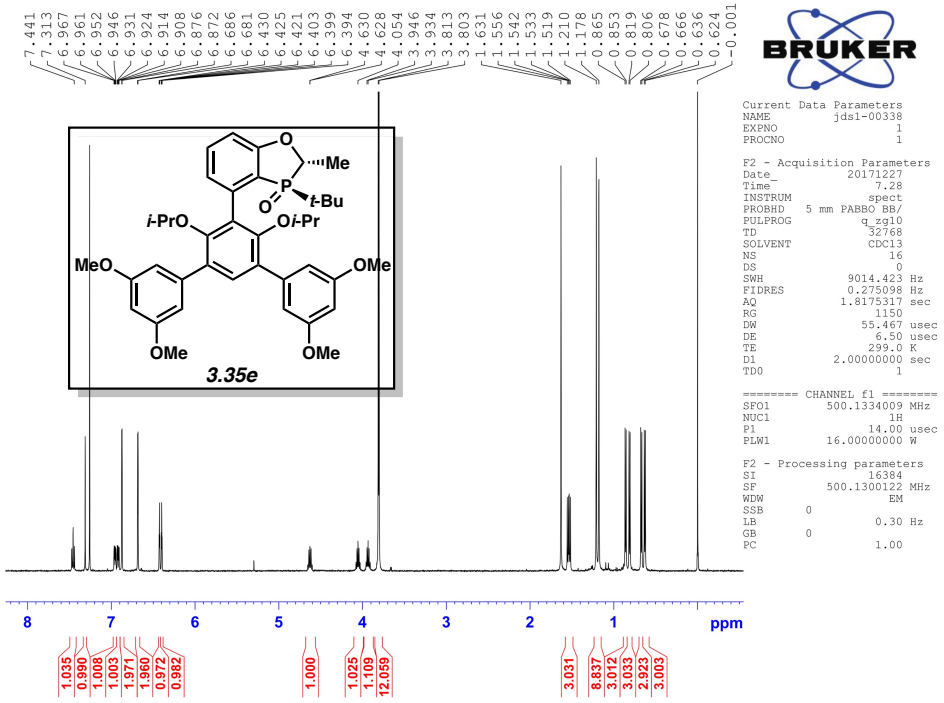

Figure 3.113 ^{1}H NMR (500 MHz, $CDCl_3$) of compound **3.35e**.

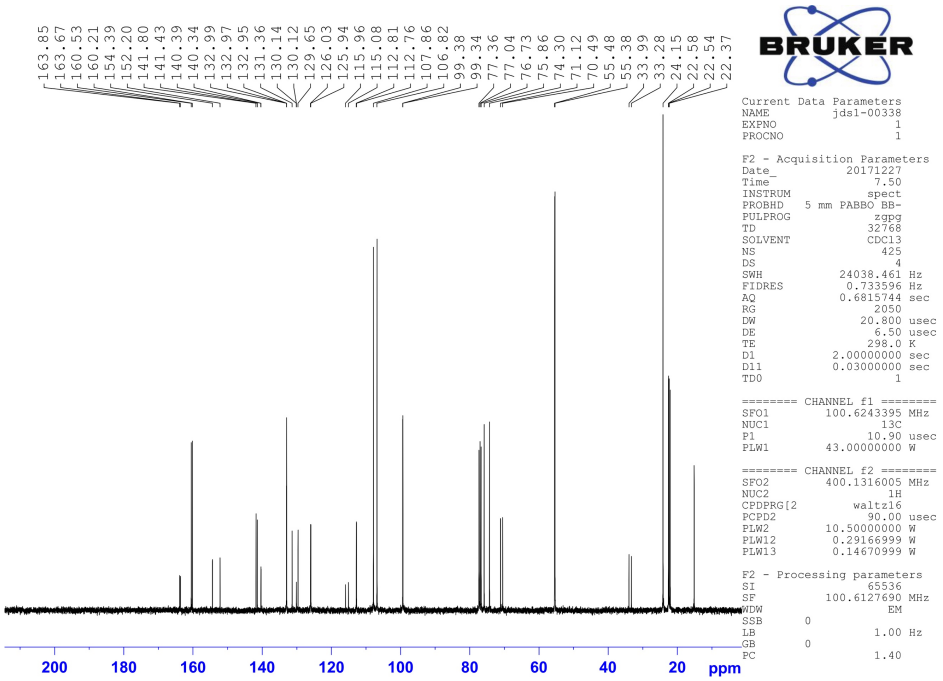

Figure 3.114 ^{13}C NMR (100 MHz, $CDCl_3$) of compound **3.35e**.

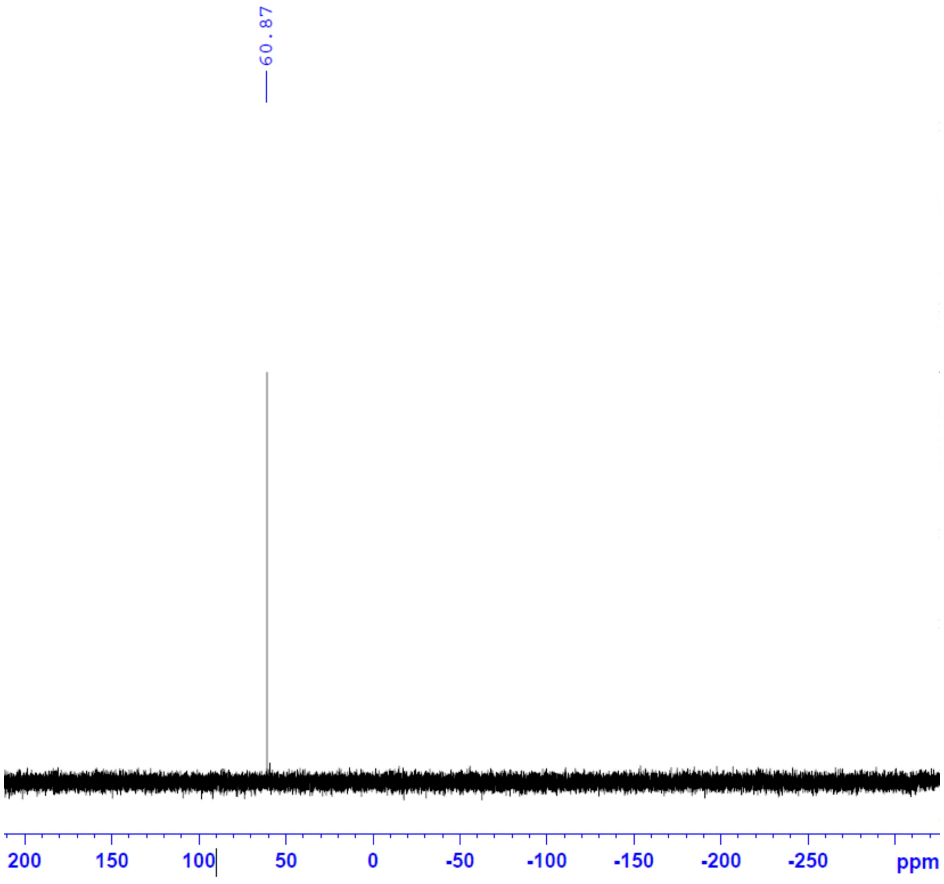

Figure 3.115 ^{31}P NMR (162 MHz, $CDCl_3$) of compound **3.35e**.

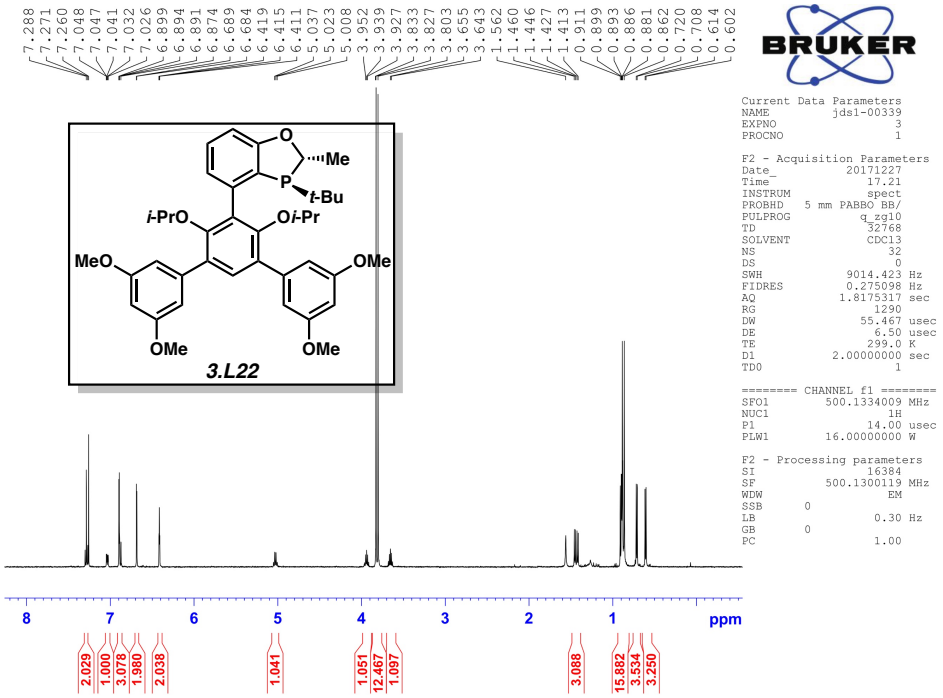

Figure 3.116 ^{1}H NMR (500 MHz, $CDCl_3$) of compound **3.L22**.

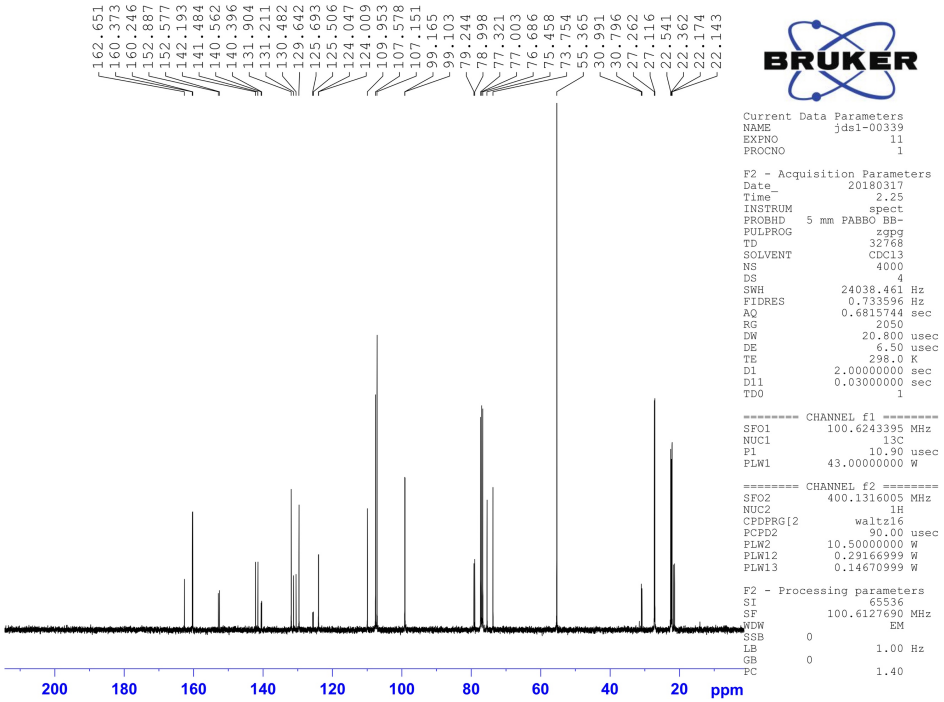

Figure 3.117 ^{13}C NMR (100 MHz, $CDCl_3$) of compound **3.L22**.

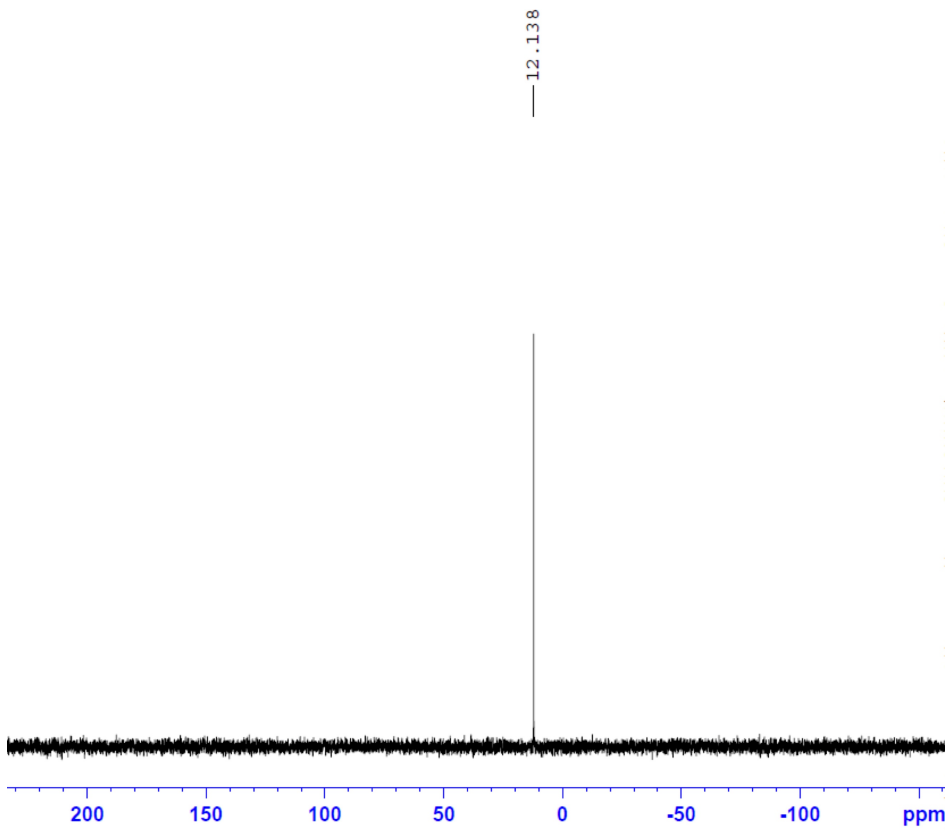

Figure 3.118 ^{13}P NMR (202 MHz, $CDCl_3$) of compound **3.L22**.

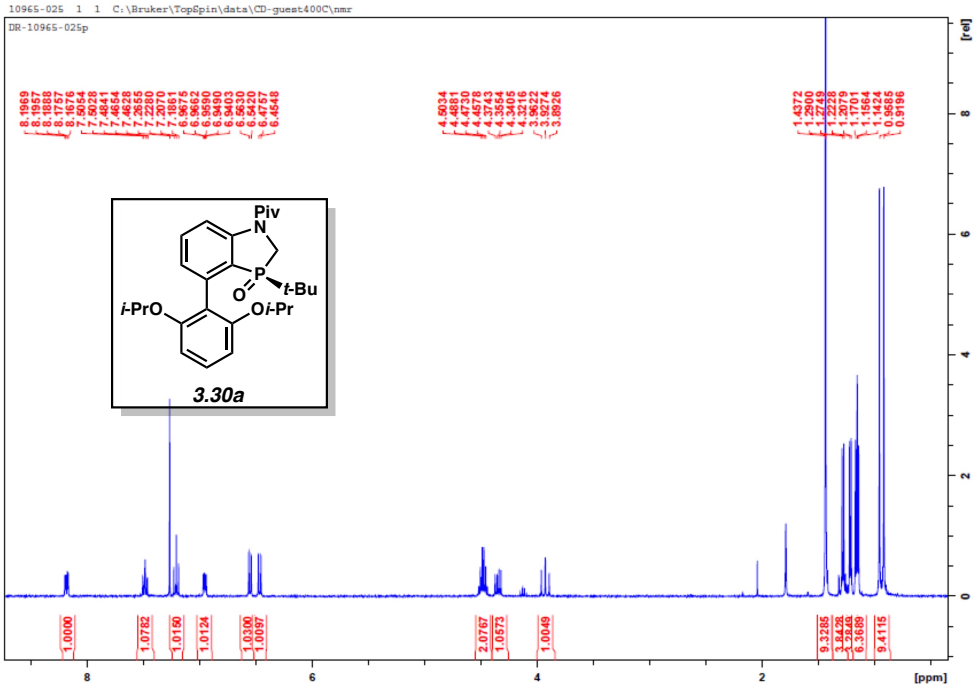

Figure 3.119 ^{1}H NMR (500 MHz, $CDCl_3$) of compound **3.30a**.

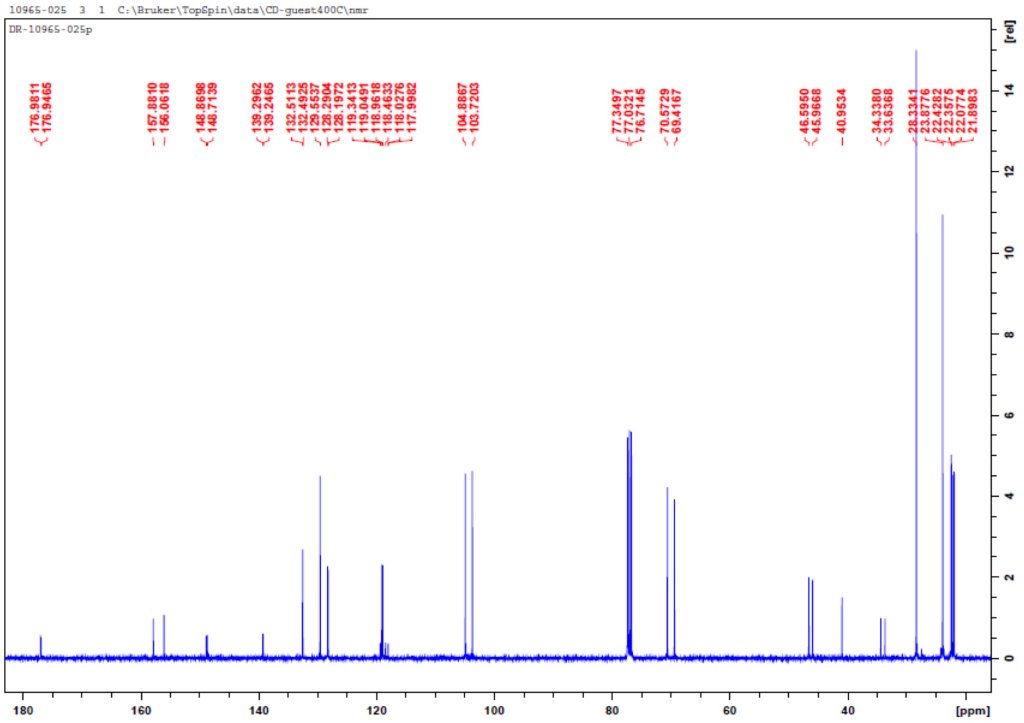

Figure 3.120 ^{13}C NMR (100 MHz, $CDCl_3$) of compound **3.30a**.

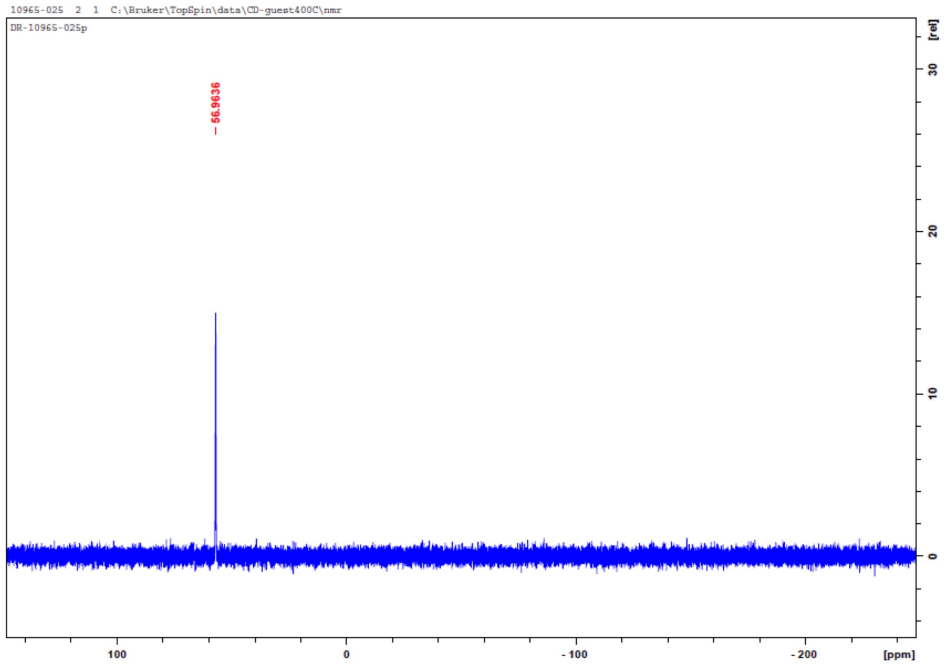

Figure 3.121 ^{31}P NMR (202 MHz, $CDCl_3$) of compound **3.30a**.

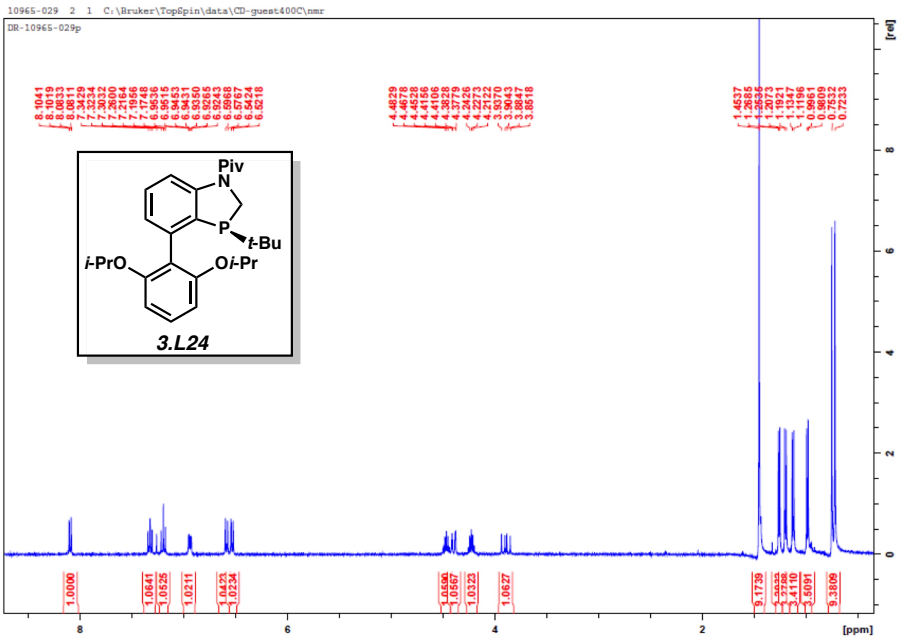

Figure 3.122 ^{1}H NMR (400 MHz, $CDCl_3$) of compound **3.L24**.

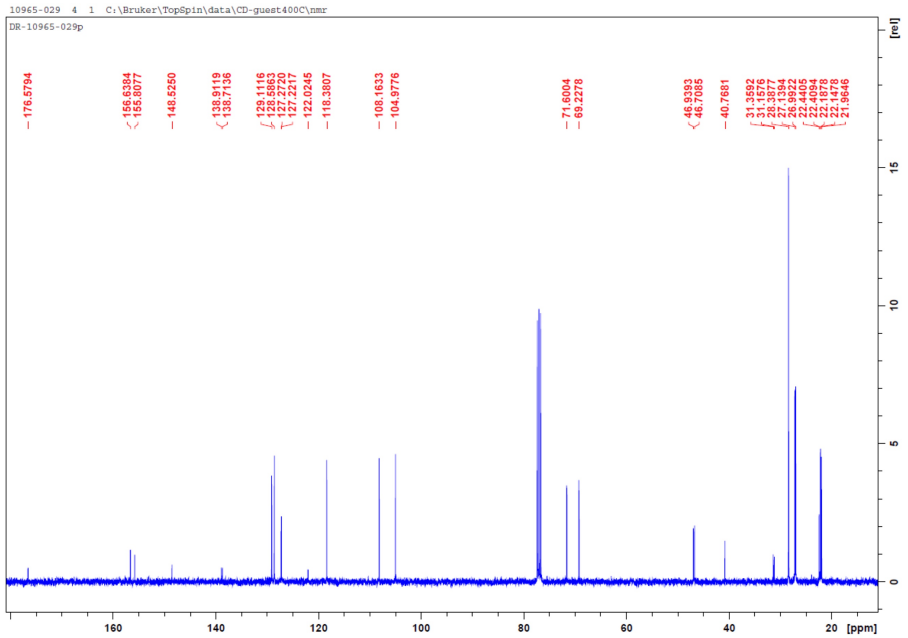

Figure 3.123 ^{13}C NMR (100 MHz, $CDCl_3$) of compound **3.L24**.

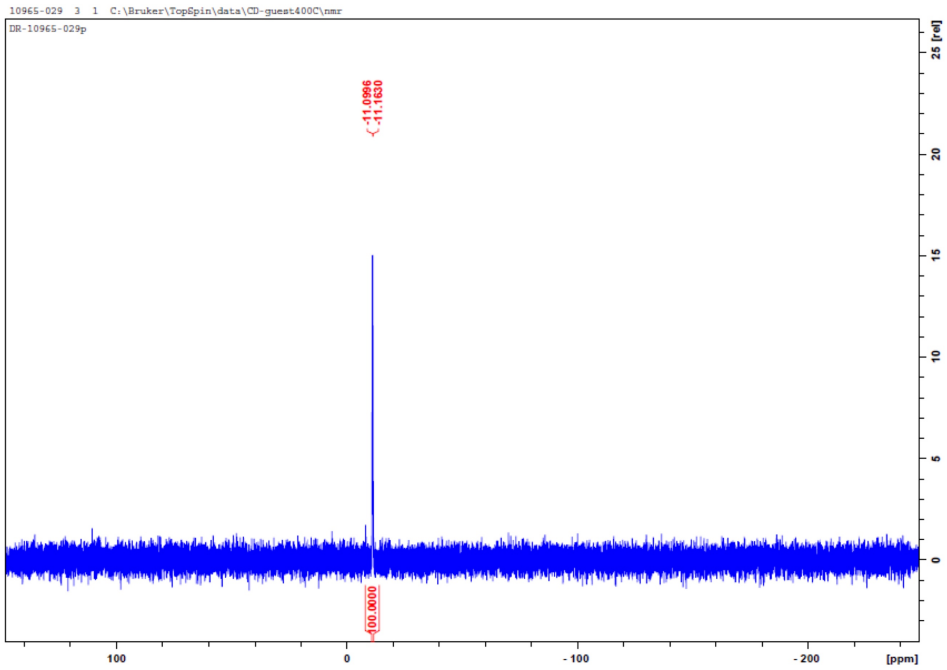

Figure 3.124 ^{31}P NMR (202 MHz, $CDCl_3$) of compound **3.L24**.

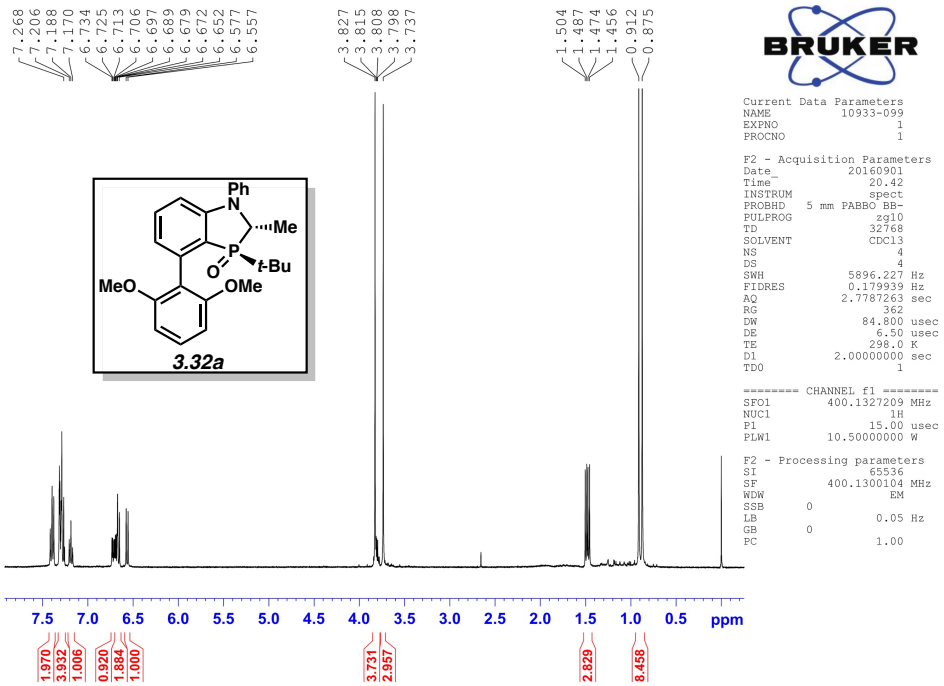

Figure 3.125 ^{1}H NMR (400 MHz, $CDCl_3$) of compound **3.32a**.

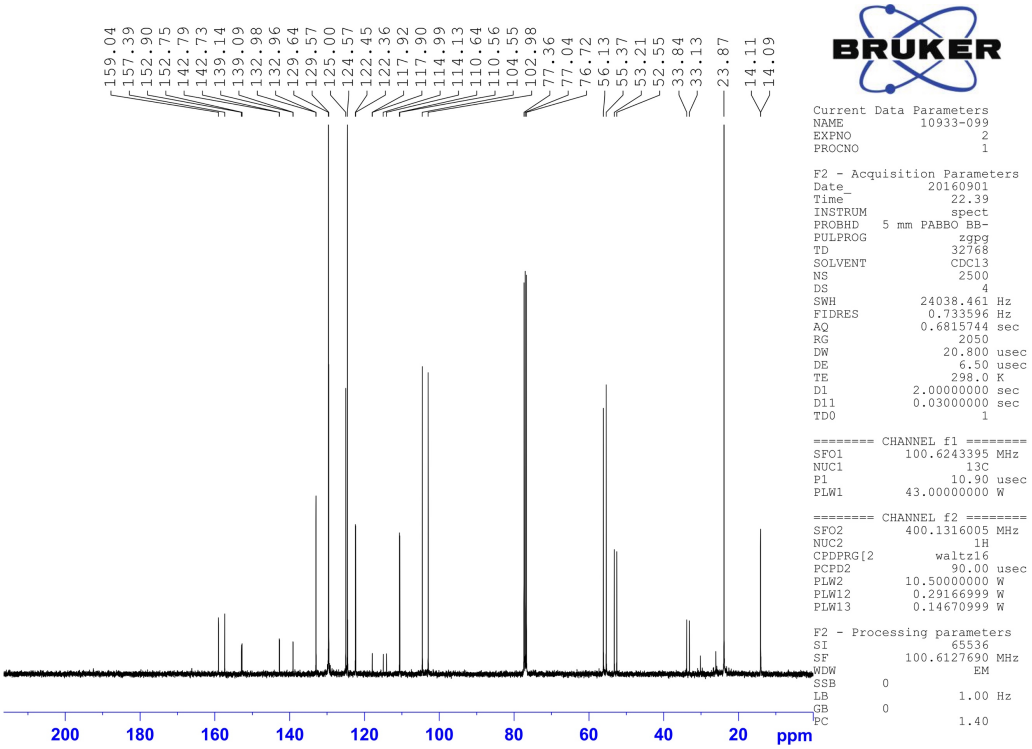

Figure 3.126 ^{13}C NMR (100 MHz, $CDCl_3$) of compound **3.32a**.

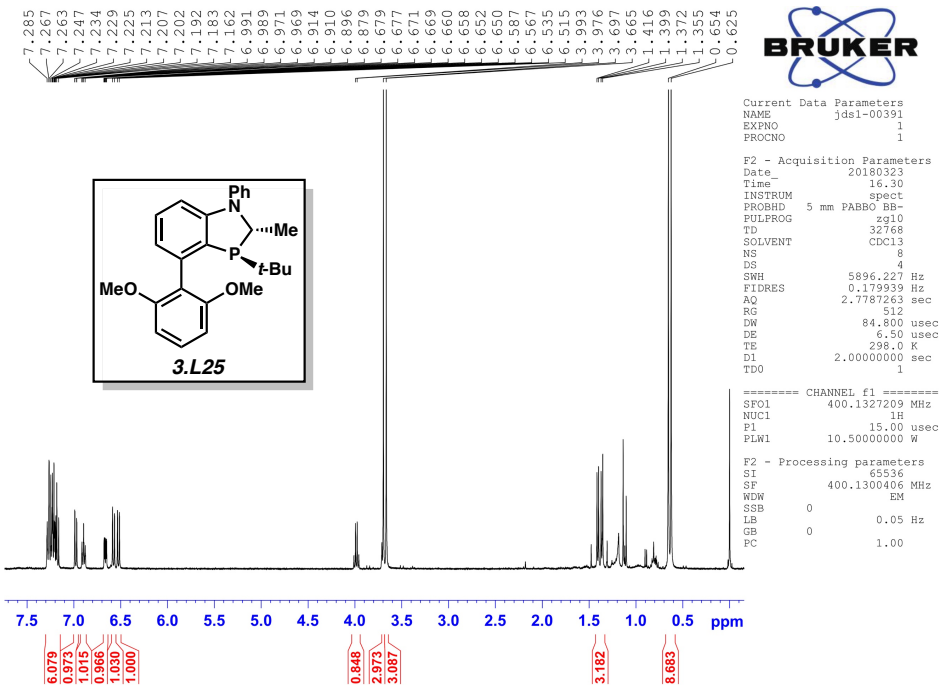

Figure 3.127 ^{1}H NMR (400 MHz, $CDCl_3$) of compound **3.L25**.

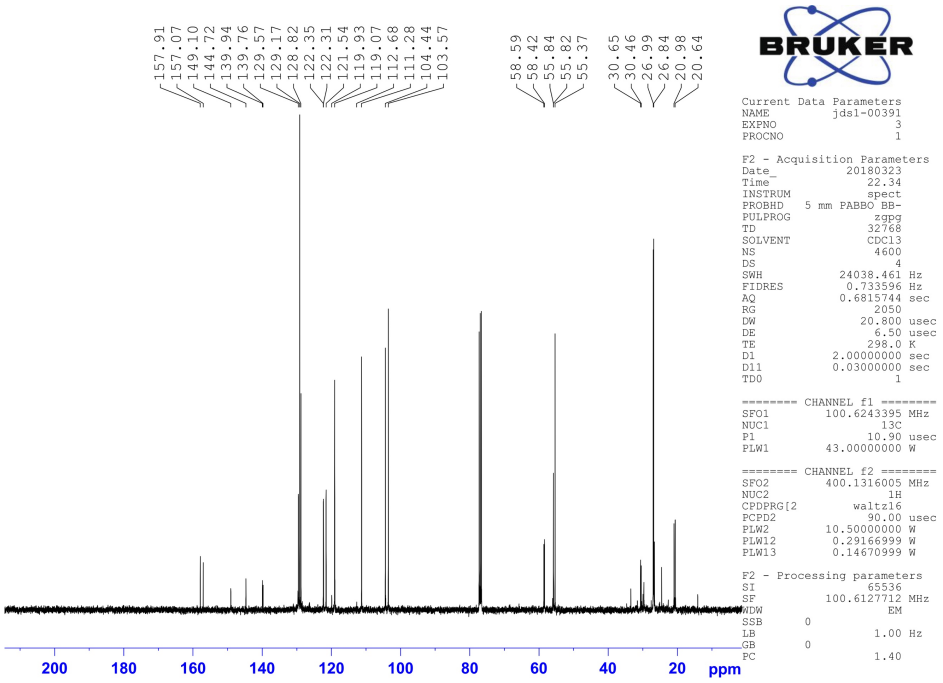

Figure 3.128 ^{13}C NMR (100 MHz, $CDCl_3$) of compound **3.L25**.

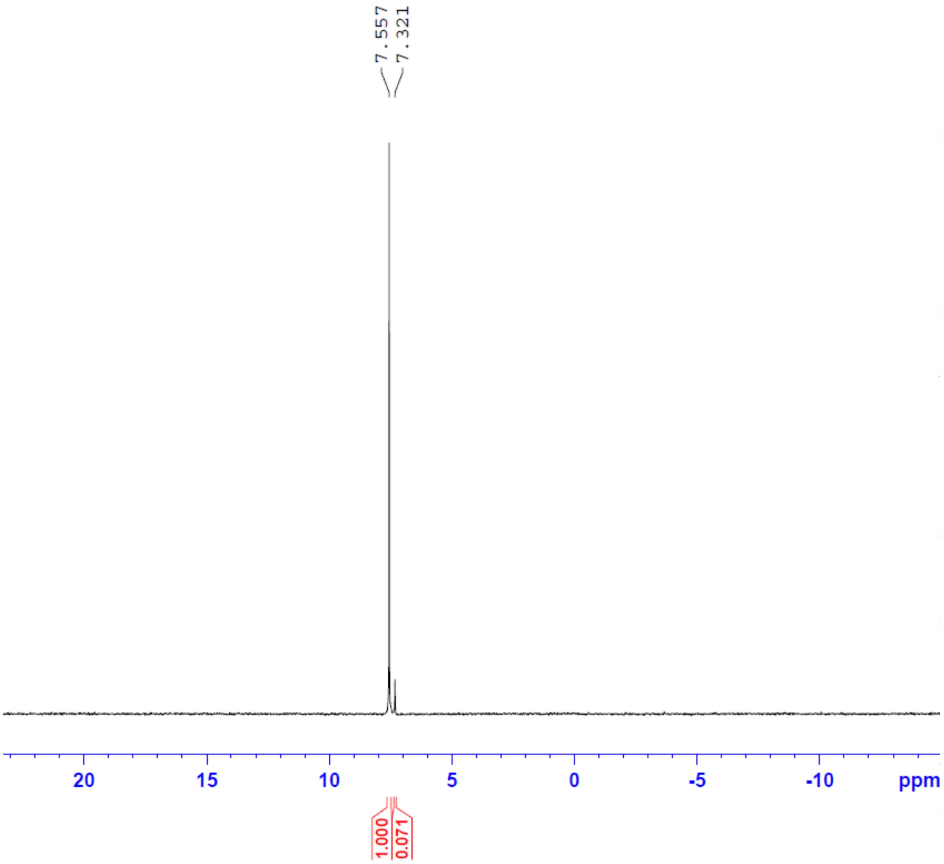

Figure 3.129 ^{31}P NMR (162 MHz, $CDCl_3$) of compound **3.L25**.

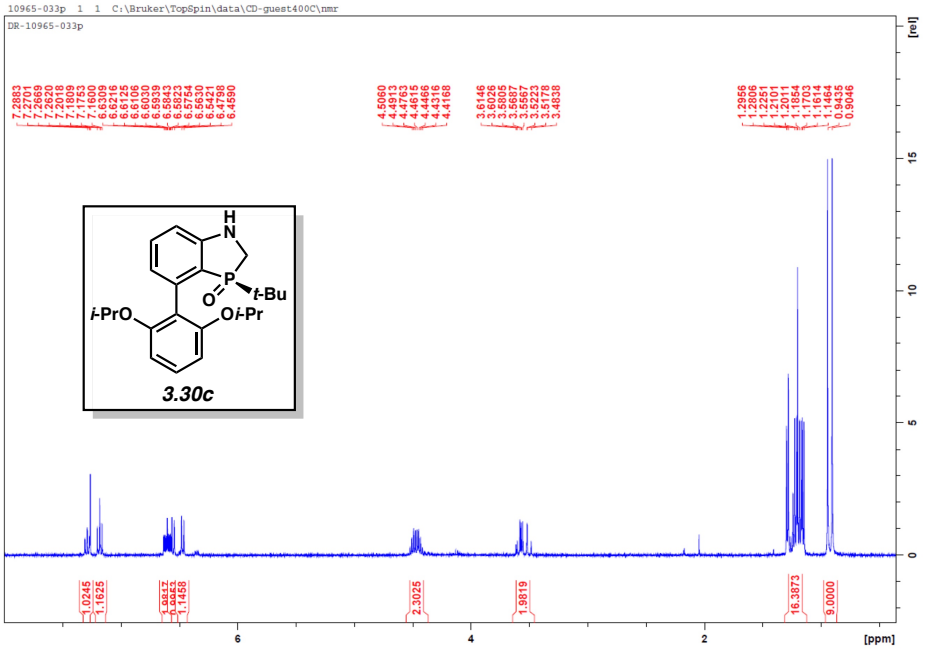

Figure 3.130 ^{1}H NMR (500 MHz, $CDCl_3$) of compound **3.30c**.

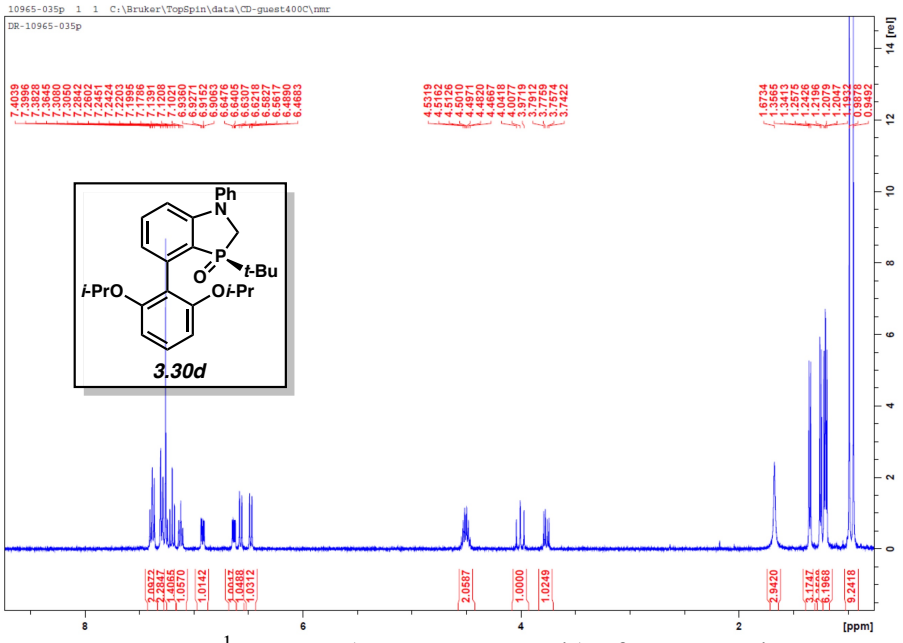

Figure 3.131 ^{1}H NMR (500 MHz, $CDCl_3$) of compound **3.30d**.

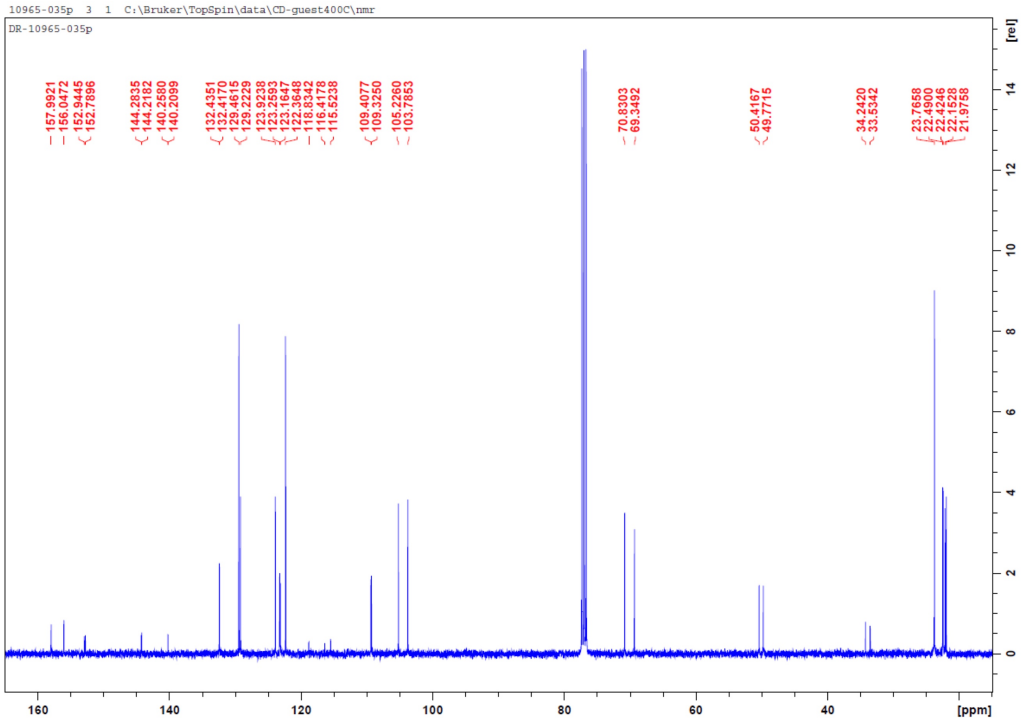

Figure 3.132 ^{13}C NMR (100 MHz, $CDCl_3$) of compound **3.30d**.

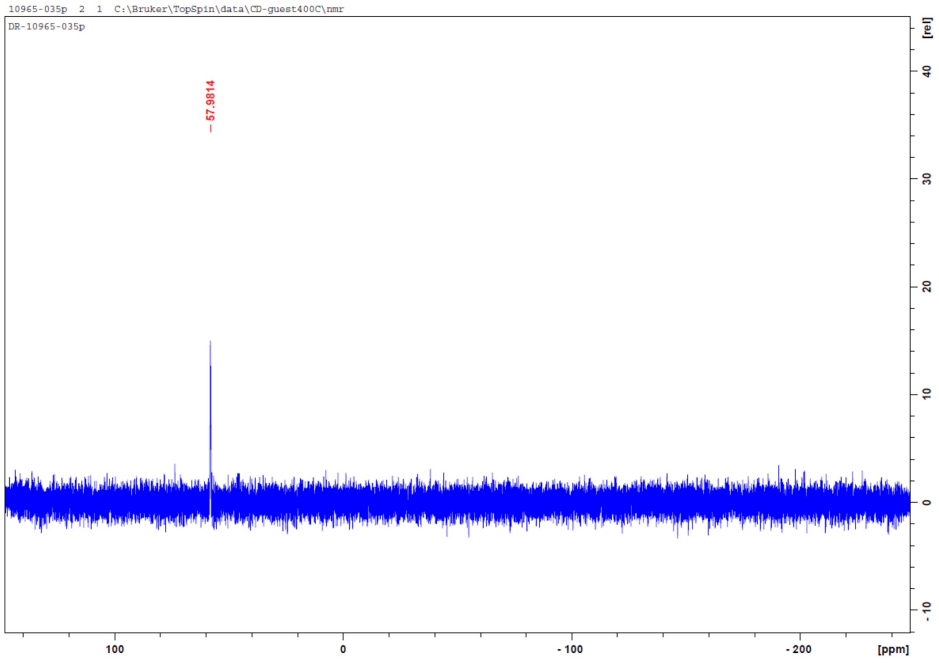

Figure 3.133 ^{31}P NMR (202 MHz, $CDCl_3$) of compound **3.30d**.

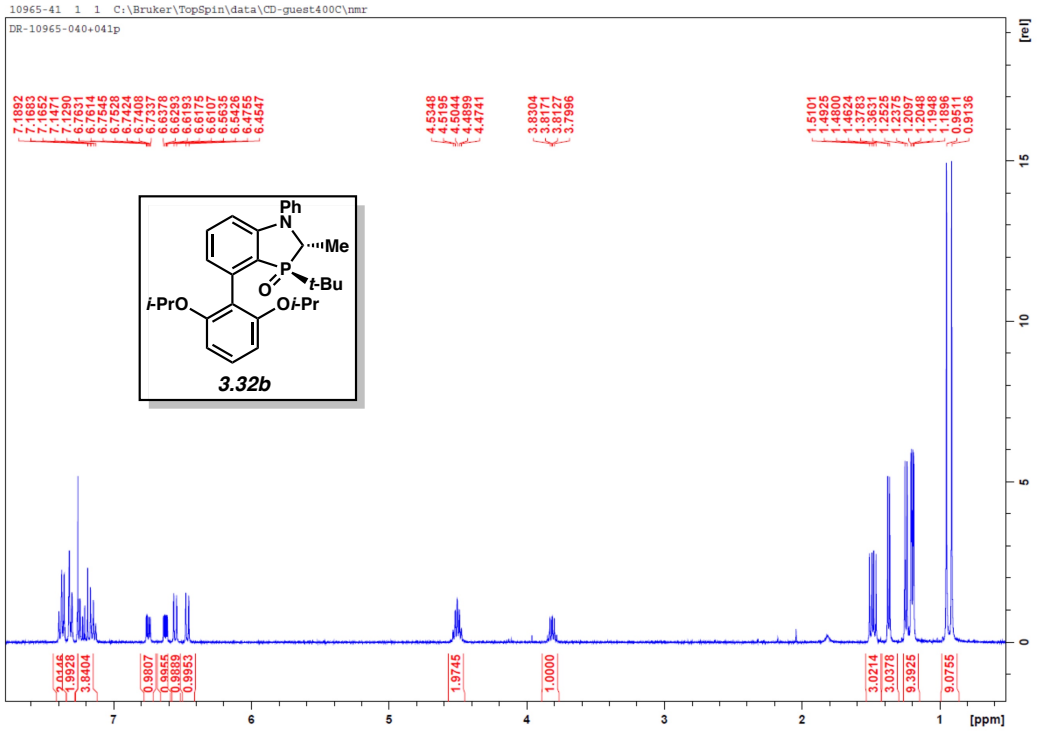

Figure 3.134 ^{1}H NMR (500 MHz, $CDCl_3$) of compound **3.32b**.

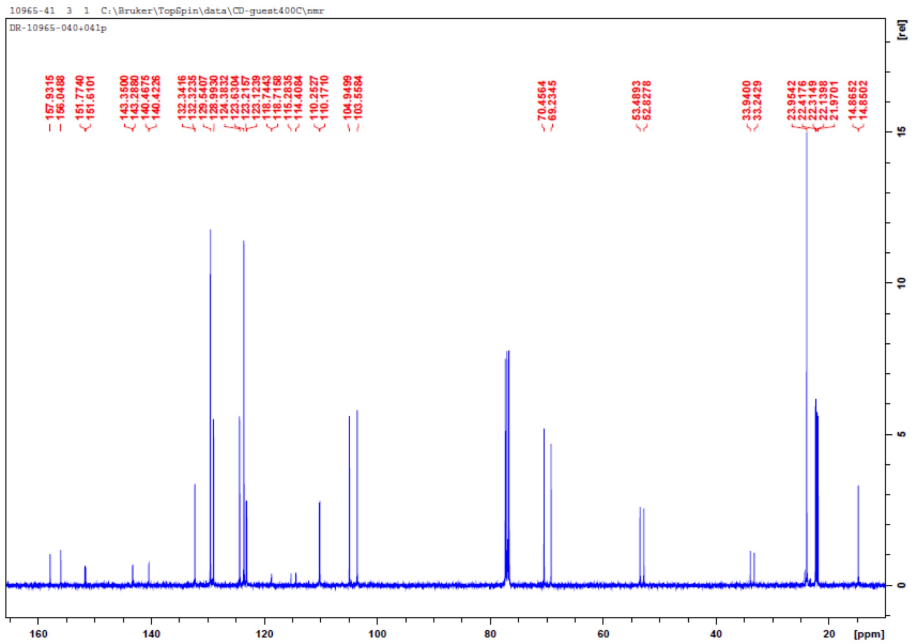

Figure 3.135 ^{13}C NMR (100 MHz, $CDCl_3$) of compound **3.32b**.

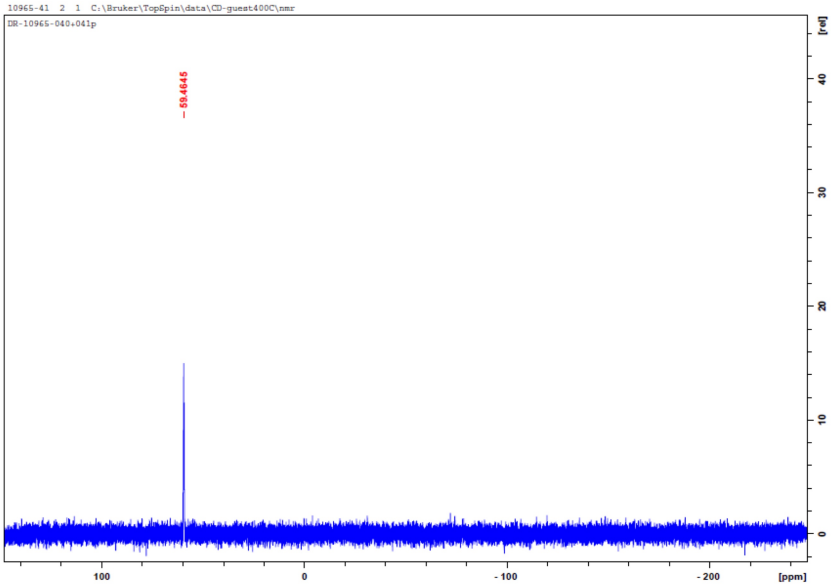

Figure 3.136 ^{31}P NMR (202 MHz, $CDCl_3$) of compound **3.32b**.

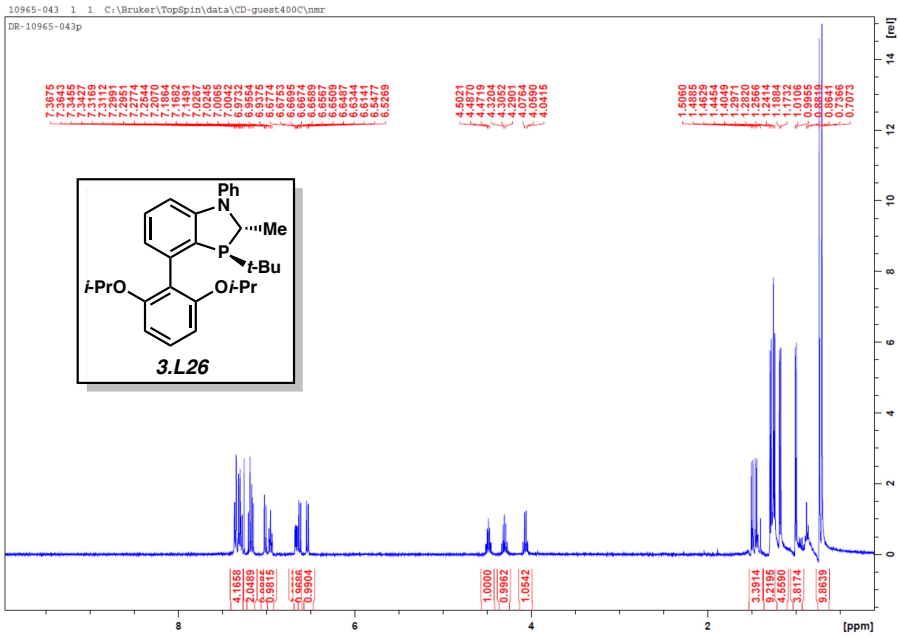

Figure 3.137 ^{1}H NMR (400 MHz, $CDCl_3$) of compound **3.L26**.

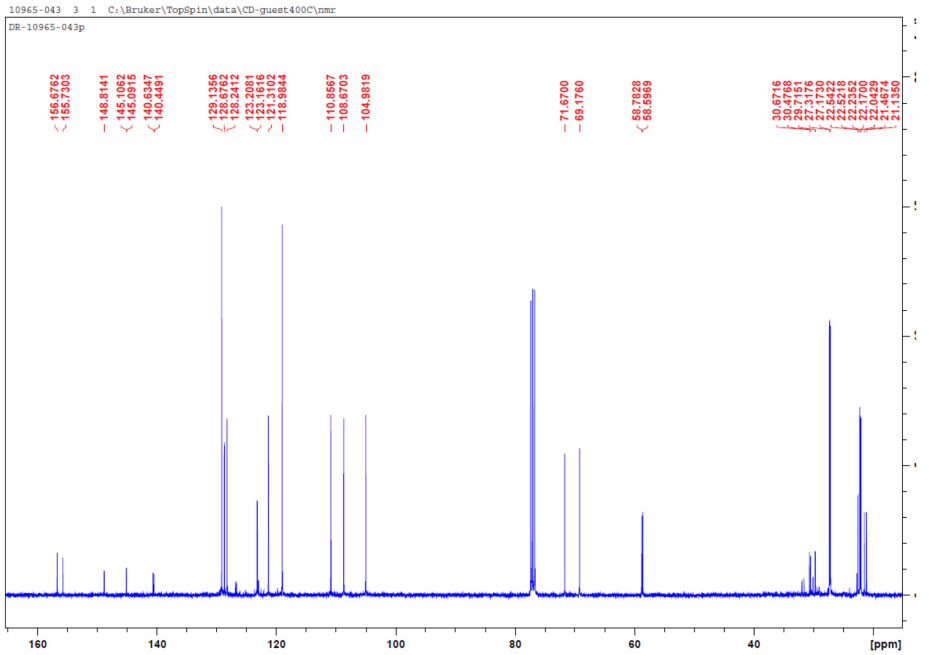

Figure 3.138 ^{13}C NMR (100 MHz, $CDCl_3$) of compound **3.L26**.

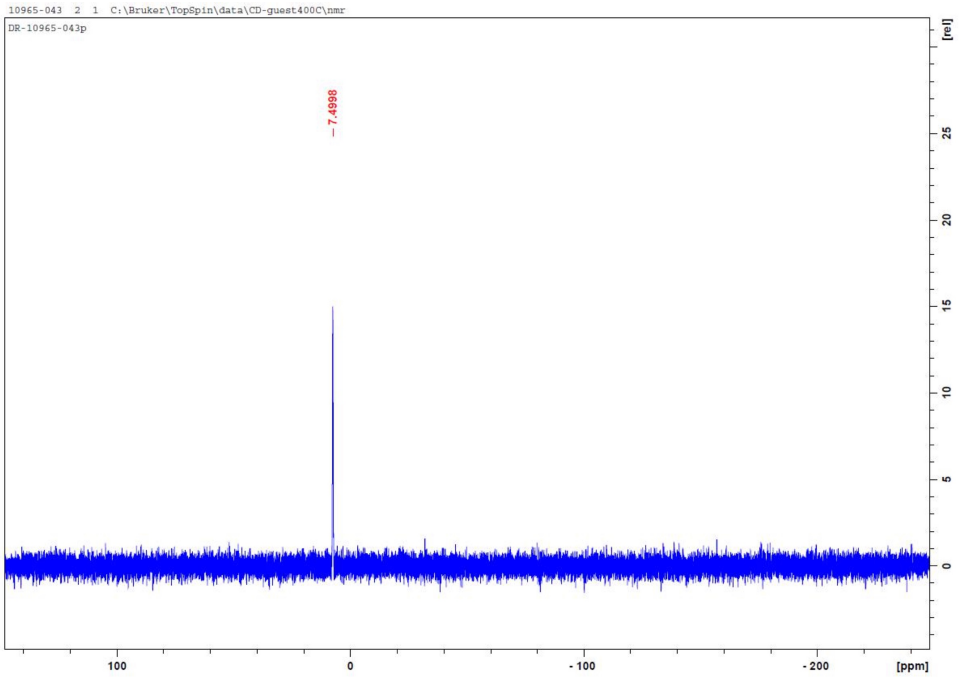

Figure 3.139 ^{31}P NMR (202 MHz, $CDCl_3$) of compound **3.L26**.

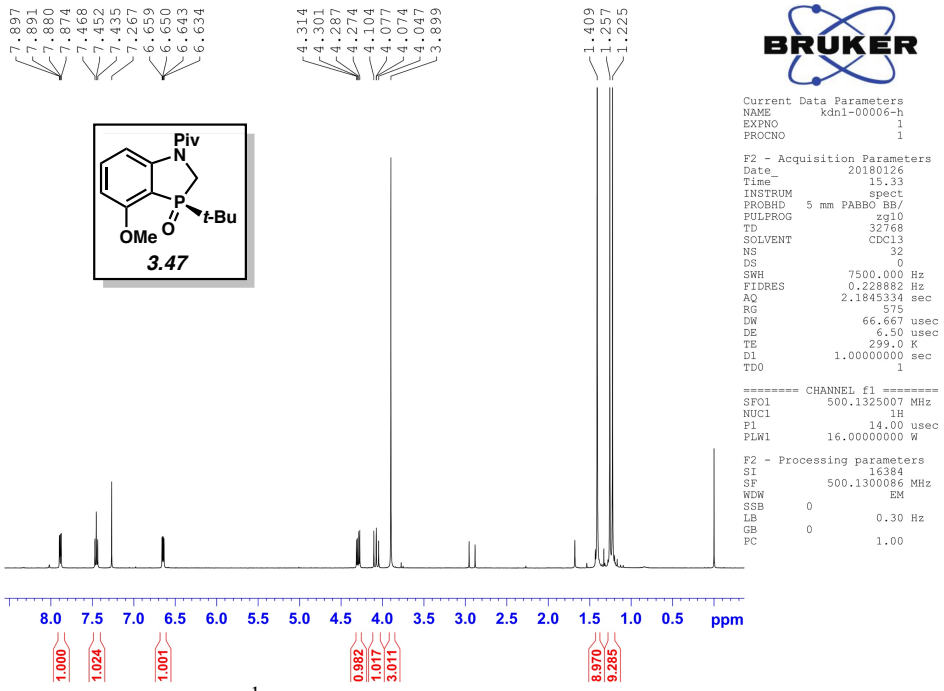

Figure 3.140 ^{1}H NMR (500 MHz, $CDCl_3$) of compound **3.47**.

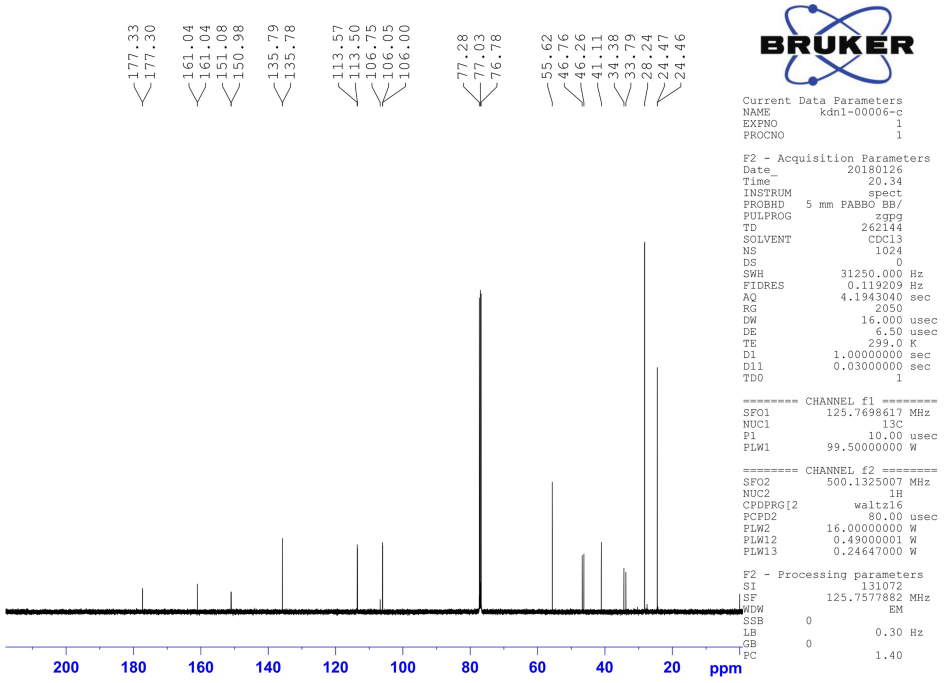

Figure 3.141 ^{13}C NMR (125 MHz, $CDCl_3$) of compound **3.47**.

Figure 3.142 ^{31}P NMR (202 MHz, $CDCl_3$) of compound **3.47**.

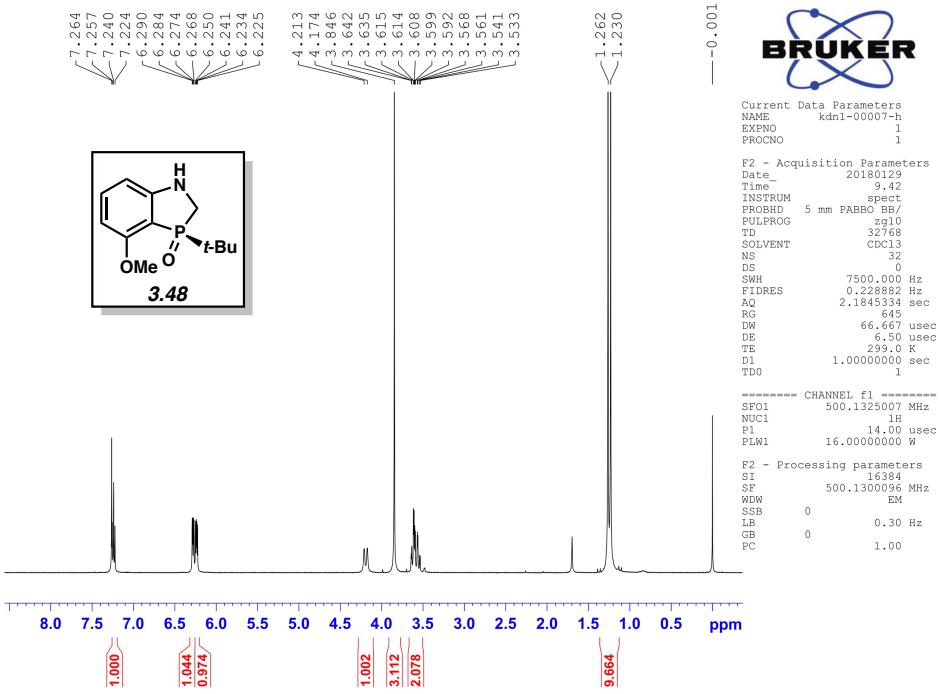

Figure 3.143 ^{1}H NMR (500 MHz, $CDCl_3$) of compound **3.48**.

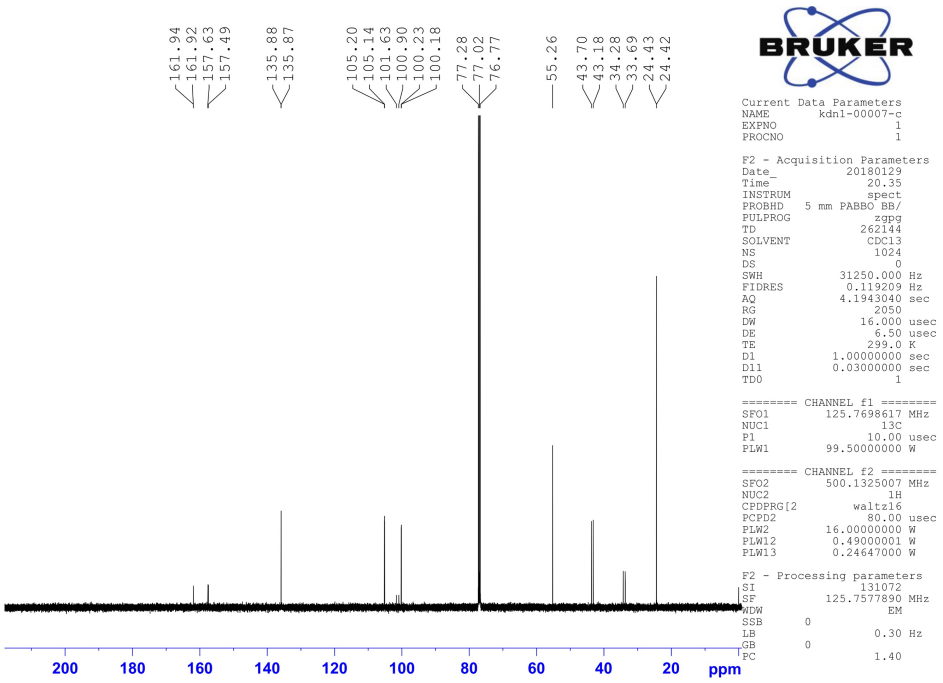

Figure 3.144 ^{13}C NMR (125 MHz, $CDCl_3$) of compound **3.48**.

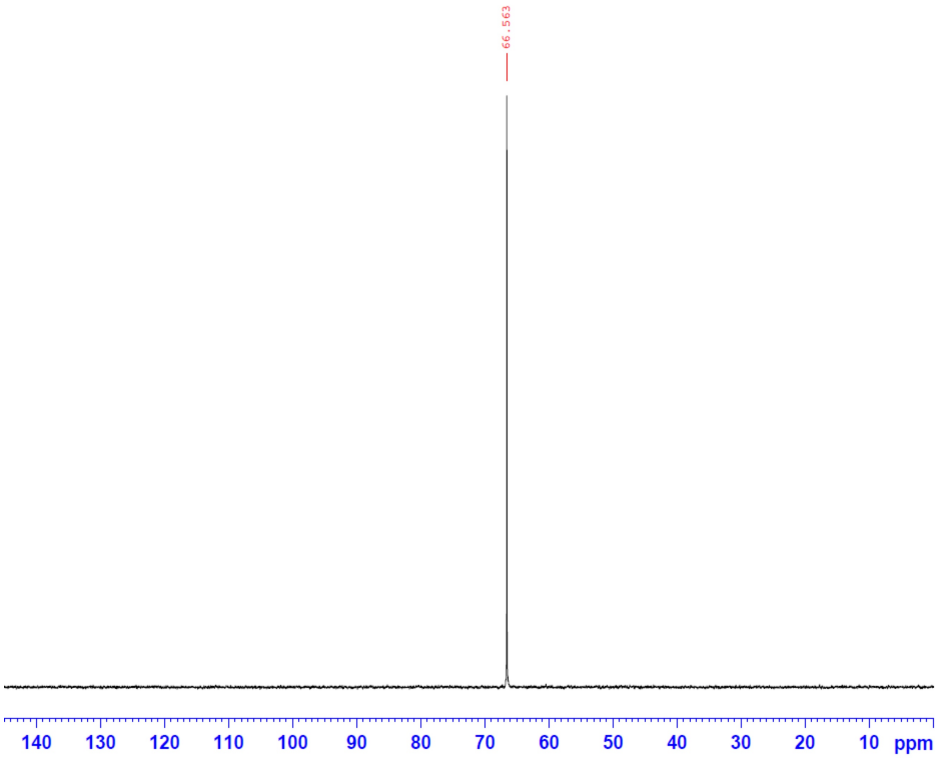

Figure 3.145 ^{31}P NMR (202 MHz, $CDCl_3$) of compound **3.48**.

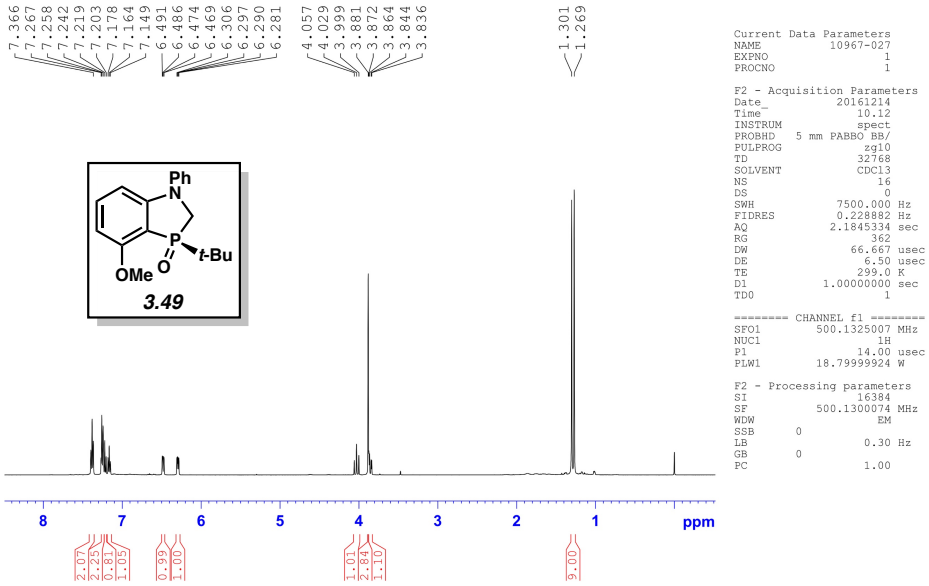

Figure 3.146 ^{1}H NMR (500 MHz, $CDCl_3$) of compound **3.49**.

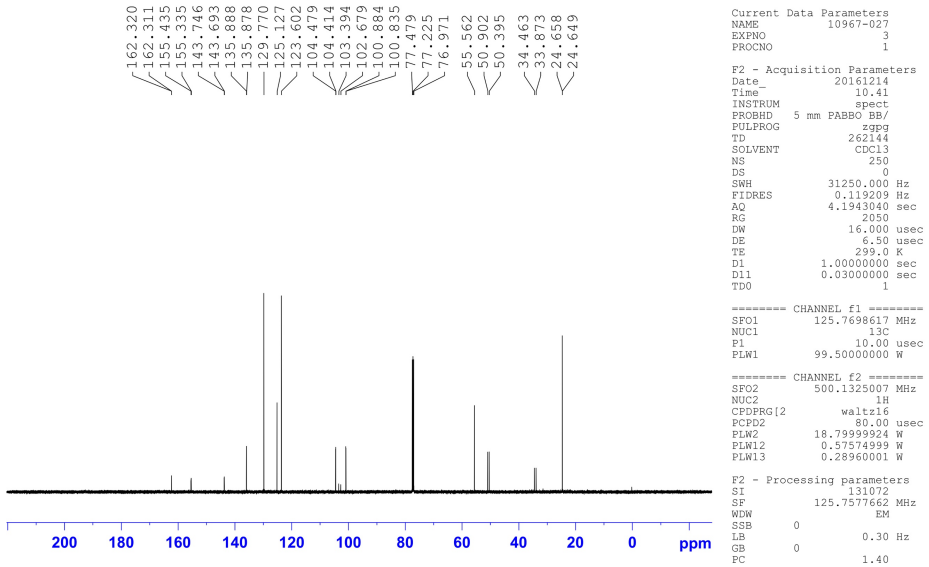

Figure 3.147 ^{13}C NMR (125 MHz, $CDCl_3$) of compound **3.49.**

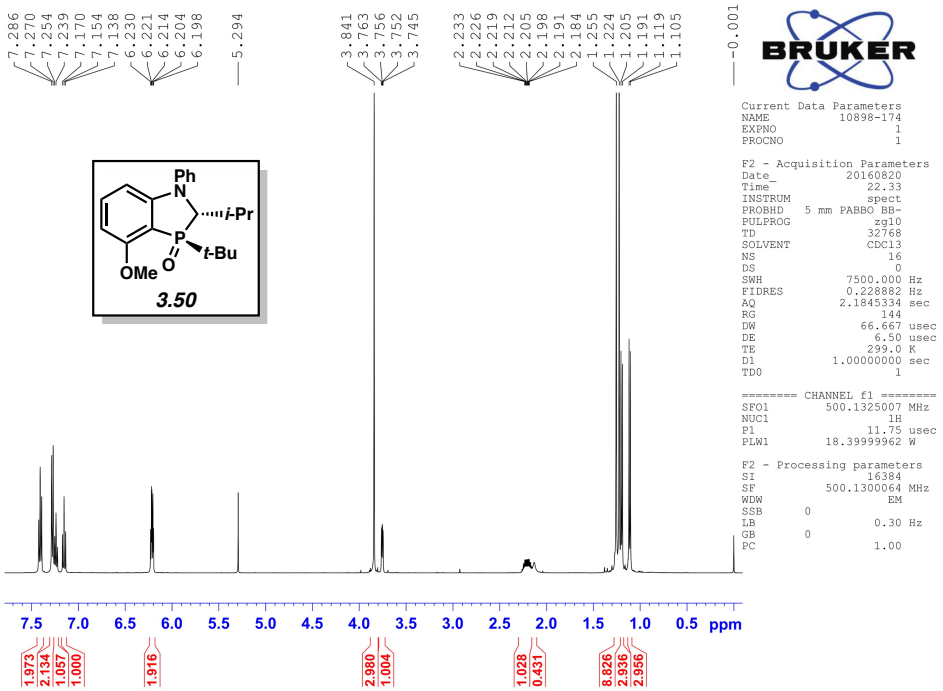

Figure 3.148 ^{1}H NMR (500 MHz, $CDCl_3$) of compound **3.50**.

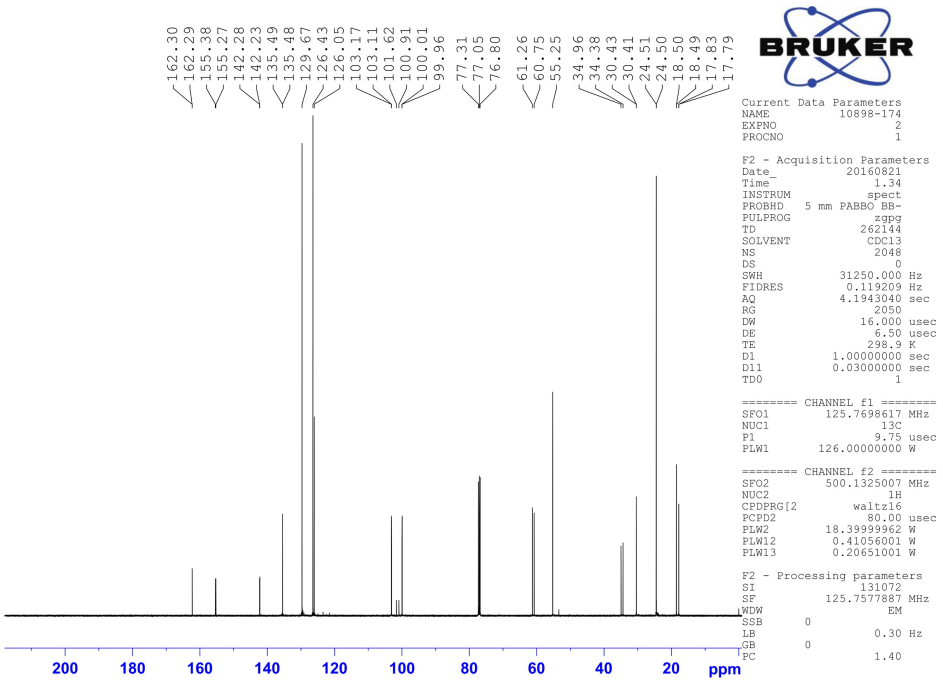

Figure 3.149 ^{13}C NMR (125 MHz, $CDCl_3$) of compound **3.50**.

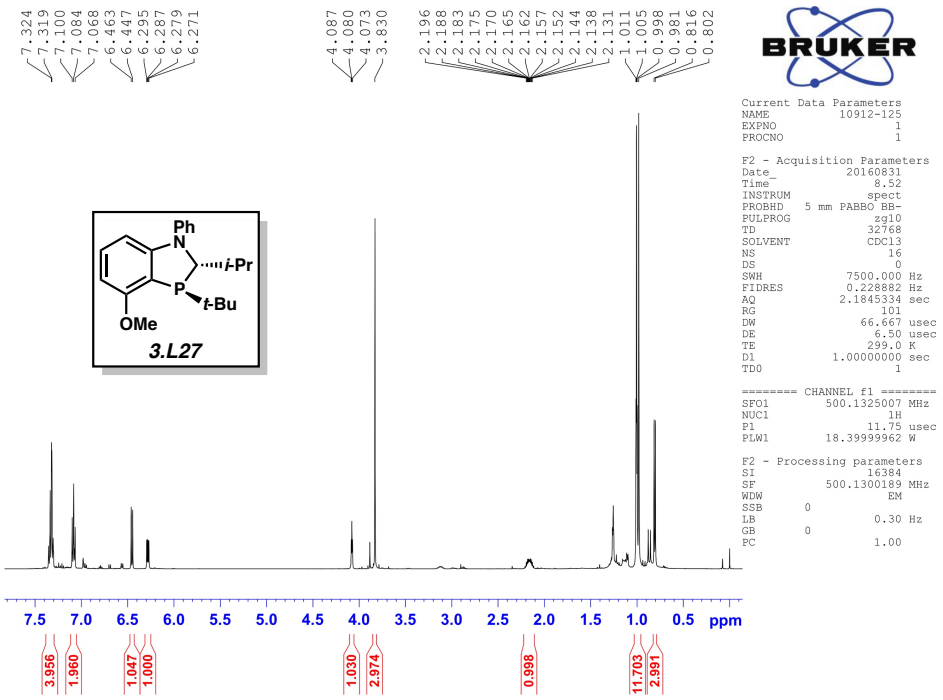

Figure 3.150 ^{1}H NMR (500 MHz, $CDCl_3$) of compound **3.L27**.

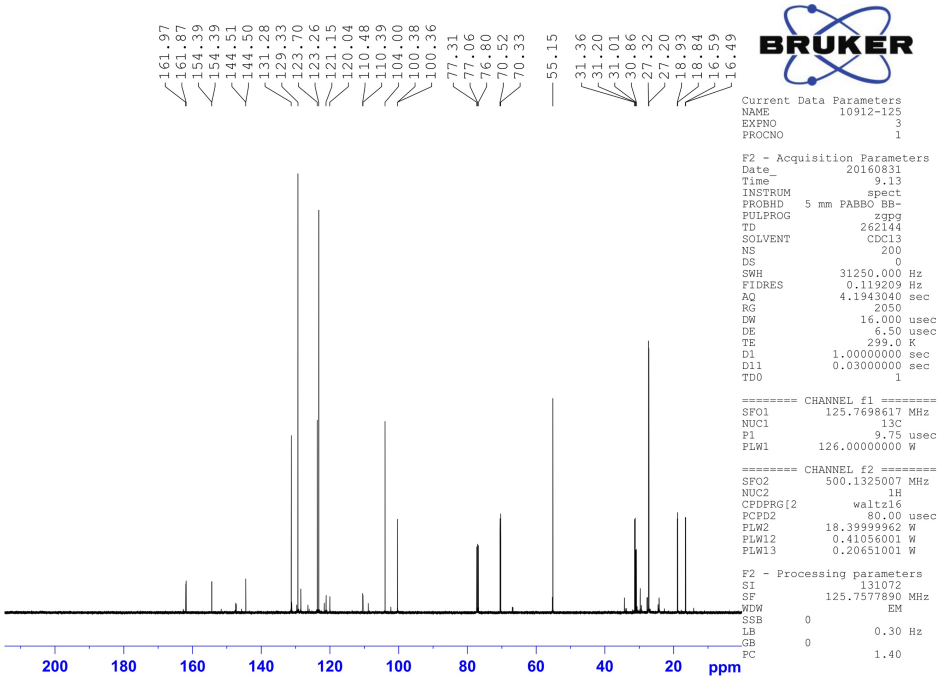

Figure 3.151 ^{13}C NMR (125 MHz, $CDCl_3$) of compound **3.L27**.

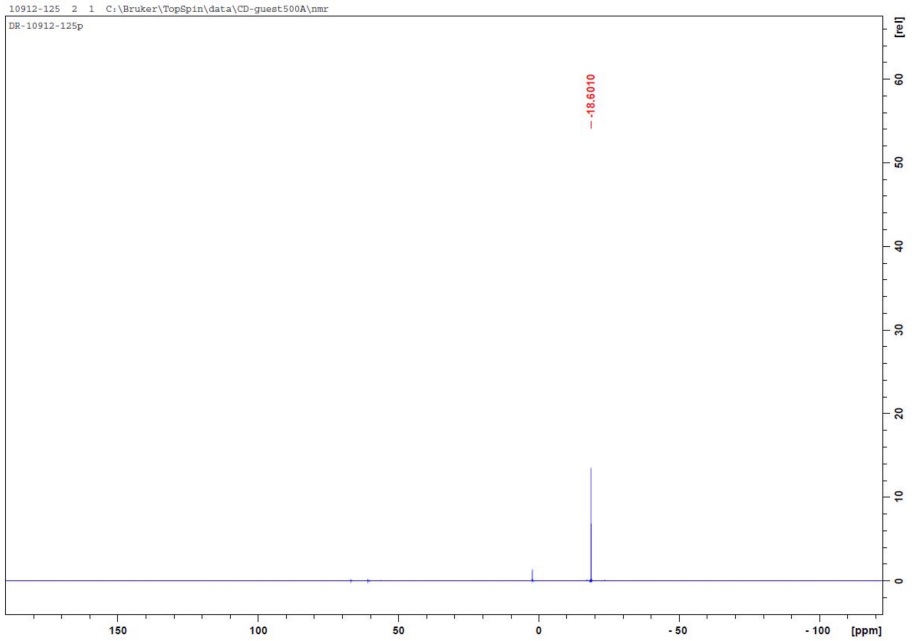

Figure 3.152 ^{31}P NMR (202 MHz, $CDCl_3$) of compound **3.L27**.

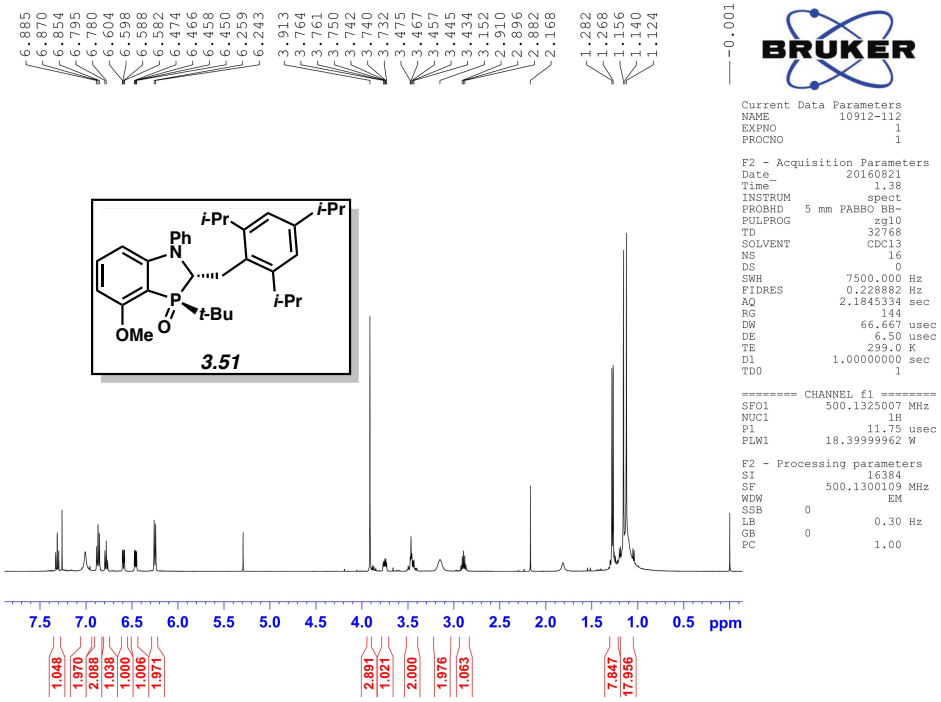

Figure 3.153 ^{1}H NMR (500 MHz, $CDCl_3$) of compound **3.51.**

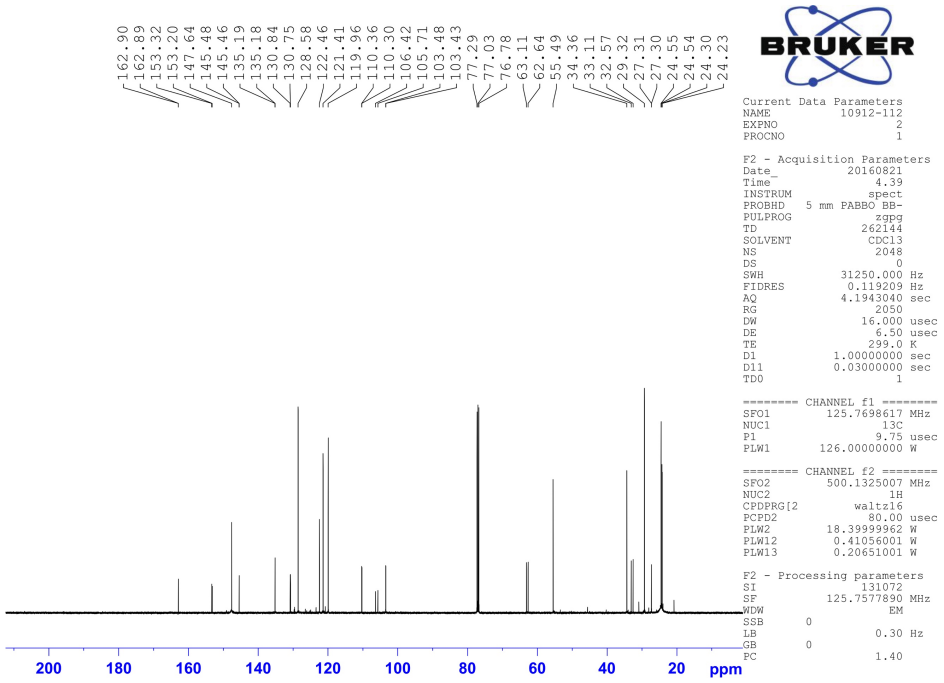

Figure 3.154 ^{13}C NMR (125 MHz, $CDCl_3$) of compound **3.51**.

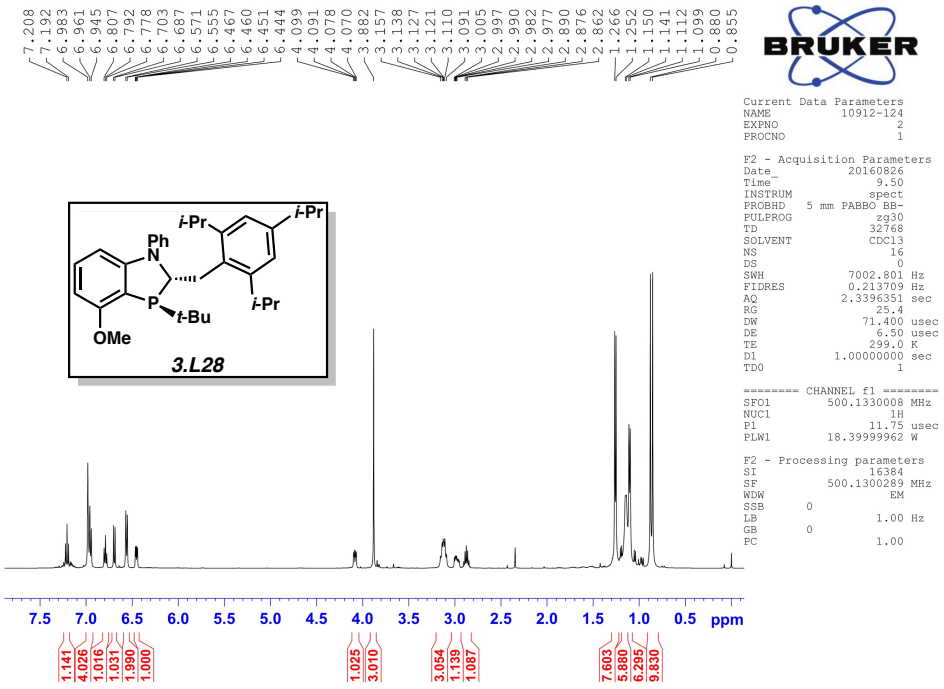

Figure 3.155 ^{1}H NMR (500 MHz, $CDCl_3$) of compound **3.L28**.

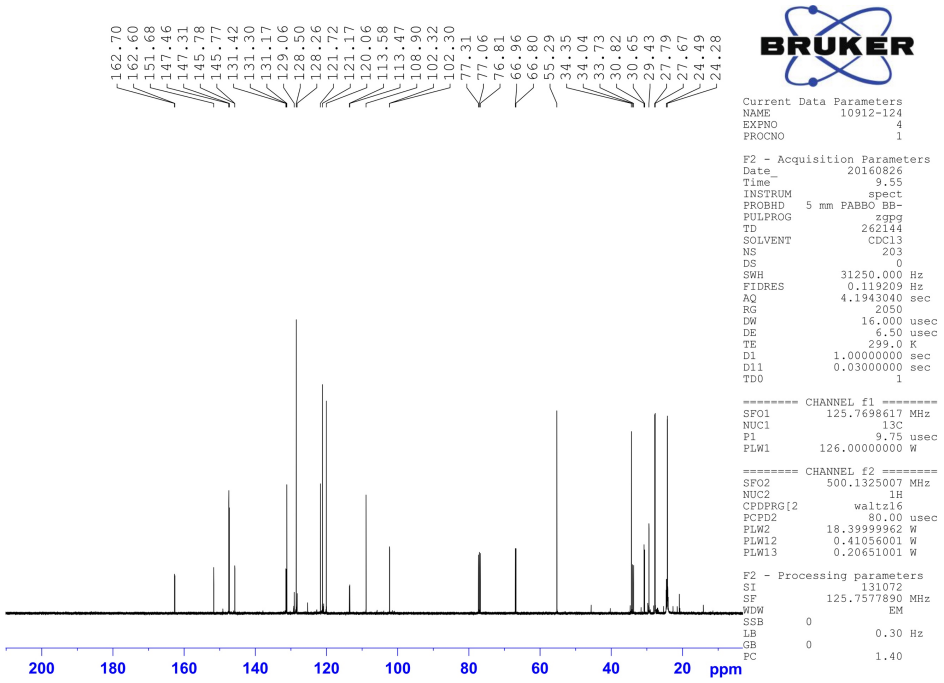

Figure 3.156 ^{13}C NMR (125 MHz, $CDCl_3$) of compound **3.L28.**

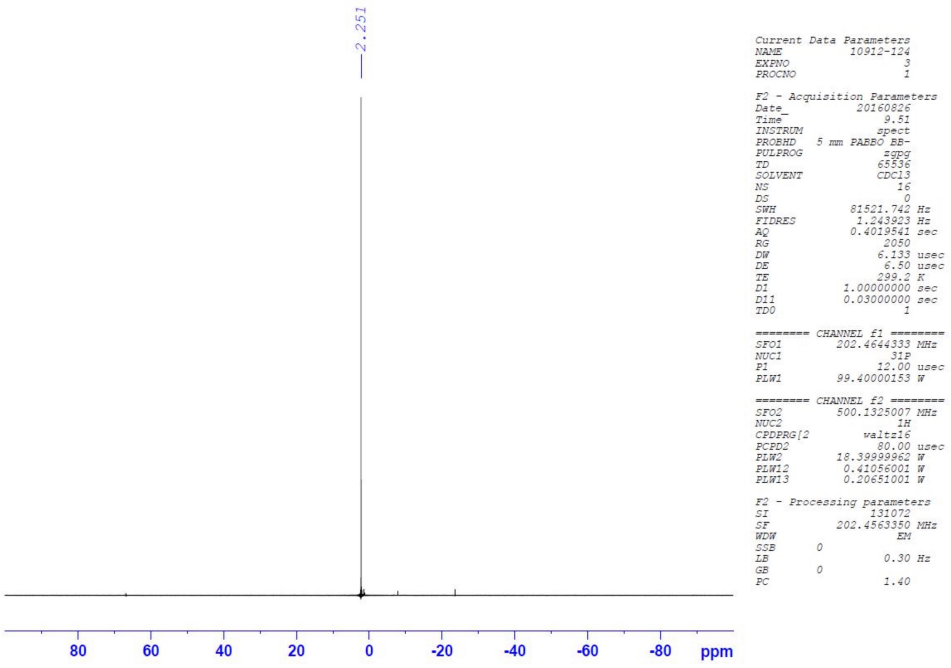

Figure 3.157 ^{31}P NMR (202 MHz, $CDCl_3$) of compound **3.L28**.

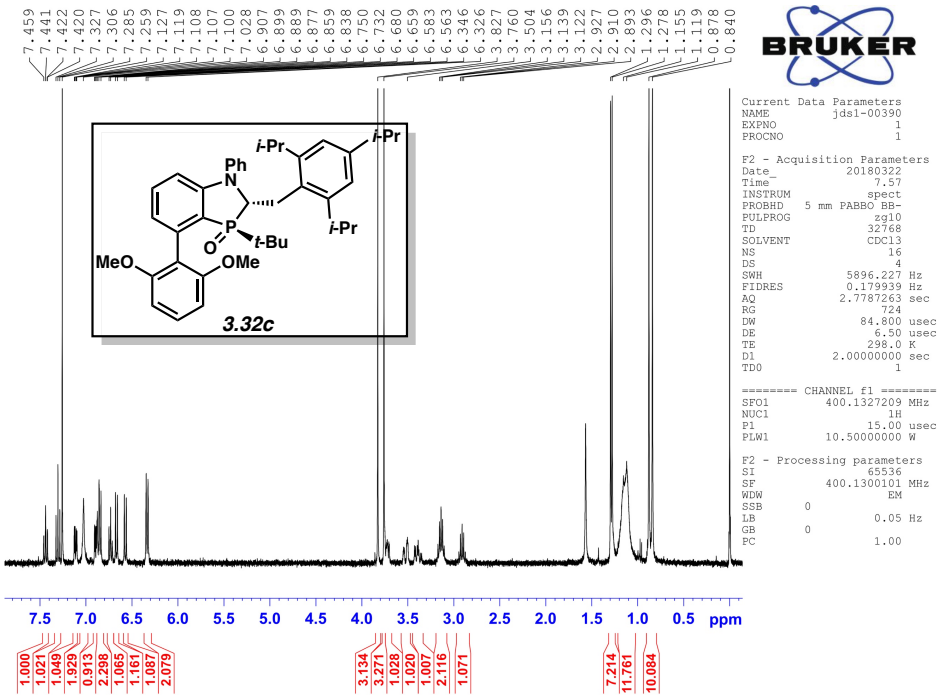

Figure 3.158 ^{1}H NMR (400 MHz, $CDCl_3$) of compound **3.32c**.

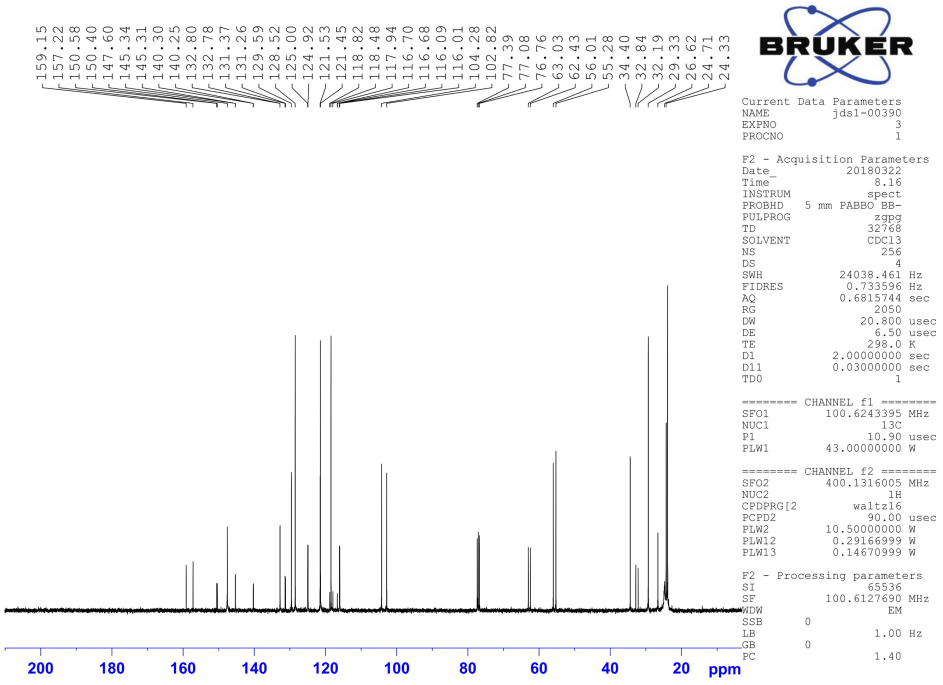

Figure 3.159 ^{13}C NMR (100 MHz, $CDCl_3$) of compound **3.32c**.

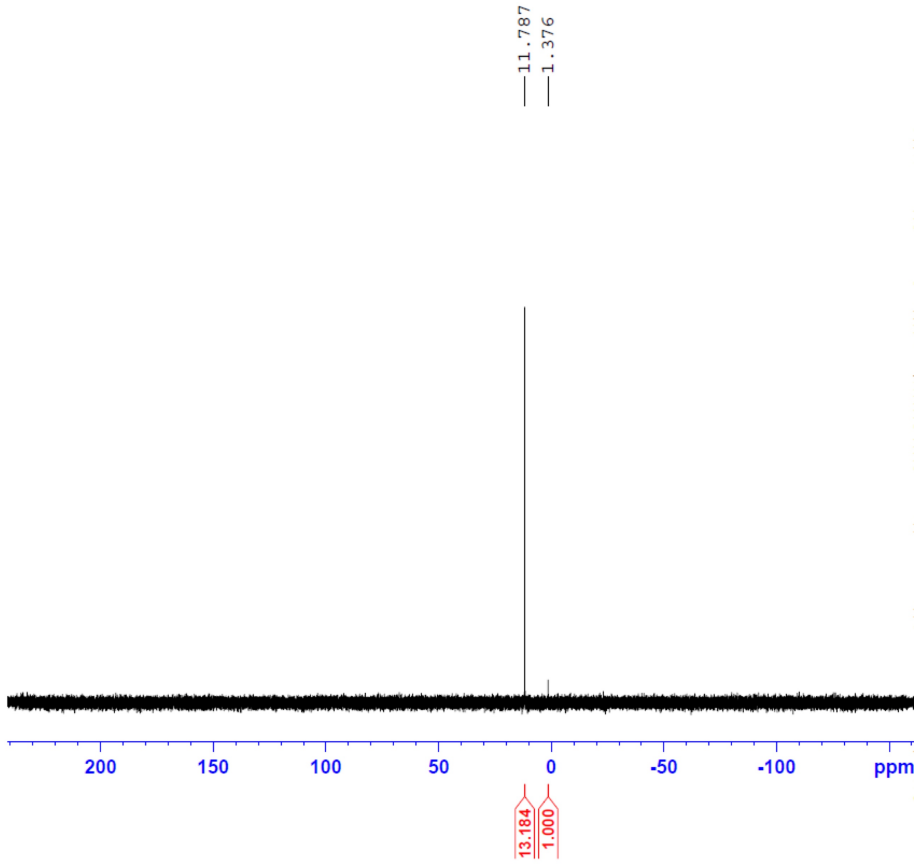

Figure 3.160 ^{31}P NMR (202 MHz, $CDCl_3$) of compound **3.32c**.

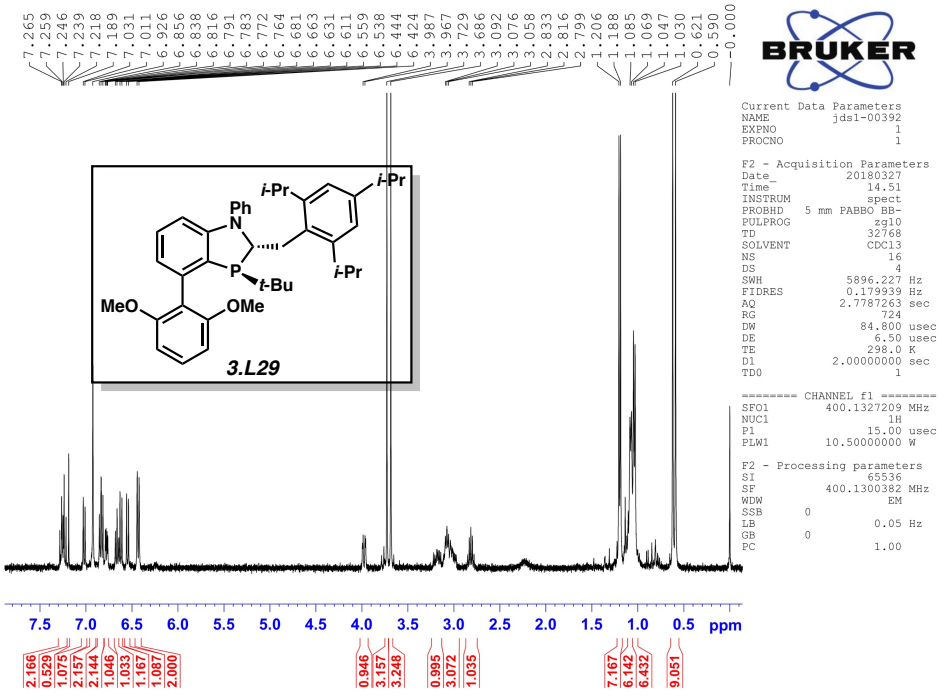

Figure 3.161 ^{1}H NMR (400 MHz, $CDCl_3$) of compound **3.L29.**

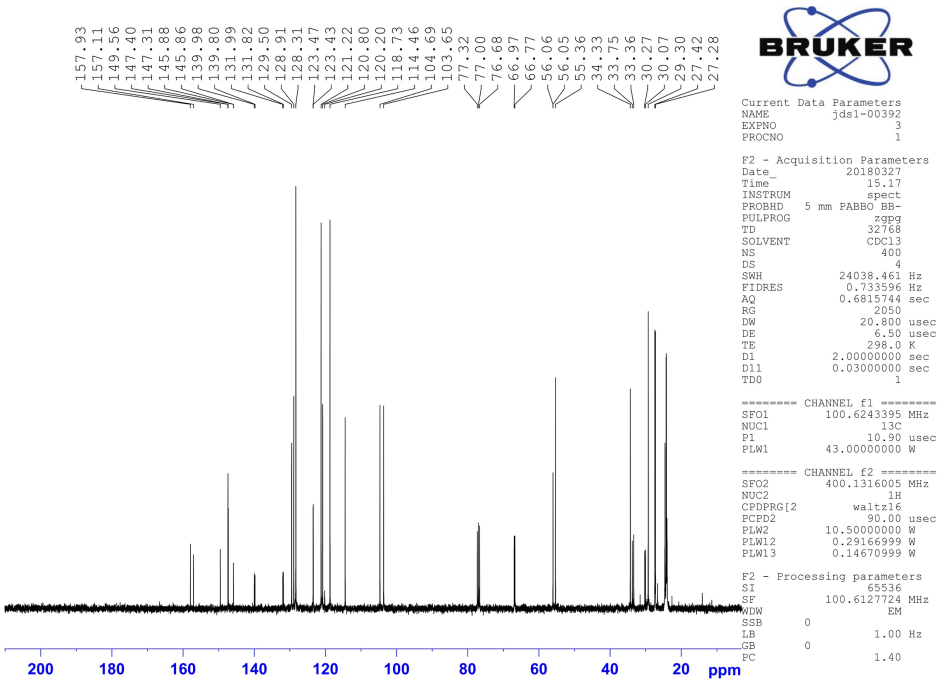

Figure 3.162 ^{13}C NMR (100 MHz, $CDCl_3$) of compound **3.L29**.

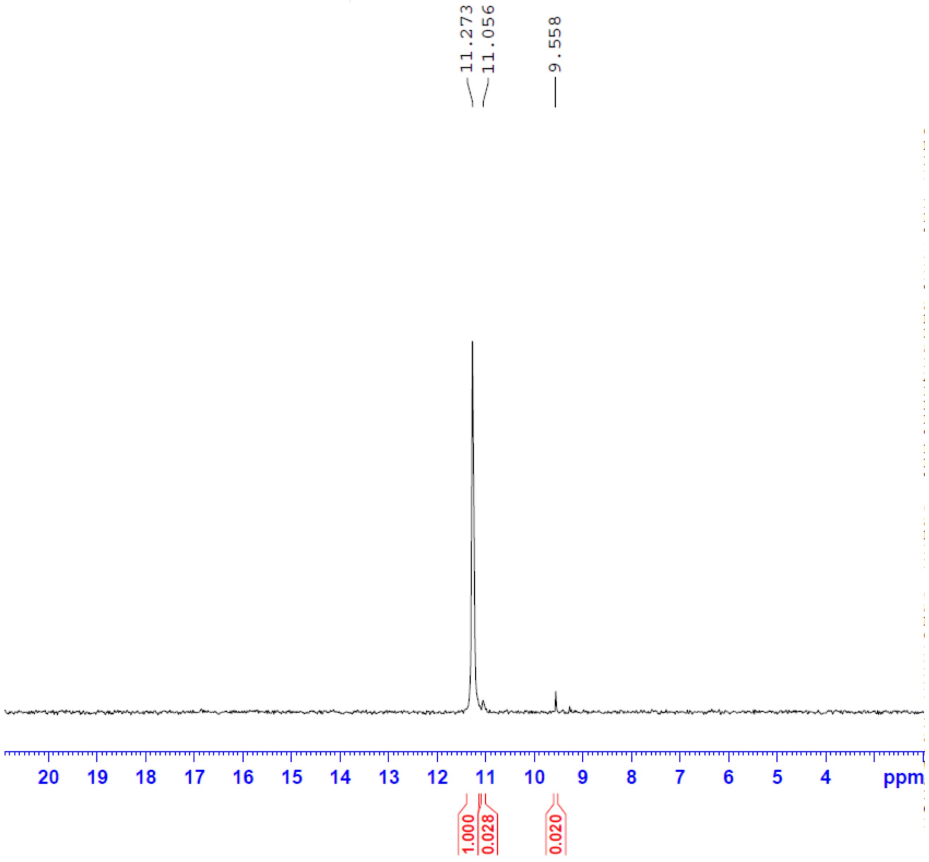

Figure 3.163 ^{31}P NMR (162 MHz, $CDCl_3$) of compound **3.L29**.

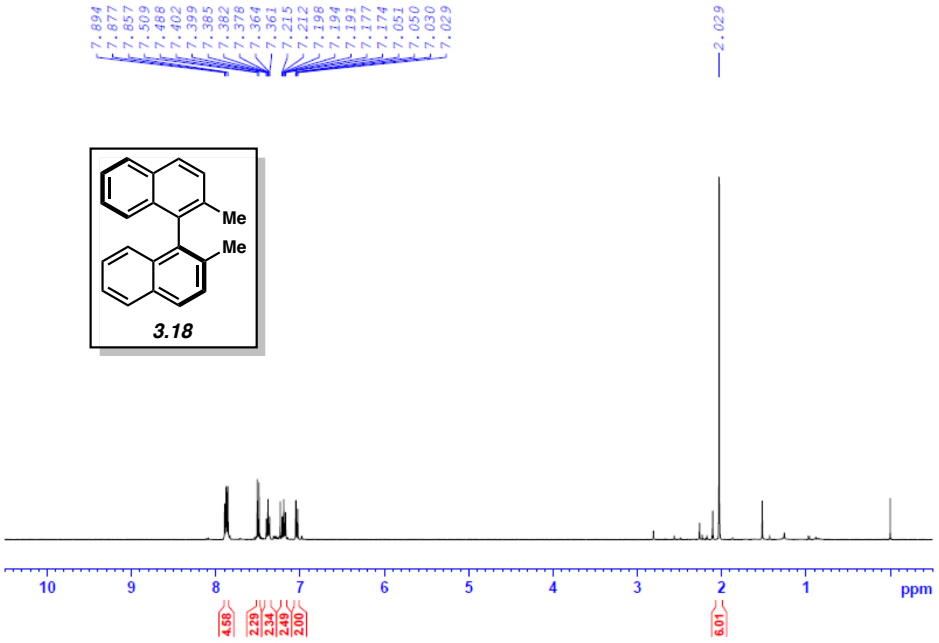

Figure 3.164 ^{1}H NMR (400 MHz, $CDCl_3$) of compound **3.18**.

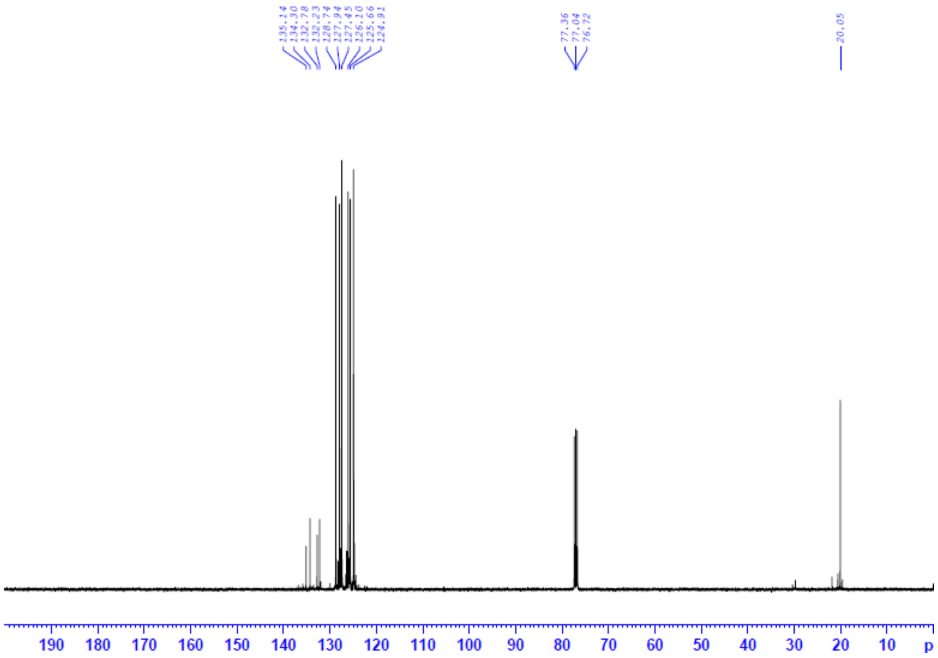

Figure 3.165 ^{13}C NMR (100 MHz, $CDCl_3$) of compound **3.18**.

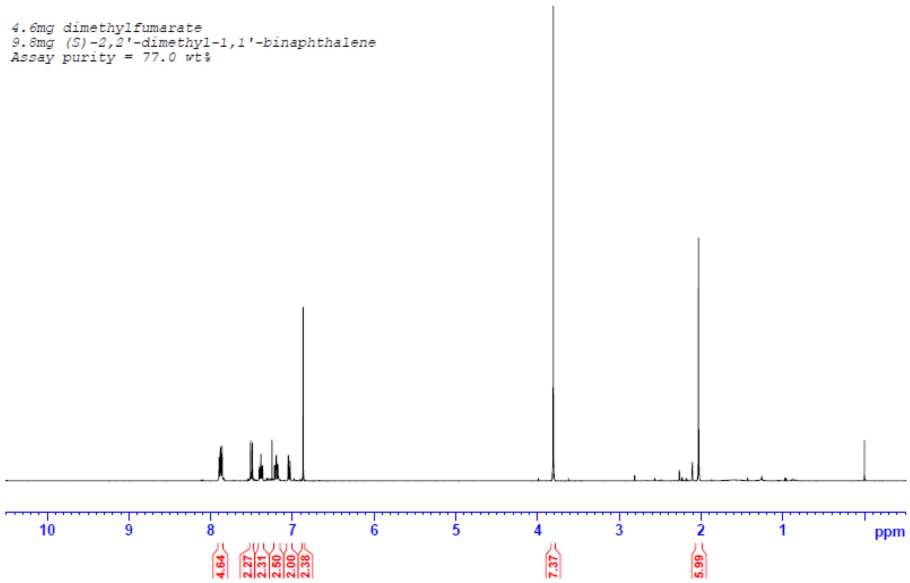

Figure 3.166 ^{1}H NMR (500 MHz, $CDCl_3$) of compound **3.18**.

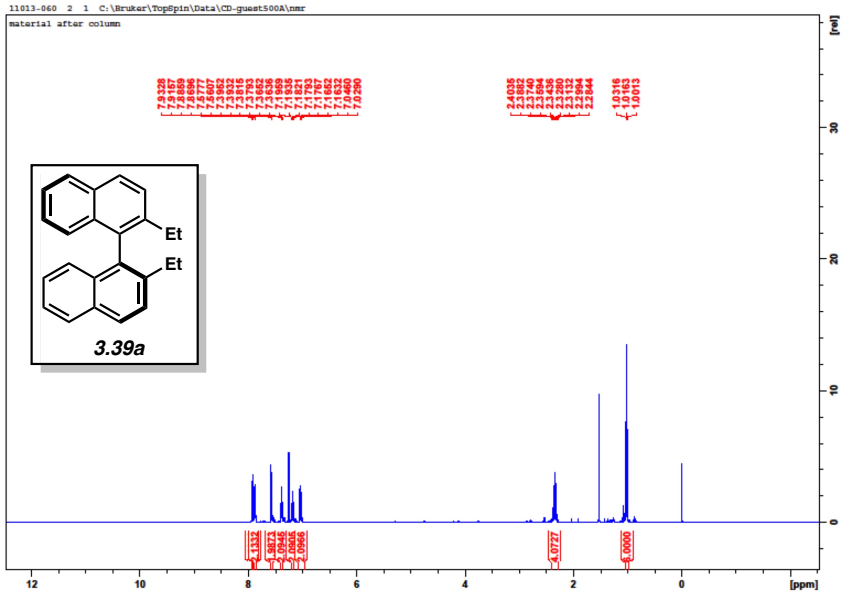

Figure 3.167 ^{1}H NMR (500 MHz, $CDCl_3$) of compound **3.39a**.

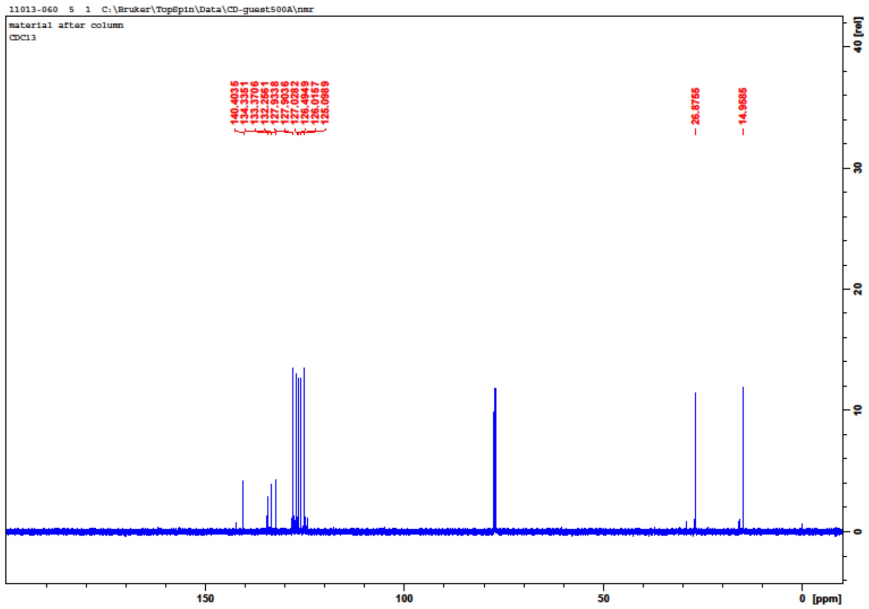

Figure 3.168 ^{13}C NMR (125 MHz, $CDCl_3$) of compound **3.39a**.

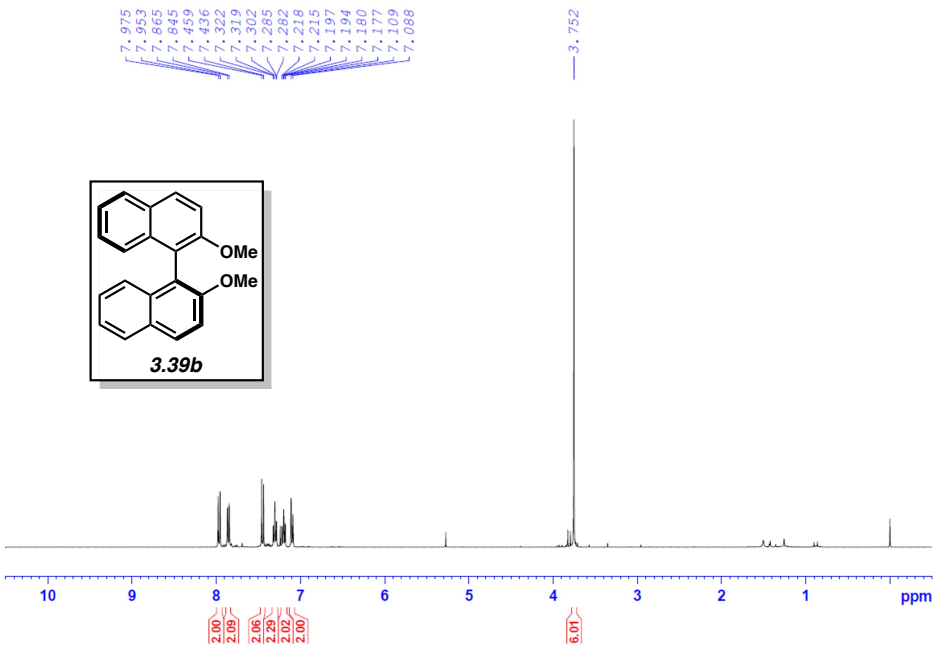

Figure 3.169 ^{1}H NMR (400 MHz, $CDCl_3$) of compound **3.39b**.

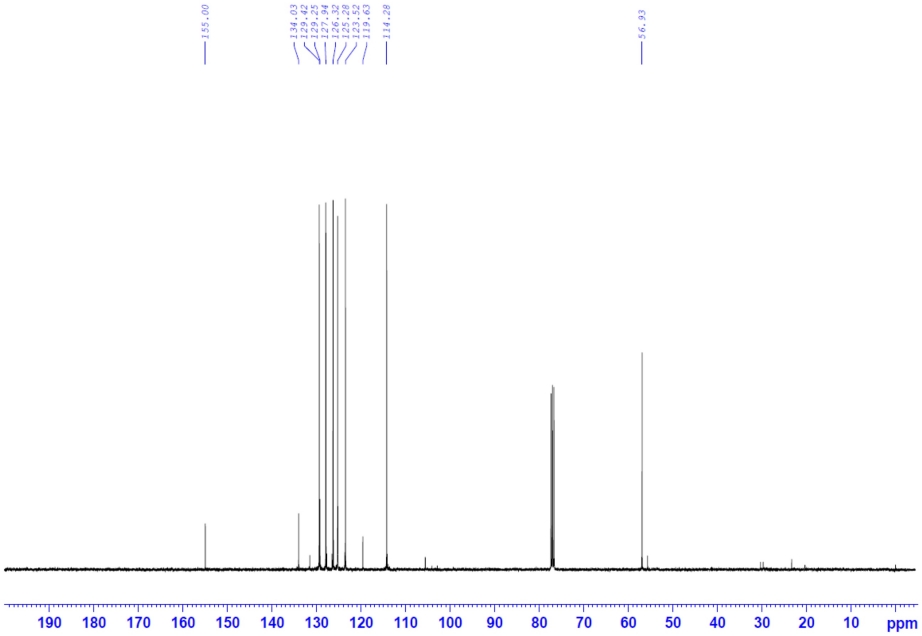

Figure 3.170 ^{13}C NMR (100 MHz, $CDCl_3$) of compound **3.39b**.

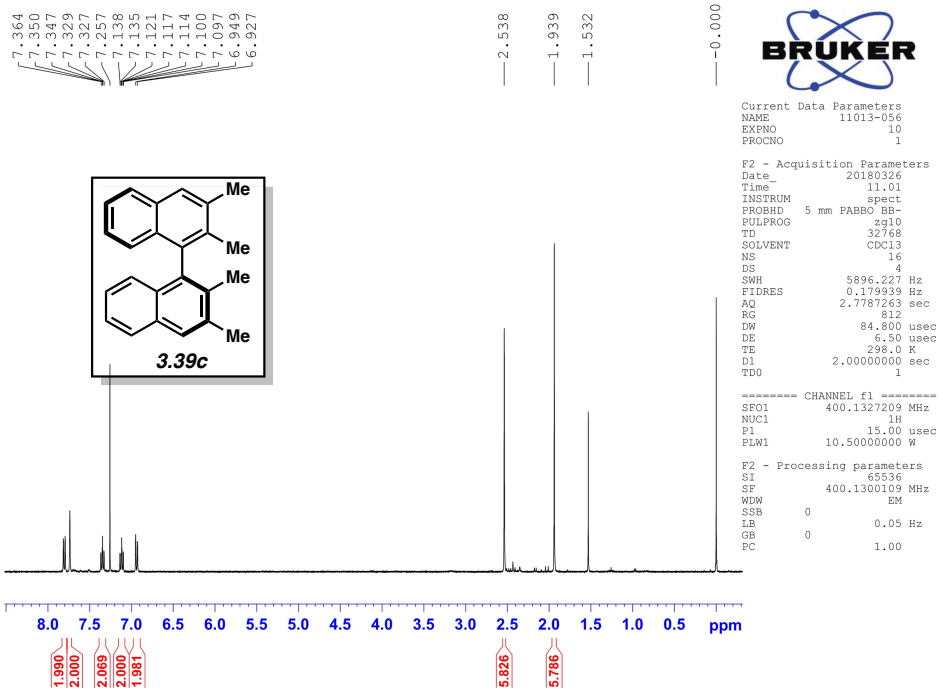

Figure 3.171 ^{1}H NMR (400 MHz, $CDCl_3$) of compound **3.39c**.

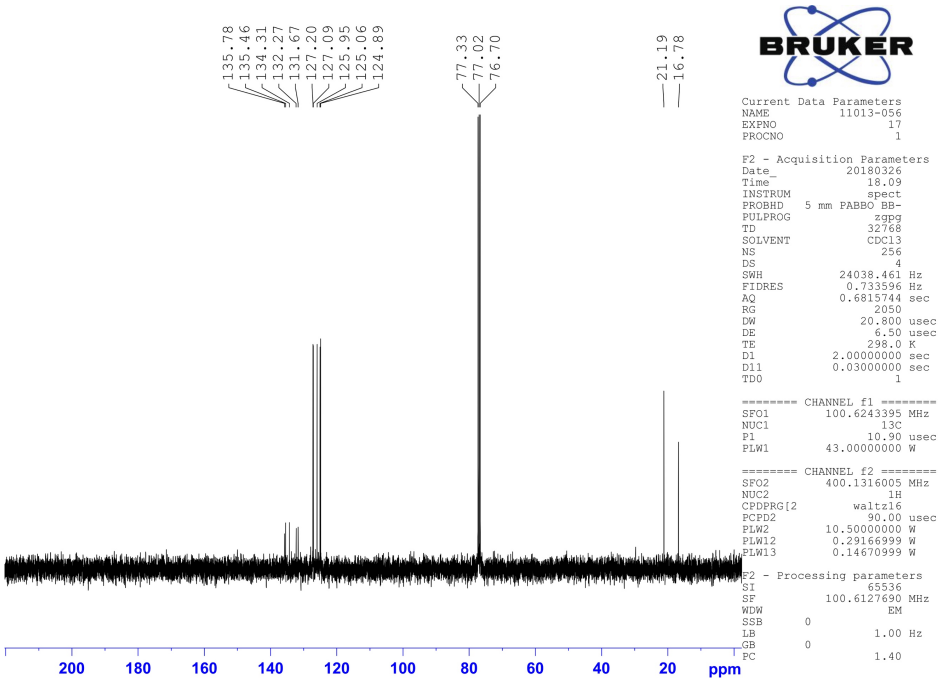

Figure 3.172 ^{13}C NMR (100 MHz, $CDCl_3$) of compound **3.39c.**

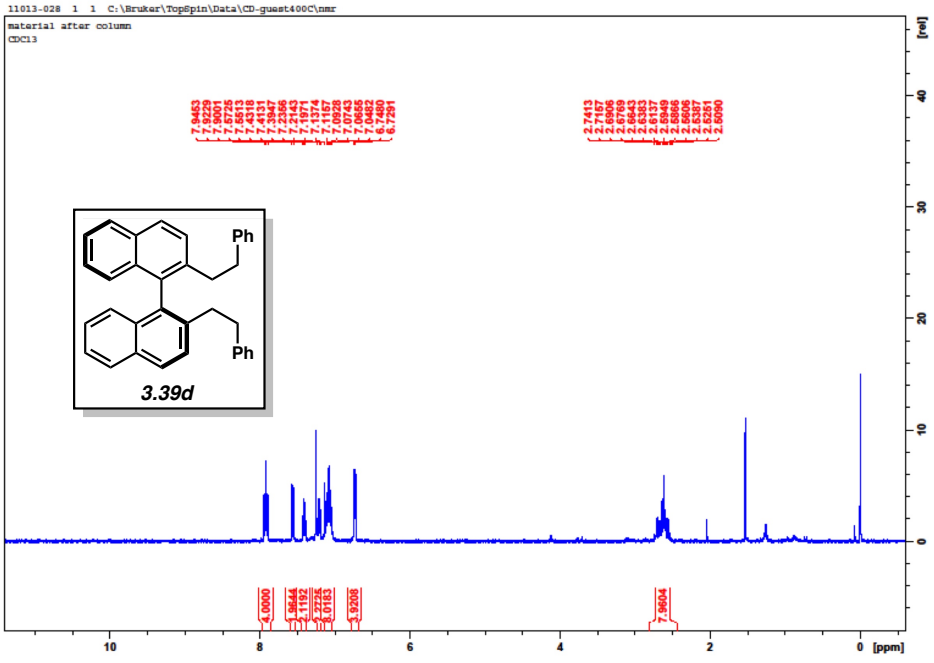

Figure 3.173 ^{1}H NMR (400 MHz, $CDCl_3$) of compound **3.39d**.

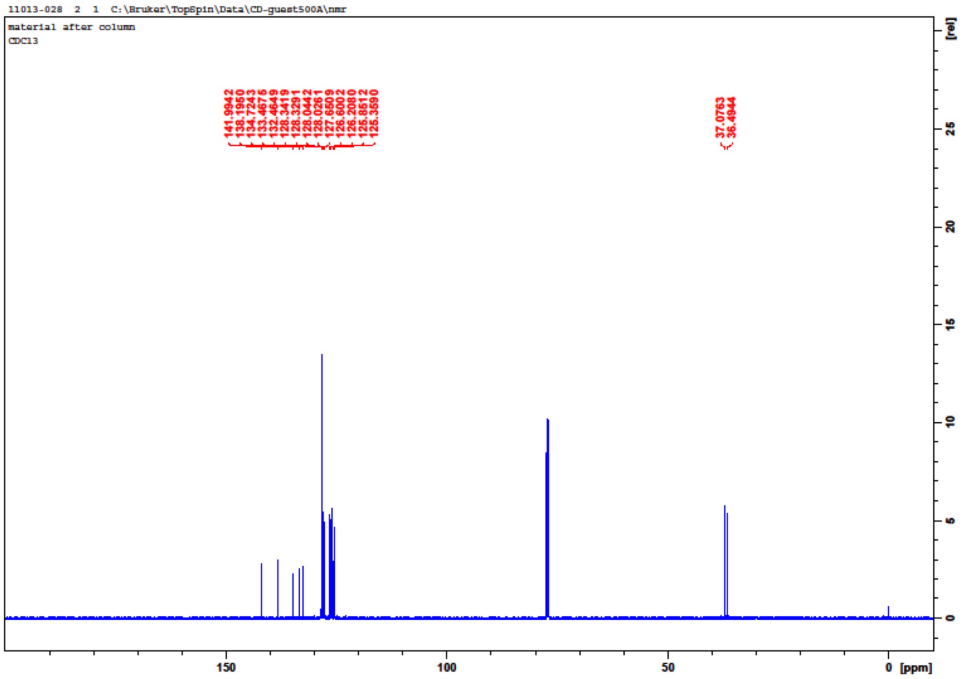

Figure 3.174 ^{13}C NMR (125 MHz, $CDCl_3$) of compound **3.39d**.

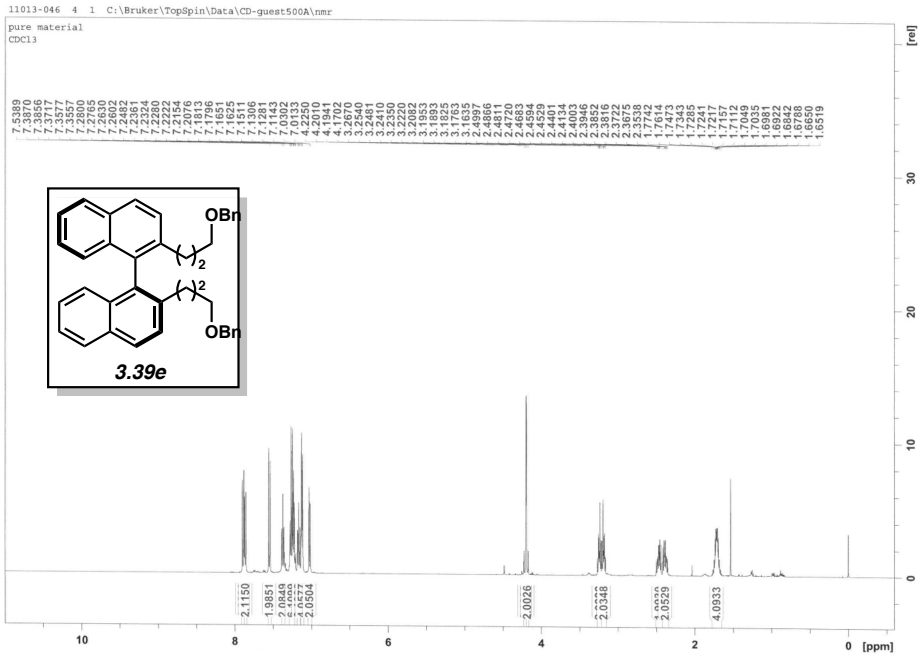

Figure 3.175 ^{1}H NMR (500 MHz, $CDCl_3$) of compound **3.39e.**

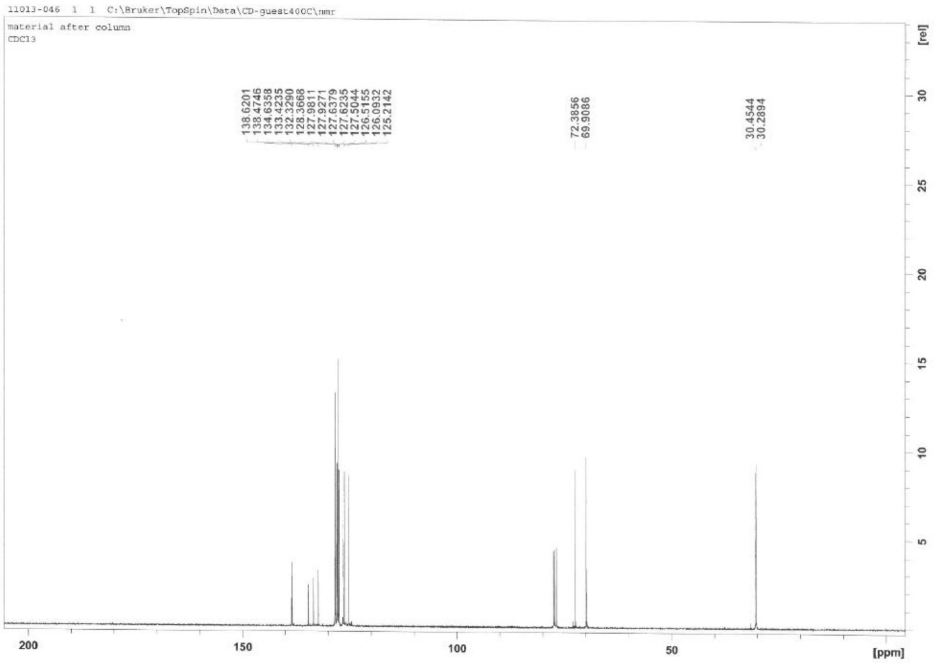

Figure 3.176 ^{13}C NMR (100 MHz, $CDCl_3$) of compound **3.39e**.

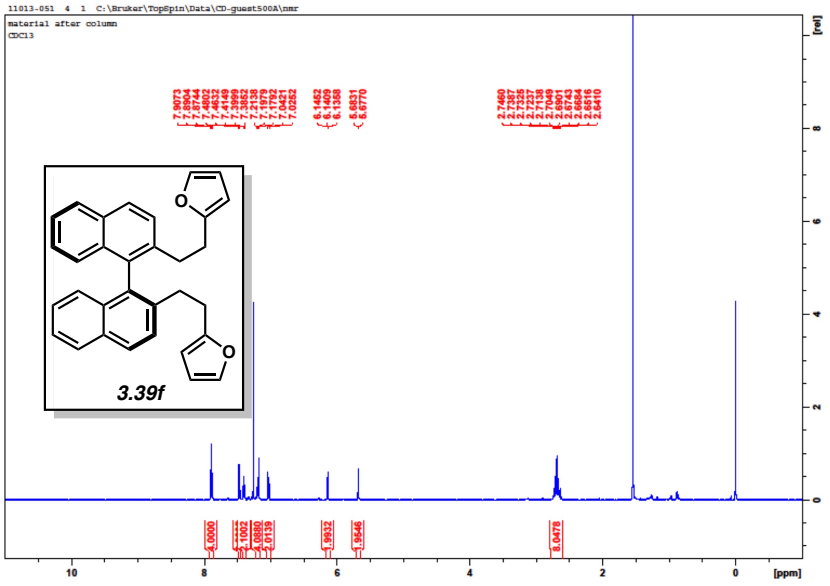

Figure 3.177 ^{1}H NMR (500 MHz, $CDCl_3$) of compound **3.39f**.

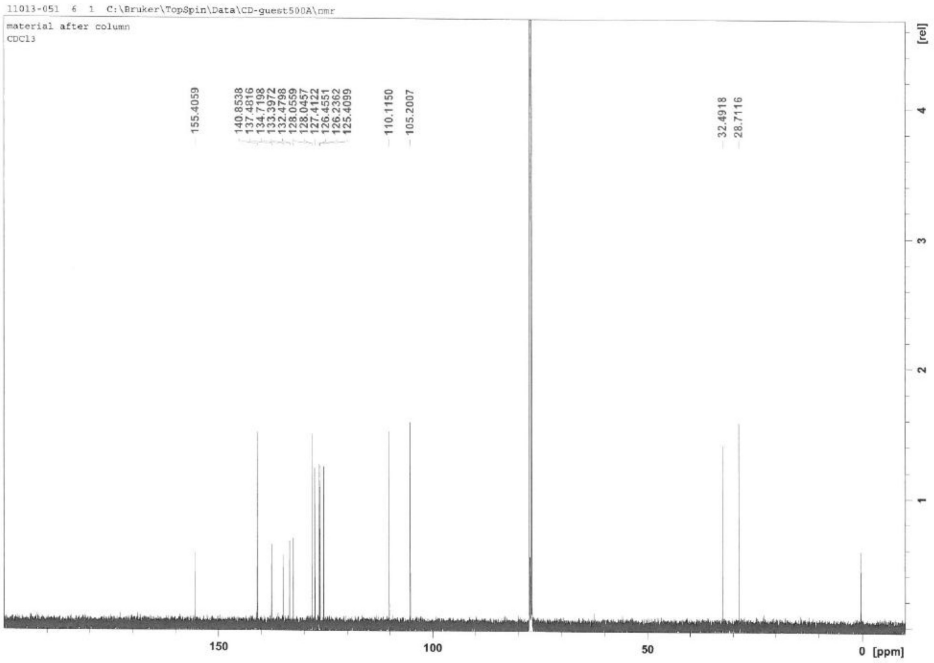

Figure 3.178 ^{13}C NMR (100 MHz, $CDCl_3$) of compound **3.39f**.

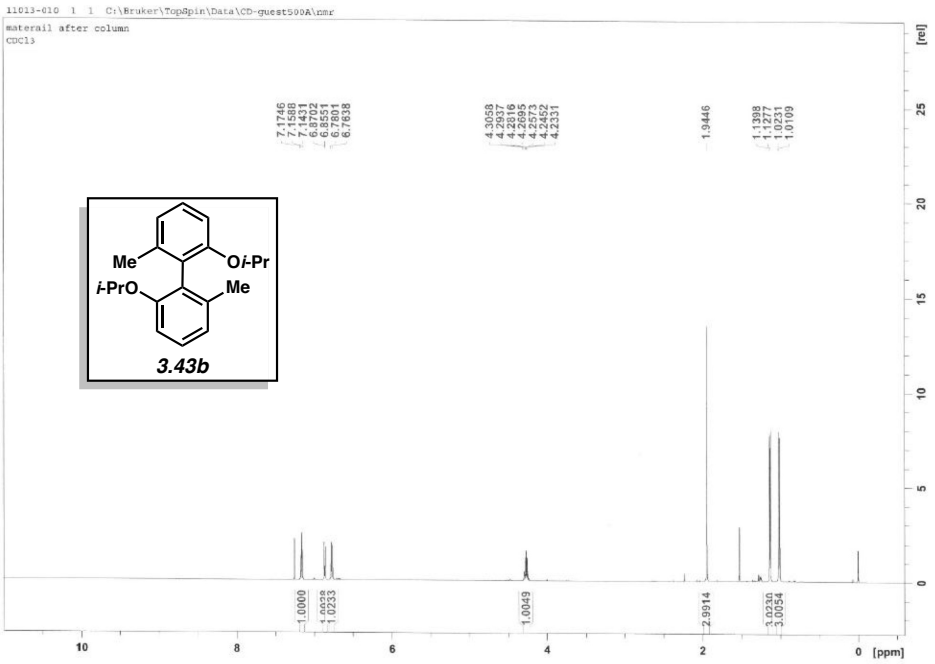

Figure 3.179 ^{1}H NMR (500 MHz, $CDCl_3$) of compound **3.43b.**

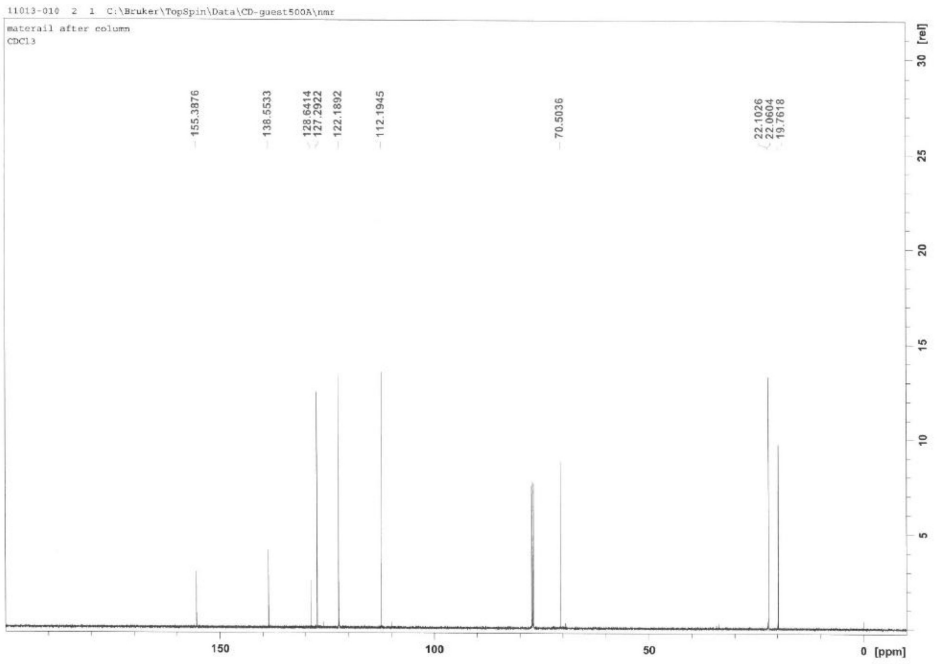

Figure 3.180 ^{13}C NMR (125 MHz, $CDCl_3$) of compound **3.43b**.

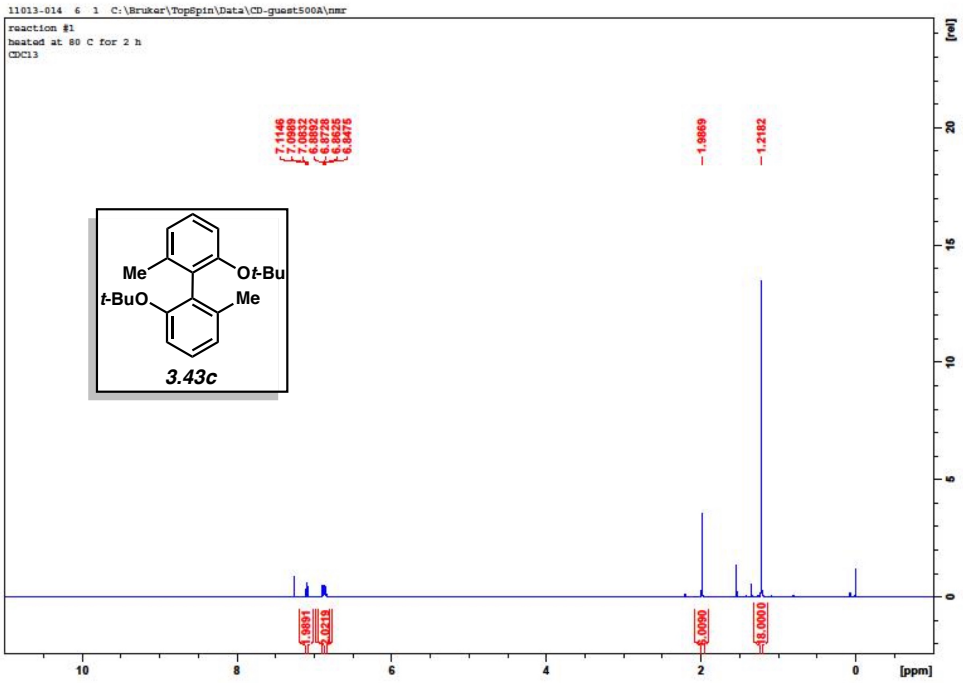

Figure 3.181 ^{1}H NMR (500 MHz, $CDCl_3$) of compound **3.43c**.

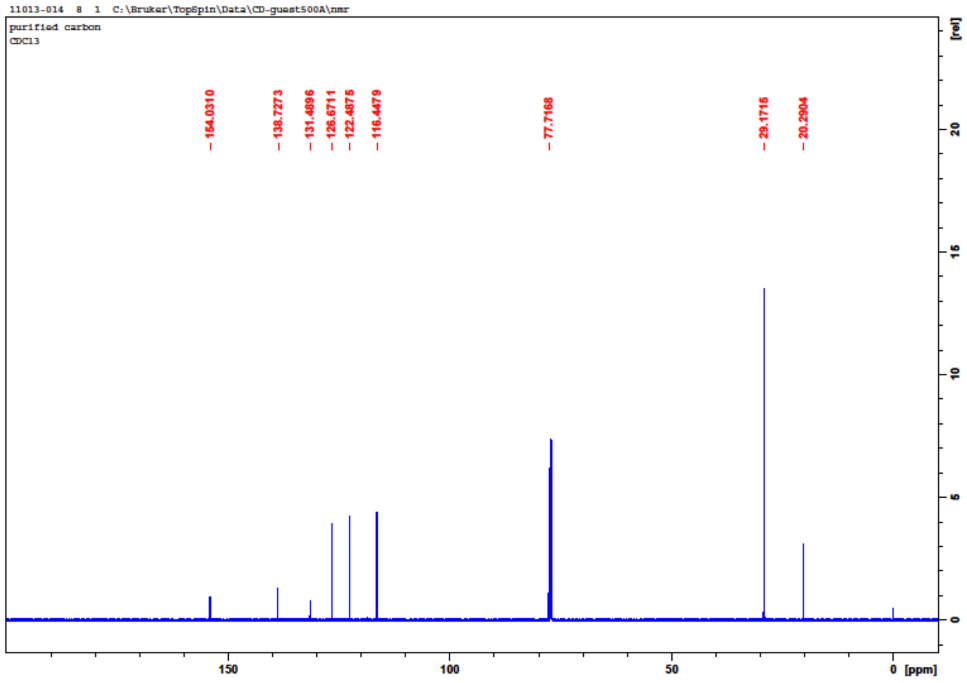

Figure 3.182 ^{13}C NMR (125 MHz, $CDCl_3$) of compound **3.43c**.

3.10 Notes and References

(1) (a) Hassan, J.; Sevignon, M.; Gozzi, C.; Schulz, E.; Lemaire, M. *Chem. Rev.* **2002**, *102*, 1359 – 1470. (b) Littke, A. F.; Fu, G. C. *Angew. Chem., Int. Ed.* **2002**, *41*, 4176 – 4211. (c) Tamao, K.; Miyaura, N. *Top. Curr. Chem*. **2002**, *219*, 1 – 9. (d) Stanforth, S. P. *Tetrahedron* **1998**, *54*, 263 – 303. (e) Diederich, F., Stang, P. J., Eds.; Wiley-VCH: New York, 1998. (f) Lessene, G. *Aust. J. Chem.* **2004**, *57*, 107. (g) Molnar, A., Ed; Wiley-VCH Verlag GmbH & Co. KGaA, Weinheim, Germany, 2013.

(2) Miyaura, N.; Yamada, K.; Suzuki, A. *Tetrahedron Lett.* **1979**, *20*, 3437 – 3440.

(3) Negishi, E.; King, A. O.; Okukado, N. *J. Org. Chem.* **1977**, *42*, 1821 – 1823.

(4) Reviews: (a) Suzuki, A. *J. Organomet. Chem.* **1999**, *576*, 147 – 168. (b) Miyaura, N.; Suzuki, A. *Chem. Rev.* **1995**, *95*, 2457 – 2483. (c) Bellina F.; Carpita, A.; Rossi, R. *Synthesis* **2004**, 2419 – 2440. (d) Christmann, U.; Vilar, R. *Angew. Chem., Int. Ed.* **2005**, *44*, 366 – 374. (e) Alonso, F.; Beletskaya, I. P.; Yus, M. *Tetrahedron* **2008**, *64*, 3047 – 3101. (f) Miyaura, N. *Top. Curr. Chem.* **2002**, *219*, 11 – 59. (g) Johansson Seechurn, C. C. C.; Kitching, M. O.; Colacot, T. J.; Snieckus, V. *Angew. Chem., Int. Ed.* **2012**, *51*, 5062 – 5085. (h) Lundgren, R. J.; Stradiotto, M. *Chem. Eur. J.* **2012**, *18*, 9758 – 9769.

(5) (a) Miura, M. *Angew. Chem., Int. Ed.* **2004**, *43*, 2201 – 2203. (b) Martin, R.; Buchwald, S. L. *Acc. Chem. Res.* **2008**, *41*, 1461 – 1473. (c) DeAngelis, A. J.; Gildner, P. G.; Chow, R.; Colacot, T. J. *J. Org. Chem.* **2015**, *80*, 6794 – 6813. (d) Kinzel, T.; Zhang, Y.; Buchwald, S. L. *J. Am. Chem. Soc.* **2010**, *132*, 14073 – 14075. (e) Yang, Y.; Oldenhuis, N. J.; Buchwald, S. L. *Angew. Chem., Int. Ed.* **2013**, *52*, 615 – 619. (f) Bruno, N. C.; Tudge, M. T.; Buchwald, S. L. *Chem. Sci.* **2013**, *4*, 916 – 920.

(6) (a) Dumrath, A.; Lubbe, C.; Beller, M. Molnar, A., Ed.; Wiley-VCH Verlag GmbH & Co. KGaA, Weinheim, Germany, 2013; pages 445 – 489. (b) Torborg, C.; Beller, M. *Adv. Synth. Catal.* **2009**, *351*, 3027 – 3043. (c) Budarin, V.; Shuttleworth, P. S.; Clark, J. H.; Luque, R. *Curr. Org. Synth.* **2010**, *7*, 614 – 627.

(7) (a) Littke, A. F.; Fu, G. C. *Angew. Chem., Int. Ed.* **1998**, *37*, 3387 – 3388. (b) Littke, A. F.; Dai, C.; Fu, G. C. *J. Am. Chem. Soc.* **2000**, *122*, 4020 – 4028. (c) Stambuli, J. P.; Kuwano, R.; Hartwig, J. F. *Angew. Chem., Int. Ed.* **2002**, *41*, 4746. (d) Fleckenstein, C. A.; Plenio, H. *Chem. Eur. J.* **2007**, *13*, 2701 – 2716. (e) Fleckenstein, C. A.; Plenio, H. *J. Org. Chem.* **2008**, *73*, 3236 – 3244. (f) Guram, A. S.; King, A. O.; Allen, J. G.; Wang, X. Schenkel, L. B.; Chan, J.; Bunel, E. E.; Faul, M. M.; Larsen, R. D.; Martinelli, M. J.; Reider, P. J. *Org. Lett.* **2006**, *8*, 1787 – 1789. (h) Hoshi, T.; Nakazawa, T.; Saitoh, I.; Mori, A.; Suzuki, T.; Sakai, J.; Hagiwara, H. *Org. Lett.* **2008**, *10*, 2063 – 2066. (i) Hoshi, T.; Saitoh, T.; Nakazawa, T.; Suzuki, T.; Sakai, J.; Hagiwara, H. *J. Org. Chem.* **2009**, *74*, 4013 – 4016. (j) Yin, J.: Rainka, M. P.; Zhang, X. –X.; Buchwald, S. L. *J. Am. Chem. Soc.* **2002**, *124*, 1162 – 1163. (k) Yin, J.; Buchwald, S. L. *J. Am. Chem. Soc.* **2000**, *122*, 12051 – 12052. (l) Walker, S. D.; Barder, T. E.; Martinelli, J. R.; Buchwald, S. L. *Angew. Chem., Int. Ed.* **2004**, *43*, 1871 – 1876. (m) Barder, T. E.; Walker, S. D.; Martinelli, J. R.; Buchwald, S. L. *J. Am. Chem. Soc.* **2005**, *127*, 4685 – 4696. (n) Billingsley, K. L.; Anderson, K. W.; Buchwald, S. L. *Angew. Chem., Int. Ed.* **2006**, *45*, 3484 – 3488. (o) Billingsley, K.; Buchwald, S. L. *J. Am. Chem. Soc.* **2007**, *129*, 3358 – 3366. (p) Bhayana, B.; Fors, B. P.; Buchwald, S. L. *Org. Lett.* **2009**, *11*, 3954 – 3957. (p) Tang, W.; Capacci, A. G.; Wei, X.; Li, W.; White, A.; Patel, N. D.; Savoie, J.; Gao, J.; Rodriguez, S.; Qu, B.; Haddad, N.; Lu, B. Z.; Krishnamurthy, D.; Yee, N. K.; Senanayake, C. H. *Angew. Chem., Int. Ed.* **2010**, *49*, 5879 –

5883. (q) Guram, A. S.; King, A. O.; Allen, J. G.; Wang, X.; Schenkel, L. B.; Chan, J. Bunel, E. E.; Faul, M. M.; Larsen, R. D.; Martinelli, M. J.; Reider, P. J. *Org. Lett.* **2006**, *8*, 1787 – 1789. (r) Milne, J. E.; Buchwald, S. L. *J. Am. Chem. Soc.* **2004**, *126*, 13028 – 13032. (s) Dai, C.; Fu, G. C. *J. Am. Chem. Soc.* **2001**, *123*, 2719 – 2724. (t) Sieber, J. D.; Qu, B.; Rodriguez, S.; Haddad, N.; Grinberg, N.; Lee, H.; Song, J. J.; Yee, N. K.; Senanayake, C. H. *J. Org. Chem.* **2016**, *81*, 729 – 736. (u) Luzung, M. R.; Patel, J. S.; Yin, J. *J. Org. Chem.* **2010**, *75*, 8330 – 8332. (v) Zhang, Y.; Lao, K. S.; Sieber, J. D.; Xu, Y.; Wu, L.; Wang, X. –J.; Desrosiers, J. –N.; Lee, H.; Haddad, N.; Han, S.; Yee, N. K.; Song, J. J.; Howell, A. R.; Senanayake, C. H. *Synthesis* **2018**, DOI: 10.1055/s-0037-1610158

(8) (a) Gstottmayr, C. W. K.; Bohm, V. P. W.; Herdtweck, E.; Grosche, M.; Herrmann, W. A A *Angew. Chem., Int. Ed.* **2002**, *41*, 1363 – 1365. (b) Navarro, O.; Kelly, R. A.; Stevens, E. D.; Nolan, S. P. *J. Am. Chem. Soc.* **2003**, *125*, 16194 – 16195. (c) Altenhoff, G.; Goddard, R.; Lehmann, C. W.; Glorius, F. *Angew. Chem., Int. Ed.* **2003**, *42*, 3690 – 3693. (d) Altenhoff, G.; Goddard, G. R.; Lehmann, C. W.; Glorius, F. *J. Am. Chem. Soc.* **2004**, *126*, 15195 – 15201. (e) Song, C.; Ma, Y.; Chai, Q.; Ma, C.; Jiang, W.; Andrus, M. B. *Tetrahedron* **2005**, *61*, 7438 – 7446. (f) Marion, N.; Navarro, O.; Mei, J.; Stevens, E. D.; Scott, N. M.; Nolan, S. P. *J. Am. Chem. Soc.* **2006**, *128*, 4101 – 4111. (g) O'Brien, C. J.; Kantchev, E. A. B.; Valente, C.; Hadei, N.; Chass, G. A.; Lough, A.; Hopkinson, A. C.; Organ, M. G. *Chem. Eur. J.* **2006**, *12*, 4743 – 4748. (h) Organ, M. G.; Calimsiz, S.; Sayah, M.; Hoi, K. H.; Lough, A. J. *Angew. Chem., Int. Ed.* **2009**, *48*, 2383 – 2387. (i) Valente, C.; Belowich, B. E.; Hadei, N.; Organ, M .G. *Eur. J. Org. Chem.* **2010**, 4343 – 4354.

(9) (a) Zhao, Q.; Li, C.; Senanayake, C. H.; Tang, W. *Chem. Eur. J.* **2013**, *19*, 2261 – 2265. (b) Demchuk, O. M.; Yoruk, B.; Blackburn, T.; Snieckus, V. *Synlett* **2006**, 2908 – 2913. (c) Lu, D. –D.; He, X. –X.; Liu, F. –S. *J. Org. Chem.* **2017**, *82*, 10898 – 10911. (d) Lesieur, M.; Slawin, A. M. Z.; Cazin, C. S. J. *Org. Biomol. Chem.* **2014**, *12*, 5586 – 5589. (e) Bastug, G.; Nolan, S. P. *Organometallics* **2014**, *33*, 1253 – 1258. (f) Tu, T.; Sun, Z.; Fang, W.; Xu, M.; Zhou, Y. *Org. Lett.* **2012**, *14*, 4250 – 4253. (g) Chartoire, A.; Lesieur, M.; Falivene, L.; Slawin, A. M. Z.; Cavallo, L.; Cazin, C. S. J.; Nolan, S. P. *Chem. Eur. J.* **2012**, *18*, 4517 – 4521. (h) Li, G. –Q.; Yamamoto, Y.; Miyaura, N. *Synlett* **2011**, *12*, 1769 – 1773. (i) Hoshi, T.; Nakazawa, T.; Saitoh, I.; Mori, A.; Suzuki, T.; Sakai, J. –I.; Hagiwara, H. *Org. Lett.* **2008**, *10*, 2063 – 2066. (j) Schaarschmidt, D.; Grumbt, M.; Hildebrandt, A.; Lang, H. *Eur. J. Org. Chem.* **2014**, 6676 – 6685. (k) Giannerini, M.; Hornillos, V.; Vila, C.; Fananas-Mastral, M.; Feringa, B. L. *Angew. Chem., Int. Ed.* **2013**, *52*, 13329 – 13333. (l) Wu, L.; Drinkel, E.; Gaggia, F.; Capolicchio, S.; Linden, A.; Falivene, L.; Cavallo, L.; Dorta, R. *Chem. Eur. J.* **2011**, *17*, 12886 – 12890. (m) Ackermann, L.; Potukuchi, H. K.; Althammer, A.; Born, R.; Mayer, P. *Org. Lett.* **2010**, *12*, 1004 – 1007.

(10) (a) Bringmann, G.; Gulder, T.; Gulder, T. A. M.; Breuning, M. *Chem. Rev.* **2011**, *111*, 563 – 639. (b) Kozlowski, M. C.; Morgan, B. J.; Linton, E. C. *Chem. Soc. Rev.* **2009**, *38*, 3193 – 3207. (c) Zask, A.; Murphy, J.; Ellestad, G. A. *Chirality* **2013**, *25*, 265 – 274. (d) Smyth, J. E.; Butler, N. M.; Keller, P. A. *Nat. Prod. Rep.* **2015**, *32*, 1562 – 1583. (e) Bringmann, G.; Price-Mortimer, A. J.; Keller, P. A.; Gresser, M. J.; Garmer, J.; Breuning, M. *Angew. Chem., Int. Ed.* **2005**, *44*, 5384 – 5427. (f) Wencel-Delord, J.; Panossian, A.; Leroux, F. R.; Colobert, F. *Chem. Soc. Rev.* **2015**, *44*, 3418 – 3430.

(11) (a) Fandrick, K. R.; Li, W.; Zhang, Y.; Tang, W.; Gao, J. Rodriguez, S.; Patel, N. D.; Reeves, D. C.; Wu, J. –P.; Sanyal, S.; Gonnella, N.; Qu, B.; Haddad, N.; Lorenz, J. C.; Sidhu, K.; Wang, J.; Ma, S.; Grinberg, N.; Lee, H.; Tsantrizos, Y.; Poupart, M. –A.; Busacca, C. A.; Yee, N. K.; Lu, B. Z.; Senanayake, C. H. *Angew. Chem., Int. Ed.* **2015**, *54*, 7144 – 7148. (b) Haddad, N.; Mangunuru, H. P. R.; Fandrick, K. R.; Qu, B.; Sieber, J. D.; Rodriguez, S.; Desrosiers, J. –N.; Patel, N. D.; Lee, H.; Kurouski, D.; Grinberg, N.; Yee, N. K.; Song, J. J.; Senanayake, C. H. *Adv. Synth. Catal.* **2016**, *358*, 3522 – 3527.

(12) Reviews on catalytic asymmetric cross-coupling: (a) Baudoin, O. *Eur. J. Org. Chem.* **2005**, 4223 – 4229. (b) Yang, H.; Yang, X.; Tang, W. *Tetrahedron* **2016**, *72*, 6143 – 6174. (c) Demchuk, O. M.; Kaplon, K.; Kacka, A.; Pietrusiewicz, K. M. *Phosphorous, Sufur, and Silicon* **2016**, *191*, 180 – 200. (d) Cherney, A. H.; Kadunce, N. T.; Reisman, S. E *Chem. Rev.* **2015**, *115*, 9587 – 9652.

(13) (a) Yin, J. J.; Buchwald, S. L. *J. Am. Chem. Soc.* **2000**, *122*, 12051 – 12052. (b) Shen, X.; Jones, G. O.; Watson, D. A.; Bhayana, B.; buchwald, S. L. *J. Am. Chem. Soc.* **2010**, *132*, 11278 – 11287. (c) Cammidge, A. N.; Crepy, K. V. L. *Chem. Commun.* **2000**, 1723 – 1724. (d) Cammidge, A. N.; Crepy, K. V. L. *Tetrahedron* **2004**, *60*, 4377 – 4386. (e) Bermejo, A.; Ros, A.; Fernandez, R.; Lassaletta, J. M. *J. Am. Chem. Soc.* **2008**, *130*, 15798 – 15799. (f) Ros, A.; Estepa, B.; Bermejo, A.; Alvarez, E.; Fernandez, R.; Lassaletta, J. M. *J. Org. Chem.* **2012**, *77*, 4740 – 4750. (g) Sawai, K.; Tatumi, R.; Nakahodo, T.; Fujihara, H. *Angew. Chem., Int. Ed.* **2008**, *47*, 6917 – 6919. (h) Zhang, S. –S.; Wang, Z. Q.; Xu ,M. –H.; Lin, G. –Q. *Org. Lett.* **2010**, *12*, 5546 – 5549. (i) Yamamoto, T.; Akai, Y.; Nagata, Y.; Suginome, M. *Angew. Chem., Int. Ed.* **2011**, *50*, 8844 – 8847. (j) Castanet, A. –S.; Colobert, F.; Broutin, P. –E.; Obringer, M.

Tetrahedron: Asymmetry **2002**, *13*, 659 – 665. (k) Herrbach, A.; Marinetti, A.; Baudoin, O.; Guenard, D.; Gueritte, F. *J. Org. Chem.* **2003**, *68*, 4897 – 4905. (l) Mikami, K.; Miyamoto, T.; Hatano, M. *Chem. Commun.* **2004**, 2082 – 2083. (m) Sun, L.; Dai, W. –M. *Tetrahedron* **2011**, *67*, 9072 – 9079. (n) Tang, W.; Patel, N. D.; Xu, G.; Xu, X.; Savoie, J.; Ma, S.; Hao, M. –H.; Keshipeddy, S.; Capacci, A. G.; Wei, X.; Zhang, Y.; Gao, J.; Li, W.; Rodriguez, S.; Lu, B. Z.; Yee, N. K. Senanayake, C. H. *Org. Lett.* **2012**, *14*, 2258 – 2261. (o) Xu, G.; Fu, W.; Liu, G.; Senanayake, C. H.; Tang, W. *J. Am. Chem. Soc.* **2014**, *136*, 570 – 573. (p) Uozumi, Y.; Matsuura, T.; Arakawa, T.; Yamada, Y. M. A. *Angew. Chem., Int. Ed.* **2009**, *48*, 2708 – 2710. (q) Jensen, J. F.; Johannsen, M. *Org. Lett.* **2003**, *5*, 3025 – 3028. (r) Genov, M.; Almorin, A.; Espinet, P. *Chem. –Eur. J.* **2006**, *12*, 9346 – 9352. (s) Meskova, M.; Putala, M. *Tetrahedron Asymmetry* **2013**, *24*, 894 – 902. (t) Castillo, A. B.; Perandones, B. F.; Zangrando, E.; Gladiali, S.; Godard, C.; Claver, C. *J. Organomet. Chem.* **2013**, *743*, 31 – 36. (u) Wang, S.; Li, J.; Miao, T.; Wu, W.; Li, Q.; Zhuang, Y.; Zhou, Z.; Qiu, L. *Org. Lett.* **2012**, *14*, 1966 – 1969. (v) Wu, W.; Wang, S.; Zhou, Y.; He, Y.; Zhuang, Y.; Li, L.; Wan, P. Wang, L.; Zhou, Z.; Qiu, L. *Adv. Synth. Catal.* **2012**, *354*, 2395 – 2402. (w) Zhou, Y.; Wang, S.; Wu, W.; Li, Q.; He, Y.; Zhuang, Y.; Li, L.; Pang, J.; Zhou, Z.; Qiu, L. *Org. Lett.* **2013**, *15*, 5508 – 5511. (x) Zhou, Y.; Zhang, X.; Liang, H.; Cao, Z.; Zhao, X.; He, Y.; Wang, S.; Pang, J.; Zhou, Z. Ke, Z.; Qiu, L. *ACS Catalysis* **2014**, *4*, 1309 – 1397. (y) Xia, W.; Li, Y.; Zhou, Z.; Chen, H.; Liang, H.; Yu, S.; He, X.; Zhang, Y.; Pang, J.; Zhou, Z.; Qiu, L. *Adv. Synth Catal.* **2017**, *359*, 1656 – 1662. (z) Chatterjee, A.; Mallin, H.; Klehr, J.; Vallapurackal, J.; Finke, A. D.; Vera, L.; Marsh, M.; Ward, T. R. *Chem. Sci* **2016**, *7*, 673 – 677. (aa) Benhamou, L.; Besnard, C.; Kundig, E. P. *Organometallics* **2014**, *33*, 260 –

266. (bb) Li, Y.; Tang, J.; Gu, J.; Wang, Q.; Sun, P.; Zhang, D. *Organometallics* **2014**, *33*, 876 – 884. (cc) Yang, X.; Xu, G.; Tang, W. *Tetrahedron* **2016**, *72*, 5178 – 5183.

(14) (a) Genov, M.; Fuentes, B.; Espinet, P.; Pelaz, B. *Tetrahedron: Asymmetry* **2006**, *17*, 2593 – 2595. (b) Genov, M.; Almorin, A.; Espinet, P. *Tetrahedron Asymmetry* **2007**, *18*, 625 – 627.

(15) (a) Hayashi, T.; Hayashizaki, K.; Kiyoi, T.; Ito, Y. *J. Am. Chem. Soc.* **1988**, *110*, 8153 – 8156. (b) Hayahsi, T.; Niizuma, S.; Kamikawa, T.; Suzuki, N.; Uozumi, Y. *J. Am. Chem. Soc.* **1995**, *117*, 9101 – 9102

(16) (a) Tamao, K.; Sumitani, K.; Kumada, M. *J. Am. Chem. Soc.* **1972**, *94*, 4374 – 4376. (b) Corriu, R. J. P.; Masse, J. P. *Chem. Commun.* **1972**, 144a. (c) Smith, R. S.; Kochi, J. K. *J. Org. Chem.* **1976**, *41*, 502 – 509. (d) Adrio, J.; Carretero, J. C. *ChemCatChem.* **2010**, *2*, 1384 – 1386. (e) Kambe, N.; Iwasaki, T.; Terao, J. *Chem. Soc. Rev.* **2011**, *40*, 4937 – 4947. (f) Heravi, M. M.; Hajiabbasi, P. *Montash Chem.* **2012**, *143*, 1575 – 1592.

(17) For an overview of the selectivity determining step in Pd-catalyzed cross-coupling reactions, see: Denmark, S. E.; Chang, W. –T. T.; Houk, K. N.; Liu, P. *J. Org. Chem.* **2015**, *80*, 313 – 366.

(18) Reviews: (a) Lipshutz, B. H.; Ghorai, S.; Cortes-Clerget, M. *Chem. Eur. J.* **2018**, *24*, 6672 – 6695. (b) Demchuk, O. M.; Jasinski, R. *Phosphorous, Sulfur, and Silicon* **2016**, *191*, 245 – 253. (c) Dallinger, D.; Kappe, C. O. *Chem. Rev.* **2007**, *107*, 2563 – 2591. (d) Lamlin, M.; Nassar-Hardy, L.; Hierso, J. C.; Fouquet, E.; Felpin, F. X. *Adv. Synth. Catal.* **2010**, *352*, 33 – 79. (e) Lipshutz, B. H.; Ghorai, S. *Aldrichimica Acta.* **2012**, *45*, 3 – 16.

(19) Selected examples: (a) Patel, N. D.; Rivalti, D.; Buono, F. G.; Chatterjee, A.; Qu, B.; Desrosiers, J. –N.; Rodriguez, S.; Sieber, J. D.; Haddad, N.; Fandrick, K. R.; Lee, H.; Yee, N. K.;

Busacca, C. A.; Senanayake, C. H. *Asian J. Org. Chem.* **2017**, *6*, 1285 – 1291. (b) Leadbeater, N. E.; Marco, M. *J. Org. Chem.* **2003**, *68*, 888 – 892. (c) Amini, M.; Tarassoli, A.; Yousefi, S.; Delsouz-Hafshejani, S.; Bigdeli, M.; Salehifar, M. *Chinese Chem. Lett.* **2014**, *25*, 166 – 168. (d) Demchuk, O. M.; Kaplon, K.; Mazur, L.; Strzelecka, D.; Pietrusiewicz, K. M. *Tetrahedron* **2016**, *72*, 6668 – 6677. (e) Li, Z.; Gelbaum, C.; Heaner, IV, W. L.; Fisk, J.; Jaganathan, A.; Holden, B.; Pollet, P.; Liotta, C. L. *Org. Process Res. Dev.* **2016**, *20*, 1489 – 1499. (f) Bumagin, N. A.; Bykov, V. V.; Beletskaya, I. P. *Bull. Acad. Sci. USSR, Div. Chem. Sci.* **1989**, *38*, 2206 – 2206. (g) Bumagin, N. A.; Bykov, V. V. *Tetrahedron* **1997**, *53*, 14437 – 14450. (h) Liu, C.; Zhang, Y. X.; Liu, N.; Qiu, J. S. *Green Chem.* **2012**, *14*, 2999 – 3003. (i) Hoffmann, I.; Blumenroder, B.; Thumann, S. O. N.; Dommer, S.; Schatz, J. *Green Chem.* **2015**, *17*, 3844 – 3857. (j) Zhou, C. S.; Wang, J. Y.; Li, L. Y.; Wang, R. H.; Hong, M. C. *Green Chem.* **2011**, *13*, 2100 – 2106. (k) Handa, S.; Wang, Y.; Gallou, F.; Lipshutz, B. H. *Science* **2015**, *349*, 1087 – 1091. (l) Botella, L.; Najera, C. *Angew. Chem., Int. Ed.* **2002**, *41*, 179 – 181. (m) Rohlich, C.; Wirth, A. S.; Kohler, K. *Chem. Eur. J.* **2012**, *18*, 15485 – 15494. (n) Lipshutz, B. H.; Abela, A. R. *Org. Lett.* **2008**, *10*, 5329 – 5332. (o) Handa, S.; Andersson, M. P.; Gallou, F.; Reilly, J.; Lipshutz, B. H. *Angew. Chem., Int. Ed.* **2016**, *55*, 4914 – 4918.

(20) (a) Breslow, R. *Handbook of Green Chemistry*; Li, C. –J. Ed.; Wiley-VCH: Weinheim, Germany, 2010; Vol. 5, pp 1 – 29. (b) Hailes, H. C. *Org. Process Res. Dev.* **2007**, *11*, 114 – 120. (c) Welton, T. *Proc. R. Soc. A* **2015**, *471*, 20150502. (d) Jessop, P. G *Green Chem.* **2011**, *12*, 1391 – 1398. (e) Clarke, C. J.; Tu, W. –C.; Levers, O.; Brohl, A.; Hallett, J. P. *Chem. Rev.* **2018**, *118*, 747 – 800. (f) Simon, M. –O.; Li, C. –J. *Chem. Soc. Rev.* **2012**, *41*, 1415 – 1427. (g) Li, C. – J.; Chen, L. Organic Chemistry in Water. *Chem. Soc. Rev.* **2006**, *35*, 68 – 82. (h) Akiya, N.;

Savage, P. E. *Chem. Rev.* **2002**, *102*, 2725 – 2750. (i) Lindstrom, U. M. *Chem. Rev.* **2002**, *102*, 2751 – 2772.

(21) Despite the recognized potential "green" properties of water for use as the reaction solvent (ref. 19), reactions run in water may or may not actually be "green." A truly green process employing water as the solvent must be designed correctly to address other important factors related to reaction concentration, waste management, and contaminated water purification/recycling, see: (a) Blackmond, D. G.; Armstrong, A.; Coombe, V.; Wells, A. *Angew. Chem., Int. Ed.* **2007**, *46*, 3798 – 3800. (b) Ni, Y.; Holtmann, D.; Hollmann, F. *ChemCatChem* **2014**, *6*, 930 – 943. (c) Dominguez de Maria, P.; Hollmann, F. *Front. Microbiol.* **2015**, *6*, 1257 – 1261. (d) Clark, J. H.; Tavener, S. J. *Org. Proc. Res. & Dev.* **2007**, *11*, 149 – 155.

(22) Two other reports of asymmetric Suzuki–Miyaura cross-coupling in water have been reported (ref. 13z, 13aa); however, these both are performed in the presence of an organic co-solvent.

(23) Qu, B.; Haddad, N.; Rodriguez, S.; Sieber, J. D.; Desrosiers, J. –N.; Patel, N. D.; Zhang, Y.; Grinberg, N.; Lee, H.; Ma, S.; Ries, U. J.; Yee, N. K.; Senanayake, C. H. *J. Org. Chem.* **2016**, *81*, 745 – 750.

(24) Rodriguez, S.; Qu, B.; Haddad, N.; Reeves, D.; Tang, W.; Krishnamurthy, D.; Senanayake, C. H. *Adv. Synth. Catal.* **2011**, *353*. 533 – 537.

(25) Tang, W.; Keshipeddy, S.; Zhang, Y.; Wei, X.; Savoie, J.; Patel, N. D.; Yee, N. K.; Senanayake, C. H. *Org. Lett.* **2011**, *13*, 1366 – 1369.

(26) Fandrick, D. R.; Fandrick, K. R.; Reeves, J. T.; Tan, Z.; Tang, W.; Capacci, A. G.; Rodriguez, S.; Song, J. J.; Lee, H.; Yee, N. K.; Senanayake, C. H. *J. Am. Chem. Soc.* **2010**, *132*, 7600 – 7601.

(27) Fandrick, D. R.; Hart, C. A.; Okafor, I. S.; Mercadante, M. A; Sanyal, S.; Masters, J. T.; Sarvestani, M.; Fandrick, K. R.; Stockdill, J. L.; Grinberg, N.; Gonnella, N.; Lee, H.; Senanayake, C. H. *Org. Lett.* **2016**, *18*, 6192 – 6195.

(28) Sieber, J. D.; Rivalti, D. R.; Herbage, M. A.; Masters, J. T.; Fandrick, K. R.; Fandrick, D. R.; Haddad, N.; Lee, H.; Yee, N. K.; Gupton, B. F.; Senanayake, C. H. *Org. Chem. Front.* **2016**, *3*, 1149 – 1153.

(29) Sieber, J. D.; Chennamadhavuni, D.; Fandrick, K. R.; Qu, B.; Han, Z. S.; Savoie, J.; Ma, S.; Samankumara, L. P.; Grinberg, N.; Lee, H.; Song, J. J.; Senanayake, C. H. *Org. Lett*. **2014**, *16*, 5494 – 5497.

(30) Sieber, J. D.; Angeles-Dunham, V. V.; Chennamadhavuni, D.; Fandrick, D. R.; Haddad, N.; Grinberg, N.; Kurouski, D.; Lee, H.; Song, J. J.; Yee, N. K.; Mattson, A. E.; Senanayake, C. H. *Adv. Synth. Catal.* **2016**, *358*, 3062 – 3068.

(31) (a) Tang, W.; Qu, B.; Capacci, A. G.; Rodriguez, S.; Wei, X.; Haddad, N.; Narayanan, B.; Ma, S.; Grinberg, N. Yee, N. K.; Krishnamurthy, D.; Senanayake, C. H. *Org. Lett.* **2010**, *12*, 176 – 179. (b) Tang, W.; Capacci, A. G.; White, A.; Ma, S.; Rodriguez, S.; Qu, B.; Savoie, J.; Patel, N. D.; Wei, X.; Haddad, N.; Grinberg, N.; Yee, N. K.; Krishnamurthy, D.; Senanayake, C. H. *Org. Lett*. **2010**, *12*, 1104 – 1108. (c) Li, G.; Zatolochnaya, O. V.; Wang, X. –J.; Rodriguez, S.; Qu, B.; Sieber, J. D.; Desrosiers, J. –N.; Mangunuru, H. P. R.; Biswas, S.; Rivalti, D.;

Karyakarte, S.; Grinberg, N.; Wu, L.; Lee, H.; Haddad, N.; Fandrick, D. R.; Yee, N. K.; Song, J. J.; Senanayake, C. H. *Org. Lett.* **2018**, *20*, 1725 - 1729.

(32) (a) Qu, B.; Samankumara, L. P.; Savoie, J.; Fandrick, D. R.; Haddad, N.; Wei, X.; Ma, S.; Lee, H.; Rodriguez, S.; Busacca, C. A.; Yee, N. K.; Song, J. J.; Senanayake, C. H. *J. Org. Chem*. **2014**, *79*, 993 – 1000. b) Qu, B.; Samankumara, L. P.; Ma, S.; Fandrick, K. R.; Desrosiers, J.-N.; Rodriguez, S.; Li, Z.; Haddad, N.; Han, Z. S.; McKellop, K.; Pennino, S.; Grinberg, N.; Gonnella, N. C.; Song, J. J.; Senanayake, C. H. *Angew. Chem., Int. Ed*. **2014**, *53*, 14428 – 14432.

(33) (a) Wei, X.; Qu, B.; Zeng, X.; Savoie, J.; Fandrick, K. R.; Desrosiers, J. –N.; Tcyrulnikov, S.; Marsini, M. A.; Buono, F. G.; Li, Z.; Yang, B. –S.; Tang, W.; Haddad, N.; Gutierrez, O.; Wang, J.; Lee, H.; Ma, S.; Campbell, S.; Lorenz, J. C.; Eckhardt, M.; Himmelsbach, F.; Peters, S.; Patel, N. D.; Tan, Z.; Yee, N. K.; Song, J. J.; Roshcanger, F.; Kozlowski, M. C.; Senanayake, C. H. *J. Am. Chem. Soc.* **2016**, *138*, 15473 – 15481. (b) Qu, B.; Mangunuru, H. P. R.; Wei, X.; Fandrick, K. R.; Desrosiers, J. –N.; Sieber, J. D.; Kurouski, D.; Haddad, N.; Samankumara, L. P.; Lee, H.; Savoie, J.; Ma, S.; Grinberg, N.; Sarvestani, M.; Yee, N. K.; Song, J. J.; Senanayake, C. H. *Org. Lett.* **2016**, *18*, 4920 – 4923. (c) Qu, B.; Mangunuru, H. P. R.; Tcyrulnikov, S.; Rivalti, D.; Zatolochnaya, O. V.; Kurouski, D.; Radomkit, S.; Biswas, S.; Karyakarte, S.; Fandrick, K. R.; Sieber, J. D.; Rodriguez, S.; Desrosiers, J. –N.; Haddad, N.; McKellop, K.; Pennino, S.; Lee, H.; Yee, N. K.; Song, J. J.; Kozlowlsi, M. C.; Senanayake, C. H. *Org. Lett.* **2018**, *20*, 1333 – 1337.

(34) Tan, R.; Zheng, X.; Qu, B.; Sader, A.; Fandrick, K. R.; Senanayake, C. H.; Zhang, X. *Org. Lett.* **2016**, *18*, 3346 – 3349.

(35) (a) Rodriguez, S.; Qu, B.; Fandrick, K. R.; Buono, F.; Haddad, N.; Xu, Y.; Herbage, M. A.; Zeng, X.; Ma, S.; Grinberg, N.; Lee, H.; Han, Z. S.; Yee, N. K.; Senanayake, C. H. *Adv. Synth. Catal.* **2014**, *356*, 301 – 307. (b) Zatolochnaya, O. V.; Rodriguez, S.; Zhang, Y.; Lao, K. S.; Tcyrulnikov, S.; Li, G.; Wang, X. –J.; Qu, B.; Biswas, S.; Mangunuru, H. P. R.; Rivalti, D.; Sieber, J. D.; Desrosier, J. –N.; Leung, J. C.; Grinber, N.; Lee, H.; Haddad, N.; Yee, N. K.; Song, J. J.; Kozlowski, M. C.; Senanayake, C. H. *Chem. Sci.* **2018**, *9*, 4505 – 4508.

(36) Thomas, A. A.; Zahrt, A. F.; Delaney, C. P.; Denmark, S. E. *J. Am. Chem. Soc.* **2018**, *140*, 4401 – 4416.

(37) Molander, G. A.; Ellis, N. *Acc. Chem. Res.* **2007**, *40*, 275 – 286.

(38) Manolikakes, S. M.; Ellwart, M.; Stathakis, C. I.; Knochel, P. *Chem. Eur. J.* **2014**, *20*, 12289 – 12297.

(39) Reviews: (a) García-Melchor, M.; Braga, A. A. C., Lledós, A., Ujaque, G., Maseras, F. *Acc. Chem. Res.* **2013**, *46*, 2626 – 2634. (b) Sperger, T., Sanhueza, I. A., Kalvet, I., Schoenebeck, F. *Chem. Rev.* **2015**, *115*, 9532 – 9586. (c) Busch, M.; Wodrich, M. D.; Corminboeuf, C. *ACS Catal.* **2017**, *7*, 5643 – 5653

(40) (a) Casares, J. A.; Espinet, P.; Fuentes, B.; Salas, G. *J. Am. Chem. Soc.* **2007**, *129*, 3508–3509. (b) Fuentes, B.; García-Melchor, M.; Lledós, A.; Maseras, F.; Casares, J. A.; Ujaque, G.; Espinet, P. *Chem. Eur. J.* **2010**, *16*, 8596 – 8599. (c) Liu, Q.; Lan, Y.; Liu, J.; Li, G.; Wu, Y. –D.; Lei, A. *J. Am. Chem. Soc.* **2009**, *131*, 10201 – 10210.

(41) Mlynarski, S. N.; Schuster, C. H.; Morken, J. P. *Nature* **2014**, *505*, 386–390.

(42) (a) Thomas, A. A.; Denmark, S. E. *Science* **2016**, *352*, 329 – 332. (b) Thomas, A. A.; Wang, H.; Zahrt, A. F.; Denmark, S. E. *J. Am. Chem. Soc.* **2017**, *139*, 3805 – 3821. (c) Carrow, B. P.;

Hartwig, J. F. *J. Am. Chem. Soc.* **2011**, *133*, 2116 – 2119. (d) Lennox, A. J. J.; Lloyd-Jones, G. C. *Angew. Chem., Int. Ed.* **2013**, *52*, 7362. (e) Amatore, C.; Jutand, A.; Le Duc, G. *Chem. Eur. J.* **2011**, *17*, 2492 – 2503. (f) Jover, J.; Fey, N.; Purdie, M.; Lloyd-Jones, G. C.; Harvey, J. N. *J. Mol. Catal. A* **2010**, *324*, 39 – 47.

(43) Jasinki, R.; Demchuk, O.M.; Babyuk, D. *J. Chem.* **2017**, Article ID 3617527, 12 pages, https://doi.org/10.1155/2017/3617527 (Accessed Jun 6, 2018).

(44) (a) Ortuno, M. A.; Lledos, A.; Maseras, F.; Ujaque, G. *ChemCatChem.* **2014**, *6*, 3132 – 3138. (b) Sicre, C., Braga, A. A. C., Maseras, F., Cid, M.M. *Tetrahedron* **2008***, 64*, 7437 – 7443. (c) Braga, A. A. C.; Morgon, N. H.; Ujaque, G.; Maseras, F. *J. Am. Chem. Soc.* **2005**, *127*, 9298 – 9307. (d) Braga, A. A. C.; Morgon, N. H.; Ujaque, G.; Lledos, A.; Maseras, F. *J. Organomet. Chem.* **2006**, *691*, 4459 – 4466. (e) Braga, A. A.; Ujaque, G.; Maseras, F. *Organometallics* **2006**, *25*, 3647 – 3658.

(45) Miyaura, N. *J. Organomet. Chem.* **2002**, *653*, 54 – 57.

(46) Zeebe, R. E.; Sanyal, A.; Ortiz, J. D.; Wolf-Gladrow, D. A. *Marine Chemistry* **2001**, *73,* 113 – 124.

(47) Davis, M. E., Davis, R. J. (2003). McGraw-Hill Higher Education, New York, NY.

(48) (a) Guan, Y., Wheeler, S. E. *Angew. Chem., Int. Ed.* **2017**, *56*, 9101 – 9105. (b) Santoro, S., Kalek, M., Huang, G., Himo, F. *Acc. Chem. Res.* **2016**, *49*, 1006 – 1018.

(49) (a) Desiraju, G. R.S., T. Oxford University Press: New York, NY, 1999. (b) Steiner, T.; Desiraju, G. R. Chem. Commun. **1998**, 891 – 892. (c) Jeffrey, G. A. Oxford University Press: New York, NY, 1997. (d) Taylor, R.; Kennard, O. *J. Am. Chem. Soc.* **1982**, *104*, 5063 – 5070. (e) Jeffrey, G. A.; Maluszynska, H. *Int. J. Biol. Macromol.* **1982**, *4*, 173 – 185.

(50) Lingenfelter, D. S.; Helgeson, R. C.; Cram, D. J. *J. Org. Chem.* **1981**, *46*, 393 – 406.

(51) Wen, J. –F.; Hong, W.; Yuan, K.; Mac, T. C. W.; Wng, H. N. C. *J. Org. Chem.* **2003**, *68*, 8918 – 8931.

(52) Gaussian 09, Revision D.01, M. J. Frisch, G. W. Trucks, H. B. Schlegel, G. E. Scuseria, M. A. Robb, J. R. Cheeseman, G. Scalmani, V. Barone, B. Mennucci, G. A. Petersson, H. Nakatsuji, M. Caricato, X. Li, H. P. Hratchian, A. F. Izmaylov, J. Bloino, G. Zheng, J. L. Sonnenberg, M. Hada, M. Ehara, K. Toyota, R. Fukuda, J. Hasegawa, M. Ishida, T. Nakajima, Y. Honda, O. Kitao, H. Nakai, T. Vreven, J. A. Montgomery, Jr., J. E. Peralta, F. Ogliaro, M. Bearpark, J. J. Heyd, E. Brothers, K. N. Kudin, V. N. Staroverov, T. Keith, R. Kobayashi, J. Normand, K. Raghavachari, A. Rendell, J. C. Burant, S. S. Iyengar, J. Tomasi, M. Cossi, N. Rega, J. M. Millam, M. Klene, J. E. Knox, J. B. Cross, V. Bakken, C. Adamo, J. Jaramillo, R. Gomperts, R. E. Stratmann, O. Yazyev, A. J. Austin, R. Cammi, C. Pomelli, J. W. Ochterski, R. L. Martin, K. Morokuma, V. G. Zakrzewski, G. A. Voth, P. Salvador, J. J. Dannenberg, S. Dapprich, A. D. Daniels, O. Farkas, J. B. Foresman, J. V. Ortiz, J. Cioslowski, and D. J. Fox, Gaussian, Inc., Wallingford CT, 2013.

(53) (a) Lee, C.; Yang, W.; Parr, R. G. *Phys. Rev. B* **1988**, *37*, 785 – 789. (b) Becke, A. D. *J. Chem. Phys.* **1993**, *98*, 5648 – 5652. (c) Becke, A. D. *J. Chem. Phys.* **1993**, *98*, 1372 – 1377.

(54) S. Grimme, J. Antony, S. Ehrlich and H. Krieg. *J. Chem. Phys.* **2010**, *132*, 154104 – 154105.

(55) (a) Braga, A. A. C., Morgon, N. H., Ujaque, G., Lledo´s, A., Maseras, F. *J. Organometallic Chem*. **2006**, *691,* 4459 – 4466. (b) Jover J., Feya, N., Purdie, M., Lloyd-Jones G. C., Harvey, J. N. *Journal of Molecular Catalysis A: Chemical* **2010***, 324,* 39 – 47.

(56) Zhao, Y.; Truhlar, D. *J. Chem. Theory Comput.* **2009**, *5*, 324 – 333. (b) Minenkov, Y., Occhipinti, G., Jensen, V. R. *J. Phys. Chem. A* **2009**, *113*, 11833 – 11844.

(57) Denmark, S. E., Chang, W-T. T., Houk, K. N., Liu, P. *J. Org. Chem.* **2015**, *80*, 313 – 366.

(58) Marenich, A. V.; Cramer, C. J.; Truhlar, D. G. *J. Phys. Chem. B* **2009**, *113*, 6378 – 6396.

(59) Zhao, Y.; Truhlar, D. *Theor. Chem. Acc.* **2008**, *120*, 215 – 241.

(60) Patel, N. D.; Sieber, J. D.; Tcyrulnikov, S.; Simmons, B. J. *et. al. ACS Catal.* **2018**, *8*, 10190–10209.

CHAPTER FOUR

Generation and Regioselective Trapping of a 3,4-Piperidyne for the Synthesis of Functionalized Heterocycles

Travis C. McMahon, Jose M. Medina, Yun-Fang Yang, Bryan J. Simmons,

K. N. Houk, and Neil K. Garg

J. Am. Chem. Soc. **2015**, *137*, 4082–4085.

4.1 Abstract

We report the generation of the first 3,4-piperidyne and its use as a building block for the synthesis of annulated piperidines. Experimental and computational studies of this intermediate are disclosed, along with comparisons to the well-known 3,4-pyridyne. The distortion/interaction model is used to explain the observed regioselectivities.

4.2 Introduction

Heterocycles containing one or more nitrogen atoms comprise nearly 60% of all small-molecule drugs that have been approved by the U.S. Food and Drug Administration.[1] The most prevalent of *N*-containing heterocycles is the piperidine ring, which is found in 72 currently marketed small-molecule drugs. Notable examples include the blockbuster drugs clopidogrel (Plavix), tadalafil (Cialis), and solifenacin (VESIcare) (Figure 4.1). Given the importance of this medicinally privileged scaffold, new methods to rapidly access annulated piperidines from simple precursors are highly sought after.

With the aim of developing a new method for the synthesis of decorated piperidines, we questioned if the unusual 3,4-piperidyne intermediate **4.1** could be generated and used as a new synthetic building block (Figure 4.1). Notably, 3,4-piperidynes have never been accessed previously. The most closely related studies have involved the isomeric 2,3-piperidyne **4.2**, which has been the subject of two seminal investigations. In 1988, Wentrup and coworkers generated **4.2** (R = H) using flash vacuum pyrolysis.[2] Although **4.2** was deemed unstable above –150 °C and was never utilized in any synthetic application, Wentrup's studies validated the notion that **4.2** could be generated. Additionally, during the preparation of this manuscript, Danheiser disclosed an efficient means to access **4.2** (R = Ts) and performed a series of synthetically useful trapping reactions.[3] Interestingly, whereas piperidynes have been rarely studied,[4] the corresponding aromatic pyridynes **4.3**[5] and **4.4**,[6] along with many other arynes and hetarynes, have been widely pursued for more than half a century.[7,8,9]

Herein we report: (a) the first generation of a 3,4-piperidyne **4.1**; (b) the strategic use of **4.1** to construct a range of functionalized piperidines, many of which possess significant aliphatic character[10] and represent new heterocyclic scaffolds; (c) regioselectivity predictions, observations, and explanations involving the 3,4-piperidyne, which are in accord with the distortion/interaction model;[7a,7d,8a] and (d) an explanation for the lack of selectivity observed in trapping experiments of the 3,4-pyridyne (**4.3**), which has been unresolved for many decades.

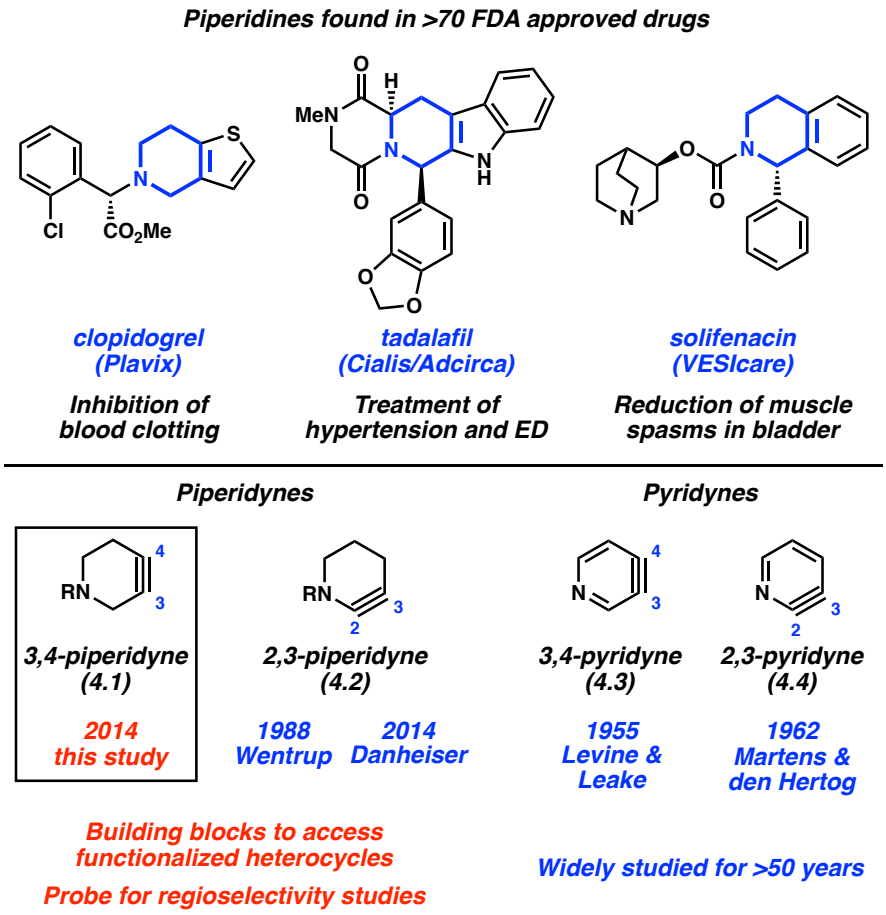

Figure 4.1. Piperidine-containing drugs, piperidynes **4.1** and **4.2**, and pyridynes **4.3** and **4.4**

4.3 Prediction of Regioselectivities Based on the Distortion/Interaction Model

We initiated our studies by applying the distortion/interaction model to our targeted piperidyne, Cbz-derivative **4.1a**,[11] in order to assess its likelihood that it would undergo regioselective trapping in reactions with nucleophiles and cycloaddition partners (Figure 4.2). In previous studies, we have shown that the degree of distortion present in the ground state of arynes and strained alkynes correlates to observed regioselectivities due to the intermediate being pre-distorted toward one of two competing transition states.[7a,7d,8a,9] Geometry optimization using DFT calculations (B3LYP/6-31G(d)) revealed that **4.1a** is significantly distorted (ca. 10°

difference in internal angles at C4 and C3) such that nucleophilic addition should occur preferentially at the more linear terminus (C4). As a key point of comparison, we also studied the 3,4-pyridyne (**4.3**), which is well-known to react with poor regioselectivity,[7a,7d,8a,12] as alluded to earlier. In contrast to **4.1a**, the geometry-optimized structure of **4.3** shows little unsymmetrical distortion. Given this interesting dichotomy, we envisioned that experimental studies of 3,4-piperidyne **4.1a** would not only test our regioselectivity predictions, but could also ultimately shed light on why the 3,4-pyridyne (**4.3**) is not significantly distorted and, accordingly, reacts with poor regioselectivity.

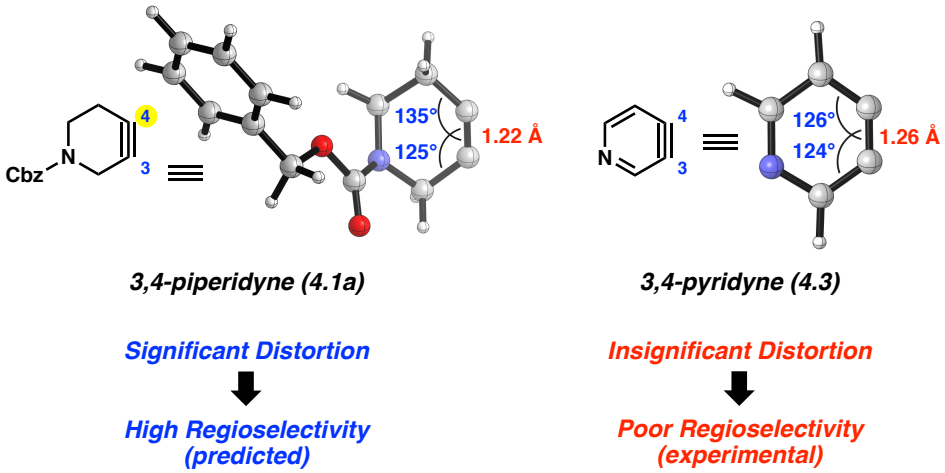

Figure 4.2. Optimized structures of **4.1a** and **4.3** obtained at the B3LYP/6-31G(d) level

4.4 Synthesis of Silyl Triflate Precursor

The success of our study would rely on the development of an efficient synthesis of a suitable 3,4-piperidyne precursor. After identifying silyl triflate **4.8** as our target,[11,13] we developed the robust and scalable three-step route shown in Scheme 4.1. Beginning from commercially available 4-methoxypyridine (**4.5**), a known procedure was employed to effect

ortho silylation to yield silyl pyridine **4.6**.[14] Next, a one-pot procedure involving reductive carbamoylation and hydrolysis[15] provided vinylogous amide **4.7** in excellent yield. Finally, conjugate reduction followed by trapping of the resultant enolate with Tf_2O[16] provided silyl triflate **4.8**. The sequence was performed on gram scale and provided **4.8** in 51% overall yield from **4.5**.[17]

Scheme 4.1. Synthesis of silyl triflate **4.8**

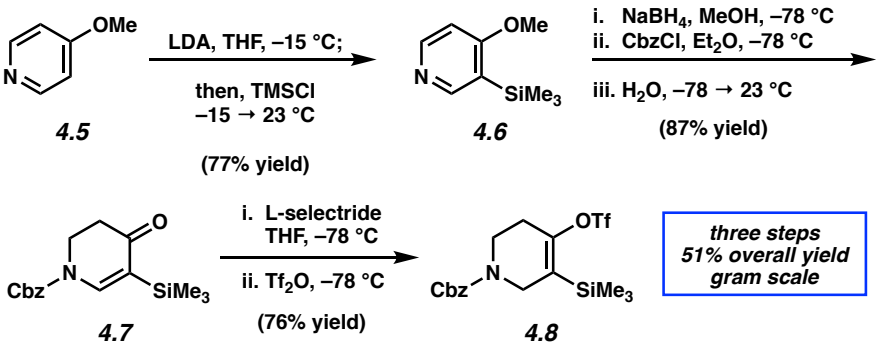

4.5 Generation & Trapping of 3,4-Piperidyne 4.1a

To validate that the 3,4-piperidyne could be generated, we performed a series of Diels–Alder trapping experiments to produce a variety of annulated products (Table 4.1). Specifically, silyl triflate **4.8** was treated with CsF in the presence of several trapping agents (3 equiv) in acetonitrile at 60 °C. The use of tetracyclone as the trapping agent delivered a tetrahydroisoquinoline product in 76% yield via cycloaddition, followed by loss of CO (entry 1). An alternate tetrahydroisoquinoline was accessed upon trapping of the intermediate 3,4-piperidyne with 2-pyrone, by way of a Diels–Alder, retro-Diels–Alder sequence with concomitant loss of CO_2 (entry 2). Additionally, cycloadditions with 2,5-dimethylfuran or *N*-

Boc-pyrrole provided the corresponding piperidine-fused [2.2.1]-bridged bicyclic products (entries 3 and 4).

Table 4.1. Diels–Alder cycloadditions of 3,4-piperidyne **4.1a**

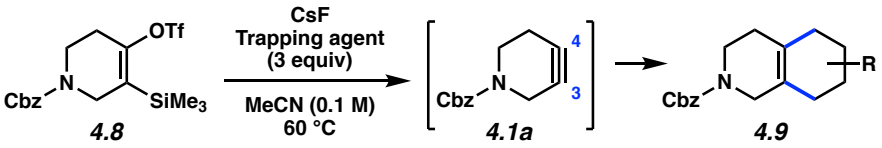

Entry	Trapping agent	Product	Yield[a]
1	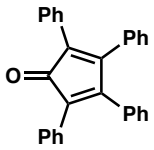	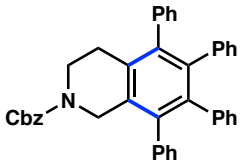	*76%*
2	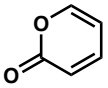	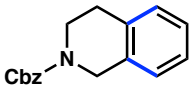	*62%*
3	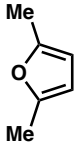	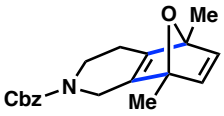	*61%*
4	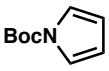	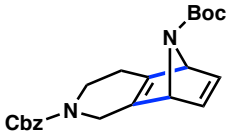	*66%*

[a] Reported yields are the average of two experiments and are based on the amount of isolated products.

Encouraged by our initial success, we carried out trapping experiments of 3,4-piperidyne **4.1a** with a variety of nucleophiles and unsymmetrical cycloaddition partners (Table 4.2). In addition to acting as a probe for our regioselectivity predictions, some of the transformations provide access to interesting heterocyclic products. Nucleophilic addition experiments were performed with imidazole and morpholine (entries 1 and 2). In both cases, addition occurred exclusively at C4, consistent with our earlier prediction and differing from the known trends of

3,4-pyridyne reactions. An analogous regiochemical preference was observed in a series of cycloaddition reactions. For example, trapping with a nitrone afforded isoxazoline products in good yield and with a significant regiochemical preference of 12.7 to 1 (entry 3). (3+2) Cycloadditions using either azide or diazo coupling partners provided triazole and pyrazole products, respectively (entries 4 and 5). Pyridine- and *N*-Ph pyrazole-containing annulated products could be obtained as well, albeit with lower selectivities (entries 6 and 7).[18]

Several salient features regarding this methodology and the products shown in Tables 4.1 and 4.2 should be noted. (a) Analogous to known reactions of arynes using silyl triflate precursors, 3,4-piperidyne trapping experiments are operationally trivial to perform and generally do not require the rigorous exclusion of oxygen or moisture. (b) Silyl triflate **4.8**, which is now being commercialized to enable its widespread use in drug discovery,[17] can be used as a single precursor in order to access a variety of annulated piperidines. This stands in contrast to more conventional strategies, which would involve developing independent syntheses of each annulated piperidine desired. (c) Several of the products accessed by our methodology represent new scaffolds, including those unique compounds shown in entries 3 and 4 in Table 4.1 and those highlighted in entries 3 and 6 of Table 4.2.[19] (d) Several of the cycloaddition adducts shown in Table 4.2 are new analogs of known medicinally important scaffolds. For example, compounds related to those in entries 4, 5, and 7 show promise for the treatment of inflammation,[20] diabetes,[21] cancer,[22] hepatitis C,[23] or other illnesses. (e) Finally, with regard to regioselectivity, it should be emphasized that 3,4-piperidyne **4.1a** uniformly reacts with a preference for initial attack occurring at C4, which is the same trend seen in reactions of the well-studied 3,4-pyridyne (**4.3**). However, the observed selectivities in the case of **4.1a** are generally greater compared to the selectivities seen in the trapping of 3,4-pyridynes.[24]

Table 4.2. Reactions of silyl triflate **4.8** with nucleophiles and cycloaddition partners

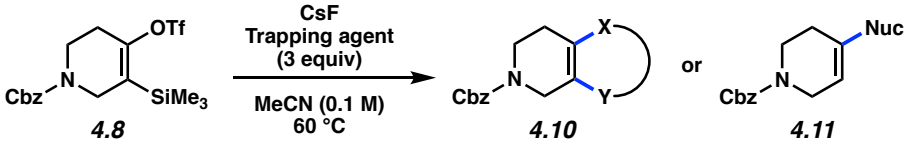

Entry	Trapping agent	Product(s)	Yield[a] (ratio)
1		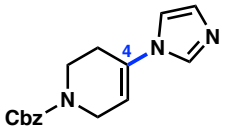	*78% (>20:1)*
2	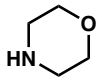	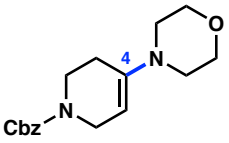	*99%[b] (>20:1)*
3	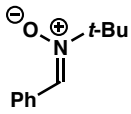	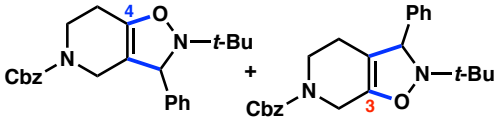	*84% (12.7:1)*
4	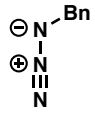	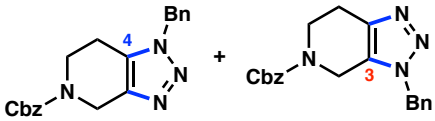	*81% (5.3:1)*
5	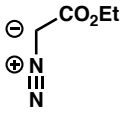	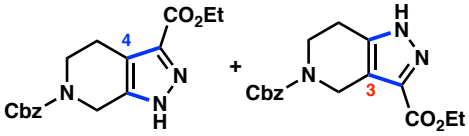	*78% (4.6:1)*
6	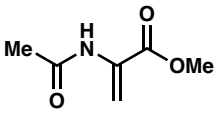	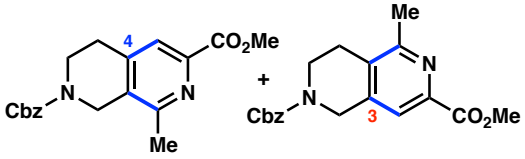	*57% (2.1:1)*
7	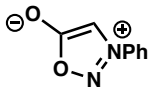	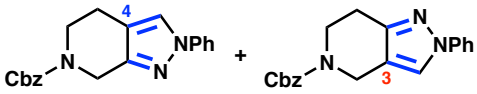	*87% (1.3:1)*

[a]Reported yields are the average of two experiments and are based on the amount of isolated products. [b]Yield was determined using 1,3,5-trimethoxybenzene as an external standard.

4.6 Comparison of Transition States & Distortion Present in 4.1a and 4.3

To understand the disparity in the regioselectivities of the reactions of the 3,4-pyridyne (**4.3**) and 3,4-piperidyne **4.1a**, we used DFT calculations to analyze the competing transition states for the nucleophilic addition of morpholine to **4.3**, and compared the results to the corresponding transition states involving **4.1a** (Figure 4.3). In the reactions of **4.3** with morpholine, the difference in energies for attack at C4 versus C3 (**TS4.1** and **TS4.2**, respectively) is negligible. This is consistent with the low regioselectivity seen experimentally.[24,25] Given that these are very early transition states, the distortion energy (ΔE^{dist}), or the energy required to alter the alkyne geometry toward the transition state, is expected to be small; in fact, we do calculate a slightly greater ΔE^{dist} of the alkyne for **TS4.2** than **TS4.1** (ca. 0.2 kcal/mol). In contrast, the addition of morpholine to C4 of 3,4-piperidyne **4.1a** (**TS4.3**) is predicted to be favored over attack at C3 (**TS4.4**) by roughly 1.7 kcal/mol. Notably, the disparity in distortion energy (ΔE^{dist}) accounts for most of the energetic difference and the resulting high regioselectivity observed experimentally (see Table 4.2, entry 2). These results validate that the distortion/interaction model correctly predicts and explains regioselectivities in reactions of both the 3,4-pyridyne (**4.3**) and 3,4-piperidyne **4.1a**.

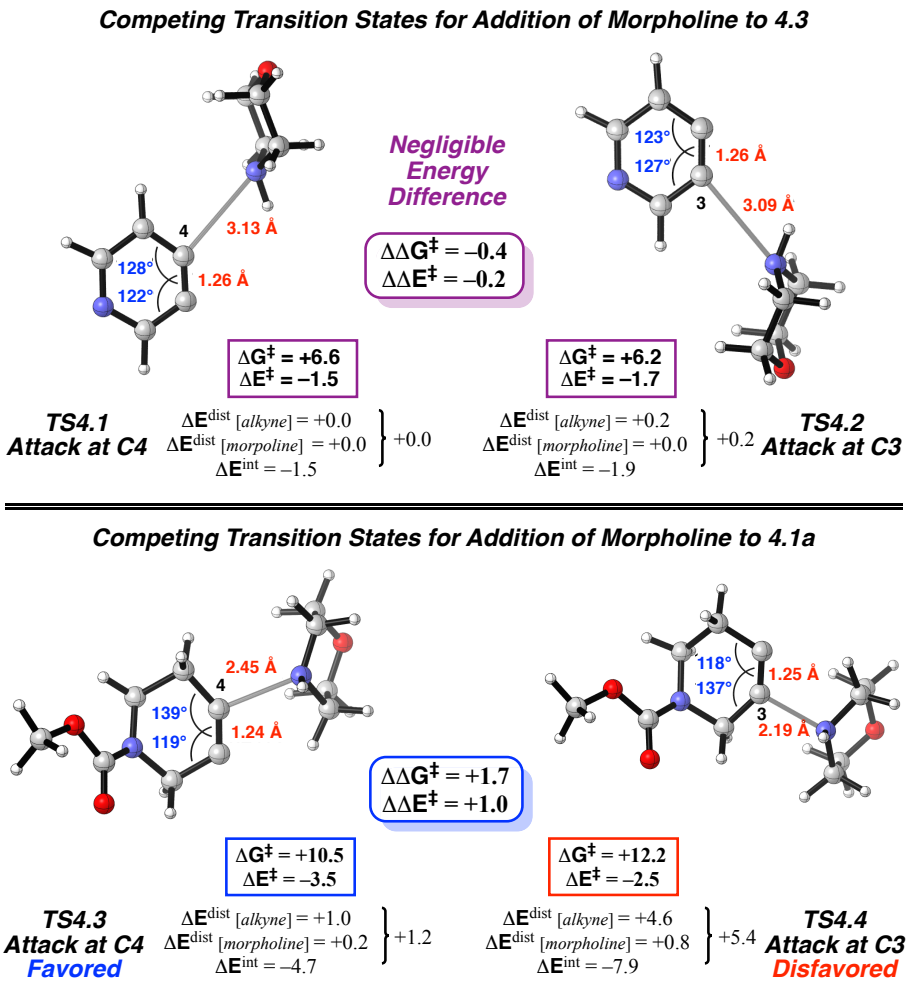

Figure 4.3. Optimized transition states for nucleophilic addition of morpholine to **4.3** and **4.1a** using B3LYP/6-31G(d). Single-point energies were calculated at the B3LYP-D3/6-311+G(d,p) level with CPCM solvent model for MeCN. Energies are provided in kcal mol^{-1}.

As noted earlier, the lack of regioselectivity seen in reactions of 3,4-pyridynes has been a long-standing problem. Thus, we sought to probe one remaining critical question: why is the 3,4-piperidyne significantly distorted, while the 3,4-pyridyne is not? The explanation is summarized in Figure 4.4. The distortion of 3,4-piperidyne **4.1a** is caused by the electronegativity of the *N*-heteroatom that deforms the triple bond as a result of Bent's rule.[26] The internal bond angle at C3 is decreased, mixing in *p* character at C3 and releasing electron density toward the electronegative *N*-atom. Although the analogous effect is also present in 3,4-pyridyne (**4.3**), it is

offset by the in-plane overlap of the nitrogen lone pair with the π and π* orbitals at C3, which causes C3 to move toward the *N*-atom (for further discussion of these competing effects, see the Experimental Section). Such an effect is not seen in **4.1a**, as the nitrogen lone pair is orthogonal to the π and π* orbitals of the alkyne.

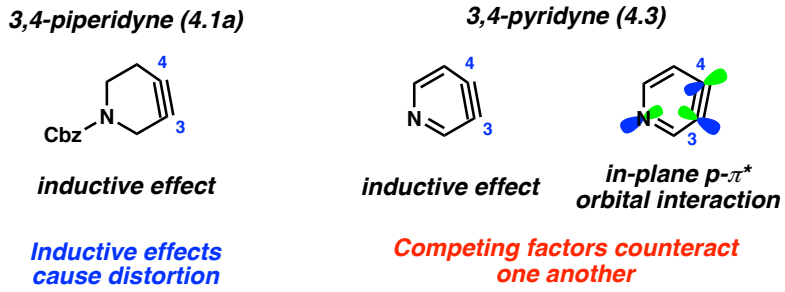

Figure 4.4. Explanation for differing distortion seen in **4.1a** and **4.3**

4.7 Conclusion

In summary, we have synthesized the first 3,4-piperidyne, **4.1a**, and demonstrated that this reactive intermediate can be utilized in a variety of cycloadditions to form annulated piperidine scaffolds. The regioselectivity trends observed in reactions of **4.1a** with nucleophiles and unsymmetrical cycloaddition partners are predicted and rationalized by the distortion/interaction model. Moreover, we have explained the inductive effect that causes the distortion seen in **4.1a**, in addition to the competing inductive effects and orbital interactions that result in the lack of regioselectivity observed in reactions of the well-studied 3,4-pyridyne (**4.3**). Our findings not only provide a new platform to access medicinally-privileged piperidine scaffolds, but also lay the foundation for further studies geared toward strategically harnessing strained heterocyclic alkynes as useful synthetic building blocks.

4.8 Experimental Section

4.8.1 Materials and Methods

Unless stated otherwise, reactions were conducted in flame-dried glassware under an atmosphere of nitrogen using anhydrous solvents (freshly distilled or passed through activated alumina columns). All commercially obtained reagents were used as received unless otherwise specified. Cesium fluoride (CsF) was obtained from Strem Chemicals. Trifluoromethanesulfonic anhydride (Tf_2O) and trimethylsilyl chloride (TMSCl) were obtained from Oakwood Products, Inc. and distilled before use. *N*-tert-butyl-α-phenylnitrone and methyl 2-acetamidoacrylate were obtained from Alfa Aesar. Ethyl diazoacetate, (trimethylsilyl)diazomethane (1 M in Et_2O), tetracyclone, 2,5-dimethylfuran, *N*-Boc-pyrrole, and L-selectride (1 M in THF) were obtained from Sigma Aldrich. Benzyl chloroformate and 2-pyrone were obtained from Acros Organics. Morpholine was obtained from Spectrum Chemical and distilled before use. Reaction temperatures were controlled using an IKAmag temperature modulator and, unless stated otherwise, reactions were performed at room temperature (rt, approximately 23 °C). Thin layer chromatography (TLC) was conducted with EMD gel 60 F254 pre-coated plates (0.25 mm) and visualized using a combination of UV light and potassium permanganate staining. Preparative thin layer chromatography (TLC) was conducted with EMD gel 60 F254 pre-coated plates (0.5 mm) and visualized using UV light. Silicycle Siliaflash P60 (particle size 0.040–0.063 mm) was used for flash column chromatography. ^{1}H NMR and 2D-NOESY spectra were recorded on Bruker spectrometers (500 MHz) and are reported relative to deuterated solvent signals. Data for ^{1}H NMR spectra are reported as follows: chemical shift (δ ppm), multiplicity, coupling constant (Hz) and integration. ^{13}C NMR spectra were recorded on Bruker spectrometers (125 MHz) and are reported relative to deuterated solvent signals. Data for ^{13}C NMR spectra are reported in

terms of chemical shift and, when necessary, multiplicity, and coupling constant (Hz). For mixtures of regioisomers, the major regioisomer is reported with the minor regioisomer in parentheses for both ^{1}H NMR and ^{13}C NMR spectra. IR spectra were obtained using a Perkin-Elmer 100 spectrometer and are reported in terms of frequency absorption (cm^{-1}). High-resolution mass spectra were obtained on Waters LCT Premier with ACQUITY LC and Thermo Scientific^{TM} Exactive Mass Spectrometers with DART ID-CUBE.

4.8.2 Experimental Procedures

4.8.2.1 Synthesis of 3,4-Piperidyne Precursor

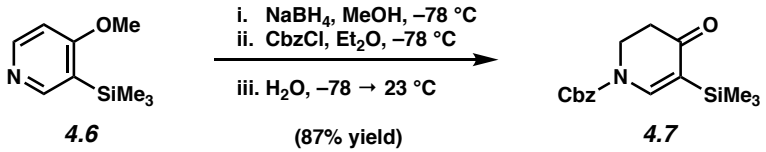

Vinylogous Amide 4.7. To a solution of known silyl pyridine **4.6**[27] (1.00 g, 5.52 mmol, 1 equiv) in MeOH (11 mL) was added $NaBH_4$ (0.230 g, 6.07 mmol, 1.1 equiv) at –78 °C. After stirring for 20 min, benzyl chloroformate (0.87 mL, 6.07 mmol, 1.1 equiv) in Et_2O (1.1 mL) was then added dropwise over 15 min. After stirring for 1 h at –78 °C, H_2O (9.2 mL) was added and the reaction was warmed to room temperature. After 1.5 h, the reaction mixture was diluted with H_2O (20 mL) and extracted with EtOAc (3 × 15 mL). The combined organic layers were washed with H_2O (2 × 20 mL) and brine (20 mL), dried over Na_2SO_4, filtered, and concentrated *in vacuo*. The resulting crude product was purified by flash chromatography (9:1 hexanes : EtOAc) to provide vinylogous amide **4.7** (1.45 g, 87% yield) as a colorless oil. Vinylogous Amide **4.7**: R_f 0.52 (4:1 hexanes : EtOAc); ^{1}H NMR (500 MHz, $CDCl_3$, 55 °C): δ 7.85 (s, 1H), 7.40–7.36 (m, 5H), 5.28 (s, 2H), 4.01 (t, J = 7.4, 2H), 2.52 (t, J = 7.3, 2H), 0.17 (s, 9H); ^{13}C NMR (125 MHz,

$CDCl_3$, 55 °C): δ 196.2, 153.1, 147.3, 135.6, 128.9, 128.8, 128.4, 116.7, 69.0, 42.9, 36.3, –1.24; IR (film): 1723, 1655, 1576, 1391, 1344, 1298 cm^{-1}; HRMS-ESI (*m/z*) $[M + H]^+$ calcd for $C_{16}H_{22}NO_3Si$, 304.1364; found 304.1350.

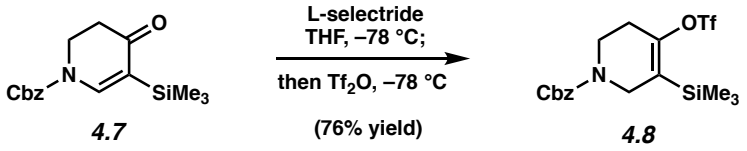

Silyl Triflate 4.8. To a stirred solution of vinylogous amide **4.7** (2.91 g, 9.56 mmol, 1 equiv) in THF (43 mL) was added L-selectride (1.0 M in THF, 10.5 mL, 10.5 mmol, 1.1 equiv) at –78 °C. After stirring for 15 min, Tf_2O (1.26 mL, 10.5 mmol, 1.1 equiv) was added dropwise over 15 min. The reaction was stirred for 20 min at –78 °C and then a saturated aqueous solution of $NaHCO_3$ (30 mL) was added and the reaction was warmed to room temperature. After stirring for 2 h, the layers were separated and the aqueous layer was extracted with EtOAc (3 × 20 mL), washed with brine (1 × 50 mL), dried over Na_2SO_4, filtered, and concentrated *in vacuo*. The resulting crude product was purified by flash chromatography with basic Brockman Grade I 58 Å Al_2O_3 (hexanes), followed by a silica gel column (3:2 hexanes : EtOAc) to give silyl triflate **4.8** (2.60 g, 76% yield) as a colorless oil. Silyl Triflate **4.8**: R_f 0.60 (4:1 hexanes : EtOAc); ^1H NMR (500 MHz, $CDCl_3$, 55 °C): δ 7.37–7.35 (m, 5H), 5.18 (s, 2H), 4.13 (t, J = 2.5, 2H), 3.68 (t, J = 5.9, 2H), 2.57–2.55 (m, 2H), 0.25 (s, 9H); ^{13}C NMR (125 MHz, $CDCl_3$, 55 °C): δ 155.1, 151.8, 136.8, 128.7, 128.3, 128.1, 126.3, 118.6 (q, J = 320.0), 67.7, 45.4, 41.0, 28.9, –1.32; IR (film): 1702, 1656, 1412, 1243, 1204, 1141 cm^{-1}; HRMS-ESI (*m/z*) $[M + H]^+$ calcd for $C_{17}H_{23}NF_3O_5SiS$, 438.1013; found, 438.0992.

4.8.2.2 Trapping Experiments of 3,4-Piperidyne

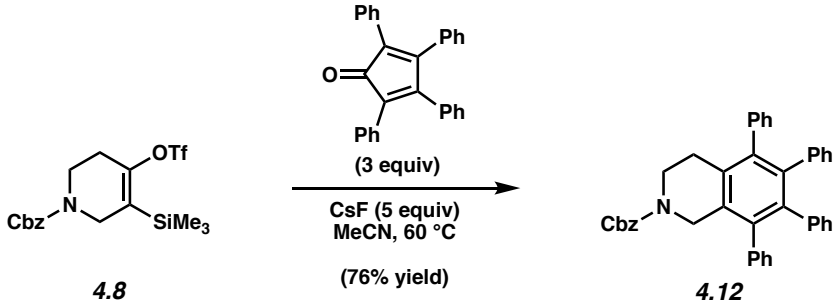

Representative Procedure (Preparation of piperidine 4.12 is used as an example). Piperidine 4.12 (Table 4.1, Entry 1). To a stirred solution of silyl triflate **4.8** (51.6 mg, 0.118 mmol, 1 equiv) and tetracyclone (133 mg, 0.345 mmol, 3.0 equiv) in MeCN (1.2 mL) was added CsF (88.0 mg, 0.575 mmol, 5.0 equiv). The reaction vessel was sealed and placed in a preheated aluminum heating block maintained at 60 °C for 3 h. After cooling to 23 °C, the reaction mixture was filtered over silica gel (EtOAc eluent, 12 mL). Evaporation under reduced pressure and further purification by preparative thin layer chromatography (6:1:1 hexanes : EtOAc : PhH) afforded **4.12** as a pale yellow oil (76% yield, average of two experiments). **4.12**: R_f 0.25 (9:1 hexanes : EtOAc); ^{1}H NMR (500 MHz, C_6D_6, 80 °C): δ 7.12–6.98 (m, 19H), 6.78–6.74 (m, 4H), 6.67–6.64 (m, 2H), 5.11 (s, 2H), 4.55 (s, 2H), 3.53 (m, 2H), 2.58 (t, J = 6.1, 2H); ^{13}C NMR (125 MHz, C_6D_6, 80 °C): δ 155.4, 141.1, 141.0, 140.8, 140.7, 140.2, 139.9, 139.8, 139.6, 137.9, 133.2, 132.3, 131.8, 130.7, 130.5, 128.6, 128.4, 128.2, 128.1, 128.1, 128.0, 127.9, 127.1, 126.9, 126.6, 125.8, 125.8, 67.2, 46.1, 42.2, 28.8; IR (film): 3034, 1702, 1478, 1442, 1428, 1269 cm^{-1}; HRMS-ESI (*m/z*) $[M + H]^+$ calcd for $C_{41}H_{34}NO_2$, 572.2584; found 572.2552.

Any modifications of the conditions shown in this representative procedure are specified in the following schemes, which depict all of the results shown in Tables 4.1 and 4.2.

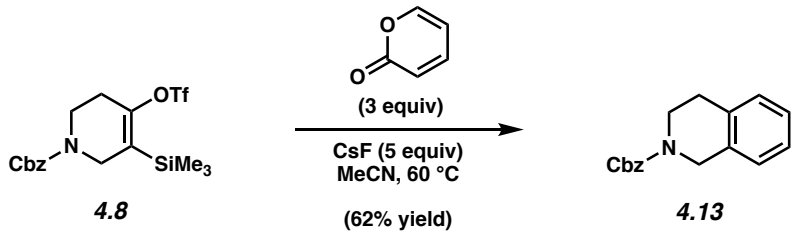

Piperidine 4.13 (Table 4.1, Entry 2). Purification by preparative thin layer chromatography (2:1 hexanes : EtOAc) afforded **4.13** (62% yield, average of two experiments) as a colorless oil. **4.13**: R_f 0.25 (9:1 hexanes : EtOAc); ^{1}H NMR (500 MHz, C_6D_6, 80 °C): δ 7.27 (d, J = 7.6, 2H), 7.14–7.11 (m, 2H), 7.08–7.05 (m, 1H), 6.96–6.92 (m, 2H), 6.81–6.79 (m, 1H), 6.74 (br s, 1H), 5.16 (d, J = 4.4, 2H), 4.50 (s, 2H), 3.46 (br s, 2H), 2.43 (app t, J = 5.3, 2H); ^{13}C NMR (125 MHz, C_6D_6, 80 °C): δ 155.5, 137.8, 135.0, 134.0, 128.9, 128.7, 128.4, 128.1, 126.6, 126.6, 126.5, 67.3, 46.2, 41.9, 29.1; IR (film): 1699, 1452, 1428, 1294, 1226, 1119 cm^{-1}; HRMS-ESI (*m/z*) $[M + H]^+$ calcd for $C_{17}H_{18}NO_2$, 268.1332; found 268.1317.

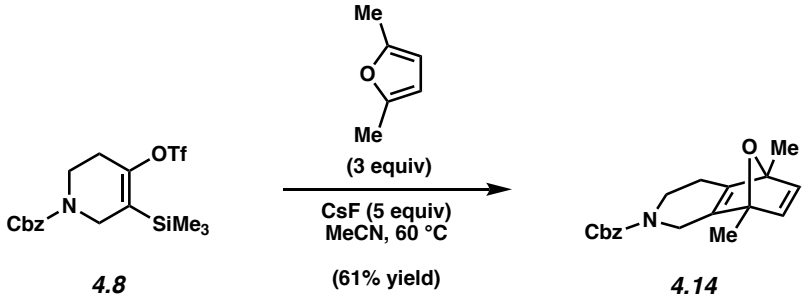

Piperidine 4.14 (Table 4.1, Entry 3). Purification by preparative thin layer chromatography (2:1 hexanes : EtOAc) afforded **4.14** (61% yield, average of two experiments) as a colorless oil. **4.14**: R_f 0.20 (4:1 hexanes : EtOAc); ^{1}H NMR (500 MHz, C_6D_6, 80 °C): δ 7.24 (d, J = 7.6, 2H), 7.11 (d, J = 7.6, 2H), 7.05 (app t, J = 7.3, 1H), 6.58 (m, 2H), 5.14 (s, 2H), 4.17 (dd, J = 15.0, 2.9, 1H), 3.74 (d, J = 17.8, 1H), 3.45–3.42 (m, 1H), 3.30–3.29 (m, 1H), 2.06–2.02 (m, 1H), 1.59–1.54 (m, 1H), 1.41 (s, 3H), 1.38 (s, 3H); ^{13}C NMR (125 MHz, C_6D_6, 80 °C): δ 155.7, 150.9, 149.3, 148.3,

148.2, 137.9, 128.7, 128.4, 128.0, 90.9, 90.3, 67.4, 43.3, 41.4, 23.5, 15.0, 14.9; IR (film): 1701, 1424, 1290, 1234, 1106, 860.1 cm^{-1}; HRMS-ESI (*m/z*) $[M + H]^+$ calcd for $C_{19}H_{22}NO_3$, 312.1594; found 312.1580.

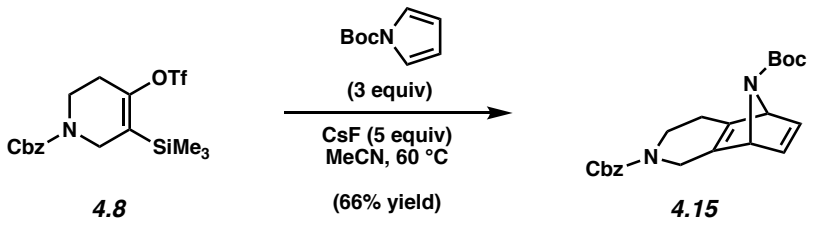

4.8 ***4.15***

Piperidine 4.15 (Table 4.1, Entry 4). Purification by preparative thin layer chromatography (4:1 hexanes : EtOAc) afforded **4.15** (66% yield, average of two experiments) as a colorless oil. **4.15**: R_f 0.25 (4:1 hexanes : EtOAc); ^{1}H NMR (500 MHz, CD_3CN, 55 °C): δ 7.38–7.31 (m, 5H), 7.02–7.00 (m, 2H), 5.13 (s, 2H), 4.95–4.91 (m, 2H), 4.28 (dt, *J* = 18.0, 3.2, 1H), 3.90 (dt, *J* = 18.0, 3.3, 1H), 3.51–3.48 (m, 2H), 2.47–2.44 (m, 1H), 2.09–2.04 (m, 1H), 1.4 (s, 9H); ^{13}C NMR (125 MHz, CD_3CN, 55 °C): δ 156.9, 156.3, 149.8, 148.0, 144.5, 144.3, 139.1, 129.9, 129.3, 129.2, 81.3, 70.4, 68.9, 68.2, 45.6, 42.7, 29.1, 26.6; IR (film): 1700, 1455, 1423, 1366, 1332, 1228 cm^{-1}; HRMS-ESI (*m/z*) $[M + H]^+$ calcd for $C_{22}H_{27}N_2O_4$, 383.1965; found 383.1947.

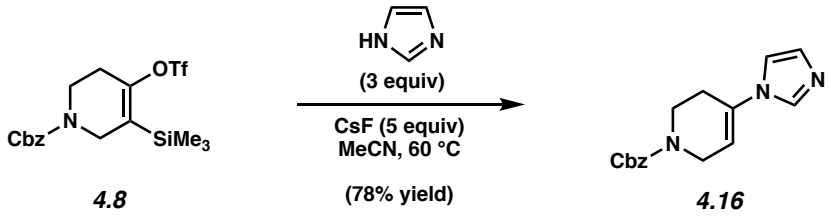

4.8 ***4.16***

Piperidine 4.16 (Table 4.2, Entry 1). Purification by preparative thin layer chromatography (9:1 CH_2Cl_2 : MeOH) afforded **4.16** (78% yield, average of two experiments) as a colorless oil. **4.16**: R_f 0.41 (9:1 CH_2Cl_2 : MeOH); ^{1}H NMR (500 MHz, CD_3CN, 55 °C): δ 7.67 (s, 1H), 7.42–7.32

(m, 5H), 7.22 (s, 1H), 7.01 (s, 1H), 5.88–5.87 (m, 1H), 5.18 (s, 2H), 4.13 (m, 2H), 3.75 (t, J = 3.8, 2H), 2.62–2.58 (m, 2H); ^{13}C NMR (125 MHz, CD_3CN, 55 °C): δ 158.5, 138.8, 136.1, 134.1, 130.7, 139.8, 129.3, 129.0, 125.1, 113.8, 68.2, 43.6, 41.7, 28.4; IR (film): 1699, 1493, 1428, 1233, 1213, 1112 cm^{-1}; HRMS-ESI (*m/z*) [M + H]$^+$ calcd for $C_{16}H_{18}N_3O_2$, 284.1394; found 284.1379.

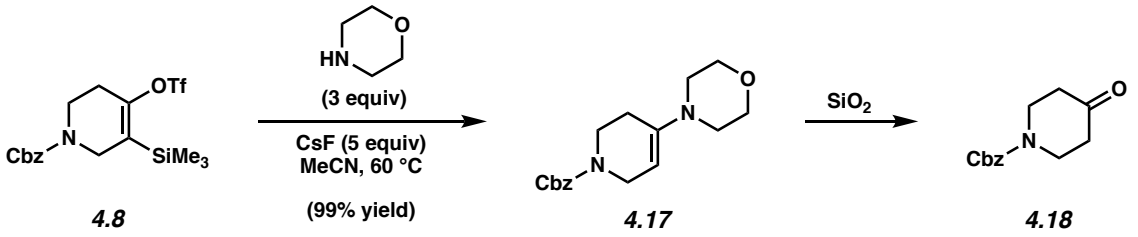

Piperidine 4.17 (Table 4.2, Entry 2). Evaporation under reduced pressure afforded **4.17** (99% yield). The yield was determined by ^{1}H NMR analysis of the crude reaction mixture using 1,3,5-trimethoxybenzene (5.6 mg, 0.72 equiv) as an external standard. **4.17** was found to hydrolyze to the corresponding ketone[28] **4.18** upon exposure to silica gel. **4.18**: R_f 0.45 (3:1 PhH : EtOAc). The regioselectivity of the nucleophilic attack was verified by the isolation of **4.18**. **4.17**: ^{1}H NMR (500 MHz, C_6D_6, 80 °C): δ 7.28 (d, J = 7.4, 2H), 7.13 (t. J = 7.5, 2H), 7.07 (t, J = 7.5, 1H), 5.18 (s, 2H), 4.23 (m, 1H), 3.99 (br s, 2H), 3.46 (t, J = 4.8, 6H), 2.41 (t, J = 4.8, 4H), 1.8 (m, 2H); ^{13}C NMR (125 MHz, CD_3CN, 55 °C): δ 146.1, 139.0, 129.8, 129.1, 129.0, 118.3, 97.4, 67.8, 67.8, 49.5, 44.1, 42.2, 41.7, 27.7, 1.88; IR (film): 1699, 1362, 1329, 1290, 1267, 1033 cm^{-1}; HRMS-ESI (*m/z*) [M + H]$^+$ calcd for $C_{17}H_{23}N_2O_3$, 303.1703; found 303.1690.

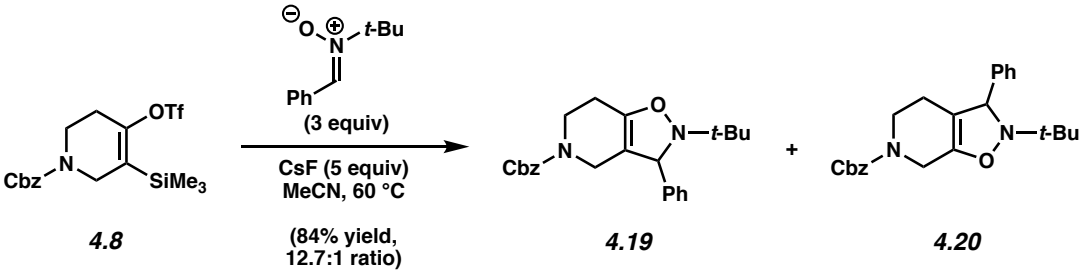

4.8 *4.19* *4.20*

Piperidines 4.19 and 4.20 (Table 4.2, Entry 3). Purification by preparative thin layer chromatography (7:3 hexanes : EtOAc) afforded **4.19** and **4.20** (84% yield, average of two experiments, 12.7:1 ratio) as a colorless oil. **4.19**: R_f 0.63 (7:3 hexanes : EtOAc); ^{1}H NMR (500 MHz, $CDCl_3$, 55 °C): δ 7.36–7.29 (m, 9H), 7.26–7.24 (m, 1H), 5.12 (s, 2H), 5.02 (br s, 1H), 3.95 (app d, J = 15.7, 1H), 3.83 (app dt, J = 13.2, 5.2, 1H), 3.55–3.47 (m, 2H), 2.29 (br s, 2H), 1.14 (s, 9H); ^{13}C NMR (125 MHz, $CDCl_3$, 55 °C): δ 155.8, 147.2, 143.0, 137.1, 128.7, 128.6, 128.1, 128.0, 127.6, 127.3, 104.5, 69.3, 67.4, 60.7, 41.1, 41.1, 25.3, 22.3; IR (film): 1700, 1454, 1423, 1286, 1212, 1132 cm^{-1}; HRMS-ESI (*m/z*) $[M + H]^+$ calcd for $C_{24}H_{29}N_2O_3$, 393.2173; found 393.2154.

The structure of **4.19** was verified by 2D-NOESY, as the following interaction was observed:

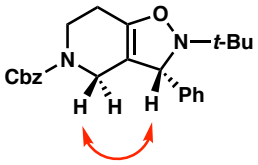

4.19

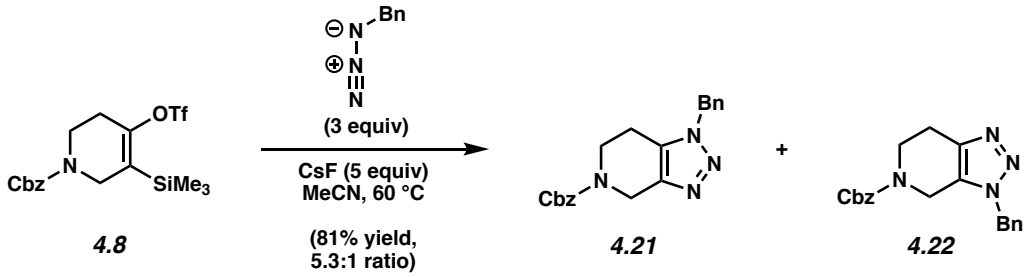

Piperidines 4.21 and 4.22 (Table 4.2, Entry 4). Purification by preparative thin layer chromatography (3:2 EtOAc : hexanes) afforded an inseparable mixture of triazoles **4.21** and **4.22** (81% yield, average of two experiments, 5.3:1 ratio) as a white solid. Compounds **4.21** and **4.22** were characterized as a mixture of regioisomers. R_f 0.40 (3:2 EtOAc : hexanes); ^{1}H NMR (500 MHz, C_6D_6, 80 °C): δ 7.21–7.20 (7.21–7.20) (m, 2H), 7.15 (7.15) (m, 1H), 7.13–7.10 (7.13–7.10) (m, 2H), 7.07–7.06 (7.07–7.06) (m, 1H), 7.01–7.00 (7.01–7.00) (m, 3H), 6.92–6.90 (6.92–6.90) (m, 2H), 5.07 (5.06) (app s, 2H), 4.92 (4.89) (s, 2H), 4.61 (4.11) (s, 2H), 3.30 (3.30) (app t, J = 5.2, 2H), 1.95 (2.56) (app t, J = 5.6, 2H); ^{13}C NMR (125 MHz, $CDCl_3$, 55 °C): δ 155.7, 155.6, 142.4, 141.3, 136.7, 136.6, 134.7, 134.2, 130.6, 129.3, 129.2, 128.8, 128.7, 128.6, 128.6, 128.3, 128.2, 128.2, 128.1, 127.9, 127.7, 127.7, 67.8, 67.7, 52.7, 52.3, 42.1, 42.0, 41.2, 40.3, 22.8, 21.0; IR (film): 1698, 1455, 1424, 1223, 1198, 1100 cm^{-1}; HRMS-ESI (*m/z*) $[M + H]^+$ calcd for $C_{20}H_{21}N_4O_2$, 349.1659; found 349.1638.

The structure of **4.21** was verified by 2D-NOESY and 2D-HMBC of the mixture, as the following interactions were observed:

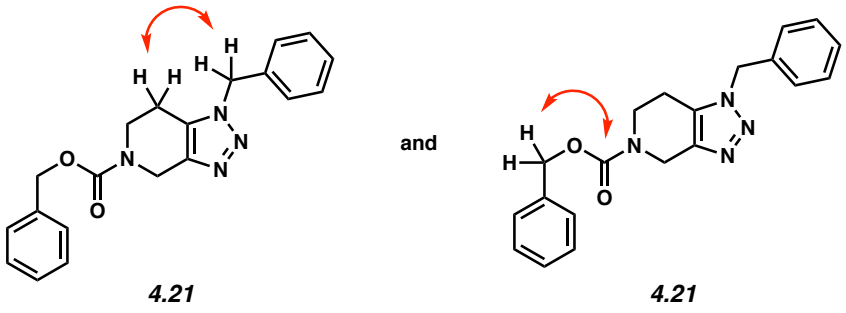

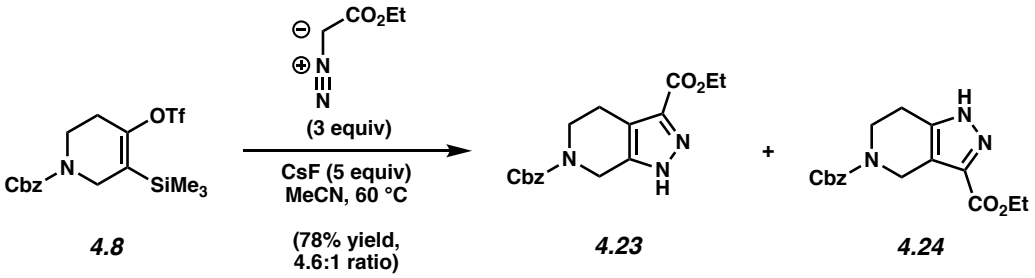

Piperidines 4.23 and 4.24 (Table 4.2, Entry 5). Purification by preparative thin layer chromatography (3:2 EtOAc : hexanes) afforded **4.23** (64% yield, average of two experiments) as a colorless oil and **4.24** (14% yield, average of two experiments) as a colorless oil. **4.23**: R_f 0.43 (3:2 EtOAc : hexanes); ^{1}H NMR (500 MHz, $CDCl_3$, 55 °C): δ 7.37–7.28 (m, 5H), 5.19 (s, 2H), 4.69 (s, 2H), 4.37 (q, J = 7.2, 2H), 3.74 (t, J = 5.8, 2H), 2.87 (t, J = 5.6, 2H), 1.36 (t, J = 7.0, 3H); ^{13}C NMR (125 MHz, $CDCl_3$, 55 °C): δ 160.3, 155.8, 145.9, 136.8, 132.1, 128.6, 128.2, 128.0, 118.2, 67.6, 61.1, 42.5, 42.0, 21.9, 14.4; IR (film): 3219, 2931, 1701, 1470, 1427, 1226 cm^{-1}; HRMS-ESI (*m/z*) $[M + H]^+$ calcd for $C_{17}H_{20}N_3O_4$, 330.1448; found 330.1426. **4.24**: R_f 0.25 (2:3 Hexanes : EtOAc); ^{1}H NMR (500 MHz, $CDCl_3$, 55 °C): δ 7.38–7.30 (m, 5H), 5.20 (s, 2H), 4.74 (s, 2H), 4.39 (q, J = 7.1, 2H), 3.79 (t, J = 5.8, 2H), 2.82 (t, J = 5.7, 2H), 1.38 (t, J = 7.0, 3H); ^{13}C NMR (125 MHz, $CDCl_3$, 55 °C): δ 160.5, 155.9, 145.9, 137.0, 132.6, 128.7, 128.2, 128.1,

117.0, 67.6, 61.3, 41.7, 41.6, 23.3, 14.4; IR (film): 3244, 2957, 1699, 1424, 1269, 1222 cm^{-1}; HRMS-ESI (*m/z*) $[M + H]^+$ calcd for $C_{17}H_{20}N_3O_4$, 330.1448; found 330.1429.

The structures of **4.23** and **4.24** were verified by 2D-HMBC, as the following interactions were observed:

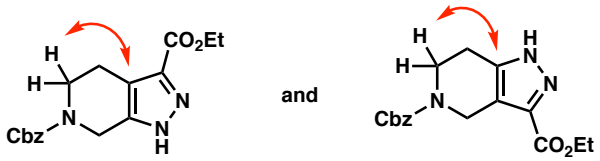

4.23 ***4.24***

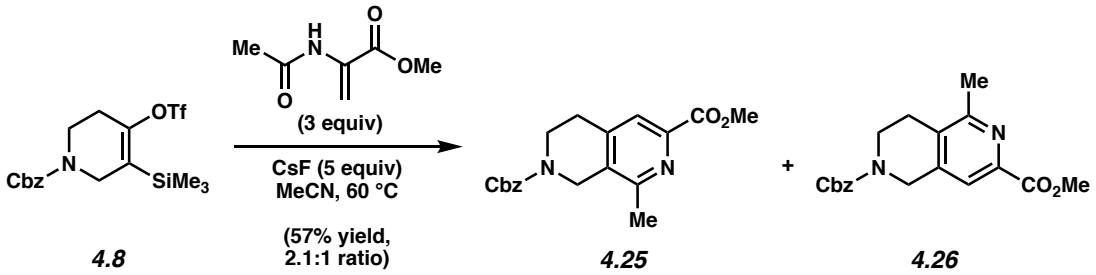

4.8 ***4.25*** ***4.26***

Piperidines 4.25 and 4.26 (Table 4.2, Entry 6). Purification by preparative thin layer chromatography (3:1 PhH : EtOAc) afforded an inseparable mixture of pyridines **4.25** and **4.26** (57% yield, average of two experiments, 2.1:1 ratio) as a colorless oil. Compounds **4.25** and **4.26** were characterized as a mixture of regioisomers. R_f 0.40 (1:1 PhH : EtOAc); ^1H NMR (500 MHz, $CDCl_3$, 55 °C): δ 7.76 (7.73) (s, 1H), 7.38–7.36 (7.35–7.32) (m, 5H), 5.21 (5.19) (s, 2H), 4.62 (4.69) (s, 2H), 3.98 (3.98) (s, 3H), 3.75 (3.80) (t, J = 5.9, 2H), 2.89 (2.81) (t, J = 5.7, 2H), 2.54 (2.56) (s, 3H); ^{13}C NMR (125 MHz, $CDCl_3$, 55 °C): δ 166.1, 166.1, 166.1, 166.1, 158.0, 155.9, 155.6, 155.4, 145.6, 145.3, 144.4, 143.1, 136.8, 136.8, 132.4, 131.5, 128.8, 128.4, 128.2, 128.2, 123.6, 120.9, 67.8, 67.8, 52.8, 52.7, 45.8, 44.1, 41.2, 40.7, 29.1, 26.2, 22.3, 21.8; IR

(film): 1740, 1702, 1433, 1340, 1242, 1217 cm^{-1}; HRMS-ESI (*m/z*) $[M + H]^+$ calcd for $C_{19}H_{21}N_2O_4$, 341.1496; found 341.1482.

The structures of **4.25** and **4.26** were verified by 2D-NOESY, as the following interactions were observed:

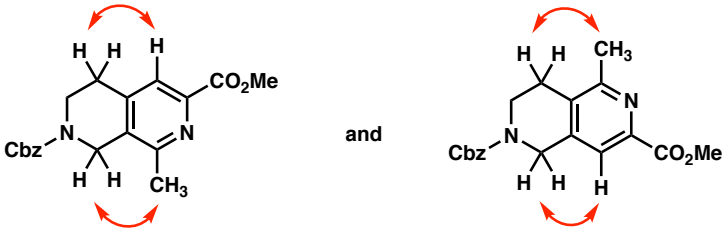

4.25 ***4.26***

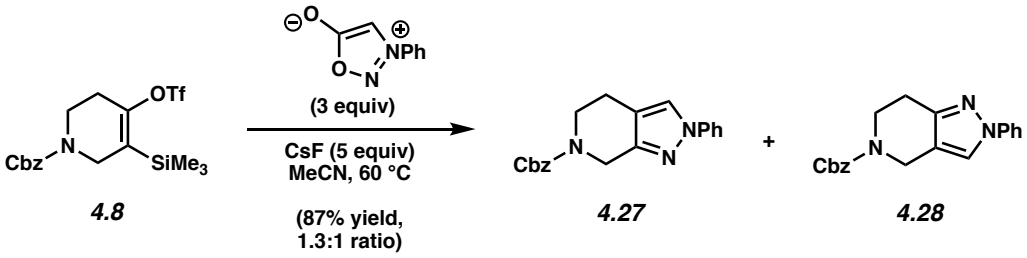

4.8 ***4.27*** ***4.28***

Piperidines 4.27 and 4.28 (Table 4.2, Entry 7). The sydnone trapping agent was synthesized using a known procedure.[29] Purification by preparative thin layer chromatography (9:1 PhH : Et_2O) afforded pyrazoles **4.27** and **4.28** (87% yield, average of two experiments, 1.3:1 ratio) both as amorphous white solids. **4.27**: R_f 0.43 (9:1 PhH : Et_2O); ^1H NMR (500 MHz, CD_3CN, 55 °C): δ 7.85 (s, 1H), 7.68–7.66 (m, 2H), 7.46–7.43 (m, 2H), 7.40–7.35 (m, 4H), 7.33–7.29 (m, 1H), 7.27 (t, *J* = 7.5, 1H), 5.15 (s, 2H), 4.64 (s, 2H), 3.72 (t, *J* = 5.8, 2H), 2.69 (t, *J* = 5.8, 2H); ^{13}C NMR (125 MHz, CD_3CN, 55 °C): δ 156.8, 148.9, 141.2, 138.7, 130.7, 129.7, 129.1, 128.9, 127.2, 125.7, 119.8, 117.5, 68.1, 44.0, 43.5, 21.8; IR (film): 2929, 1698, 1599, 1504, 1425, 1385 cm^{-1}; HRMS-ESI (*m/z*) $[M + H]^+$ calcd for $C_{20}H_{20}N_3O_2$, 334.1550; found 334.1537. **4.28**: R_f 0.42

(9:1 PhH : Et_2O); ^1H NMR (500 MHz, CD_3CN, 55 °C): δ 7.86 (s, 1H), 7.68–7.66 (m, 2H), 7.45–7.43 (m, 2H), 7.39–7.35 (m, 4H), 7.32–7.29 (m, 1H), 7.26 (t, J = 7.4, 1H), 5.15 (s, 2H), 4.58 (s, 2H), 3.78 (t, J = 5.8, 2H), 2.79, (t, J = 5.9, 2H); ^{13}C NMR (125 MHz, CD_3CN, 55 °C): δ 156.7, 149.8, 141.7, 138.7, 130.7, 129.7, 129.2, 128.9, 127.2, 124.2, 119.7, 116.7, 68.1, 43.3, 41.6, 24.7; IR (film): 1698, 1599, 1505, 1426, 1384, 1223 cm^{-1}; HRMS-ESI (m/z) $[M + H]^+$ calcd for $C_{20}H_{20}N_3O_2$, 334.1550; found 334.1530.

The structures of **4.27** and **4.28** were verified by 2D-NOESY, as the following interactions were observed:

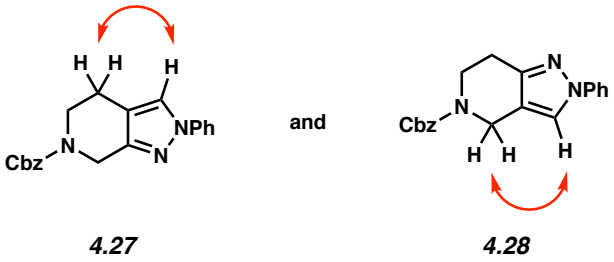

4.27 *4.28*

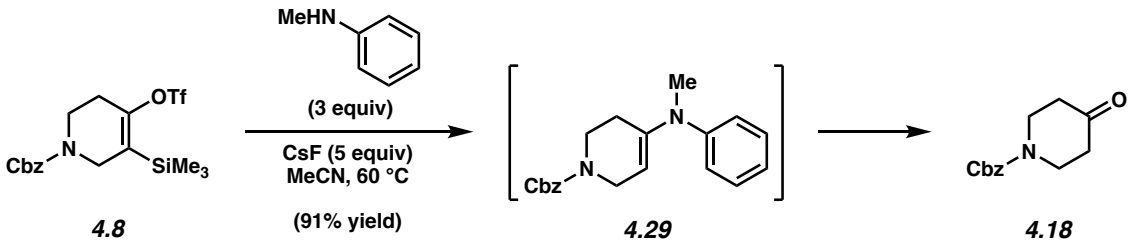

4.8 *4.29* *4.18*

Piperidine 4.29. Evaporation under reduced pressure afforded **4.18** (91% yield). The yield was determined by ^1H NMR analysis of the crude reaction mixture using trimethoxybenzene (5.3 mg, 0.75 equiv) as an external standard. **4.29** was not observed; however, its intermediacy was inferred by the isolation of the hydrolysis product, known ketone **4.18**.[28] **4.18**: R_f 0.45 (3:1 PhH : EtOAc). The regioselectivity of the nucleophilic attack was verified by the isolation of **4.18**.

4.8.3 Computational Methods

All calculations were carried out with the Gaussian 09 package.[30] Geometry optimization and energy calculations were performed with B3LYP.[31] The 6-31G (d) basis set[32] was used for all of the atoms. Frequency analysis was conducted at the same level of theory to verify the stationary points to be real minima or saddle points and to obtain the thermodynamic energy corrections. A quasiharmonic correction was applied during the entropy calculation by setting all positive frequencies that are less than 100 cm^{-1} to 100 cm^{-1}.[33] This method has been found to give relatively accurate energetics for cycloadditions. Single-point energies were calculated at the B3LYP-D3[34]/6-311+G(d,p) level. Solvent effect (solvent = acetonitrile) was calculated by using the CPCM[35] solvation model. Computed structures are illustrated using CYLVIEW.[36]

4.8.3.1 Bent´s Rule & Alkyne Distortion Determine Regioselectivity of Nucleophilic Addition

Bent's rule, as stated in 1961, is that *"atomic s character concentrates in orbitals directed toward electropositive substituents."* In other words, bonds between elements of different electronegativities are polarized in a way such that the electron density will be shifted towards the more electronegative element. Due to the inherent higher stability of *s* orbitals, the hybrid orbitals from the more electronegative atoms will increase their *s* character in order to stabilize the withdrawn electron density. To compensate for this shift in electron density, the less electronegative atoms will direct hybrid orbitals with an increased *p* character toward the more electronegative atoms to which they are bound, without a significant energic penalty. As a result, the hybrid orbitals that constitute these polarized bonds deviate from ideal sp^n (n = 1, 2 or 3) hybridizations, which translates into distorted geometries.

4.8.3.2 *n*→*p interaction in 3,4-pyridyne** The delocalization of the lone pair of electrons (*n*) from the nitrogen atom to the antibonding orbital (*p**) of the alkyne moiety is an attractive electronic interaction that stabilizes 3,4-pyridyne. Figure 4.5 shows this favorable two-electron, two-orbital interaction between the nitrogen lone pair (*n*) and the antibonding orbital (*p**) of the alkyne. The result of this interaction is the formation of a lower energy orbital, (*n*+*p**), and a higher energy orbital, (*n*-*p**). The (*n*+*p**) orbital is computed to be HOMO-2, and it is stabilized by the favorable orbital overlap between the nitrogen lone pair (*n*) and the *p* orbital at C-3 of the antibonding orbital (*p**), which is in closer proximity compared with that of C-4. The maximum stabilization occurs in the system when there is greater orbital overlap between *n* and C3. As a result, the alkyne reorients itself in a manner where C3 of the alkyne moves toward the nitrogen atom to maximize this stabilizing interaction. This counteracts the inductive effect of the electronegative nitrogen atom, which would distort the alkyne in the opposite manner in accord with Bent's rule (see: Figure 4.4). It is the sum of these two opposing effects that leads to the two internal angles at C3 and C4 (124° and 126°) being very similar and showing little distortion, and consequently, no significant regioselectivity in nucleophilic additions.

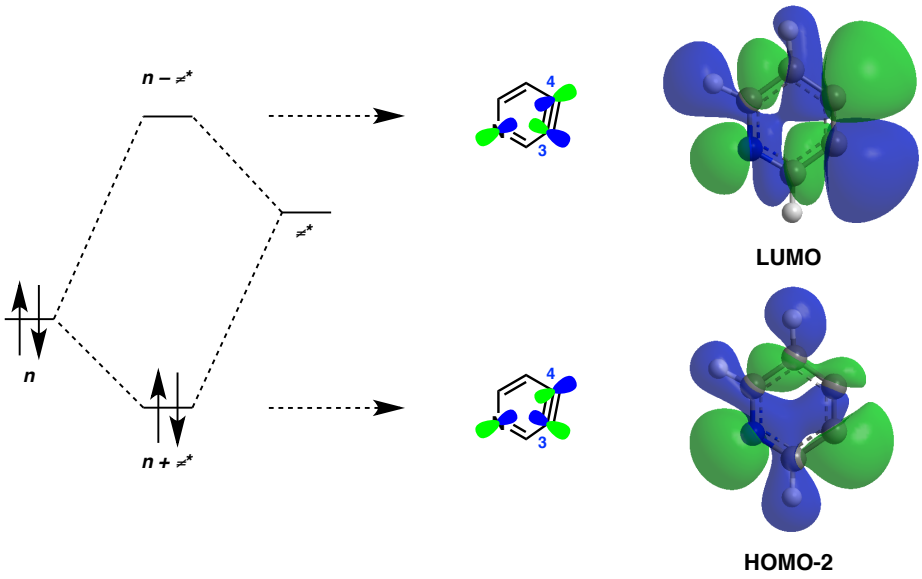

Figure 4.5. *n→p** interaction in 3,4-pyridyne

4.8.3.3 Energies, Enthalpies, and Free Energies

Table 4.3. Energies, enthalpies, and free energies of the structures calculated at the B3LYP-D3/6-311+G(d,p)(CPCM^{MeCN})//B3LYP/6-31G(d).

Structures	ZPE	DE	DH	DG	E	H	G	Imaginary Frequency
4.3	0.154569	0.164225	0.165169	0.11937	-477.409844	-477.244675	-477.290474	–
TS4.1	0.200137	0.211205	0.212149	0.170824	-534.923275	-534.711126	-534.752451	-41.505
TS4.2	0.200204	0.211238	0.212182	0.163959	-534.923580	-534.711398	-534.759621	-42.130
4.1a	0.063685	0.067966	0.068910	0.036450	-247.022283	-246.953373	-246.985833	–
TS4.3	0.291685	0.307621	0.308565	0.245795	-765.314031	-765.005466	-765.068236	-21.426
TS4.4	0.292273	0.307920	0.308864	0.247304	-765.312285	-765.003421	-765.064981	-68.745

4.8.3.4 Cartesian Coordinates of the Relevant Structures

Cartesian coordinates for the optimized structures were reported in the literature.[37]

4.9 Spectra Relevant to Chapter Four:

Generation and Regioselective Trapping of a 3,4-Piperidyne for the Synthesis of Functionalized Heterocycles

Travis C. McMahon, Jose M. Medina, Yun-Fang Yang, Bryan J. Simmons, K. N. Houk, and Neil K. Garg

J. Am. Chem. Soc. **2015**, *137*, 4082–4085.

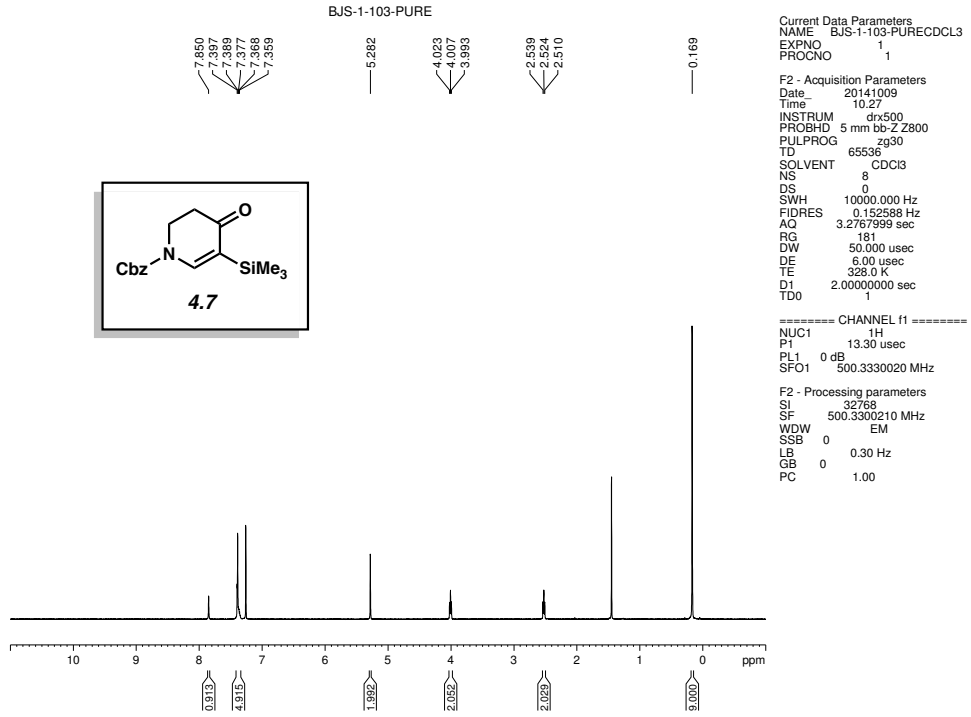

Figure 4.6 ^{1}H NMR (500 MHz, $CDCl_3$) of compound **4.7**.

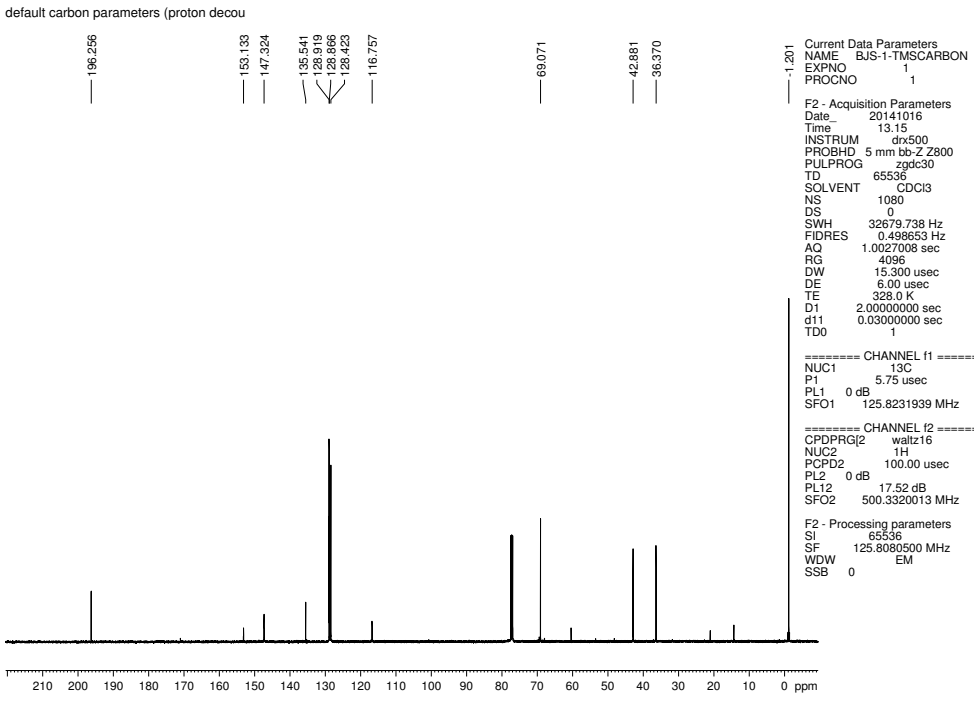

Figure 4.7 ^{13}C NMR (125 MHz, $CDCl_3$) of compound **4.7**.

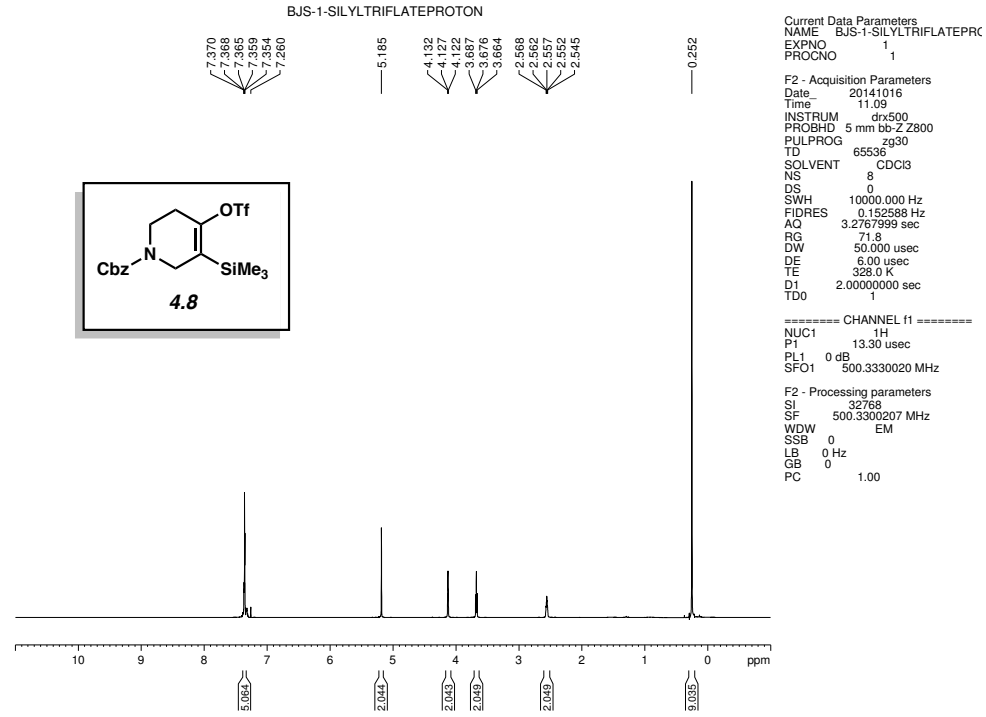

Figure 4.8 ^{1}H NMR (500 MHz, $CDCl_3$) of compound **4.8**.

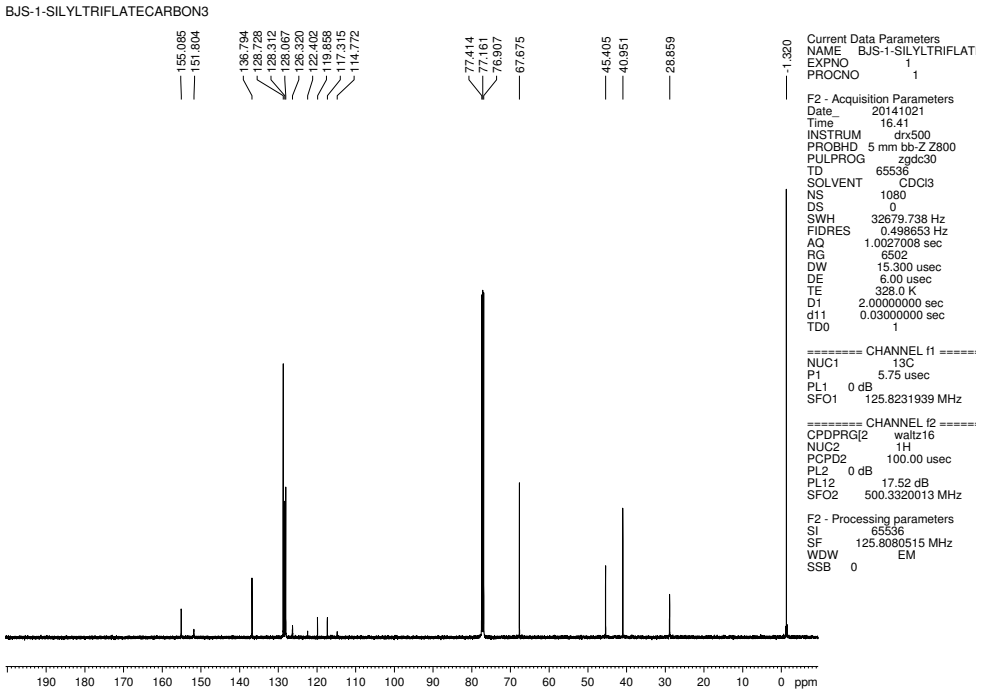

Figure 4.9 ^{13}C NMR (125 MHz, $CDCl_3$) of compound **4.8**.

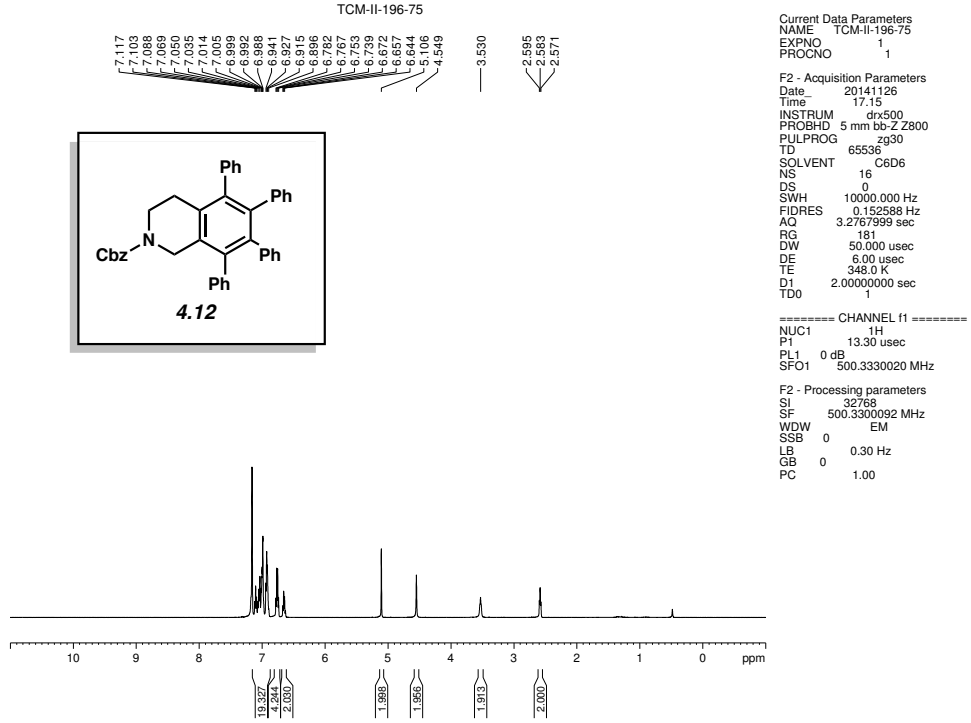

Figure 4.10 ^{1}H NMR (500 MHz, C_6D_6) of compound **4.12**.

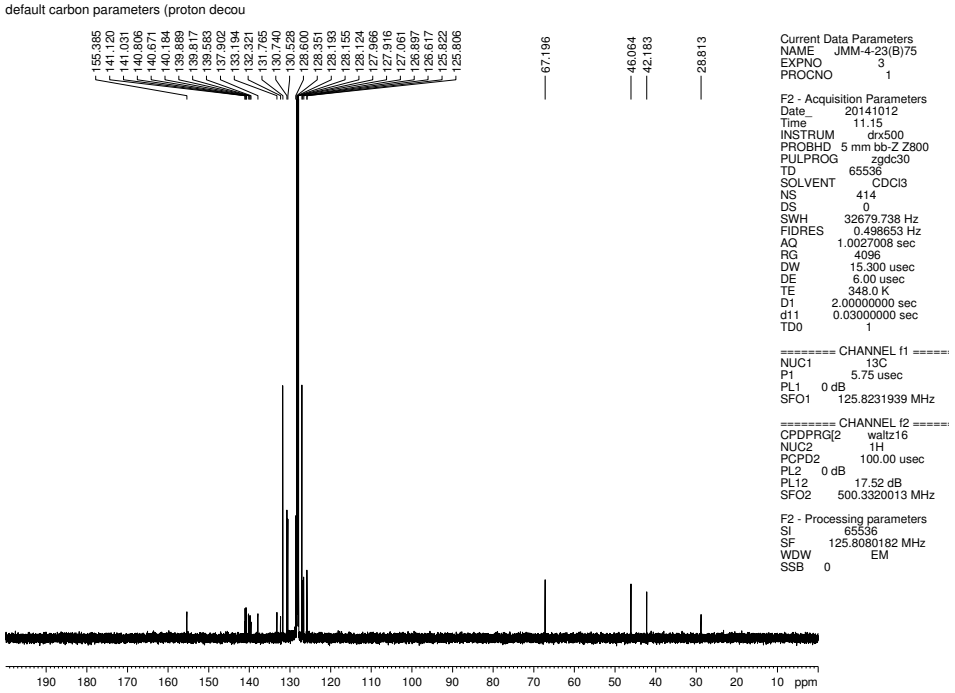

Figure 4.11 ^{13}C NMR (125 MHz, $CDCl_3$) of compound **4.12**.

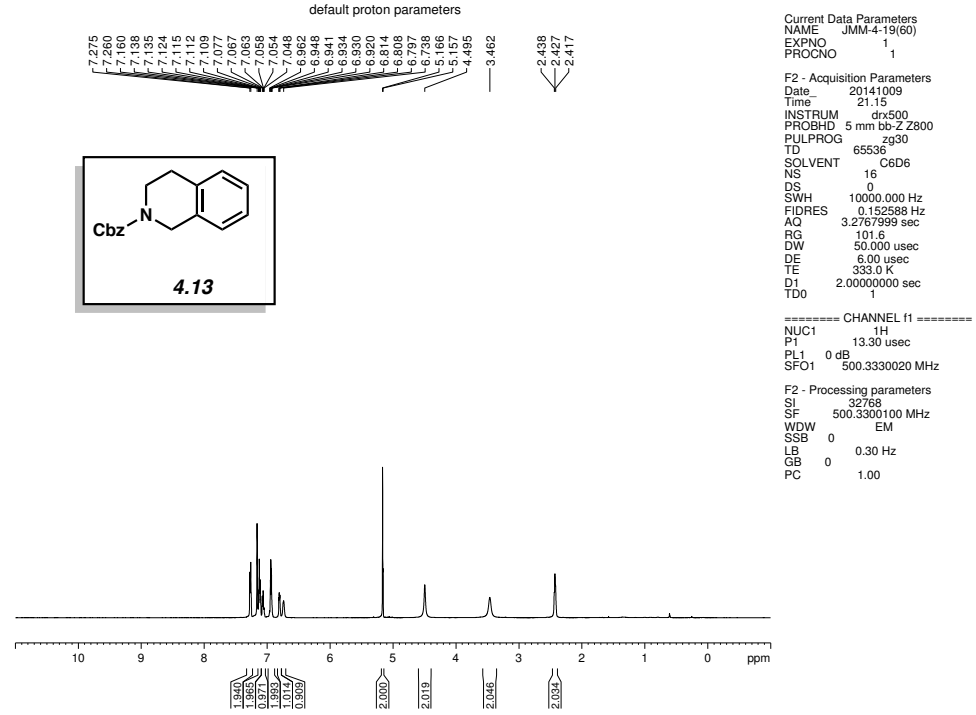

Figure 4.12 ^{1}H NMR (500 MHz, C_6D_6) of compound **4.13**.

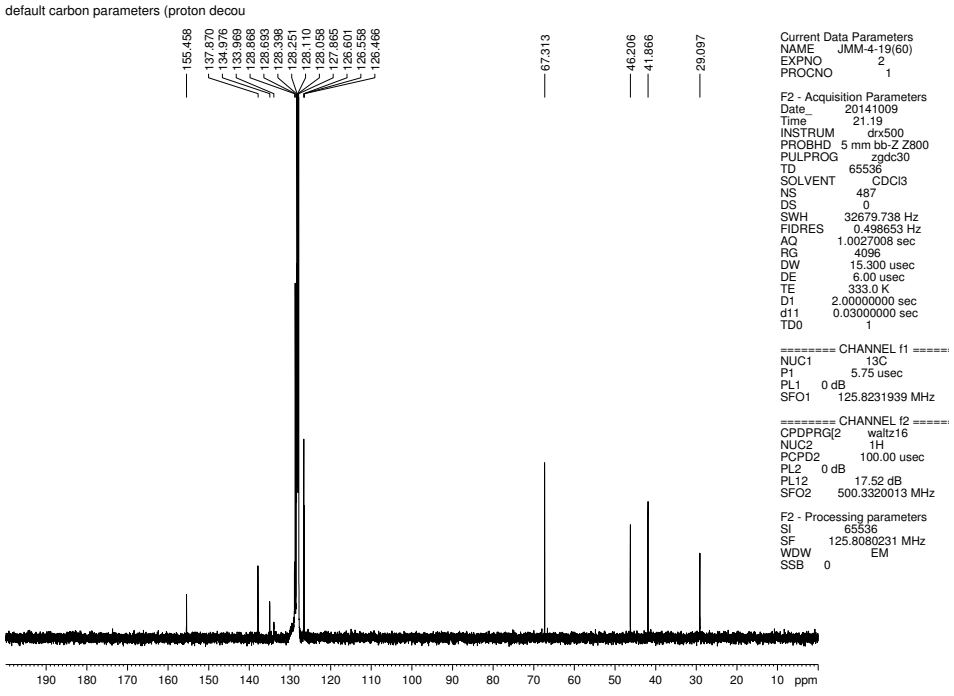

Figure 4.13 ^{13}C NMR (125 MHz, $CDCl_3$) of compound **4.13**.

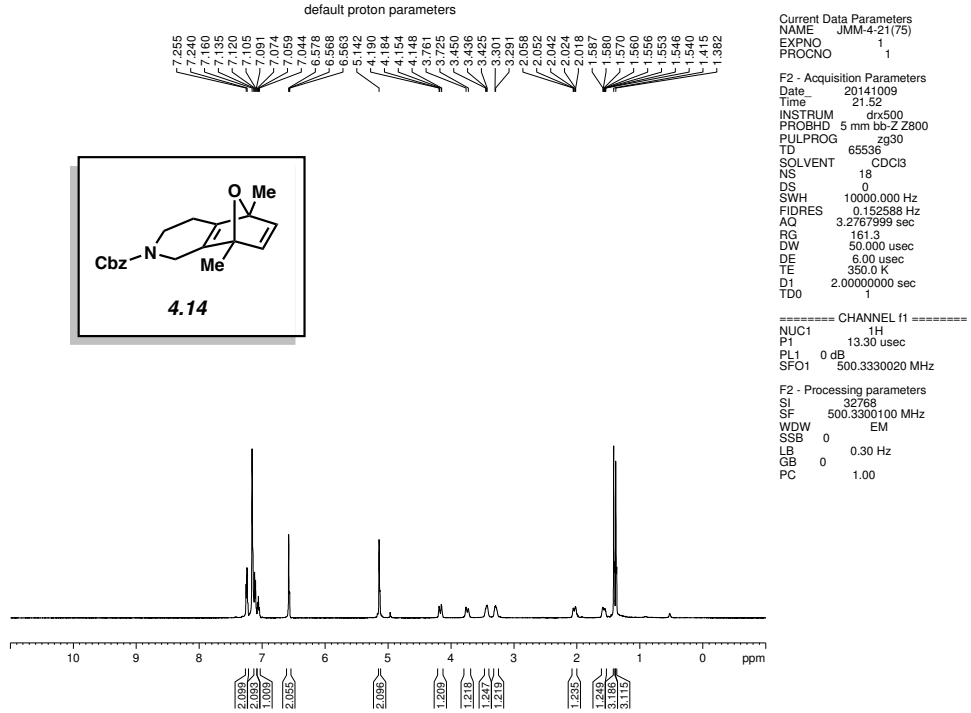

Figure 4.14 ^{1}H NMR (500 MHz, $CDCl_3$) of compound **4.14**.

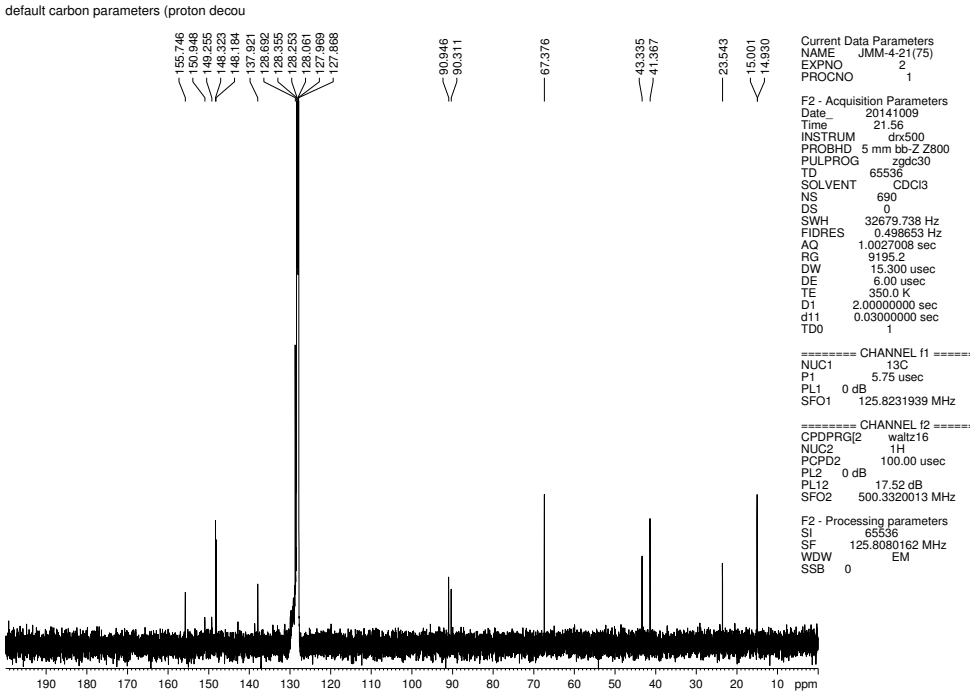

Figure 4.15 ^{13}C NMR (125 MHz, $CDCl_3$) of compound **4.14**.

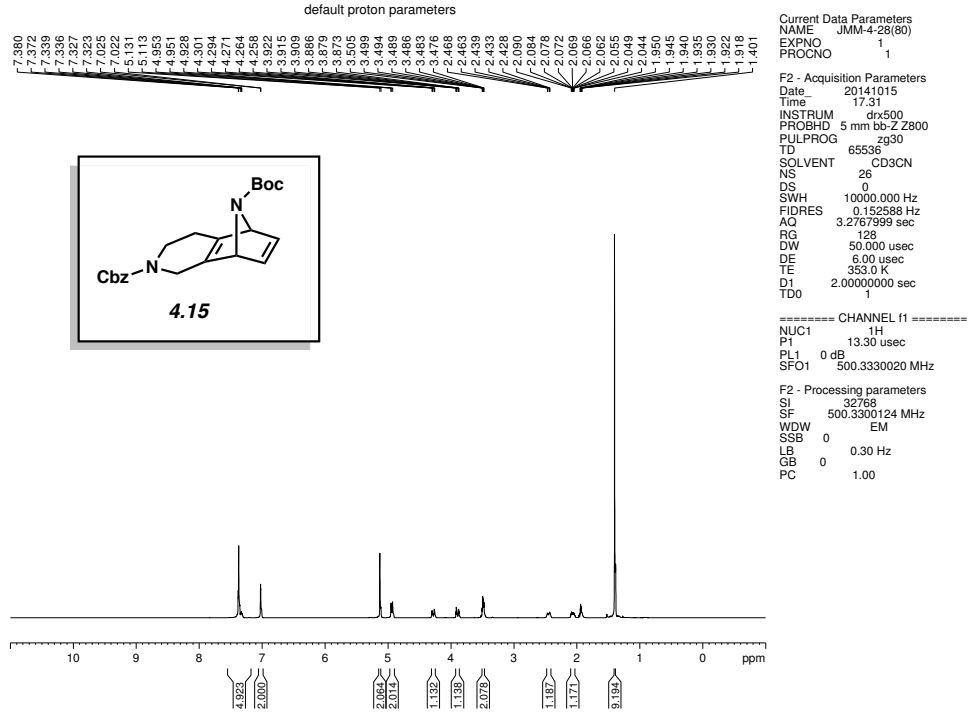

Figure 4.16 ^{1}H NMR (500 MHz, CD_3CN) of compound **4.15**.

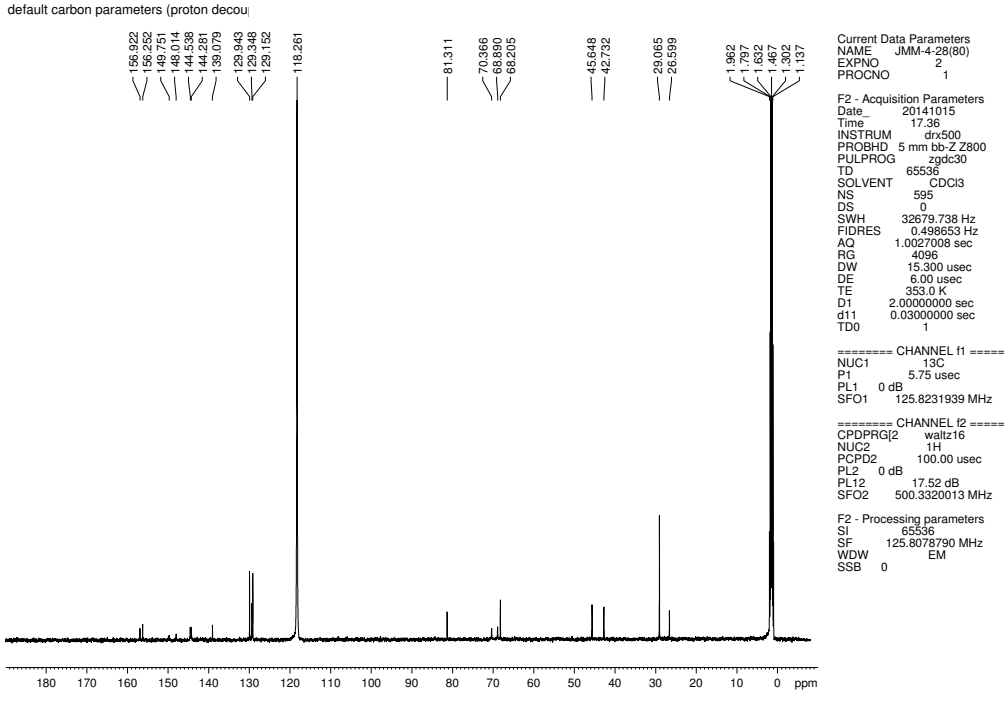

Figure 4.17 ^{13}C NMR (125 MHz, $CDCl_3$) of compound **4.15**.

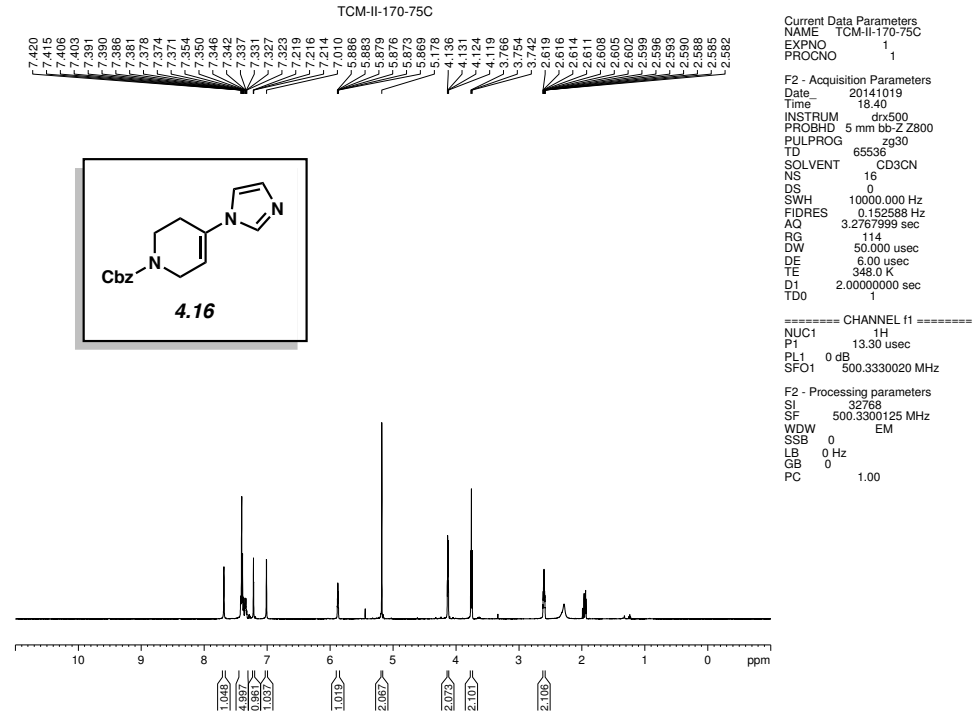

Figure 4.18 ^{1}H NMR (500 MHz, CD_3CN) of compound **4.16**.

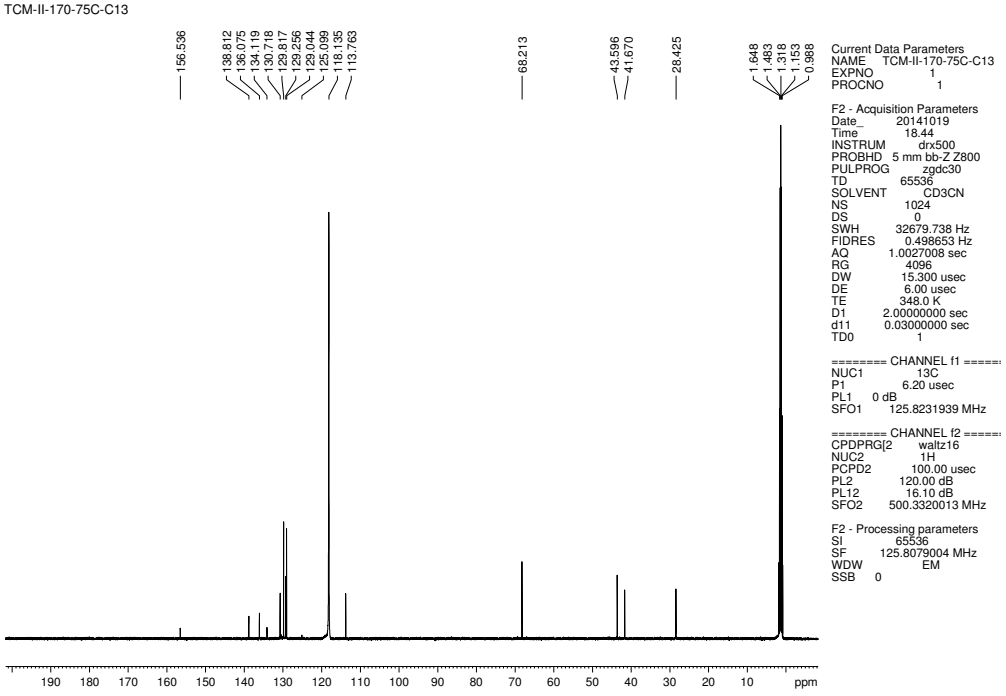

Figure 4.19 ^{13}C NMR (125 MHz, CD_3CN) of compound **4.16**.

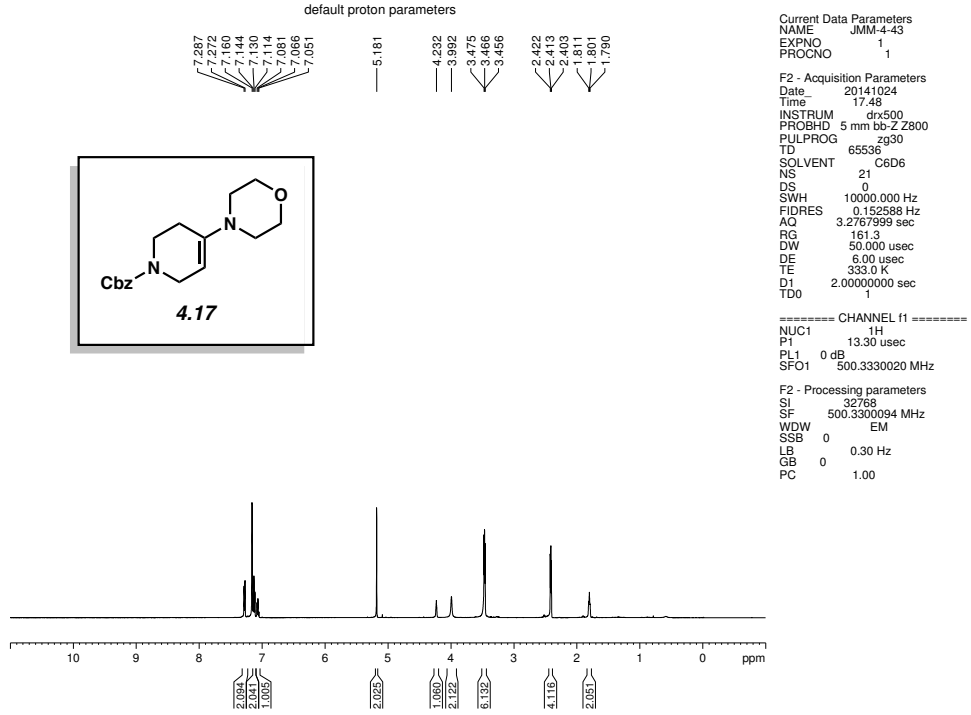

Figure 4.20 ^{1}H NMR (500 MHz, C_6D_6) of compound **4.17**.

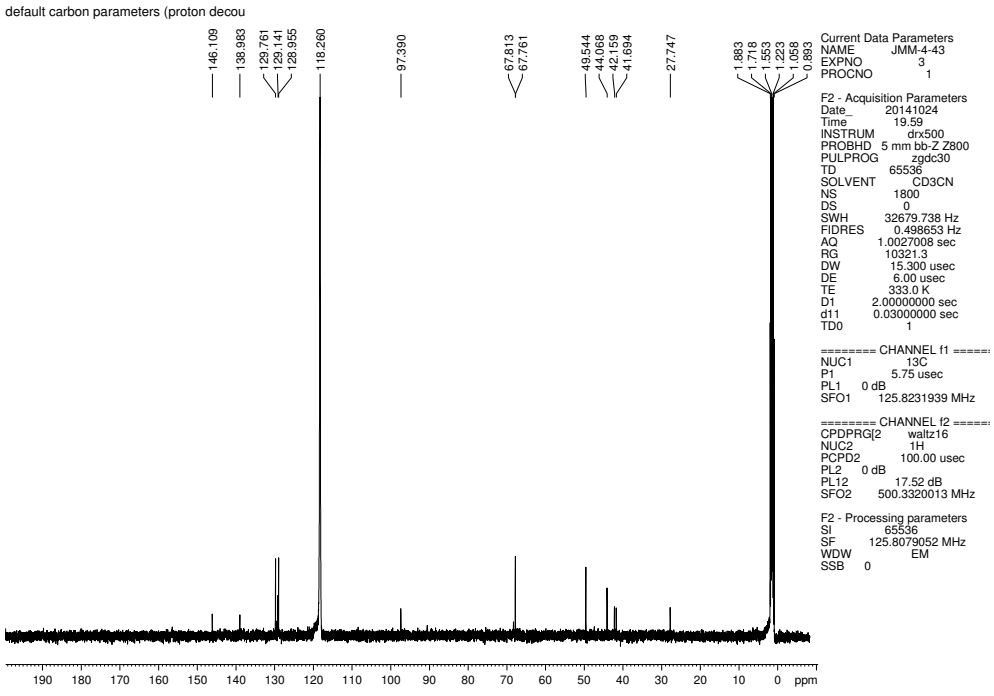

Figure 4.21 ^{13}C NMR (125 MHz, CD_3CN) of compound **4.17**.

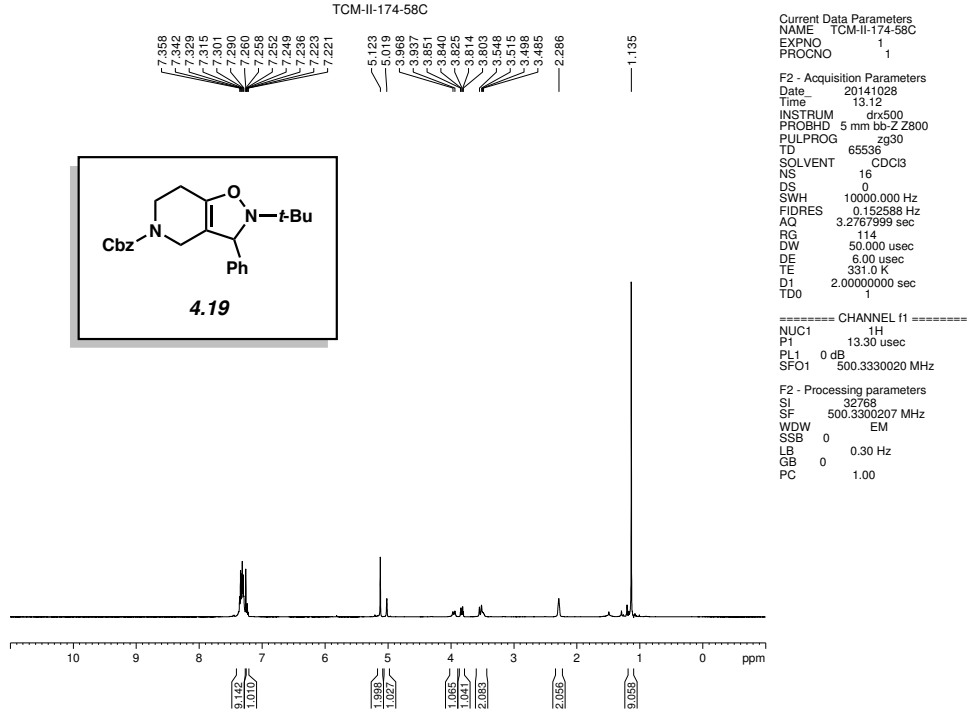

Figure 4.22 ^{1}H NMR (500 MHz, $CDCl_3$) of compound **4.19**.

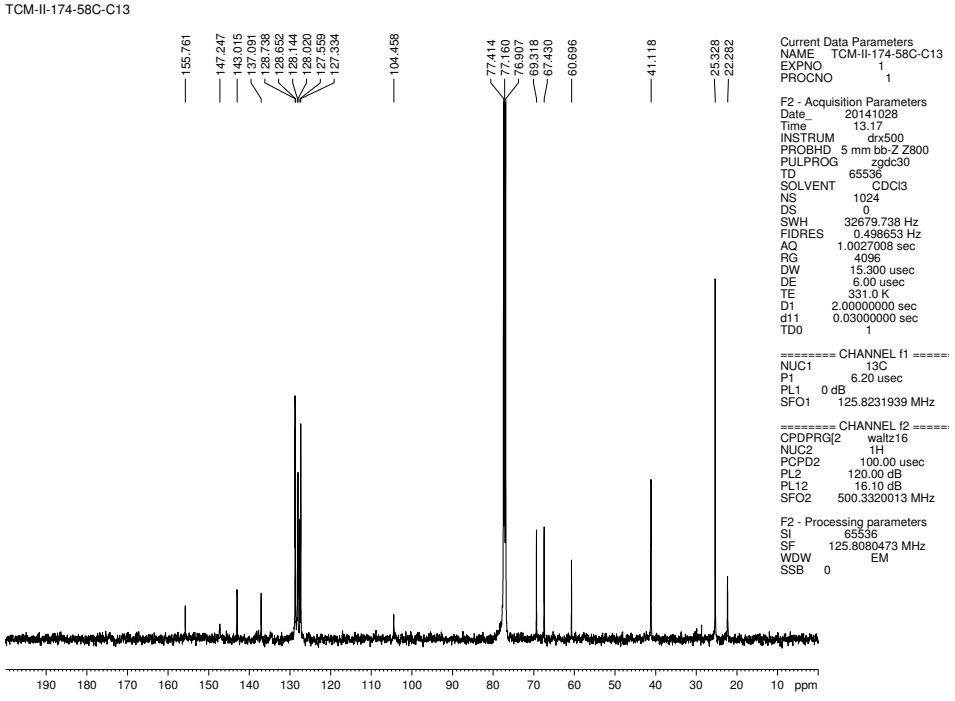

Figure 4.23 ^{13}C NMR (125 MHz, $CDCl_3$) of compound **4.19**.

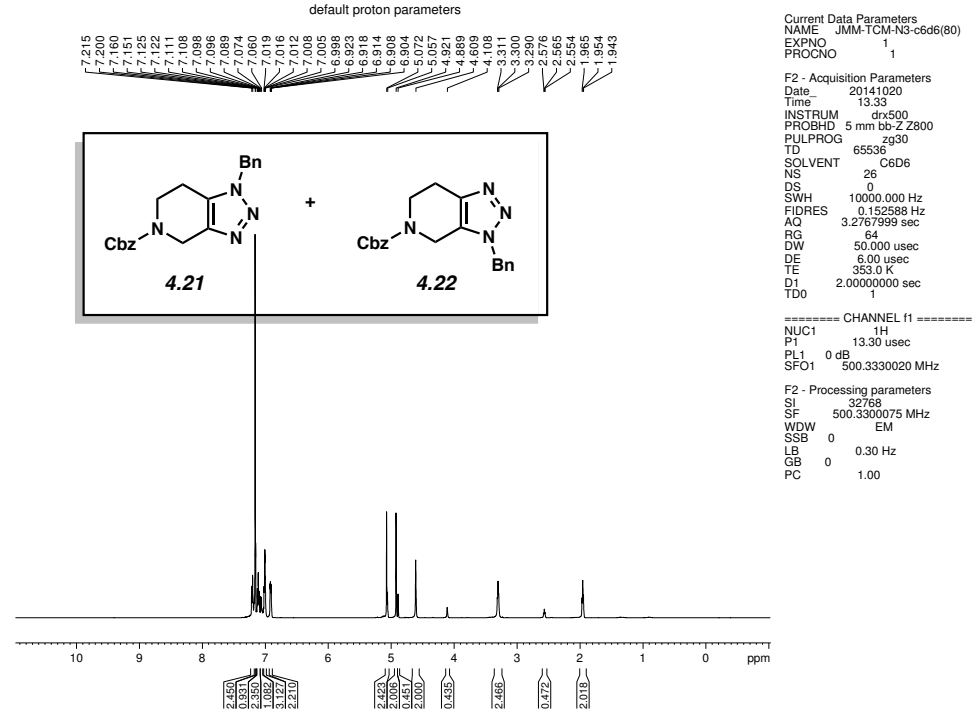

Figure 4.24 ^{1}H NMR (500 MHz, C_6D_6) of compound **4.21** and **4.22**.

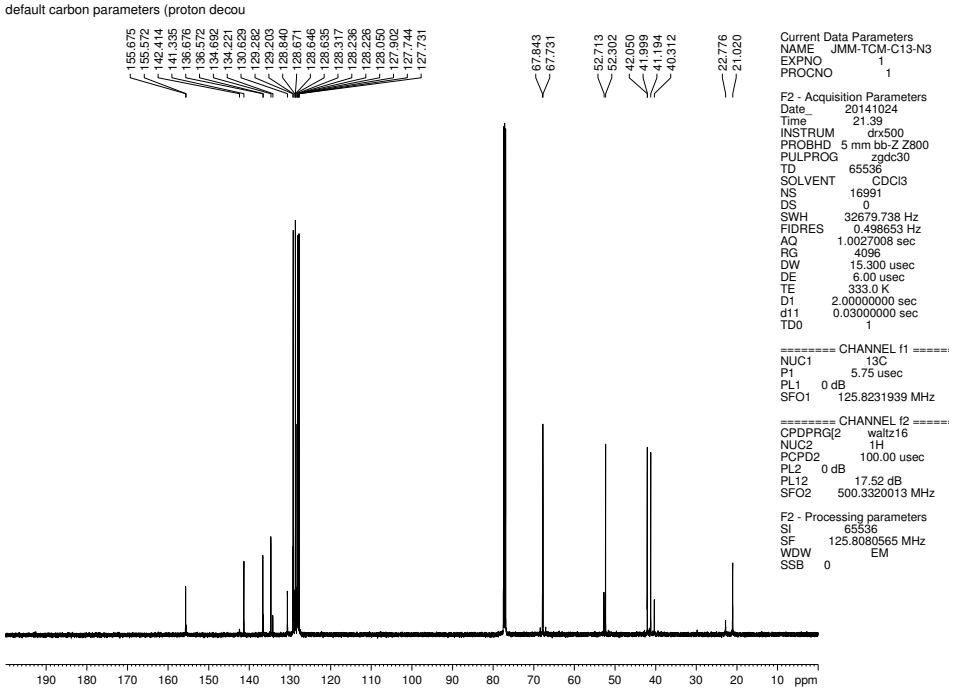

Figure 4.25 ^{13}C NMR (125 MHz, $CDCl_3$) of compound **4.21** and **4.22**.

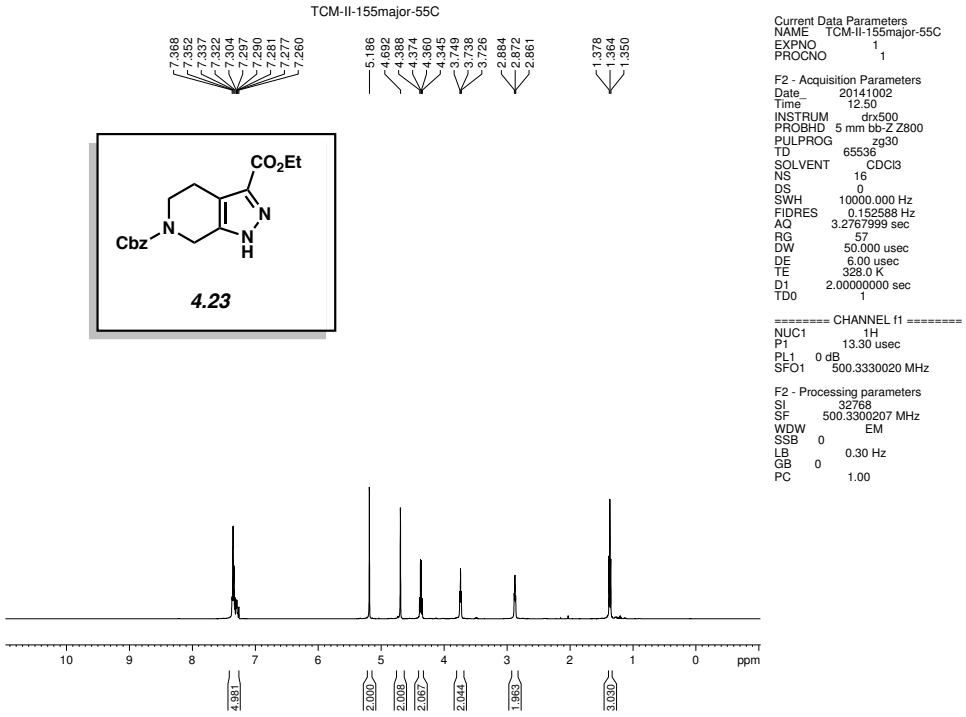

Figure 4.26 ^{1}H NMR (500 MHz, $CDCl_3$) of compound **4.23**.

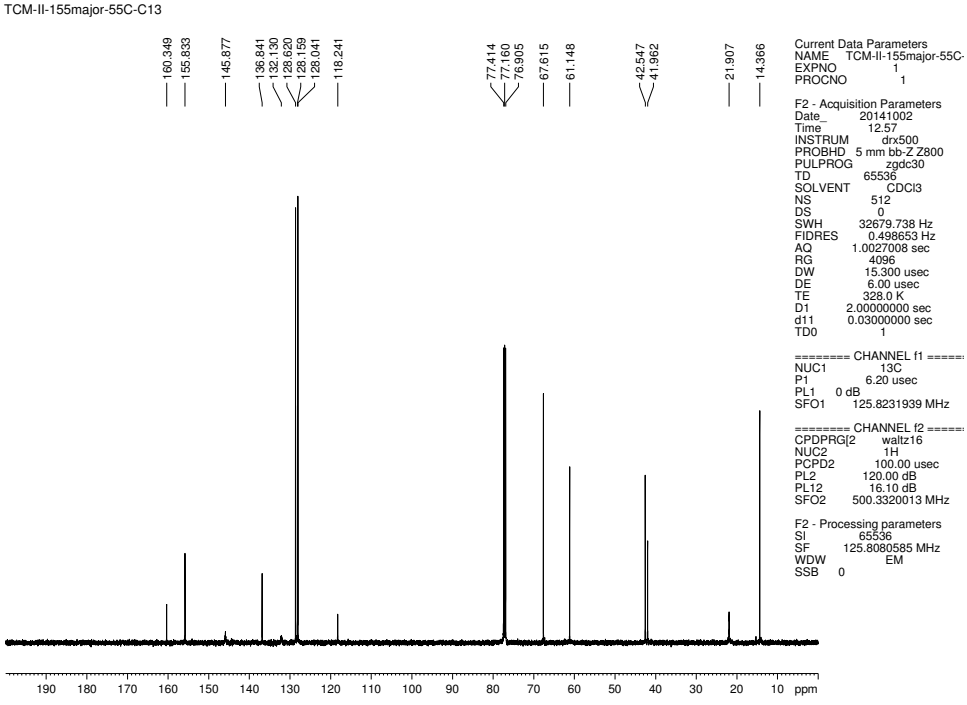

Figure 4.27 ^{13}C NMR (125 MHz, $CDCl_3$) of compound **4.23**.

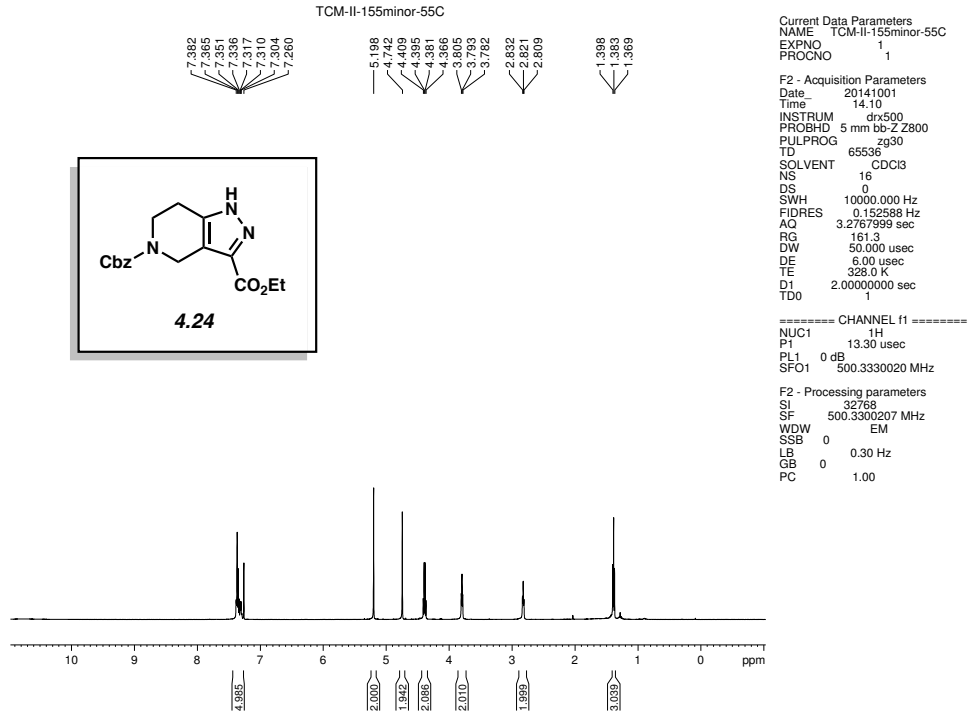

Figure 4.28 ^{1}H NMR (500 MHz, $CDCl_3$) of compound **4.24**.

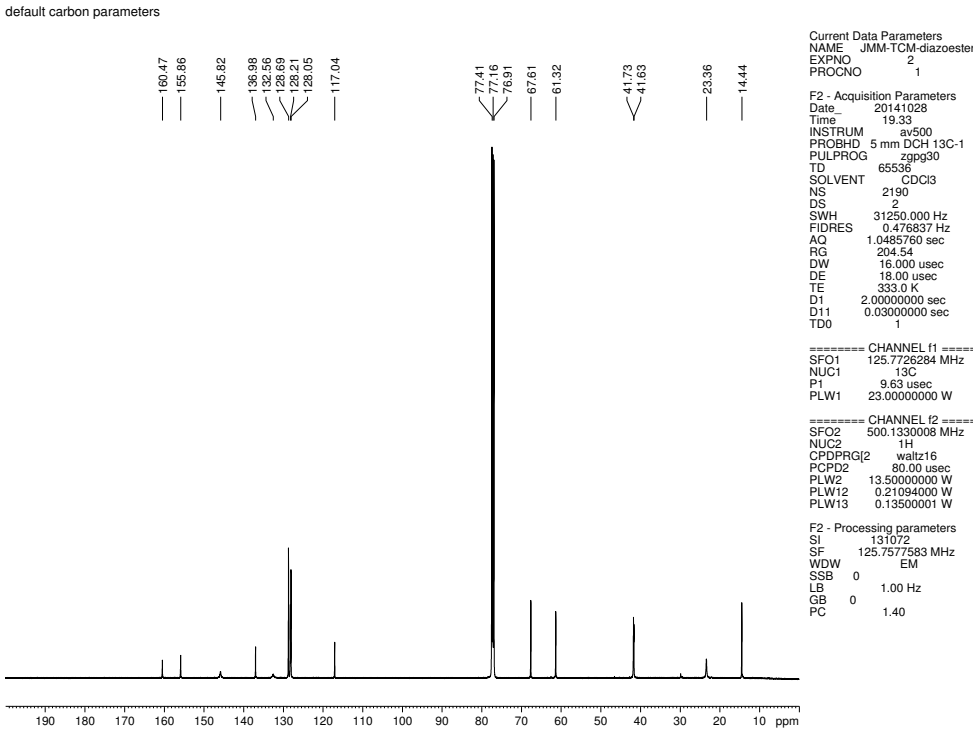

Figure 4.29 ^{13}C NMR (125 MHz, $CDCl_3$) of compound **4.24**.

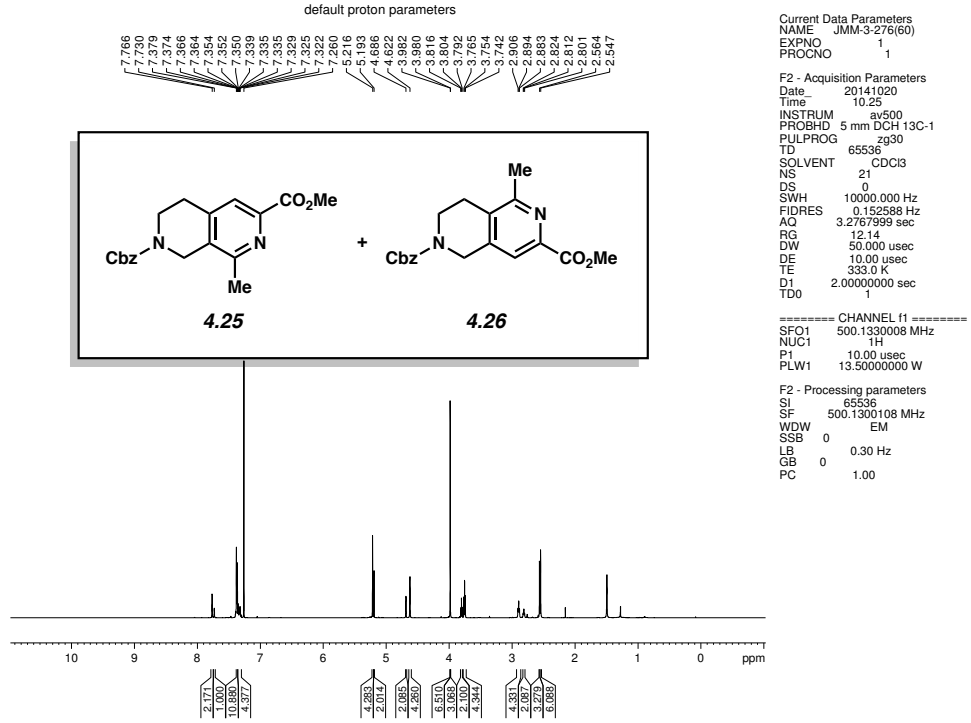

Figure 4.30 ^{1}H NMR (500 MHz, $CDCl_3$) of compound **4.25** and **4.26**.

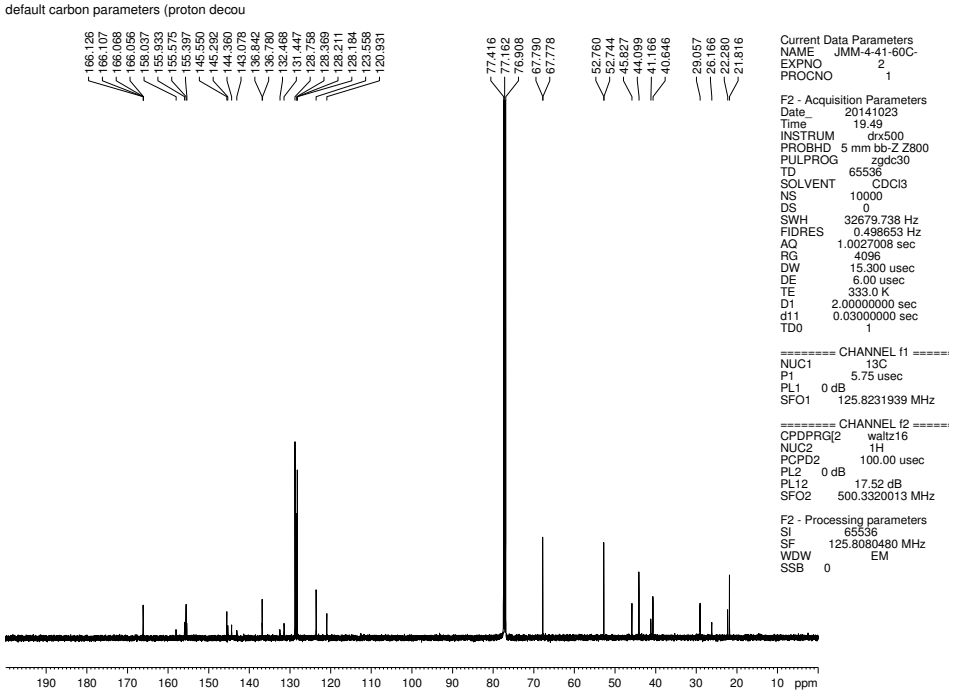

Figure 4.31 ^{13}C NMR (125 MHz, $CDCl_3$) of compound **4.25** and **4.26**.

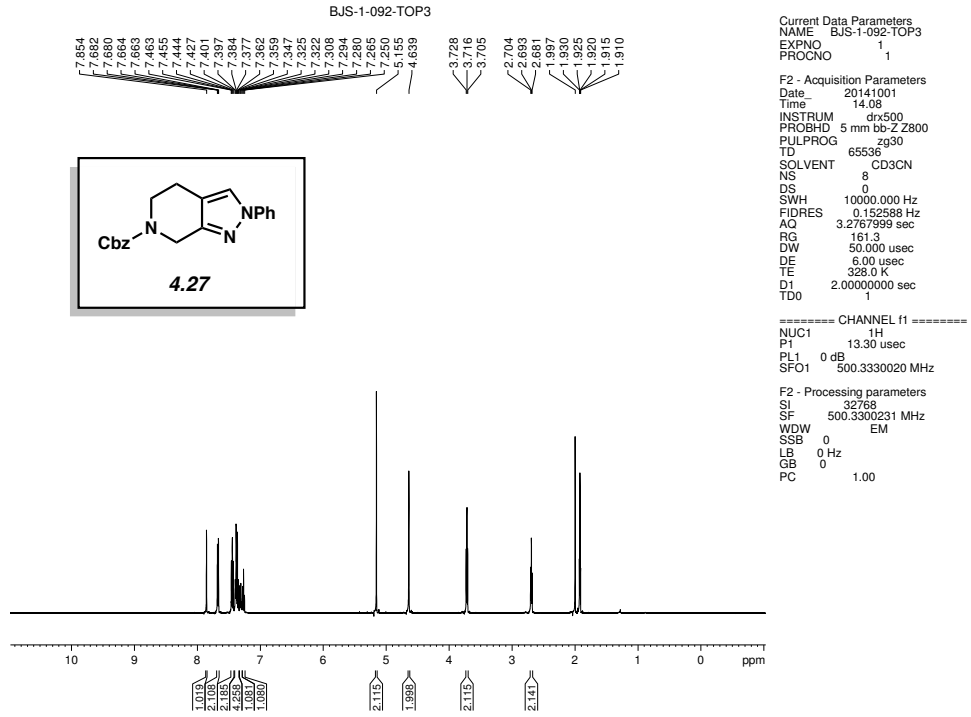

Figure 4.32 ^{1}H NMR (500 MHz, CD_3CN) of compound **4.27**.

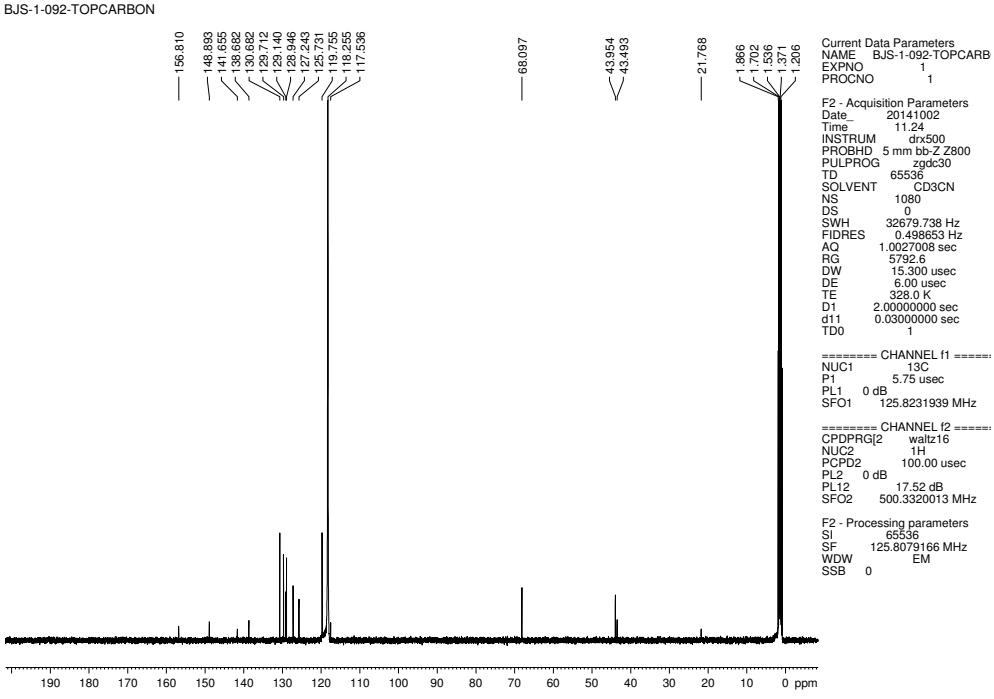

Figure 4.33 ^{13}C NMR (125 MHz, CD_3CN) of compound **4.27**.

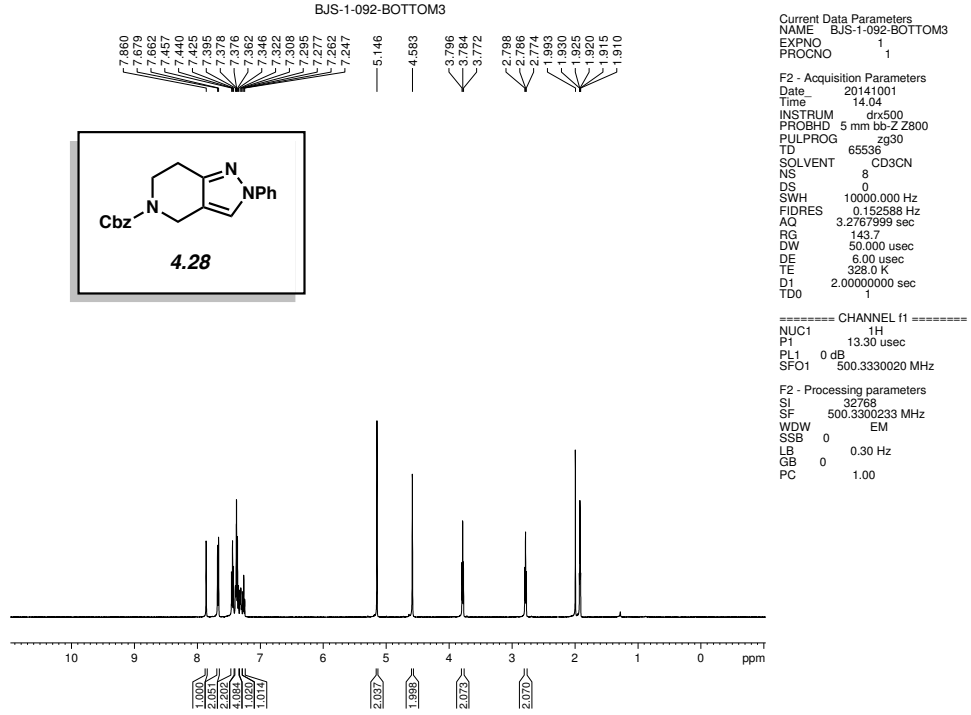

Figure 4.34 ^{1}H NMR (500 MHz, CD_3CN) of compound **4.28**.

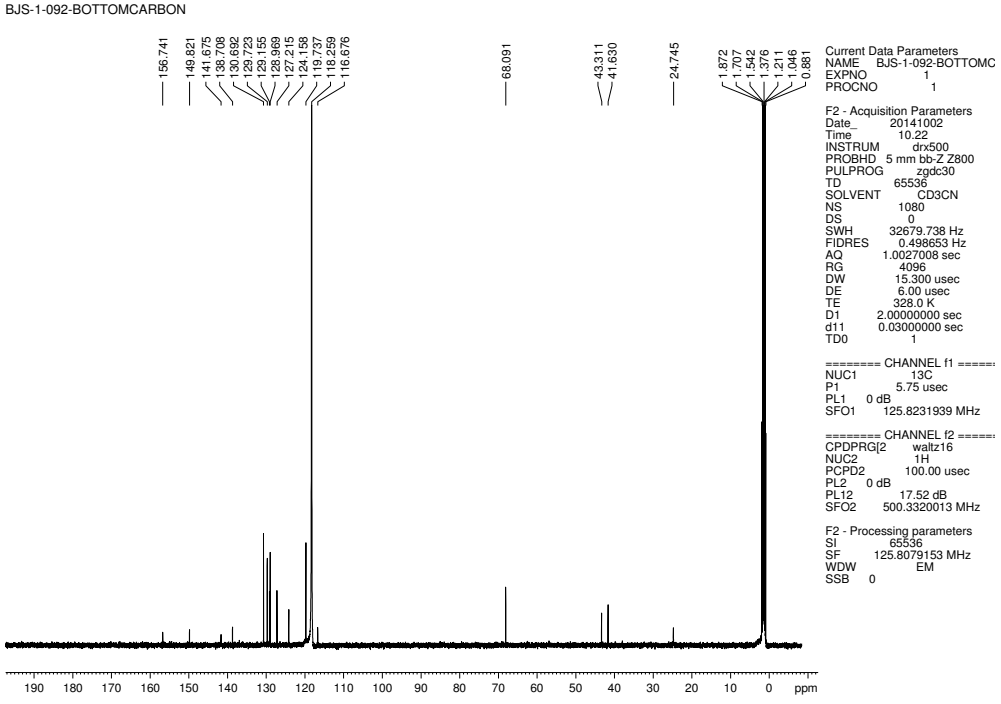

Figure 4.35 ^{13}C NMR (125 MHz, CD_3CN) of compound **4.28**.

4.10 Notes and References

(1) Vitaku, E.; Smith, D. T.; Njardarson, J. T. *J. Med. Chem.* **2014**, *57*, 10257–10274.

(2) Wentrup, C.; Blanch, R.; Briehl, H.; Gross, G. *J. Am. Chem. Soc.* **1988**, *110*, 1874–1880.

(3) Tlais, S. F.; Danheiser, R. L. *J. Am. Chem. Soc.* **2014**, *136*, 15489–15492.

(4) Medium sized *N*-containing cycloalkynes have been used in bioorthogonal click chemistry by Bertozzi and others. For a pertinent review, see: Sletten, E. M.; Bertozzi, C. R. *Angew. Chem., Int. Ed.* **2009**, *48*, 6974–6998.

(5) Levine, R.; Leake, W. W. *Science* **1955**, *121*, 780.

(6) Martens, R. J.; den Hertog, H. J. *Tetrahedron Lett.* **1962**, *3*, 643–645.

(7) For recent reviews of arynes and hetarynes, see: (a) Bronner, S. M.; Goetz, A. E.; Garg, N. K. *Synlett* **2011**, 2599–2604. (b) Tadross, P. M.; Stoltz, B. M. *Chem. Rev.* **2012**, *112*, 3550–3577. (c) Gampe, C. M.; Carreira, E. M. *Angew. Chem., Int. Ed.* **2012**, *51*, 3766–3778. (d) Goetz, A. E.; Garg, N. K. *J. Org. Chem.* **2014**, *79*, 846–851. (e) Goetz, A. E.; Shah, T. K.; Garg, N. K. *Chem. Commun.* **2015**, *51*, 34–45.

(8) For recent studies from our laboratory, see: (a) Goetz, A. E.; Garg, N. K. *Nat. Chem.* **2013**, *5*, 54–60. (b) Medina, J. M.; Mackey, J. L.; Garg, N. K.; Houk, K. N. *J. Am. Chem. Soc.* **2014**, *136*, 15798–15805.

(9) For a recent study of cyclohexynes and cyclopentyne, see: Medina, J. M.; McMahon, T. C.; Jiménez-Osés, G.; Houk, K. N.; Garg, N. K. *J. Am. Chem. Soc.* **2014**, *136*, 14706–14709.

(10) The ability to access heterocyclic scaffolds with significant aliphatic character is an important direction in modern drug discovery; see: (a) Lovering, F.; Bikker, J.; Humblet, C. *J.*

Med. Chem. **2009**, *52*, 6752–6756. (b) Ritchie, T. J.; Macdonald, S. J. F. *Drug Discovery Today* **2009**, *14*, 1011–1020.

(11) The carboxybenzyl (Cbz) protecting group was chosen because of its pronounced stability and its ability to be selectively cleaved.

(12) For recent examples of 3,4-pyridyne regioselectivities, see: (a) Enamorado, M. F.; Ondachi, P. W.; Comins, D. L. *Org. Lett.* **2010**, *12*, 4513–4515. (b) Saito, N.; Nakamura, K.-i.; Shibano, S.; Ide, S.; Minami, M.; Sato, Y. *Org. Lett.* **2013**, *15*, 386–389. (c) Saito, N.; Nakamura, K.-i.; Sato, Y. *Heterocycles* **2014**, *88*, 929–937.

(13) Given the widespread use of silyl triflates in aryne and cycloalkyne trapping experiments (using mild fluoride-based conditions), we deemed silyl triflate **4.8** an ideal target.

(14) Comins, D. L.; Joseph, S. P.; Goehring, R. R. *J. Am. Chem. Soc.* **1994**, *116*, 4719–4728.

(15) Knapp, S.; Yang, C.; Pabbaraja, S.; Rempel, B.; Reid, S.; Withers, S. G. *J. Org. Chem.* **2005**, *70*, 7715–7720.

(16) Atanes, N.; Escudero, S.; Pérez, D.; Guitián, E.; Castedo, L. *Tetrahedron Lett.* **1998**, *39*, 3039–3040.

(17) Aldrich Chemical Co, Inc. is currently commercializing silyl triflate **4.8**.

(18) For entry 6, substantial mass is lost to non-productive reaction pathways, which may render regioselectivity data unreliable. In the case of entry 7, the lack of regioselectivity can be attributed to the sydnone trappings occurring through concerted, highly synchronous transition states, with low activation barriers. Larock and Shi have reported similarly modest regioselectivities using 3-methoxybenzyne with the sydnone trapping agent; see: Fang, Y.; Wu, C.; Larock, R. C.; Shi, F. *J. Org. Chem.* **2011**, *76*, 8840–8851.

(19) Structural similarity searches were performed using SciFinder Scholar. Other scaffolds, including the minor adduct from the diazoester cycloaddition (Table 4.2, entry 5) and the major product from the sydnone cycloaddition (Table 4.2, entry 7) are also difficult to access.

(20) Vaca, M. J. A.; Gil, J. I. A.; Chrovian, C. C.; Coate, H. R.; Angelis, M. D.; Dvorak, C. A.; Gelin, C. F.; Letavic, M. A.; Savall, B. M.; Soyode-Johnson, A.; Stenne, B. M.; Swanson, D. M. P2X7 Modulators, US 20140275015, September 18, 2014.

(21) Ashton, W. T.; Caldwell, C. G.; Mathvink, R. J.; Ok, H. O.; Reigle, L. B.; Weber, A. E. 3-Amino-4-Phenylbutanoic Acid Derivatives as Dipeptidyl Peptidase Inhibitors for the Treatment or Prevention of Diabetes, WO 2004064778, August 05, 2004.

(22) Fabienne, T.; Patrick, M.; Teresa, D.; Pierre, C. M.; Francois, C. New Tetrahydropyrazolo (3,4-c)pyridine Derivatives are Kinase Modulators Used Especially for Treating Cancer, FR 2857362, January 14, 2005.

(23) Blatt, L. M.; Seiwert, S.; Beigelman, L.; Kercher, T.; Kennedym, A. L.; Andrews, S. W. Novel Inhibitors of Hepatitis C Virus Replication, WO 2008005511, January 10, 2008.

(24) Comparative regioselectivity data for the reactions of 3,4-pyridyne (**4.3**) and 3,4-piperidyne **4.1a** are summarized below (C4 attack favored in all cases). For piperidyne regioselectivity data, see: Table 4.2 and the Experimental Section. For pyridyne regioselectivity data: A. E. Goetz, N. K. Garg, Unpublished Results, UCLA; see also ref 8a. For additional pyridyne azide cycloaddition regioselectivity data, see ref 12c.

Reactive Species	*Regioselectivity with Morpholine*	*Regioselectivity with N-Me-Aniline*	*Regioselectivity with Nitrone*	*Regioselectivity with Azide*
5.3	*1.3 : 1*	*1.9 : 1*	*1.9 : 1*	*1.7 : 1*
5.1a	*>20 : 1*	*>20 : 1*	*12.7 : 1*	*5.3 : 1*

(25) Considering the standard error associated with computations and that the transition states are very early with low barriers, we consider the computational and experimental findings to be in reasonable accord.

(26) Bent, H. A. *Chem. Rev.* **1961**, *61*, 275–311.

(27) Comins, D. L.; Joseph, S. P.; Goehring, R. R. *J. Am. Chem. Soc.* **1994**, *116*, 4719–4728.

(28) The corresponding ketone is a commercially available compound, CAS: 19099-93-5. For known spectral data, see: Sasano, Y.; Nagasawa, S.; Yamazaki, M.; Shibuya, M.; Park, J.; Iwabuchi, Y. *Angew. Chem.* **2014**, *126*, 3300–3304.

(29) Thoman, C. J.; Voaden, D. J. *Org. Synth*. **1965**, *45*, 96.

(30) Frisch, M. J.; Trucks, G. W.; Schlegel, H. B.; Scuseria, G. E.; Robb, M. A.; Cheeseman, J. R.; Scalmani, G.; Barone, V.; Mennucci, B.; Petersson, G. A.; Nakatsuji, H.; Caricato, M.; Li, X.; Hratchian, H. P.; Izmaylov, A. F.; Bloino, J.; Zheng, G.; Sonnenberg, J. L.; Hada, M.; Ehara, M.; Toyota, K.; Fukuda, R.; Hasegawa, J.; Ishida, M.; Nakajima, T.; Honda, Y.; Kitao, O.; Nakai, H.; Vreven, T.; Montgomery, J. A.; Peralta, J. E.; Ogliaro, F.; Bearpark, M.; Heyd, J. J.; Brothers, E.; Kudin, K. N.; Staroverov, V. N.; Kobayashi, R.; Normand, J.; Raghavachari, K.; Rendell, A.; Burant, J. C.; Iyengar, S. S.; Tomasi, J.; Cossi, M.; Rega, N.; Millam, J. M.; Klene, M.; Knox, J. E.; Cross, J. B.; Bakken, V.; Adamo, C.; Jaramillo, J.; Gomperts, R.; Stratmann, R. E.; Yazyev, O.; Austin, A. J.; Cammi, R.; Pomelli, C.; Ochterski, J. W.; Martin, R. L.; Morokuma, K.; Zakrzewski, V. G.; Voth, G. A.; Salvador, P.; Dannenberg, J. J.; Dapprich, S.; Daniels, A. D.; Farkas, Ö.; Foresman, J. B.; Ortiz, J. V.; Cioslowski J.; Fox, D. J. *Gaussian 09, Revision D.01*, *Vol.* Gaussian, Inc., Wallingford CT, 2010.

(31) (a) Becke, A. D. *J. Chem. Phys.* **1993**, *98*, 5648–5652. (b) Lee, C.; Yang, W.; Parr, R. G. *Phys. Rev. B* **1988**, *37*, 785–789. (c) Becke, A. D. *J. Chem. Phys.* **1993**, *98*, 1372–1377. (d) Stephens, P. J.; Devlin, F. J.; Chabalowski, C. F.; Frisch, M. J. *J. Phys. Chem.* **1994**, *98*, 11623–11627.

(32) (a) Ditchfield, R.; Hehre, W. J.; Pople, J. A. *J. Chem. Phys.* **1971**, *54*, 724–728. (b) Hehre, W. J.; Ditchfield, R.; Pople, J. A. *J. Chem. Phys.* **1972**, *56*, 2257–2261. (c) Hariharan, P. C.; Pople, J. A. *Theor. Chim. Acta.* **1973**, *28*, 213–222.

(33) (a) Zhao, Y.; Truhlar, D. G. *Phys. Chem. Chem. Phys*. **2008**, *10*, 2813–2818. (b) Ribeiro, R. F.; Marenich, A. V.; Cramer, C. J.; Truhlar, D. G. *J. Phys. Chem. B* **2011**, *115*, 14556–14562.

(34) (a) Grimme, S. *J. Comput. Chem.* **2006**, *27*, 1787–1799. (b) Grimme, S.; Antony, J.; Ehrlich, S.; Krieg, H. *J. Chem. Phys.* **2010**, *132*, 154104–154122.

(35) (a) Barone, V.; Cossi, M. *J. Phys. Chem. A* **1998**, *102*, 1995–2001. (b) Cossi, M.; Rega, N.; Scalmani, G.; Barone, V. *J. Comput. Chem.* **2003**, *24*, 669–681. (c) Takano, Y.; Houk, K. N. *J. Chem. Theory Comput.* **2005**, *1*, 70–77.

(36) Legault, C. Y. CYLView, 1.0b; Université de Sherbrooke, Canada, **2009**; http://www.cylview.org

(37) McMahon, T. C.; Medina, J. M.; Yang, Y.-F.; Simmons, B. J.; Houk, K. N.; Garg, N. K. *J. Am. Chem. Soc*. **2015**, *137*, 4082–4085.

CHAPTER FIVE

Understanding and Interrupting the Fischer Azaindolization Reaction

Bryan J. Simmons, Marie Hoffmann, Pier Alexandre Champagne, Elias Picazo,

Katsuya Yamakawa, Lucas A. Morrill, K. N. Houk, and Neil K. Garg.

J. Am. Chem. Soc. **2017**, *139*, 14833–14836.

5.1 Abstract

Experimental and computational studies pertaining to the Fischer azaindolization reaction are reported. These studies explain why pyridylhydrazines are poorly reactive in Fischer indolization reactions, in addition to the origin of hydrazine substituent effects. Additionally, an interrupted variant of Fischer azaindolization methodology is disclosed, which provides a synthetic entryway into fused azaindoline scaffolds.

5.2 Introduction

The Fischer indolization reaction, first described in 1883,[1] remains a powerful tool in modern chemical synthesis.[2] The transformation, which typically involves the acid-mediated reaction of aryl hydrazines with ketones or aldehydes to give indoles, has many applications in medicinal chemistry.[2] The Fischer indolization has also been used extensively in natural product synthesis, including several recent examples, to generate remarkable structural complexity.[3]

One deficiency associated with the Fischer indolization involves the variant in which pyridylhydrazines are employed to furnish azaindole products (a.k.a., Fischer azaindolization).[4] This transformation was first tested over 100 years ago.[5] It is now known, particularly via the

studies of Parrick[4a,b] and Robinson[4c] that the azaindolization can proceed under extreme thermal conditions. For the corresponding acid-mediated process to take place, certain substituents on the hydrazine (e.g., methoxy, halides) can be used to improve reactivity, but the origins of such beneficial effects have remained unknown.[4d–g]

The present study answers two key questions. (A) What factors govern the success or failure of the Fischer azaindolization reaction? (B) Could a general "interrupted" variant of the Fischer azaindolization[6] be developed as a method to access fused azaindoline scaffolds? Although fused azaindoline frameworks are uncommon,[7] the parent azaindole heterocycle serves as a bioisostere for indoles[8] and is present in compounds of medicinal relevance. In fact, more than 74,000 bioactive azaindoles are known,[9] including the currently marketed drugs Zelboraf (**5.1**, Figure 5.1) and Venclexta.[10] Fused indolines are present in more than 22,000 bioactive molecules, more than 870 of which are natural products (e.g., **5.2**).[6c,9,11] We now report mechanistic insights into the Fischer azaindolization reaction, the scope of the interrupted variant (**5.3** + **5.4** → **5.5**), and the use of this methodology to access aza-analogues of bioactive compounds.

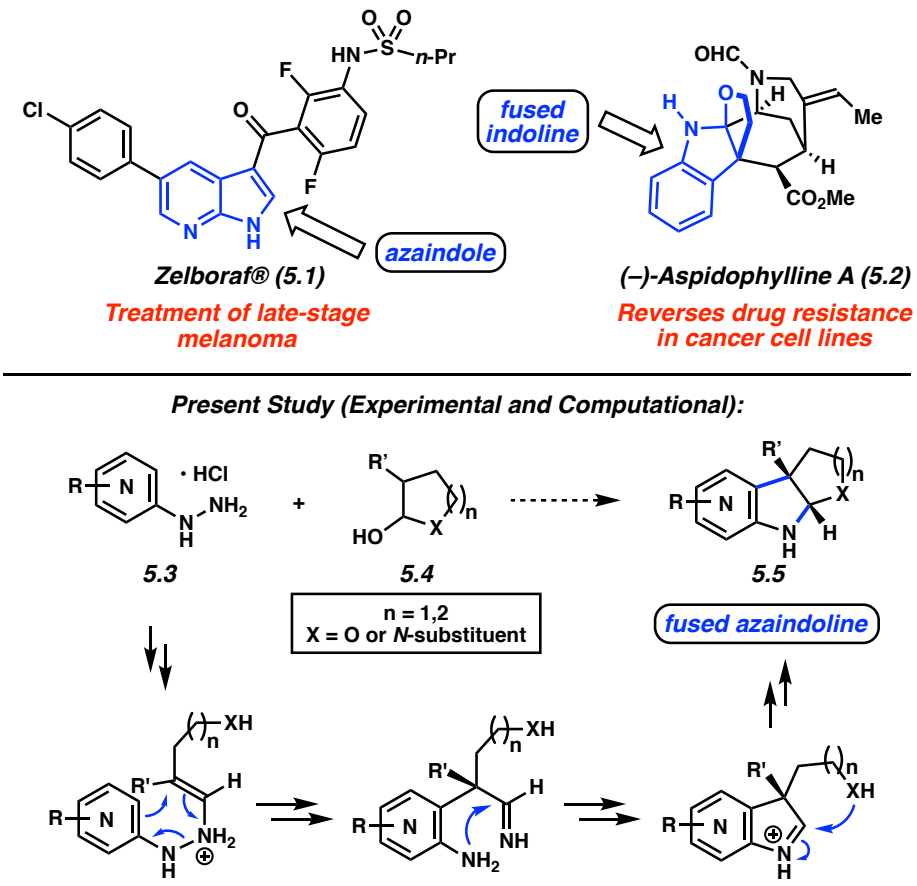

Figure 5.1 Zelboraf (**5.1**), (–)-aspidophylline A (**5.2**), and interrupted Fischer azaindolization reaction.

5.3 Computational Study of the Fischer Azaindolization Reaction

With the goal of understanding the factors that lead to success or failure of the Fischer azaindolization reaction, we performed a series of SCS-MP2 calculations.[12] We first investigated if the activation barrier for [3,3]-sigmatropic rearrangement varies significantly based on the aryl hydrazine employed. Thus, as summarized in Figure 5.2, the $\Delta G^{\ddagger}$ was calculated for this step under four scenarios:[13] (a) the neutral phenylhydrazone, (b) protonation of the β-nitrogen of phenylhydrazone,[14] (c) protonation of the β-nitrogen of 3-pyridylhydrazone, and (d) protonation of the β-nitrogen of methoxy-substituted 3-pyridylhydrazone. In all cases, we used propionaldehyde as the Fischer indolization reaction partner. For three of the scenarios

(transition states **5.6**, **5.7**, and **5.9**), the calculations were in good accord with experimental trends. However, for transition state **5.8** involving the experimentally problematic 3-pyridylhydrazine, the activation barrier was calculated to be reasonable (i.e., 13.5 kcal/mol). Thus, we sought an alternative explanation for the poor reactivity of 3-pyridylhydrazones in Fischer indolization reactions.

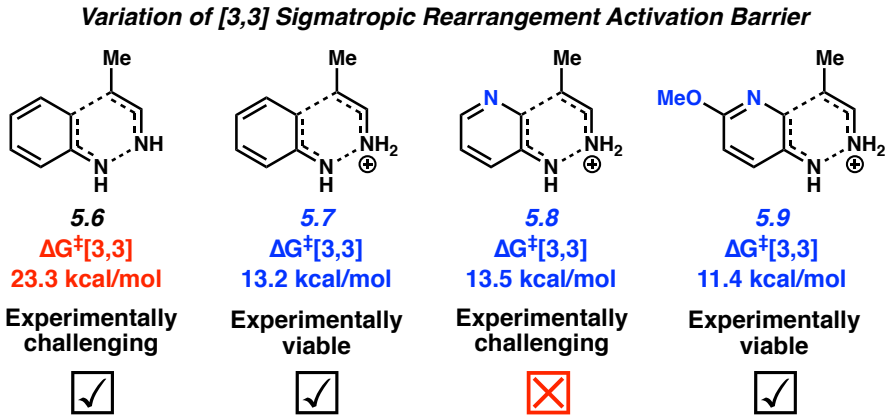

Figure 5.2 [3,3]-sigmatropic rearrangement transition states of various arylhydrazines.

We next considered if the pyridine nitrogen might be protonated (Figure 5.3). Indeed, protonation of this nitrogen is much preferred over hydrazone protonation, and pyridinium salt **5.10** is the global minimum of the pathway. To convert **5.10** to **5.11** requires 21.8 kcal/mol, leading to a high total barrier of 35.3 kcal/mol for the tautomerization and [3,3]-sigmatropic rearrangement (**5.10** → **5.8**). As noted earlier, it is known that introduction of a methoxy substituent on the pyridylhydrazine (e.g., see **5.9**, Figure 5.2) leads to improved yields in experimental studies.[4d–g] This has previously been rationalized by a "push/ pull" effect[4d] which, in turn, makes the [3,3]-sigmatropic rearrangement more favorable. Instead, we suggest that the methoxy group reduces the basicity of the pyridine nitrogen, thus rendering the proton

transfer/tautomerization more feasible. We calculate that the tautomerization between the 2-methoxy analogues of **5.10** and **5.11** is only 14.9 kcal/mol (versus 21.8 kcal/mol for **5.10** to **5.11**).[12] Consequently, the better performance in Fischer azaindolizations of methoxy-substituted pyridylhydrazines compared to the parent pyridylhydrazines can be attributed to the diminished basicity of the pyridine nitrogen in the former case.

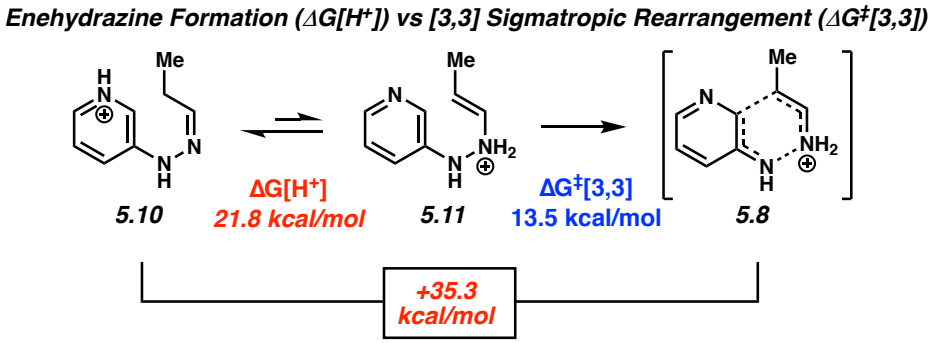

Figure 5.3 Unfavorable equilibrium between **5.10** and **5.11**.

5.4 Interrupted Fischer Azaindolization Reaction

We also explored the interrupted variant of the Fischer azaindolization to access fused azaindolines since only a single example of this transformation is available in the literature[6d] and no methodology studies have been reported. To initiate our efforts in this area, we used methoxy-substituted pyridylhydrazine salt **5.12** (Table 5.1), due to its previously established favorable reactivity in Fischer azaindolization reactions. Following an initial survey of reaction conditions, mainly involving variation of solvent, acid sources, time, and temperature, we found that **5.12** underwent interrupted Fischer azaindolization with a variety of aldehyde surrogates to give fused 4-azaindoline products **5.13**. Of note, the transformation introduces two stereocenters, one of which is quaternary. Results are depicted based on optimization of individual substrates. Upon

treatment of **5.12** with lactol **5.14**, furanoazaindoline **5.15** was obtained in 97% yield (entry 1). Alternate substituents on the lactol were tolerated, as demonstrated by the successful interrupted Fischer azaindolization of phenyl lactol **5.16** and allyl lactol **5.18** to furnish adducts **5.17** and **5.19**, respectively (entries 2 and 3). The 6-membered lactol **5.20** was also deemed a suitable reaction partner, as demonstrated by the formation of 6,5,6-tricycle **5.21** (entry 4). In addition, we evaluated several hemiaminal substrates for the synthesis of azapyrrolidinoindolines. The use of methyl substituted *N*-Ts hemiaminal **5.22** led to **5.23** (entry 5), whereas employment of allyl derivative **5.24** gave azaindoline **5.25** (entry 6). Lastly, we evaluated carbamate-containing hemiaminal substrate **5.26**, which furnished **5.27** in 82% yield (entry 7).

Table 5.1 Scope of the aldehyde surrogate in the interrupted Fischer azaindolization.

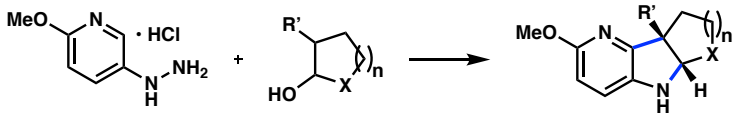

5.12 + *5.4* → *5.13*

Entry	Aldehyde Surrogate	Product	Condition Yield (%)
1	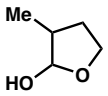 *5.14*	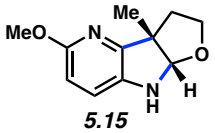 *5.15*	H_2O, 100 °C, 1 h *97% yield*
2	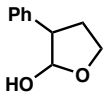 *5.16*	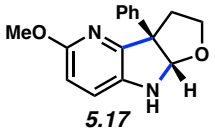 *5.17*	4% aq H_2SO_4 60 °C, 5 h *80% yield*
3	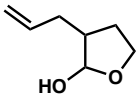 *5.18*	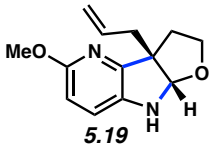 *5.19*	4% aq H_2SO_4 60 °C, 5 h *74% yield*
4	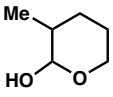 *5.20*	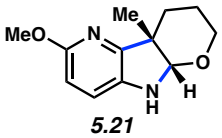 *5.21*	4% aq H_2SO_4 23 °C, 24 h *62% yield*
5	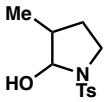 *5.22*	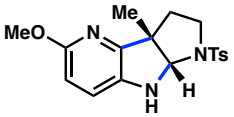 *5.23*	H_2O, 100 °C, 1 h *94% yield*
6	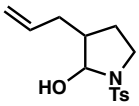 *5.24*	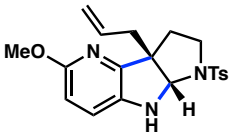 *5.25*	AcOH, 90 °C, 1 h *58% yield*
7	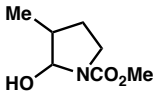 *5.26*	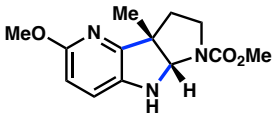 *5.27*	4% aq H_2SO_4 120 °C, 1 h *82% yield*

Having established the tolerance of the interrupted Fischer azaindolization methodology toward variation in the aldehyde surrogate, we shifted our attention to assessing changes in the hydrazine component (Table 5.2). Halohydrazines **5.29** and **5.31** underwent interrupted Fischer

azaindolization with lactol **5.14** to deliver 4-azaindoline products **5.30** and **5.32**, respectively (entries 1 and 2). Interestingly, the use of methoxyhydrazine **5.33** led to azaindoline product **5.34**, albeit in a lower yield (entry 3).[15] Efforts to further optimize this transformation were unsuccessful. Isomeric hydrazines **5.35**, **5.37**, and **5.39** were also evaluated with the hopes of accessing 5-, 6-, and 7-substituted azaindolines. Whereas the interrupted Fischer azaindolization reaction failed to produce 5-azaindoline **5.36** (entry 4), the methodology furnished 6-azaindoline **5.38** (entry 5) and 7-azaindoline **5.40** (entry 6), albeit with a modest yield in the latter case. Finally, unsubstituted 3-pyridylhydrazine **5.41** was tested as a point of comparison (entry 7). Consistent with expectations based on the literature[4] and our calculations (see Figure 5.3), the transformation proved problematic and gave **5.42** in a poor yield of 11%.[16]

Table 5.2 Scope of hydrazine and correlation to calculated free energies.

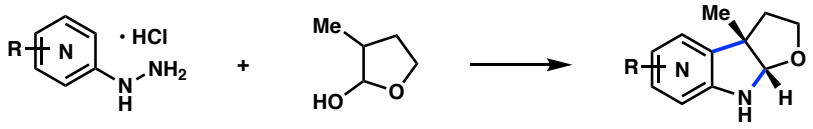

5.3 *5.14* *5.28*

Entry	Hydrazine	Product	Condition Yield (%)	$\Delta G[H^+]^b$ $\Delta G^{\ddagger}[3,3]$
1	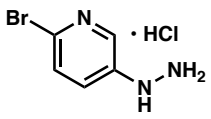 *5.29*	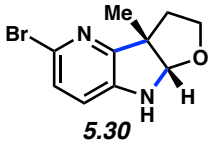 *5.30*	4% aq H_2SO_4 120 °C, 1 h *62% yield*	*+12.1* *+14.7*
2	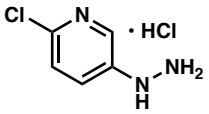 *5.31*	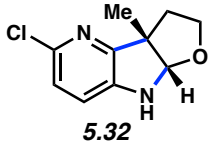 *5.32*	4% aq H_2SO_4 120 °C, 1 h *72% yield*	*+12.5* *+15.1*
3	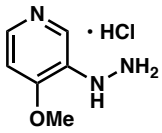 *5.33*	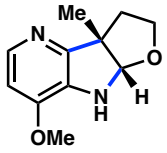 *5.34*	4% aq H_2SO_4 120 °C, 3 h *48% yield*	+20.1 +14.4
4	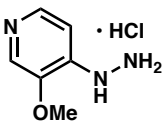 *5.35*	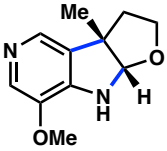 *5.36*	4% aq H_2SO_4 120 °C, 3 h *No Reaction*	+23.7 +16.6
5	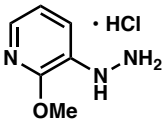 *5.37*	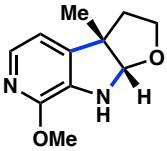 *5.38*	4% aq H_2SO_4 120 °C, 1 h *70% yield*	+11.5 +14.1
6	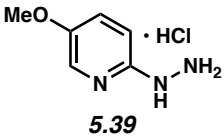 *5.39*	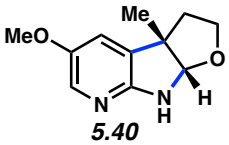 *5.40*	4% aq H_2SO_4 120 °C, 3 h *53% yield*	+18.8 +13.4
7	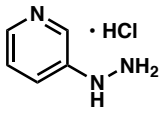 *5.41*	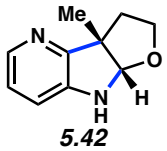 *5.42*	4% aq H_2SO_4 120 °C, 3 h *11% yield*	*+21.8* +13.5

To complement these experimental studies, calculations were performed for the reaction of each hydrazine depicted in Table 5.2, with propionaldehyde as a model aldehyde under acidic conditions.[12] Earlier, we hypothesized that the success or failure of the Fischer azaindolization methodology hinges on the feasibility of enehydrazine formation, rather than [3,3]-sigmatropic rearrangement. Consistent with this notion, we found the computed activation barriers for [3,3]-sigmatropic rearrangement ($\Delta G^{\ddagger}$[3,3]) were uniformly accessible and ranged from 13.4 to 16.6 kcal/mol. On the other hand, the calculated tautomerization equilibria ($\Delta G[H^+]$) varied considerably between 11.5 and 23.7 kcal/mol. In cases where the calculated $\Delta G[H^+]$ is high, the reaction is experimentally problematic (entries 4 and 7). In the cases of entries 3 and 6, the $\Delta G[H^+]$ is slightly more favorable leading to modest yields of product. However, if $\Delta G[H^+]$ is sufficiently low (i.e., less than 15 kcal/mol), the reaction proceeds more efficiently (Table 5.2, entries 1, 2, 5, and Table 5.1). Overall, hydrazines with poorly basic pyridine nitrogens had the smallest $\Delta G[H^+]$.

5.5 Interrupted Fischer Azaindolization Reaction in Bioactive Molecule Synthesis

The interrupted Fischer azaindolization methodology can be used to synthesize new aza-analogues of bioactive molecules (Figure 5.4). Treatment of benzyloxyhydrazine **5.43** with lactol **5.14** under acidic conditions delivered furanoazaindoline **5.44** in 81% yield. Using a straightforward 3-step sequence, **5.44** was elaborated to carbamate **5.45**, a new analogue of the potent acetylcholinesterase inhibitor phensvenine.[17] Switching to a significantly more complex system, we performed the interrupted Fischer azaindolization of hydrazine **5.12** and known[3j] ketolactone **5.46**. Following the acid-mediated rearrangement and subsequent hydrolysis in the

same pot, a straightforward methylation gave pentacycle **5.47**. In turn, azaindoline **5.47** was converted in two steps to **5.48**, an analogue of the anticancer agent (–)-aspidophylline A.[11]

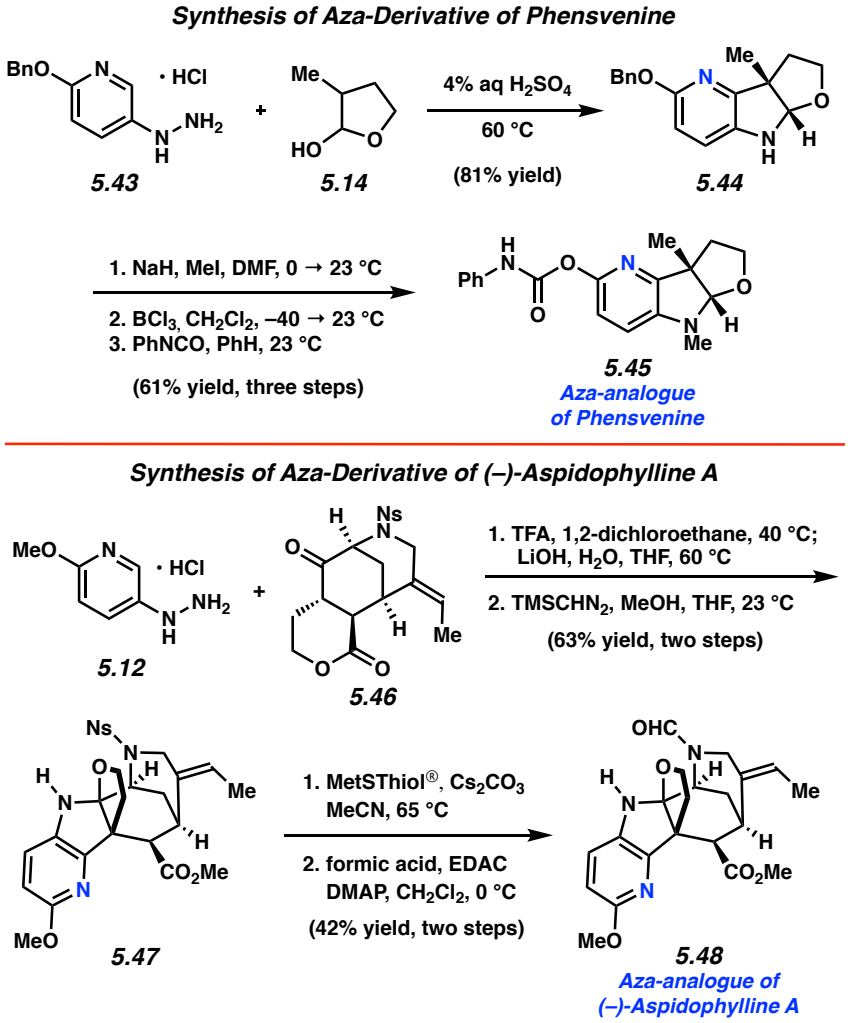

Figure 5.4 Synthesis of aza-analogues.

5.6 Conclusion

We have performed an experimental and computational study of the Fischer azaindolization reaction, related to a transformation first attempted more than 100 years ago. Calculations were used to explain the difficulty in employing pyridylhydrazines in Fischer

indolizations, in addition to the origin of hydrazine substituent effects. Rather than the [3,3]-sigmatropic rearrangement step being the single determining factor, we find that reactions suffer if the pyridine nitrogen is too basic, making the tautomerization step prohibitively challenging. We have also developed an interrupted Fischer azaindolization methodology, which provides a synthetic entryway into fused azaindoline scaffolds. The syntheses of new aza-analogues of phensvenine and (–)-aspidophylline A underscore the potential of this methodology to deliver new aza-derivatives of medicinally privileged fused indoline-containing compounds.

5.7 Experimental Section

5.7.1 Materials and Methods

Unless stated otherwise, reactions were conducted in flame-dried glassware under an atmosphere of air and commercially obtained reagents were used as received. Di-*tert*-buyl hydrazodiformate (**5.52**), amine **5.50**, boronate ester **5.57**, $Pd_2(dba)_3$, $Cu(OAc)_2$, and dppf were obtained from Sigma-Aldrich and used as received. Di-*tert*-butyl azodicarboxylate (**5.55**), bromopyridines **5.51**, **5.60**, amine **5.49**, and boronate ester **5.62** were obtained from Combi-Blocks and used as received. Amines **5.59** and **5.61** were obtained from Oakwood and used as received. Boronic acid **5.54** was obtained from Frontier Scientific and used as received. Solid supported thiol-resin MetSThiol® was obtained from SiliCycle (Product # R51030B). Reaction temperatures were controlled using an IKAmag temperature modulator, and unless stated otherwise, reactions were performed at elevated temperatures (approximately 120 °C). Thin-layer chromatography (TLC) was conducted with EMD gel 60 F254 pre-coated plates (0.25 mm for analytical chromatography and 0.50 mm for preparative chromatography) and visualized using a combination of UV, anisaldehyde, iodine, and potassium permanganate staining

techniques. Silicycle Siliaflash P60 (particle size 0.040–0.063 mm) was used for flash column chromatography. ^{1}H NMR spectra were recorded on Bruker spectrometers (at 300, 400 and 500 MHz) and are reported relative to residual solvent signals. Data for ^{1}H NMR spectra are reported as follows: chemical shift (δ ppm), multiplicity, coupling constant (Hz), integration. Data for ^{13}C NMR are reported in terms of chemical shift (at 100 and 125 MHz). IR spectra were recorded on a Perkin-Elmer UATR Two FT-IR spectrometer and are reported in terms of frequency absorption (cm^{-1}). DART-MS spectra were collected on a Thermo Exactive Plus MSD (Thermo Scientific) equipped with an ID-CUBE ion source and a Vapur Interface (IonSense Inc.). Both the source and MSD were controlled by Excalibur software v. 3.0. The analyte was spotted onto OpenSpot sampling cards (IonSense Inc.) using volatile solvents (e.g. chloroform, dichloromethane). Ionization was accomplished using UHP He (Airgas Inc.) plasma with no additional ionization agents. The mass calibration was carried out using Pierce LTQ Velos ESI (+) and (–) Ion calibration solutions (Thermo Fisher Scientific). Optical rotations were measured with a Rudolf Autopol III Automatic Polarimeter.

5.7.2 Experimental Procedures

Note: Experimental information for compounds **5.14**[18], **5.16**[18], **5.18**[18], **5.20**[18], **5.22**[18], **5.24**[18], **5.26**[19], and **5.46**[3d] have previously been reported.

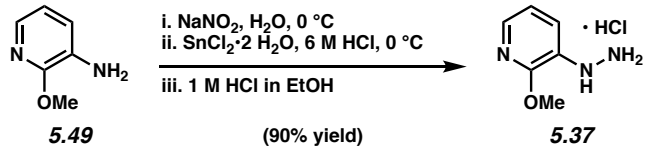

5.49 **(90% yield)** ***5.37***

Representative Procedure A for the synthesis of hydrazine substrates from Tables 5.1 and 5.2. (5.37 is used as an example). Hydrazine 5.37. To a solution of aniline **5.49** (200.0 mg, 1.60

mmol, 1.0 equiv) in 6 M HCl (3.0 mL, 0.5 M) at 0 °C was added dropwise a solution of $NaNO_2$ (107.0 mg, 1.55 mmol, 1.0 equiv) in deionized H_2O (4.0 mL, 0.4 M) over 1 min under an air atmosphere. After stirring at 0 °C for 30 min, a solution of $SnCl_2$•2 H_2O (878.0 mg, 3.90 mmol, 2.5 equiv) in 6 M HCl (3.0 mL, 1.3 M) was added dropwise over 1 min. The reaction was allowed to stir at 0 °C for 1 h, then quenched with a solution of 40% w/w KOH in deionized H_2O until a pH of 12 had been reached (ca. 10 mL). The solution was transferred to a separatory funnel and extracted with EtOAc (4 x 20 mL). The organic layers were combined, dried over $MgSO_4$, and the volatiles were removed under reduced pressure. The resulting crude residue was taken up in EtOAc (6.0 mL) and cooled to 0 °C. Next, 1 M HCl in EtOH (8.0 mL, 0.2 M) was added dropwise over 1 min. The resulting precipitate was collected by filtration through a vacuum filter. The solid residue was washed with CH_2Cl_2 (5 mL) and dried under reduced pressure to yield hydrazine **5.37** as a solid (252.8 mg, 90% yield). Hydrazine **5.37**: mp: 151–152 ºC; R_f 0.57 (EtOAc); ^{1}H NMR (500 MHz, DMSO-d_6): δ 10.40 (br. s, 3H), 8.09 (br. s, 2H), 7.72 (dd, J = 5.1, 1.5, 1H), 7.40 (dd, J = 7.7, 1.5, 1H), 6.94 (dd, J = 7.7, 5.1, 1H) 3.90 (s, 3H); ^{13}C NMR (125 MHz, DMSO-d_6): δ 152.3, 138.0, 129.4, 120.8, 117.0, 53.4; IR (film): 3347, 3091, 2589, 1565, 788 cm^{-1}; HRMS-APCI (*m/z*) [M + H]$^+$ calcd for $C_6H_{10}N_3O^+$, 140.0818; found 140.0816.

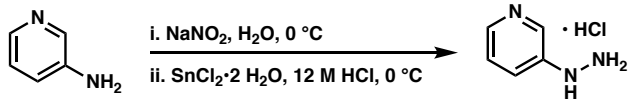

5.50 **(67% yield)** ***5.41***

Representative Procedure B for the synthesis of hydrazine substrates from Table 5.2 (5.41 is used as an example). Hydrazine 5.41. To a solution of aniline **5.50** (1.0 g, 10.60 mmol, 1.0

equiv) in 12 M HCl (10.0 mL, 1.1 M) at 0 °C was added dropwise a solution of $NaNO_2$ (768.0 mg, 11.10 mmol, 1.0 equiv) in deionized H_2O (10.0 mL, 1.1 M) over 1 min under an air atmosphere. After stirring at 0 °C for 30 min, a solution of $SnCl_2$•2 H_2O (6.0 g, 26.50 mmol, 2.5 equiv) in 12 M HCl (10.0 mL, 2.6 M) was added dropwise over 1 min. The reaction was allowed to stir at 0 °C for 30 min. The precipitate was then removed by vacuum filtration. The filtrate was left to evaporate over 48 h allowing crystals to form. The resulting solid was transferred to a filter paper, washed with Et_2O (10 mL), and dried under reduced pressure to yield hydrazine **5.41** as a solid (1.03 g, 67% yield). Hydrazine **5.41**: mp: 181–183 ºC; R_f 0.08 (EtOAc); ^{1}H NMR (500 MHz, DMSO-d_6): δ 11.45 (br. s, 3H), 9.54 (br. s, 1H), 8.45–8.43 (m, 2H), 8.04–8.02 (m, 1H), 7.96–7.93 (m, 1H); ^{13}C NMR (125 MHz, DMSO-d_6): δ 144.9, 133.8, 129.3, 127.3, 126.8; IR (film): 3500, 3060, 2656, 1548, 787 cm^{-1}; HRMS-APCI (*m/z*) $[M + H]^+$ calcd for $C_5H_8N_3^+$, 110.0713; found 110.0711.

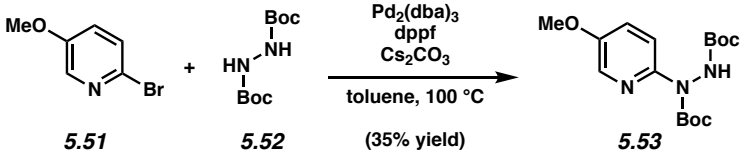

5.51 *5.52* *5.53*

Representative Procedure C for the synthesis of hydrazine substrates from Table 5.2. (5.39 is used as an example). Boc-Hydrazine 5.53. To a A 1-dram vial charged with a magnetic stir bar and Cs_2CO_3 (876.7 mg, 2.69 mmol, 1.25 equiv) was flame-dried under reduced pressure, and allowed to cool under a N_2 atmosphere. Bromide **5.51** (505.9 mg, 2.69 mmol, 1.25 equiv) and di-*tert*-butyl hydrazodiformate (**5.52**) (500.0 mg, 2.15 mmol, 1.0 equiv) were added and the vial was flushed with N_2 for 5 min. The vial was taken into a glovebox and charged with $Pd_2(dba)_3$ (98.5 mg, 0.11 mmol, 0.05 equiv), dppf (179.1 mg, 0.32 mmol, 0.15 equiv), and toluene (3.6 mL,

0.75 M). The vial was then capped with a Teflon-lined screw cap and taken out of the glovebox where it was placed in a pre-heated aluminum block and allowed to stir at 100 °C for 24 h. After cooling to room temperature, the reaction mixture was diluted with CH_2Cl_2 (15 mL) and filtered through a plug of celite (30 mL of CH_2Cl_2 as eluent). The organics were transferred to a separatory funnel and washed sequentially with deionized water (2 x 15 mL), saturated aqueous NaCl (15 mL), and dried over Na_2SO_4. The volatiles were removed under reduced pressure. The resulting crude residue was purified by flash chromatography (1:1 Hexanes:EtOAc) to yield Boc-hydrazine **5.53** (253.9 mg, 35% yield) as a light brown solid.

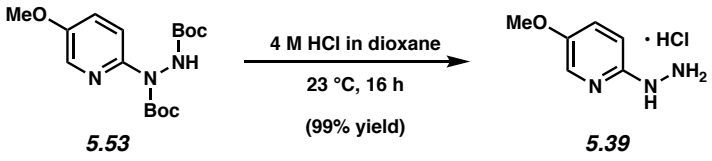

5.53 *5.39*

Hydrazine 5.39. A 20 mL scintillation vial equipped with a magnetic stir bar was charged with Boc-hydrazine **5.53** (269.5 mg, 0.79 mmol, 1.0 equiv) and 4 M HCl in dioxane (5.3 mL, 0.15 M). After stirring at 23 °C for 16 h, the volatiles were removed under reduced pressure. The resulting crude solid was transferred to a filter paper, washed with EtOAc (5 mL), and dried under reduced pressure to yield hydrazine **5.39** (141.1 mg, 99% yield) as a yellow solid. Hydrazine **5.39**: mp: 198–200 ºC; R_f 0.09 (EtOAc); ^{1}H NMR (500 MHz, DMSO-d_6): δ 9.71 (br. s, 3H), 9.03 (br. s, 1H), 7.88 (d, J = 2.8, 1H), 7.44 (dd, J = 9.1, 2.8, 1H), 6.88 (app. dd, J = 9.1, 2.8, 1H), 3.78 (s, 3H); ^{13}C NMR (125 MHz, DMSO-d_6): 150.8, 150.3, 130.3, 126.6, 110.6, 56.0; IR (film): 3308, 2940, 2646, 1620, 1584 cm^{-1}; HRMS-APCI (*m/z*) $[M + H]^+$ calcd for $C_6H_{10}N_3O^+$, 140.0818; found 140.0816.

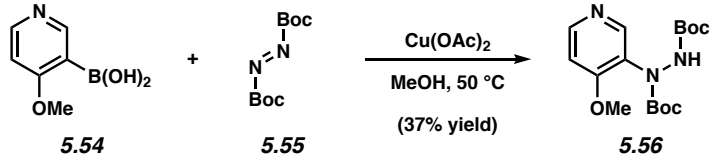

Representative Procedure D for the synthesis of hydrazine substrates from Table 5.2. (5.33 is used as an example). Boc-Hydrazine 5.56. A 20 mL scintillation vial was charged with a magnetic stir bar, flame-dried under reduced pressure, and allowed to cool under a N_2 atmosphere. Boronic acid **5.54** (300.0 mg, 1.76 mmol, 1.0 equiv), di-*tert*-butyl azodicarboxylate (**5.55**) (444.6 mg, 1.93 mmol, 1.1 equiv), $Cu(OAc)_2$ (31.9 mg, 0.17 mmol, 0.10 equiv), and MeOH (7.0 mL, 0.25 M) were added under an atmosphere of air. The vial was capped with a Teflon-lined screw cap, placed in a pre-heated aluminum block, and allowed to stir at 50 °C for 3 h. After cooling to room temperature, the volatiles were removed under reduced pressure. The reaction mixture was then transferred to a separatory funnel with deionized water (5 mL) and CH_2Cl_2 (5 mL). The layers were separated and the aqueous layer was extracted with CH_2Cl_2 (3 x 5 mL). The organic layers were combined, washed with saturated aqueous NaCl (15 mL), and then dried over Na_2SO_4. The volatiles were removed under reduced pressure. The resulting crude residue was purified by flash chromatography (1:10 Hexanes:EtOAc, 2% Et_3N) to yield Boc-hydrazine **5.56** (221.7 mg, 37% yield) as a white solid.

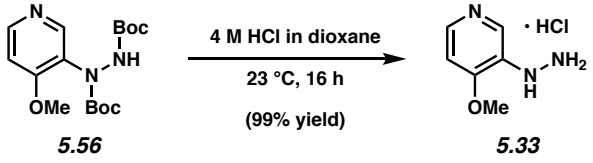

Hydrazine 5.33. A 20 mL scintillation vial equipped with a magnetic stir bar was charged with Boc-hydrazine **5.56** (221.7 mg, 0.65 mmol, 1.0 equiv) and 4 M HCl in dioxane (4.4 mL, 0.15 M). After stirring at 23 °C for 16 h, the volatiles were removed under reduced pressure. The

resulting crude residue was transferred to a filter paper, washed with EtOAc (5 mL), and dried under reduced pressure to yield hydrazine **5.33** (140.4 mg, 99% yield) as a light brown solid. Hydrazine **5.33**: mp: 178–180 ºC; R_f 0.07 (EtOAc); ^{1}H NMR (500 MHz, DMSO-d_6): δ 8.81 (br. s, 1H), 8.52 (dd, J = 6.5, 0.7, 1H), 8.42 (d, J = 0.7, 1H), 7.59 (d, J = 6.5, 1H), 4.14 (s, 3H); ^{13}C NMR (125 MHz, DMSO-d_6): 158.9, 136.7, 134.2, 124.1, 108.3, 58.1; IR (film): 3382, 3206, 2851, 2051, 1505 cm^{-1}; HRMS-APCI (*m/z*) $[M + H]^+$ calcd for $C_6H_{10}N_3O^+$, 140.0818; found 140.0817.

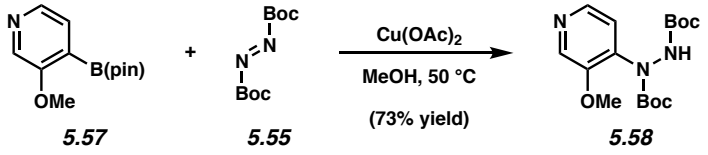

Representative Procedure E for the synthesis of hydrazine substrates from Table 5.2. (5.35 is used as an example). Boc-Hydrazine 5.58. A 20 mL scintillation vial was charged with a magnetic stir bar, flame-dried under reduced pressure, and allowed to cool under a N_2 atmosphere. Boronate ester **5.57** (300.0 mg, 1.28 mmol, 1.0 equiv), di-*tert*-butyl azodicarboxylate (**5.55**) (326.0 mg, 1.40 mmol, 1.1 equiv), $Cu(OAc)_2$ (23.2 mg, 0.13 mmol, 0.10 equiv), and MeOH (5.1 mL, 0.25 M) were added under an atmosphere of air. The vial was capped with a Teflon-lined screw cap, placed in a pre-heated aluminum block, and then allowed to stir at 50 °C for 3 h. After cooling to room temperature, the volatiles were removed under reduced pressure. The reaction mixture was then transferred to a separatory funnel with deionized water (5 mL) and CH_2Cl_2 (5 mL). The layers were separated and the aqueous layer was extracted with CH_2Cl_2 (3 x 5 mL). The organic layers were combined, washed with saturated aqueous NaCl (15 mL), and then dried over Na_2SO_4. The volatiles were removed under reduced pressure. The resulting crude residue was purified by flash chromatography (1:10

Hexanes: EtOAc, 2% Et_3N) to yield Boc-hydrazine **5.58** (316.3 mg, 73% yield) as a colorless foam.

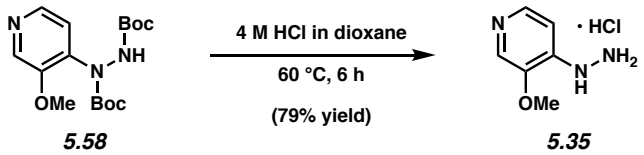

5.58 *5.35*

Hydrazine 5.35. A 20 mL scintillation vial equipped with a magnetic stir bar was charged with Boc-hydrazine **5.58** (131.8 mg, 0.39 mmol, 1.0 equiv) and 4 M HCl in dioxane (2.6 mL, 0.15 M). The vial was then capped with a Teflon-lined screw cap and was placed in a pre-heated aluminum block at 60 °C for 6 h. Once at room temperature, the volatiles were removed under reduced pressure. The resulting crude residue was transferred to a filter paper, washed with EtOAc (5 mL), and dried under reduced pressure to yield hydrazine **5.35** (53.7 mg, 79% yield) as a yellow solid. Hydrazine **5.35**: mp: 225–228 ºC; R_f 0.00 (EtOAc); ^{1}H NMR (500 MHz, DMSO-d_6): δ 9.70 (br. s, 1H), 8.19 (d, J = 6.6, 1H), 8.08 (s, 1H), 7.21 (d, J = 6.6, 1H), 3.94 (s, 3H); ^{13}C NMR (125 MHz, DMSO-d_6): 149.1, 141.9, 135.7, 120.0, 104.0, 57.2; IR (film): 3366, 3215, 2834, 1631, 1536 cm^{-1}; HRMS-APCI (*m/z*) $[M + H]^+$ calcd for $C_6H_{10}N_3O^+$, 140.0818; found 140.0816.

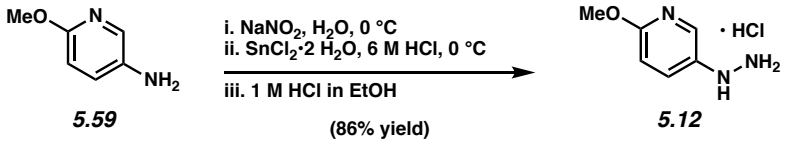

5.59 *5.12*

Hydrazine 5.12. Following representative procedure A yielded hydrazine **5.12** (2.42 g, 86% yield) as a light brown solid. Hydrazine **5.12**: mp: 175–178 ºC; R_f 0.27 (EtOAc); ^{1}H NMR (500 MHz, DMSO-d_6): δ 10.45 (br. s, 4H), 7.99 (d, J = 2.8, 1H), 7.65 (dd, J = 9.1, 2.8, 1H), 6.90 (d, J

= 9.1, 1H), 3.83 (s, 3H); ^{13}C NMR (125 MHz, DMSO-d_6): 158.8, 136.7, 132.4, 130.3, 110.7, 54.0; IR (film): 3368, 3201, 2564, 1627, 1562 cm^{-1}; HRMS-APCI (*m/z*) [M + H]$^+$ calcd for $C_6H_{10}N_3O^+$, 140.0818; found 140.0815.

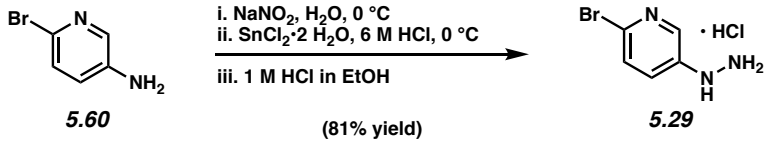

Hydrazine 5.29. Following representative procedure A yielded hydrazine **5.29** (280.7 mg, 81% yield) as an orange solid. Hydrazine **5.29**: mp: 211–213 ºC; R_f 0.37 (EtOAc); ^{1}H NMR (500 MHz, DMSO-d_6): δ 10.43 (br. s, 3H), 8.69 (br. s, 1H), 8.08 (d, J = 3.0, 1H), 7.56 (d, J = 8.5, 1H), 7.35 (dd, J = 8.5, 3.0, 1H); ^{13}C NMR (125 MHz, DMSO-d_6): 142.1, 136.9, 132.0, 127.7, 125.4; IR (film): 3070, 2883, 2645, 1927, 1619 cm^{-1}; HRMS-APCI (*m/z*) [M + H]$^+$ calcd for $C_5H_7N_3Br^+$, 187.9818; found 187.9814.

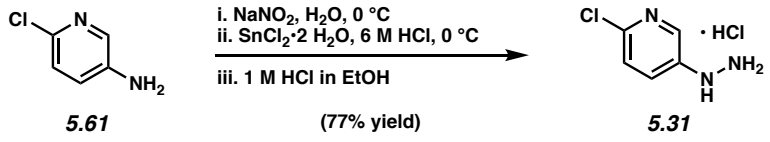

Hydrazine 5.31. Following representative procedure A yielded hydrazine **5.31** (215.3 mg, 77% yield) as a light brown solid. Hydrazine **5.31**: mp: 208–209 ºC; R_f 0.37 (EtOAc); ^{1}H NMR (500 MHz, DMSO-d_6): δ 10.45 (br. s, 3H), 8.72 (br. s, 1H), 8.10–8.09 (m, 1H), 7.47–7.43 (m, 2H); ^{13}C NMR (125 MHz, DMSO-d_6): 141.9, 141.6, 136.1, 125.5, 124.0; IR (film): 3378, 3197, 2662, 1617, 1470 cm^{-1}; HRMS-APCI (*m/z*) [M + H]$^+$ calcd for $C_5H_7N_3Cl^+$, 144.0323; found 144.0320.

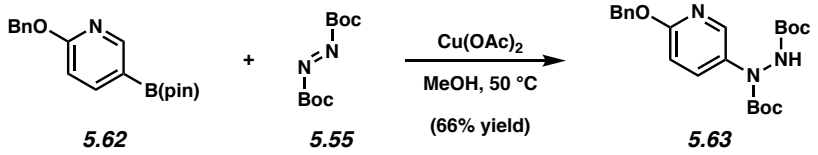

5.62 *5.55* *5.63*

Boc-Hydrazine 5.63. Following representative procedure E. Purification by flash chromatography (5:1 Hexanes:EtOAc) yielded Boc-hydrazine **5.63** (560.0 mg, 66% yield) as a light yellow solid.

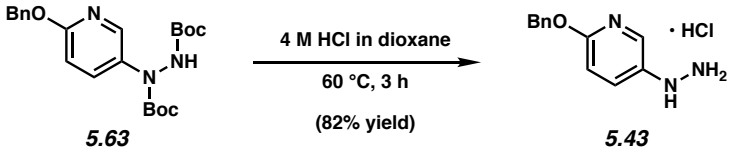

5.63 *5.43*

Hydrazine 5.43. Following representative procedure E yielded hydrazine **5.43** (280.1 mg, 82% yield) as a yellow solid. Hydrazine **5.43**: mp: 125–128 ºC; R_f 0.33 (EtOAc); ^{1}H NMR (500 MHz, DMSO-d_6): δ 10.11 (br. s, 3H), 9.90 (br. s, 1H), 7.89 (d, J = 2.5, 1H), 7.47 (app. dt, J = 8.8, 2.5, 1H), 7.38 (d, J = 7.3, 2H), 7.33 (t, J = 7.3, 2H), 7.27 (t, J = 7.3, 1H), 6.84 (d, J = 8.8, 1H), 5.26 (s, 2H); ^{13}C NMR (125 MHz, DMSO-d_6): 158.8, 137.4, 136.5, 133.8, 129.2, 128.4, 127.8, 127.7, 110.8, 67.0; IR (film): 3389, 2894, 2646, 1946, 1556 cm^{-1}; HRMS-APCI (*m/z*) $[M + H]^+$ calcd for $C_{12}H_{14}N_3O^+$, 216.1131; found 216.1128.

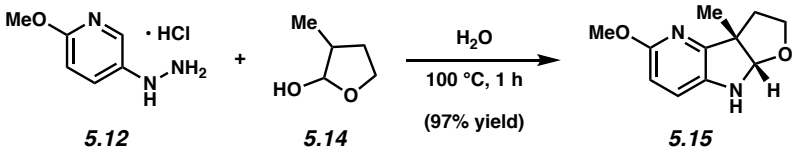

5.12 *5.14* *5.15*

Representative Procedure (azaindoline 5.15 is used as an example). Azaindoline 5.15. A scintillation vial containing a magnetic stir bar was charged with lactol **5.14** (23.6 mg, 0.231 mmol, 1.0 equiv) and deionized H_2O (4.6 mL, 0.05 M). Hydrazine **5.12** (60.9 mg, 0.347 mmol, 1.5 equiv) was added and the vial was capped with a Teflon-lined screw cap. The reaction mixture was then placed in a pre-heated aluminum block and allowed to stir at 100 °C for 1 h. After cooling to room temperature, the reaction mixture was transferred to a separatory funnel with deionized H_2O (3 mL) and EtOAc (3 mL). The reaction mixture was then basified to a pH of 12 by the addition of 40% w/w KOH in deionized H_2O (ca. 4 mL). The layers were separated and the aqueous layer was extracted with EtOAc (3 x 5 mL). The combined organic layers were washed with saturated aqueous NaCl (5 mL), and then dried over Na_2SO_4. The volatiles were removed under reduced pressure, and the crude residue was purified by preparative thin-layer chromatography (2:1 Hexanes:EtOAc) to yield azaindoline **5.15** (97% yield, average of two experiments) as a yellow oil. Azaindoline **5.15**: R_f 0.55 (1:1 Hexanes:EtOAc); ^{1}H NMR (500 MHz, $CDCl_3$): δ 6.88 (d, *J* = 8.4, 1H), 6.43 (d, *J* = 8.4, 1H), 5.27 (s, 1H), 3.96 (ddd, *J* = 8.9, 7.6, 1.7, 1H), 3.87 (s, 3H), 3.53 (ddd, *J* = 10.9, 8.9, 5.3, 1H), 2.40 (ddd, *J* = 12.1, 5.3, 1.7, 1H), 2.03 (ddd, *J* = 12.1, 10.9, 7.6, 1H), 1.48 (s, 3H); ^{13}C NMR (125 MHz, $CDCl_3$): 159.7, 151.2, 136.8, 119.7, 107.4, 99.1, 67.6, 54.3, 53.8, 39.6, 22.6; IR (film): 3347, 2961, 2867, 1603, 1471 cm^{-1}; HRMS-APCI (*m/z*) $[M + H]^+$ calcd for $C_{11}H_{15}N_2O_2^+$, 207.1128; found 207.1124.

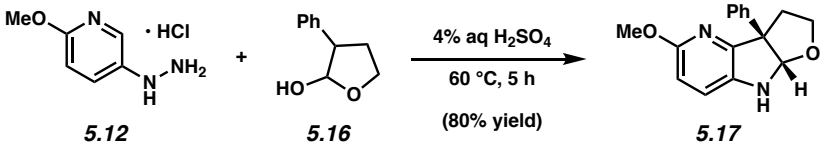

5.12 *5.16* *5.17*

Azaindoline 5.17. Purification by preparative thin-layer chromatography (2:1 Hexanes:EtOAc) yielded azaindoline **5.17** (80% yield, average of two experiments) as an amorphous solid.

Azaindoline **5.17**: R_f 0.63 (1:1 Hexanes:EtOAc); ^{1}H NMR (500 MHz, $CDCl_3$): δ 7.42 (d, J = 7.8, 2H), 7.32 (t, J = 7.8, 2H), 7.26–7.21 (m, 1H), 6.94 (d, J = 8.6, 1H), 6.47 (d, J = 8.6, 1H), 5.69 (s, 1H), 4.39 (s, 1H), 4.18–4.15 (m, 1H), 3.85 (s, 3H), 3.67–3.62 (m, 1H), 2.85–2.82 (m, 1H), 2.65–2.59 (m, 1H); ^{13}C NMR (125 MHz, $CDCl_3$): 159.8, 149.1, 142.6, 137.6, 128.6, 126.9, 126.5, 120.5, 108.4, 99.7, 68.6, 62.4, 53.8, 39.7; IR (film): 3341, 2866, 2973, 1602, 1470 cm^{-1}; HRMS-APCI (*m/z*) $[M + H]^+$ calcd for $C_{16}H_{17}N_2O_2^+$, 269.1285; found 269.1269.

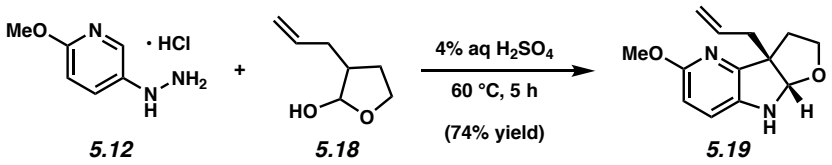

5.12 *5.18* *5.19*

Azaindoline 5.19. Purification by preparative thin-layer chromatography (3:2 Hexanes:EtOAc) yielded azaindoline **5.19** (74% yield, average of two experiments) as a red oil. Azaindoline **5.19**: R_f 0.62 (1:1 Hexanes:EtOAc); ^{1}H NMR (400 MHz, $CDCl_3$): δ 6.88–6.86 (m, 1H), 6.45–6.42 (m, 1H), 5.75–5.65 (m, 1H), 5.39 (s, 1H), 5.10–5.06 (m, 1H), 5.03–4.99 (m, 1H), 3.98–3.93 (m, 1H), 3.87 (s, 3H), 3.53 (ddd, J = 11.2, 8.8, 5.3, 1H), 2.75–2.69 (m, 1H), 2.52–2.47 (m, 1H), 2.34–2.29 (m, 1H), 2.09 (app. ddd, J = 11.2, 11.2, 7.4, 1H); ^{13}C NMR (100 MHz, $CDCl_3$): 159.8, 149.9, 137.7, 134.4, 119.9, 118.0, 107.8, 96.8, 67.3, 58.1, 53.9, 40.9, 37.9; IR (film): 3343, 2973, 2947, 1603, 1471 cm^{-1}; HRMS-APCI (*m/z*) $[M + H]^+$ calcd for $C_{13}H_{17}N_2O_2^+$, 233.1285; found 233.1279.

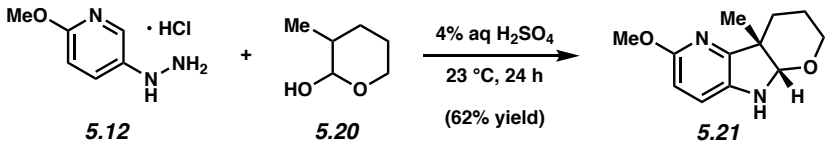

5.12 *5.20* *5.21*

Azaindoline 5.21. Purification by preparative thin-layer chromatography (3:2 Hexanes:EtOAc) yielded azaindoline **5.21** (62% yield, average of two experiments) as an amorphous solid. Azaindoline **5.21**: R_f 0.59 (1:1 Hexanes:EtOAc); ^{1}H NMR (400 MHz, $CDCl_3$): δ 6.93 (d, *J* = 8.1, 1H), 6.41 (d, *J* = 8.1, 1H), 4.74 (s, 1H), 4.04 (br. s, 1H), 3.87 (s, 3H), 3.75 (dddd, *J* = 11.2, 4.0, 4.0, 1.6, 1H), 3.40 (ddd, *J* = 11.2, 10.0, 3.0, 1H), 2.45 (dddd, *J* = 13.3, 4.0, 4.0, 1.6, 1H), 1.62 (ddd, *J* = 13.6, 11.8, 4.7, 1H), 1.55–1.47 (m, 1H), 1.47–1.36 (m, 1H), 1.17 (s, 3H); ^{13}C NMR (100 MHz, $CDCl_3$): 159.7, 153.0, 136.4, 120.5, 106.2, 94.9, 63.0, 54.0, 44.2, 29.2, 24.7, 22.2; IR (film): 3319, 2950, 2851, 1603, 1464 cm^{-1}; HRMS-APCI (*m/z*) $[M + H]^+$ calcd for $C_{12}H_{17}N_2O_2^+$, 221.1285; found 221.1278.

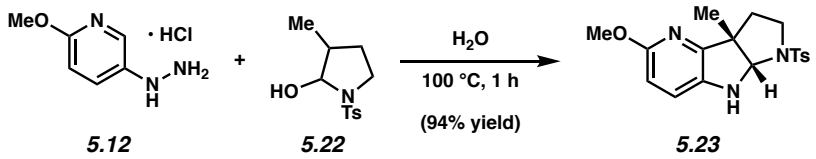

5.12 *5.22* *5.23*

Azaindoline 5.23. Purification by preparative thin-layer chromatography (2:1 Hexanes:EtOAc) yielded azaindoline **5.23** (94% yield, average of two experiments) as a colorless oil. Azaindoline **5.23**: R_f 0.77 (1:1 Hexanes:EtOAc); ^{1}H NMR (400 MHz, $CDCl_3$): δ 7.74 (d, *J* = 8.3, 2H), 7.32 (d, *J* = 8.3, 2H), 6.90 (d, *J* = 8.4, 1H), 6.44 (d, *J* = 8.4, 1H), 4.98 (s, 1H), 3.84 (s, 3H), 3.39 (ddd, *J* = 10.5, 8.2, 2.3, 1H), 3.10 (ddd, *J* = 10.5, 10.5, 6.4, 1H), 2.44 (s, 3H), 2.41 (ddd, *J* = 12.5, 6.4, 2.3, 1H), 1.70 (ddd, *J* = 12.5, 10.5, 8.2, 1H), 1.27 (s, 3H); ^{13}C NMR (100 MHz, $CDCl_3$): 159.9, 150.2, 143.8, 136.3, 136.0, 129.9, 127.2, 120.9, 107.9, 84.1, 54.6, 53.9, 47.7, 36.1, 22.4, 21.7; IR (film): 3375, 2963, 2867, 1597, 1470 cm^{-1}; HRMS-APCI (*m/z*) $[M + H]^+$ calcd for $C_{18}H_{22}N_3O_3S^+$, 360.1376; found 360.1363.

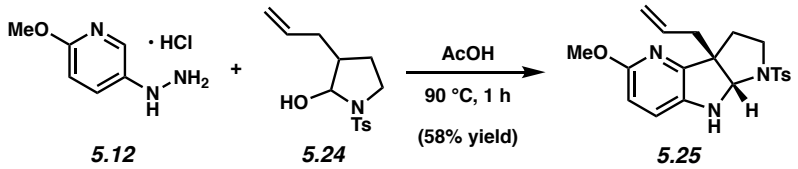

5.12 *5.24* *5.25*

Azaindoline 5.25. Purification by preparative thin-layer chromatography (2:1 Hexanes:EtOAc) yielded azaindoline **5.25** (58% yield, average of two experiments) as a colorless oil. Azaindoline **5.25**: R_f 0.70 (1:1 Hexanes:EtOAc); ^{1}H NMR (500 MHz, $CDCl_3$): δ 7.74 (d, *J* = 7.8, 2H), 7.32 (d, *J* = 7.8, 2H), 6.89 (d, *J* = 8.4, 1H), 6.45 (d, *J* = 8.4, 1H), 5.54 (dddd, *J* = 17.4, 10.0, 7.4, 7.4, 1H), 5.11 (s, 1H), 4.98–4.93 (m, 2H), 4.52 (br. s, 1H), 3.84 (s, 3H), 3.38 (ddd, *J* = 10.3, 8.3, 2.3, 1H), 3.10 (ddd, *J* = 10.3, 10.3, 6.2, 1H), 2.44 (s, 3H), 2.41–2.38 (m, 1H), 2.32–2.27 (m, 2H), 1.78 (ddd, *J* = 12.2, 10.2, 8.3, 1H); ^{13}C NMR (125 MHz, $CDCl_3$): 159.8, 149.0, 143.8, 137.0, 136.0, 133.5, 129.9, 127.3, 120.8, 118.5, 108.2, 81.6, 58.2, 53.9, 47.5, 40.5, 34.2, 21.7; IR (film): 3376, 3072, 2950, 1598, 1471 cm^{-1}; HRMS-APCI (*m/z*) $[M + H]^+$ calcd for $C_{20}H_{24}N_3O_3S^+$, 386.1533; found 386.1511.

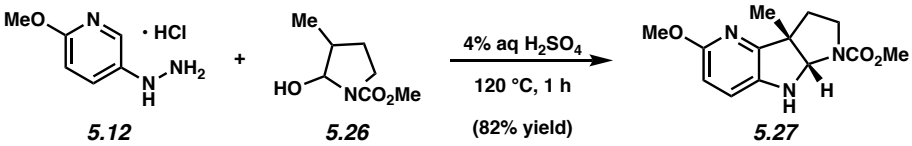

5.12 *5.26* *5.27*

Azaindoline 5.27. Purification by preparative thin-layer chromatography (1:1 Hexanes:EtOAc) yielded azaindoline **5.27** (82% yield, average of two experiments) as an amorphous solid. Azaindoline **5.27**: R_f 0.46 (1:1 Hexanes:EtOAc); ^{1}H NMR (500 MHz, $CDCl_3$, 58 °C): δ 6.85 (d, *J* = 8.3, 1H), 6.43 (d, *J* = 8.3, 1H), 5.10 (br. s, 1H), 3.88 (s, 3H), 3.72–3.64 (m, 4H), 3.09–3.04 (m, 1H), 2.53–2.49 (m, 1H), 2.02–1.95 (m, 1H), 1.42 (s, 3H); ^{13}C NMR (125 MHz, C_6D_6, **Major rotational isomer**): 160.0, 155.4, 150.2, 137.0, 120.7, 109.0, 82.1, 53.4, 53.2, 51.9, 45.9, 35.4, 22.2; ^{13}C NMR (125 MHz, C_6D_6, **Minor rotational isomer**, 11 of 13 peaks seen): 160.2, 154.4,

150.3, 136.6, 120.6, 109.1, 81.4, 54.6, 52.1, 46.4, 22.7; IR (film): 3360, 2956, 2869, 1696, 1605 cm^{-1}; HRMS-APCI (*m/z*) $[M + H]^+$ calcd for $C_{13}H_{18}N_3O_3^+$, 264.1343; found 264.1330.

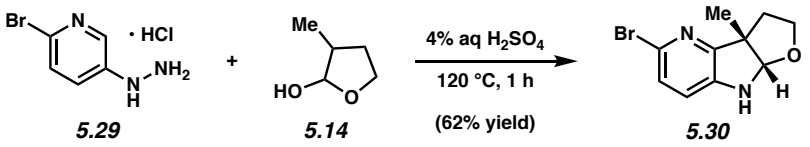

Azaindoline 5.30. Purification by preparative thin-layer chromatography (1:1 Hexanes:EtOAc) yielded azaindoline **5.30** (62% yield, average of two experiments) as a light brown solid. Azaindoline **5.30**: mp: 170–171 ºC; R_f 0.50 (1:1 Hexanes:EtOAc); ^{1}H NMR (500 MHz, $CDCl_3$): δ 7.08 (d, *J* = 8.3, 1H), 6.89 (d, *J* = 8.3, 1H), 5.29 (s, 1H), 4.64 (br. s, 1H), 3.98 (ddd, *J* = 8.9, 7.6, 1.6, 1H), 3.52 (dddd, *J* = 11.3, 8.9, 5.3, 1H), 2.43 (ddd, *J* = 12.3, 5.3, 1.6, 1H), 2.05 (ddd, *J* = 12.3, 11.3, 7.6, 1H), 1.50 (s, 3H); ^{13}C NMR (125 MHz, $CDCl_3$): 156.1, 142.2, 129.8, 126.2, 116.7, 98.5, 67.7, 54.2, 39.9, 22.8; IR (film): 3328, 2963, 2866, 1595, 1426 cm^{-1}; HRMS-APCI (*m/z*) $[M + H]^+$ calcd for $C_{10}H_{12}N_2OBr^+$, 255.0128; found 255.0128.

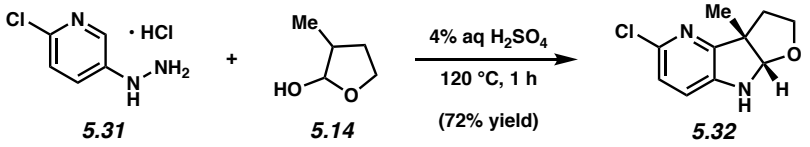

Azaindoline 5.32. Purification by preparative thin-layer chromatography (1:1 Hexanes:EtOAc) yielded azaindoline **5.32** (72% yield, average of two experiments) as a brown solid. Azaindoline **5.32**: mp: 143–145 ºC; R_f 0.50 (1:1 Hexanes:EtOAc); ^{1}H NMR (500 MHz, $CDCl_3$): δ 6.95 (d, *J* = 8.3, 1H), 6.77 (d, *J* = 8.3, 1H), 5.31 (s, 1H), 4.62 (br. s, 1H), 3.99 (ddd, *J* = 8.9, 7.6, 1.6, 1H), 3.53 (ddd, *J* = 11.3, 8.9, 5.3, 1H), 2.43 (ddd, *J* = 12.3, 5.3, 1.6, 1H), 2.06 (ddd, *J* = 12.3, 11.3, 7.6, 1H), 1.51 (s, 3H); ^{13}C NMR (125 MHz, $CDCl_3$): 155.3, 141.8, 140.5, 122.5, 116.7, 98.6,

67.7, 54.2, 39.9, 22.8; IR (film): 3319, 2965, 2867, 1596, 1430 cm^{-1}; HRMS-APCI (*m/z*) $[M + H]^+$ calcd for $C_{10}H_{12}N_2OCl^+$, 211.0633; found 211.0633.

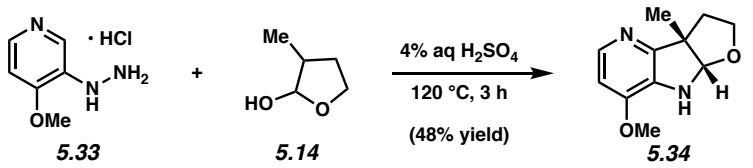

Azaindoline 5.34. Purification by preparative thin-layer chromatography (EtOAc) yielded azaindoline **5.34** (48% yield, average of two experiments) as an amorphous solid. Azaindoline **5.34**: R_f 0.26 (EtOAc); ^1H NMR (500 MHz, $CDCl_3$): δ 7.94 (d, *J* = 5.3, 1H), 6.61 (d, *J* = 5.3, 1H), 5.33 (s, 1H), 4.51 (br. s, 1 H), 3.99 (ddd, *J* = 8.8, 7.6, 1.5, 1H), 3.88 (s, 3H), 3.54 (ddd, *J* = 11.2, 8.8, 5.5, 1H), 2.45 (ddd, *J* = 12.2, 5.5, 1.5, 1H), 2.08 (ddd, *J* = 12.2, 11.2, 7.6, 1H), 1.53 (s, 3H); ^{13}C NMR (125 MHz, $CDCl_3$): 154.2, 149.8, 141.9, 132.3, 105.7, 98.8, 67.9, 55.5, 54.9, 39.8, 22.8; IR (film): 3308, 2926, 2867, 1614, 1498 cm^{-1}; HRMS-APCI (*m/z*) $[M + H]^+$ calcd for $C_{11}H_{15}N_2O_2^+$, 207.1128; found 207.1121.

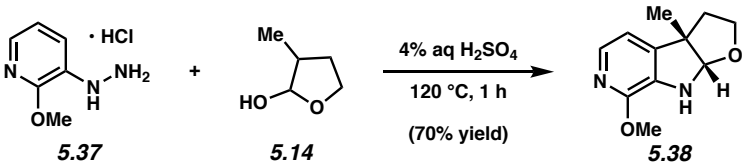

Azaindoline 5.38. Purification by preparative thin-layer chromatography (2:1 Hexanes:EtOAc) yielded azaindoline **5.38** (70% yield, average of two experiments) as a colorless solid. Azaindoline **5.38**: mp: 143–145 ºC; R_f 0.51 (1:1 Hexanes:EtOAc); ^1H NMR (500 MHz, $CDCl_3$): δ 7.64 (d, *J* = 5.1, 1H), 6.70 (d, *J* = 5.1, 1H), 5.34 (s, 1H), 4.48 (br. s, 1H), 3.99–3.95 (m, 4H), 3.54 (ddd, *J* = 11.2, 8.7, 5.1, 1H), 2.16 (ddd, *J* = 12.3, 5.1, 1.6, 1H), 2.07 (ddd, *J* = 12.3, 11.2, 7.3, 1H), 1.47 (s, 3H); ^{13}C NMR (125 MHz, $CDCl_3$): 150.0, 142.3, 137.1, 132.9, 112.3, 99.9,

67.6, 55.1, 53.2, 40.8, 23.9; IR (film): 3328, 2956, 2867, 1611, 1471 cm^{-1}; HRMS-APCI (*m/z*) $[M + H]^+$ calcd for $C_{11}H_{15}N_2O_2^+$, 207.1128; found 207.1126.

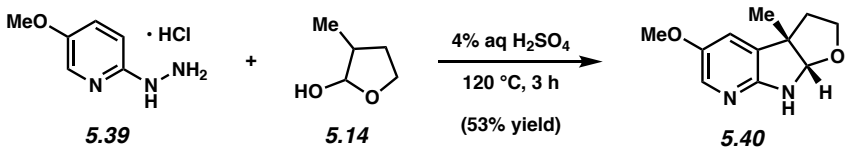

Azaindoline 5.40. Purification by preparative thin-layer chromatography (1:1 Hexanes:EtOAc) yielded azaindoline **5.40** (53% yield, average of two experiments) as a yellow solid. Azaindoline **5.40**: mp: 87–90 ºC; R_f 0.13 (1:1 Hexanes:EtOAc); ^{1}H NMR (500 MHz, $CDCl_3$): δ 7.56 (d, *J* = 2.7, 1H), 6.95 (d, *J* = 2.7, 1H), 5.31 (s, 1H), 5.11 (br. s, 1H), 3.97 (ddd, *J* = 8.8, 7.0, 1.6, 1H), 3.78 (s, 3H), 3.58 (ddd, *J* = 10.9, 8.8, 5.4, 1H), 2.13–2.03 (m, 2H), 1.47 (s, 3H); ^{13}C NMR (125 MHz, $CDCl_3$): 156.7, 150.5, 130.9, 128.8, 120.6, 98.0, 67.2, 56.8, 52.6, 41.5, 24.7; IR (film): 3206, 2956, 2866, 1627, 1480 cm^{-1}; HRMS-APCI (*m/z*) $[M + H]^+$ calcd for $C_{11}H_{15}N_2O_2^+$, 207.1128; found 207.1121.

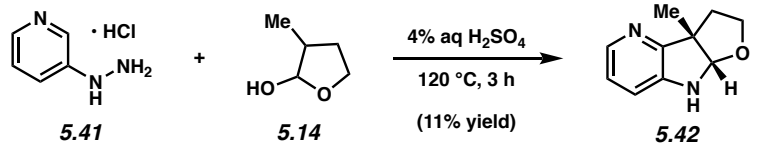

Azaindoline 5.42. Purification by preparative thin-layer chromatography (98:2 EtOAc:Et_3N) yielded azaindoline **5.42** (11% yield, average of two experiments) as an amorphous solid. Azaindoline **5.42**: R_f 0.44 (EtOAc); ^{1}H NMR (500 MHz, $CDCl_3$): δ 7.95 (dd, *J* = 5.1, 1.4, 1H), 6.93 (dd, *J* = 7.9, 5.1, 1H), 6.79 (dd, *J* = 7.9, 1.4, 1H), 5.31 (s, 1H), 4.59 (br. s, 1H), 3.99 (ddd, *J* = 8.9, 7.6, 1.6, 1H), 3.53 (ddd, *J* = 11.2, 8.9, 5.3, 1H), 2.43 (ddd, *J* = 12.2, 5.3, 1.6, 1H), 2.09 (ddd, *J* = 12.2, 11.2, 7.6, 1H), 1.52 (s, 3H); ^{13}C NMR (125 MHz, $CDCl_3$): 155.0, 142.7, 140.1,

122.5, 113.9, 98.3, 67.7, 54.0, 40.1, 22.9; IR (film): 3330, 2961, 2867, 1602, 1436 cm^{-1}; HRMS-APCI (*m/z*) $[M + H]^+$ calcd for $C_{10}H_{13}N_2O^+$, 177.1022; found 177.1009.

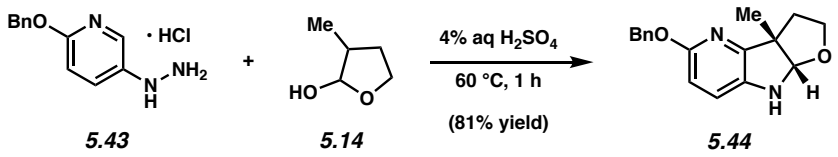

Azaindoline 5.44. A round-bottom flask containing a magnetic stir bar was charged with lactol **5.14** (37.2 mg, 0.364 mmol, 1.0 equiv) and 4% aqueous H_2SO_4 (7.3 mL, 0.05 M). Hydrazine **5.43** (274.3 mg, 1.092 mmol, 3.0 equiv) was added and the flask equipped with an air condenser. The reaction mixture was then placed in a pre-heated oil bath and allowed to stir at 60 °C for 1 h. After cooling to room temperature, the reaction mixture was transferred to a separatory funnel with deionized H_2O (5 mL) and EtOAc (5 mL). The reaction mixture was then basified to a pH of 9 with saturated aqueous $NaHCO_3$ (ca. 10 mL). The layers were separated and the aqueous layer was extracted with EtOAc (3 x 10 mL). The combined organic layers were washed with saturated aqueous NaCl (10 mL), and then dried over Na_2SO_4. The volatiles were removed under reduced pressure, and the crude residue was purified by flash chromatography (2:1 Hexanes:EtOAc) to yield azaindoline **5.44** (83.2 mg, 81% yield) as a yellow oil. Azaindoline **5.44**: R_f 0.54 (1:1 Hexanes:EtOAc); ^1H NMR (500 MHz, $CDCl_3$): δ 7.46 (d, *J* = 7.2, 2H), 7.35 (t, *J* = 7.2, 2H), 7.30–7.28 (m, 1H), 6.87 (d, *J* = 8.5, 1H), 6.48 (d, *J* = 8.5, 1H), 5.31 (s, 1H), 5.30 (s, 1H), 5.27 (s, 1H), 4.25 (br. s, 1H), 3.97 (ddd, *J* = 9.1, 7.7, 1.7, 1H), 3.53 (ddd, *J* = 11.1, 9.1, 5.1. 1H), 2.39 (ddd, *J* = 12.1, 5.1, 1.7, 1H), 2.04 (ddd, *J* = 12.1, 11.1 7.7, 1H), 1.48 (s, 3H); ^{13}C NMR (125 MHz, $CDCl_3$): 159.1, 151.0, 138.1, 137.1, 128.5, 128.3, 127.8, 119.9, 108.6, 99.2, 68.1, 67.7, 54.5, 39.7, 22.8; IR (film): 3348, 2963, 2930, 1603, 1447 cm^{-1}; HRMS-APCI (*m/z*) $[M + H]^+$ calcd for $C_{17}H_{19}N_2O_2^+$, 283.1441; found 283.1434.

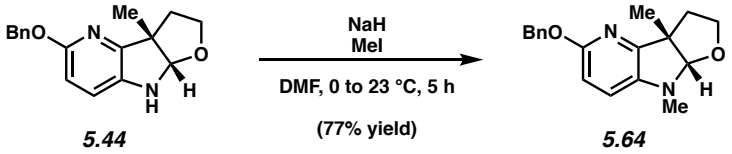

Azaindoline 5.64. A 1-dram vial was charged with a magnetic stir bar, flame-dried under reduced pressure, and allowed to cool under a N_2 atmosphere. Azaindoline **5.44** (83.0 mg, 0.294 mmol, 1.0 equiv) was added and the vial was flushed with N_2 for 5 min. DMF (294 μL, 1.0 M) was added and the reaction mixture cooled to 0 °C under an N_2 atmosphere. NaH (60% dispersion in mineral oil, 26.0 mg, 0.647 mmol, 2.2 equiv) was added in one portion and the reaction was left to stir for 30 min at 0 °C. MeI (44 μL, 0.706 mmol, 2.4 equiv) was then added dropwise over 1 min. After 30 min stirring at 0 °C, the reaction mixture was warmed to 23 °C and allowed to stir for 4 h. The reaction mixture was then transferred to a separatory funnel with deionized H_2O (3 mL) and CH_2Cl_2 (3 mL). The layers were separated and the aqueous layer was extracted with CH_2Cl_2 (3 x 5 mL). The combined organic layers were washed sequentially with deionized H_2O (3 x 3 mL) and saturated aqueous NaCl (10 mL), and then dried over Na_2SO_4. The volatiles were removed under reduced pressure, and the crude residue was purified by flash chromatography (3:1 Hexanes:EtOAc) to yield azaindoline **5.64** (61.0 mg, 77% yield) as a colorless oil. Azaindoline **5.64**: R_f 0.46 (3:1 Hexanes:EtOAc); ^{1}H NMR (500 MHz, $CDCl_3$): δ 7.46 (d, *J* = 7.5, 2H), 7.35 (t, *J* = 7.5, 2H), 7.30–7.27 (m, 1H), 6.64 (d, *J* = 8.3, 1H), 6.50 (d, *J* = 8.3, 1H), 5.32–5.27 (m, 2H), 5.04 (s, 1H), 3.96 (ddd, *J* = 9.0, 7.6, 1.6, 1H), 3.43 (ddd, *J* = 11.2, 9.0, 5.6, 1H), 2.88 (s, 3H), 2.36 (ddd, *J* = 12.2, 5.6, 1.6, 1H), 2.02 (ddd, *J* = 12.2, 11.2, 7.6, 1H), 1.47 (s, 3H); ^{13}C NMR (125 MHz, $CDCl_3$): 157.9, 151.5, 139.7, 138.2, 128.4, 128.3, 127.7, 115.8, 108.0, 104.3, 68.2, 67.7, 53.4, 39.7, 32.0, 22.7; IR (film): 2930, 2864, 1595, 1457, 1421 cm^{-1}; HRMS-APCI (*m/z*) $[M + H]^+$ calcd for $C_{18}H_{21}N_2O_2^+$, 297.1598; found 297.1596.

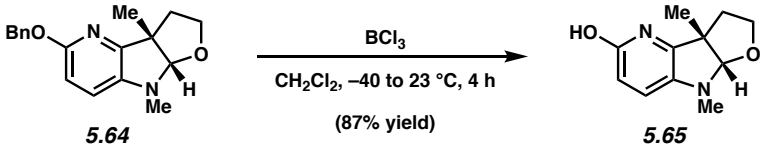

Hydroxyazaindoline 5.65. A 1-dram vial was charged with a magnetic stir bar, flame-dried under reduced pressure, and allowed to cool under a N_2 atmosphere. Azaindoline **5.64** (3.3 mg, 0.011 mmol, 1.0 equiv) was added and the vial was flushed with N_2 for 5 min. CH_2Cl_2 (222 μL, 0.05 M) was added and the reaction mixture cooled to –40 °C. BCl_3 (1 M in CH_2Cl_2, 78.0 μL, 0.078 mmol, 7.0 equiv) was added dropwise over 1 min and the reaction mixture was stirred at –40 °C. After 5 min, the reaction mixture was warmed to 23 °C and allowed to stir for 4 h. The reaction mixture was then transferred to separatory funnel containing ice-cold deionized H_2O (5 mL). The reaction mixture was basified to a pH of 9 with saturated aqueous $NaHCO_3$ (5 mL) and then extracted with EtOAc (5 x 3 mL). The combined organic layers were washed with saturated aqueous NaCl (10 mL), and subsequently dried over Na_2SO_4. The volatiles were removed under reduced pressure, and the crude residue was purified by preparative thin-layer chromatography (EtOAc) to yield hydroxyazaindoline **5.65** (1.9 mg, 87% yield) as a brown solid. Hydroxyazaindoline **5.65**: mp: 169–170 ºC; R_f 0.36 (EtOAc); ^{1}H NMR (500 MHz, $CDCl_3$): δ 6.77 (d, *J* = 8.5, 1H), 6.49 (d, *J* = 8.5, 1H), 5.01 (s, 1H), 3.97 (ddd, *J* = 8.8, 7.4, 1.6, 1H), 3.47 (ddd, *J* = 11.2, 8.8, 5.2, 1H), 2.88 (s, 3H), 2.44 (ddd, *J* = 12.2, 5.2, 1.6, 1H), 2.08 (ddd, *J* = 12.2, 11.2, 7.4, 1H), 1.53 (s, 3H); ^{13}C NMR (125 MHz, $CDCl_3$): 159.2, 148.9, 138.5, 118.9, 109.2, 104.5, 67.9, 53.2, 39.5, 32.3, 22.7; IR (film): 2964, 2926, 2669, 1614, 1488 cm^{-1}; HRMS-APCI (*m/z*) $[M + H]^+$ calcd for $C_{11}H_{15}N_2O_2^+$, 207.1128; found 207.1123.

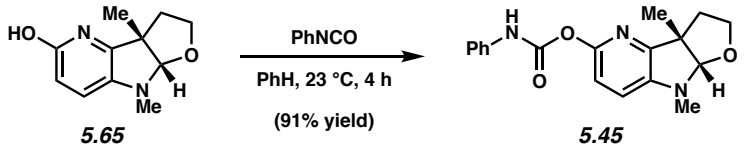

5.65 *5.45*

Aza-phensvenine 5.45. A 1-dram vial was charged with a magnetic stir bar, flame-dried under reduced pressure, and allowed to cool under a N_2 atmosphere. Hydroxyazaindoline **5.65** (5.0 mg, 0.024 mmol, 1.0 equiv) was added and the vial was flushed with N_2 for 5 min. The vial was then charged with a stock solution of PhNCO (1.7 uL, 0.022 mmol, 0.92 equiv) in PhH (200 µL, 0.075 M), and the reaction mixture was allowed to stir at 23 °C under an N_2 atmosphere. After 4 h, the volatiles were removed under reduced pressure to yield aza-phensvenine **5.45** (7.2 mg, 91% yield) as an amorphous solid. Aza-phensvenine **5.45**: R_f 0.40 (1:1 Hexanes:EtOAc); ^{1}H NMR (500 MHz, C_6D_6): δ 7.27 (d, *J* = 8.0, 2H), 7.05–7.02 (m, 2H), 6.83–6.80 (m, 1H), 6.77 (d, *J* = 8.1, 1H), 6.61 (br. s, 1H), 6.13 (d, *J* = 8.1, 1H), 4.86 (s, 1H), 3.65 (ddd, *J* = 8.9, 7.6, 1.6, 1H), 3.25 (ddd, *J* = 11.2, 8.9, 5.4, 1H), 2.52 (s, 3H), 2.26 (ddd, *J* = 12.2, 5.4, 1.6, 1H), 1.67 (ddd, *J* = 12.2, 11.2, 7.6, 1H), 1.32 (s, 3H); ^{13}C NMR (125 MHz, C_6D_6): 154.0, 152.0, 150.6, 143.5, 138.4, 129.1, 123.7, 119.0, 114.9, 113.0, 103.9, 67.4, 53.2, 40.2, 30.8, 22.7; IR (film): 3281, 2926, 1746, 1646, 1597 cm^{-1}; HRMS-APCI (*m/z*) $[M + H]^+$ calcd for $C_{18}H_{20}N_3O_3^+$, 326.1499; found 326.1490.

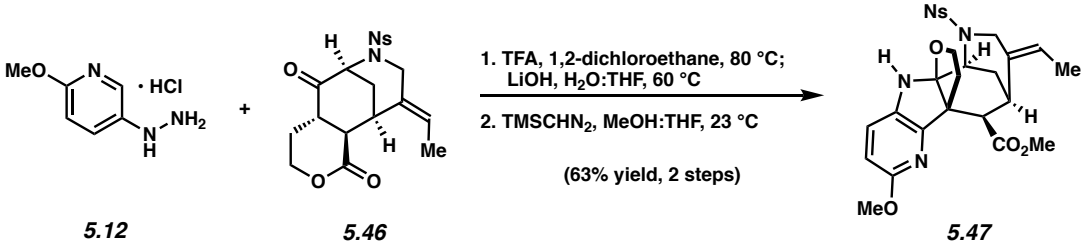

5.12 *5.46* *5.47*

Aza-furoindoline 5.47. A 1-dram vial was charged with a magnetic stir bar, flame-dried under reduced pressure, and allowed to cool under a N_2 atmosphere. Ketolactone **5.46** (10.0 mg, 0.0238

mmol, 1.0 equiv) was added and suspended in 1,2-dichloroethane (1.0 mL, 0.020 M). Hydrazine **5.12** (35.0 mg, 0.119 mmol, 5.0 equiv) and TFA (10.0 μL, 0.119 mmol, 5.0 equiv) were added to the reaction vial. The mixture was degassed via the freeze-pump-thaw method using a –78 °C dry ice/acetone bath. After warming to 23 °C, the reaction vessel was placed into a pre-heated 80 °C aluminum heating block and allowed to stir for 12 h. After cooling to room temperature, the reaction mixture was filtered over Na_2SO_4, washed with CH_2Cl_2 (10 mL), and concentrated under reduced pressure. The resultant residue was suspended in 1:1 THF/H_2O (1.0 mL, 0.02 M) in a 1-dram vial. LiOH (5.0 mg, 0.238 mmol, 10.0 equiv) was added and the reaction vessel was placed into a pre-heated 60 °C aluminum heating block. Upon stirring for 2 h at 60 °C, the reaction was cooled to 23°C. The layers were separated and the aqueous layer was extracted with CH_2Cl_2 (4 x 2 mL). The organic layers were combined, dried over Na_2SO_4, and concentrated under reduced pressure. The resultant residue was suspended in 1:1 THF/MeOH (1.0 mL, 0.02 M) in a 1-dram vial. $TMSCHN_2$ (77.0 μL, 0.046 mmol, 2.0 equiv) was added and the resultant solution stirred at room temperature. Upon stirring for 1.5 h, the reaction was diluted with 2 mL of H_2O and the layers were separated. The aqueous layer was extracted with EtOAc (4 x 2 mL). The organic layers were combined, dried over Na_2SO_4, and then concentrated under reduced pressure. The crude residue was purified by flash chromatography (9:1 Hexanes:EtOAc → 7:3 Hexanes:EtOAc) to afford aza-furoindoline **5.47** (8.0 mg, 63% yield) as a yellow oil. Aza-furoindoline **5.47:** R_f 0.50 (1:1 Hexanes:EtOAc); ^{1}H NMR (500 MHz, $CDCl_3$): δ 8.07–8.03 (m, 1H), 7.69–7.61 (m, 3H), 6.88 (d, *J* = 8.5, 1H), 6.44 (d, *J* = 8.2, 1H), 5.53 (q, *J* = 7.0, 1H), 4.38 (br. s, 1H), 4.04 (d, *J* = 15.0, 1H), 3.93 (d, *J* = 15.0, 1H), 3.78 (br. s, 4H), 3.67 (s, 3H), 3.35–3.28 (m, 1H), 3.21 (q, *J* = 3.8, 1H), 3.08–3.00 (m, 1H), 2.90 (d, *J* = 4.8, 1H), 2.47 (dd, *J* = 13.6, 5.6, 1H), 2.06 (dt, *J* = 13.5, 3.7, 1H), 1.96 (dt, *J* = 13.3, 2.6, 1H), 1.52 (dd, *J* = 6.9, 1.8, 3H); ^{13}C

NMR (125 MHz, $CDCl_3$): 171.8, 159.8, 151.2, 148.1, 134.4, 134.0, 133.1, 131.5, 131.1, 129.5, 125.0, 124.4, 120.4, 108.9, 100.8, 68.5, 54.5, 54.2, 53.4, 52.0, 51.7, 48.5, 34.4, 31.2, 30.1, 12.7; IR (film): 3360, 2950, 2872, 1742, 1163 cm^{-1}; HRMS-APCI (*m/z*) $[M + H]^+$ calcd for $C_{26}H_{29}N_4O_8S^+$, 557.1701; found 557.1691; $[\alpha]^{25.9}_D$ –165.33° (c = 0.1, CH_2Cl_2).

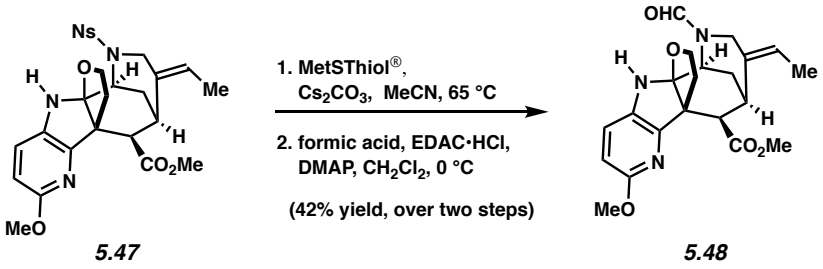

5.47 *5.48*

(–)-10-Methoxy-9-aza-aspidophylline A (5.48). To a 1-dram vial, a suspension of aza-furoindoline **5.47** (10.0 mg, 0.017 mmol, 1.0 equiv) and Cs_2CO_3 (18.0 mg, 0.0539 mmol, 3.2 equiv) in MeCN (1.0 mL, 0.02 M) was added MetSThiol® (58.0 mg, 0.0718 mmol, 4.2 equiv). The reaction vessel was placed in an aluminum block and heated to 65 °C. After stirring for 12 h, the reaction was cooled to 23 °C and filtered through a plug of celite (100 mg) and washed with 10 mL of MeCN. The filtrate was concentrated under reduced pressure to afford the corresponding secondary amine, which was used subsequently without further purification.

In a 20 mL scintillation vial, HCOOH (9.6 μL, 0.255 mmol, 15.0 equiv) was added to a solution of DMAP (44 mg, 0.358 mmol, 20.0 equiv) and EDAC•HCl (34 mg, 0.179 mmol, 10.0 equiv) in CH_2Cl_2 (3.8 mL, 0.005 M) at 0 °C. This mixture was stirred at 0 °C for 15 min, at which point a 400 μL aliquot of this stock solution was added to the crude denosylated product in a 1-dram vial equipped with a magnetic stir bar. The reaction mixture was cooled to 0 °C and stirred for 1.5 h. The reaction mixture was then quenched with saturated aqueous $NaHCO_3$ (2 mL). The layers were separated and the aqueous layer was extracted with CH_2Cl_2 (4 x 2 mL).

The organic layers were combined, dried over Na_2SO_4, and concentrated under reduced pressure. The crude mixture was purified via flash chromatography (1:1 Hexanes:EtOAc → 1:9 Hexanes:EtOAc) to afford (–)-10-methoxy-9-aza-aspidophylline A (**5.48**) as a colorless oil (3.0 mg, 42% yield). (–)-10-methoxy-9-aza-aspidophylline A (**5.48**) was observed as a 5:1 mixture of rotational isomers in $CDCl_3$. (–)-10-methoxy-9-aza-aspidophylline A (**5.48**) **(Major rotational isomer)**: R_f 0.27 (1:9 Hexanes:EtOAc); ^{1}H NMR (500 MHz, $CDCl_3$): δ 8.12 (s, 1H), 6.95 (d, *J* = 8.5, 1H), 6.49 (d, *J* = 8.5, 1H), 5.62 (q, *J* = 6.8, 1H), 4.38 (d, *J* = 18.0, 1H), 4.01–3.96 (m, 2H), 3.85 (t, *J* = 3.0, 1H), 3.80 (s, 3H), 3.70 (d, *J* = 3.2, 1H), 3.69 (s, 3H), 3.55–3.47 (m, 1H), 3.31 (q, *J* = 4.1, 1H), 2.95–2.86 (m, 1H), 2.82 (d, *J* = 4.8, 1H), 2.67 (dd, *J* = 13.6, 5.6, 1H), 2.10 (dt, *J* = 13.3, 2.7, 1H), 2.00 (dt, *J* = 13.5, 3.8, 1H), 1.54 (br. s, 3H); ^{13}C NMR (125 MHz, $CDCl_3$): 171.6, 164.3, 160.1, 151.6, 134.1, 129.1, 124.3, 121.4, 109.7, 101.2, 69.2, 54.3, 54.2, 53.5, 52.0, 51.8, 44.6, 33.2, 30.8, 30.4, 12.9; IR (film): 3318, 2927, 2862, 1744, 1421 cm^{-1}; HRMS-APCI (*m/z*) $[M + H]^+$ calcd for $C_{21}H_{26}N_3O_5^+$, 400.18670; found 400.18560; $[\alpha]^{28.5}_D$ –4.00° (c = 0.1, CH_2Cl_2).

5.8 Computational Section

5.8.1 Computational Details

Ab initio calculations were performed with Gaussion 09.[20] Geometries were optimized and their vibrational frequencies obtained at the MP2/6-31G(d) level of theory, with the SMD solvation model for water.[21] MP2 energies were corrected using the "spin-component-scaled" (SCS) approach, pioneered by Grimme,[22] such as E(SCS-MP2) = E(SCF) + 1.2*(αβ) + (1/3)*(αα+ββ) where αα, ββ, and αβ are the "alpha-alpha", "beta-beta" and "alpha-beta" spin contributions, respectively, found in the Gaussian output. In the case of closed-shell calculations such as those used in the current study, αα and ββ are identical. This SCS- MP2 correction was

found to greatly improve the performance of MP2 calculations, notably for sigmatropic rearrangements.[23] This SCS-MP2/6-31G(d)/SMD(water)//MP2/6-31G(d)/SMD(water) method was also chosen as we have previously shown that it accurately reproduces experimental rates of Fischer indolization reactions.[24] Normal mode frequency analysis was used to confirm that stationary points were either minima (no imaginary frequency) or saddle-points (TS, one (1) imaginary frequency) on the potential energy surface. All saddle-points were further analyzed with the Intrinsic Reaction Coordinate (IRC) tools to verify that they connected the expected minima. ZPE, enthalpy and free energy corrections were obtained using a standard state of 1 atmosphere of pressure and 298 K. Free energies were computed using Truhlar's quasiharmonic oscillator approximation, setting all frequencies below 100 cm^{-1} to 100 cm^{-1}.[25] The free energies reported in this study are thus obtained by adding the quasiharmonic free energy corrections to the SCS-MP2 electronic energies. Reported structures are the result of extensive conformation sampling on all evaluated compounds. Structures were illustrated using CYLview.[26] To obtain atomic charges, natural bond orbital (NBO) analysis (pop=nbo keyword in Gaussian 09) was performed at the MP2/6-311+G(d,p) level (gas phase) on the MP2/6-31G(d)/SMD(water)-optimized structures.

5.8.2 Additional Schemes and Discussion

To study the effects of protonation and substituents on the barriers of the [3,3]-sigmatropic rearrangement typical of Fischer indolization reactions, we chose a model system based on the combination of aryl/pyridyl hydrazines with propanal **5.67**. We have previously shown that in the case of aryl hydrazines, the [3,3]-sigmatropic rearrangement is the rate-limiting step of the reaction and occurs with the substrates being monoprotonated.[24]

Scheme 5.1 Thermal (unprotonated) Fischer indolization reaction of model system.

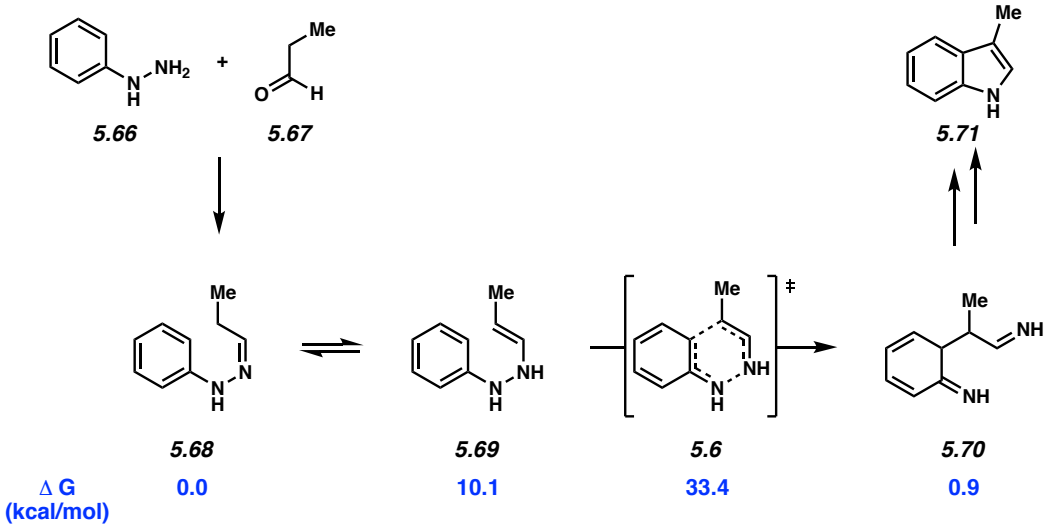

In the thermal Fischer indolization reaction (Scheme 5.1), hydrazone **5.68** (formed from the condensation of aryl hydrazine **5.66** with propanal (**5.67**) first tautomerizes to ene- hydrazine **5.69**, which can then undergo a [3,3]-sigmatropic rearrangement to form diimine **5.70**. This intermediate then rearomatizes and goes on to form the indole product **5.71**. When all compounds are neutral, reaching **5.6** from the hydrazone costs 33.4 kcal/mol. This barrier is much higher than what is known experimentally for such reactions.[24]

In the acid-catalyzed (monoprotonated) reaction (Scheme 5.2), two pathways are available to the substrates. The hydrazone with its α nitrogen protonated, **5.72**, is the global minimum of the system, but **5.7** has the smallest barrier for the rearrangement. In this case, the activation free energy of the reaction is then 23.8 kcal/mol, which is in agreement with experimental rates.[24]

Scheme 5.2 Acid-catalyzed (monoprotonated) Fischer indolization reaction of model system.

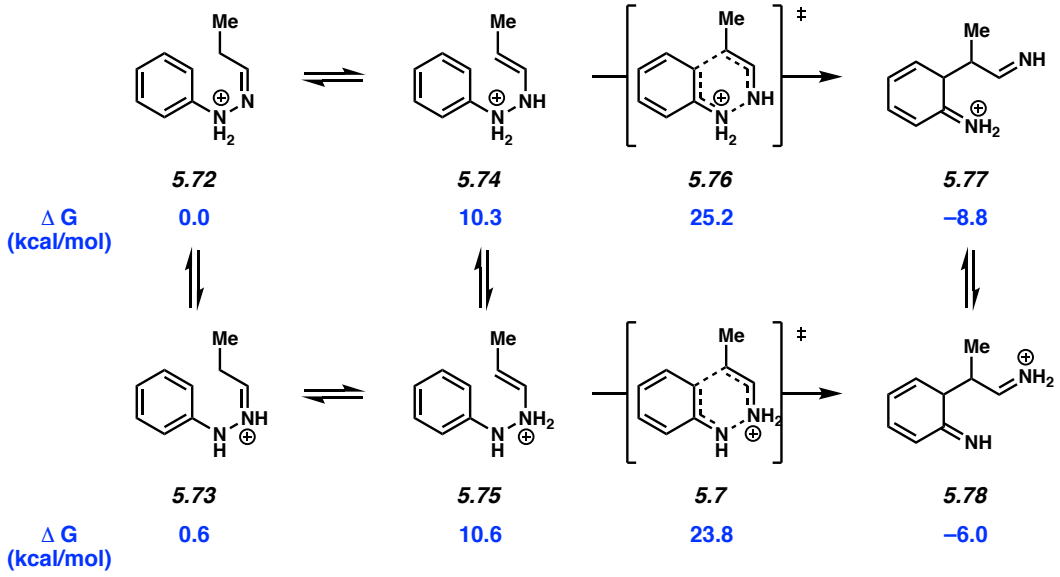

Therefore, all other systems that we studied were singly protonated. For all pyridyl hydrazines, three different nitrogen atoms can be protonated on any intermediate or transition state. Moreover, in most cases the [3,3]-sigmatropic rearrangement can occur on two different carbons, meaning two transition states and two diimine products are possible for each protonation state. The full pathway for the parent pyridyl hydrazine is presented below in Scheme 5.3.

The free energy for the pathway of α-methylpyridine hydrazone is found in Scheme 5.4. Once again, the hydrazone protonated at the pyridine nitrogen is the global minimum of the system, and because of the increased basicity of the methyl-substituted ene-hydrazine α nitrogen, the best transition state goes through with protonation of the α-nitrogen.

Scheme 5.3 Reaction pathway for protonated 3-pyridylhydrazine. Free energies in kcal/mol.

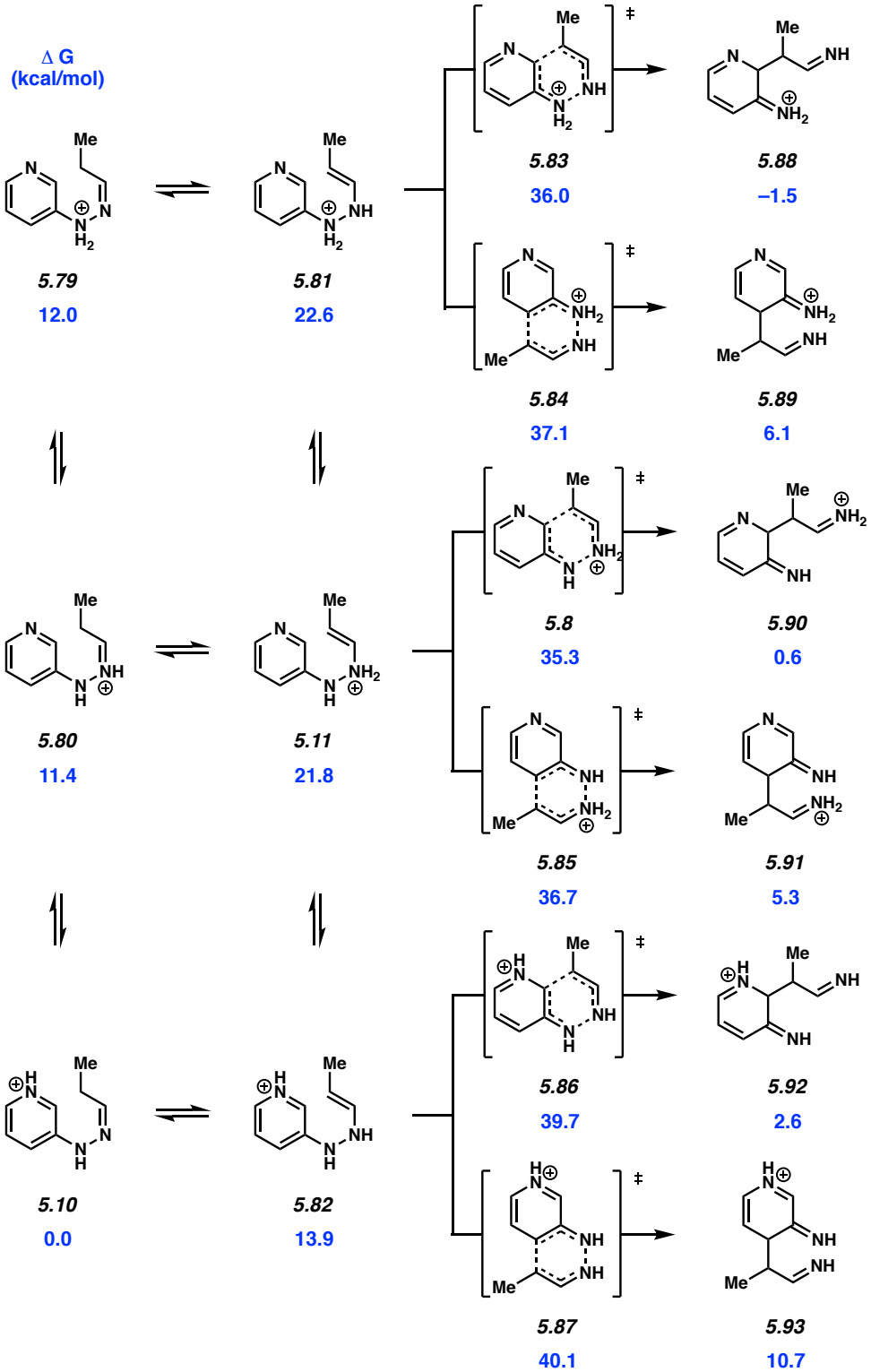

Scheme 5.4 Reaction pathway for 3-(1-methylhydrazinyl)pyridine. Free energies in kcal/mol.

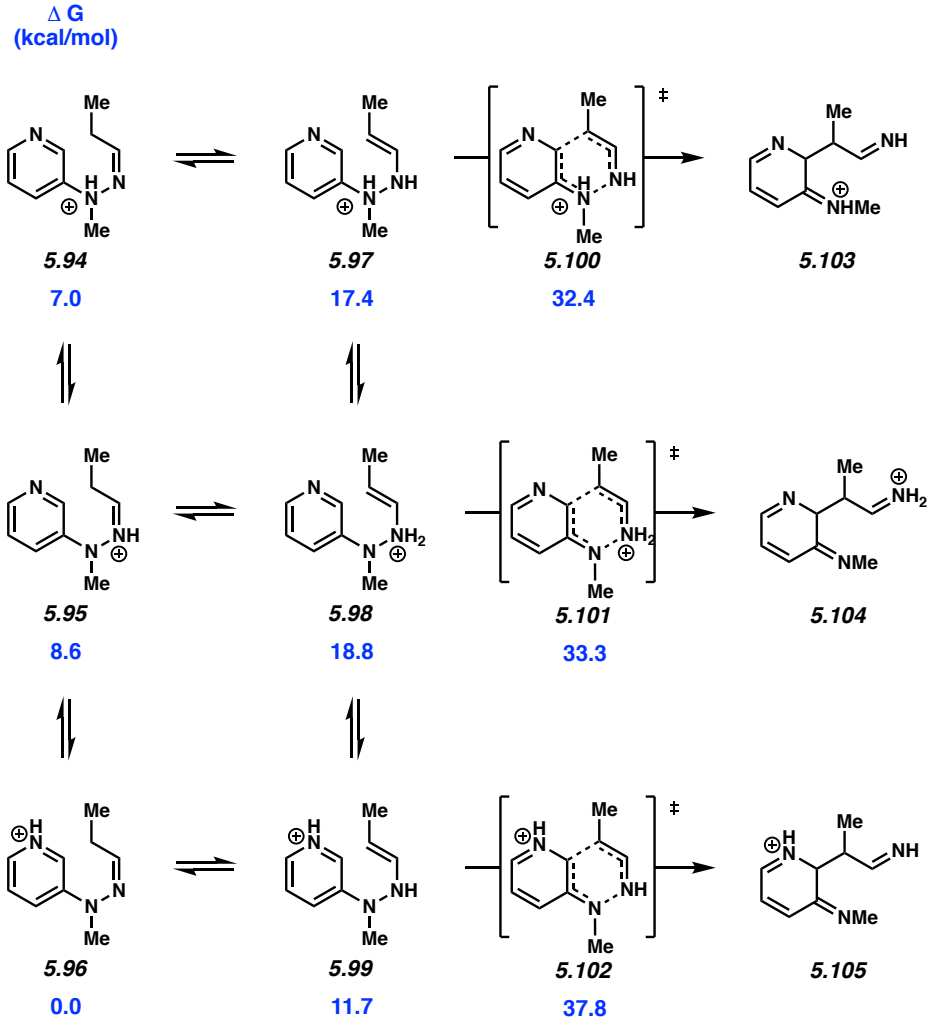

Relative free energies for all other computed systems can be found in Table 5.3. In all cases the global minimum is the hydrazone protonated at the pyridine nitrogen. Moreover, in all but one case, the most favored transition state goes through protonation at the β-nitrogen of the hydrazone.

Table 5.3 Relative free energies (kcal/mol) for each intermediate or transition state on the potential energy pathways of different monoprotonated pyridyl hydrazones formed by pyridyl hydrazines and propanal.

	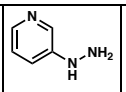		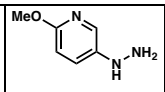		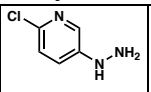		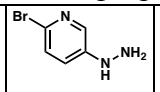		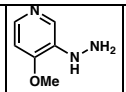		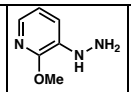		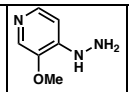		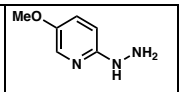	
	cmpd #	ΔG	cmpd #	ΔG	cmpd #	ΔG	cmpd #	ΔG	cmpd #	ΔG	cmpd #	ΔG	cmpd #	ΔG	cmpd #	ΔG
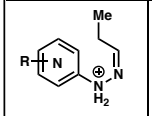	***5.79***	12.0	***5.106***	6.5	***5.123***	4.8	***5.141***	4.5	***5.159***	13.0	***5.171***	4.2	***5.183***	17.4	***5.195***	10.2
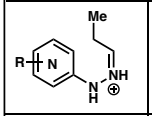	***5.80***	11.4	***5.107***	5.7	***5.124***	2.9	***5.142***	2.1	***5.160***	12.0	***5.172***	3.4	***5.184***	15.4	***5.196***	8.6
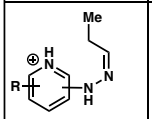	***5.10***	0.0	***5.108***	0.0	***5.125***	0.0	***5.143***	0.0	***5.161***	0.0	***5.173***	0.0	***5.185***	0.0	***5.197***	0.0
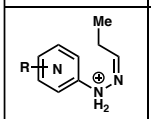	***5.81***	22.6	***5.109***	16.5	***5.126***	15.4	***5.144***	14.8	***5.162***	23.1	***5.174***	15.8	***5.186***	28.2	***5.198***	21.8
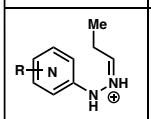	***5.11***	21.8	***5.110***	14.9	***5.127***	12.5	***5.145***	12.1	***5.163***	20.1	***5.175***	11.5	***5.187***	23.7	***5.199***	18.8
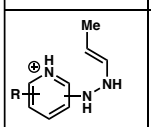	***5.82***	13.9	***5.111***	13.9	***5.128***	14.3	***5.146***	14.2	***5.164***	14.6	***5.176***	12.8	***5.188***	15.3	***5.200***	13.3
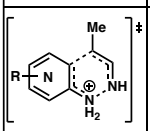	***5.83***	36.0	***5.112***	27.8	***5.129***	28.6	***5.147***	27.9	***5.165***	35.5	***5.177***	25.6	***5.189***	42.0	***5.201***	35.2
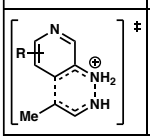	***5.84***	37.1	***5.113***	32.4	***5.130***	30.5	***5.148***	29.7	–	–	–	–	–	–	–	–
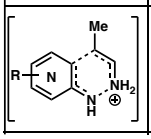	***5.8***	35.3	***5.9***	26.3	***5.131***	27.6	***5.149***	26.8	***5.166***	34.5	***5.178***	34.5	***5.190***	40.3	***5.202***	32.2

Table 5.3 Continued

	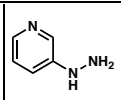		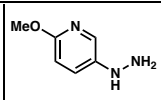		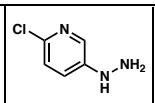		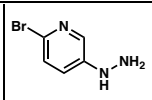		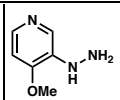		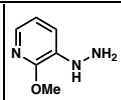		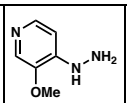		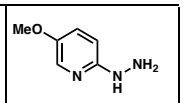	
	cmpd #	**ΔG**	**cmpd #**	**ΔG**	**cmpd #**	**ΔG**	**cmpd #**	**ΔG**	**cmpd #**	**ΔG**	**cmpd #**	**ΔG**	**cmpd #**	**ΔG**	**cmpd #**	**ΔG**
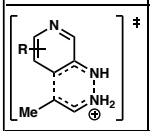	***5.85***	36.7	***5.114***	31.2	***5.132***	29.1	***5.150***	28.4	–	–	–	–	–	–	–	–
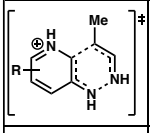	***5.86***	39.7	***5.115***	35.9	***5.133***	39.6	***5.151***	40.0	***5.167***	37.7	***5.179***	35.3	***5.191***	45.0	***5.203***	41.7
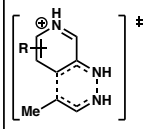	***5.87***	40.1	***5.116***	40.0	***5.134***	40.5	***5.152***	40.5	–	–	–	–	–	–	–	–
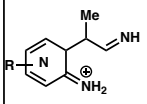	***5.88***	–1.5	***5.117***	–10.2	***5.135***	–8.8	***5.153***	–9.3	***5.168***	–0.1	***5.180***	–4.3	***5.192***	5.5	***5.204***	0.7
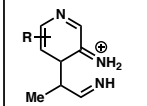	***5.89***	6.1	***5.118***	8.3	***5.136***	0.6	***5.154***	–0.4	–	–	–	–	–	–	–	–
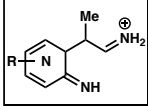	***5.90***	0.6	***5.119***	–9.2	***5.137***	–8.7	***5.155***	–9.3	***5.169***	0.5	***5.181***	–5.9	***5.193***	7.0	***5.205***	1.4
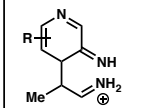	***5.91***	5.3	***5.120***	2.7	***5.138***	–1.6	***5.156***	–2.5	–	–	–	–	–	–	–	–
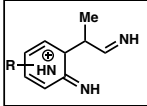	***5.92***	2.6	***5.121***	–6.7	***5.139***	1.8	***5.157***	2.6	***5.170***	0.0	***5.182***	0.7	***5.194***	11.3	***5.206***	10.0
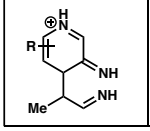	***5.93***	10.7	***5.122***	–4.3	***5.140***	–7.3	***5.158***	–8.6	–	–	–	–	–	–	–	–

5.8.3 Origin of Regioselectivity

Fischer indolization reactions with aza-substituted substrates are regioselective. The calculations support these results. In the case of the 2-methoxy-5-hydrazinylpyridine, the [3,3]-

sigmatropic rearrangement at the 6-position is favored by 4.9 kcal/mol over the rearrangement at the 4-position of the pyridine ring.

The [3,3]-sigmatropic rearrangements are, for all but one aza-substituted system, favored by protonation at the β nitrogen. In the only case where the α-protonated TS is favored, it is only 0.2 kcal/mol lower than the β-protonated TS. We propose the following explanation for the regioselectivity (Scheme 5.5). In the transition state, N–N bond cleavage creates two "pieces" of the substrate: a neutral enamine piece and a cationic aromatic ring. This ring is attacked at either the carbon alpha or gamma from the pyridine nitrogen.

Scheme 5.5 [3,3]-sigmatropic rearrangement with protonated β-nitrogen of ene-hydrazine.

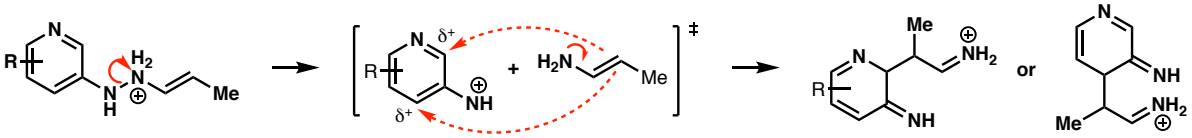

5.207 *5.208* *5.209* *5.210* *5.211*

The preference for attack at either position can be predicted from the extent of positive charge on these carbons, before or at the transition state. Using NBO analysis, the charge at these carbons for the aza-substituted substrate and those with a substituent at the 2-position were calculated. The same charges for the two transition states leading to regioisomeric products were also calculated. These data are listed below in Table 5.4.

Table 5.4 Relative free energies (kcal/mol, from their respective global minima) and NBO charges of the β-protonated ene-hydrazine and transition states, for the various 2- substituted 5-pyridylhydrazines.

		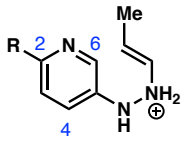			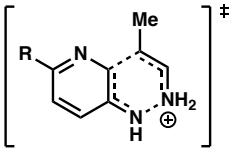			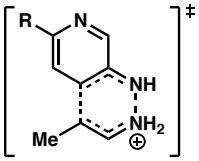		
entry	**R**	**ΔG**	**z (C4)**	**z (C6)**	**ΔG**	**z (C4)**	**z (C6)**	**ΔG**	**z (C4)**	**z (C6)**
1	H	21.8	–0.132	0.108	35.3	–0.082	0.164	36.7	–0.061	0.182
2	OMe	14.9	–0.110	0.146	26.3	–0.075	0.212	31.2	–0.021	0.225
3	Cl	12.5	–0.127	0.123	27.6	–0.072	0.178	29.1	–0.051	0.207
4	Br	12.1	–0.132	0.117	26.8	–0.073	0.177	28.4	–0.053	0.205

For the unsubstituted case (entry 1), the positive charge at C6 is much greater than that of C4, both in the ene-hydrazine and in the transition states. Even more important is that this difference is very similar in both transition states, even though they lead to different products. The greater positive charge at C6 is presumably caused by the proximity of the pyridine nitrogen, which acts as an electronegative element.

For the methoxy-substituted substrate (entry 2), the difference between the partial positive charge at the C6 and C4 positions is even greater. Thus, the regioselectivity would be predicted to be higher, which is what the calculated activation barriers predict. The increased difference is attributed to the methoxy substituent at the 2-position. Indeed, this group is located at the meta position of both C4 and C6 and provides a strong electron-withdrawing effect. For C6, both the pyridine nitrogen and 2-methoxy combine to make attack at this position much easier than at C4.

For the halogenated substrates (entries 3 and 4), the same explanation is true. The electronegative substituents make the charge at C6 more positive, in line with these substrates being slightly more regioselective than the unsubstituted case. Once again, the extent of positive

charge do not vary significantly if the TS happens at C4 or C6, and are very similar to that observed in the ene-hydrazine intermediate.

Therefore, for these Fischer indolization reactions with aza-substituted compounds, analysis of the charges on the reactant are a good way to determine which will be the most favored regiosiomer formed during the [3,3]-sigmatropic rearrangement.

5.8.4 Cartesian Coordinates for Reactants and Transition States

Cartesian coordinates for the optimized structures were reported in the literature.[27]

5.9 Spectra Relevant to Chapter Five:

Understanding and Interrupting the Fischer Azaindolization Reaction

Bryan J. Simmons, Marie Hoffmann, Pier Alexandre Champagne, Elias Picazo, Katsuya Yamakawa, Lucas A. Morrill, K. N. Houk, and Neil K. Garg.

J. Am. Chem. Soc. **2017**, *139*, 14833–14836.

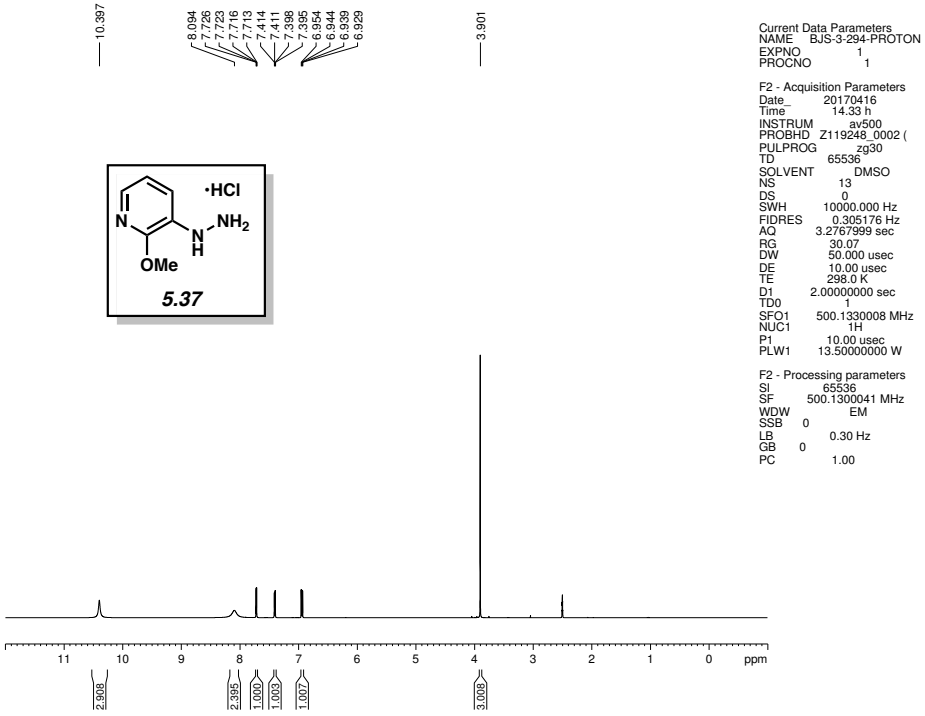

Figure 5.5 ^{1}H NMR (500 MHz, DMSO-d_6) of compound **5.37**.

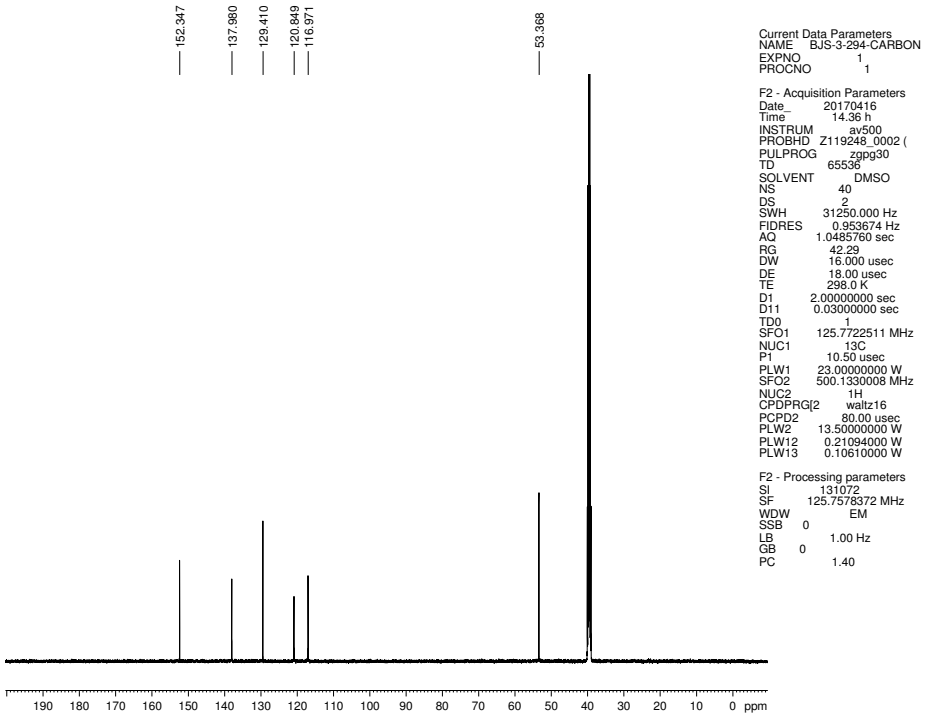

Figure 5.6 ^{13}C NMR (125 MHz, DMSO-d_6) of compound **5.37**.

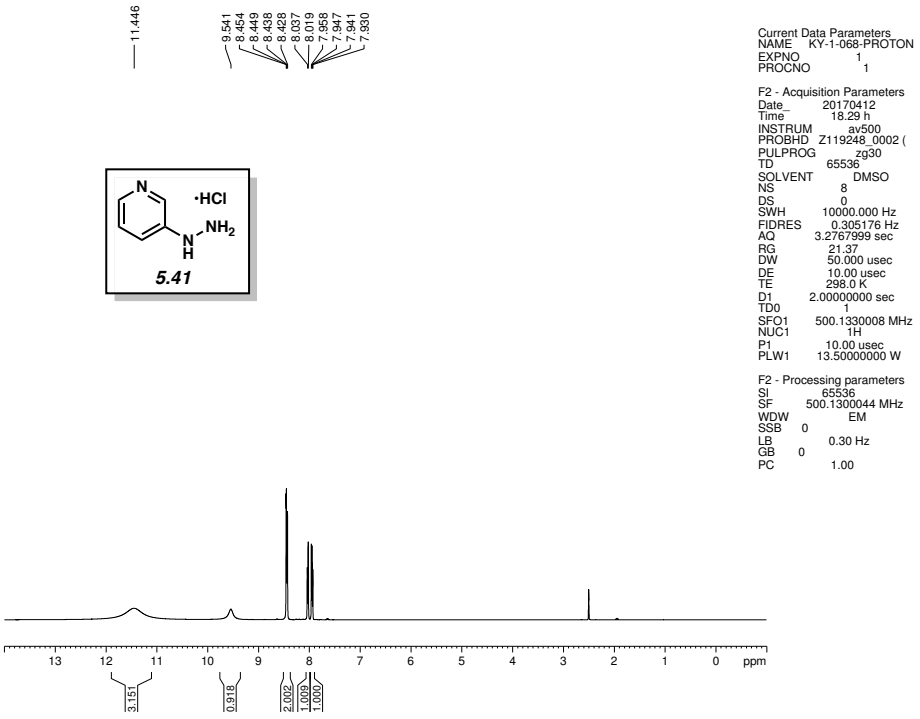

Figure 5.7 ^{1}H NMR (500 MHz, DMSO-d_6) of compound **5.41**.

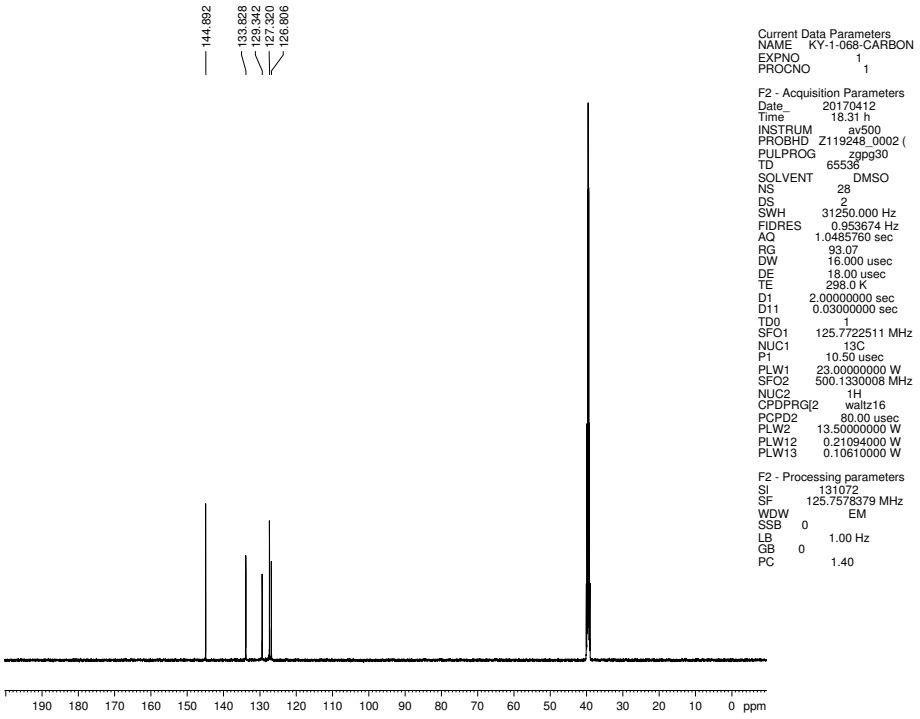

Figure 5.8 ^{13}C NMR (125 MHz, DMSO-d_6) of compound **5.41**.

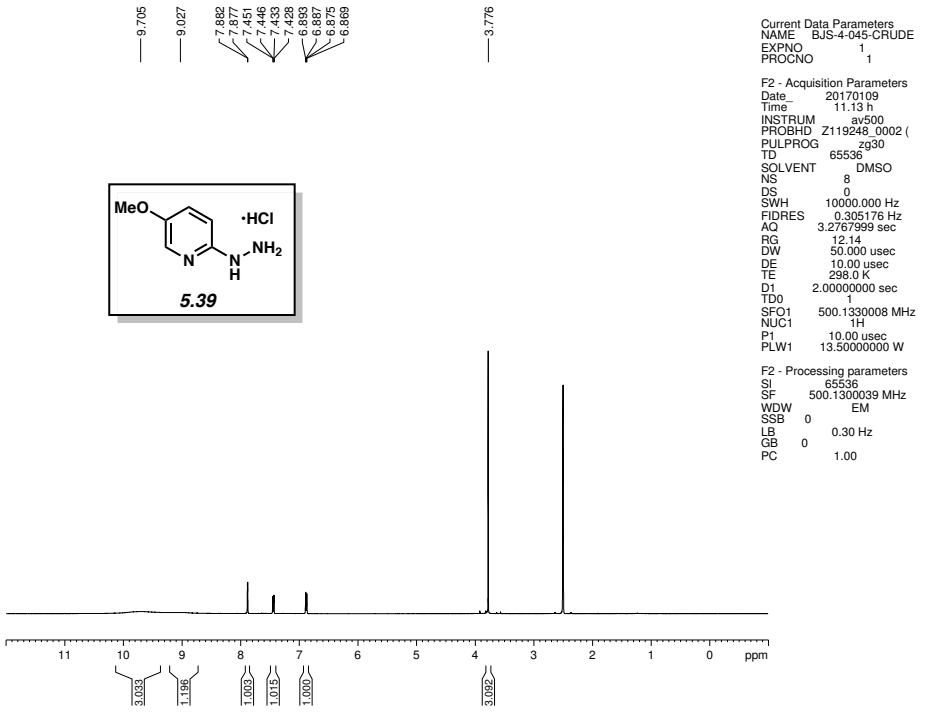

Figure 5.9 ^{1}H NMR (500 MHz, DMSO-d_6) of compound **5.39**.

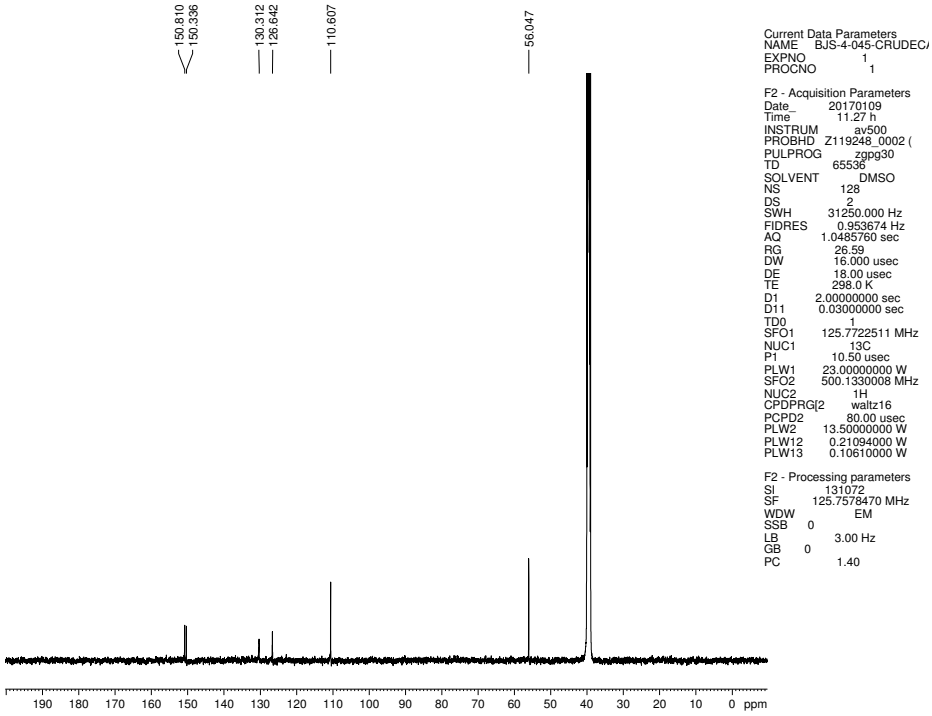

Figure 5.10 ^{13}C NMR (125 MHz, DMSO-d_6) of compound **5.39**

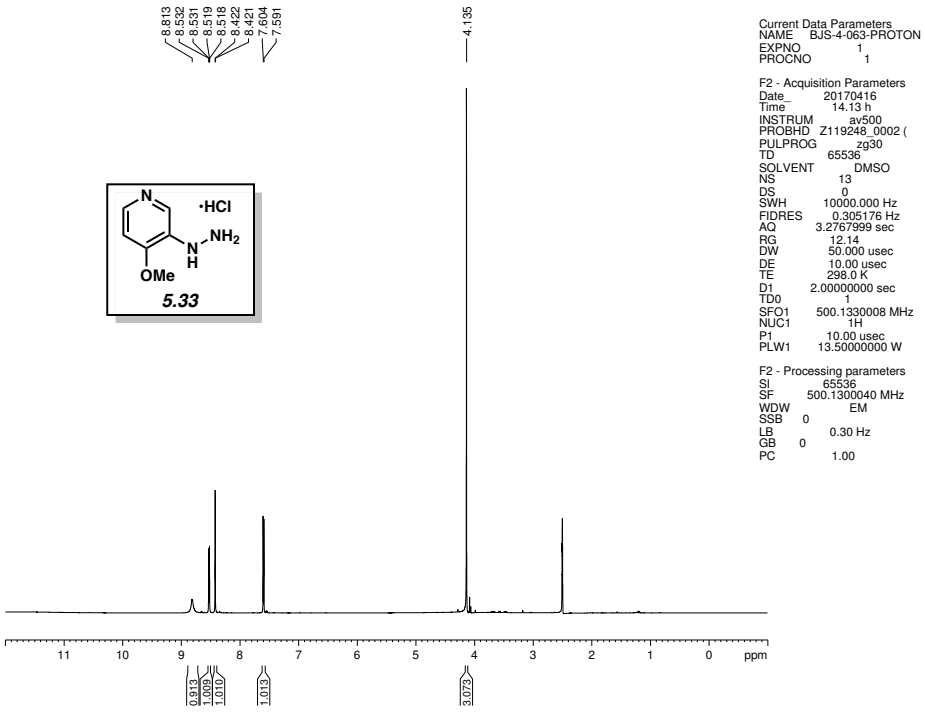

Figure 5.11 ^{1}H NMR (500 MHz, DMSO-d_6) of compound **5.33**.

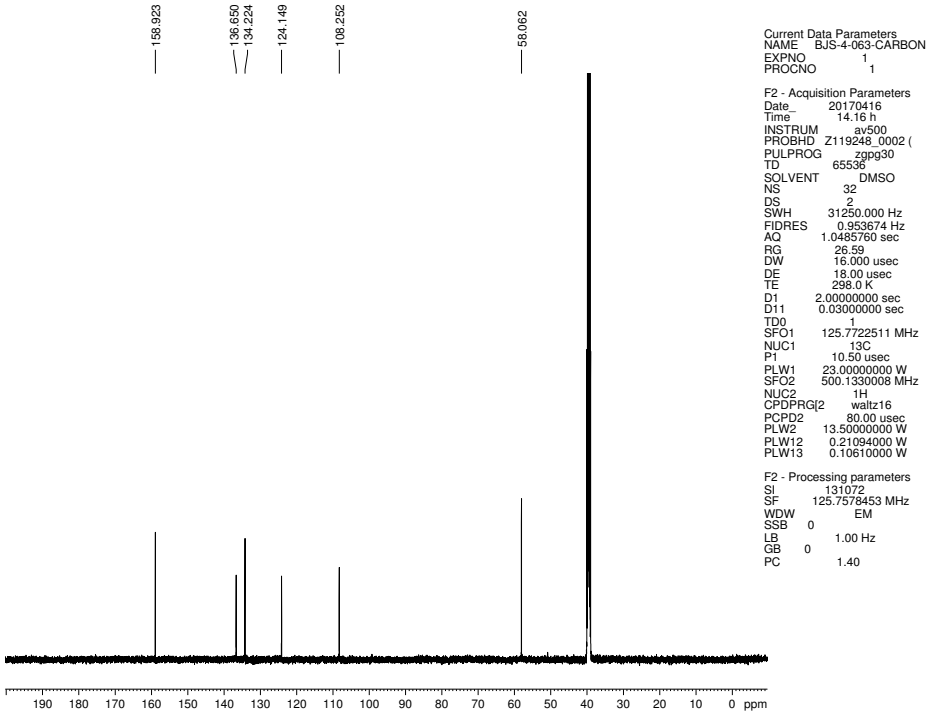

Figure 5.12 ^{13}C NMR (125 MHz, DMSO-d_6) of compound **5.33**.

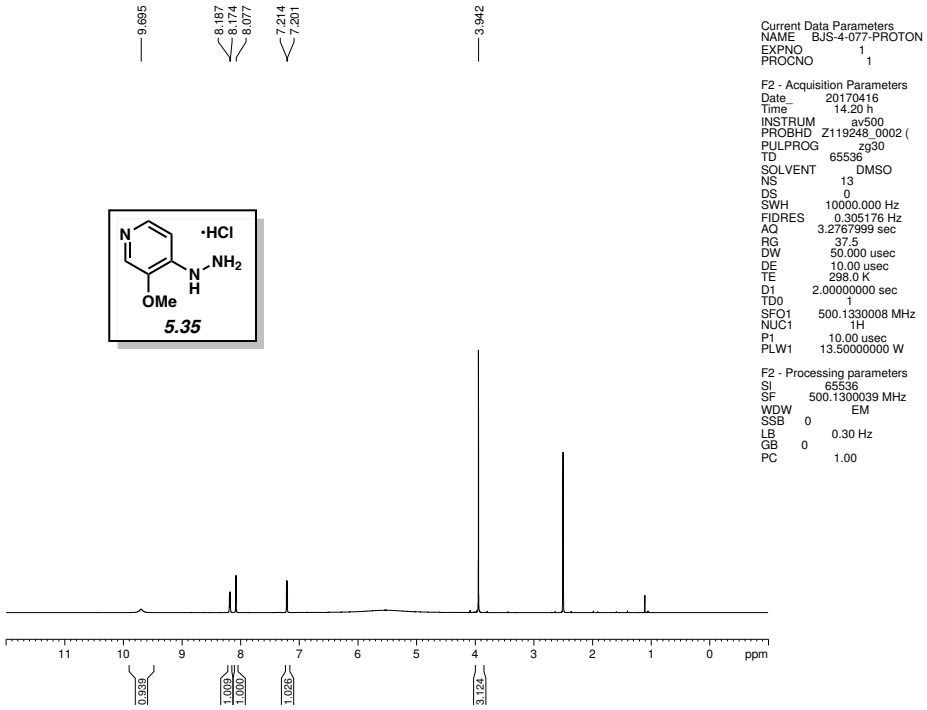

Figure 5.13 ^{1}H NMR (500 MHz, DMSO-d_6) of compound **5.35**.

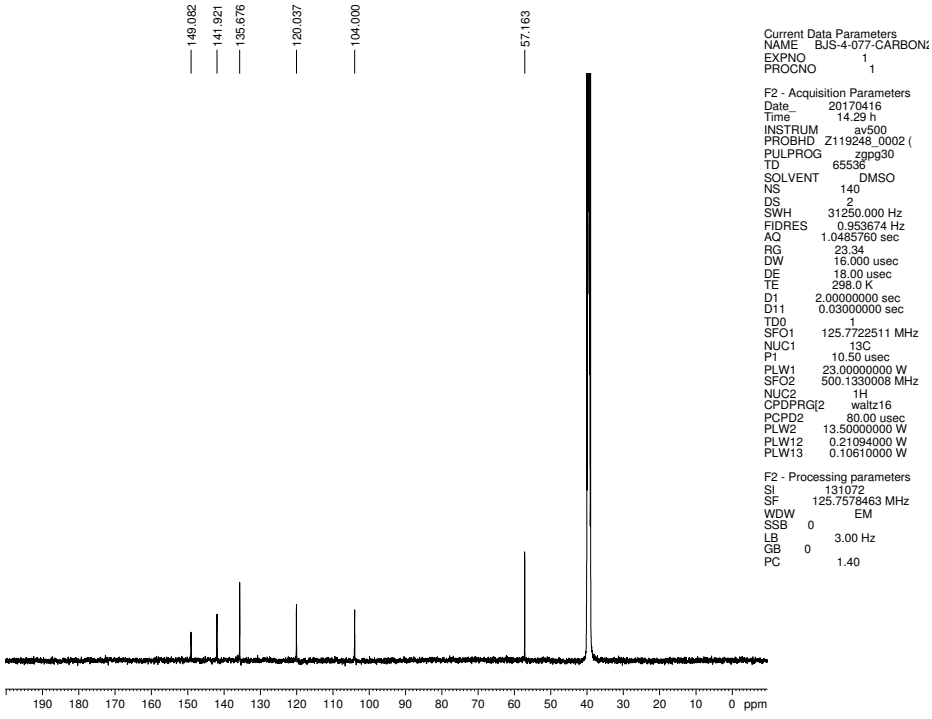

Figure 5.14 ^{13}C NMR (125 MHz, DMSO-d_6) of compound **5.35**.

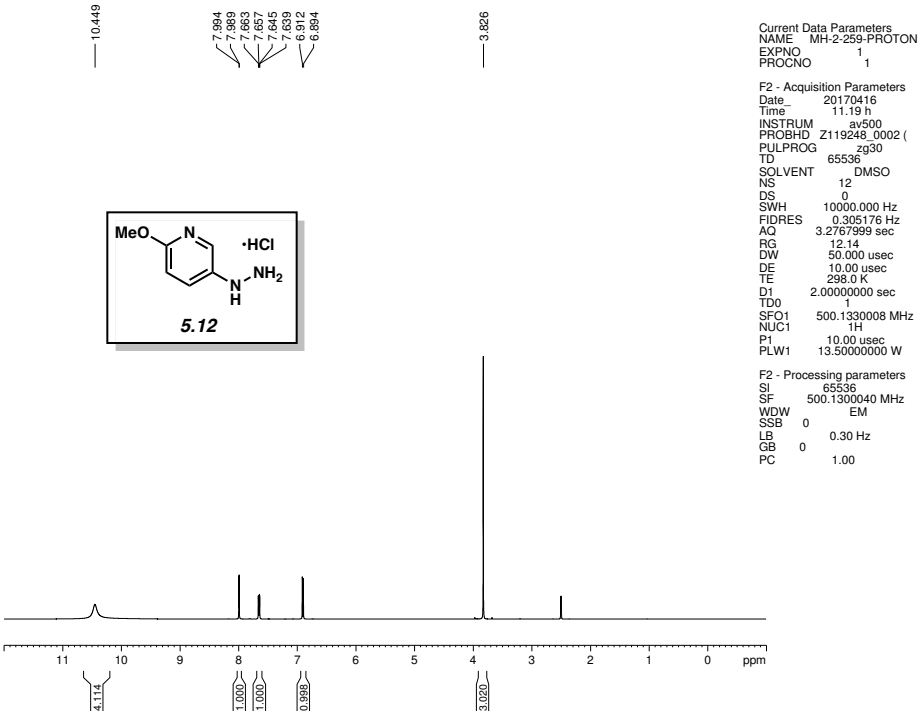

Figure 5.15 ^{1}H NMR (500 MHz, DMSO-d_6) of compound **5.12**.

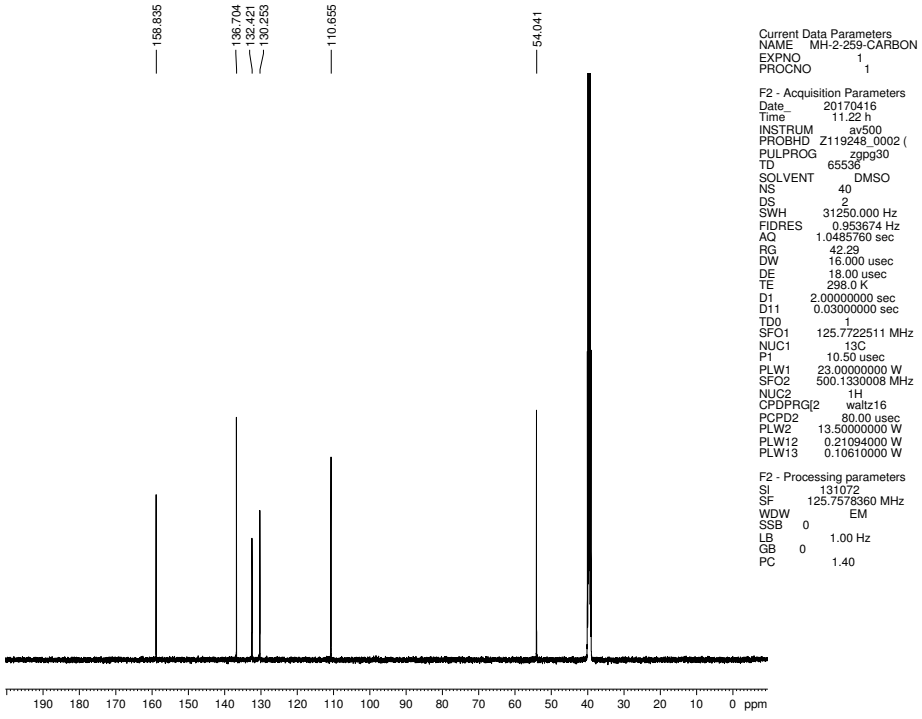

Figure 5.16 ^{13}C NMR (125 MHz, DMSO-d_6) of compound **5.12**.

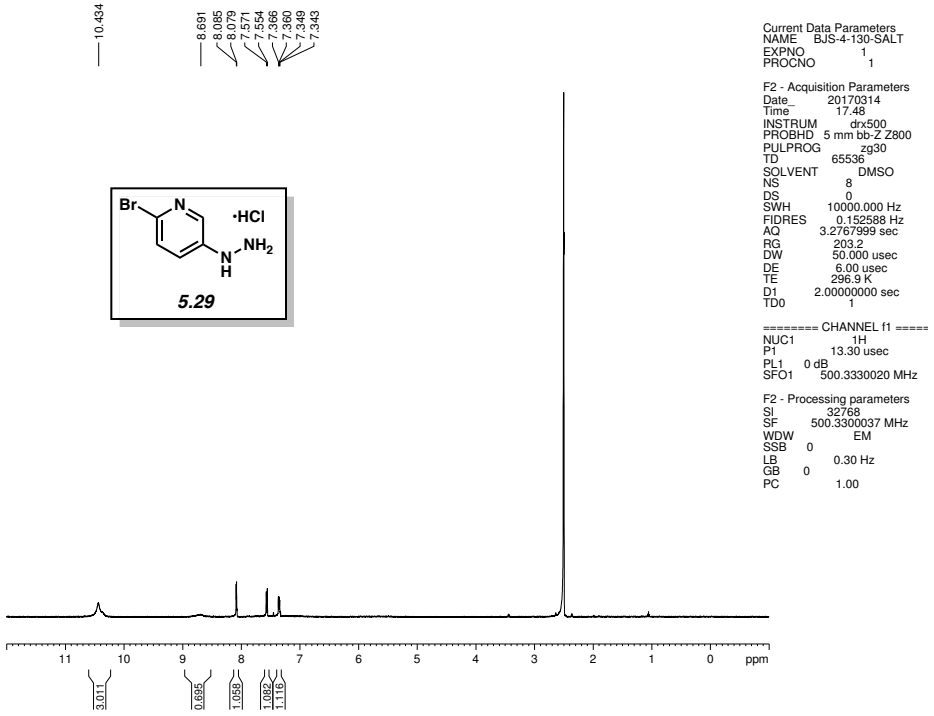

Figure 5.17 ^{1}H NMR (500 MHz, DMSO-d_6) of compound **5.29**.

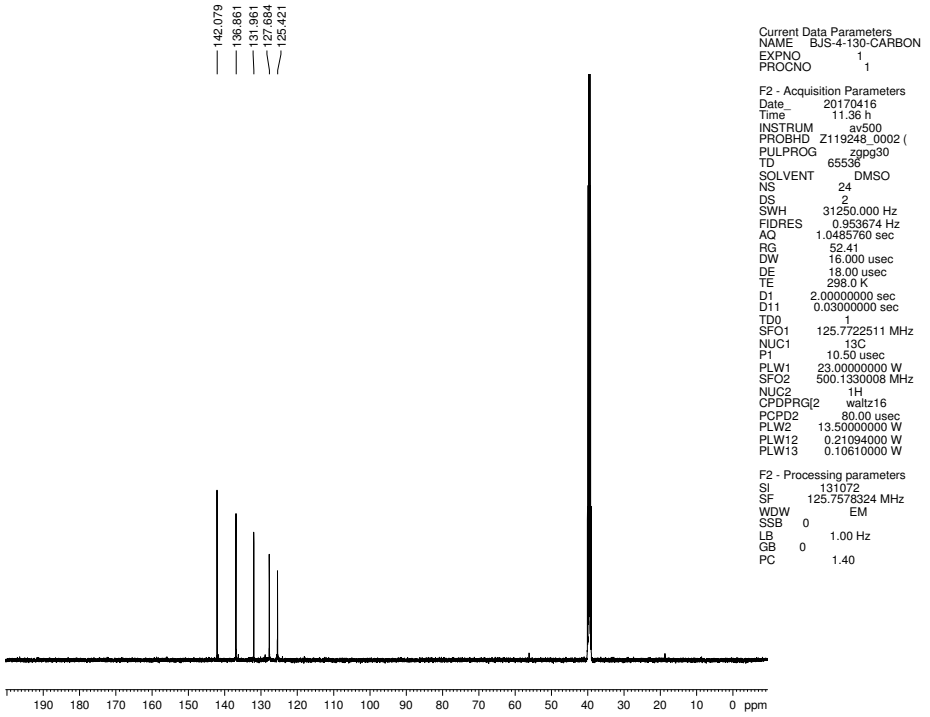

Figure 5.18 ^{13}C NMR (125 MHz, DMSO-d_6) of compound **5.29**.

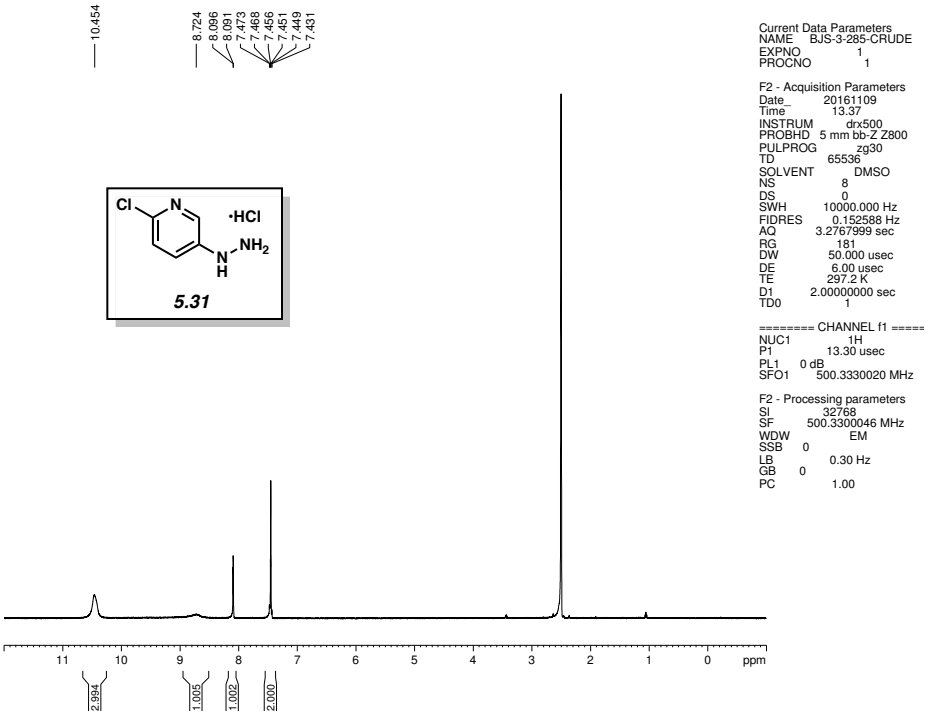

Figure 5.19 ^{1}H NMR (500 MHz, DMSO-d_6) of compound **5.31**.

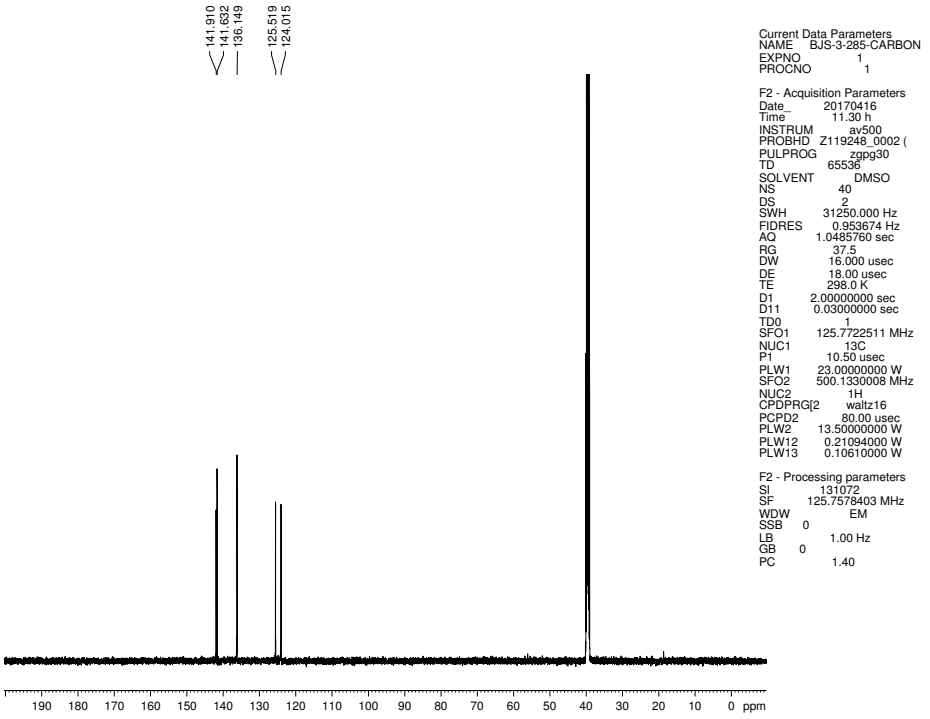

Figure 5.20 ^{13}C NMR (125 MHz, DMSO-d_6) of compound **5.31**.

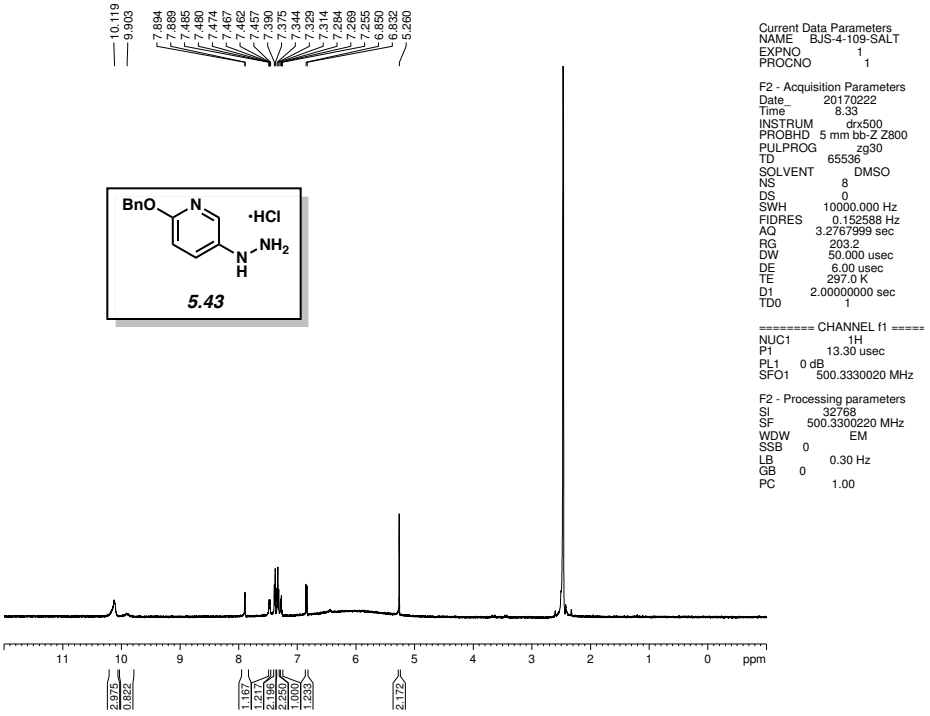

Figure 5.21 ^{1}H NMR (500 MHz, DMSO-d_6) of compound **5.43**.

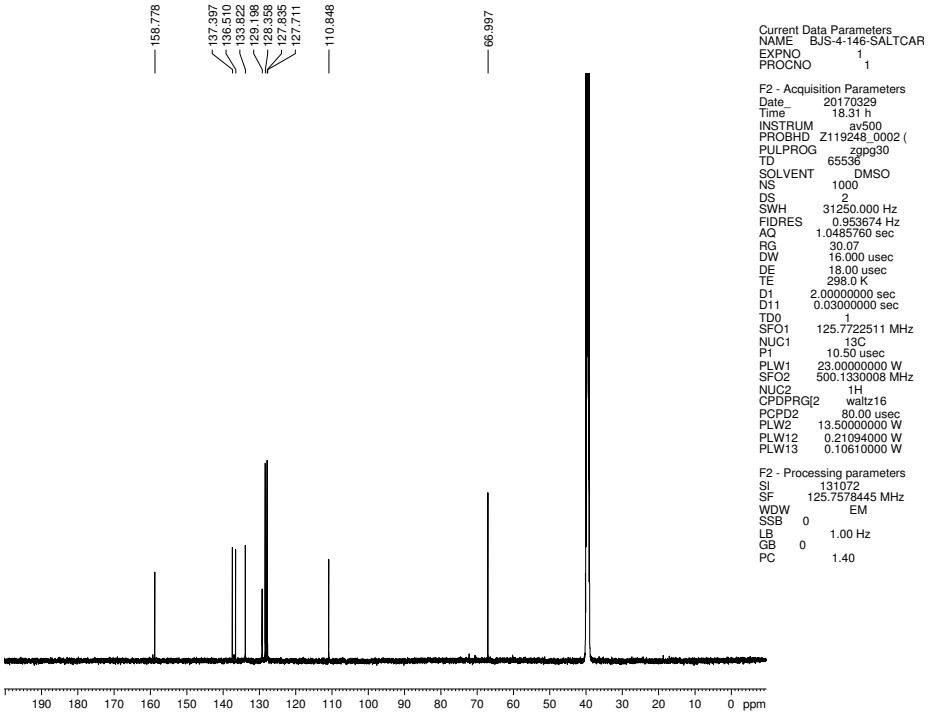

Figure 5.22 ^{13}C NMR (125 MHz, DMSO-d_6) of compound **5.43**.

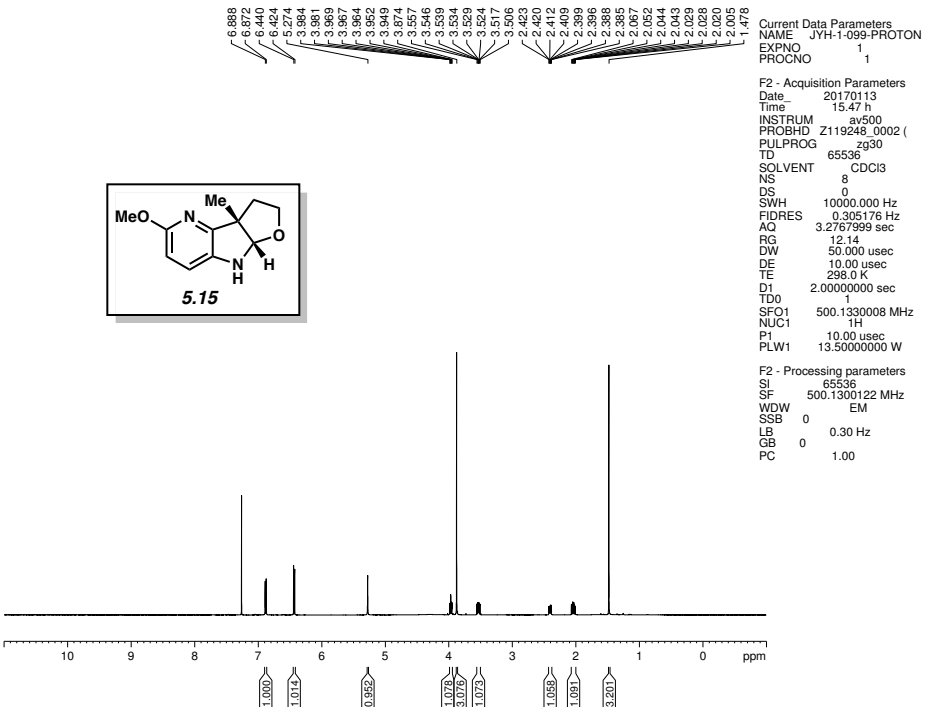

Figure 5.23 ^{1}H NMR (500 MHz, $CDCl_3$) of compound **5.15**.

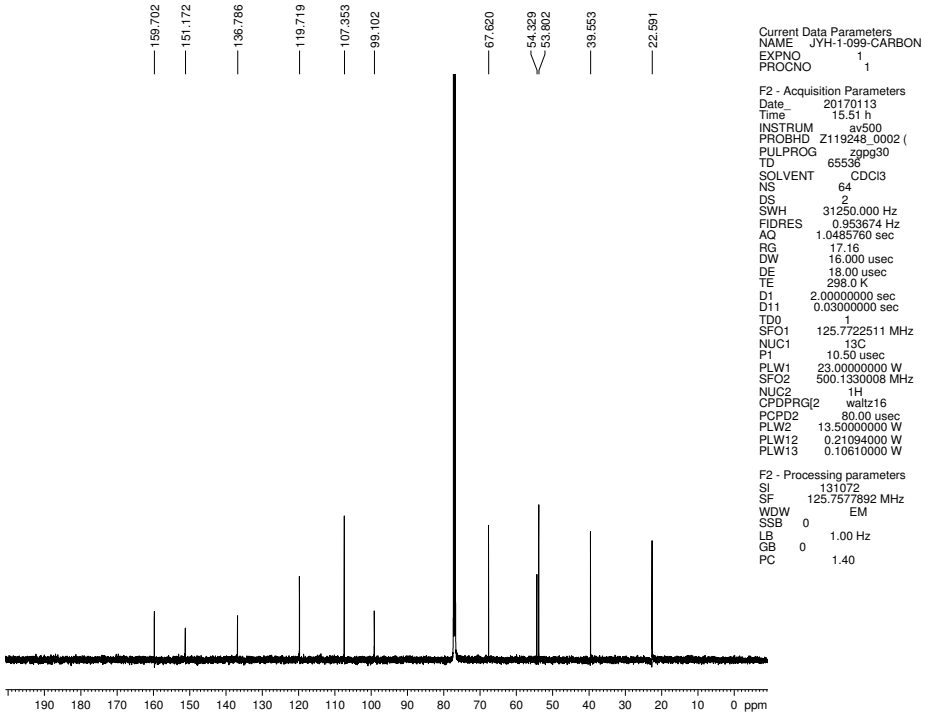

Figure 5.24 ^{13}C NMR (125 MHz, $CDCl_3$) of compound **5.15**.

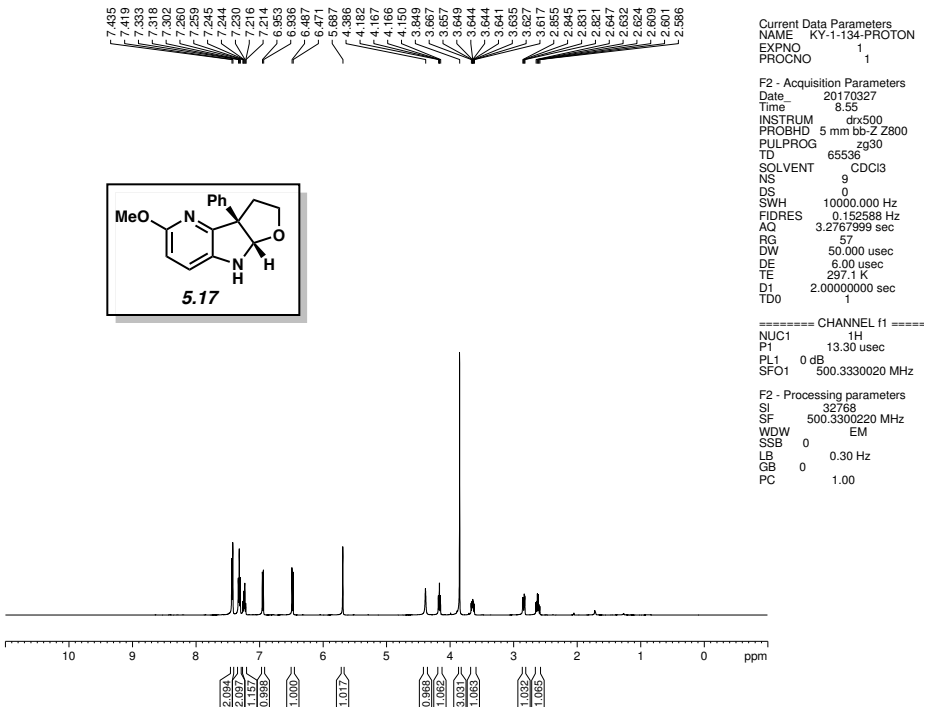

Figure 5.25 ^{1}H NMR (500 MHz, $CDCl_3$) of compound **5.17**.

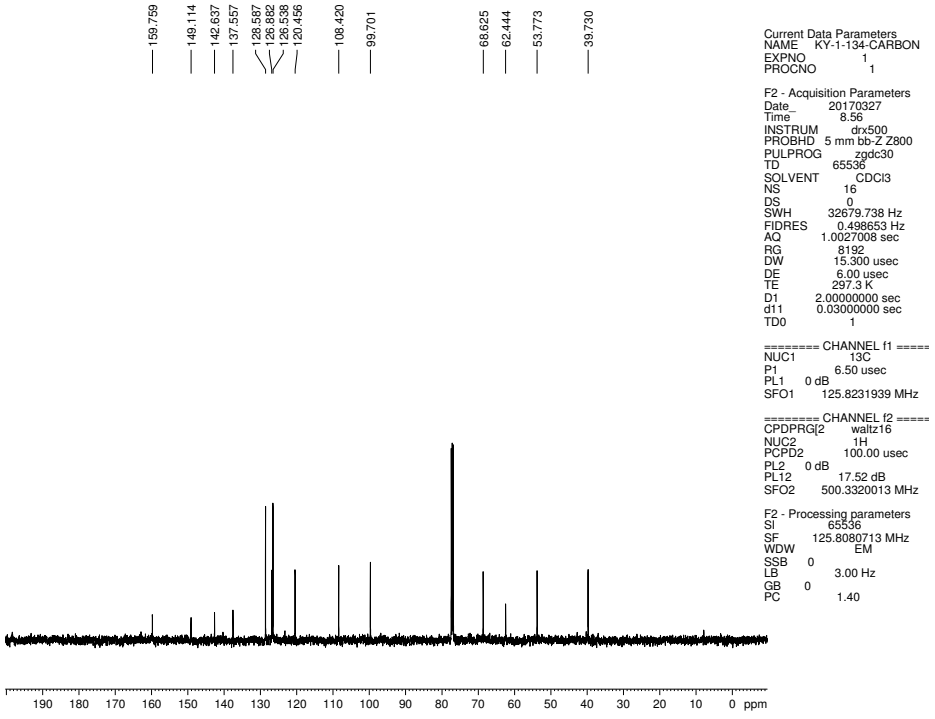

Figure 5.26 ^{13}C NMR (125 MHz, $CDCl_3$) of compound **5.17**.

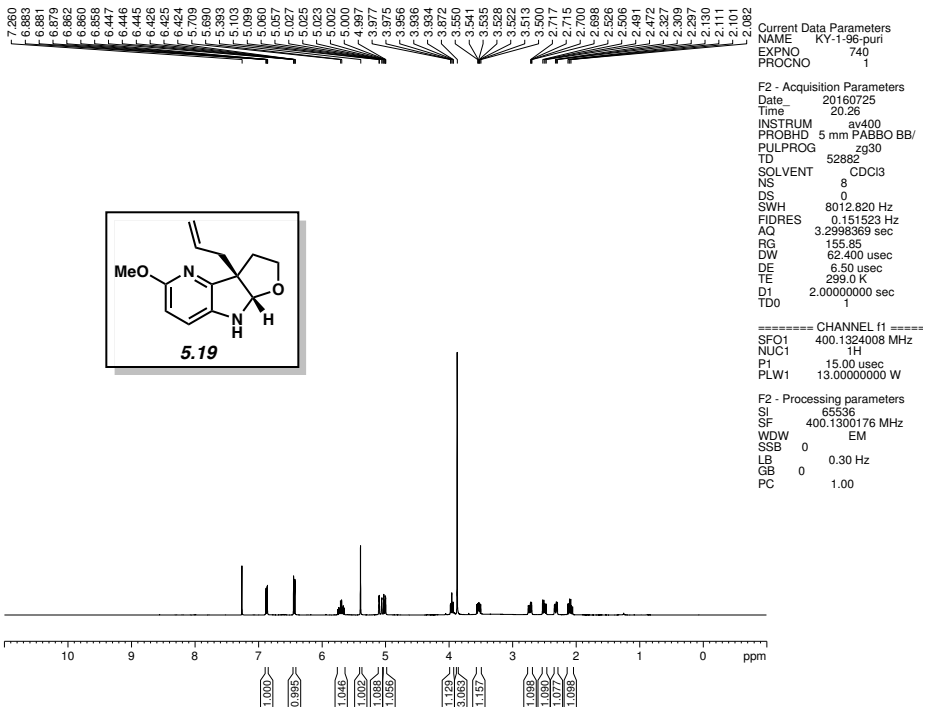

Figure 5.27 ^{1}H NMR (500 MHz, $CDCl_3$) of compound **5.19**.

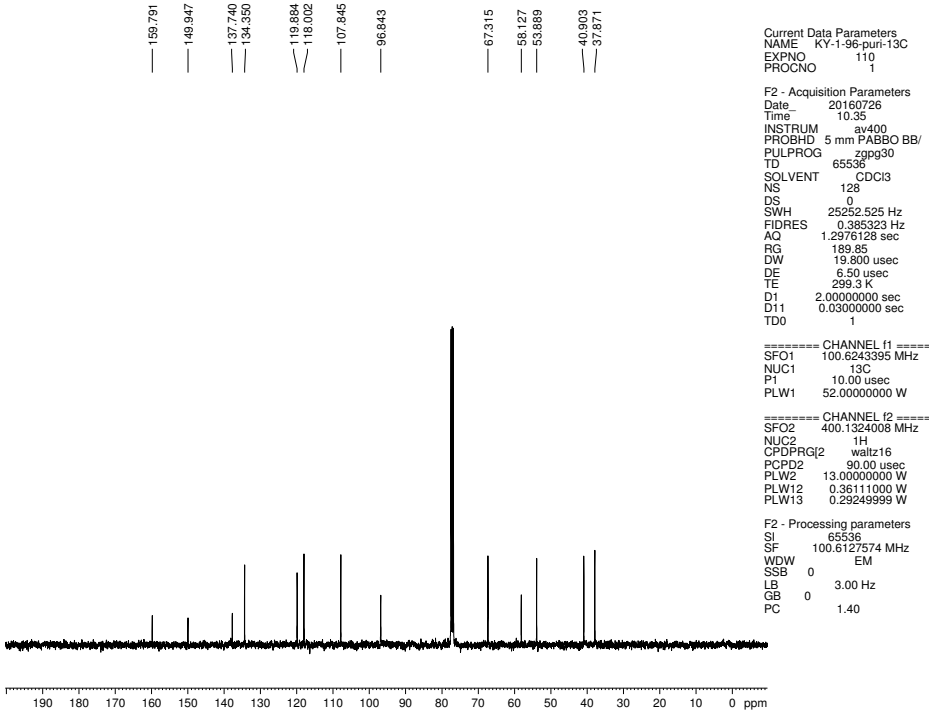

Figure 5.28 ^{13}C NMR (125 MHz, $CDCl_3$) of compound **5.19**.

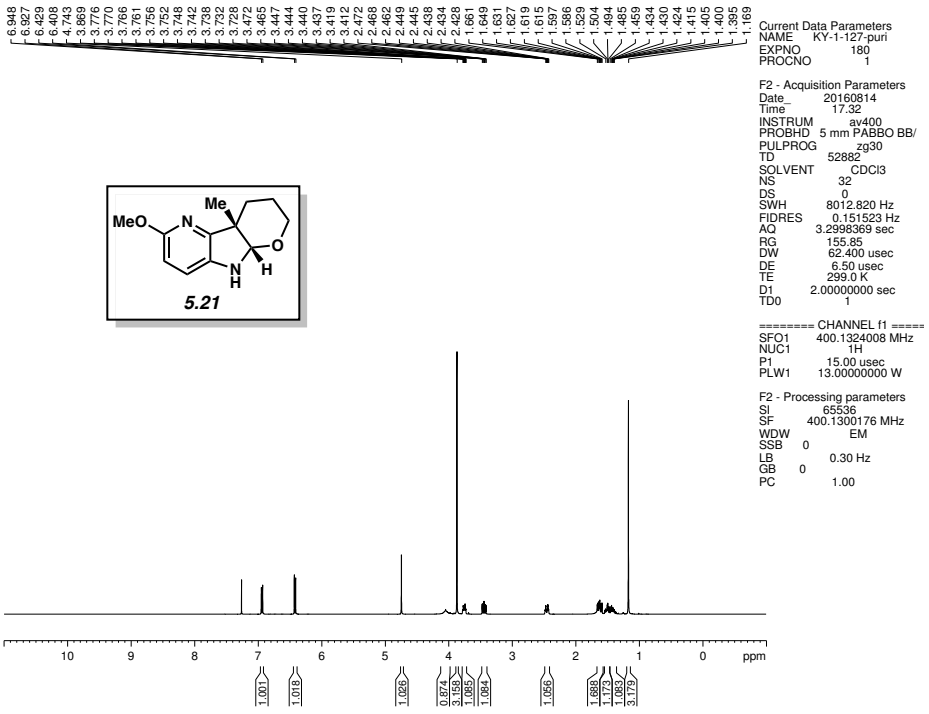

Figure 5.29 ^{1}H NMR (500 MHz, $CDCl_3$) of compound **5.21**.

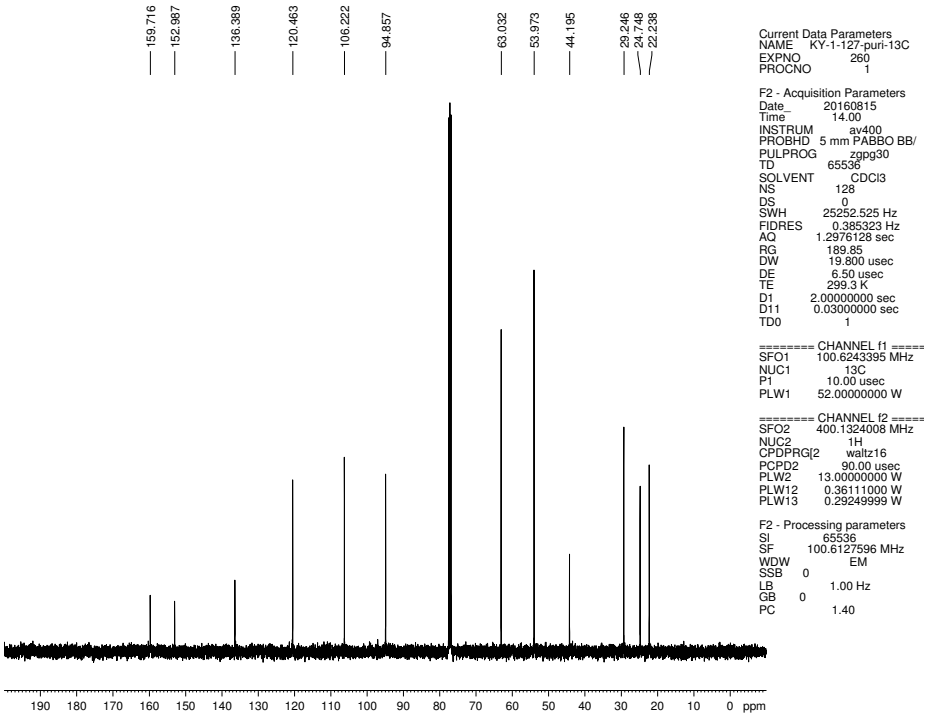

Figure 5.30 ^{13}C NMR (125 MHz, $CDCl_3$) of compound **5.21**.

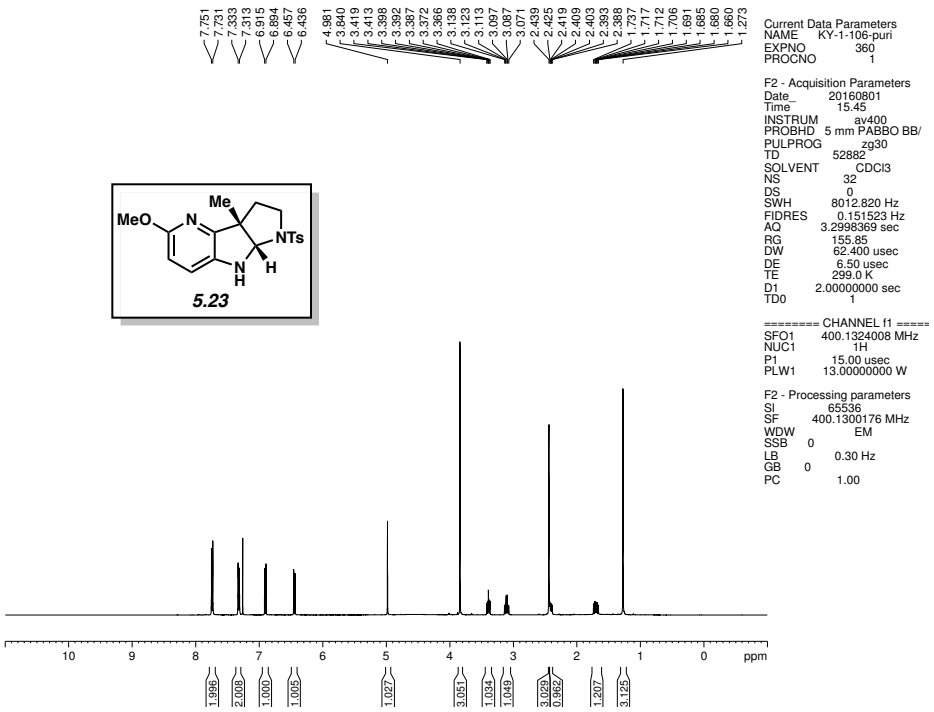

Figure 5.31 ^{1}H NMR (500 MHz, $CDCl_3$) of compound **5.23**.

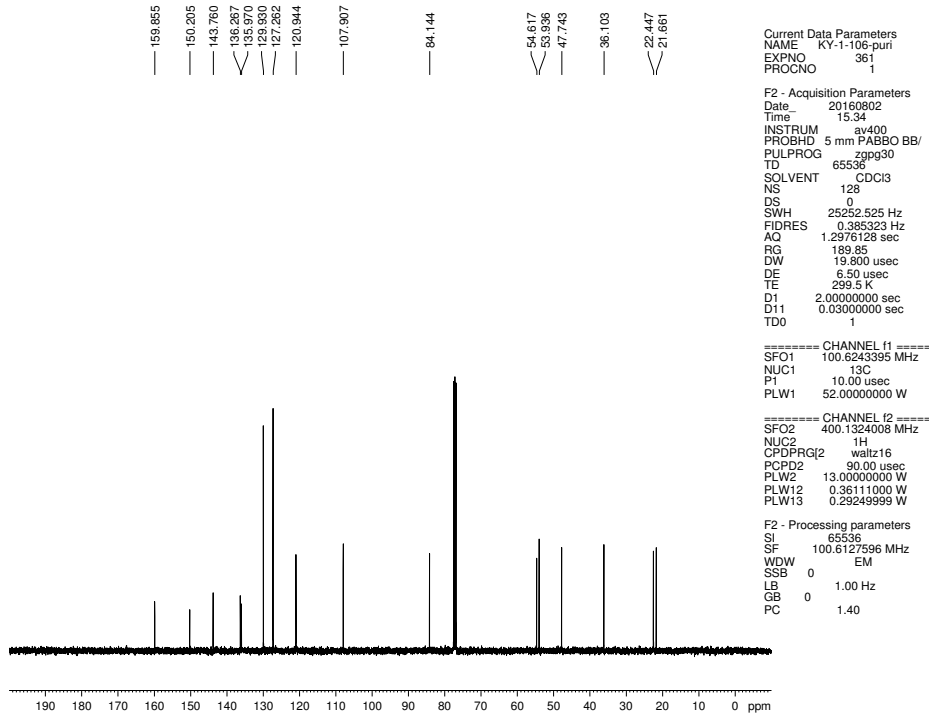

Figure 5.32 ^{13}C NMR (125 MHz, $CDCl_3$) of compound **5.23**.

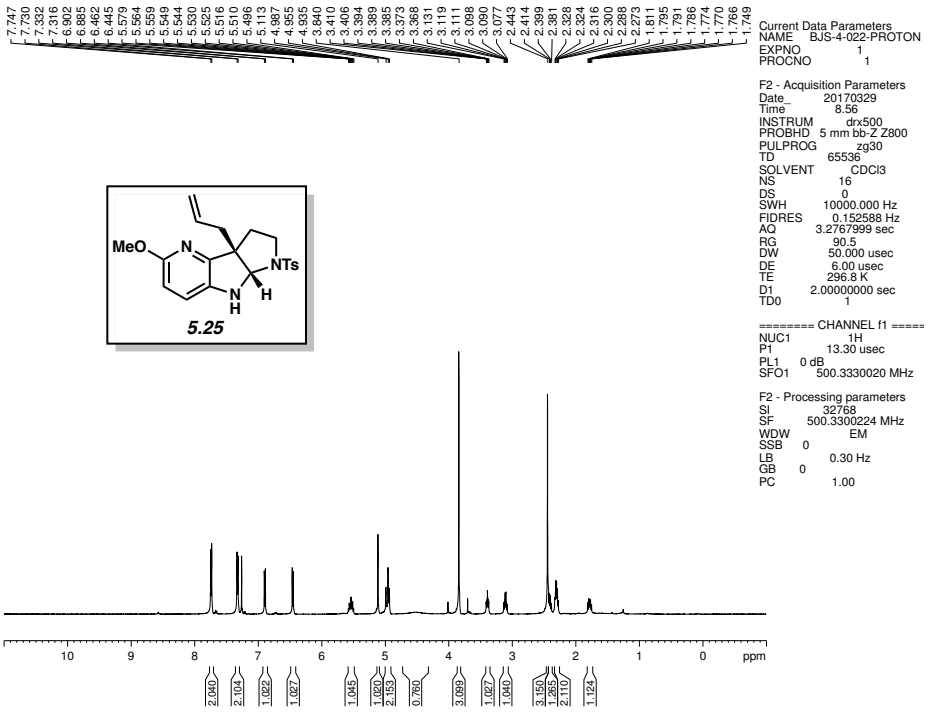

Figure 5.33 ^{1}H NMR (500 MHz, $CDCl_3$) of compound **5.25**.

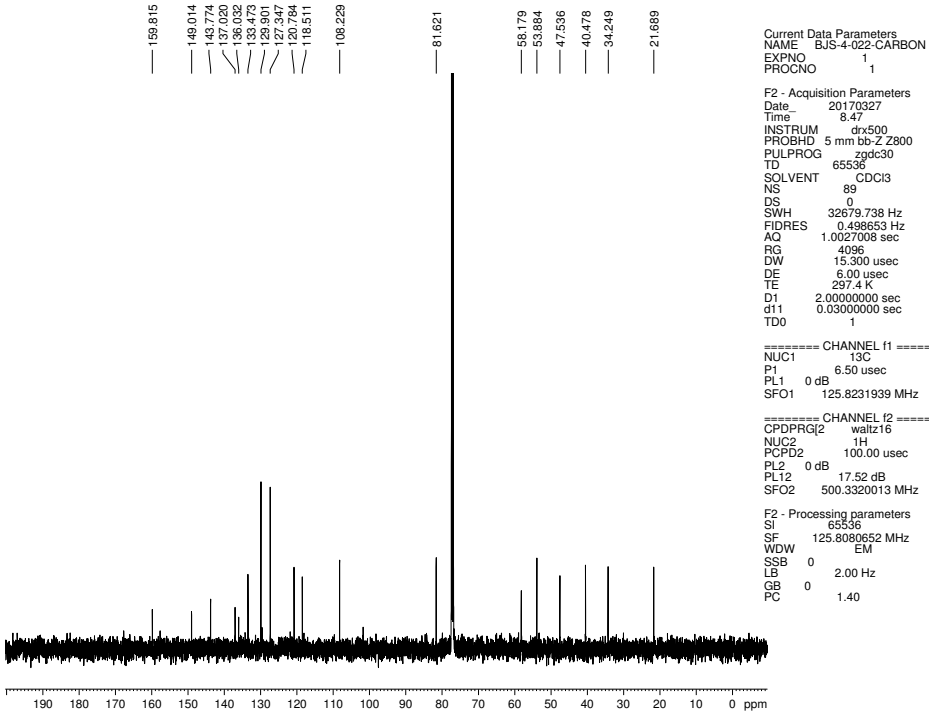

Figure 5.34 ^{13}C NMR (125 MHz, $CDCl_3$) of compound **5.25**.

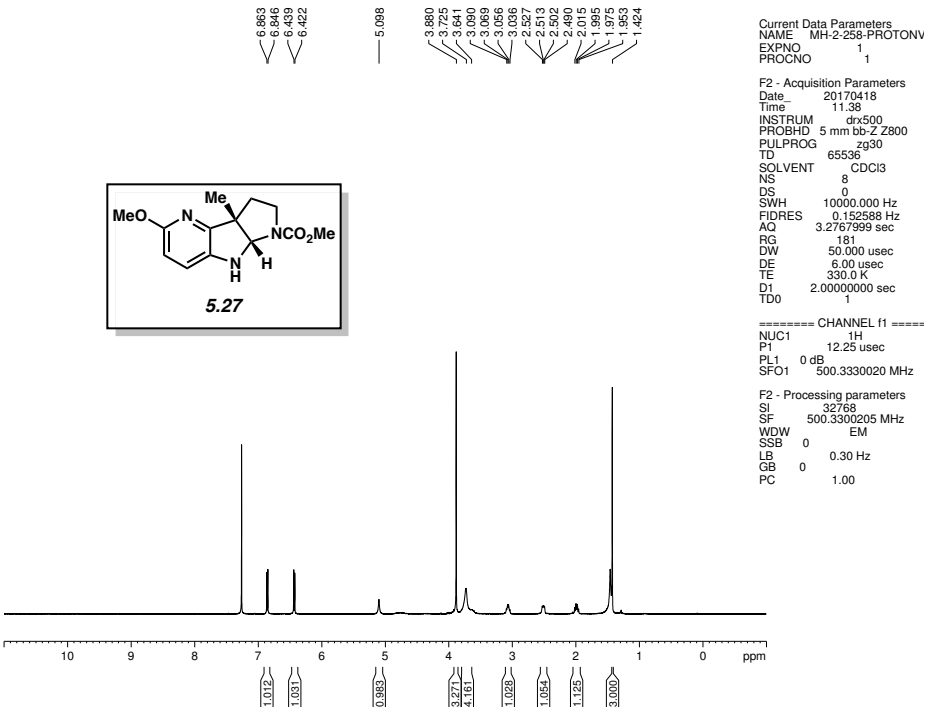

Figure 5.35 ^{1}H NMR (500 MHz, $CDCl_3$) of compound **5.27**.

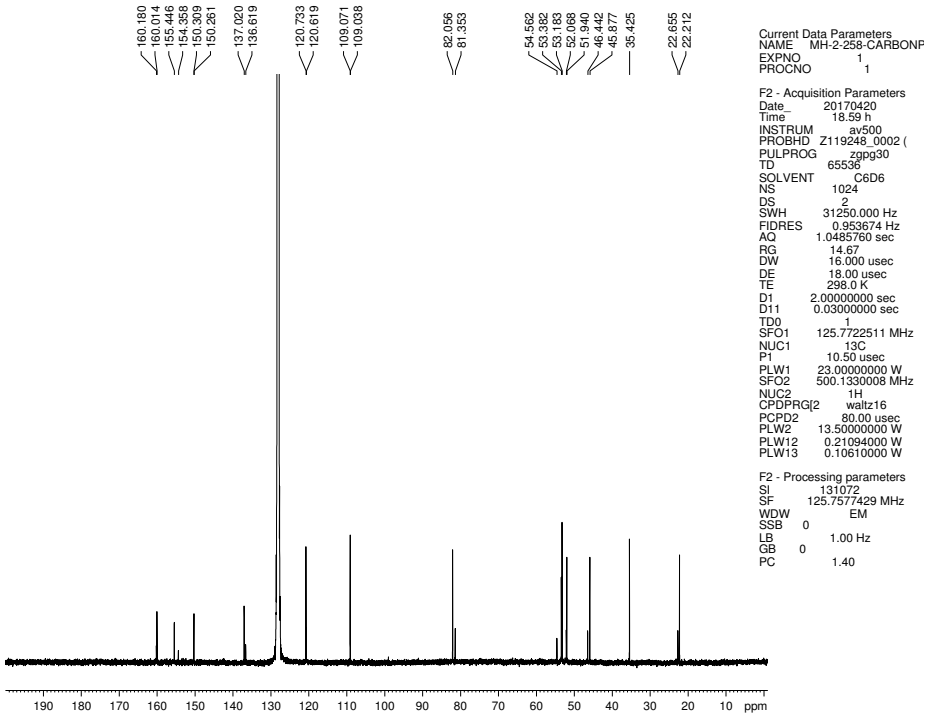

Figure 5.36 ^{13}C NMR (125 MHz, C_6D_6) of compound **5.27**.

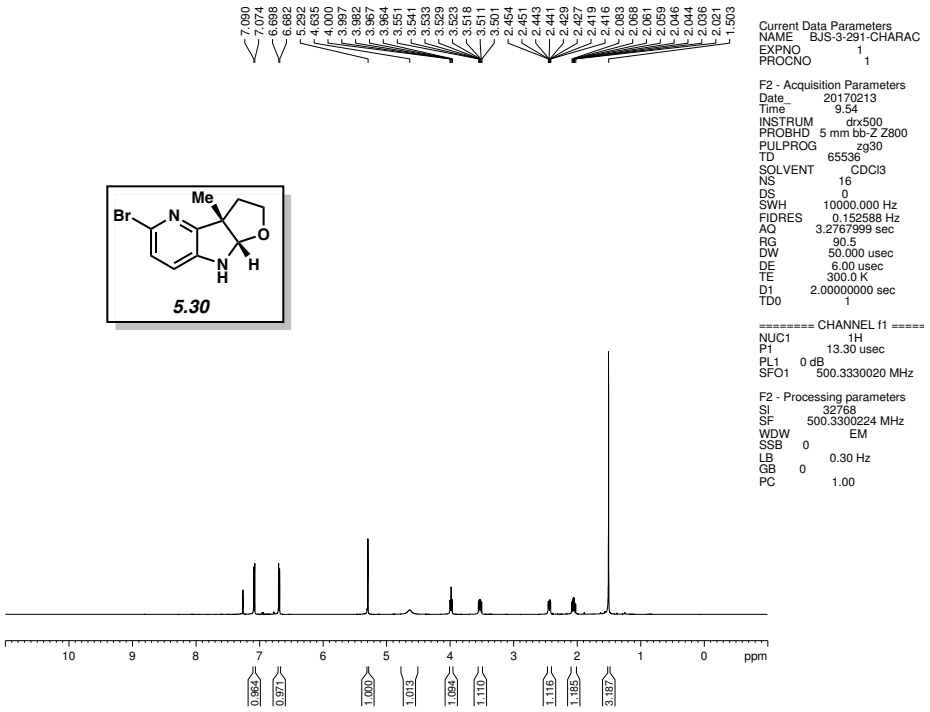

Figure 5.37 ^{1}H NMR (500 MHz, $CDCl_3$) of compound **5.30**.

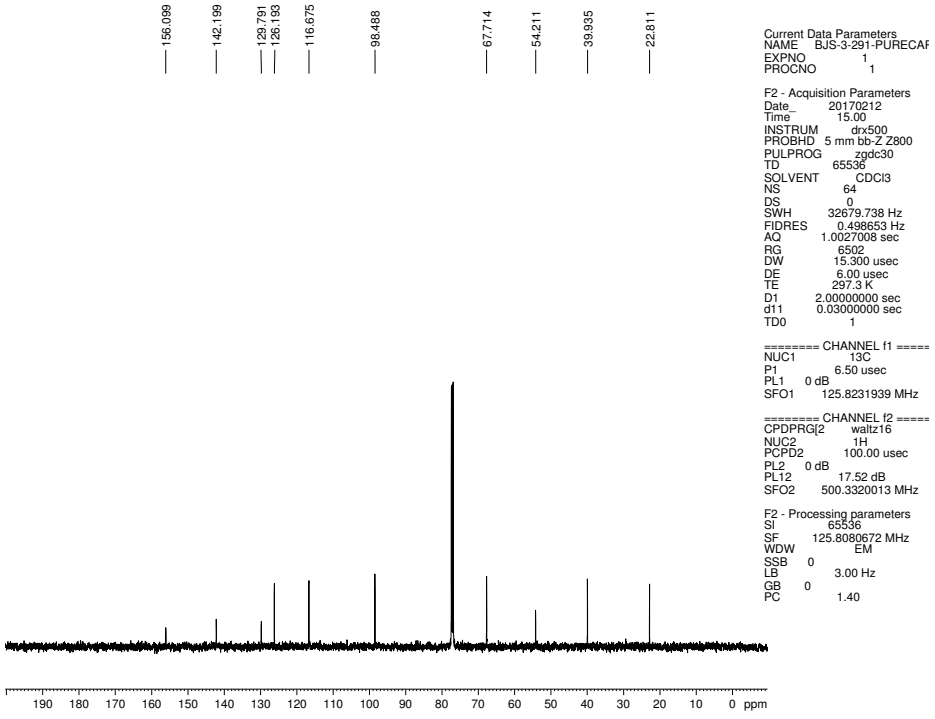

Figure 5.38 ^{13}C NMR (125 MHz, $CDCl_3$) of compound **5.30**.

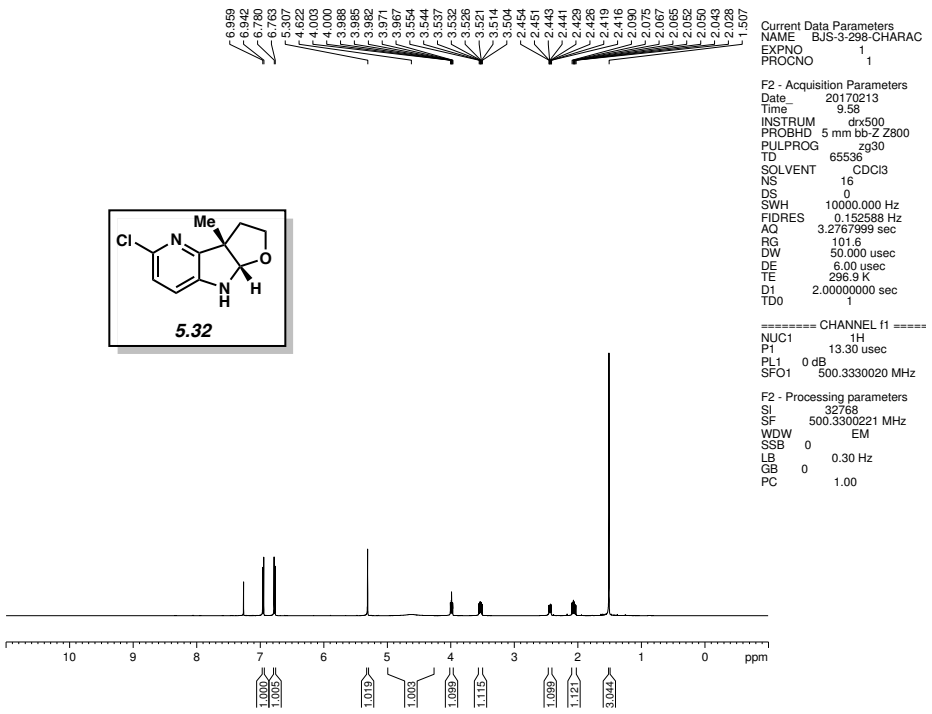

Figure 5.39 ^{1}H NMR (500 MHz, $CDCl_3$) of compound **5.32**.

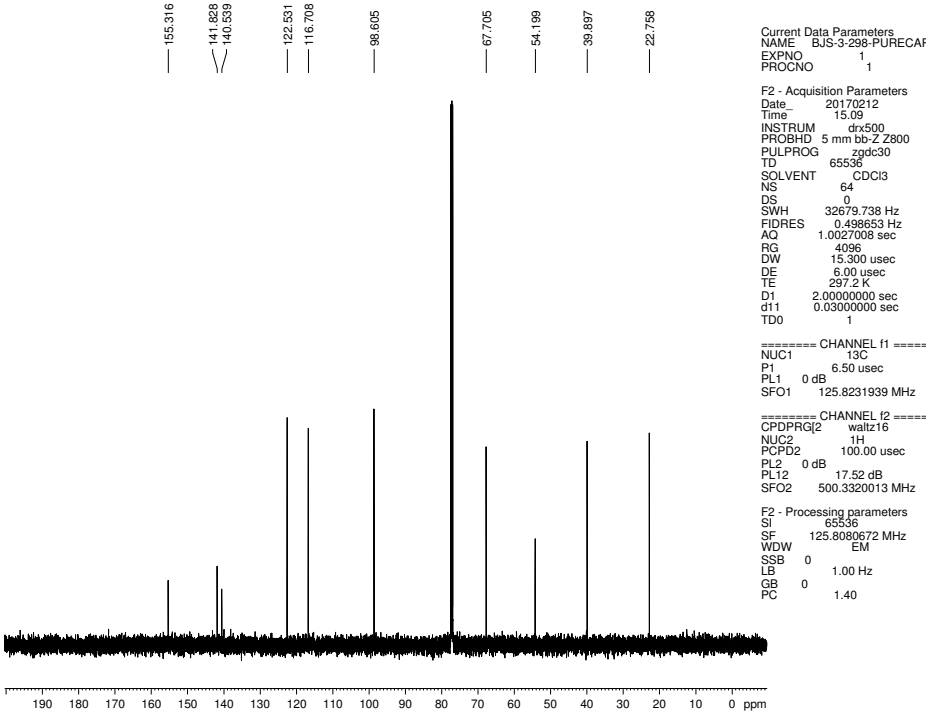

Figure 5.40 ^{13}C NMR (125 MHz, $CDCl_3$) of compound **5.32**

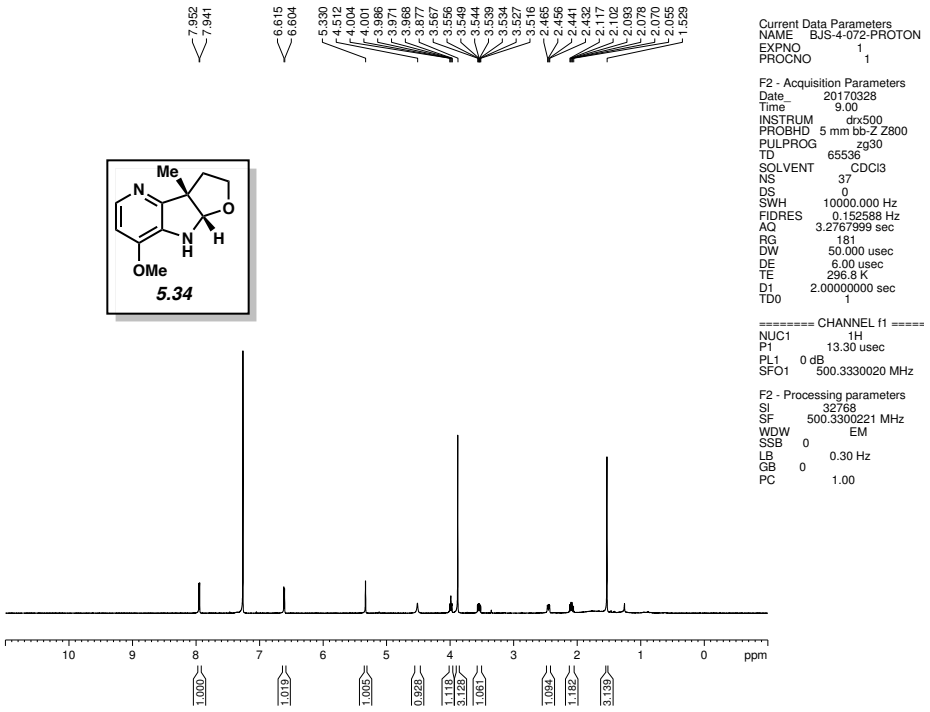

Figure 5.41 ^{1}H NMR (500 MHz, $CDCl_3$) of compound **5.34**.

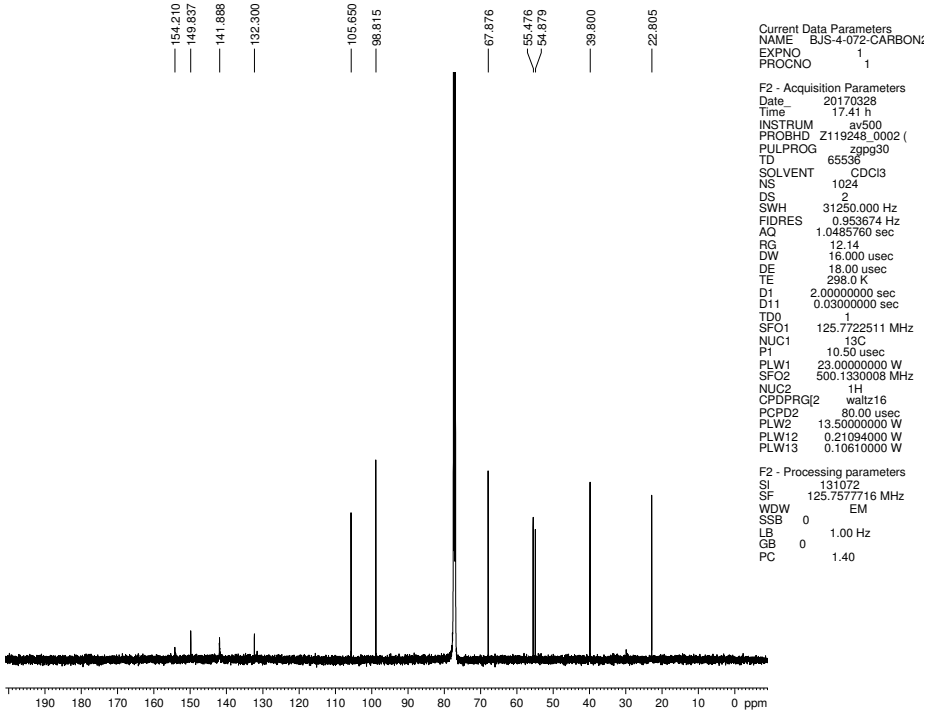

Figure 5.42 ^{13}C NMR (125 MHz, $CDCl_3$) of compound **5.34**.

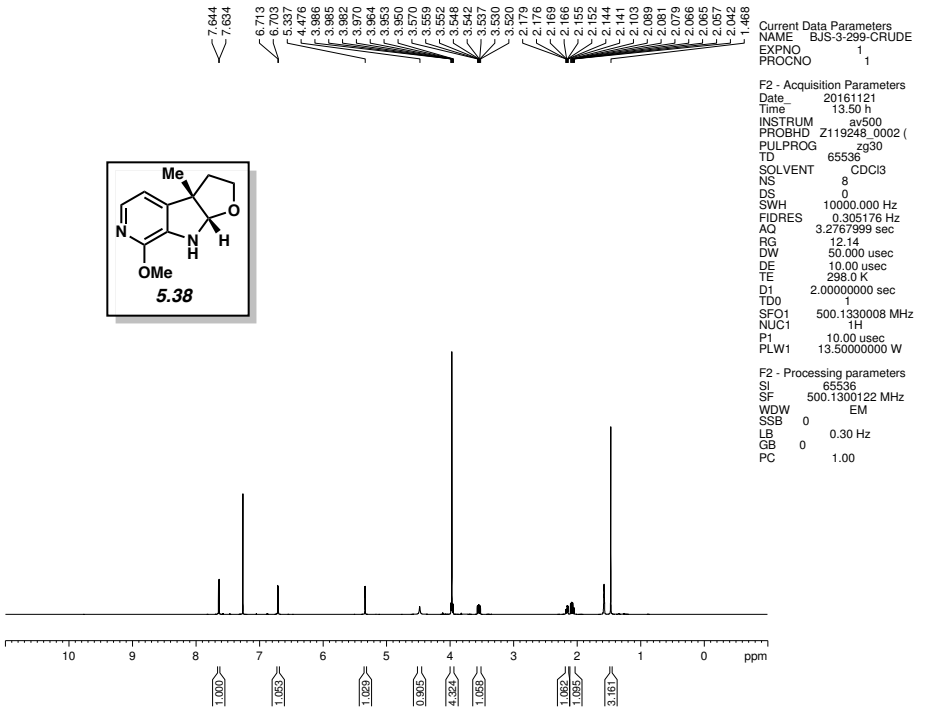

Figure 5.43 ^{1}H NMR (500 MHz, $CDCl_3$) of compound **5.38**.

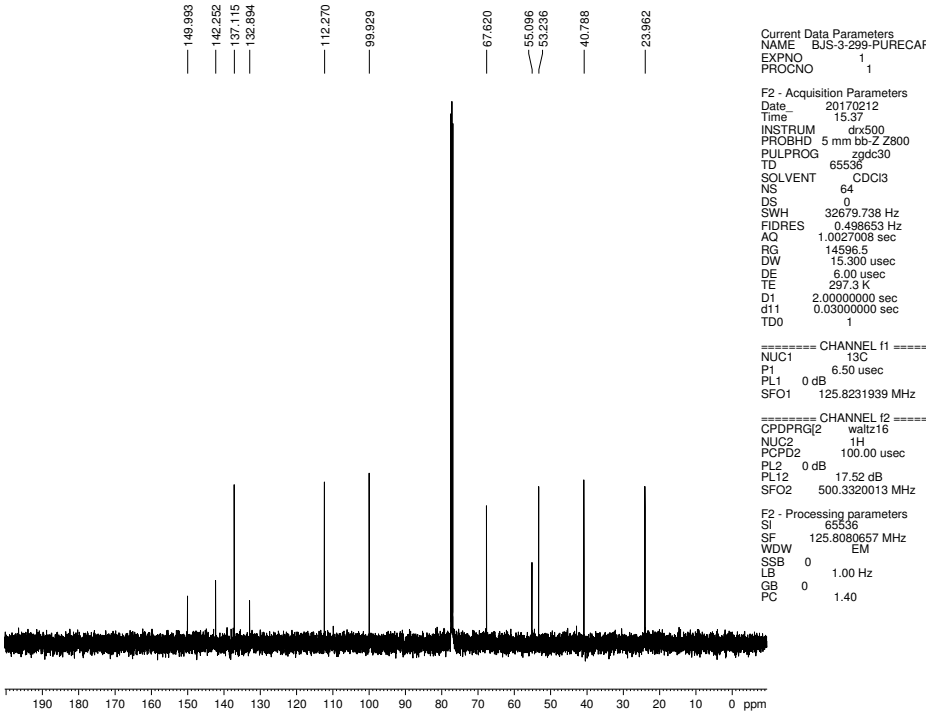

Figure 5.44 ^{13}C NMR (125 MHz, $CDCl_3$) of compound **5.38**.

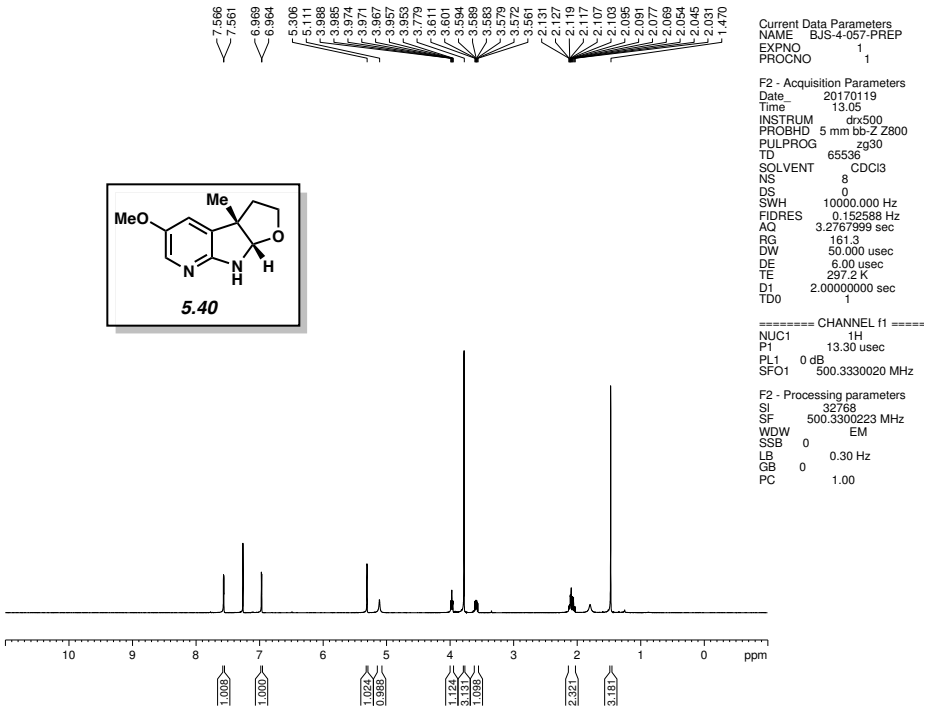

Figure 5.45 ^{1}H NMR (500 MHz, $CDCl_3$) of compound **5.40**.

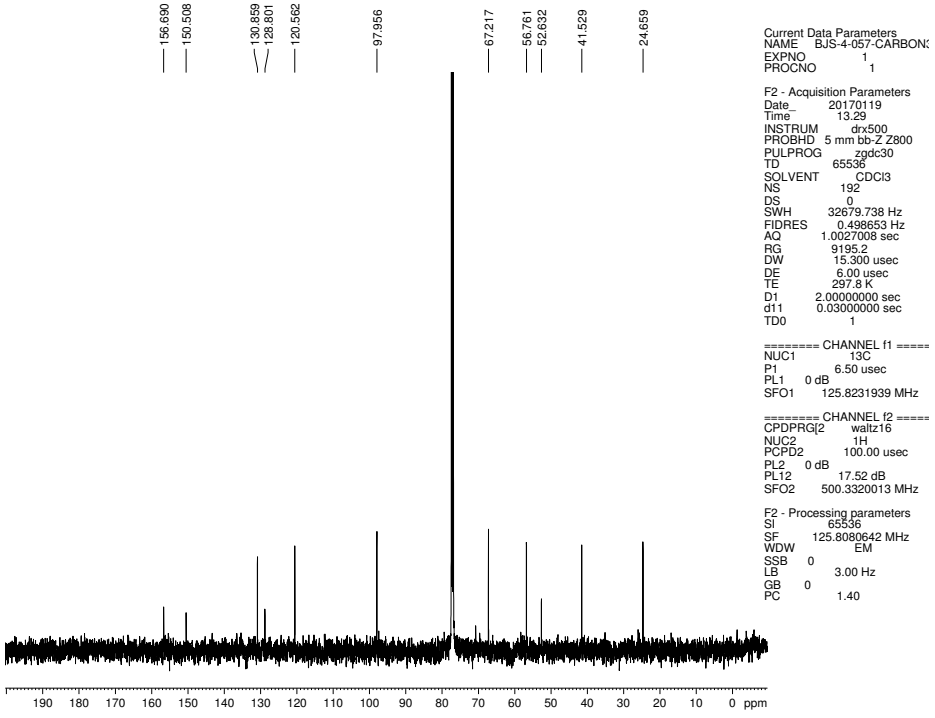

Figure 5.46 ^{13}C NMR (125 MHz, $CDCl_3$) of compound **5.40**.

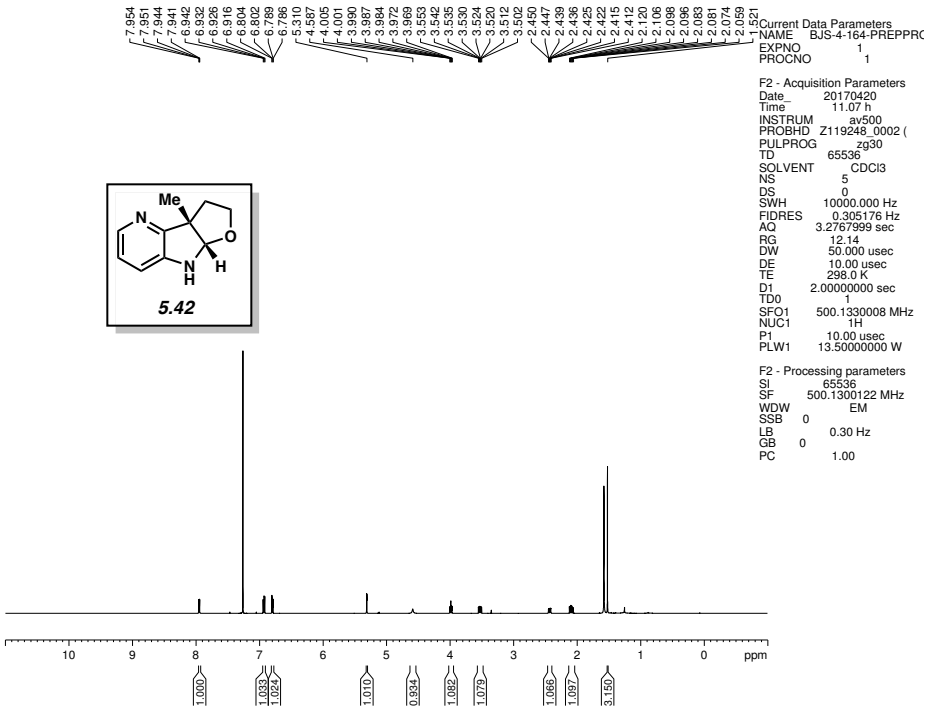

Figure 5.47 ^{1}H NMR (500 MHz, $CDCl_3$) of compound **5.42**.

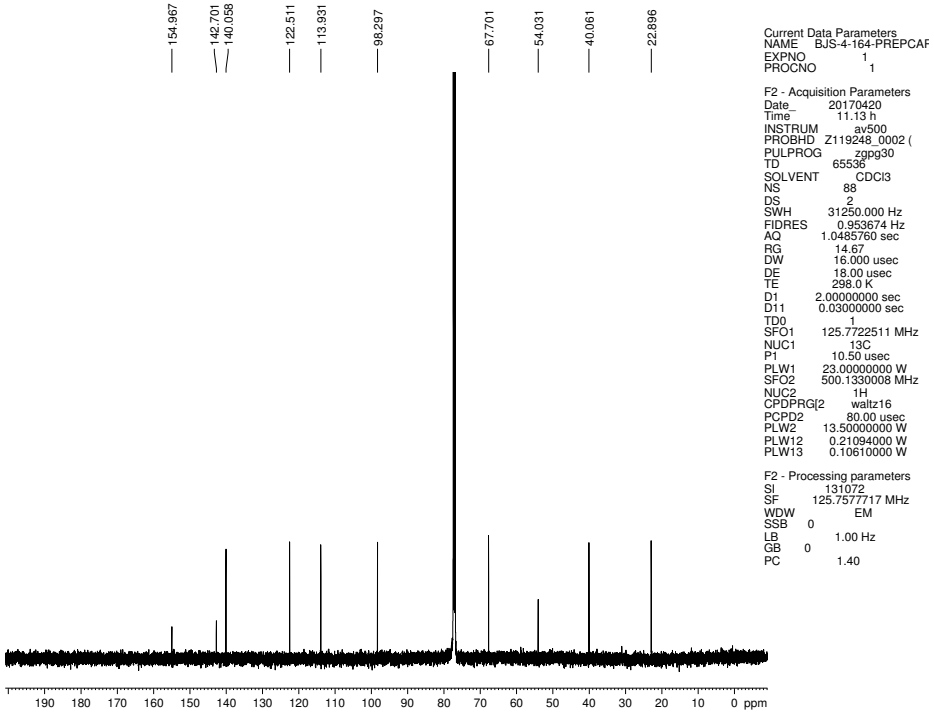

Figure 5.48 ^{13}C NMR (125 MHz, $CDCl_3$) of compound **5.42**.

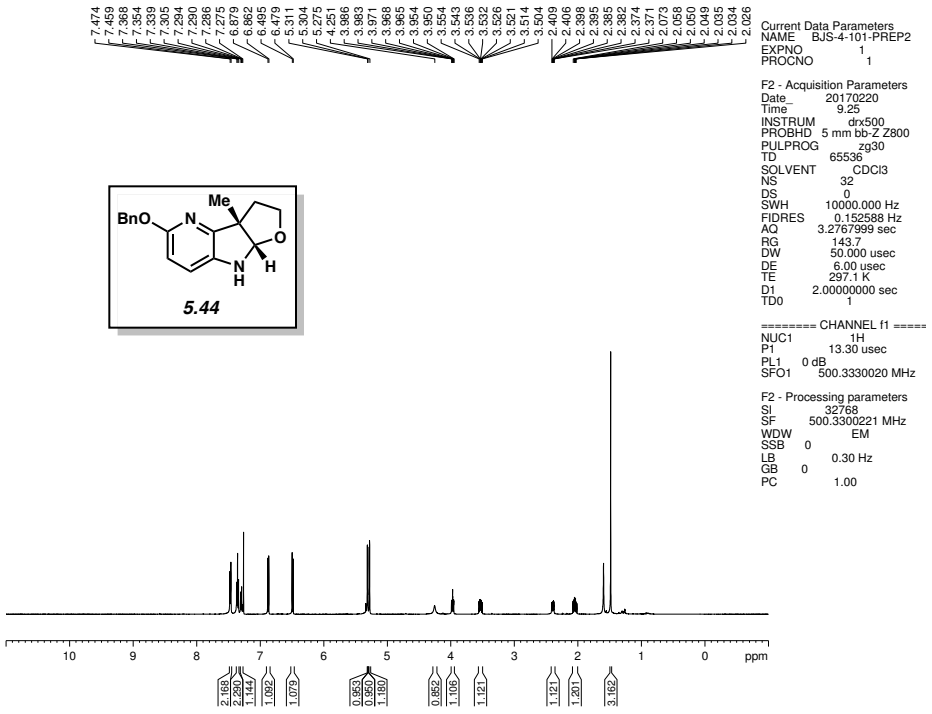

Figure 5.49 ^{1}H NMR (500 MHz, $CDCl_3$) of compound **5.44**.

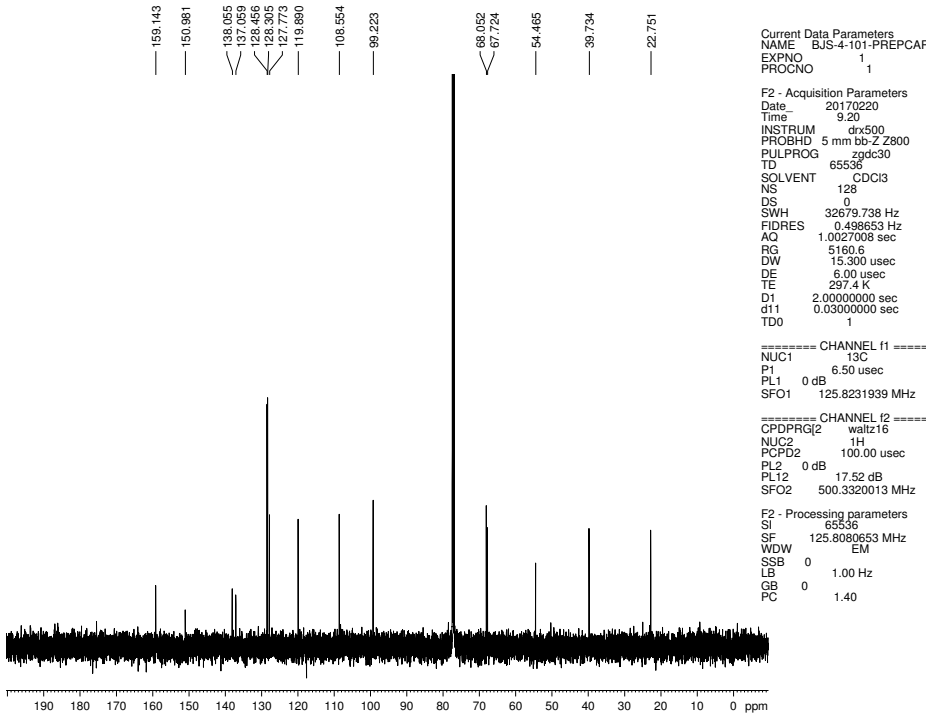

Figure 5.50 ^{13}C NMR (125 MHz, $CDCl_3$) of compound **5.44**.

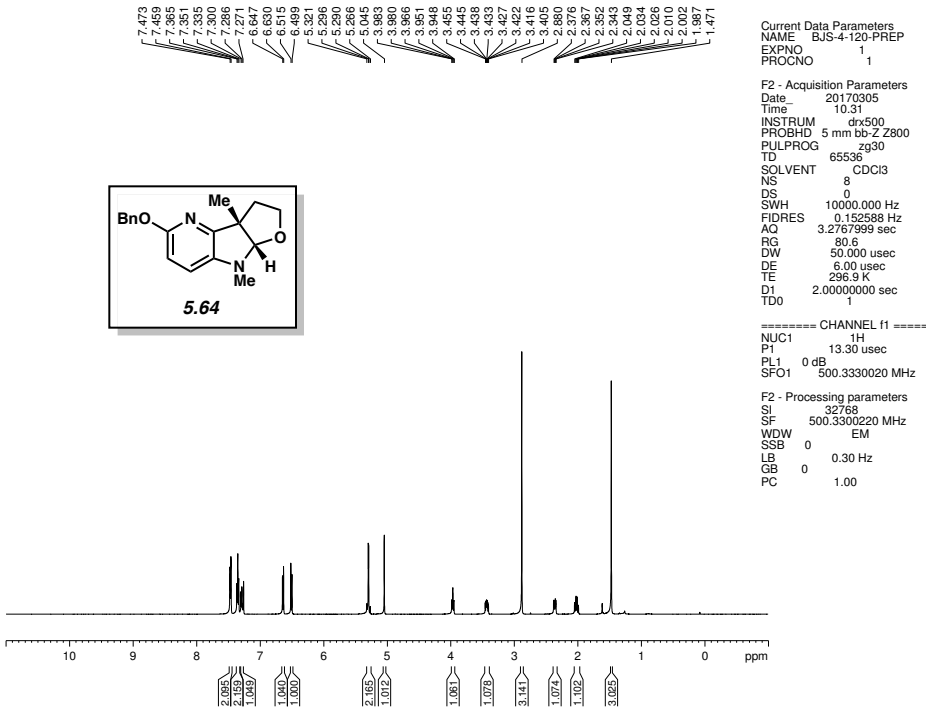

Figure 5.51 ^{1}H NMR (500 MHz, $CDCl_3$) of compound **5.64**.

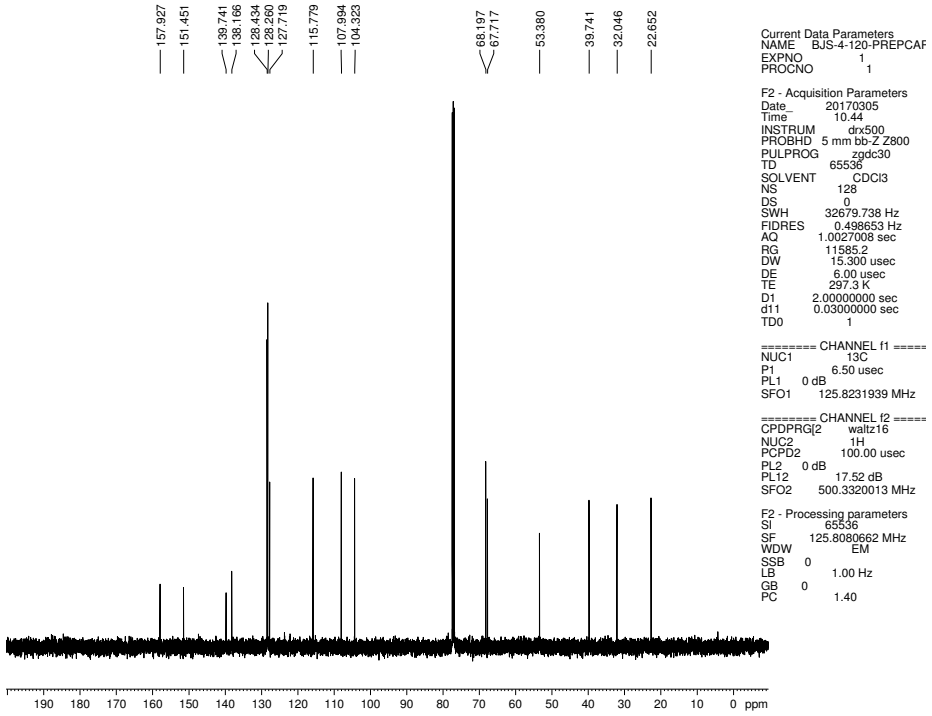

Figure 5.52 ^{13}C NMR (125 MHz, $CDCl_3$) of compound **5.64**.

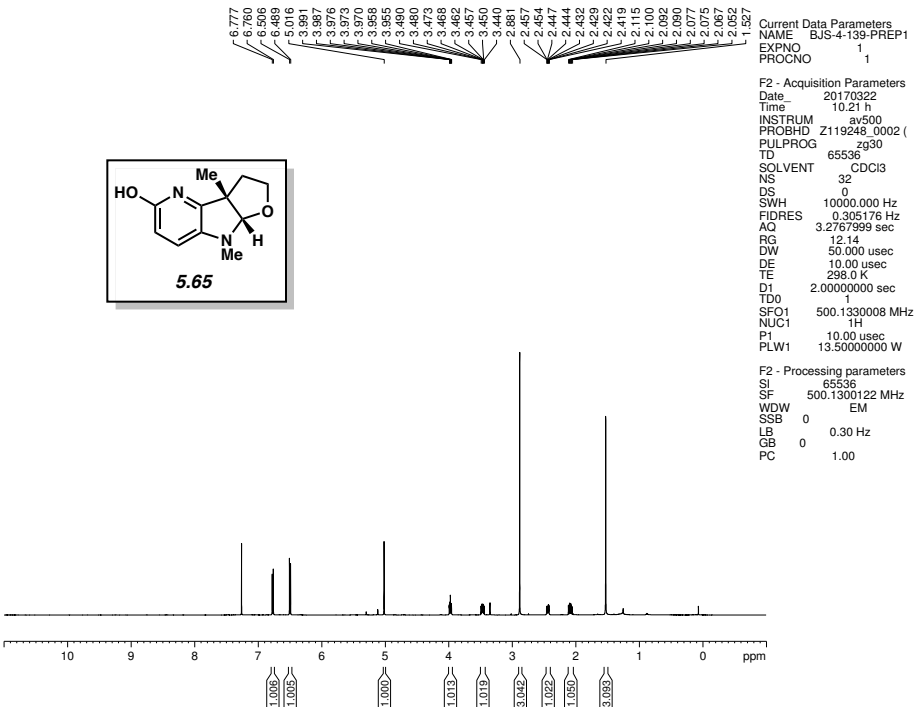

Figure 5.53 ^{1}H NMR (500 MHz, $CDCl_3$) of compound **5.65**.

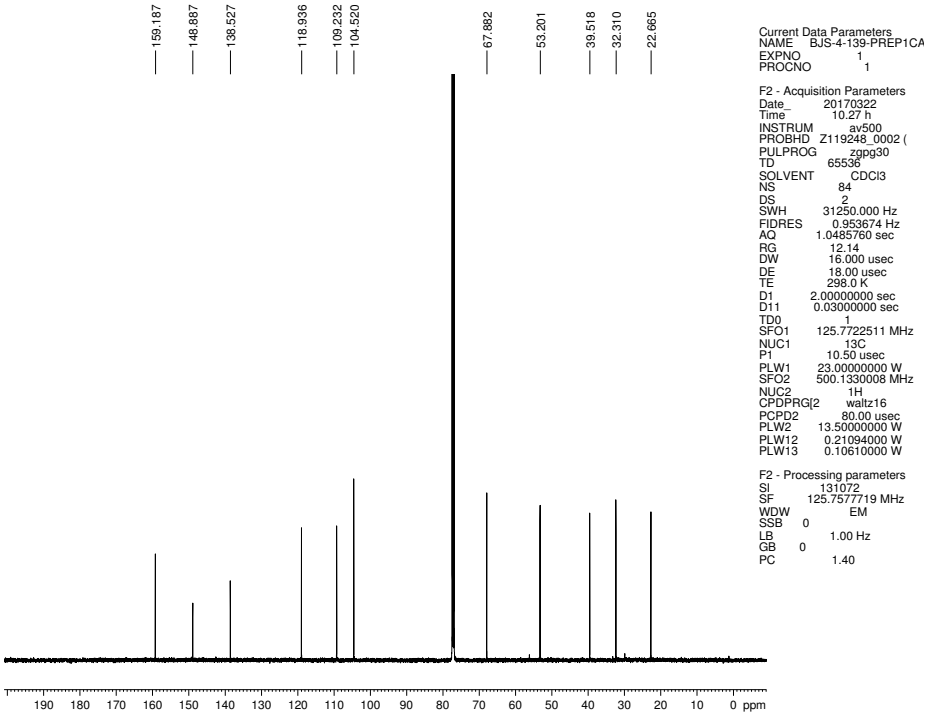

Figure 5.54 ^{13}C NMR (125 MHz, $CDCl_3$) of compound **5.65**.

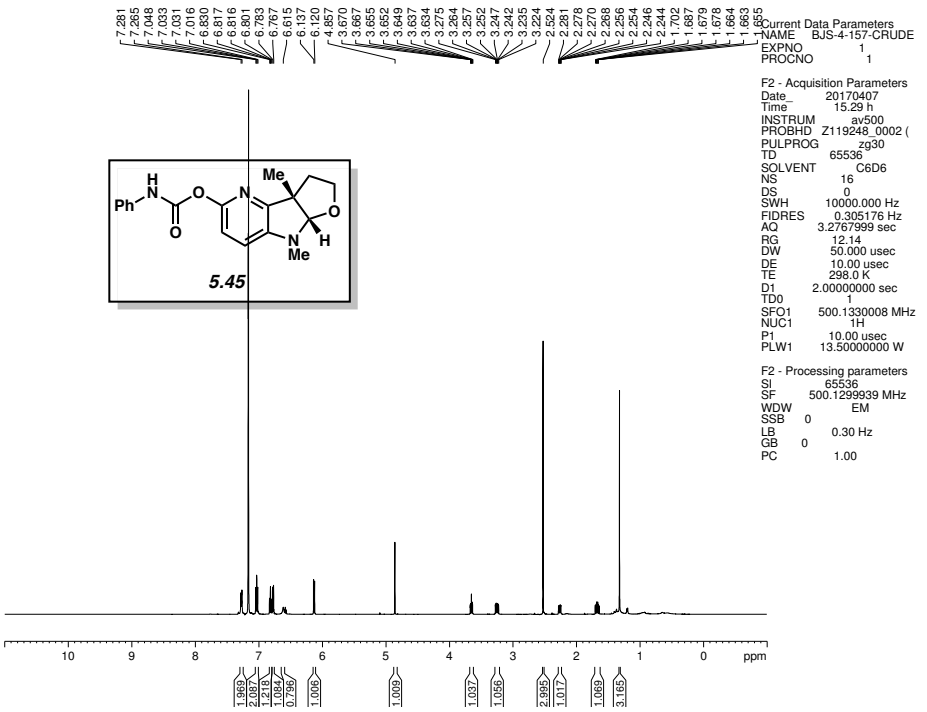

Figure 5.55 ^{1}H NMR (500 MHz, $CDCl_3$) of compound **5.45**.

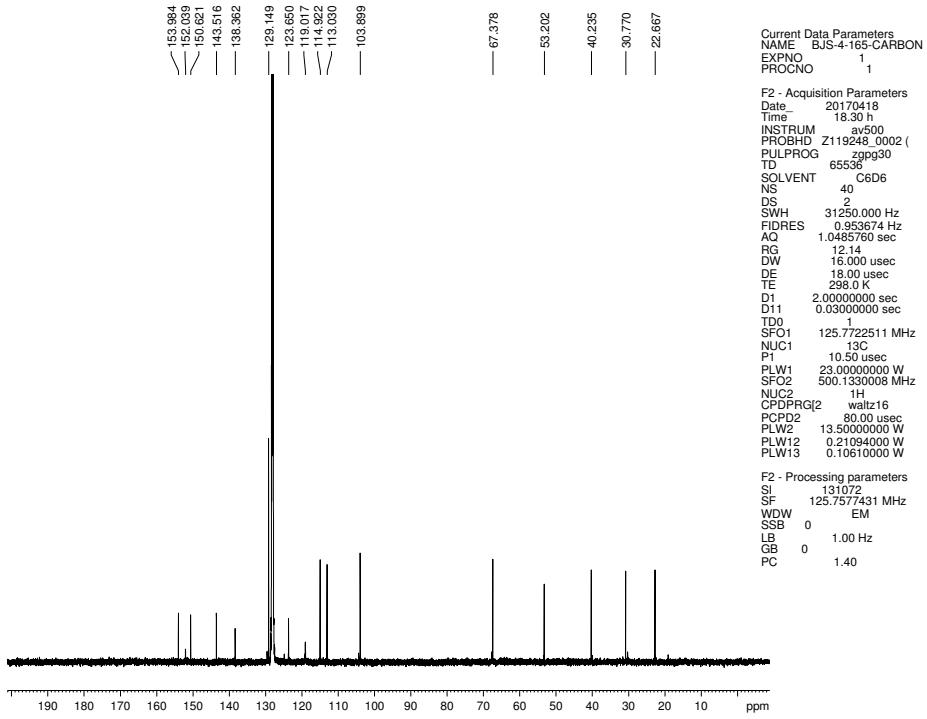

Figure 5.56 ^{13}C NMR (125 MHz, $CDCl_3$) of compound **5.45**.

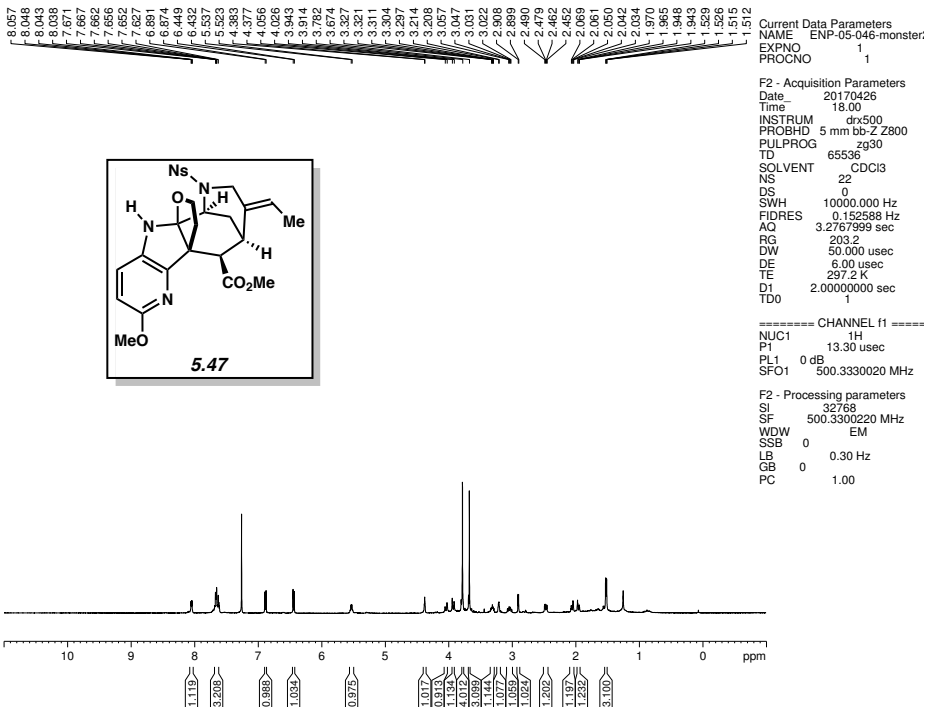

Figure 5.57 ^{1}H NMR (500 MHz, $CDCl_3$) of compound **5.47**.

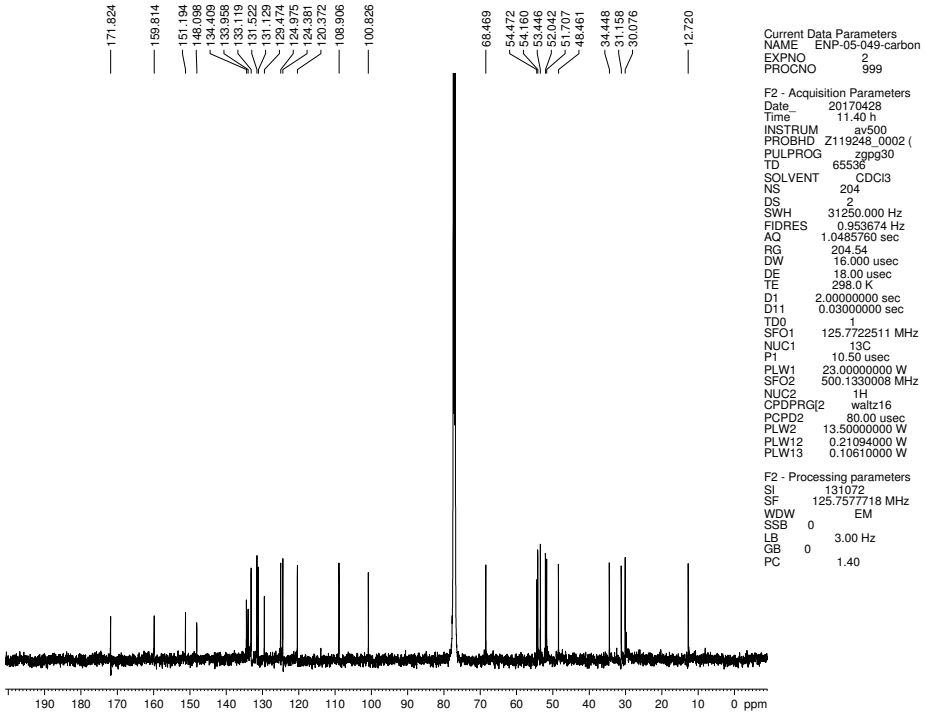

Figure 5.58 ^{13}C NMR (125 MHz, $CDCl_3$) of compound **5.47**.

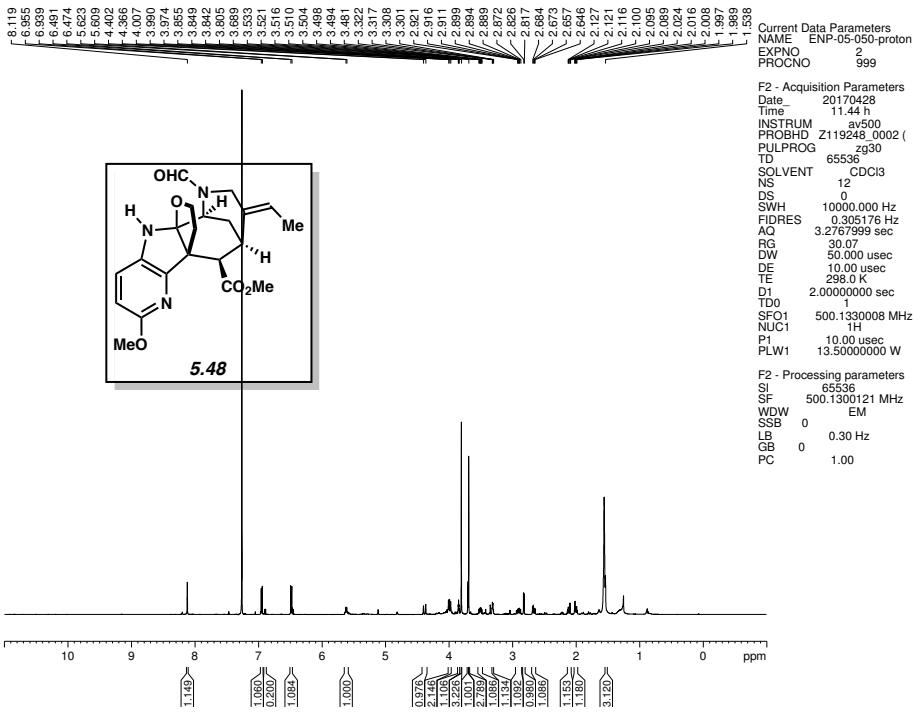

Figure 5.59 ^{1}H NMR (500 MHz, $CDCl_3$) of compound **5.48**.

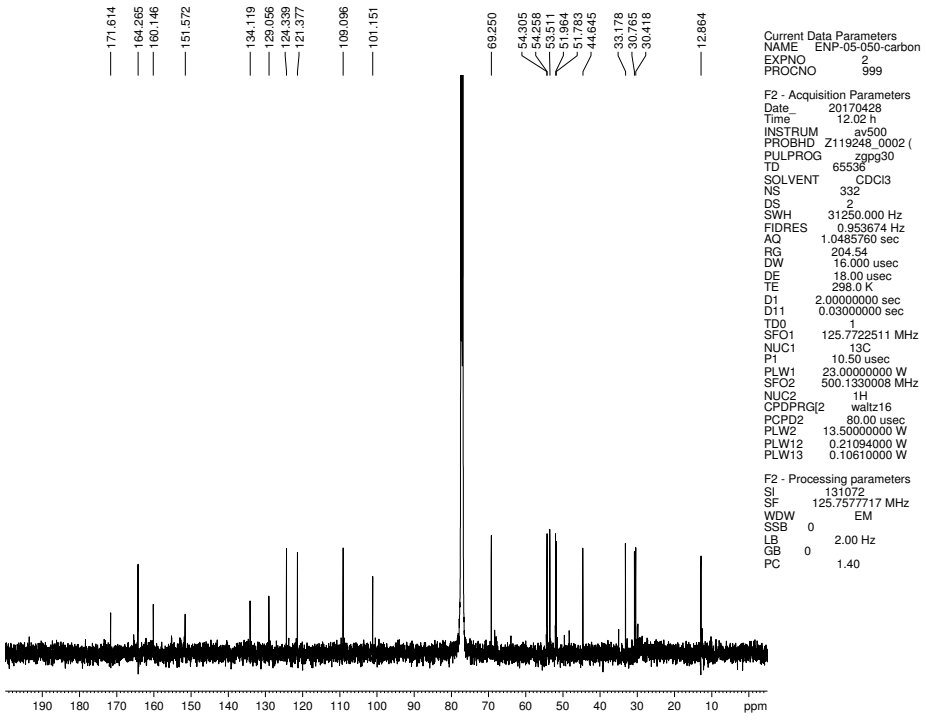

Figure 5.60 ^{13}C NMR (125 MHz, $CDCl_3$) of compound **5.48**.

5.10 Notes and References

(1) (a) Fischer, E.; Jourdan, F. *Ber. Dtsch. Chem. Ges.* **1883**, *16*, 2241–2245. (b) Fischer, E.; Hess, O. *Ber. Dtsch. Chem. Ges.* **1884**, *17*, 559–568.

(2) (a) Robinson, B. *Chem. Rev.* **1963**, *63*, 373–401. (b) Robinson, B. *Chem. Rev.* **1969**, *69*, 227–250. (c) Humphrey, G. R.; Kuethe, J. T. *Chem. Rev.* **2006**, *106*, 2875–2911. (d) Hughes, D. L. *Org. Prep. Proced. Int.* **2009**, *25*, 607–632.

(3) (a) Krüger, S.; Gaich, T. *Angew. Chem., Int. Ed.* **2015**, *54*, 315−317. (b) Park, J.; Kim, D.-H.; Das, T.; Cho, C.-G. *Org. Lett.* **2016**, *18*, 5098−5101. (c) Smith, J. M.; Moreno, J.; Boal, B. W.; Garg, N. K. *J. Am. Chem. Soc.* **2014**, *136*, 4504−4507. (d) Moreno, J.; Picazo, E.; Morrill, L. A.; Smith, J. M.; Garg, N. K. *J. Am. Chem. Soc.* **2016**, *138*, 1162−1165. (e) Ueda, H.; Satoh, H.; Matsumoto, K.; Sugimoto, K.; Fukuyama, T.; Tokuyama, H. *Angew. Chem., Int. Ed.* **2009**, *48*, 7600−7603. (f) Satoh, H.; Ueda, H.; Tokuyama, H. *Tetrahedron* **2013**, *69*, 89−95. (g) Wang, D.; Hou, M.; Ji, Y.; Gao, S. *Org. Lett.* **2017**, *19*, 1922−1925. (h) Adams, G. L.; Carroll, P. J.; Smith, A. B., III *J. Am. Chem. Soc.* **2012**, *134*, 4037−4040. (i) Adams, G. L.; Carroll, P. J.; Smith, A. B., III *J. Am. Chem. Soc.* **2013**, *135*, 519−528.

(4) (a) Kelly, A. H.; McLeod, D. H.; Parrick, J. *Can. J. Chem.* **1965**, *43*, 296–301. (b) Kelly, A. H.; Parrick, J. *Can. J. Chem.* **1966**, *44*, 2455–2459. (c) Crooks, P. A.; Robinson, B. *Can. J. Chem.* **1969**, *47*, 2061–2067. (d) Jeanty, M.; Blu, J.; Suzenet, F.; Guillaumet, G. *Org. Lett.* **2009**, *11*, 5142–5145. (e) Pin, F.; Buron, F.; Saab, F.; Colliandre, L.; Bourg, S.; Schoentgen, F.; Guevel, R. L.; Guillouzo, C.; Routier, S. *Med. Chem. Commun.* **2011**, *2*, 899–903. (f) Inman, M.; Carbone, A.; Moody, C. J. *J. Org. Chem.* **2012**, *77*, 1217–1232. (g) Thomae, D.; Jeanty, M.; Coste, J.; Guillaumet, G.; Suzenet, F. *Eur. J. Org. Chem.* **2013**, 3328–3336. (h) Alekseyev, R. S.;

Amirova, S. R.; Kabanova, E. V.; Terenin, V. I. *Chem. Heterocycl. Compd. (N.Y.)* **2014**, *50*, 1305–1315.

(5) Perkin, W. H.; Robinson, R. *J. Chem. Soc., Trans.* **1913**, *103*, 1973–1985.

(6) In the interrupted Fischer azaindolization, rather than re-aromatization occurring to give an azaindole heterocycle, the transient iminium species generated is trapped by a pendant nucleophile (see mechanism for **5.3** + **5.4** → **5.5** in Figure 5.1). For reviews on the parent interrupted Fischer indolization reaction (non-aza version), see: (a) Li, S.; Han, J.; Li, A. *Huaxue Xuebao* **2013**, *71*, 295–298. (b) Mo, Y.; Zhao, J.; Chen, W.; Wang, Q. *Res. Chem. Intermediat.* **2015**, *41*, 5869–5877. (c) Susick, R. B.; Morrill, L. A.; Picazo, E.; Garg, N. K. *Synlett* **2017**, *28*, 1–11. One example of the Fischer azaindolization has been reported for the synthesis of a tetracyclic pyrrolidino-4-azaindoline; see: (d) de Graaff, C.; Bensch, L.; Boersma, S. J.; Cioc, R. C.; van Lint, M. J.; Janssen, E.; Turner, N. J.; Orru, R. V. A.; Ruijter, E. *Angew. Chem., Int. Ed.* **2015**, *54*, 14133–14136.

(7) Only four azaindoline compounds of the type **5.5** are known in the literature. For two furano-4-azaindolines prepared by a Pd-catalyzed intermolecular carboamination approach, see: (a) Bizet, V.; Borrajo-Calleja, G. M.; Besnard, C.; Mazet, C. *ACS Catal.* **2016**, *6*, 7183–7187. For a pyrrolidino-7-azaindoline derived from a [3+2] alkene / isocyanate cycloaddition, see: (b) Huang, L.; Cheng, H.; Zhang, R.; Wang, M.; Xie, C. *Adv. Synth. Catal.* **2014**, *356*, 2477–2484. (c) Cheng, H.; Zhang, R.; Yang, S.; Wang, M.; Zeng, X.; Xie, L.; Xie, C.; Wu, J.; Zhong, G. *Adv. Synth. Catal.* **2016**, *358*, 970–976. See also reference 6d.

(8) Mérour, J.-Y.; Buron, F.; Plé, K.; Bonnet, P.; Routier, S. *Molecules* **2014**, *19*, 19935–19979.

(9) A structural search using Reaxys was used to obtain these statistics (accessed June, 2017).

(10) Bollag, G.; Tsai, J.; Zhang, J.; Zhang, C.; Ibrahim, P.; Nolop, K.; Hirth, P. *Nat. Rev. Drug Discov.* **2012**, *11*, 873–886.

(11) Subramaniam, G.; Hiraku, O.; Hayashi, M.; Koyano, T.; Komiyama, K.; Kam, T.-S. *J. Nat. Prod.* **2007**, *70*, 1783−1789.

(12) See Experimental Section (Section 5.7) for details.

(13) $\Delta G^{\ddagger}$[3,3] is the difference between the transition state energy of the sigmatropic rearrangement step and the energy of the enehydrazine precursor.

(14) [3,3]-Sigmatropic rearrangement in the Fischer indolization is thought to proceed more favorably via protonation of the β-nitrogen. For prior computational studies, see: Çelebi-Olcüm, N.; Boal, B. W.; Huters, A. D.; Garg, N. K.; Houk, K. N. *J. Am. Chem. Soc.* **2011**, *133*, 5752–5755.

(15) Considering the higher basicity of 4-methoxypyridine compared to pyridine itself, this result may seem counterintuitive. However, this result underscores the need to take into account the relative basicities of the corresponding enehydrazine intermediates. We estimate that the enehydrazine derivative of 4-methoxypyridine is roughly 2 orders of magnitude more basic compared to the enehydrazine derivative of pyridine itself based on calculations. See the Experimental Section (Section 5.7) for details.

(16) We also predicted that the use of N-methylhydrazine **5.212** would perform more favorably compared to hydrazine **5.41**, largely due to a more favorable tautomerization equilibrium ($\Delta G[H^+]$). Despite the high estimated overall barrier of 32.4 kcal/mol, we found that Fischer azaindolization of **5.212** + **5.14** gave **5.213** in 44% yield. Under identical conditions, the corresponding indolization of **5.41** gave only 12% yield of product **5.42**.

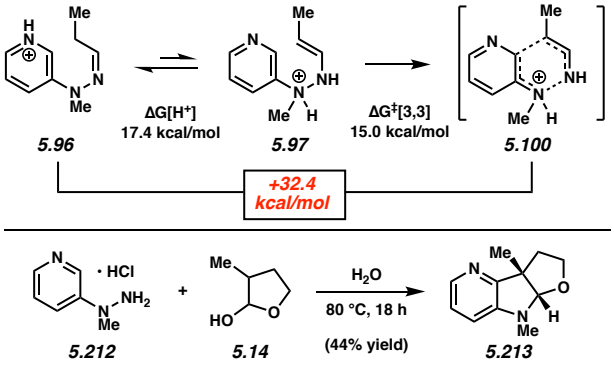

(17) Yu, Q.; Liu, C.; Brzostowska, M.; Chrisev, L.; Brossi, A.; Greig, N. H.; Atack, J. R.; Soncrant, T. T.; Rapoport, S. I.; Radunz, H. E. *Helv. Chim. Acta* **1991**, *74*, 761–766. Schammel, A. W.; Boal, B. W.; Zu, L.; Mesganaw, T.; Garg, N. K. *Tetrahedron* **2010**, *66*, 4687–4695.

(18) Boal, B. W.; Schammel, A. W.; Garg, N. K. *Org. Lett.* **2009**, *11*, 3458–3461.

(19) Schammel, A. W.; Boal, B. W.; Zu, L.; Mesganaw, T.; Garg, N. K. *Tetrahedron* **2010**, *66*, 4687–4695.

(20) Gaussian 09, *Revision D.01*, M. J. Frisch, G. W. Trucks, H. B. Schlegel, G. E. Scuseria, M. A. Robb, J. R. Cheeseman, G. Scalmani, V. Barone, B. Mennucci, G. A. Petersson, H. Nakatsuji, M. Caricato, X. Li, H. P. Hratchian, A. F. Izmaylov, J. Bloino, G. Zheng, J. L. Sonnenberg, M. Hada, M. Ehara, K. Toyota, R. Fukuda, J. Hasegawa, M. Ishida, T. Nakajima, Y. Honda, O. Kitao, H. Nakai, T. Vreven, J. A. Montgomery, Jr., J. E. Peralta, F. Ogliaro, M. Bearpark, J. J. Heyd, E. Brothers, K. N. Kudin, V. N. Staroverov, T. Keith, R. Kobayashi, J. Normand, K. Raghavachari, A. Rendell, J. C. Burant, S. S. Iyengar, J. Tomasi, M. Cossi, N. Rega, J. M. Millam, M. Klene, J. E. Knox, J. B. Cross, V. Bakken, C. Adamo, J. Jaramillo, R. Gomperts, R. E. Stratmann, O. Yazyev, A. J. Austin, R. Cammi, C. Pomelli, J. W. Ochterski, R. L. Martin, K. Morokuma, V. G. Zakrzewski, G. A. Voth, P. Salvador, J. J. Dannenberg, S. Dapprich, A. D.

Daniels, O. Farkas, J. B. Foresman, J. V. Ortiz, J. Cioslowski, and D. J. Fox, Gaussian, Inc., Wallingford CT, 2013.

(21) Marenich, A. V.; Cramer, C. J.; Truhlar, D. G. *J. Phys. Chem. B* **2009**, *113*, 6378–6396.

(22) (a) Grimme, S. *J. Chem. Phys.* **2003**, *118*, 9095–9102. (b) Gerenkamp, M.; Grimme, S. *Chem. Phys. Lett.* **2004**, *392*, 229–235.

(23) Goumans, T. P. M.; Ehlers, A. W.; Lammertsma, K.; Würthwein, E.-U.; Grimme, S. *Chem. Eur. J.* **2004**, *10*, 6468–6475.

(24) Çelebi-Ölçüm, N.; Boal, B. W.; Huters, A. D.; Garg, N. K.; Houk, K. N. *J. Am. Chem. Soc.* **2011**, *133,* 5752–5755.

(25) (a) Ribeiro, R. F.; Marenich, A. V.; Cramer, C. J.; Truhlar, D. G. *J. Phys. Chem. B* **2011**, *115*, 14556–14562. (b) Zhao, Y.; Truhlar, D. G. *Phys. Chem. Chem. Phys.* **2008**, *10*, 2813–2818.

(26) CYLview, 1.0b; Legault, C. Y., Université de Sherbrooke, 2009 (http://www.cylview.org).

(27) Simmons, B. J.; Hoffmann, M.; Champagne, P. A.; Picazo, E.; Yamakawa, K.; Morrill, L. A.; Houk, K. N.; Garg, N. K. *J. Am. Chem. Soc.* **2017**, *139*, 14833–14836.

CHAPTER SIX

Synthesis of Fused Indolines by Interrupted Fischer Indolization in a Microfluidic Reactor

Alexander Tuan-Huy Duong, Bryan J. Simmons, Mohammad Parvez Alam, Jesus Campagna, Neil K. Garg, Varghese John.

Tetrahedron Lett. **2019**, *60*, 322–326.

6.1 Abstract

This study describes our development of a microfluidic reaction scheme for the synthesis of fused indoline ring systems found in several bioactive compounds. We have utilized a continuous-flow microfluidic reactor for the reaction of hydrazines with latent aldehydes through the interrupted Fischer indolization reaction to form fused indoline and azaindoline products. We have identified optimal conditions and evaluated the scope of this microfluidic reaction using various hydrazine and latent aldehyde surrogates. This green chemistry approach can be of general utility to rapidly produce indoline scaffolds and intermediates in a continuous manner.

6.2 Introduction

The discovery and development of efficient methods using microfluidic flow chemistry to rapidly synthesize bioactive molecules is of great value for hit-to-lead optimization efforts.[1,2,3] However, microfluidic transformations of basic reactions are still limited due to engineering feasibility for translating heterogeneous reactions in a flow reactor.[4,5,6,7,8] A vast majority of low molecular weight bioactive molecules are heterocyclic, and often comprised of several connected

heterocyclic rings.[9,10,11] A small subset of molecules that have received substantial interest due to their medicinal properties are furoindoline and pyrrolidinoindoline that possess a fused indoline motif as shown in Figure 6.1. These scaffolds are present in many naturally occurring alkaloids.[12,13,14,15,16,17,18,19]

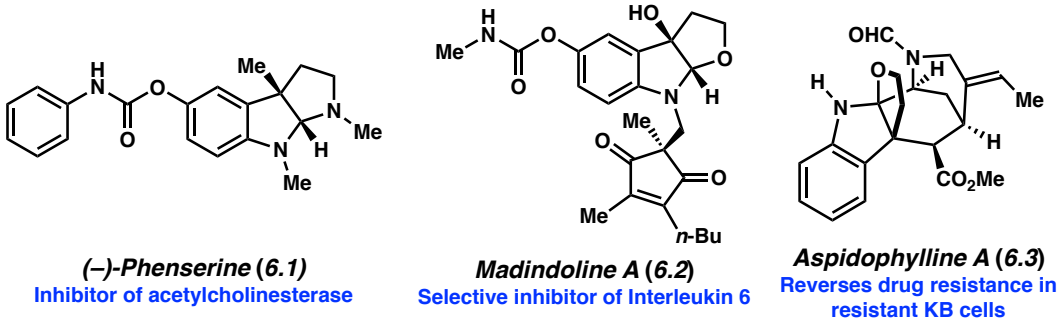

Figure 6.1. Example of representative bioactive compounds containing fused indolines.

The Fischer indolization reaction is an efficient way to construct fused indoline ring-systems, although several alternate methods have also been developed to access these biologically important motifs.[19,20,21] A variant of this reaction, the Garg interrupted Fischer indolization, has the advantage of producing three new bonds, two heterocyclic rings and two stereogenic centers, in one reaction.[15,16] This methodology is convergent, broad in scope, proceeds under mild reaction conditions, and can be used to synthesize a variety of natural products.[15] In one such example, this transformation has been recently utilized in the total synthesis of Aspidophylline A (**6.3**) and its aza-analog.[18,22]

Continuous-flow microfluidic reactor based approaches allow for rapid synthesis of products in a green chemistry mode.[2] While there are few reports on Fischer indolization reactions using a microfluidic reactor, this is not the case with the interrupted Fisher indolization reaction to the best of our knowledge.[23,24,25] We describe here the development of a microfluidic

reactor process for the preparation of indoline and azaindoline compounds using the interrupted Fischer indolization reaction, which complements known batch chemistry (Scheme 6.1).[15] This microfluidic reaction allows for the synthesis of indoline-containing products by the reaction of hydrazines and latent aldehydes under mildly acidic conditions. The methodology allows for efficient reagent mixing, smaller reaction volumes, optimal heat transfer, precise reaction (retention) times, and the possibility to conduct multistep reactions in a single or continuous sequence. Thus, this microfluidic approach can be of general utility for synthesis of such biologically relevant molecules in a safe, environmentally friendly, and cost effective manner that could be amenable to large scale manufacturing.

Scheme 6.1. General flow reactor scheme.

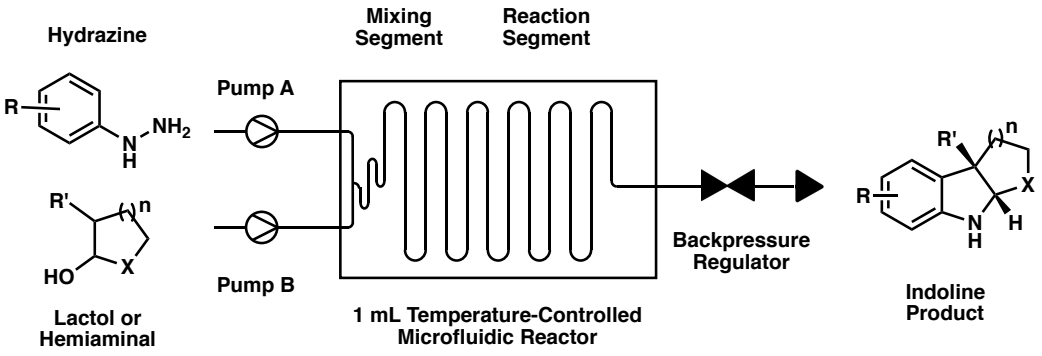

6.3 Results and Discussion

Our approach to obtain indoline scaffolds in the microfluidic reactor using the interrupted Fischer indole synthesis is shown in Table 6.1.[15] As part of developing this transformation we initially tried the reaction of phenyl-hydrazine (**6.4**) and lactol (latent aldehyde) **6.5** in the reactor using (1:1) AcOH:H_2O at 60 °C and 1 bar pressure to determine if we could obtain furoindoline **6.6**. Unfortunately, we did not get any product under these conditions. Next, we changed the

temperature, pressure and retention time in the microfluidic reactor to determine the reaction outcome. After several variations we found that successful interrupted Fischer indolization reaction occurred at 80 °C, 2 bar pressure, and 20 min retention time in the microfluidic reactor affording the desired furoindoline **6.6** in 84% yield (entry 5). Further increasing the temperature, pressure and retention time in the microfluidic reactor led to the optimal conditions of 120 °C, 3 bar pressure and 5 min retention time in the microfluidic reactor affording a 97% yield of **6.6** as determined by HPLC (entry 8). Scale up and purification of the product by flash chromatography gave furoindoline **6.6** in 65% isolated yield.

Table 6.1. Optimization of interrupted Fischer indolization in a microfluidic reactor.[a]

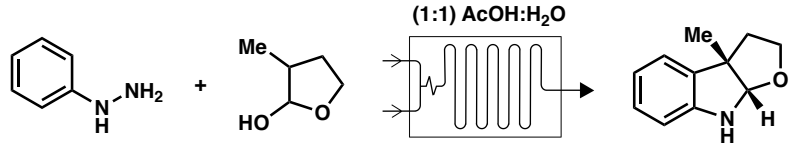

6.4 ***6.5*** ***6.6***

Entry	Pressure (bar)	Temperature (°C)	Flow Rate[b] (μL/min)	Retention Time[c] (min)	Yield[d] (%)
1	1	60	500	2	0
2[e]	2	70	500	2	0
3[e]	2	70	200	5	0
4[e]	2	80	200	5	0
5[e]	2	80	50	20	84
6[e]	2	100	50	20	97
7[f]	3	120	100	10	97
8[f]	3	120	200	5	97[g]

[a] Synthesis of compound **6.6** was done under varying conditions (entry 1–8); two solutions were prepared and introduced by Pump A & B into the Asia microfluidic reactor; one contained the phenyl hydrazine **6.4** (1.0 equiv) in AcOH:H_2O (2.5 mL, 1:1 v/v) and the other contained latent aldehyde **6.5** (1.1 equiv) in AcOH:H_2O (2.5 mL, 1:1 v/v). [b] Combined flow rate from both pumps. [c] Residence time in microfluidic chip reactor (1000 mL volume). [d] HPLC yield from microfluidic flow reactor. [e] Hydrazine added at 0.2 M. Latent aldehyde at 1.1 equiv. [f] Hydrazine added at 0.5 M. Latent aldehyde at 1.1 equiv. [g] Scale-up of reaction yielded furoindoline **6.6** in 65% yield (details in Supplementary Data).

After identifying the optimal microfluidic conditions for the interrupted Fischer indolization, we next conducted the reaction using different hydrazines while keeping the latent aldehyde (**6.5**) constant. As shown in Table 6.2, the reaction is broad in scope with respect to the hydrazine surrogates. Both para- and ortho- substituents were tolerated under the microfluidic reaction condition (entries 1, 2, 4, 5 and 6) and afforded the corresponding furoindoline products in good yields. The *N*-methyl-substituted hydrazine **6.9** was shown to be a competent coupling partner (entry 3) and afforded the desired N-methyl furoindoline **6.16** in 68% yield while use of the *p*-methoxypyridylhydrazine salt **6.13** afforded the furanoazaindoline **6.20** in moderate 40% yield (entry 7). Several of the products such as the haloindolines (entries 2, 5, 6), are setup for further functionalization by transition-metal-catalyzed cross-coupling chemistry.

Table 6.2. Hydrazine variants in the microfluidic interrupted Fischer indolization reaction.[a]

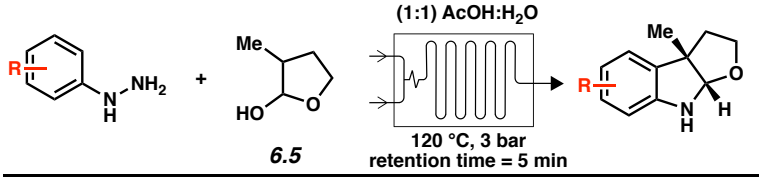

6.5

Entry	Hydrazine Variant	Product	Yield
1	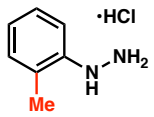 **6.7**	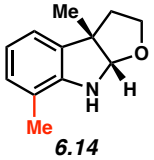 **6.14**	78%
2	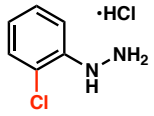 **6.8**	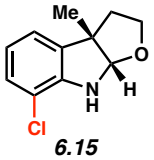 **6.15**	57%
3	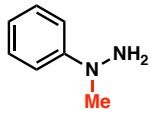 **6.9**	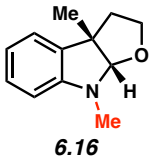 **6.16**	68%
4	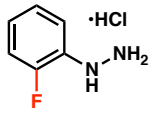 **6.10**	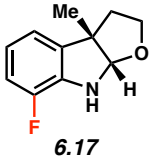 **6.17**	34%
5	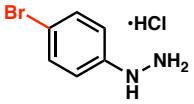 **6.11**	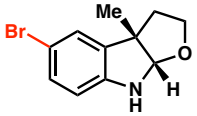 **6.18**	55%
6	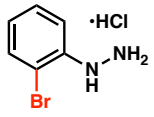 **6.12**	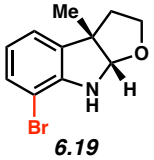 **6.19**	56%
7	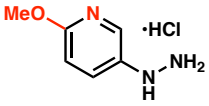 **6.13**	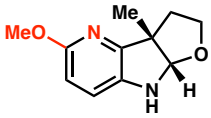 **6.20**	40%

[a] The reactions were performed using optimized condition (see Table 6.1, entry 8); two solutions were prepared and introduced by Pump A & B into the Asia microfluidic reactor; one contained the different hydrazine surrogates (**6.7**–**6.13**) (1.0 equiv) in AcOH:H_2O (2.5 mL, 1:1 v/v) and the other contained latent aldehyde **6.5** (1.1 equiv) in AcOH:H_2O (2.5 mL, 1:1 v/v). Average isolated yields from at least two trials for products (**6.14**–**6.20**) are reported.

We further evaluated the scope of the transformation with nitrogen- or oxygen-containing latent aldehyde coupling partners using phenyl hydrazine **6.4** (Table 6.3). The use of five-membered oxygen- or nitrogen-containing latent aldehydes afforded the corresponding furoindoline **6.24** and pyrrolidinoindoline **6.25** in 49% and 42% yield, respectively. Interestingly, even the six-membered homolog (**6.26**) of the pyrrolidinoindoline framework was obtained using this methodology, although in lower yield.

Table 6.3. Variations of the latent aldehyde surrogate in the microfluidic reaction.[a]

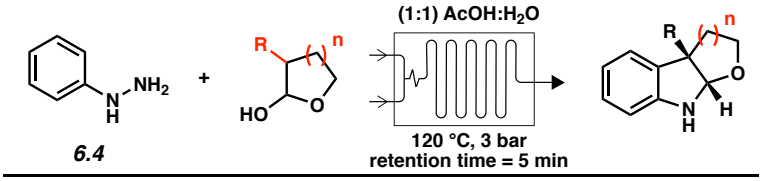

6.4

Entry	Lactol Variant	Product	Yield
1[b]	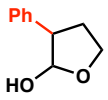 ***6.21***	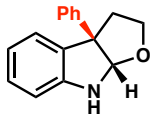 ***6.24***	49%
2[c]	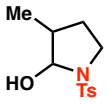 ***6.22***	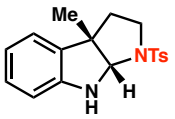 ***6.25***	42%
3[d]	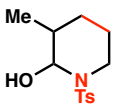 ***6.23***	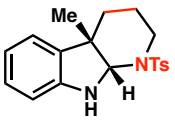 ***6.26***	21%

[a] The reactions were performed using optimized conditions (see Table 6.1, entry 8); two solutions were prepared and introduced by Pump A & B into the Asia microfluidic reactor; one contained the phenyl hydrazine (**6.4**) (1.0 equiv) in AcOH:H_2O (0.5 mL, 1:1 v/v) and the other contained lactol variant (**6.21**–**6.23**) (1.1 equiv) in AcOH:H_2O or AcOH (0.5 mL, 1:1 v/v). Average isolated yields from at least two trials for products (**6.24**–**6.26**) are reported. [b] Hydrazine added at 0.4 M. Latent aldehyde at 1.1 equiv due to insolubility of latent aldehyde **6.21**. [c] Hydrazine added at 0.1 M. Latent aldehyde at 1.1 equiv due to insolubility of latent aldehyde **6.22**. [d] Hydrazine added at 0.4 M. Latent aldehyde at 1.1 equiv due to insolubility of latent aldehyde **6**.**23** & reaction performed in AcOH.

6.4 Conclusion

The use of a microfluidic reactor for the interrupted Fischer indolization resulted in short reaction times and led to indoline and azaindoline products in reasonable yields. We were able to accelerate the microfluidic reaction by increasing temperature and pressure to achieve yields up to 97% with 5 minutes residence time in the reactor. This rapid green chemistry methodology should facilitate continuous synthesis of fused indoline ring systems that can potentially be coupled with additional microfluidic reactors for multistep synthesis. This approach allows for rapid synthesis of these important scaffolds as dual enzyme inhibitors and should prove useful for the discovery of new drug candidates.

6.5 Experimental Section

6.5.1 Materials and Methods

All chemicals used for synthesis were used as received from commercial sources. Phenylhydrazine (**6.4**), 4-bromophenylhydrazine hydrochloride (**6.11**), 2-fluorophenylhydrazine hydrochloride (**6.10**), and 2-bromophenylhydrazine hydrochloride hydrate (**6.12**) were obtained from TCI. All other chemicals were synthesized as previously reported[17] from the Garg lab. Analytical thin–layer chromatographic separations were carried out on silica gel (60 Å particle size, 250 μm thickness, F-254, Silicycle) coated glass plates; spots were visualized with UV light. HPLC data was gathered using an Agilent 1260 Infinity instrument and an Agilent Poroshell-120 column (2.7 um particle size, 4.6 mm diameter x 50 mm length) using a gradient method of 60:40 (Acetonitrile:H_2O) to 98:2 (Acetonitrile:H_2O) over 5 minutes. ^{1}H NMR spectra were recorded using a 400 MHz Bruker spectrometer and reported in parts per million (ppm, δ) relative to chemical residual ^{1}H

resonance of the solvent $CDCl_3$ at 7.26 ppm. Data for ^1H NMR spectra are reported as follows: chemical shift (ppm, δ), multiplicity, coupling constant (Hz), and integration. ^{13}C NMR spectra are reported in terms of chemical shift (ppm, δ), relative to the central line of $CDCl_3$ at 77.16 ppm.

6.5.2 General Information for Flow Reactor Setup

The experiments were conducted using the commercially available Asia continuous-flow system from Syrris. The system configuration consisted of an Asia Pressurized Input Store, Syringe Pump, Reagent Injector, Chip Climate Controller, and Pressure Controller, all connected via PTFE tubing (1.6 mm OD x 0.5 mm ID) purchased from Syrris. The Pressurized Input Store allowed storage of our mobile solvent phase under an inert nitrogen atmosphere. From the Store, solvent would flow to two separate Syringe pumps, then to the Reagent Injector, Chip Climate Controller, and Backpressure Regulator. The system's modular design allowed for independent modification to each reaction parameter. Individual flow rates could be independently changed at each Syringe Pump, which determined residence and reaction time through the reactor. This time derived from the reactor chip volume, divided by the combined flow rate through it. Reaction temperatures could be controlled through the Chip Climate Controller, which houses the microfluidic chip reactor, and reaction pressure could be changed (as in Table 6.1) through the Backpressure Regulator.

Scheme 6.2. Asia flow reactor scheme.

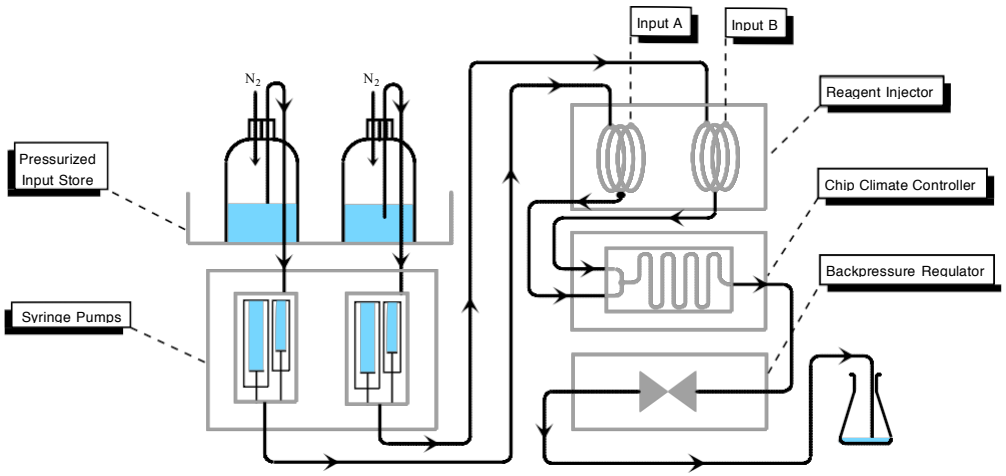

Figure 6.2. Flow reactor setup.

6.5.3 General Procedure for Flow Reactor Syntheses and Purification

Unless stated otherwise, reactions were performed in a Syrris 1000 μL glass microfluidic chip reactor (part number 2100146). Prepared stock solutions of the phenylhydrazine and lactol were charged into separate 1 mL syringes and injected into the Reagent Injector Inputs A and B. In cases when reagents did not readily dissolve, sonication and heating were used until the reagents were fully dissolved. Reagents were then introduced into the microfluidic chip reactor by Pumps A and B. The mixture was pumped through the reactor at a predetermined flow rate to achieve desired residence times. Crude product was then purified via flash chromatography using a Combiflash R_f200 instrument and prepacked silica gel (300–400 mesh) cartridges (Hexanes, 5 minutes; 100% Hexanes → 5:95 (EtOAc:Hexanes), 10 minutes; 5:95 (EtOAc:Hexanes), 5 minutes; 5:95 (EtOAc:Hexanes) → 1:4 (EtOAc:Hexanes), 10 minutes; 1:4 (EtOAc:Hexanes) → 7:3 (EtOAc:Hexanes), 5 minutes). Fractions corresponding to the product were combined and isolated under vacuum.

6.5.4 Optimization of Flow Parameters and Substrate Synthesis

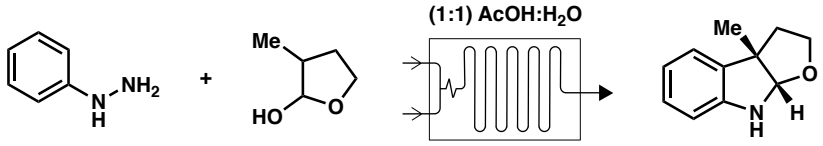

6.4 *6.5* *6.6*

Representative Procedure. Synthesis of Indoline 6.6 (Table 6.1, entries 1–6). Phenylhydrazine **6.4** (0.2 M in AcOH/H_2O (1:1 v/v), 50 μL, 0.01 mmol, 1 equiv) was injected into Pump A. Lactol **6.5 (**0.22 M in AcOH/H_2O (1:1 v/v), 50 μL, 0.011 mmol, 1.1 equiv) was injected into Pump B. Temperature, pressure, and flow rates were changed to achieve designated reaction conditions. The chip was flushed with AcOH/H_2O (1:1 v/v) to elute the

product. Crude product was collected in a flask. Product yields were determined by HPLC. Yield was obtained by percent ratio of the product peak to that for the starting materials.

Representative Procedure. Synthesis of Indoline 6.6 (Table 6.1, entry 7). Phenylhydrazine **6.4** (0.5 M in AcOH/H_2O (1:1 v/v), 50 μL, 0.025 mmol, 1 equiv) was injected into Pump A. Lactol **6.5** (0.55 M in AcOH/H_2O (1:1 v/v), 50 μL, 0.028 mmol, 1.1 equiv) was injected into Pump B. Chip reactor was preheated to 120 °C and pressure was set to 3 bar. Pumps A and B were both set to 50 μL/min flow rates to achieve a 10 min residence time. The chip was flushed with AcOH/H_2O (1:1 v/v) to elute the product. Crude product was collected in a flask. Product yield was determined by HPLC to be 97%.

Representative Procedure. Synthesis of Indoline 6.6 (Table 6.1, entry 8). Phenylhydrazine **6.4** (0.5 M in AcOH/H_2O (1:1 v/v), 5 mL, 2.5 mmol, 1 equiv) was injected into Pump A. Lactol **6.5** (0.55 M in AcOH/H_2O (1:1 v/v), 5 mL, 2.75 mmol, 1.1 equiv) was injected into Pump B. Chip reactor was preheated to 120 °C and pressure was set to 3 bar. Pumps A and B were both set to 100 μL/min flow rates to achieve a final 200 μL/min flow rate and 5 min residence time in the reactor. Crude product was collected in a flask, and crude yield was determined by HPLC. The crude product was quenched with a solution of sat. aq. $NaHCO_3$ (2 x 30 mL) and extracted with EtOAc (2 x 60 mL). Combined organic phases were dried over Na_2SO_4 and concentrated under reduced pressure. Purification by flash chromatography afforded furoindoline **6.6** **(**(3a*S*,8a*S*)-3a-methyl-3,3a,8,8a-tetrahydro-2*H*-furo[2,3-*b*]indole**)** as a brown oil (285 mg, 65% yield). R*f* 0.3 (3:1 Hexanes:EtOAc); ^{1}H NMR (400 MHz, $CDCl_3$) δ 7.12–7.03 (m, 2H), 6.77 (t, *J*= 7.4 Hz, 1H), 6.59 (d, *J* = 7.8 Hz, 1H), 5.29 (s, 1H), 3.97 (ddd, *J* = 8.7, 7.2, 1.6 Hz,

1H), 3.58 (ddd, *J*= 11.1, 8.6, 5.2 Hz, 1H), 2.21–2.06 (m, 2H), 1.48 (s, 3H). Spectral data match those previously reported.[15]

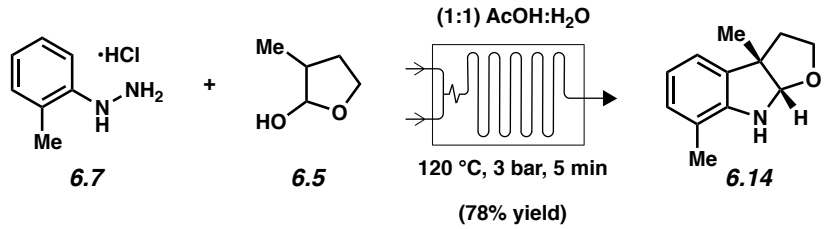

Representative Procedure. Synthesis of Indoline 6.14 (Table 6.2, entry 1) is used as an example. Phenylhydrazine **6.7** (0.5 M in AcOH/H_2O (1:1 v/v), 500 uL, 0.25 mmol, 1.0 equiv) was injected into Pump A. Lactol **6.5** (0.55 M in AcOH/H_2O (1:1 v/v), 500 uL, 0.28 mmol, 1.1 equiv) was injected into Pump B. Chip reactor was preheated to 120 °C and pressure was set to 3 bar. Pumps A and B were both set to 100 μL/min flow rates to achieve a 5 min residence time. The crude product was quenched with a solution of sat. aq. $NaHCO_3$ (20 mL) and extracted with EtOAc (3 x 20 mL). Combined organic phases were dried over Na_2SO_4 and concentrated under reduced pressure. Purification by flash chromatography afforded furoindoline **6.14** ((3a*S*,8a*S*)-3a,7- dimethyl-3,3a,8,8a-tetrahydro-2*H*-furo[2,3-*b*]indole) as a brown solid (78% yield, average of two experiments). R*f* 0.4 (3:1 Hexanes:EtOAc); ^{1}H NMR (400 MHz, $CDCl_3$) δ 6.95 (d, *J* = 7.9 Hz, 1H), 6.91 (d, *J* = 6.4 Hz, 1H), 6.72 (t, *J* = 7.4 Hz, 1H), 5.32 (s, 1H), 3.95 (ddd, *J* = 8.8, 7.2, 1.7 Hz, 1H), 3.68–3.45 (m, 1H), 2.21–2.17 (m, 1H), 2.15 (s, 3H), 2.13–2.04 (m, 1H), 1.48 (s, 3H). Spectral data match those previously reported.[15]

Any modifications of the conditions shown in this representative procedure are specified in the following schemes, which depict all of the reactions in Table 6.2.

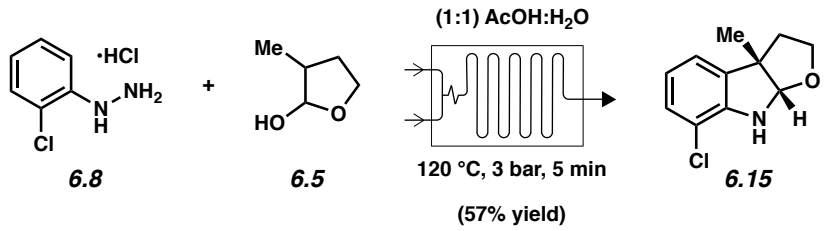

Indoline 6.15 (Table 6.2, entry 2). Purification by flash chromatography afforded furoindoline **6.15** ((3a*S*,8a*S*)-7-chloro-3a-methyl-3,3a,8,8a-tetrahydro-2*H*-furo[2,3-*b*]indole) as a yellow solid (57% yield, average of two experiments). R*f* 0.4 (3:1 Hexanes:EtOAc); ^{1}H NMR (400 MHz, $CDCl_3$) δ 7.05 (d, *J* = 9.1 Hz, 1H), 6.96 (d, *J* = 8.4 Hz, 1H), 6.71–6.65 (m, 1H), 5.33 (s, 1H), 3.97 (ddd, *J* = 8.8, 7.1, 1.7 Hz, 1H), 3.57 (ddd, *J* = 11.1, 8.7, 5.2 Hz, 1H), 2.16 (ddd, *J* = 11.7, 5.2, 1.4 Hz, 1H), 2.13–2.04 (m, 1H), 1.48 (s, 3H). Spectral data match those previously reported. [15]

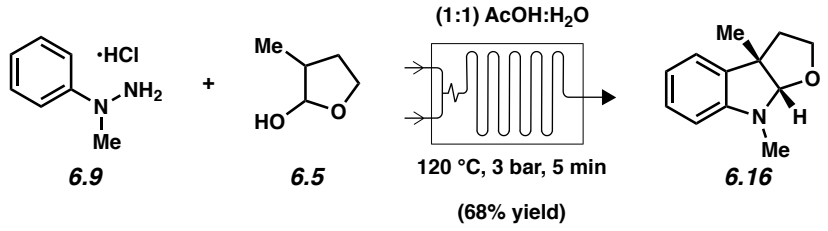

Indoline 6.16 (Table 6.2, entry 3). Purification by flash chromatography afforded furoindoline **6.16** ((3a*S*,8a*S*)-3a,8-dimethyl-3,3a,8,8a-tetrahydro-2*H*-furo[2,3-*b*]indole) as a colorless oil (68% yield, average of two experiments). R*f* 0.5 (3:1 Hexanes:EtOAc); ^{1}H NMR (400 MHz, $CDCl_3$) δ 7.14–7.08 (m, 1H), 7.05 (d, *J* = 6.4 Hz, 1H), 6.68 (t, *J* = 7.8 Hz, 1H), 6.37 (d, *J* = 7.8 Hz, 1H), 5.07 (s, 1H), 3.95 (ddd, *J* = 8.7, 7.2, 1.6 Hz, 1H), 3.46 (ddd, *J* = 11.0, 8.6, 5.3 Hz, 1H), 2.93 (s, 3H), 2.29–1.91 (m, 2H), 1.46 (s, 3H). Spectral data match those previously reported. [15]

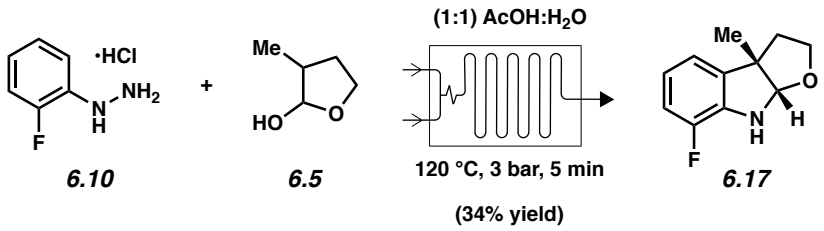

Indoline 6.17 (Table 6.2, entry 4). Purification by flash chromatography afforded furoindoline **6.17** ((3a*S*,8a*S*)-7-fluoro-3a-methyl-3,3a,8,8a-tetrahydro-*H*-furo[2,3-*b*]indole) as a brown amorphous solid (34% yield, average of two experiments). R*f* 0.4 (3:1 Hexanes:EtOAc); ^{1}H NMR (400 MHz, $CDCl_3$) δ 6.88–6.81 (m, 2H), 6.69 (ddd, *J* = 8.2, 7.3, 4.6 Hz, 1H), 5.33 (s, 1H), 3.97 (ddd, *J* = 8.8, 7.2, 1.7 Hz, 1H), 3.57 (ddd, *J* = 11.1, 8.7, 5.2 Hz, 1H), 2.18 (ddd, *J* = 12.0, 5.2, 1.7 Hz, 1H), 2.09 (ddd, *J* = 12.0, 11.1, 7.2 Hz, 1H), 1.48 (s, 3H); ^{13}C NMR (101 MHz, $CDCl_3$) δ 147.73 ($J_{C\text{-}F}$ = 2.39), 137.69 ($J_{C\text{-}F}$ = 0.05), 136.16 ($J_{C\text{-}F}$ = 0.13), 119.54 ($J_{C\text{-}F}$ = 0.06), 118.55 ($J_{C\text{-}F}$ = 0.03), 114.63 ($J_{C\text{-}F}$ = 0.17), 100.23, 67.77, 54.83, 41.55, 24.69; ^{19}F NMR (376 MHz, $CDCl_3$) δ –136.09 (two minor peaks seen in ^{19}F NMR spectrum could be inseperable isomers likely from impurities in the starting hydrazine). HRMS-ESI (m/z) $[M + H]^+$ calcd for $C_{11}H_{13}FNO^+$, 194.09757; found, 194.09755.

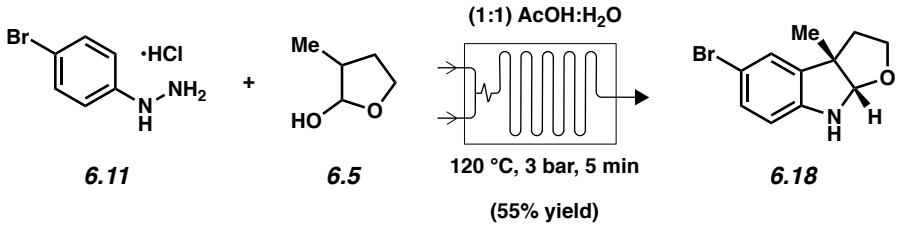

Indoline 6.18 (Table 6.2, entry 5). Phenylhydrazine **6.11** (0.25 M in AcOH/H_2O (1:1 v/v), 500 uL, 1 equiv) was injected into Pump A. Lactol **6.5** (0.275 M in AcOH/H_2O (1:1 v/v), 500 uL, 1.1 equiv) was injected into Pump B. Chip reactor was preheated to 120 °C and pressure was set to 3 bar. Pumps A and B were both set to 100 μL/min flow rates to achieve a 5 min residence

time. The crude product was quenched with a solution of sat. aq. $NaHCO_3$ (20 mL) and extracted with EtOAc (3 x 20 mL). Combined organic phases were dried over Na_2SO_4 and concentrated under reduced pressure. Purification by flash chromatography afforded furoindoline **6.18** ((3a*S*,8a*S*)-5-bromo-3a-methyl-3,3a,8,8a-tetrahydro-2*H*-furo[2,3-*b*]indole) as a yellow oil (55% yield, average of two experiments). R*f* 0.3 (3:1 Hexanes:EtOAc); ^{1}H NMR (400 MHz, $CDCl_3$) δ 7.16 (d, *J* = 1.7 Hz, 1H), 7.13 (dd, *J* = 8.2, 2.0 Hz, 1H), 6.45 (d, *J* = 8.4 Hz, 1H), 5.26 (s, 1H), 3.96 (ddd, *J* = 8.8, 7.1, 1.7 Hz, 1H), 3.61–3.48 (m, 1H), 2.19–2.12 (m, 1H), 2.11–2.03 (m, 1H), 1.46 (s, 3H); ^{13}C NMR (101 MHz, $CDCl_3$) δ 148.08, 136.58, 130.78, 126.31, 110.52, 109.72, 99.92, 67.57, 54.19, 41.56, 24.74; HRMS-ESI (m/z) $[M + H]^+$ calcd for $C_{11}H_{13}BrNO^+$, 254.01750; found, 254.01751.

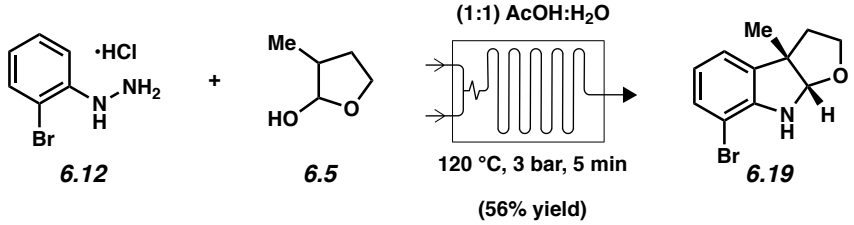

Indoline 6.19 (Table 6.2, entry 6). Purification by flash chromatography afforded furoindoline **6.19 (**(3a*S*,8a*S*)-7-bromo-3a-methyl-3,3a,8,8a-tetrahydro-2*H*-furo[2,3-*b*]indole**)** as a yellow solid (56% yield, average of two experiments). Melting point 39–43 °C; R*f* 0.4 (3:1 Hexanes:EtOAc); ^{1}H NMR (400 MHz, $CDCl_3$) δ 7.19 (d, *J* = 8.0 Hz, 1H), 6.99 (d, *J* = 8.3 Hz, 1H), 6.67–6.59 (m, 1H), 5.32 (s, 1H), 3.97 (ddd, *J* = 8.7, 7.1, 1.7 Hz, 1H), 3.62–3.53 (m, 1H), 2.20–2.13 (m, 1H), 2.12– 2.04 (m, 1H), 1.48 (s, 3H); ^{13}C NMR (101 MHz, $CDCl_3$) δ 147.55, 135.38, 130.59, 121.92, 120.08, 101.79, 98.91, 67.62, 55.48, 41.73, 24.85; HRMS-ESI (m/z) $[M+ H]^+$ calcd for $C_{11}H_{13}BrNO^+$, 254.01750; found, 254.01755.

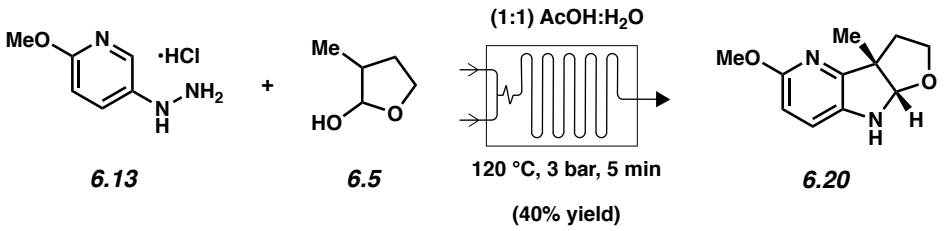

6.13 *6.5* *6.20*

Indoline 6.20 (Table 6.2, entry 7). Purification by flash chromatography afforded furoindoline **6.20** ((3a*S*,8a*S*)-5-methoxy-3a-methyl-3,3a,8,8a-tetrahydro-2*H*-furo[3',2':4,5]pyrrolo[3,2-*b*]pyridine) as a yellow solid (40% yield, average of two experiments). R*f* 0.3 (3:1 Hexanes:EtOAc); ^{1}H NMR (500 MHz, $CDCl_3$) δ 6.88 (d, *J* = 8.4 Hz, 1H), 6.43 (d, *J* = 8.4 Hz, 1H), 5.27 (s, 1H), 3.97 (ddd, *J* = 9.0, 7.5, 1.7 Hz, 1H), 3.87 (s, 3H), 3.53 (ddd, *J* = 11.1, 8.7, 5.3 Hz, 1H), 2.40 (ddd, *J* = 12.1, 5.3, 1.5 Hz, 1H), 2.08–1.98 (m, 1H), 1.47 (s, 3H). Spectral data match those previously reported.[18]

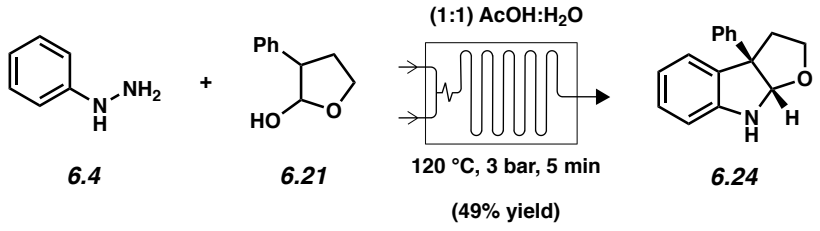

6.4 *6.21* *6.24*

Representative Procedure. Synthesis of Indoline 6.24 (Table 6.3, entry 1) is used as an example. Due to insolublity issues with the lactol, a more dilute solution of the starting materials were used (Table 6.3, entry 1-3). Phenylhydrazine **6.4** (0.4 M in AcOH/H_2O (1:1 v/v), 500 uL, 1 equiv) was injected into Pump A. Lactol **6.21** (0.44 M in AcOH/H_2O (1:1 v/v), 500 uL, 1.1 equiv) into Pump B. Chip reactor was preheated to 120 °C and pressure was set to 3 bar. Pumps A and B were both set to 100 μL/min flow rates to achieve a 5 min residence time. The crude product eluted and quenched with a solution of sat. aq. $NaHCO_3$ (20 mL) and extracted with EtOAc (3 x 20 mL). Combined organic phases were dried over Na_2SO_4 and concentrated under

reduced pressure. Purification by flash chromatography a forded furoindoline **6.24** ((3a*R*,8a*S*)-3a-phenyl-3,3a,8,8a-tetrahydro-2*H*-furo[2,3-*b*]indole) as a colorless oil (49% yield, average of two experiments). R*f* 0.4 (3:1 Hexanes:EtOAc); ^{1}H NMR (400 MHz, $CDCl_3$) δ 7.37–7.28 (m, 4H), 7.25–7.20 (m, 1H), 7.12–7.07 (m, 1H), 7.05–7.01 (m, 1H), 6.76 (td, *J* = 7.4, 1.0 Hz, 1H), 6.67 (d, *J* = 7.8 Hz, 1H), 5.62 (s, 1H), 4.19–4.13 (m, 1H), 3.75–3.62 (m, 1H), 2.83–2.68 (m, 1H), 2.52 (dd, *J* = 11.9, 4.4 Hz, 1H). Spectral data match those previously reported. [15]

Any modifications of the conditions shown in this representative procedure are specified in the following schemes, which depict all of the reactions in Table 6.3.

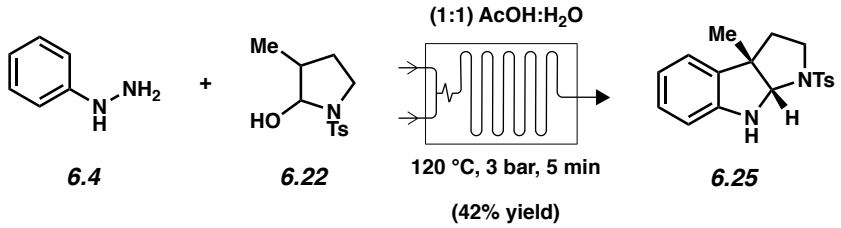

Indoline 6.25 (Table 6.3, entry 2). Phenylhydrazine **6.4** (0.1 M in AcOH/H_2O (1:1 v/v), 500 uL, 1 equiv) was injected into Pump A. Hemiaminal **6.22** (0.11 M in AcOH/H_2O (1:1 v/v), 500 uL, 1.1 equiv) was injected into Pump B. Chip reactor was preheated to 120 °C and pressure was set to 3 bar. Pumps A and B were both set to 100 μL/min flow rates to achieve a 5 min residence time. The crude product was quenched with a solution of sat. aq. $NaHCO_3$ (20 mL) and extracted with EtOAc (3 x 20 mL). Combined organic phases were dried over Na_2SO_4 and concentrated under reduced pressure. Purification by flash chromatography afforded pyrrolidinoindoline **6.25 (**(3a*S*,8a*S*)-3a-methyl-1-tosyl-1,2,3,3a,8,8a-hexahydropyrrolo[2,3-*b*]indole**)** as a yellow solid (42% yield, average of two experiments). R*f* 0.4 (3:1

Hexanes:EtOAc); ^{1}H NMR (400 MHz, $CDCl_3$) δ 7.74 (d, *J* = 8.3 Hz, 2H), 7.32 (d, *J* = 8.4 Hz, 2H), 7.07 (td, *J* = 7.7, 1.3 Hz, 1H), 7.02–6.98 (m, 1H), 6.76 (td, *J* = 7.4, 0.9 Hz, 1H), 6.62 (d, *J* = 7.8 Hz, 1H), 5.03 (s, 1H), 3.41 (ddd, *J* = 10.4, 7.9, 2.6 Hz, 1H), 3.13 (td, *J* = 10.2, 6.1 Hz, 1H), 2.44 (s, 3H), 2.19–2.12 (m, 1H), 1.78 (ddd, *J* = 12.5, 10.1, 7.9 Hz, 1H), 1.27 (s, 3H). Spectral data match those previously reported. [15]

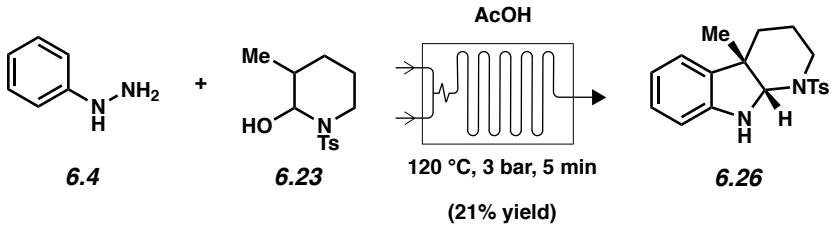

Indoline 6.26 (Table 6.3, entry 3). Phenylhydrazine **6.4** (0.4 M in AcOH, 500 uL, 1 equiv) was injected into Pump A. Hemiaminal **6.23** (0.44 M in AcOH, 500 uL, 1.1 equiv) was injected into Pump B. Chip reactor was preheated to 120 °C and pressure was set to 3 bar. Pumps A and B were both set to 100 μL/min flow rates to achieve a 5 min residence time. The crude product was quenched with a solution of sat. aq. $NaHCO_3$ (20 mL) and extracted with EtOAc (3 x 20 mL). Combined organic phases were dried over Na_2SO_4 and concentrated under reduced pressure. Purification by flash chromatography forded pyrrolidinoindoline **6.26** ((4a*S*,9a*S*)-4a-methyl-1-tosyl-2,3,4,4a,9,9a-hexahydro-1*H*-pyrido[2,3-*b*]indole) as a yellow amorphous solid (21% yield, average of two experiments). R*f* 0.5 (3:1 Hexanes:EtOAc); ^{1}H NMR (400 MHz, $CDCl_3$) δ 7.75 (d, *J* = 8.3 Hz, 2H), 7.34 (d, *J* = 8.0 Hz, 2H), 7.06–7.00 (m, 1H), 6.96 (d, *J* = 7.3 Hz, 1H), 6.75 (t, *J* = 7.9 Hz, 1H), 6.59 (d, *J* = 7.7 Hz, 1H), 5.18 (s, 1H), 3.75–3.61 (m, 1H), 3.27–3.12 (m, 1H), 2.45 (s, 3H), 1.72–1.41 (m, 4H), 1.26 (s, 3H). Spectral data match those previously reported. [15]

6.6 Spectra Relevant to Chapter Six:

Synthesis of Fused Indolines by Interrupted Fischer Indolization in a Microfluidic Reactor

Alexander Tuan-Huy Duong, Bryan J. Simmons, Mohammad Parvez Alam, Jesus Campagna, Neil K. Garg, Varghese John.

Tetrahedron Lett. **2019**, *60*, 322–326.

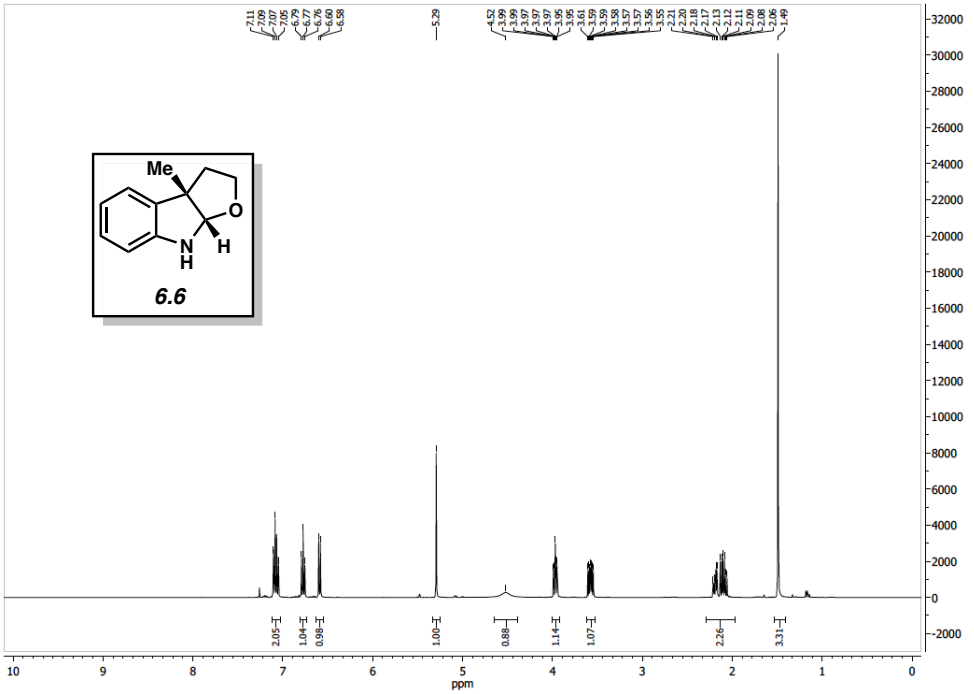

Figure 6.3 ^{1}H NMR (400 MHz, $CDCl_3$) of compound **6.6**.

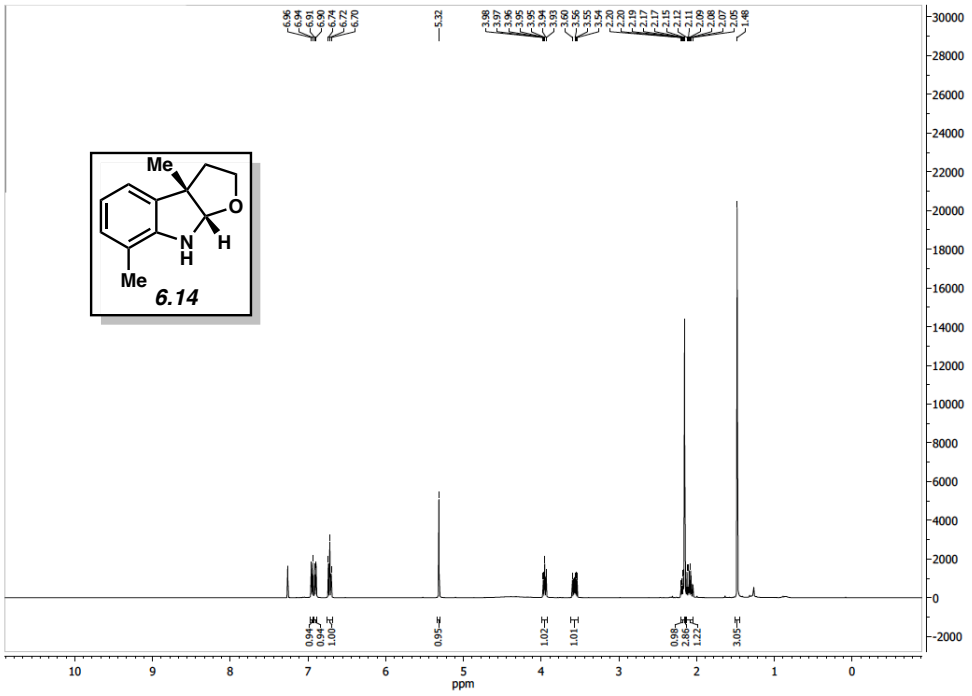

Figure 6.4 ^{1}H NMR (400 MHz, $CDCl_3$) of compound **6.14**.

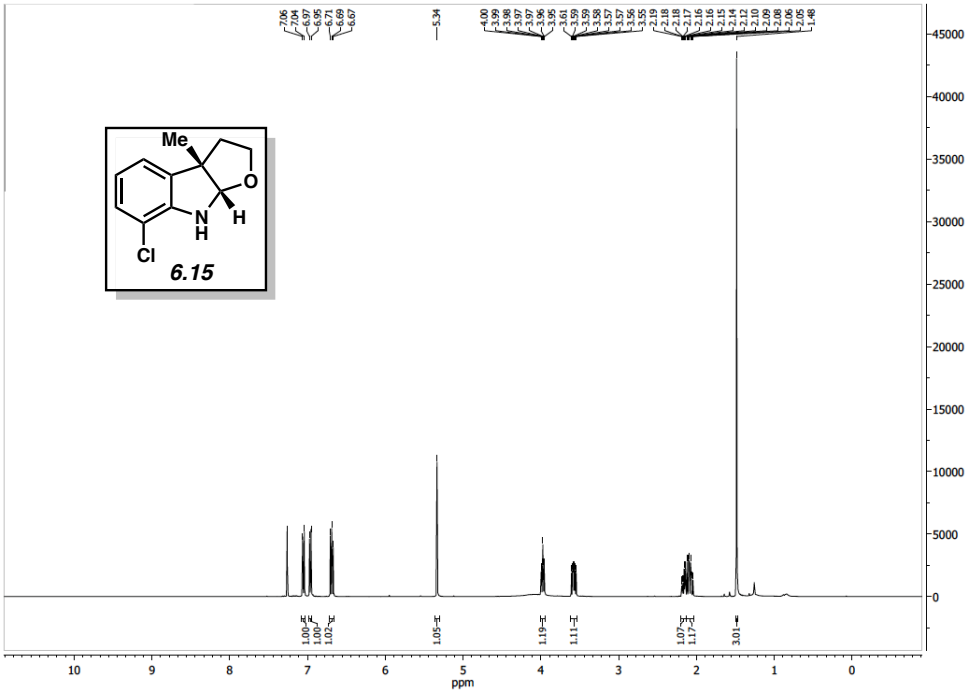

Figure 6.5 ^{1}H NMR (400 MHz, $CDCl_3$) of compound **6.15**.

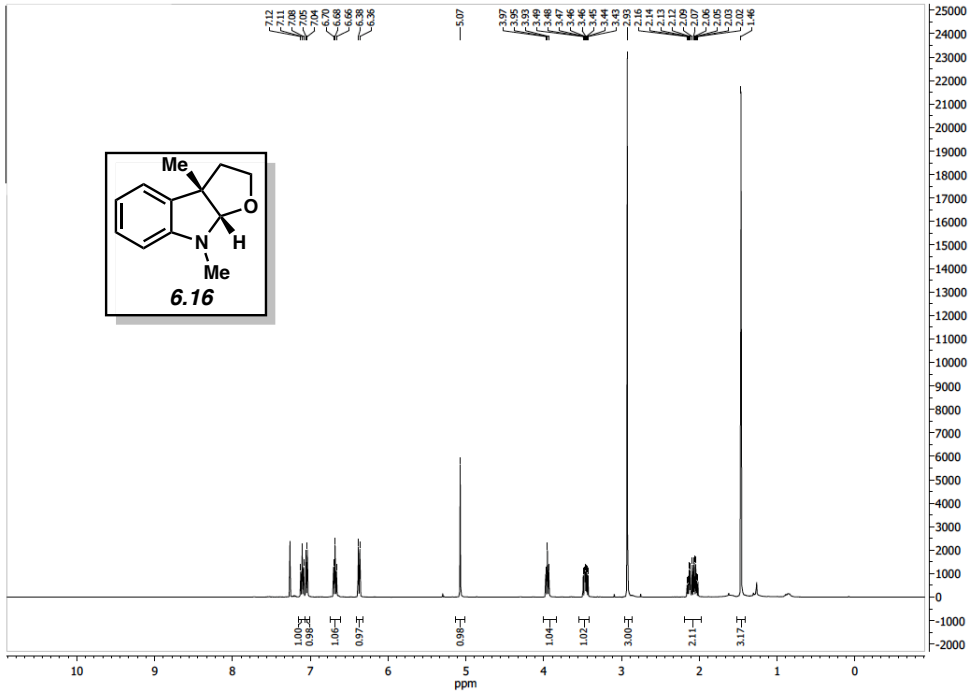

Figure 6.6 ^{1}H NMR (400 MHz, $CDCl_3$) of compound **6.16**.

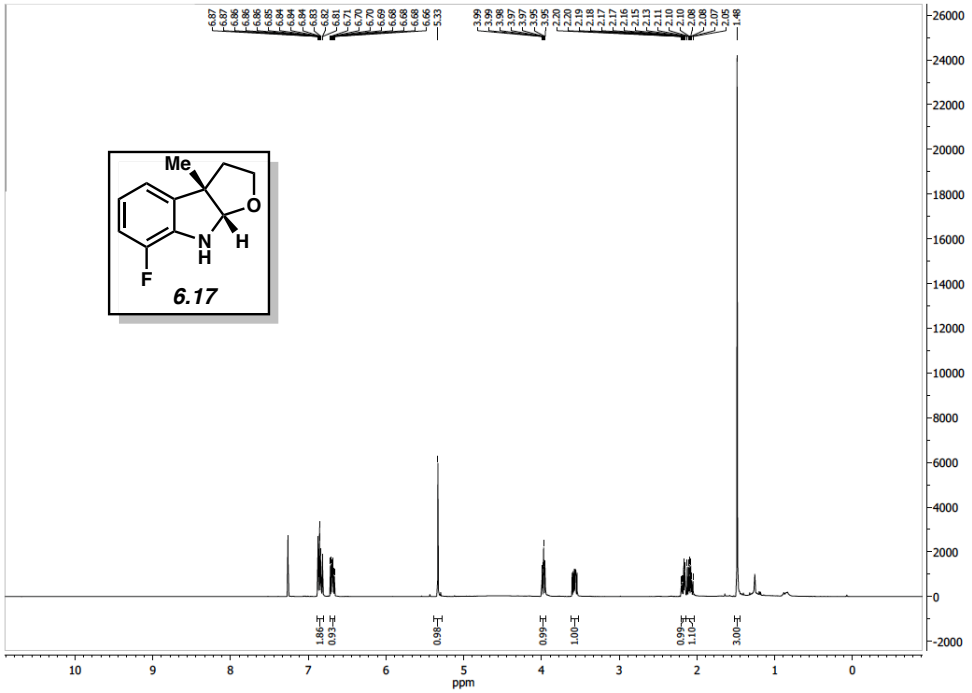

Figure 6.7 ^{1}H NMR (400 MHz, $CDCl_3$) of compound **6.17**.

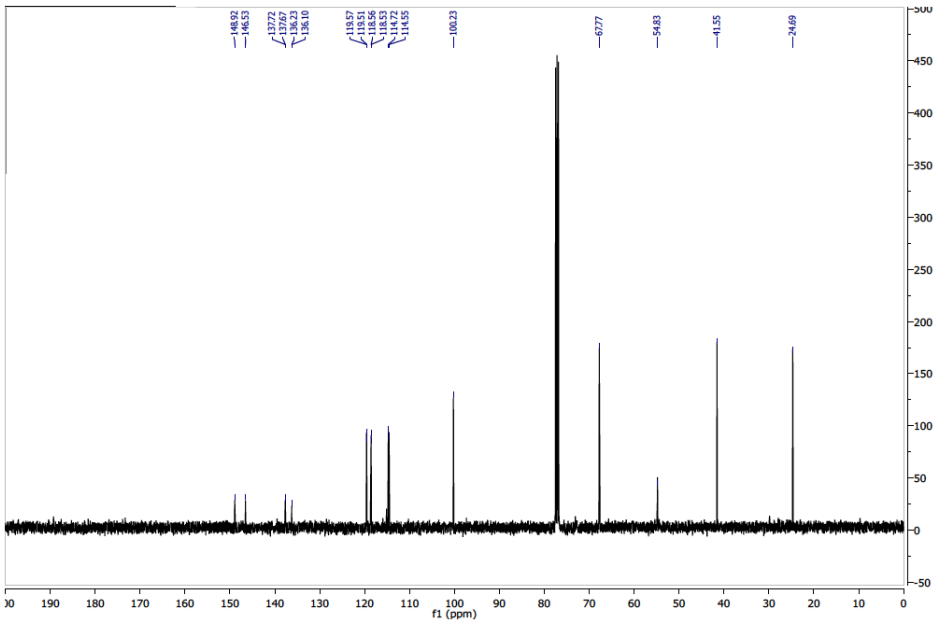

Figure 6.8 ^{13}C NMR (101 MHz, $CDCl_3$) of compound **6.17**.

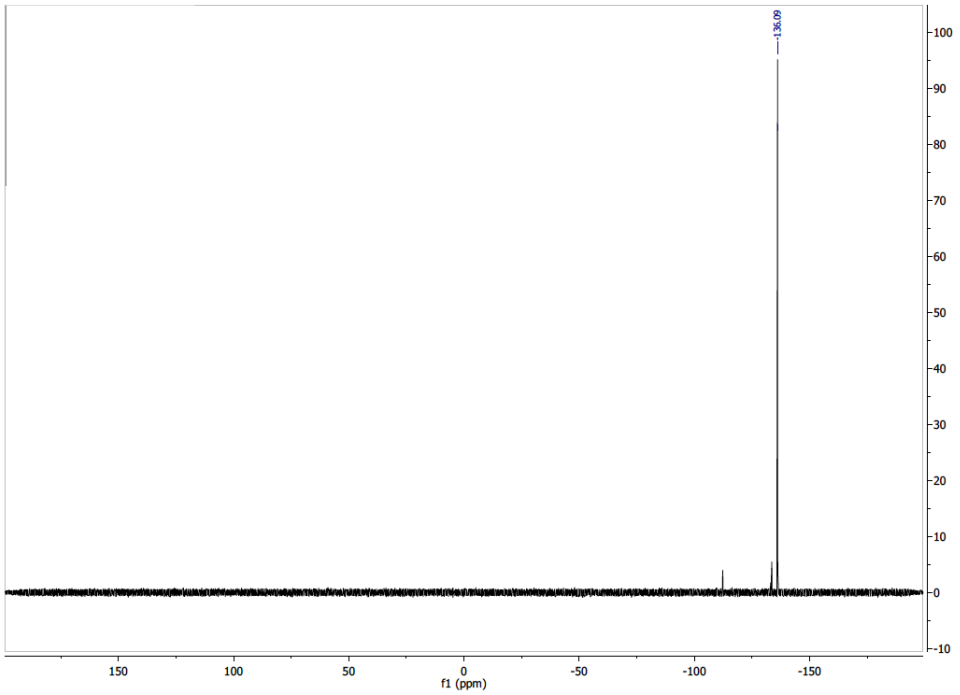

Figure 6.9 ^{19}F NMR (376 MHz, $CDCl_3$) of compound **6.17**.

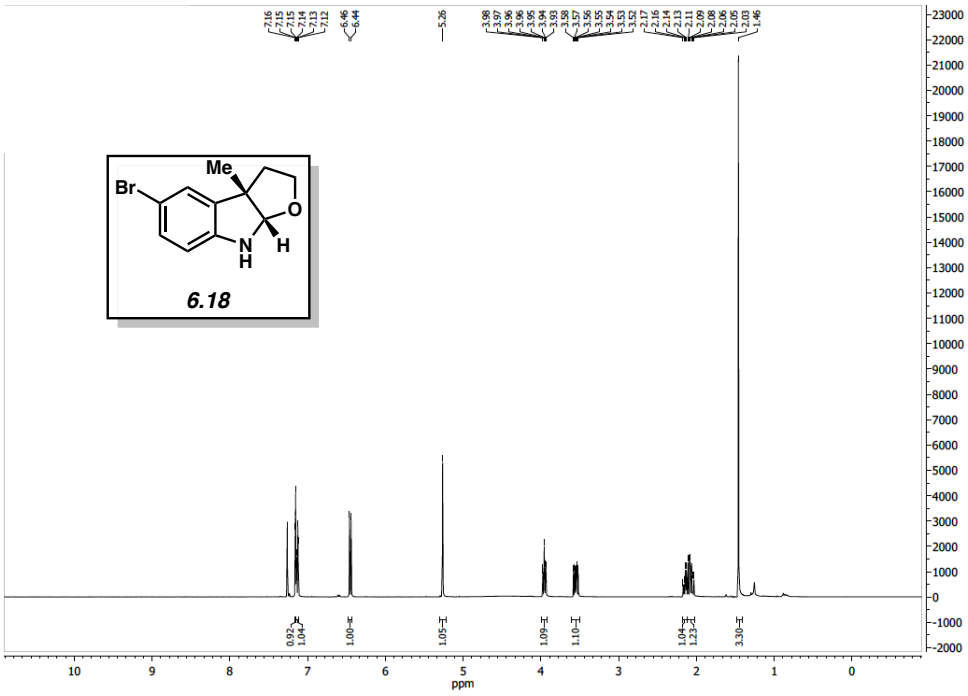

Figure 6.10 ^{1}H NMR (400 MHz, $CDCl_3$) of compound **6.18**.

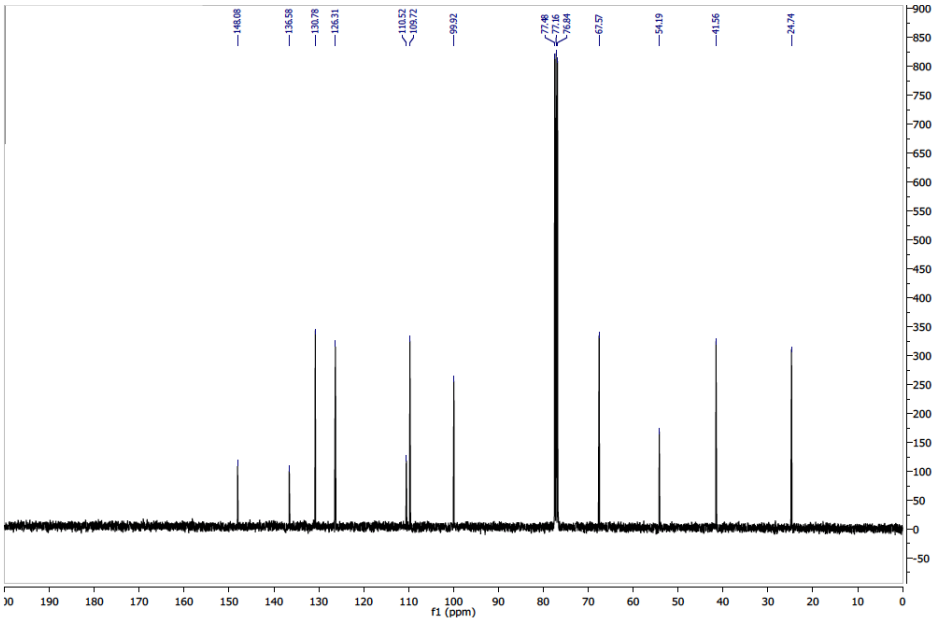

Figure 6.11 ^{13}C NMR (101 MHz, $CDCl_3$) of compound **6.18**.

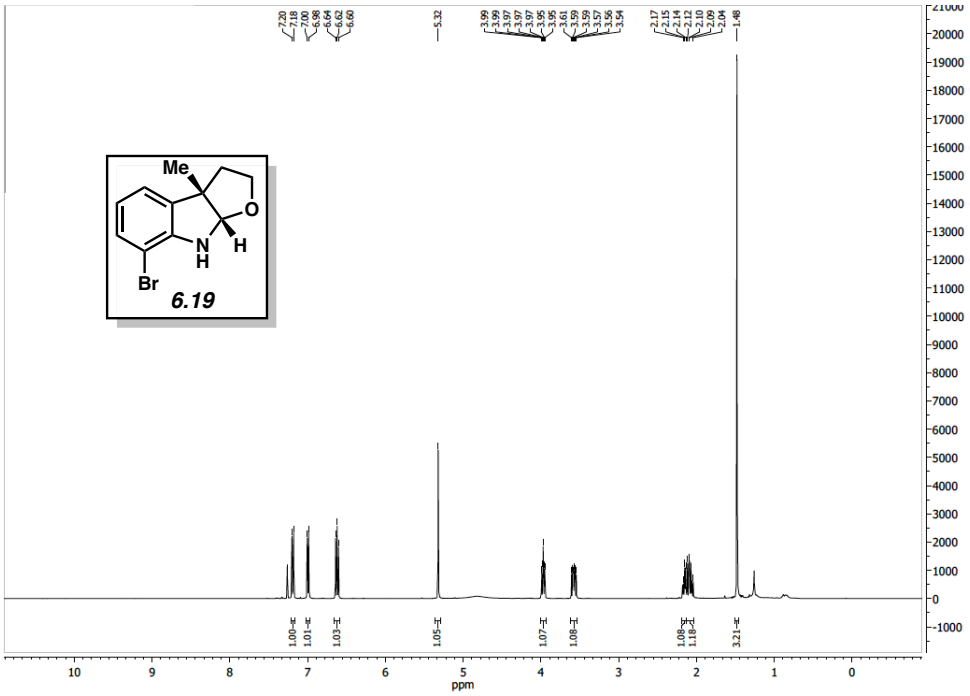

Figure 6.12 ^{1}H NMR (400 MHz, $CDCl_3$) of compound **6.19**.

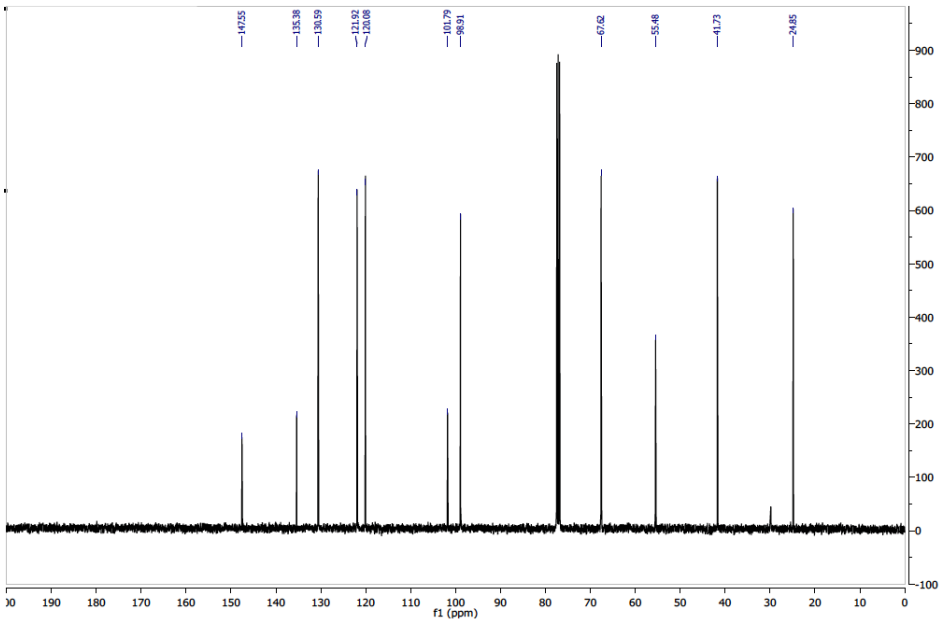

Figure 6.13 ^{13}C NMR (101 MHz, $CDCl_3$) of compound **6.19**.

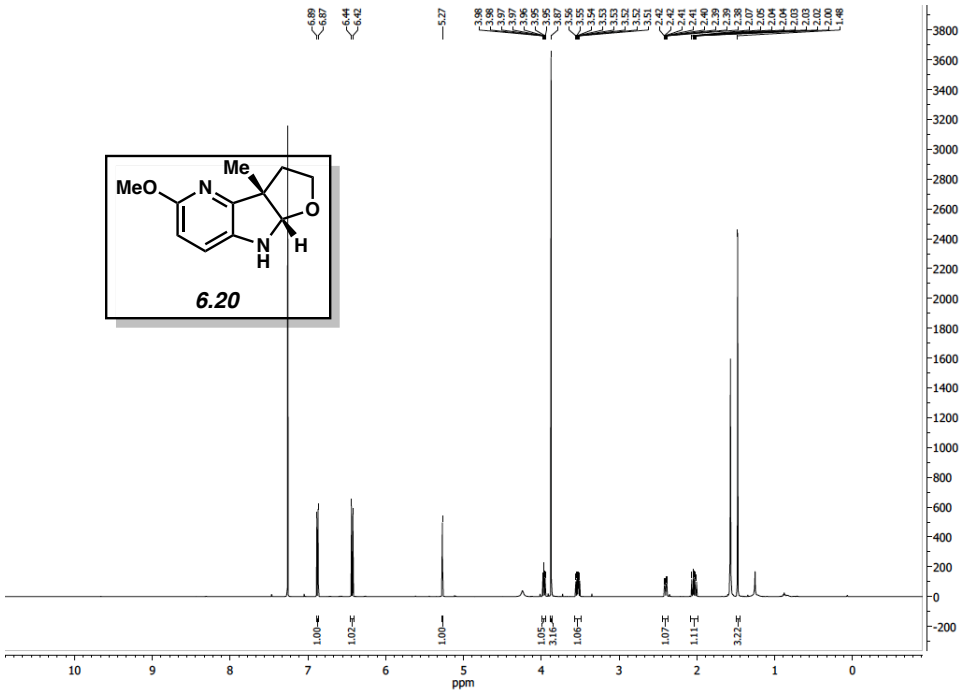

Figure 6.14 ^{1}H NMR (400 MHz, $CDCl_3$) of compound **6.20**.

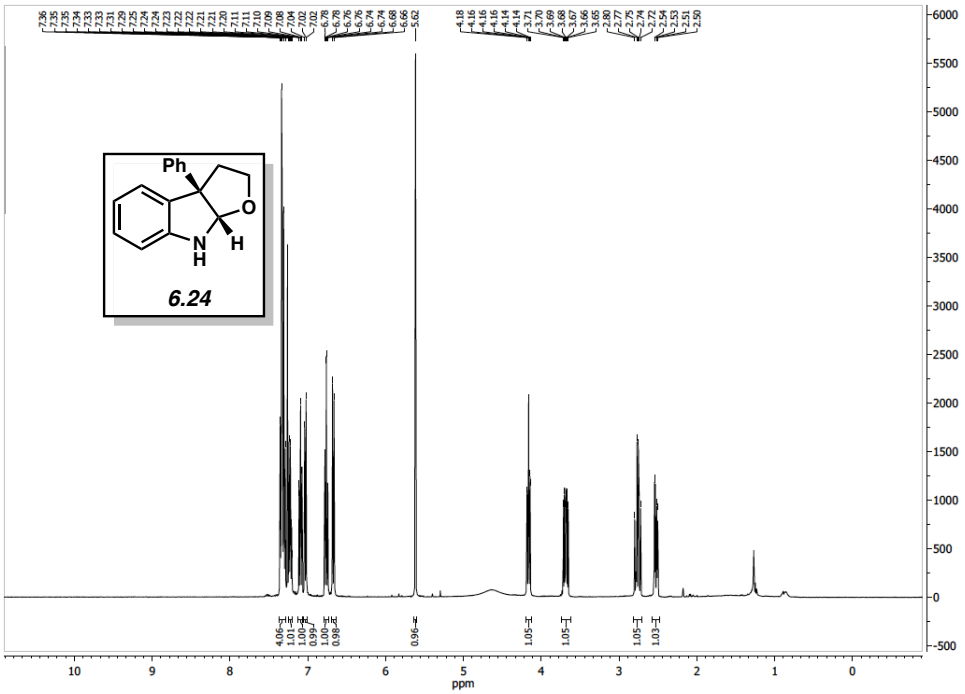

Figure 6.15 ^{1}H NMR (400 MHz, $CDCl_3$) of compound **6.24**.

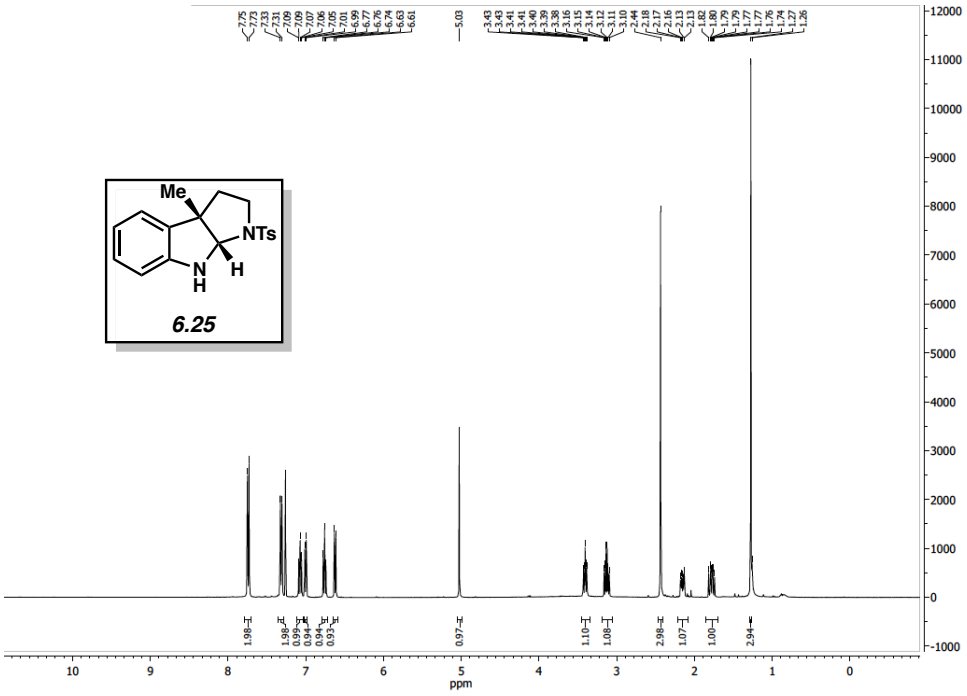

Figure 6.16 ^{1}H NMR (400 MHz, $CDCl_3$) of compound **6.25**.

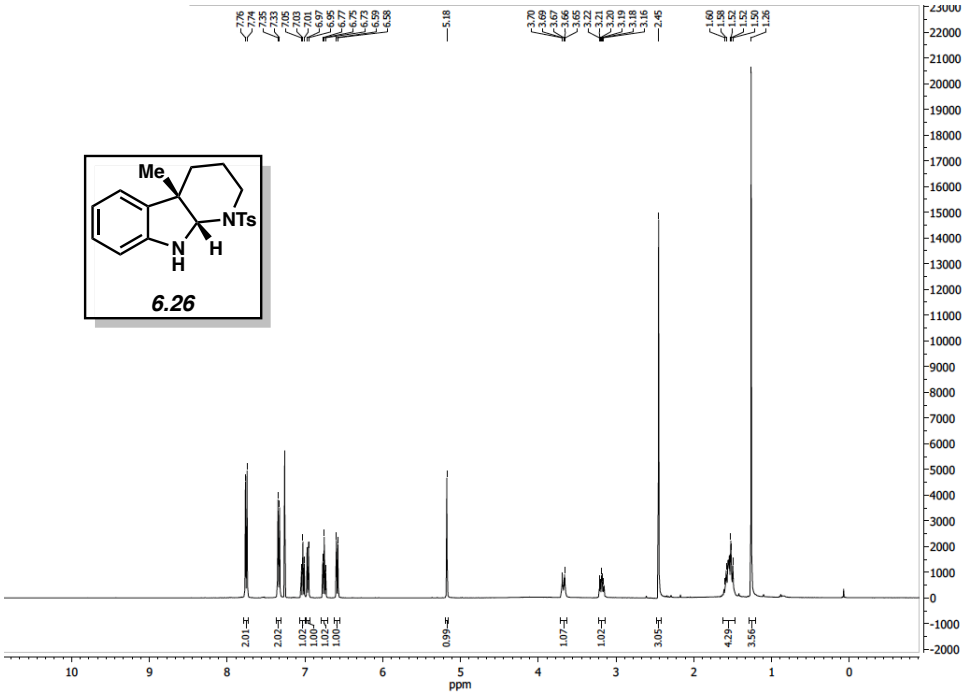

Figure 6.17 ^{1}H NMR (400 MHz, $CDCl_3$) of compound **6.26**.

6.7 Notes and References

(1) Polshettiwar, V.; Varma, R. S. *Curr. Opin. Drug Discov. Devel.* **2007**, *10*, 723.

(2) Lummiss, J. A. M.; Morse, P. D.; Beingessner, R. L.; Jamison, T. F. *Chem. Rec.* **2017**, *17*, 667.

(3) Brozowski, M.; O'Brien, M.; Ley, S. V.; Polyzos, A. *Acc. Chem. Res.* **2015**, *48*, 349.

(4) *Flow Chemistry;* Darvas, F.; Hessel, V.; Dormán, G., Eds.; De Gruyter: Berlin, 2014; Vols. 1 & 2.

(5) Fanelli, F.; Parisi, G.; Degennaro, L.; Luisi, R. *Beilstein J. Org. Chem.* **2017**, *13*, 520.

(6) Gérardy, R.; Emmanuel, N.; Toupy, T.; Kassin, V.-E.; Tshibalonza, N. N.; Schmitz, M.; Monbaliu, J.-C. M. *Eur. J. Org. Chem.* **2018**, *2018*, 2301.

(7) Hartman, R. L.; McMullen, J. P.; Jensen, K. F. *Angew. Chem., Int. Ed.* **2011**, *50*, 7502.

(8) Pieber, B.; Gilmore, K.; Seeberger, P. H. *J. Flow Chem.* **2017**, *7*, 129.

(9) Myers, R. M.; Fitzpatrick, D. E.; Turner, R. M.; Ley, S. V. *Chem. - A Eur. J.* **2014**, *20*, 12348.

(10) Gutmann, B.; Cantillo, D.; Kappe, C. O. *Angew. Chem., Int. Ed.* **2015**, *54*, 6688.

(11) Baumann, M.; Baxendale, I. R. *Beilstein J. Org. Chem.* **2015**, *11*, 1194.

(12) Klein, J. *Expert Opin. Investig. Drugs* **2007**, *16*, 1087.

(13) Sunazuka, T.; Hirose, T.; Shirahata, T.; Harigaya, Y.; Hayashi, M.; Komiyama, K.; Omura, S.; Smith, A. B. *J. Am. Chem. Soc.* **2000**, *122*, 2122.

(14) Ren, W.; Wang, Q.; Zhu, J. *Chem.- Int. Ed.* **2014**, *53*, 1818.

(15) Boal, B. W.; Schammel, A. W.; Garg, N. K. *Org. Lett.* **2009**, *11*, 3458.

(16) For a pertinent review of the Garg laboratory's Fischer indolization studies, see: Susick, R. B.; Morrill, L. A.; Picazo, E.; Garg, N. K. *Synlett* **2017**, *28*, 1.

(17) Schammel, A. W.; Boal, B. W.; Zu, L.; Mesganaw, T.; Garg, N. K. *Tetrahedron* **2010**, *66*, 4687.

(18) Simmons, B. J.; Hoffmann, M.; Champagne, P. A.; Picazo, E.; Yamakawa, K.; Morrill, L. A.; Houk, K. N.; Garg, N. K. *J. Am. Chem. Soc.* **2017**, *139*, 14833.

(19) *Flow Chemistry for the Synthesis of Heterocycles*; Van Mileghem, S.; Veryser, C.; De Borggraeve, W. M.; Sharma, U. K., Eds; Van der Eycken E. V., Eds. Springer: Cham, 2018; pp 133–159.

(20) Fischer, E.; Jourdan, F. Ueber Die Hydrazine Der Brenztraubensäure. *Berichte der Dtsch. Chem. Gesellschaft* **1883**, *16*, 2241.

(21) Fischer, E.; Hess, O. *Berichte der Dtsch. Chem. Gesellschaft* **1884**, *17*, 559.

(22) Zu, L.; Boal, B. W.; Garg, N. K. *J. Am. Chem. Soc.* **2011**, *133*, 8877.

(23) Gutmann, B.; Gottsponer, M.; Elsner, P.; Cantillo, D.; Roberge, D. M.; Kappe, C. O. *Org. Process Res. Dev.* **2013**, *17*, 294.

(24) Wahab, B.; Ellames, G.; Passey, S.; Watts, P. *Tetrahedron* **2010**, *66*, 3861.

(25) Xu, J.; Yu, J.; Jin, Y.; Li, J.; Yu, Z.; Lv, Y. *Chem. Eng. Process. Process Intensif.* **2017**, *121*, 144.